BioMed Research International

Advances in Prostate Cancer Research and Treatment

Guest Editors: Giovanni Luca Gravina, Lorenzo Livi, Andrea M. Isidori, and David Sherris

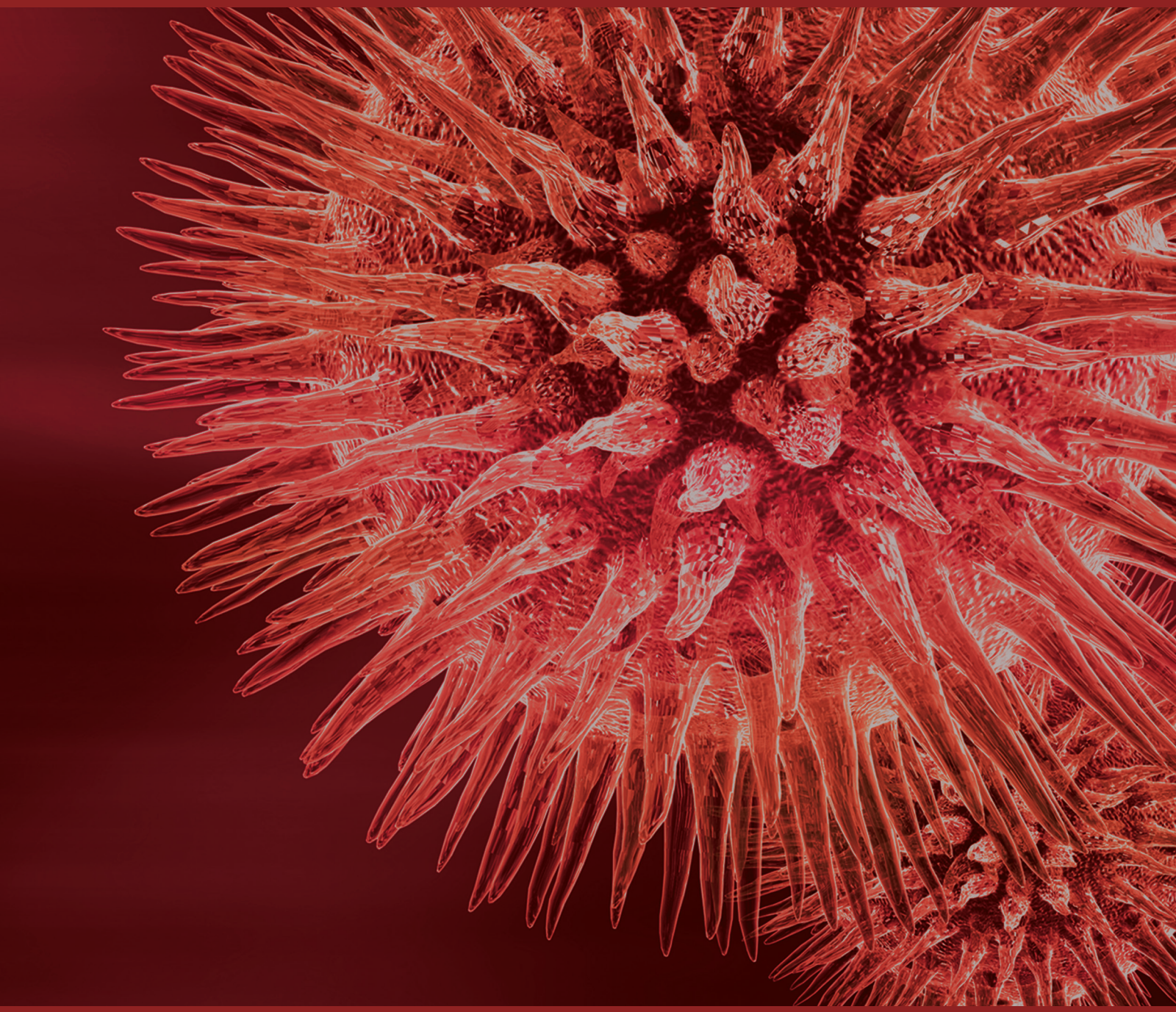

Advances in Prostate Cancer Research and Treatment

BioMed Research International

Advances in Prostate Cancer Research and Treatment

Guest Editors: Giovanni Luca Gravina, Lorenzo Livi, Andrea M. Isidori, and David Sherris

Contents

Hindawi Publishing Corporation
BioMed Research International
Volume 2014, Article ID 708383, 3 pages
http://dx.doi.org/10.1155/2014/708383

Editorial

Advances in Prostate Cancer Research and Treatment

Lorenzo Livi,[1] Andrea M. Isidori,[2] David Sherris,[3] and Giovanni Luca Gravina[2,4]

[1] *Radiotherapy Unit, Department of Experimental and Clinical Biomedical Sciences, University of Florence, Largo Brambilla 3, 50134 Firenze, Italy*
[2] *Department of Experimental Medicine, Sapienza University, 00161 Rome, Italy*
[3] *RestorGenex Pharmaceuticals, Inc., 37 Neillian Crescent, Jamaica Plain, MA 02130, USA*
[4] *Laboratory of Radiobiology and Division of Radiotherapy, Department of Applied, Clinical and Biotechnological Sciences, University of L'Aquila, Via Vetoio, Coppito 2, 67100 L'Aquila, Italy*

Correspondence should be addressed to Giovanni Luca Gravina; giovanniluca.gravina@uniroma1.it

Received 23 July 2014; Accepted 23 July 2014; Published 18 August 2014

It is becoming a truism to state that the progress in computer technologies and nanotechnologies, biomedical imaging, and molecular biology has made it possible to switch from a population treatment approach to a concept based on personalized medicine [1]. The shift from population to individual patient treatment implies the use of information derived from different actors and disciplines which individually do not have the capacity to propose a comprehensive offer [2]. This is particularly true in the field of radiation and medical oncology as well as in clinical and molecular radiology. The main advantage of combining information derived from different clinical and preclinical fields lies in the possibility of selecting a specific population of subjects who, most likely, will benefit from a particular pharmacological or nonpharmacological treatment in accordance with their "molecular profile" at a given time-point [1, 2]. At the same time this information may conversely be used to select patients for whom the risk of adverse effects may be higher [1, 2].

Prostate cancer (Pca) is one of the most commonly diagnosed cancers in men and surgery [3] and radiotherapy (RT) [3–5] remain the gold standard for the treatment of localized or locally advanced Pca. Radiotherapy is configured as a powerful treatment approach with outstanding oncological results and with impressive technical improvements over the last two decades [6]. We now have a greater understanding of mechanisms sustaining the biological processes responsible for tumor progression [7–12] or towards a biological aggressive or radio resistant phenotype [13–15]. However, we are aware that the improvement in oncological outcome of men who remain at high risk for systemic failure may be achieved by improving each diagnostic and therapeutic step including the diagnostic performances of conventional imaging modalities [16]. To date, conventional anatomic imaging techniques of computed tomography (CT), ultrasound, magnetic resonance imaging (MRI), single-photon emission computed tomography (SPECT), and positron emission tomography (PET) are currently used in the common clinical practice to stage men suffering from Pca [17–20]. All these diagnostic tools have peculiar advantages and disadvantages although they play a rather limited role in monitoring men with Pca [17–20]. These limitations are attributable to the incapacity to distinguish malignant from the surrounding nonmalignant tissue [16–20]. The close integration between molecular biology and clinical imaging may ease the development of new molecular imaging agents useful in monitoring a number of biological events that, until a few years ago, were studied by conventional molecular assays [17]. With regard to Pca, progress in quantification, characterization, and timing of biological processes may be obtained overcoming problems related to the amplification of low level signals of in vivo biological events, the development of integrated imaging platforms with sufficiently high spatial and temporal resolution [18], and the need to reach the target in vivo to achieve satisfactory specificity [16–20].

The advances in the molecular based approaches in radiology are specifically evident in oncological treatments [19]. One of the most striking examples of foregoing statements is attested by the development of the enormous amount

of specific drugs and inhibitors, the ability to genetically modify cellular systems, and the introduction of a multitude of diagnostic tools able to monitor individual molecular and biological processes [17]. These achievements have dramatically augmented our understanding of molecular oncology and this body of knowledge can now be translated into new drugs or agents for molecular imaging by allowing detection of patients with specific molecular profiles and improving patient care [20].

Finally a significant advance has been achieved with the theranostics which represents a research field integrating two distinct approaches that both encompass all steps of patients' management [21–23]. Of course, medical imaging is the prerequisite for such approach. However, the other mainstay of this approach is the use of molecular biomarkers which are important in the diagnostic processes, in determining the best course of treatment, in monitoring the patient's response and in detecting potential recurrence of the disease, and in anticipating potential adverse effects. Basically, theranostics has three distinct fields of application. They include (1) selection of patients for a specific treatment, (2) the prediction for drug response, resistance, and safety, and (3) monitoring of the therapeutic response [21–23].

This and much more are the heart of this special issue on the advances in diagnosis and treatment of prostate cancer. This special issue encompasses articles on the state of the art, advantages, and disadvantages, current limitations, and future perspectives of Pca monitoring and treatment methods. G. L. Gravina et al., *"Strategies for imaging androgen receptor signaling pathway in prostate cancer: implications for hormonal manipulation and radiation treatment,"* D. Junker et al., *"Evaluation of the PI-RADS scoring system for classifying mpMRI findings in men with suspicion of prostate cancer,"* S. F. Carbone et al., *"Diffusion-weighted magnetic resonance diagnosis of local recurrences of prostate cancer after radical prostatectomy: preliminary evaluation on twenty-seven cases,"* and V. Panebianco et al., *"Advanced imaging for the early diagnosis of local recurrence prostate cancer after radical prostatectomy,"* present advanced clinical and molecular imaging methods in clinical follow-up of response to therapy. T. Gondek et al., *"Evaluation of 12-lipoxygenase (12-LOX) and plasminogen activator inhibitor 1 (PAI-1) as prognostic markers in prostate cancer,"* M. Srivastava et al., *"Diverse effects of ANXA7 and p53 on LNCaP prostate cancer cells are associated with regulation of SGK1 transcription and phosphorylation of the SGK1 target FOXO3A,"* F. Zazzeroni et al., "*KCTD11 tumor suppressor gene expression is reduced in prostate adenocarcinoma,*" D. Gianfrilli et al., *"Sex steroid metabolism in benign and malignant intact prostate biopsies: individual profiling of prostate intracrinology,"* M. Lanciotti et al., *"The role of M1 and M2 macrophages in prostate cancer in relation to extracapsular tumor extension and biochemical recurrence after radical prostatectomy,"* I. Giusti and V. Dolo, "*Extracellular vesicles in prostate cancer: new future clinical strategies?,*" T. Van den Broeck et al., *"The role of single nucleotide polymorphisms in predicting prostate cancer risk and therapeutic decision making,"* A. Dimakakos et al., *"Novel tools for prostate cancer prognosis, diagnosis, and follow-up,"* and A. Irelli et al., *"Bioclinical parameters driving decision-making of subsequent lines of treatment in metastatic castration-resistant prostate cancer,"* offer new insight into the use of some traditional and less well established cancer biomarkers in clinical and laboratory practice. The works of C. Festuccia et al., *"Antitumor effects of saffron-derived carotenoids in prostate cancer cell models,"* S. Taurin et al., *"A novel role for raloxifene nanomicelles in management of castrate resistant prostate cancer,"* and A. Colciago et al., *"In vitro chronic administration of ERbeta selective ligands and prostate cancer cell growth: hypotheses on the selective role of 3beta-adiol in AR-positive RV1 cells,"* deal with the use of innovative pharmacological treatments. Of special interest are the articles that report on novel focal treatments, hypofractionated or modulated and intensified adjuvant radiation treatments for the management of prostate cancer, by A. M. Hirst et al., "*Low temperature plasma: a novel focal therapy for localized prostate cancer?,*" M. Valeriani et al., *"Image-guided hypofractionated radiotherapy in low-risk prostate cancer patients,"* G. Mantini et al., *"Intensified adjuvant treatment of prostate carcinoma: feasibility analysis of a phase I/II trial,"* S. Barra et al., *"Image guided hypofractionated radiotherapy by helical tomotherapy for prostate carcinoma: toxicity and impact on Nadir PSA,"* and M. Mangoni et al., *"Hypofractionation in prostate cancer: radiobiological basis and clinical appliance."*

Authors' Contribution

Lorenzo Livi and Andrea M. Isidori equally contributed to this paper.

Acknowledgment

We would like to thank all authors who contributed to this special issue for their excellent work and we hope that this issue will be useful to the experts of all profiles dealing with prostate cancer in both clinical and preclinical settings.

Lorenzo Livi
Andrea M. Isidori
David Sherris
Giovanni Luca Gravina

References

[1] L. Patel, B. Parker, D. Yang, and W. Zhang, "Translational genomics in cancer research: converting profiles into personalized cancer medicine," *Cancer Biology & Medicine*, vol. 10, no. 4, pp. 214–220, 2013.

[2] P. Malaney, S. V. Nicosia, and V. Davé, "One mouse, one patient paradigm: new avatars of personalized cancer therapy," *Cancer Letters*, vol. 344, no. 1, pp. 1–12, 2014.

[3] R. Siegel, C. DeSantis, K. Virgo et al., "Cancer treatment and survivorship statistics, 2012," *CA: A Cancer Journal for Clinicians*, vol. 62, no. 4, pp. 220–241, 2012.

[4] M. di Staso, P. Bonfili, G. L. Gravina et al., "Late morbidity and oncological outcome after radical hypofractionated radiotherapy in men with prostate cancer," *BJU International*, vol. 106, no. 10, pp. 1458–1462, 2010.

[5] V. Tombolini, M. Di Staso, P. Bonfili et al., "Subjective and objective measures of late genitourinary morbidity following

hypofractionated radiotherapy in men with prostate cancer," *Prostate Cancer and Prostatic Diseases*, vol. 13, no. 1, pp. 34–38, 2010.

[6] V. Valentini, B. Glimelius, and V. Frascino, "Quality assurance and quality control for radiotherapy/medical oncology in Europe: guideline development and implementation," *European Journal of Surgical Oncology*, vol. 39, no. 9, pp. 938–944, 2013.

[7] G. L. Gravina, F. Marampon, D. Sherris et al., "Torc1/Torc2 inhibitor, Palomid 529, enhances radiation response modulating CRM1-mediated survivin function and delaying DNA repair in prostate cancer models," *Prostate*, vol. 74, no. 8, pp. 852–868, 2014.

[8] C. Festuccia, G. L. Gravina, A. Mancini et al., "Trifluoroibuprofen inhibits α-methylacyl coenzyme A racemase (AMACR/P504S), reduces cancer cell proliferation and inhibits in vivo tumor growth in aggressive prostate cancer models," *Anti-Cancer Agents in Medicinal Chemistry*, vol. 14, no. 7, 2014.

[9] G. L. Gravina, F. Marampon, P. Muzi et al., "PXD101 potentiates hormonal therapy and prevents the onset of castration-resistant phenotype modulating androgen receptor, HSP90, and CRM1 in preclinical models of prostate cancer," *Endocrine-Related Cancer*, vol. 20, no. 3, pp. 321–337, 2013.

[10] G. L. Gravina, F. Marampon, M. Piccolella et al., "Hormonal therapy promotes hormone-resistant phenotype by increasing DNMT activity and expression in prostate cancer models," *Endocrinology*, vol. 152, no. 12, pp. 4550–4561, 2011.

[11] G. L. Gravina, F. Marampon, F. Petini et al., "The TORC1/TORC2 inhibitor, palomid 529, reduces tumor growth and sensitizes to docetaxel and cisplatin in aggressive and hormone-refractory prostate cancer cells," *Endocrine-Related Cancer*, vol. 18, no. 4, pp. 385–400, 2011.

[12] G. L. Gravina, C. Festuccia, F. Marampon et al., "Biological rationale for the use of DNA methyltransferase inhibitors as new strategy for modulation of tumor response to chemotherapy and radiation," *Molecular Cancer*, vol. 9, pp. 305–317, 2010.

[13] J. Ni, P. J. Cozzi, J. L. Hao et al., "CD44 variant 6 is associated with prostate cancer metastasis and chemo-/radioresistance," *The Prostate*, vol. 74, no. 6, pp. 602–617, 2014.

[14] L. Chang, P. H. Graham, J. Hao et al., "Emerging roles of radioresistance in prostate cancer metastasis and radiation therapy," *Cancer Metastasis Reviews*, vol. 33, no. 2-3, pp. 469–496, 2014.

[15] J. Bartek, M. Mistrik, and J. Bartkova, "Androgen receptor signaling fuels DNA repair and radioresistance in prostate cancer," *Cancer Discovery*, vol. 3, no. 11, pp. 1222–1224, 2013.

[16] G. L. Gravina, V. Tombolini, M. D. Staso et al., "Advances in imaging and in non-surgical salvage treatments after radiorecurrence in prostate cancer: what does the oncologist, radiotherapist and radiologist need to know?" *European Radiology*, vol. 22, no. 12, pp. 2848–2858, 2012.

[17] L. Fass, "Imaging and cancer: a review," *Molecular Oncology*, vol. 2, no. 2, pp. 115–152, 2008.

[18] M. G. Pomper, "Translational molecular imaging for cancer," *Cancer Imaging A*, vol. 5, pp. S16–S26, 2005.

[19] S. Kumar, A. Mohan, and R. Guleria, "Biomarkers in cancer screening, research and detection: present and future: a review," *Biomarkers*, vol. 11, no. 5, pp. 385–405, 2006.

[20] D. A. Mankoff, "Molecular imaging to select cancer therapy and evaluate treatment response," *Quarterly Journal of Nuclear Medicine and Molecular Imaging*, vol. 53, no. 2, pp. 181–192, 2009.

[21] J. M. Street and J. W. Dear, "The application of mass-spectrometry-based protein biomarker discovery to theragnostics," *The British Journal of Clinical Pharmacology*, vol. 69, no. 4, pp. 367–378, 2010.

[22] D. Majumdar, X. Peng, and D. M. Shin, "The medicinal chemistry of theragnostics, multimodality imaging and applications of nanotechnology in cancer," *Current Topics in Medicinal Chemistry*, vol. 10, no. 12, pp. 1211–1226, 2010.

[23] V. I. Shubayev, T. R. Pisanic II, and S. Jin, "Magnetic nanoparticles for theragnostics," *Advanced Drug Delivery Reviews*, vol. 61, no. 6, pp. 467–477, 2009.

Hindawi Publishing Corporation
BioMed Research International
Volume 2014, Article ID 464869, 8 pages
http://dx.doi.org/10.1155/2014/464869

Research Article

Sex Steroid Metabolism in Benign and Malignant Intact Prostate Biopsies: Individual Profiling of Prostate Intracrinology

Daniele Gianfrilli,[1] Silvia Pierotti,[1] Riccardo Pofi,[1] Costantino Leonardo,[2] Mauro Ciccariello,[3] and Federica Barbagallo[1]

[1] *Department of Experimental Medicine, Sapienza University, Viale del Policlinico 155A, 00161 Rome, Italy*
[2] *Department of Urology, Sapienza University, 00161 Rome, Italy*
[3] *Department of Radiology, Sapienza University, 00161 Rome, Italy*

Correspondence should be addressed to Daniele Gianfrilli; daniele.gianfrilli@uniroma1.it

Received 2 May 2014; Accepted 18 June 2014; Published 13 August 2014

Academic Editor: Giovanni Luca Gravina

In vitro studies reveal that androgens, oestrogens, and their metabolites play a crucial role in prostate homeostasis. Most of the studies evaluated intraprostatic hormone metabolism using cell lines or preprocessed specimens. Using an *ex vivo* model of intact tissue cultures with preserved architecture, we characterized the enzymatic profile of biopsies from patients with benign prostatic hyperplasia (BPH) or cancer (PC), focusing on 17β-hydroxy-steroid-dehydrogenases (17β-HSDs) and aromatase activities. Samples from 26 men who underwent prostate needle core biopsies (BPH $n = 14$; PC $n = 12$) were incubated with radiolabeled ^{3}H-testosterone or ^{3}H-androstenedione. Conversion was evaluated by TLC separation and beta-scanning of extracted supernatants. We identified three major patterns of conversion. The majority of BPHs revealed no active testosterone/oestradiol conversion as opposed to prostate cancer. Conversion correlated with histology and PSA, but not circulating hormones. Highest Gleason scores had a higher androstenedion-to-testosterone conversion and expression of 17β-HSD-isoenzymes-3/5. *Conclusions*. We developed an easy tool to profile individual intraprostatic enzymatic activity by characterizing conversion pathways in an intact tissue environment. In fresh biopsies we found that 17β-HSD-isoenzymes and aromatase activities correlate with biological behaviour allowing for morphofunctional phenotyping of pathology specimens and clinical monitoring of novel enzyme-targeting drugs.

1. Introduction

Prostate cancer is the most common cancer in men. An increasing trend in prostate cancer incidence, a disease associated with age, has been described and partially attributed to better screening procedures [1] and awareness [2]. A significant number of prostate cancers, however, remain indolent and, if untreated, do not alter life quality and expectancy. For this reason the burden of universal treatment of confined asymptomatic disease should be weighed against the economic socioeconomic costs of overtreatment, the complications associated with the currently available treatments (including androgen-deprivation therapy), and the overall quality/life expectancy of affected subjects [3, 4].

Improvements in prostate cancer diagnosis, classification, and treatment witnessed in the past 20 years have not been paralleled by improvement in preoperative prognostic grading of the disease which still relies on morphological appearance of random biopsies. A functional prognostic presurgical characterization of the disease is needed to identify those subjects who require aggressive treatment and those who can be managed conservatively. Furthermore, a function profiling of prostate tissue will also be very useful to monitor unoperated patients during radiotherapy (RT) and androgen-deprivation therapy (ADT) to follow up changes in prostate tissue responsiveness and aggressiveness.

It is widely accepted that androgens play a central role in the biology of the prostate. Estrogens, however, can also modulate prostatic growth and development [5, 6]. Taken together, observations from many studies on murine models imply that both androgens and estrogens are needed to induce proliferative, precancerous lesions and prostate

cancer. Indeed, the balance between androgen induced cell proliferation and apoptosis is thought to be a major regulator of growth of the normal and cancerous prostate. Epidemiological studies, however, showed that there is no association between circulating steroid hormone levels and prostate cancer [7]. *In vitro* studies reveal that intratissual levels of sex steroids may diverge from their plasmatic counterpart due to complex enzymatic equipment expressed by prostate cells that can interconvert steroids [8]. Labrie et al. was the first to describe the "intracrinology" of the prostate gland [9, 10].

Prostate tissue contains a variety of steroid metabolizing enzymes required for the local production of active androgens and estrogens from their precursors provided by the adrenals [10–12]. The main enzymes involved in local steroid metabolism are steroid sulfatases, 3β-hydroxysteroid dehydrogenases (3β-HSDs), 17β-hydroxysteroid dehydrogenases (17β-HSDs), 5β-reductases, and aromatase. In normal conditions a steady state exists between synthesis and inactivation of active androgens; however tissue transformation can be associated with an alteration of this balance. Increasing evidences suggest that prostate cancer cells alter local and paracrine steroid hormone metabolism. In the past decade, a growing number of studies tried to explore the role of local androgen production in cancer progression and transformation into castrate-resistant tumours (CRPC) [13, 14].

In the present work we provide evidences that intraprostatic hormonal profiling, some sort of individual metabolic fingerprint, can be easily obtained. One of the most innovative features of the present study is that we analysed the metabolism of prostate cells directly "*ex vivo*" on fresh specimens from biopsy or surgical resection. The aim of the current work is (1) to set up a reproducible, rapid, and easy approach to define the enzymatic profiling of the normal, hyperplastic (BPH), and cancerous prostate cell (PC) (2) to correlate the patterns with steroid enzymes' expression and tumour's histology.

2. Methods

2.1. Patients and Tissues. Specimens were obtained from 26 patients (14 BPH and 12 PC) who underwent transrectal ultrasound-guided prostate biopsy followed by prostate surgery (radical for cancer or transurethral for enlargement) between 2009 and 2012 at the Department of Urology, Sapienza University. The clinical characteristics are reported in Table 1.

All patients examined in this study did not receive radiation, chemotherapy, or hormone therapy before surgery. Clinical data, including patient age, serum prostate specific antigen (PSA) concentration, clinical stage according to the International TNM classification, lymph node status, and Gleason's score, were retrieved for all patients. All procedures were performed using commercially available ultrasound equipment with 7.5 MHz probes (Philips IU22); biopsy samples were obtained using an automatic spring-loaded biopsy gun with an 18-gauge needle.

Specimens upon collection were placed on saline buffer and immediately processed (Figure 1). The protocol was reviewed and approved by the local board and funded by study Grants MIUR 2008NY72SJ and RBFR10URHP.

Table 1: Characteristics of enrolled subjects.

	BPH ($n = 14$)	PC ($n = 12$)
AGE		
Mean ± SD	67 ± 7	70 ± 7
(Range)	(56–79)	(68–84)
PSA	3.02 ± 1.58 ng/mL	9.13 ± 5.47 ng/mL
Gleason score	n.a.	Gleason < 8 (60%) Gleason ≥ 8 (40%)
Therapies	2/14 on α-lytic agents (no pts. on hormonal treatment)	No pts. on hormonal treatment
Additional notes	3/14 with chronic inflammation	

2.2. Enzymatic Assays. Unprocessed samples were split into three parts, one for enzymatic activity, one for mRNA gene expression studies, and one sent to the pathologist for confirmation. One hundred milligrams of intact tissue was exposed to physiological concentrations of different H_3-labeled compounds (Sigma-Aldrich), to explore the capability of these cells to metabolize these substances, in serum-free buffering medium under controlled temperature and atmosphere. One hundred microliters of media was collected at different time points (30 min, 1 h, 2 h, 4 h, 8 h, and 16 h) after incubation of various H_3-labeled steroids and total lipids were extracted with 400 μL Folch reagent (chloroform/methanol: 2 : 1 vol/vol), vortexed, and spun at 14,000 ×g for 5 min. The organic phase was collected and evaporated in a speed-vac. Dried extracts were redissolved in 40 μL of ethanol and spotted onto TLC plates (Whatman). The plates were developed twice in chloroform-ethyl acetate (4 : 1 vol/vol). Steroid metabolites were quantified using a BioScan AR-2000 Imaging System (Bioscan). Bidimensional acquisition of β-emission was obtained using dedicated software (Bioscan).

2.3. Reverse Transcriptase-Polymerase Chain Reaction (RT-PCR). RNA was extracted from tissue samples using GenElute TM Mammalian Total RNA Miniprep kit according to the manufacturer's instructions (Sigma-Aldrich). 1 μg of total RNA was retrotranscribed in a total volume of 50 μL using random primers (F. Hoffmann-La Roche, Basel, Switzerland) and M-MLV reverse transcriptase (Invitrogen, Carlsbad, CA) and used as template for real-time polymerase chain reaction. Real-time quantitative PCRs (qPCR) was performed using 2 μL of cDNA, 18 μM for each primer, 5 μM for probe (Applied Biosystems), TaqMan GenEX Master Mix (Applied Biosystems), and iQCycler (Bio-Rad Laboratories) according to the manufacturer's instructions. 17β-HSD1, 17β-HSD2, 17β-HSD3, 17β-HSD4, 17β-HSD5, 17β-HSD7, 17β-HSD8, 17β-HSD10, aromatase, and beta-actin (actb) human primers were used. Data were analyzed using the standard curve method. The relative quantities of transcripts were calculated

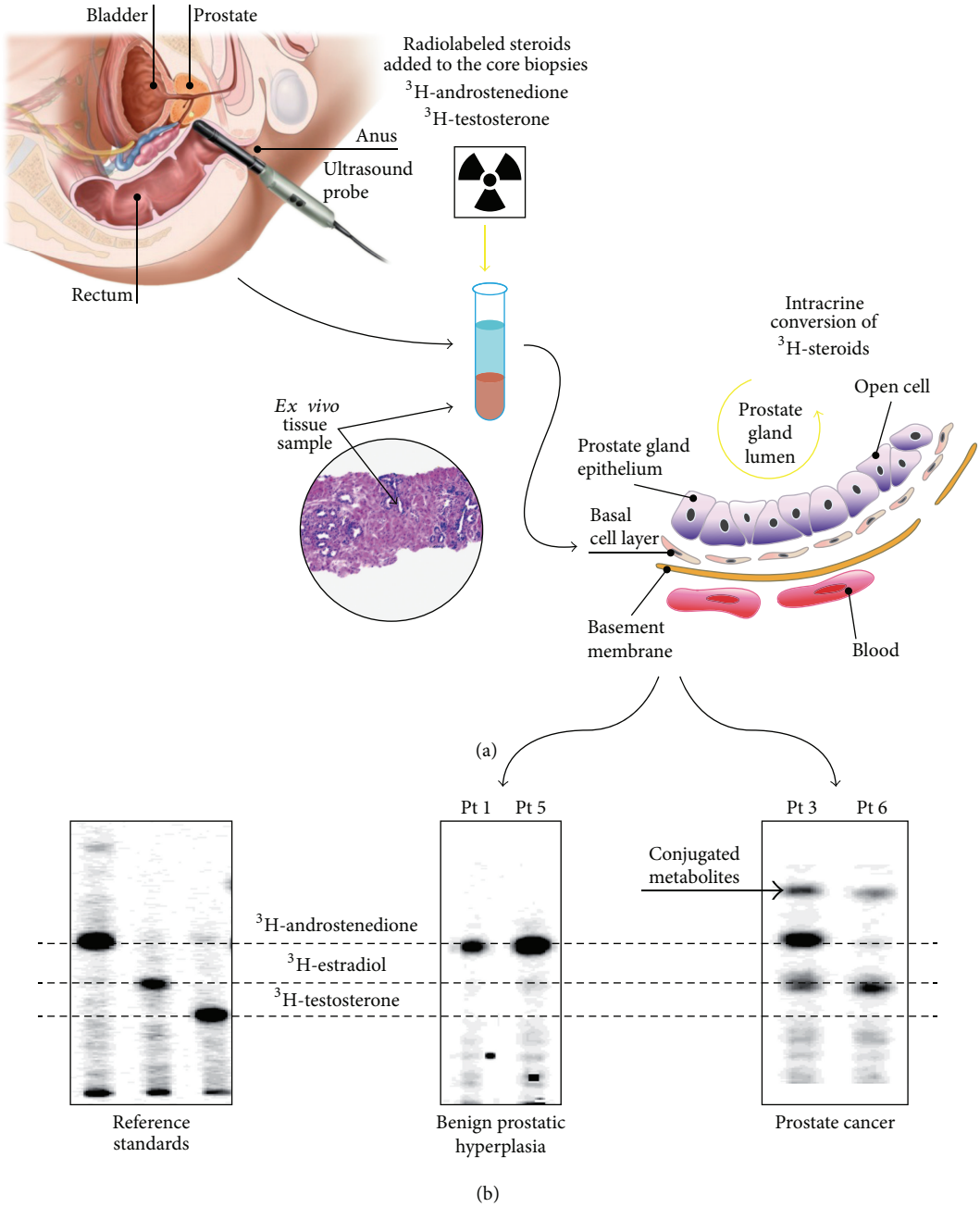

Figure 1: (a) Unique features of our "*ex vivo*" model: samples were histologically confirmed on-site, part of each sample was immediately dry frozen for subsequent RNA analysis, and part was fixed and embedded for paraffin section analysis. The core biopsies guaranteed tissue integrity that is crucial to maintain enzyme kinetics and directionality closer to what occurs in *in vivo*; specifically the stromal-to-epithelial interaction remains unaltered, allowing appraisal of the contribution of tumor microenvironment. (b) Examples of different TCL patterns (steroid fingerprint) in patients with BPH or PC (monodimensional development). Of notice is that patients with different stage PC exhibit different steroid maps (patient 3 had a Gleason 6, while patient 6 a Gleason 8). Incubation time: 24 hours. BPH: benign prostatic hyperplasia; PC: prostate cancer.

from triplicate samples after normalization of the data against the housekeeping gene (actb).

2.4. Data Analysis and Statistical Methods. Differences between experimental groups were analyzed by the Student's *t*-test and chi-square test. Spearman's correlation coefficients were used to assess the relationship between experimental variables. Multiple comparisons were performed using a one-way ANOVA and Turkey's post hoc test. The test was two-sided and $P \leq 0.05$ was considered significant. All analyses were performed using SPSS version 17.0 PC version (SPSS Inc., Chicago, IL, USA).

3. Results

Clinical features of the enrolled patients are reported in Table 1. None of the recruited patients were taking steroid hormones or chemotherapy or received previous external beam radiation. Two PBH patients were on α-adrenolytic treatment of lower urinary tract symptoms.

To determine the efficiency whereby various precursors undergo intraprostatic conversion to more potent steroids, an operation protocol has been designed as follows: normal and cancerous cells derived from bioptic specimens were exposed to physiological concentrations of different labelled compounds (herein described for ^{3}H-androstenedione or ^{3}H-testosterone) as described in methods. Enzymatic products were then separated by two-dimensional TLC (2D-TLC) by sequential use of two customized mobile phases in order to discriminate molecular compounds that may differ for a single atom of hydrogen. The 2D procedure started with a classical monodimensional TLC (as shown in Figure 1) that, when necessary, could be followed by a further separation based on the affinity with the second mobile phase run orthogonally to the first one. Because it is unlikely that two molecules will be similar in two distinct repartition properties, molecules are more effectively separated in 2D-TLC than in 1D-TLC. As a result the products of hormone metabolism spread out across the whole chromatographic surface. In respect to the current analysis of androstenedione/testosterone conversion into estrogens or testosterone a 1D-TLC was sufficient to discriminate the various steroids. Subsequent scanning of the developed TLC sheet, by means of the Argon-Methane enhanced β-emission scanner, will allow the identification of substrate-product(s) emitting spots and the measurement of CPM from each spot. Bioscan software renders an image that is equivalent to a "metabolic fingerprint" of each prostatic specimen (Figure 1(b)).

A representative pattern of conversion that has been observed in BPH and in PC is shown in Figure 1(b). When PC samples were exposed to ^{3}H-androstenedione the most frequent observed pattern was estradiol conversion (66%), while 17% of tissue revealed testosterone formation and the remaining 17% showed no conversion activity (Figure 2). On the contrary the majority of BPH samples showed no conversion (60%) or estrogen formation (30%); only 10% of samples exhibited some testosterone production. When PC samples were exposed to ^{3}H-testosterone, the majority (66%) revealed estrogen formation or no conversion (34%); none showed formation of conjugated byproducts. On the contrary in BPH samples 60% of subjects showed formation of conjugated steroids, while estrogen formation was observed in 22% and 18% exhibited no conversion (Figure 2).

The synthesis of testosterone from precursor molecules occurs via a well-established sequence of reversible reactions. Since androgen levels may be affected by both changes in synthetic and degradative enzyme expression, gene expression analyses of 17β-HSD types 5 and 7 isoenzymes with predominant reductase activity versus types 4, 8, and 10 with a predominant oxidase activity were performed in BPH and PC (Figure 3). Compared to normal tissue, BPH showed a significant lower expression level of the 17β-HSD types 5, 7, and 10 enzymes, consistently with a reduced de novo enzymatic production of androgens; in respect to PC, all samples showed lower levels of expression for all enzymes, compared to BPH tissue. This finding is in apparent contrast with the enzymatic conversion activities reported in Figure 2. Indeed, PC showed a predominant reduction in the expression of the 17β-HSDs with reductase activity compared to oxidizing ones, when compared with BPH or normal tissue.

Moreover none of the PC samples expressed 17β-HSD type 2, compared to BPH, while maintaining an efficient expression of 17β-HSD type 3 enzymes and aromatase transcripts (Figure 4).

In Figure 5 estradiol and testosterone generation in all samples (compared to the maximum conversion achieved set to 10) is reported. Despite the relatively small cohort number, a greater enzymatic activity is seen in PC samples with a high grade Gleason score compared to low Gleason score (histology) ($P < 0.05$).

4. Discussion

Prostate cancer is considered a "hormone-dependent" disease because the prostate requires testicular androgens for its secretory function and cancerous cells retain this sensitivity to androgens. Cell growth and survival of early stage prostate cancer can in fact respond to androgens and this evidence is the background of the androgen-deprivation therapy (ADT). Although plasma concentrations of testosterone have been shown to decrease by more than 90% following castration, androgen levels in prostate cancer tissues decreased only by 50–60%, suggesting the importance of in situ androgen production in prostate cancers [6, 15, 16]. In addition, ADT is associated with severe systemic adverse events such as cardiac, metabolic, hepatic, bone, sexual, and cognitive complications that eventually lead to an increased mortality rate compared to the risk related to prostatic cancer itself [3, 4]. ADT is successful until the tumour enters an androgen-refractory state, leading to the failure of such long-term strategy.

So far it has been impossible to associate high levels of circulating androgens with the progression of prostate cancer [7]. This is in strong agreement with the decline of plasmatic testosterone with age, which would ultimately lead to an inverse relationship between circulating androgens and the risk of developing prostate cancer. As a matter of fact, intratissual levels of sex steroids may diverge from their plasmatic counterpart due to enzymatic equipment that can interconvert and metabolize steroids [9, 10, 15]. The local steroid metabolism is therefore the main determinant of the intraprostatic hormonal profile. Androgens level variation as sole determinants of prostate cancer development and progression has led to neglecting the evidence that the onset of malignancy is accompanied by an estrogen-sensitive condition where tumour growth and spread is stimulated and maintained by an increase in the cellular levels of androgen aromatization into estrogens, in a manner similar to that described in breast cancer [6, 11]. Moreover, animal models

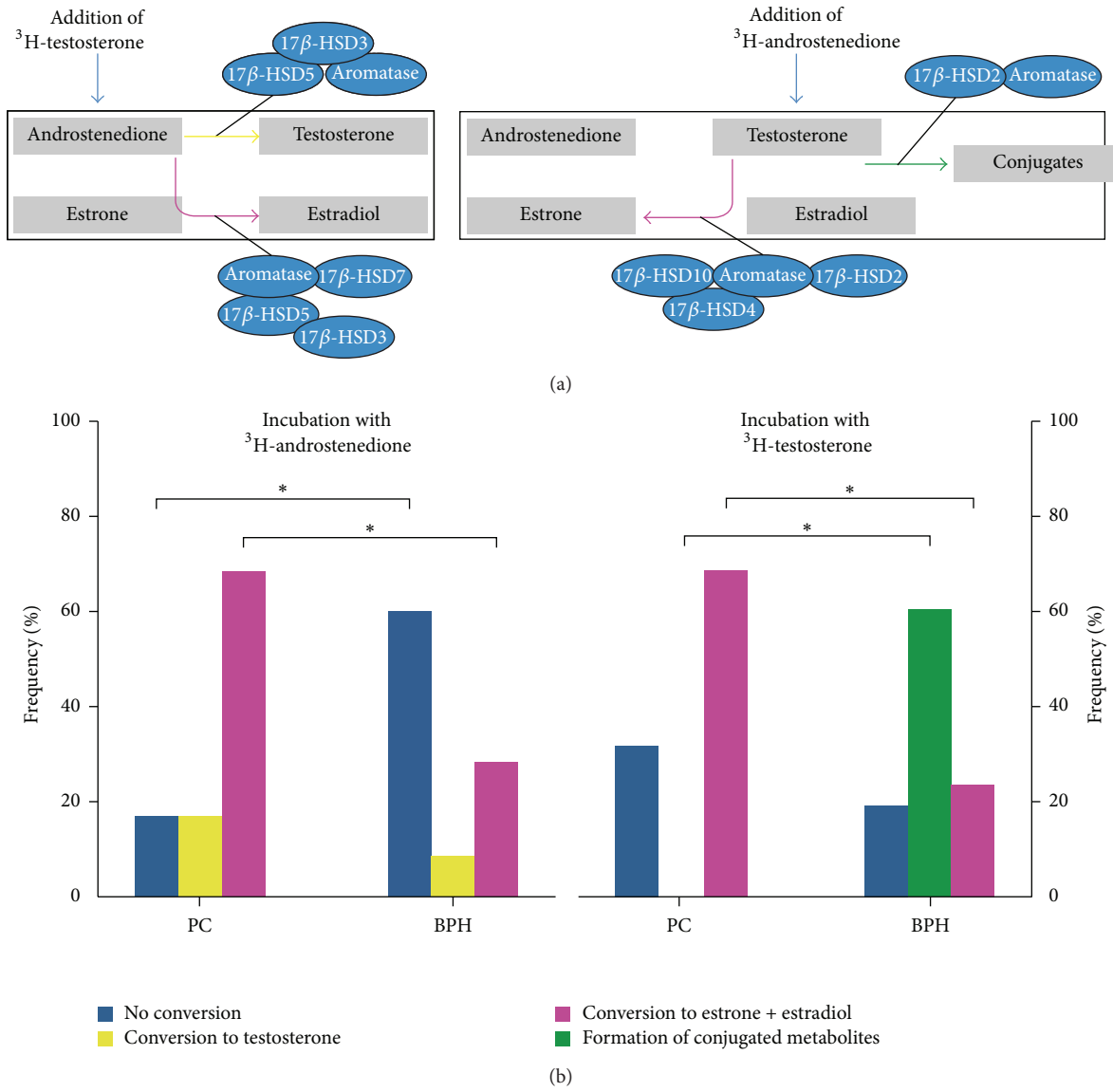

FIGURE 2: (a) Schematic representation of the different pathways evaluated by TLC byproducts formation after exposure to ^{3}H-androstenedione or ^{3}H-testosterone. (b) Frequency of the major pattern of conversions observed during incubation in all subjects (more than one conversion reaction can be observed in the same subject). $^*P < 0.05$; BPH: benign prostatic hyperplasia ($n = 14$); PC: prostate cancer ($n = 12$).

have clearly showed that supraphysiological levels of estrogens and androgens are each separately capable of altering the normal growth of the prostate, but individually they do not induce prostatic malignancy. As neither hormone by itself is able to induce malignant changes in the prostate, the balance between sex steroids is critical in inducing premalignant and malignant lesions. In this respect, an altered profile of prostatic enzymes that metabolize steroids has to be invoked in the acquisition of aggressiveness of prostate cancer. At present, we barely know the exact molecular mechanisms underlining the progression of the prostatic disease and the acquisition of the metastatic behaviour.

Classical monitoring factors of prostate cancer, such as PSA levels, stadiation, and Gleason score, are losing their reliability in the attempt to discriminate among multiple stages of the disease. New prognostic and diagnostic markers are needed. Our goal was to develop novel methods to acquire data on the enzymatic profile (and its changes) in intact prostate tissue in order to characterize the history of the disease with respect to follow-up, medical, surgical, and radiotherapeutic procedures.

In addition, there is a recent growing interest toward several metabolites that could be bioactivated into more active steroids with high affinity binding to androgen receptor (AR) or estrogen receptor (ER) [17]. An interesting observation is that androgenic activity of the C11-keto forms of A4, T, and DHT are more androgenic than their respective 11-hydroxy forms [17]. This implicates that the activity of

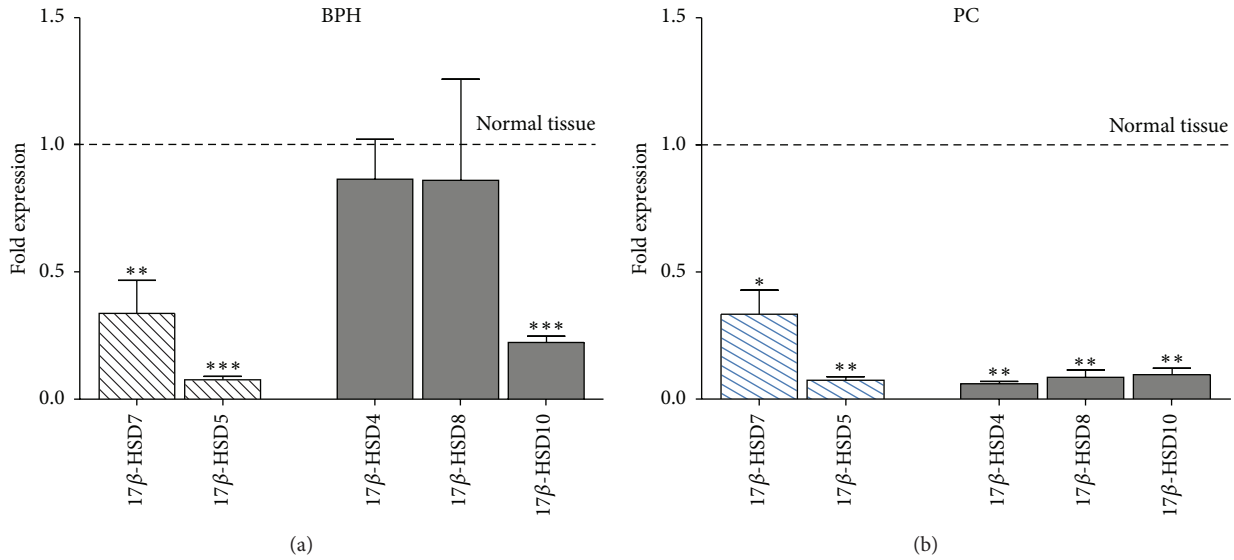

Figure 3: Quantitative gene expression in examined tissue relative to whole (normal) prostate tissue (fold change) of 17β-HSDs with predominant reductase activity (types 5 and 7, yellow) versus 17β-HSDs with a predominant oxidase activity (types 4, 8, and 10, green). BPH: benign prostatic hyperplasia ($n = 11$); PC: prostate cancer ($n = 7$). Statistical significance is represented versus whole normal tissue $^{***}P \leq 0.001$; $^{**}P < 0.01$.

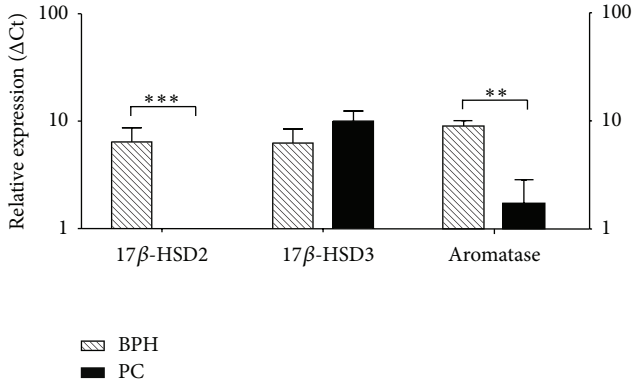

Figure 4: Quantitative gene expression in examined tissue relative to whole (normal) prostate tissue (normal set to 1) of 17β-HSD type 2 and type 3 and aromatase. BPH: benign prostatic hyperplasia ($n = 11$); PC: prostate cancer ($n = 7$).

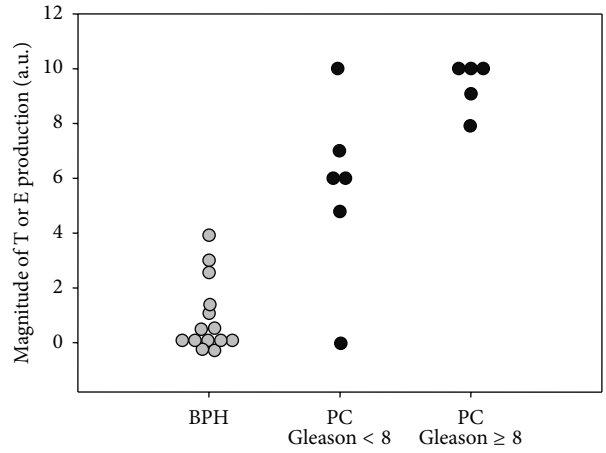

Figure 5: Correlation between conversion efficiency toward testosterone or estradiol and histological grading of tissue samples; BPH: benign prostatic hyperplasia (gray circle, $n = 14$); PC: prostate cancer (solid circle, $n = 12$).

the 11β-HSDs family, which interconvert 11-hydroxy and 11-keto steroids, could be another regulatory point in the activation or inactivation of 11-hydroxy and 11-keto androgens in the prostate [17]. The involvement of 11b-HSD in prostate physiology deserves future studies as it has already been shown to be crucial in several clinical conditions [18, 19].

The most extensively studied intracrinology pathways, nowadays, are those related to the 17β-HSDs.

Precise measurements of relative enzymatic activity of this family are complicated by the requirement for optimal pH and nicotinamide adenine dinucleotide cofactors that requires intact cell models. In this respect we believe that our model has the advantage of assessing this in the best way. In androgen and estrogen metabolism, 17HSDs catalyze the reactions between the active 17β-hydroxysteroids and less active 17-ketosteroids. At present, several 17HSD isoenzymes have been characterized [20]; specifically types 1, 3, 5, and 7 are reductive enzymes, whereas types 2, 4, 8, 10, and 11 are oxidative enzymes. Very recently Fankhauser and colleagues showed that upregulation of 17HSD17B is the predominant source of signalling androgens in hormone refractory prostate cancer, much greater than either the so-called "backdoor" or the "5-α dione" pathway [14].

Our findings document that in an *ex vivo* model of intact prostate tissue, an enhanced reductive pathway is a feature of PC, compared to BPH. These data are consistent with those

by Nakamura et al., demonstrating that in human prostate cancer 17β-HSD5 immunoreactivity was detectable in 77% of cases with a stronger staining correlated to more advanced clinical stages (TNM stage pT3 versus pT2) [21].

The current idea is that the progression of prostate cancer in the setting of castrate androgen levels is not due to the development of an androgen insensitive tumour clone but rather to the fact that the cancer has evolved mechanisms to escape systemic androgen deprivation while still taking advantage of signalling through AR [6, 13–15, 22].

The recognition of the fact that intratumoural androgen synthesis and activity are biologically relevant and that overexpression of the AR is a consistent feature of prostate cancer progression has led to the development of several new therapeutic approaches. One example is the utilization of abiraterone acetate, an inhibitor of 17α-hydroxylase and C17, 20 lyase (CYP17A1) for advanced CRPC treatment. Blockade of CYP17A1 activity by abiraterone suppresses androstenedione, dehydroepiandrosterone (DHEA), testosterone, and oestradiol formation, as well as other metabolites [23]. We believe that our approach could be useful to monitor intracrinology changes of patients under novel enzyme-targeting drugs.

In the innovation of the methodological approach, we rely on several facts: (1) because of the high sensitivity of the detection system, the enzymatic activity can be determined using exceedingly low amounts of labelled compounds mimicking the *in vivo* conditions; (2) the number of cells required to test the activity is also very small allowing test on biopsies; (3) enzymatic activity is assessed in the optimal pH and nicotinamide adenine dinucleotide cofactors concentration; (4) tissues can be subsequently processed for other uses.

The present work, however, has also some limitations. One limitation is that we did not measure DHT levels that could have been altered by both type 1 and type 2 5-α reductase activity [21]. However, taking into account that patients with BPH or prostate cancer often use specific 5-α inhibitors (2 out of 14 in our series) this was not possible. Another limitation of the present study is that we did not address the role 17β-HSD6. This enzyme has been recently considered the backdoor pathway of DHT synthesis in patients undergoing ADT [24] since it exerts a key role in androstanediol bioactivation to the downstream pathway leading to DHT formation from adrenal steroids [25]. However, *in vitro* assessment of 17β-HSD6 activity is very problematic and most of studies simply rely only on mRNA expression, that, as we have shown, does not necessarily reflect protein levels and activities. In addition, a recent study revealed that 17β-HSD6 is expressed in ERβ-positive epithelial cells of the human prostate but that in prostate cancers of Gleason grade higher than 3, both ERβ and 17βHSD6 become undetectable [26], suggesting that formation of 3β-Adiol via 17βHSD6 from DHT could be considered an important growth regulatory pathway, but not a marker of prostate cancer aggressiveness [26]. Finally, future studies are ongoing to characterize the phase two metabolism of steroids derivatives that are understudied and could be a future target for castrate-resistant prostate cancer [27].

In summary, we developed an easy tool to profile individual intraprostatic enzymatic activity (steroid map or fingerprint) by characterizing conversion pathways in an intact tissue environment from fresh biopsies. Using this novel approach we found that 17β-HSD-isoenzymes and aromatase activity in prostate tissue cultures correlate with biological behaviour. This approach could be a novel useful tool for clinical monitoring of novel enzyme-targeting drugs.

Conflict of Interests

The authors declare that there is no conflict of interests regarding the publication of this paper.

Authors' Contribution

Daniele Gianfrilli and Silvia Pierotti equally contributed to the paper.

Acknowledgment

The study was supported by Ministry of Research MIUR Grants PRIN 2008 no. 2008NY72SJ and FIRB 2010 no. RBFR10URHP.

References

[1] J. M. Correas, E. Drakonakis, A. M. Isidori et al., "Update on ultrasound elastography: miscellanea. Prostate, testicle, musculo-skeletal," *European Journal of Radiology*, vol. 82, no. 11, pp. 1904–1912, 2013.

[2] A. Aversa, A. M. Isidori, D. Gianfrilli et al., "Are subjects with erectile dysfunction aware of their condition? Results from a retrospective study based on an Italian free-call information service," *Journal of Endocrinological Investigation*, vol. 27, no. 6, pp. 548–556, 2004.

[3] A. M. Isidori, J. Buvat, and G. Corona, "A critical analysis of the role of testosterone in erectile function: from pathophysiology to treatment—a systematic review," *European Urology*, vol. 65, no. 1, pp. 99–112, 2014.

[4] F. Saad, A. Aversa, A. M. Isidori, L. Zafalon, M. Zitzmann, and L. Gooren, "Onset of effects of testosterone treatment and time span until maximum effects are achieved," *European Journal of Endocrinology*, vol. 165, no. 5, pp. 675–685, 2011.

[5] R. J. Santen, H. Brodie, E. R. Simpson, P. K. Siiteri, and A. Brodie, "History of aromatase: saga of an important biological mediator and therapeutic target," *Endocrine Reviews*, vol. 30, no. 4, pp. 343–375, 2009.

[6] G. P. Risbridger, I. D. Davis, S. N. Birrell, and W. D. Tilley, "Breast and prostate cancer: more similar than different," *Nature Reviews Cancer*, vol. 10, no. 3, pp. 205–212, 2010.

[7] K. K. Tsilidis, R. C. Travis, P. N. Appleby et al., "Interactions between genome-wide significant genetic variants and circulating concentrations of insulin-like growth factor 1, sex hormones, and binding proteins in relation to prostate cancer risk in the National Cancer Institute breast and prostate cancer cohort consortium," *The American Journal of Epidemiology*, vol. 175, no. 9, pp. 926–935, 2012.

[8] P. Soronen, M. Laiti, S. Törn et al., "Sex steroid hormone metabolism and prostate cancer," *Journal of Steroid Biochemistry and Molecular Biology*, vol. 92, no. 4, pp. 281–286, 2004.

[9] F. Labrie, A. Dupont, J. Simard, V. Luu-The, and A. Belanger, "Intracrinology: the basis for the rational design of endocrine therapy at all stages of prostate cancer," *European Urology*, vol. 24, supplement 2, pp. 94–105, 1993.

[10] F. Labrie, V. Luu-The, S. Lin et al., "The key role of 17β-hydroxysteroid dehydrogenases in sex steroid biology," *Steroids*, vol. 62, no. 1, pp. 148–158, 1997.

[11] G. P. Risbridger, J. J. Bianco, J. S. Ellem, and J. S. McPherson, "Oestrogens and prostate cancer," *Endocrine-Related Cancer*, vol. 10, no. 2, pp. 187–191, 2003.

[12] W. A. Ricke, S. J. McPherson, J. J. Bianco, G. R. Cunha, Y. Wang, and G. P. Risbridger, "Prostatic hormonal carcinogenesis is mediated by in situ estrogen production and estrogen receptor alpha signaling," *The FASEB Journal*, vol. 22, no. 5, pp. 1512–1520, 2008.

[13] P. Härkönen, S. Törn, R. Kurkela et al., "Sex hormone metabolism in prostate cancer cells during transition to an androgen-independent state," *Journal of Clinical Endocrinology and Metabolism*, vol. 88, no. 2, pp. 705–712, 2003.

[14] M. Fankhauser, Y. Tan, G. Macintyre et al., "Canonical androstenedione reduction is the predominant source of signalling androgens in hormone refractory prostate cancer," *Clinical Cancer Research*, 2014.

[15] J. A. Locke, E. S. Guns, A. A. Lubik et al., "Androgen Levels increase by intratumoral de novo steroidogenesis during progression of castration-resistant prostate cancer," *Cancer Research*, vol. 68, no. 15, pp. 6407–6415, 2008.

[16] A. Mizokami, E. Koh, H. Fujita et al., "The adrenal androgen androstenediol is present in prostate cancer tissue after androgen deprivation therapy and activates mutated androgen receptor," *Cancer Research*, vol. 64, no. 2, pp. 765–771, 2004.

[17] K. Storbeck, L. M. Bloem, D. Africander, L. Schloms, P. Swart, and A. C. Swart, "11β-Hydroxydihydrotestosterone and 11-ketodihydrotestosterone, novel C19 steroids with androgenic activity: A putative role in castration resistant prostate cancer?" *Molecular and Cellular Endocrinology*, vol. 377, no. 1-2, pp. 135–146, 2013.

[18] A. M. Isidori, G. A. Kaltsas, L. Perry, J. M. Burrin, G. M. Besser, and J. P. Monson, "The effect of growth hormone replacement therapy on adrenal androgen secretion in adult onset hypopituitarism," *Clinical Endocrinology*, vol. 58, no. 5, pp. 601–611, 2003.

[19] S. Pierotti, L. Gandini, A. Lenzi, and A. M. Isidori, "Prereceptorial regulation of steroid hormones in bone cells: insights on glucocorticoid-induced osteoporosis," *Journal of Steroid Biochemistry and Molecular Biology*, vol. 108, no. 3–5, pp. 292–299, 2008.

[20] J. Adamski and F. J. Jakob, "A guide to 17β-hydroxysteroid dehydrogenases," *Molecular and Cellular Endocrinology*, vol. 171, no. 1-2, pp. 1–4, 2001.

[21] Y. Nakamura, T. Suzuki, M. Nakabayashi et al., "In situ androgen producing enzymes in human prostate cancer," *Endocrine-Related Cancer*, vol. 12, no. 1, pp. 101–107, 2005.

[22] H. I. Scher, G. Buchanan, W. Gerald, L. M. Butler, and W. D. Tilley, "Targeting the androgen receptor: improving outcomes for castration-resistant prostate cancer," *Endocrine-Related Cancer*, vol. 11, no. 3, pp. 459–476, 2004.

[23] G. Attard, A. H. Reid, T. A. Yap et al., "Phase I clinical trial of a selective inhibitor of CYP17, abiraterone acetate, confirms that castration-resistant prostate cancer commonly remains hormone driven," *Journal of Clinical Oncology*, vol. 26, no. 28, pp. 4563–4571, 2008.

[24] F. Ishizaki, T. Nishiyama, T. Kawasaki et al., "Androgen deprivation promotes intratumoral synthesis of dihydrotestosterone from androgen metabolites in prostate cancer," *Scientific Reports*, vol. 3, Article ID 1528, 2013.

[25] J. L. Mohler, M. A. Titus, S. Bai et al., "Activation of the androgen receptor by intratumoral bioconversion of androstanediol to dihydrotestosterone in prostate cancer," *Cancer Research*, vol. 71, no. 4, pp. 1486–1496, 2011.

[26] S. Muthusamy, S. Andersson, H. Kim et al., "Estrogen receptor β and 17β-hydroxysteroid dehydrogenase type 6, a growth regulatory pathway that is lost in prostate cancer," *Proceedings of the National Academy of Sciences of the United States of America*, vol. 108, no. 50, pp. 20090–20094, 2011.

[27] K. M. McNamara, Y. Nakamura, Y. Miki, and H. Sasano, "Phase two steroid metabolism and its roles in breast and prostate cancer patients," *Frontiers in Endocrinology*, vol. 4, article 116, 2013.

Hindawi Publishing Corporation
BioMed Research International
Volume 2014, Article ID 480725, 8 pages
http://dx.doi.org/10.1155/2014/480725

Clinical Study

Intensified Adjuvant Treatment of Prostate Carcinoma: Feasibility Analysis of a Phase I/II Trial

Giovanna Mantini,[1] Sergio Fersino,[1] Anna Rita Alitto,[1] Vincenzo Frascino,[1] Mariangela Massaccesi,[2] Bruno Fionda,[1] Vincenzo Iorio,[3] Stefano Luzi,[1] Mario Balducci,[1] Gian Carlo Mattiucci,[1] Francesco Di Nardo,[4] Antonio De Belvis,[4] Alessio Giuseppe Morganti,[1,2] and Vincenzo Valentini[1]

[1] *Unità Operativa di Radioterapia, Dipartimento di Bio-Immagini e Scienze Radiologiche, Università Cattolica del Sacro Cuore, Policlinico Gemelli, Largo A. Gemelli 8, 00168 Roma, Italy*
[2] *Unità Operativa di Radioterapia, Fondazione di Ricerca e Cura "Giovanni Paolo II", Università Cattolica del Sacro Cuore, Crt. Tappino 35, 86100 Campobasso, Italy*
[3] *Dipartimento di Diagnostica per Immagini e Radioterapia, Policlinico Federico II, Via Pansini 5, 80131 Napoli, Italy*
[4] *Istituto di Igiene e Medicina Preventiva, Università Cattolica del Sacro Cuore, Policlinico Gemelli, Largo A. Gemelli 8, 00168 Roma, Italy*

Correspondence should be addressed to Anna Rita Alitto; ar_alitto@yahoo.it

Received 9 April 2014; Accepted 31 May 2014; Published 30 June 2014

Academic Editor: Giovanni Luca Gravina

Purpose. To perform a preliminary feasibility acute and late toxicity evaluation of an intensified and modulated adjuvant treatment in prostate cancer (PCa) patients after radical prostatectomy. *Material and Methods*. A phase I/II has been designed. Eligible patients were 79 years old or younger, with an ECOG of 0–2, previously untreated, histologically proven prostate adenocarcinoma with no distant metastases, pT2–4 N0-1, and with at least one of the following risk factors: capsular perforation, positive surgical margins, and seminal vesicle invasion. All patients received a minimum dose on tumor bed of 64.8 Gy, or higher dose (70.2 Gy; 85.4%), according to the pathological stage, pelvic lymph nodes irradiation (57.7%), and/or hormonal therapy (69.1%). *Results*. 123 patients were enrolled and completed the planned treatment, with good tolerance. Median follow-up was 50.6 months. Grade 3 acute toxicity was only 2.4% and 3.3% for genitourinary (GU) and gastrointestinal (GI) tract, respectively. No patient had late grade 3 GI toxicity, and the GU grade 3 toxicity incidence was 5.8% at 5 years. 5-year BDSF was 90.2%. *Conclusions*. A modulated and intensified adjuvant treatment in PCa was feasible in this trial. A further period of observation can provide a complete assessment of late toxicity and confirm the BDSF positive results.

1. Introduction

The incidence rates of prostatic carcinoma (PCa) increased in nearly all countries except in a few high-income countries. In contrast, the increase in PCa mortality rates mainly occurred in lower-resource settings, with declines largely confined to high-resource countries [1].

Radical prostatectomy (RP) is a common initial treatment for PCa. However, depending on tumor stage, 15–60% of patients develop a rise in PSA following radical prostatectomy [2]. Radiotherapy (RT) to the prostate bed has been used both adjuvantly and for salvage. There continues to be an active debate regarding when radiation should be administered, although 3 recent randomized trials show a consistent improvement in biochemical disease-free survival (BDFS) when adjuvant radiotherapy is administered as compared with radical prostatectomy alone [3–5]. Furthermore, RP, followed by postoperative RT in selected "high risk" patients, can be considered a treatment policy alternative to full radiation treatment for cure.

Based on a systematic review, adjuvant RT after RP improves overall survival and reduces the rate of distant

metastases with longer follow-up and at 5 and 10 years it improves local control and reduces the risk of biochemical failure [6]. Because the morbidity of postoperative radiotherapy is relatively low, when pathologic high risk factors are present adjuvant radiotherapy is recommended by international guidelines [7, 8].

The EORTC-22911 trial was the first randomized clinical trial to demonstrate the advantage in terms of BDFS achievable by adjuvant RT [9]. However, even in patients receiving adjuvant RT the trial showed a 5-year biochemical failure rate higher than 25%. In that study, RT was administered only on the prostate bed with a total dose of 60 Gy. In order to improve these results in our centers a phase I/II has been designed to assess the possible impact of both modulated and intensified adjuvant treatment.

This study included the use of a higher dose in case of positive resection margins and/or perineural infiltration, considering the greater risk of failure in these patient categories [10, 11]. In addition, the dose given to the prostate bed was superior to that used in the EORTC study, based on preliminary data showing a better clinical outcome by means of doses higher than 61.5 Gy [12]. Moreover, whereas the presence of occult pelvic lymph node involvement may explain the failure of treatments targeted only to the prostate bed [13], elective irradiation of pelvic lymph nodes (ENI) was planned in high risk patients. Finally, on the basis of some evidence on the possibility of improving the results of postoperative RT by means of adjuvant hormonal therapy (AHT) [14, 15], the study included the use of AHT in patients with increased risk of treatment failure.

However, there is no evidence on the tolerability of an intensified adjuvant treatment as that provided in this study. The use of doses higher than those tested in randomized trials and the use of ENI can obviously worsen treatment tolerability. In addition, an increased RT-induced toxicity in patients undergoing pelvic surgery has been demonstrated [16]. Finally, some studies suggest that even the use of AHT may increase RT-induced toxicity [17, 18]. On the basis of this background, the aim of this analysis is to perform a preliminary feasibility evaluation of an intensified adjuvant treatment in terms of acute and late toxicity.

2. Material and Methods

2.1. Study Objectives. The primary study end point was biochemical disease-free survival, defined as the time from RP to first evidence of biochemical relapse. In particular, the primary objective of the study was to demonstrate an increase of 5-year BDSF from 75% to 90%. Biochemical relapse was defined as a PSA level exceeding 0.2 ng/mL after enrollment for those with a postsurgical PSA level of 0.2 ng/mL or lower and as two consecutive PSA increases for patients with a postsurgical PSA level of >0.2. Secondary outcomes included acute and late toxicity, local control, and metastasis-free survival, defined as the first evidence of any pelvic recurrence or extrapelvic recurrence of disease, respectively. Patients without the event of interest were censored at their last contact date (last PSA assessment date for PSA relapse).

2.2. Study Design. A phase I/II study was planned. Prior data [9] indicated that the success rate (5-year BDFS) among controls is around 0.75. If the true success rate for experimental subjects is 0.90, we would need to study 100 experimental subjects to be able to reject the null hypothesis that the success rates for experimental and control subjects are equal with probability (power) 0.8. Type I error probability associated with this test of this null hypothesis is 0.05. We used an uncorrected chi-squared statistic to evaluate this null hypothesis. Some overrecruitment was planned to allow for a continuous drop-out process of up to 20% during the follow-up period.

2.3. Inclusion Criteria. Eligible patients were 79 years old or younger, with an ECOG performance status of 0–2 and previously untreated, histologically proven adenocarcinoma of the prostate with no known distant metastases, and pathological stage pT2–4 N0-1, with at least one of the following risk factors: capsular perforation, positive surgical margins, or seminal vesicle invasion. A pelvic lymphadenectomy and an undetectable PSA level after RP were not required. Patients who underwent salvage RT were excluded from this analysis. Patients must have had evidence of adequate bone marrow and liver function. Previous radiotherapy or chemotherapy for prostate cancer was not allowed. Patients must not have had intraoperative rectal injury, persistent urinary extravasation, or pelvic infection. Tumor stage was determined according to the 1997 International Union Against Cancer criteria [19]. Before enrollment, all patients underwent pre- and postoperative PSA test, bone scan, CT scan or MRI of abdomen-pelvis, and chest radiography.

2.4. Radiotherapy. Simulation and treatment were performed in prone position using the up-down table (UDT), a special device aimed at reducing small bowel volume in the treatment field [20]. Patients were instructed to achieve stable conditions of bladder and rectal filling. Before CT simulation and before each therapy fraction patients were invited to (1) empty the bladder 2 hours prior to the procedure and drink 2 glasses of water right after and to (2) empty the bowel over the 2 hours prior to the procedure. RT was planned based on CT simulation performed after oral administration of contrast with 5 mm apart slices. Clinical target volume (CTV) definition was performed as follows: in the CTV1 the prostatic area with the sites occupied before surgery by the prostate and seminal vesicles was included. The lower margin of CTV1 was set at the cranial extremity of cavernous bulbs. The upper limit was defined based on the cranial extremity of seminal vesicles evaluated on preoperative CT or MRI. In the CTV2, obturator, external and internal iliac, and presacral (above S2-S3) to the sacral promontory were included. The planning target volume 1 (PTV1) was obtained by adding to the CTV1 a 5 mm margin posteriorly and an 8 mm margin in all other directions. The PTV2 was obtained by adding to the CTV2 an 8 mm margin in all directions. Conformal 3D plans were obtained with box technique and 6-beam technique for PTV2 and PTV1, respectively. Beams $\geq$ 10 MV collimated with standard multileaf collimators (2×40 leaves,

Table 1: Prescribed treatment based on patients/tumor characteristics.

Treatment modulation	Patient/tumor characteristics
Higher dose (70.2 Gy) to the tumor bed	(i) Positive resection margin (ii) Perineural infiltration (iii) Postoperative PSA > 0.2 ng/mL
ENI	(i) pN1 (ii) Lymph node risk > 15%* and <10 resected lymph nodes (iii) Gleason score > 7
Short-term (6 months) AHT	(i) pT > 2 (ii) Gleason score = 7
Long-term (24 months) AHT	(i) pN1 (ii) Preoperative PSA > 20 ng/mL (iii) Gleason score > 7

*Based on Roach 3rd [22]. ENI: elective nodal irradiation; AHT: adjuvant hormonal therapy.

width 1 cm at the isocenter) were used. The dose was specified according to the guidelines of the International Commission on Radiation Units [21]. Treatment was provided once a day, 5 days a week. Depending on tumor characteristics (Table 1), prescribed doses were the following:

(1) pelvic node irradiation (45 Gy; 1.8 Gy/fraction) followed by boost on the prostate bed (19.8–25.2 Gy; 1.8 Gy/fraction; total dose: 64.8–70.2 Gy) or

(2) exclusive prostate area irradiation (64.8–70.2 Gy; 1.8 Gy/fraction).

2.5. Adjuvant Hormonal Therapy. AHT was prescribed as indicated in Table 1. AHT was started simultaneously with the start of postoperative RT. The duration of ART was 6 months or 24 months depending on the risk category (Table 1). Patients were informed about the different characteristics and side effects of available hormonal therapies. It was then allowed to choose between the following adjuvant hormonal treatments:

(1) LH-RH analogue: leuprorelin, 3.75 every month or 11.25 mg every 3 months, intramuscularly, or

(2) antiandrogen agent: bicalutamide, 150 mg per day.

2.6. Statistical Analysis. A descriptive analysis of the sample was carried out by means of mean and standard deviation (SD) for continuous variables and absolute and relative frequencies for qualitative ones. All patients were analyzed for radiotherapy toxicity. Toxicity was monitored weekly during radiotherapy. Clinical examinations including digital rectal examinations and PSA tests were done every 3 months for 2 years, then every 6 months until the end of the fifth year, and then every year. Additional staging studies (e.g., bone scans) were performed as clinically indicated. Acute adverse effects of RT were scored according to the Radiation Therapy Oncology Group (RTOG) scale [23]. The Late Radiation Morbidity Scoring Scheme of the RTOG/European Organization for Research and Treatment of Cancer (EORTC) was used to assess late toxicity [23]. Differences in toxicity were studied by means of chi-squared and Fisher's exact tests. Analyzed variables were age at diagnosis (stratified as below or equal to 65 and higher than 65), ENI (yes versus no), prostate bed dose (64.8 versus 70.2), and AHT (no versus antiandrogen versus LH-RH analogue). Even a BDFS analysis was performed. The analysis was performed using SPSS software version 12.0 for Windows. Statistical significance level was set at $P = 0.05$.

2.7. Ethical Issues. Written informed consent was obtained from all patients. The study was approved by the institutional review boards of the participating institutions.

3. Results

One hundred twenty-three patients were enrolled in the study, and they completed the planned adjuvant treatment. Median follow-up was 50.6 months (interquartile range, 29.2–80.0 months). Characteristics of study participants and treatment characteristics are displayed in Table 2. Ninety-one patients were treated at the Catholic University of Rome and 32 at the "Fondazione Giovanni Paolo II" in Campobasso. Eighteen patients had a pathological stage pN1 disease (14.6%), 4 patients had a pathological stage pT4 tumor (3.3%), and 9 patients had a postoperative PSA level > 0.2 ng/mL (7.3%).

Table 3(a) shows the results in terms of acute toxicity, and Tables 3(b) and 3(c) show the impact of age, dose to tumor bed, ENI, and AHT on acute gastrointestinal and genitourinary toxicity, respectively. Only a trend between ENI and gastrointestinal toxicity ($P = 0.072$) has been observed. For acute genitourinary toxicity a trend was observed for both ENI (0.071) and AHT ($P = 0.05$), with a higher incidence ($G \geq 2$: 24.3%) in patients treated with LH-RH analogue. However, on multivariate analysis a trend was confirmed only for AHT (ENI: odds ratio: 1.941, CI 95%: 0.567–6.650, and P: 0.291; AHT: odds ratio: 1.961, CI 95%: 0.928–4.146, and P: 0.078).

Table 4(a) shows the results in terms of late toxicity, and Table 4(b) shows the impact of age, dose to tumor bed, ENI, and AHT on late gastrointestinal and genitourinary toxicity. None of these factors showed a significant correlation with late toxicity. However, it may be noted that none of the patients who received a dose of 64.8 Gy showed grade > 1 late toxicity. Also AHT duration (6 months versus 24 months) did not show a correlation with late toxicity (data not shown).

At the last observation, 1 patient had local recurrence (0.8%), 6 patients had distant metastases (4.9), and 4 patients died (3.3%); in 2 cases, death was due to PCa (1.6%). Actuarial 5-year BDSF was 90.2%.

4. Discussion

To improve the results of standard postoperative RT, a phase I/II based on the modulation of adjuvant therapy has been designed. Therefore, different doses on different targets, with eventual drug therapy of varying length, were prescribed

Table 2: Patients and treatment characteristics.

	Number	%
All patients	123	100
Age (median, range), years	64, 46–78	
pT		
1c	0	0
2a	1	0.8
2b	2	1.6
2c	14	11.4
3a	61	49.6
3b	41	33.3
4	4	3.3
pN		
0	79	64.2
1	18	14.6
X	26	21.1
Perineural infiltration		
No	47	38.2
Yes	76	61.8
PSA before surgery (median, range), μg/L	8.8, 0.4–55.0	
PSA after surgery (median, range), μg/L	0.06, 0.01–0.90	
Histopathologic grade, Gleason score		
2–6	23	18.7
7	69	56.1
8–10	31	25.2
Lymphadenectomy		
No	26	21.1
Yes	97	78.9
Interval surgery-radiotherapy (median, range), months	4 (2–9)	
Radiotherapy dose to prostatic bed, Gy		
64.8	18	14.6
70.2	105	85.4
Elective nodal irradiation		
No	52	42.3
Yes	71	57.7
Adjuvant hormonal therapy		
No	38	30.9
Bicalutamide	48	39.0
LH-RH analogue	37	30.1

depending on pathological assessment. This preliminary analysis was designed to assess the toxicity of this treatment.

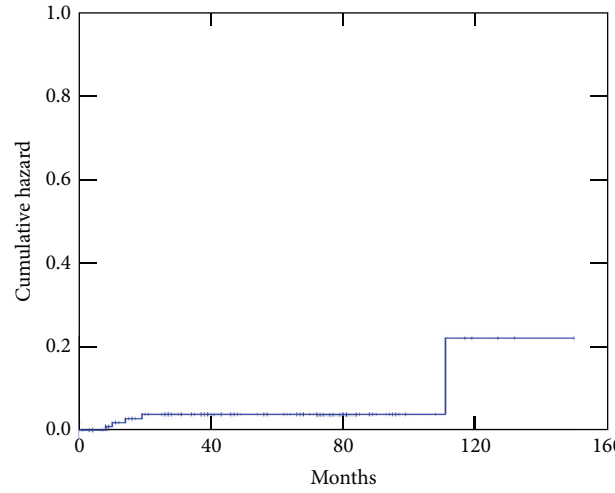

Figure 1: Actuarial cumulative incidence of gastrointestinal (grade > 1) toxicity.

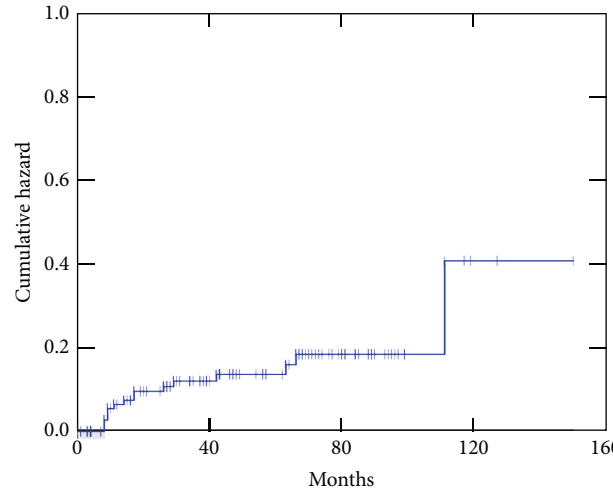

Figure 2: Actuarial cumulative incidence of genitourinary (grade > 1) toxicity.

Overall, the treatment was well tolerated. The incidence of grade 3 acute toxicity was only 2.4% and 3.3% for genitourinary and gastrointestinal toxicity, respectively (see Figures 1 and 2). No patient had late grade 3 gastrointestinal toxicity, and the actuarial 5-year cumulative incidence of grade 3 genitourinary toxicity was 5.8%.

The study has some obvious limitations. The analysis of the correlation between the different parameters of treatment with toxicity is limited by the low number of patients in the different subgroups and the duration of follow-up (median 50.6 months) may be too short for an accurate assessment of late toxicity. It should be noted, however, that 80% of cases of late gastrointestinal toxicity of grade ≥ 2 and 75% of cases of late genitourinary toxicity of grade ≥ 2 occurred in the first 3 years of follow-up. Another problem is that the potential link between comorbidity and toxicity has not been examined. Even the side effects caused by AHT were

Table 3: (a) Acute toxicity (RTOG). (b) Patients and treatment parameters: impact on gastrointestinal acute toxicity. (c) Patients and treatment parameters: impact on genitourinary acute toxicity.

(a)

	Grade				
	0	1	2	3	4
Gastrointestinal	64 (52.0%)	43 (35.0%)	13 (10.6%)	3 (2.4%)	0 (0.0%)
Genitourinary	60 (48.8%)	47 (38.2%)	12 (9.8%)	4 (3.3%)	0 (0.0%)

(b)

	Number of patients	Grade			Grade		
		0-1	≥2	$P =$	0–2	≥3	$P =$
Age							
≤65 years	72	60 (83.3%)	12 (16.7%)	0.152	70 (97.2%)	2 (2.8%)	0.772
>65 years	51	47 (92.2%)	4 (7.8%)		50 (98.0%)	1 (2.9%)	
Dose							
64.8 Gy	18	14 (77.8%)	4 (22.2%)	0.185	18 (100.0%)	0 (0.0%)	0.619
70.2 Gy	105	93 (88.6%)	12 (11.4%)		102 (97.1%)	3 (2.9%)	
ENI							
No	52	48 (92.3%)	4 (7.7%)	0.072	52 (100.0%)	0 (0.0%)	0.189
Yes	71	59 (83.1%)	12 (16.9%)		68 (95.8%)	3 (4.2%)	
AHT							
No	38	34 (89.5%)	4 (10.5%)	0.758	37 (97.4%)	1 (2.6%)	0.276
Bicalutamide	48	42 (87.5%)	6 (12.5%)		48 (100.0%)	0 (0.0%)	
LH-RH agonist	37	31 (83.8%)	6 (16.2%)		35 (94.6%)	2 (5.4%)	

ENI: elective nodal irradiation; AHT: adjuvant hormonal therapy.

(c)

	Number of patients	Grade			Grade		
		0-1	≥2	$P =$	0–2	≥3	$P =$
Age							
≤65 years	72	62 (86.1%)	10 (13.9%)	0.730	69 (95.8%)	3 (4.2%)	0.497
>65 years	51	45 (88.2%)	6 (11.8%)		50 (98.0%)	1 (2.0%)	
Dose							
64.8 Gy	18	17 (94.4%)	1 (5.6%)	0.278	18 (100.0%)	0 (0.0%)	0.527
70.2 Gy	105	90 (85.7%)	15 (14.3%)		101 (96.2%)	4 (3.8%)	
ENI							
No	52	48 (92.3%)	4 (7.7%)	0.071	50 (96.2%)	2 (3.8%)	0.566
Yes	71	59 (83.1%)	12 (16.9%)		69 (97.2%)	2 (2.8%)	
AHT							
No	38	35 (92.1%)	3 (7.9%)	0.050	37 (97.4%)	1 (2.6%)	0.264
Bicalutamide	48	44 (91.7%)	4 (8.3%)		45 (93.8%)	3 (6.3%)	
LH-RH agonist	37	28 (75.7%)	9 (24.3%)		37 (100.0%)	0 (0.0%)	

ENI: elective nodal irradiation; AHT: adjuvant hormonal therapy.

not analyzed. Finally, another limitation is related to the inhomogeneity of the prescribed AHT. However, the use in a group of patients of antiandrogen therapy was justified by the desire to avoid the side effects of androgen deprivation therapy in patients potentially suffering from the side effects of RP and RT. Second, the results of the RTOG 96-01 trial showed that in patients, with locally advanced disease, bicalutamide 150 mg adjuvant to postoperative radiotherapy demonstrates significant clinical benefits in terms of overall survival, disease-free survival, and BDFS compared with RT alone [27].

Even considering these limitations, there were no significant correlations between dose and ENI with the radiation-induced toxicity. The use of the UDT with prone positioning of the patient and of the 3D technique may at least partially explain the lack of gastrointestinal toxicity in patients who received ENI or a higher dose to the tumor bed.

Table 5 shows the results of our study in comparison with those of the randomized trials. This comparison is not easy because in those studies acute toxicity was not recorded and in two studies the used scale of toxicity was not specified [4, 5]. However, it can be observed that, despite the use of a

Table 4: (a) Actuarial 5-year late toxicity-free survival (RTOG-EORTC). (b) Impact of treatment parameters on 5-year late toxicity-free survival (RTOG-EORTC); values are in percentages.

(a)

Toxicity	Grade			
	1	2	3	4
Gastrointestinal	85.4%	96.3%	100.0%	100.0%
Genitourinary	76.5%	87.3%	94.2%	100.0%

(b)

Toxicity	Age (years)			Dose (Gy)			ENI			AHT			
	≤65	>65	$P =$	64.8	70.2	$P =$	No	Yes	$P =$	No	BIC	LRA	$P =$
GI ≥ 2	95.2	97.9	0.538	100	95.7	0.348	97.7	95.3	0.425	97.1	94.8	97.2	0.849
GU ≥ 2	86.3	89.0	0.584	100	85.2	0.097	85.2	88.4	0.634	87.7	90.6	85.0	0.893
GU ≥ 3	94.0	95.4	0.781	100	93.2	0.356	93.1	95.4	0.243	95.8	97.7	90.3	0.380

BIC: bicalutamide; ENI: elective nodal irradiation; AHT: adjuvant hormonal therapy; LRA: LH-RH agonists; and ys: years.

Table 5: Results (toxicity) comparison with randomized studies.

Study	Number of pts	Adjuvant therapy	Toxicity scores	Acute toxicity		Late toxicity	
				GI	GU	GI	GU
Thompson et al., 2006 [5]	214	RT: 60–64 Gy (2 Gy/fraction) to prostatic fossa and periprostatic tissue	NR	NR	NR	Proctitis and/or rectal bleeding: 3.3% *	Urethral stricture: 17.8%; total urinary incontinence: 6.5% *
Wiegel et al., 2009 [3] (ARO 96-02/AUO AP 09/95)	114	RT: 60 Gy (2 Gy/fraction) to prostatic fossa and region of seminal vesicles with 1 cm margin	Acute: RTOG Late: RTOG-EORTC	NR	NR	G2: 1.4% G3: 0% †	G2: 2%; G3: 0.7%; urethral stricture: 1.4% †
Bolla et al., 2012 [4] (EORTC 22911)	502	RT: 50 Gy (2 Gy/fraction) to prostatic fossa and region of seminal vesicles and periprostatic area + 10 Gy to prostatic fossa	NR	NR	NR	G ≥ 2: 2.5% ‡ Late GI-GU G ≥ 1: 70.8% Late GI-GU G3: 5.3% Late GI-GU G4: 0% ‡	G ≥ 2: 21.3% ‡
Present series	123	RT: 64.8–70.2 Gy (1.8 Gy/fraction) to prostatic fossa and region of seminal vesicles with 1 cm margin ± ENI, 45 Gy ± AHT	Acute: RTOG Late: RTOG-EORTC	G3: 2.4% G4: 0.0%	G3: 3.3% G4: 0.0%	G ≥ 2: 3.7% G ≥ 3: 0.0% G ≥ 4: 0.0% §	G ≥ 2: 12.7% G ≥ 3: 5.8% G ≥ 4: 0.0% §

ENI: elective nodal irradiation; GI: gastrointestinal; GU: genitourinary; AHT: adjuvant hormonal therapy; NR: not reported; pts: patients; *: crude (median follow-up: 10.6 years); †: crude (median follow-up: 53.7 months); ‡: 10-year cumulative incidence; and §: 5-year actuarial cumulative incidence.

higher dose and of ENI in 58% of patients, gastrointestinal G2 toxicity (3.7%) was similar to that reported in the randomized studies (1.4%–3.3%). Even the late genitourinary G2 toxicity (12.7%) was in the range (2%–21.3%) recorded in two randomized studies [3, 4]. Even the overall (gastrointestinal and genitourinary) grade 3 late toxicity (5.8%) is comparable with the results (5.3%) of the EORTC study [4]. Also, in this case, the low toxicity despite higher dose and ENI can find an explanation in the use of 3D technique, of UDT, and of slightly lower dose fractionation (1.8 Gy/fraction versus 2.0 Gy/fraction).

Table 6 shows the results of our study compared with those of recent studies on high-dose postoperative RT [24–26]. It is possible to observe that acute gastrointestinal G2 toxicity (10.6%) was similar to the results reported by Nath and coworkers and less than that recorded by van Praet and colleagues (42%). However, the latter prescribed a higher dose both to the tumor bed (75 Gy) and to the pelvic lymph

Table 6: Results (toxicity) comparison with nonrandomized studies using high-dose radiotherapy.

Study	Number of pts	Adjuvant therapy	RT technique	Toxicity scores	Acute toxicity		Late toxicity		Notes
					GI	GU	GI	GU	
Nath et al., 2010 [24]	50	RT (median dose: 68 Gy)	IMRT-IGRT	CTC 3.0	G2: 8% G3: 0%	G2: 14% G3: 0%	G2: 2% *	G2: 16% G3: 2% *	IMRT-IGRT may reduce RT-induced toxicity
Cozzarini et al., 2012 [25]	556	RT (median dose: 70.2 Gy) ± ENI	2D or 3D	CTC 3.0	NR	G2: 19% G3: 8%	NR	G2: 23.9% G3: 12% †	Younger and hypertensive pts: higher rate of severe GU late sequelae
van Praet et al., 2013 [26]	48 (pN1)	RT (75 Gy to prostate bed + ENI: 54 Gy) + ADT	IMAT	In-house developed scale	G2: 42% G3: 0%	G2: 35% G3: 4%	G2: 25% G3: 0% ‡	G2: 36% G3: 7% G4: 2% ‡	Acute and late GI toxicity higher following ENI
Present series	123	RT (64.8–70.2 Gy to prostate bed ± ENI) ± AHT	3D CRT	Acute: RTOG Late: RTOG-EORTC	G2: 10.6% G3: 2.4% G4: 0%	G2: 9.8% G3: 3.3% G4: 0%	G ≥ 2: 3.7% G ≥ 3: 0% G ≥ 4: 0% §	G ≥ 2: 12.7% G ≥ 3: 5.8% G ≥ 4: 0% §	No significant effect on toxicity by age, dose, ENI, and AHT

3D CRT: 3-dimensional conformal radiation therapy; ADT: androgen deprivation therapy; AHT: adjuvant hormonal therapy; ENI: elective nodal irradiation; GI: gastrointestinal; GU: genitourinary; IGRT: image guided radiation therapy; IMAT: intensity-modulated arc therapy; IMRT: intensity-modulated radiation therapy; pts: patients; *: crude, median follow-up: 24 months; †: 8-year risk; ‡: crude (only patients with ≥12-month follow-up); and §: 5-year actuarial cumulative incidence.

nodes (54 Gy). Similar results are those concerning late gastrointestinal G2 toxicity. Even in this case our results (3.7%) are similar to those of the study of Nath and colleagues (2%) and lower than those recorded by van Praet and collaborators (25%), again probably due to the different doses administered in this latest study.

Acute genitourinary G2 toxicity (10%) was similar to that reported in the study by Nath and colleagues (14%) and lower than that recorded by Cozzarini and coworkers (19%), probably due to the use of 2D technique in a group of patients, and less than that recorded by van Praet and collaborators (35%), again probably due to the different prescribed doses. Similar results were recorded for late genitourinary G2 toxicity (13%), again similar to that of Nath and colleagues (16%) and lower than that of Cozzarini and coworkers (23.9%) and van Praet and collaborators (36%). Again these differences can be explained by the different technique used by Cozzarini and by the different doses prescribed by van Praet.

In terms of late grade 3 genitourinary toxicity, our results (6%) are in the range of those reported in other studies (2–12%). Finally, unlike our study, in the study of van Praet and colleagues a negative impact on the toxicity of ENI was registered. Even in this case, the explanation may come from the different dose used in that study (54 Gy) compared to ours (45 Gy).

An improvement of the results in terms of toxicity may arise in the future by the use of intensity-modulated techniques. For example, a series of our parallel studies showed that the use of postoperative IMRT significantly reduces rectum and bladder irradiation compared to 3D RT [28]. In addition, hypofractionated high-dose IMRT delivered with simultaneous integrated boost (SIB) enables reduction of the overall treatment time, with an acute toxicity profile which compares favourably with that of conventionally fractionated high-dose 3D RT [29, 30].

The positive results of our study may also depend on the use of ENI. This finding confirms a previous observation on the improvement of biochemical recurrence-free survival in patients with high risk PCa undergoing prostate bed plus nodal irradiation after RP [31].

In conclusion, a modulated and intensified adjuvant treatment in PCa was feasible in this phase I/II trial. A further period of observation can provide a complete assessment of late toxicity and confirm the positive results in terms of BDSF.

Conflict of Interests

No actual or potential conflict of interests does exist regarding the publication of this paper.

References

[1] M. M. Center, A. Jemal, J. Lortet-Tieulent et al., "International variation in prostate cancer incidence and mortality rates," *European Urology*, vol. 61, no. 6, pp. 1079–1092, 2012.

[2] D. Bottke and T. Wiegel, "Prevention of local recurrence using adjuvant radiotherapy after radical prostatectomy. Indications, results, and side effects," *Urologe—Ausgabe A*, vol. 45, no. 10, pp. 1251–1254, 2006.

[3] T. Wiegel, D. Bottke, U. Steiner et al., "Phase III postoperative adjuvant radiotherapy after radical prostatectomy compared with radical prostatectomy alone in pT3 prostate cancer with postoperative undetectable prostate-specific antigen: ARO 96-02/AUO AP 09/95," *Journal of Clinical Oncology*, vol. 27, no. 18, pp. 2924–2930, 2009.

[4] M. Bolla, H. Van Poppel, B. Tombal et al., "Postoperative radiotherapy after radical prostatectomy for high-risk prostate

cancer: long-term results of a randomised controlled trial (EORTC trial 22911)," *The Lancet*, vol. 380, no. 9858, pp. 2018–2027, 2012.

[5] I. M. Thompson Jr., C. M. Tangen, J. Paradelo et al., "Adjuvant radiotherapy for pathologically advanced prostate cancer: a randomized clinical trial," *Journal of the American Medical Association*, vol. 296, no. 19, pp. 2329–2335, 2006.

[6] T. Daly, B. E. Hickey, M. Lehman, D. P. Francis, and A. M. See, "Adjuvant radiotherapy following radical prostatectomy for prostate cancer," *Cochrane Database of Systematic Reviews*, vol. 12, Article ID CD007234, 2011.

[7] A. Heidenreich, P. J. Bastian, J. Bellmunt et al., "EAU guidelines on prostate cancer—part 1: screening, diagnosis, and local treatment with curative intent-update," *European Urology*, vol. 65, pp. 124–137, 2014.

[8] I. M. Thompson, R. K. Valicenti, P. Albertsen et al., "Adjuvant and salvage radiotherapy after prostatectomy: AUA/ASTRO guideline," *Journal of Urology*, vol. 190, no. 2, pp. 441–449, 2013.

[9] M. Bolla, H. Van Poppel, L. Collette et al., "Postoperative radiotherapy after radical prostatectomy: a randomised controlled trial (EORTC trial 22911)," *The Lancet*, vol. 366, no. 9485, pp. 572–578, 2005.

[10] G. Ploussard, M. A. Agamy, O. Alenda et al., "Impact of positive surgical margins on prostate-specific antigen failure after radical prostatectomy in adjuvant treatment-naïve patients," *BJU International*, vol. 107, no. 11, pp. 1748–1754, 2011.

[11] K. Aumayr, M. Breitegger, P. R. Mazal et al., "Quantification of extraprostatic perineural spread and its prognostic value in pT3a pN0 M0 R0 prostate cancer patients," *Prostate*, vol. 71, no. 16, pp. 1790–1795, 2011.

[12] R. K. Valicenti, L. G. Gomella, M. Ismail, S. Grant Mulholland, R. O. Petersen, and B. W. Corn, "Effect of higher radiation dose on biochemical control after radical prostatectomy for pT3N0 prostate cancer," *International Journal of Radiation Oncology Biology Physics*, vol. 42, no. 3, pp. 501–506, 1998.

[13] S. Revannasiddaiah, M. K. Gupta, R. K. Seam, and I. Madabhavi, "Pelvic nodal radiotherapy in patients with unfavorable intermediate and high-risk prostate cancer: evidence, rationale, and future directions," *International Journal of Radiation Oncology Biology Physics*, vol. 80, pp. 6–16, 2011.

[14] B. W. Corn, K. Winter, and M. V. Pilepich, "Does androgen suppression enhance the efficacy of postoperative irradiation? A secondary analysis of RTOG 85-31," *Urology*, vol. 54, no. 3, pp. 495–502, 1999.

[15] H. Miyake, I. Sakai, K.-I. Harada, I. Hara, and H. Eto, "Long-term results of adjuvant hormonal therapy plus radiotherapy following radical prostatectomy for patients with pT3N0 or pT3N1 prostate cancer," *International Journal of Urology*, vol. 11, no. 6, pp. 397–401, 2004.

[16] C. Fiorino, G. Fellin, T. Rancati et al., "Clinical and dosimetric predictors of late rectal syndrome after 3D-CRT for localized prostate cancer: preliminary results of a multicenter prospective study," *International Journal of Radiation Oncology Biology Physics*, vol. 70, no. 4, pp. 1130–1137, 2008.

[17] S. J. Feigenberg, A. L. Hanlon, E. M. Horwitz, R. G. Uzzo, D. Eisenberg, and A. Pollack, "Long-term androgen deprivation increases Grade 2 and higher late morbidity in prostate cancer patients treated with three-dimensional conformal radiation therapy," *International Journal of Radiation Oncology Biology Physics*, vol. 62, no. 2, pp. 397–405, 2005.

[18] M. Feng, A. L. Hanlon, T. M. Pisansky et al., "Predictive factors for late genitourinary and gastrointestinal toxicity in patients with prostate cancer treated with adjuvant or salvage radiotherapy," *International Journal of Radiation Oncology Biology Physics*, vol. 68, no. 5, pp. 1417–1423, 2007.

[19] L. H. Sobin and I. D. Fleming, "TNM classification of malignant tumors, fifth edition," *Cancer*, vol. 80, no. 9, pp. 1803–1804, 1997.

[20] C. Capirci, C. Polico, and G. Mandoliti, "Dislocation of small bowel volume within box pelvic treatment fields, using new "up down table" device," *International Journal of Radiation Oncology Biology Physics*, vol. 51, no. 2, pp. 465–473, 2001.

[21] N. Hodapp, "The ICRU Report No. 83: prescribing, recording and reporting photon-beam intensity-modulated radiation therapy (IMRT)," *Strahlentherapie und Onkologie*, vol. 188, no. 1, pp. 97–99, 2012.

[22] A. W. Partin, J. Yoo, H. B. Carter et al., "The use of prostate specific antigen, clinical stage and Gleason score to predict pathological stage in men with localized prostate cancer," *The Journal of Urology*, vol. 150, no. 6, pp. 1923–1924, 1993.

[23] J. D. Cox, J. Stetz, and T. F. Pajak, "Toxicity criteria of the Radiation Therapy Oncology Group (RTOG) and the European Organization for Research and Treatment of Cancer (EORTC)," *International Journal of Radiation Oncology Biology Physics*, vol. 31, no. 5, pp. 1341–1346, 1995.

[24] S. K. Nath, A. P. Sandhu, B. S. Rose et al., "Toxicity analysis of postoperative image-guided intensity-modulated radiotherapy for prostate cancer," *International Journal of Radiation Oncology*, vol. 78, no. 2, pp. 435–441, 2010.

[25] C. Cozzarini, C. Fiorino, L. F. da Pozzo et al., "Clinical factors predicting late severe urinary toxicity after postoperative radiotherapy for prostate carcinoma: a single-institute analysis of 742 patients," *International Journal of Radiation Oncology Biology Physics*, vol. 82, no. 1, pp. 191–199, 2012.

[26] C. van Praet, P. Ost, N. Lumen et al., "Postoperative high-dose pelvic radiotherapy for N+ prostate cancer: toxicity and matched case comparison with postoperative prostate bed-only radiotherapy," *Radiotherapy and Oncology*, 2013.

[27] W. A. See and C. J. Tyrrell, "The addition of bicalutamide 150 mg to radiotherapy significantly improves overall survival in men with locally advanced prostate cancer," *Journal of Cancer Research and Clinical Oncology*, vol. 132, no. 1, pp. S7–S16, 2006.

[28] C. Digesú, S. Cilla, A. de Gaetano et al., "Postoperative intensity modulated radiation therapy in high risk prostate cancer: a dosimetric comparison," *Medical Dosimetry*, vol. 36, no. 3, pp. 231–239, 2011.

[29] E. Ippolito, N. Cellini, C. Digesù et al., "Postoperative intensity-modulated radiotherapy with simultaneous integrated boost in prostate cancer: a dose-escalation trial," *Urologic Oncology: Seminars and Original Investigations*, vol. 31, no. 1, pp. 87–92, 2013.

[30] M. Massaccesi, S. Cilla, F. Deodato et al., "Hypofractionated intensity-modulated radiotherapy with simultaneous integrated boost after radical prostatectomy: preliminary results of a phase II trial," *Anticancer Research*, vol. 33, no. 6, pp. 2785–2790, 2013.

[31] M. T. Spiotto, S. L. Hancock, and C. R. King, "Radiotherapy after prostatectomy: improved biochemical relapse-free survival with whole pelvic compared with prostate bed only for high-risk patients," *International Journal of Radiation Oncology Biology Physics*, vol. 69, no. 1, pp. 54–61, 2007.

Hindawi Publishing Corporation
BioMed Research International
Volume 2014, Article ID 380398, 9 pages
http://dx.doi.org/10.1155/2014/380398

Research Article

KCTD11 Tumor Suppressor Gene Expression Is Reduced in Prostate Adenocarcinoma

Francesca Zazzeroni,[1] Daniela Nicosia,[1] Alessandra Tessitore,[1] Rita Gallo,[1] Daniela Verzella,[1] Mariafausta Fischietti,[1] Davide Vecchiotti,[1] Luca Ventura,[2] Daria Capece,[1] Alberto Gulino,[3] and Edoardo Alesse[1]

[1] *Department of Biotechnological and Applied Clinical Sciences, University of L'Aquila, Via Vetoio, Coppito 2, 67100 L'Aquila, Italy*
[2] *Department of Pathology, San Salvatore Hospital, 67100 L'Aquila, Italy*
[3] *Department of Molecular Medicine, "Sapienza" University of Rome, Via Regina Elena 291, 00161 Rome, Italy*

Correspondence should be addressed to Francesca Zazzeroni; francesca.zazzeroni@univaq.it

Received 7 February 2014; Revised 28 April 2014; Accepted 29 April 2014; Published 19 June 2014

Academic Editor: Giovanni Luca Gravina

Prostate cancer is the most common noncutaneous cancer among men in the United States. A genetic contribution to prostate cancer risk has been documented, but knowledge of the molecular mechanisms involved in prostate cancer initiation is still not well understood. Loss of heterozygosity (LOH) of chromosomal regions is crucial in tumor progression. In human prostate cancer, several chromosomal regions demonstrating a high frequency of LOH have been previously identified. *KCTD11 (REN)* is a tumor suppressor gene mapping on human chromosome 17p13.2, whose expression is frequently lost in human medulloblastoma and in several other cancer types. KCTD11 acts as a negative regulator of the Hedgehog (Hh) signaling. Here, we demonstrated that *KCTD11* LOH is a common genetic lesion in human prostate adenocarcinoma. Indeed, nuclear KCTD11 protein expression is strongly reduced in primary prostate cancer, and this event correlated with overexpression of proteins acting into the Hedgehog pathway. Low levels of *KCTD11* mRNA have been also observed in prostatic cancer cells, and ectopic overexpression of KCTD11 led to growth arrest. Our study demonstrates and supports that KCTD11, as well as negatively regulated downstream effectors belonging to Hh signaling, plays a role in prostate cancer pathogenesis. This could be suitable to characterize new diagnostic and therapeutic markers.

1. Introduction

Prostate cancer (CaP) is the most common noncutaneous cancer among men in the United States. The American Cancer Society estimated approximately 240.000 new diagnosed cases and 30.000 deaths due to this neoplasm in 2013 [1]. The introduction in clinical practice of PSA in the 1980s has influenced prostate cancer incidence, by permitting early diagnosis in some patients before symptoms develop or before abnormalities on physical examination are detectable [2]. The three most important risk factors are age, race, and family history. A genetic contribution to prostate cancer risk has been documented, but knowledge of the molecular mechanisms involved in prostate cancer initiation is still not well understood. In fact, carcinogenesis of prostate epithelial cells results from a complex series of initiation and progression events under environmental and genetic factors [3]. Sequence variants in several genes, such as SRD5A (steroid-5-alpha-reductase alpha polypeptide) [4], androgen receptor [5], estrogen receptor-β [6], E-cadherin [7], and toll-like receptors [8–10], have been associated with prostate cancer. Fusion of TMPRSS2 and ETS transcription factors genes occurs in approximately 50% of prostate cancer patients [11]. Moreover, BRCA1/2 [12], MMR genes [13], and HOXB13 [14] show potential clinical relevance in prostate cancer risk. Some studies showed LOH and chromosomal aberrations in prostate tumors [15–17]. Among these, Saric et al. demonstrated that the microsatellite D17S960 marker

on the 17p13 chromosomal region is more markedly subjected to LOH in primary prostate carcinoma (43%) with respect to prostatic intraepithelial neoplasia (PIN) (18%) cases [15].

KCTD11 (REN) was originally identified by our group as a murine gene, playing a role in neural progenitor cell growth arrest and differentiation [18, 19]. Importantly, *KCTD11* has been further characterized as a tumor suppressor gene mapping on human chromosome 17p13.2, whose expression is frequently lost in human medulloblastoma and in several other cancer types due to both LOH and epigenetic events [20, 21]. In addition, it has been demonstrated that KCTD11 acts as a negative regulator of the Hedgehog (Hh) signaling in human medulloblastoma [20, 22].

Hedgehog signaling plays a key role in stem cell plasticity and in many developmental, physiological, and pathogenic processes [23]. Binding of the Hedgehog ligand to the Patched 1 (Patch1) receptor triggers a cascade of intracellular signaling activations that leads to the binding of downstream transcription factors (Gli1, Gli2, and Gli3) to their target sequences and then to the expression of target genes involved in the control of cell division or differentiation [24]. Aberrant Hh signaling activation has been implicated in prostate tumorigenesis in both human individuals and mouse models [25–32].

Here, we demonstrated that *KCTD11* LOH is a common genetic lesion also in human prostate adenocarcinoma. Indeed, nuclear KCTD11 protein expression is strongly decreased in primary prostate cancer, and this event is correlated to overexpression of proteins acting into the Sonic Hedgehog pathway. KCTD11 expression in prostatic cancer cells was also quite low, and ectopic overexpression of KCTD11 determined growth arrest through cyclin-dependent kinase inhibitors' upregulation and Hedgehog/Gli target genes' downregulation.

2. Materials and Methods

2.1. Prostate Adenocarcinoma Tissue Samples. Prostate Cancer-Normal Tissue Array (CA3) was purchased by SuperBioChips Tissue Array (Tema Ricerca Srl).

Eleven formalin-fixed, paraffin-embedded (FFPE) prostate adenocarcinoma tissue samples with Gleason between 5 and 10 and their matched normal counterparts were provided by the Pathology Unit of San Salvatore Hospital of L'Aquila. Tissue samples were microdissected in order to analyze just tumoral cells. Work was conducted in accordance with the Declaration of Helsinki.

2.2. DNA Extraction and LOH Analysis. Genomic DNA was extracted by using the Dinamite tissue kit (Labogen sas), according to the manufacturer's instructions. The microsatellite marker LOH analysis was performed by using the following primers: D17S960 FW 5′-TGATGCATATACATGCGTG-3′; D17S960REV 5′-TAGCGACTCTTCTGGCA-3′ (UniSTS:70862); D4S174 FW 5′-AAGAACCATGCGATACGACT-3′; D4S174 REV 5′-CATTCCTAGATGGGTAAAGC-3′ (UniSTS:3637). The reverse primers were ^{32}P-labeled at 5′-end by T4 polynucleotide kinase. PCR was performed by using 100 ng of genomic DNA, 0.4 μM each primer, 5% DMSO, and Taq DNA polymerase 2.5 U. PCR products were run onto a denaturing 5% polyacrylamide gel (7 M urea).

2.3. Cell Cultures. ALVA31 human prostate cancer cell line and Phoenix Ampho packaging cells were cultured in DMEM and supplemented with 10% FBS. Human prostate cancer cell lines PC3 and TSU were cultured in RPMI 1640 and supplemented with 10% FBS. LnCAP were cultured in RPMI 1640 medium containing 20% FBS, HEPES 1 mM, and glucose 4.5 g/L. All media were supplemented with glutamine 2 mM, streptomicyn 100 U/mL, and penicillin 100 U/mL.

2.4. Constructs, Transfections, and Transduction. The bicistronic retroviral construct MIGR1, expressing GFP, was obtained by MSCV vector [33]. MIGR-human KCTD11 was obtained by inserting a 1.5 Kb EcoRI fragment from pcRII-human KCTD11. Transfection of Phoenix Ampho packaging cells and infection of prostatic cancer cell lines were performed as previously described [33]. Infection efficiency was monitored by flow cytometry (FCM) and fluorescence microscopy. pCXN2-human KCTD11 [22] was transfected by using Fugene HD (Promega) according to the manufacturer's specifications. Transfection efficiency was monitored by flow cytometry (FCM) and fluorescence microscopy.

2.5. RNA Extraction and Q-RT-PCR. RNA was extracted by the use of Trizol reagent (Life Technologies) according to the manufacturer's specifications and reverse transcribed using the GeneAmp Gold RNA PCR Reagent Kit (Life Technologies). cDNA were amplified by using the following primers: KCTD11 FW 5′-GACACCTTCCGAAGCCAACC-3′, KCTD11 REV 5′-CCACTGCCACACCAAAT-3′; GLI1 FW 5′-GTGAGCCTGAATCTGTGTATGA-3′, GLI1 REV 5′-TGTGCTCGCTGTTGATGT-3′; PATCH1 FW 5′-CAGAATGGGTCCACGACAAA-3′, PATCH1 REV 5′-GTAGAAAGGGAACTGGGCATAC-3′; IGF-2 FW 5′-GTGCTGCATTGCTGCTTAC-3′, IGF-2 REV 5′-GGGCCTGCTGAAGTAGAAG-3′; Cyclin D2 FW 5′-CTGTGTGCCACCGACTTTA-3′, and Cyclin D2 REV 5′-GCGAGCTCACTTCCTCATC-3′. Q-RT-PCR was run on an Mx3000P (Statagene). Brilliant SYBR Green QPCR master mix 1x (Statagene) was used (GAPDH endogenous control). Quantitative analysis was performed by Mx3000P software.

2.6. Proliferation Assay. MIGR-hKCTD11-infected prostate cancer cell lines were cultured onto a 12 mm diameter glass. After 24 hrs, BrdU was added (BrdU labeling and detection kit, Boehringer Mannheim) according to the manufacturer's instructions. Cells were incubated for 8 and for 24 hours and then fixed in 4% paraformaldehyde for 10 min, permeabilized with 0.25% Triton X in PBS, washed, and incubated with primary antibody (anti-GFP, Santa Cruz Biotechnology). After 1 hr, cells were washed and incubated with goat anti-rabbit Alexa Flour 488 (Santa Cruz Biotech) secondary antibody for 45 min. Cells were treated with 4% paraformaldehyde and then 2 N HCl. After three washes, cells were incubated with 1 : 10 primary anti-BrdU (BrdU labeling and detection kit, Boehringer Mannheim) and, afterward, with goat anti-mouse

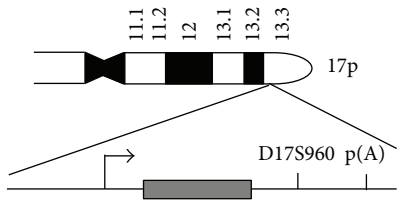

(a)

Locus	Location	Number of LOH/number of informative cases (%)	Candidate gene
D17S960	17p13	5/11 (45%)	KCTD11
D4S174 (background marker)	4p13-11	2/11 (18%)	None

(b)

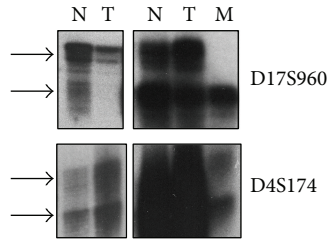

(c)

Figure 1: *KCTD11* loss of heterozygosity (LOH) analysis in prostate cancer samples matched with paired normal tissues. (a) Schematic representation of human *KCTD11* locus. D17S960 microsatellite marker position is shown. (b) *KCTD11* LOH frequency in prostate adenocarcinoma samples (D17S960, specific microsatellite marker, D4S174, background marker). (c) Representative images of *KCTD11* LOH in prostate adenocarcinoma (N normal tissues, T tumoral tissue, and M metastasis).

IgG TRITC (Sigma-Aldrich) secondary antibody. Hoechst was used for nuclear staining. Cells were analyzed by using a Zeiss Axioplan 2 (Carl Zeiss) fluorescence microscope.

2.7. Immunohistochemistry. Immunohistochemistry analysis was performed on tissue arrays from prostate cancers and normal tissues (SuperBioChips Tissue Array) and on FFPE prostate adenocarcinoma samples from the Unit of Pathology of L'Aquila San Salvatore hospital. Analysis was performed as previously described [21]. Primary antibodies were as follows: anti-α-REN antibody [18, 21], α-Gli1 (sc-6153, Santa Cruz Biotechnology), and α-Patch1 (sc-6149, Santa Cruz Biotechnology). All antibodies were diluted in ultrAb diluent (Lab Vision) and incubated overnight at 4°C. Tissues were analyzed by using a Nikon Eclipse E200 microscope. Negative controls were performed by omitting primary antibodies.

Immunostaining for KCTD11 was semiquantitatively scored as "–" (no or less than 5% positive cells), "+" (5–25% positive cells), "++" (26–50% positive cells), "+++" (51–75% positive cells), and "++++"(75–100% positive cells). Quantitative analysis was performed by counting positive cells in three different fields (magnification ×40).

2.8. Western Blot. Cell lysates were obtained as previously described [18]. Primary antibodies used were anti-p21 (mouse monoclonal, Calbiochem), anti-p27 (mouse monoclonal, Transduction Laboratories), anti-COOH1 [18, 21], and anti-actin (Santa Cruz Biotechnology). Secondary antibodies: anti-mouse-HRP, anti-rabbit-HRP, and anti-goat-HRP (Santa Cruz Biotechnology).

2.9. Statistical Analysis. Statistical analysis was performed using the unpaired 2-tailed Student's t-test. P values less than 0.05 were considered significant.

3. Results

3.1. KCTD11 LOH in Prostate Adenocarcinoma. A previous work showed that LOH of microsatellite D17S960 marker occurs in 18% of prostatic intraepithelial neoplasia (PIN), 43% of primary, and 57% of metastatic prostate cancer (CaP) lesions [15], thus identifying the loss of tumor suppressor genes on chromosomal arm 17p as an early event in CaP evolution. The authors suggested that p53 and hypermethylated in carcinoma 1 (HIC1) genes as tumor suppressors were potentially deleted because they were located close to the D17S960 chromosomal locus.

As shown in Figure 1(a) and as previously described [20], microsatellite D17S960 marker is set at the 3′-UTR of *KCTD11* single-exon tumor suppressor gene. To determine the role of *KCTD11* gene in CaP, we first decided to seek for LOH of *KCTD11* in 11 human primary CaP tissues. Tumoral and normal samples were obtained from the same FFPE tissue block by microdissection. LOH analysis revealed that 45% of our cases showed allelic deletion (Figures 1(b) and 1(c)). LOH of microsatellite D4S174 was used as a background marker. This result is in accordance with the data of Saric et al. [15], demonstrating that *KCTD11* deletion represents a genetic alteration of CaP.

3.2. KCTD11 Expression Is Downregulated in Prostate Adenocarcinoma. To extend our analysis at protein level, a commercially available Prostate Cancer-Normal Tissue Array containing 40 samples of prostate adenocarcinoma and 7 samples of normal prostatic tissue was analyzed for KCTD11 expression. Diagnosis, Gleason, and stage of each tissue were provided by the manufacturer (http://www.tissue-array.com/) and reported in Table 1. Normal prostate epithelial cells showed a high nuclear expression of KCTD11 (Table 1)

Table 1: KCTD11 expression in prostate adenocarcinoma tissues.

No.	Diagnosis	Gleason	Stage	KCTD11 expression	KCTD11 nuclear expression
1	Adenocarcinoma	9	III	++	−
2	Adenocarcinoma	7	II	−	−
3	Adenocarcinoma	9	III	−	−
4	Adenocarcinoma	10	III	+	−
5	Adenocarcinoma	9	III	−	−
6	Adenocarcinoma	8	IV	−	−
7	Adenocarcinoma	7	II	−	−
8	Adenocarcinoma	7	II	+	−
9	Adenocarcinoma	7	II	+++	+
10	Adenocarcinoma	9	III	+++	−
11	Adenocarcinoma	9	III	−	−
12	Adenocarcinoma	7	III	−	−
13	Adenocarcinoma	7	IV	−	−
14	Adenocarcinoma	9	III	−	−
15	Adenocarcinoma	9	IV	−	−
16	Adenocarcinoma	7	III	++++	++
17	Adenocarcinoma	9	IV	−	−
18	Adenocarcinoma	7	III	+++	+
19	Adenocarcinoma	7	III	−	−
20	Adenocarcinoma	9	III	++	−
21	Adenocarcinoma	7	III	++	+
22	Adenocarcinoma	7	II	++	−
23	Adenocarcinoma	7	III	−	−
24	Adenocarcinoma	6	II	−	−
25	Adenocarcinoma	9	III	++	−
26	Adenocarcinoma	9	III	+	−
27	Adenocarcinoma	8	III	−	−
28	Adenocarcinoma	6	III	++++	−
29	Adenocarcinoma	7	II	++++	+
30	Adenocarcinoma	8	III	++++	+
31	Adenocarcinoma	10	IV	−	−
32	Adenocarcinoma	7	IV	−	−
33	Adenocarcinoma	8	IV	−	−
34	Adenocarcinoma	8	III	++++	−
35	Adenocarcinoma	9	III	+	−
36	Adenocarcinoma	9	IV	+	−
37	Adenocarcinoma	9	IV	−	−
38	Adenocarcinoma	9	IV	++++	−
39	Adenocarcinoma	8	III	++++	+
40	Adenocarcinoma	7	III	++++	+
42	Normal (match of #9)	—	—	+++	+++
43	Normal (match of #12)	—	—	+	+
44	Normal (match of #14)	—	—	+++	+++
45	Normal (match of #18)	—	—	++	++
47	Normal (match of #29)	—	—	+++	+++
48	Normal (match of #31)	—	—	+++	+++
49	Normal (match of #40)	—	—	++++	++++

List of prostate adenocarcinoma and normal tissues analyzed (SuperBioChips Tissue Array). Staging and grading of each sample were obtained from manufacturer (http://www.tissue-array.com/). Evaluation of total KCTD11 expression (5th column) or nuclear KCTD11 expression (6th column) in prostate adenocarcinoma tissues was shown. Scores were as follows: "−" <5%; "+" 1–25%; "++" 25–50%; "+++" 50–75%; "++++" 75–100%.

with a positive cells mean corresponding to 60% (Figures 2(a) and 2(b) and Figure 2(d) panel (A)), suggesting a role for this gene in prostate physiology. On the contrary, in CaP tissues KCTD11 protein expression was found to be reduced (Table 1 and Figure 2(a)), with only 32% of prostatic cells expressing KCTD11. Notably, in most CaP tissues KCTD11 expression was completely lost (Table 1 and Figure 2(d) panel (D)) and in those tumoral tissues showing positivity KCTD11 expression was observed mainly in the cytoplasm (Figures 2(c) and 2(d) panel (G)). Indeed, considering just nuclear KCTD11-positive cells, CaP tissues showed a strong and significant reduction of expression of this tumor suppressor gene (Figure 2(b)).

3.3. Reduced Expression of KCTD11 Correlates with Increased Expression of Sonic Hedgehog Signaling Proteins. KCTD11 was previously identified as a suppressor of Hedgehog signaling [20, 22], and deregulation of this pathway has been extensively implicated in prostate tumorigenesis [25–31]. Therefore, contextually to KCTD11, we analyzed the expression level of Patch1 and Gli1 in the same CaP tissues setting. As shown in Figure 2(d), normal prostate epithelial cells showed low expression levels of both Patch1 and Gli1 (Figure 2(d) panels (B) and (C)), whereas in prostate cancers, in which KCTD11 was either lost or expressed in the cytoplasm, both Patch1 and Gli1 resulted to be overexpressed (Figure 2(d) panels (E)-(F), (H)-(I)).

3.4. KCTD11 Inhibits Prostate Cell Proliferation In Vitro. It has been previously shown that KCTD11 inhibits cell proliferation [18–20]. To clarify the role of KCTD11 gene in prostatic cell growth, we analyzed PC3, TSU, ALVA31, and LnCAP prostate cell lines. Firstly, *KCTD11* basal expression was assessed in these cell lines, showing significantly low levels of this transcript (Figure 3(a)). This data demonstrated that KCTD11 downregulation occurs also in prostatic cell lines. As reference, HACAT cell line showing high KCTD11 expression levels was used. Next, we generated KCTD11-GFP-overexpressing prostate cell lines by retroviral infection. High expression levels of KCTD11-GFP were confirmed both by flow cytometry analysis [data not shown] and western blot (Figure 3(d), upper panel). The effect of KCTD11 overexpression on cell proliferation was measured by BrdU incorporation (Figures 3(b) and 3(c)). All tested cell lines showed a decrease in cell growth ranging from 40 to 60%. Growth inhibition correlated with upregulation of cyclin-dependent kinase inhibitors $p21^{WAF1}$ and $p27^{KIP1}$ (Figure 3(d)). In addition, KCTD11 overexpressing prostate cancer cells (Figure 3(e)) displayed a reduction of cell proliferation-related genes, which are known direct targets of Hedgehog/Gli1, such as Cyclin D2 and IGF-2 (Figure 3(f)). Moreover, a decrease of both Patch1 and Gli1 was also observed (Figure 3(f)). Together, these data indicated that KCTD11 upregulation is necessary for inhibiting cell proliferation in prostate cells, through its ability to upregulate cyclin-dependent kinase inhibitors and downregulate Hedgehog/Gli target genes.

4. Discussion

Although prostate cancer is associated with a longer natural history than most other tumor types and most of the men diagnosed with prostate cancer every year do not die from the disease, it remains the second leading cause of cancer death in men [1]. Despite an improved understanding of prostate tumor biology, the reason why certain prostate tumors behave more aggressively than others is still not clear. Furthermore, all patients with prostate cancer are treated similarly once metastases have developed, and patients vary widely in their response to therapies. Understanding the molecular alterations driving prostate cancer can aid in the development of new biomarkers as well as therapeutic targets.

Substantial progress has been made in the last decade to understand the genetic landscape of prostatic cancer. For example, one of the most common genetic alterations discovered is the fusion of TMPRSS2 with ETS gene family of transcription factors [11]. These gene fusions occur at the early stage of the disease pathogenesis, being present in high-grade prostate intraepithelial cancer [34, 35]. In addition, they are prostate-specific and therefore not present in benign prostatic hyperplasia or any other tumor type. This discovery has major implications in prostate cancer diagnosis. In fact, the TMPRSS2-ERG fusion is now being prospectively evaluated as a diagnostic urinary test to complement prostate-specific antigen (PSA) screening [36]. Several other genetic lesions have been identified in prostate cancer, such as SRD5A (steroid-5-alpha-reductase alpha polypeptide) [4], androgen receptor [5], estrogen receptor-β [6], E-cadherin [7], and toll-like receptors [8–10].

Loss of heterozygosity (LOH) of chromosomal regions is crucial in tumor progression. In human prostate cancer, several chromosomal regions demonstrating a high frequency of LOH have been previously identified. LOH has been reported on chromosomes 1p, 3p, 5q, 7q, 6q, 8p, 8q, 10q, 11p-q, 13q, 16q, 17p, 17q, 18q, and 19p [15–17].

Human *KCTD11 (REN)* has been described as a novel tumor suppressor gene located in the short arm of chromosome 17, at the 17p13.2 locus. *KCTD11 (REN)* was isolated by our group as a murine immediate-early gene induced by neurogenic stimuli (NGF, EGF, and retinoic acid) in pluripotent embryonal stem cells and neural progenitor cell lines [18]. *KCTD11* upregulation has been associated with neurotypic differentiation, growth arrest, and $p27^{Kip1}$ induction [17, 18]. In addition, its expression is tightly regulated during development. In fact, *KCTD11* is strongly expressed in E7.5-E8.5 mouse embryo with levels decreasing thereafter and it localizes preferentially to neuroectodermal cells [18].

Importantly, the human orthologue of murine *KCTD11* has been shown to be frequently lost in human medulloblastoma (MB). In fact, *KCTD11* LOH occurs in 39% of human sporadic MB. Furthermore, all diploid and hemizygous MBs showed a strong reduction of *KCTD11* expression, suggesting that silencing of this gene is a pivotal event in MB tumorigenesis [20]. Notably, *KCTD11* expression is frequently downregulated in several human cancers, including larynx, esophagus, stomach, colon-rectum, urinary bladder, lung, breast, gallbladder, and endometrium and its promoter was

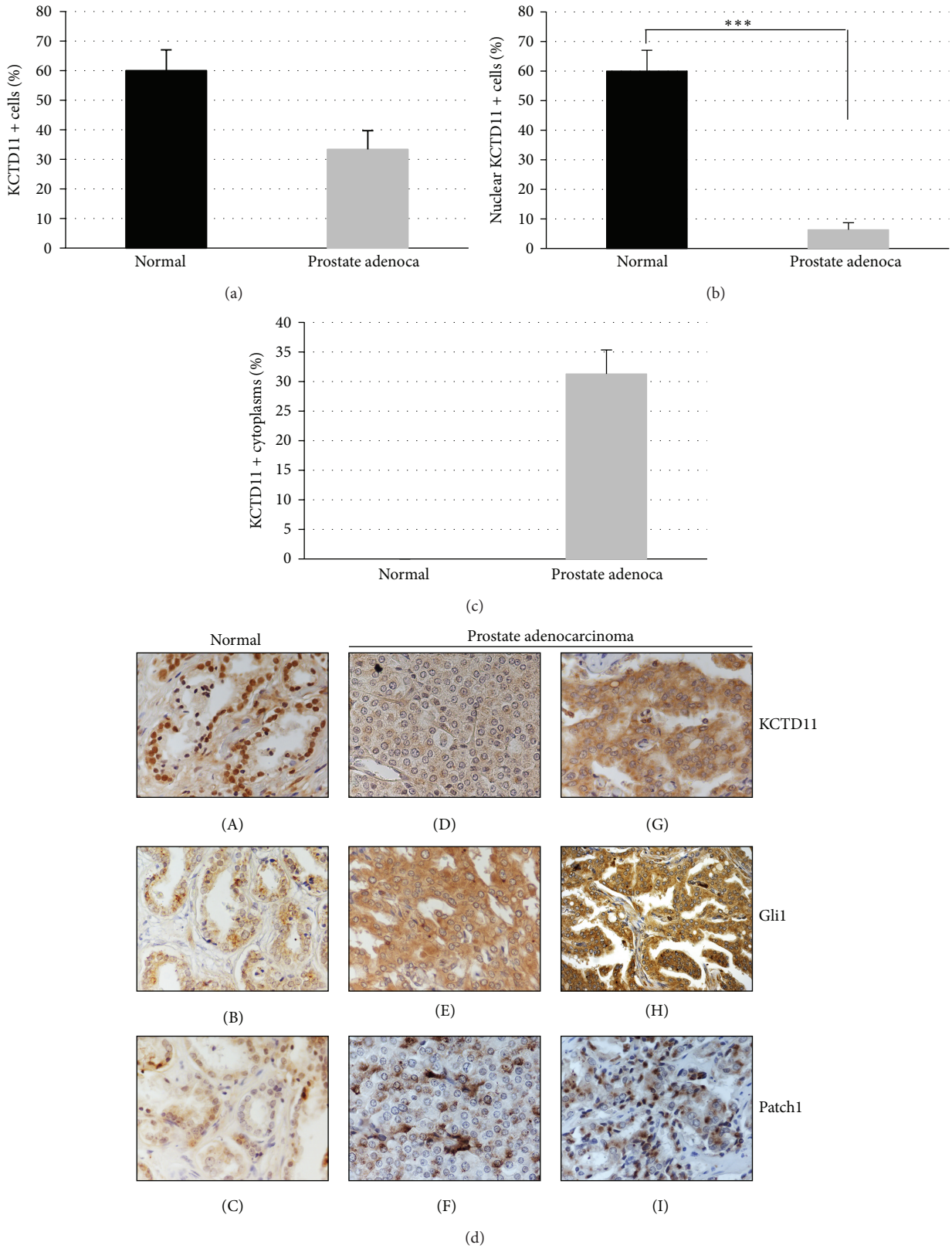

Figure 2: KCTD11 expression in prostate cancer cells compared to normal cells. (a) Total KCTD11-positive cells in normal and prostate adenocarcinoma tissues. (b) Nuclear KCTD11-positive cells in normal and prostate adenocarcinoma tissues. ($^{***}P < 0.005$) (c) Cytoplasmic KCTD11-positive cells in normal and prostate adenocarcinoma tissues. ((a)–(c)) Data are mean ± S.D. (d) KCTD11, Gli1, and Patch1 expressions in normal ((A), (B), and (C)) and prostate adenocarcinoma ((D)–(I)). Magnification 40x.

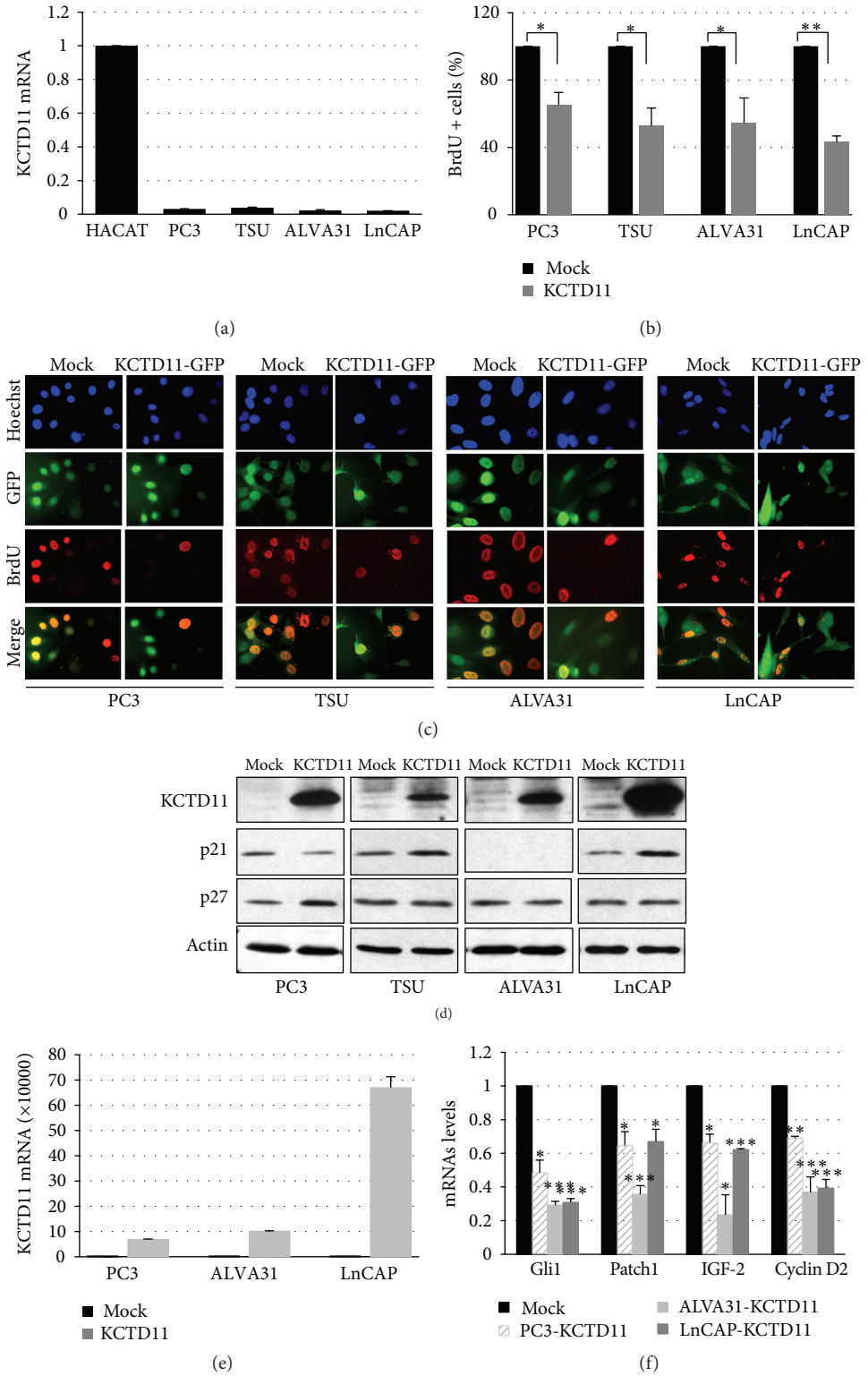

Figure 3: KCTD11 inhibits cellular proliferation. (a) Q-RT-PCR analysis of *KCTD11* mRNA expression in prostate cancer cell lines. (GAPDH was used as endogenous control.) Data are mean ± S.D. of triplicate wells. (b) BrdU-positive cells in KCTD11 overexpressing cell lines. Data are mean ± S.D. from three replicates ($^{*}P < 0.05$; $^{**}P < 0.01$). (c) Representative images of BrdU immunofluorescence assay in prostatic cells stably transfected with KCTD11-GFP. (d) Western blot showing p21 and p27 expression levels in prostate cell lines overexpressing KCTD11. (e) Q-RT-PCR analysis of *KCTD11* mRNA expression in pCXN2-human KCTD11 transfected prostate cancer cell lines. (GAPDH was used as endogenous control.) Data are mean ± S.D. of triplicate wells. (f) Q-RT-PCR analysis of *Gli1, Patch1, IGF-2, and Cyclin D2* mRNA expressions in KCTD11 overexpressing cells. Data are mean ± S.D. of triplicate wells. ($^{*}P < 0.05$; $^{**}P < 0.01$, and $^{***}P < 0.005$.)

found to be methylated in cancer [21]. Regarding its molecular activity, *KCTD11* has been shown to encode for a novel adaptor of Cullin3 ubiquitin E3 ligase complex targeting histone deacetylase 1 and able to inhibit the Hedgehog signaling pathway [20, 22]. Gli1 and Gli2 are transcription factors activated by Hedgehog signaling. They are acetylated proteins and their HDAC-mediated deacetylation promotes transcriptional activation and sustains a positive autoregulatory loop through Hedgehog-induced upregulation of HDAC1. This mechanism is turned off by HDAC1 degradation through an E3 ubiquitin ligase complex formed by Cullin3 and KCTD11 [22]. In this work, we identified *KCTD11* as a gene frequently lost in prostate cancer, showing both LOH and decreased protein expression. Our data are in accordance with KCTD11 LOH data from the Cancer Genome Atlas (TCGA) resource database (http://www.cbioportal.org/), in which deletion of KCTD11 gene is reported to occur in prostate adenocarcinoma. In most CaP tissues, KCTD11 nuclear expression was completely lost, whereas LOH was observed only in 45% of analyzed tissues. Previous work from our group demonstrated that epigenetic events, such as methylation, downregulate KCTD11 in cancer [21]. Moreover, in around 30% of prostate tumoral tissues, KCTD11 expression was observed mainly in the cytoplasm, suggesting that in these cases the protein could be mutated or sequestered by a deregulated protein interactor.

Notably, KCTD11 downregulation is associated with Gli1 and Patch1 overexpression, demonstrating that *KCTD11* tumor suppressor gene acts as an inhibitor of Hedgehog signaling not only in medulloblastoma [20] but also in prostate cancer. Moreover, aberrant Hh signaling activation has been implicated in prostate tumorigenesis in both human subjects and mouse models [25–32], and preclinical data have shown that inhibition of Hh signaling has the potential to reduce prostate cancer invasiveness and metastasis spreading [33]. However, acquired drug resistance has already been described in other cancers upon long-term treatment with Hh inhibitors. Therefore, the identification of factors involved in Hh signaling regulation, which are subjected to alterations and/or genetic lesions, might open a new scenario for designing new target therapies in prostate cancer.

5. Conclusions

Prostate cancer is one of the most common malignant diseases among men in developed countries, which has become a major public health challenge. Traditionally considered as a disease of elderly men, an increasing proportion of prostate cancer cases now occur in men of preretirement ages. New markers for identifying high-risk populations as well as novel strategies for early detection and preventive care are urgently needed.

The mechanism of prostate tumorigenesis is still not fully understood. Here, we showed both LOH and decreased protein expression of the tumor suppressor gene *KCTD11* in prostate cancer, which is associated with increased expression of Hh proteins. KCTD11 expression in prostate cancer cells was also quite low, and ectopic overexpression of KCTD11 determined growth arrest through cyclin-dependent kinase inhibitors upregulation and Hedgehog/Gli target genes' downregulation. Taken together, these data suggest that KCTD11 can be considered a potential candidate to be used for diagnostic and therapeutic application in prostate cancer.

Conflict of Interests

The authors declare that there is no conflict of interests regarding the publication of this paper.

Authors' Contribution

Francesca Zazzeroni and Daniela Nicosia have contributed equally to this work.

Acknowledgments

This work was supported by MIUR-FIRB Grant no. RBAP10A9H9 to Alesse Edoardo and to Gulino Alberto, by grants to Alesse Edoardo from the Ministry of University and Research and to Gulino Alberto from the Associazione Italiana per la Ricerca sul Cancro, the Telethon Grant GGP07118, the Ministry of University and Research, the Ministry of Health, the Center of Excellence for Biology, and Molecular Medicine and the Rome Oncogenomic Center.

References

[1] American Cancer Society, *Cancer Facts and Figures 2013*, American Cancer Society, Atlanta, Ga, USA, 2013.

[2] A. S. Obort, M. B. Ajadi, and O. Akinloye, "Prostate-specific antigen: any successor in sight?" *Reviews in Urology*, vol. 15, no. 3, pp. 97–107, 2013.

[3] J. S. Witte, "Prostate cancer genomics: towards a new understanding," *Nature Reviews Genetics*, vol. 10, no. 2, pp. 77–82, 2009.

[4] E. Lévesque, I. Laverdière, L. Lacombe et al., "Importance of 5α-reductase gene polymorphisms on circulating and intraprostatic androgens in prostate cancer," *Clinical Cancer Research*, vol. 20, no. 3, pp. 576–584, 2014.

[5] G. Fromont, M. Yacoub, A. Valeri et al., "Differential expression of genes related to androgen and estrogen metabolism in hereditary versus sporadic prostate cancer," *Cancer Epidemiology Biomarkers and Prevention*, vol. 17, no. 6, pp. 1505–1509, 2008.

[6] C. Thellenberg-Karlsson, S. Lindström, B. Malmer et al., "Estrogen receptor β polymorphism is associated with prostate cancer risk," *Clinical Cancer Research*, vol. 12, no. 6, pp. 1936–1941, 2006.

[7] L. X. Qiu, R. T. Li, J. B. Zhang et al., "The E-cadherin (CDH1) -160 C/A polymorphism and prostate cancer risk: a meta-analysis," *European Journal of Human Genetics*, vol. 17, no. 2, pp. 244–249, 2009.

[8] I. Cheng, S. J. Plummer, G. Casey, and J. S. Witte, "Toll-like receptor 4 genetic variation and advanced prostate cancer risk," *Cancer Epidemiology Biomarkers and Prevention*, vol. 16, no. 2, pp. 352–355, 2007.

[9] J. Sun, F. Wiklund, S. L. Zheng et al., "Sequence variants in toll-like receptor gene cluster (TLR6-TLR1-TLR10) and prostate cancer risk," *Journal of the National Cancer Institute*, vol. 97, no. 7, pp. 525–532, 2005.

[10] V. L. Stevens, A. W. Hsing, J. T. Talbot et al., "Genetic variation in the toll-like receptor gene cluster (TLR10-TLR1-TLR6) and prostate cancer risk," *International Journal of Cancer*, vol. 123, no. 11, pp. 2644–2650, 2008.

[11] S. A. Tomlins, D. R. Rhodes, S. Perner et al., "Recurrent fusion of TMPRSS2 and ETS transcription factor genes in prostate cancer," *Science*, vol. 310, no. 5748, pp. 644–648, 2005.

[12] A. Liede, B. Y. Karlan, and S. A. Narod, "Cancer risks for male carriers of germline mutations in BRCA1 or BRCA2: a review of the literature," *Journal of Clinical Oncology*, vol. 22, no. 4, pp. 735–742, 2004.

[13] C. Soravia, H. van der Klift, M.-A. Bründler et al., "Prostate cancer is part of the hereditary non-polyposis colorectal cancer (HNPCC) tumor spectrum," *The American Journal of Medical Genetics*, vol. 121, no. 2, pp. 159–162, 2003.

[14] J. Xu, E. M. Lange, L. Lu et al., "HOXB13 is a susceptibility gene for prostate cancer: results from the International Consortium for Prostate Cancer Genetics (ICPCG)," *Human Genetics*, vol. 132, no. 1, pp. 5–14, 2013.

[15] T. Saric, Z. Brkanac, D. A. Troyer et al., "Genetic pattern of prostate cancer progression," *International Journal of Cancer*, vol. 81, no. 2, pp. 219–224, 1999.

[16] R. S. Verma, M. Manikal, R. A. Conte, and C. J. Godec, "Chromosomal basis of adenocarcinoma of the prostate," *Cancer Investigation*, vol. 17, no. 6, pp. 441–447, 1999.

[17] C. I. Dumur, C. Dechsukhum, J. L. Ware et al., "Genome-wide detection of LOH in prostate cancer using human SNP microarray technology," *Genomics*, vol. 81, no. 3, pp. 260–269, 2003.

[18] R. Gallo, F. Zazzeroni, E. Alesse et al., "REN: a novel, developmentally regulated gene that promotes neural cell differentiation," *Journal of Cell Biology*, vol. 158, no. 4, pp. 731–740, 2002.

[19] B. Argenti, R. Gallo, L. di Marcotullio et al., "Hedgehog antagonist RENKCTD11 regulates proliferation and apoptosis of developing granule cell progenitors," *Journal of Neuroscience*, vol. 25, no. 36, pp. 8338–8346, 2005.

[20] L. di Marcotullio, E. Ferretti, E. de Smaele et al., "REN(KCTD11) is a suppressor of Hedgehog signaling and is deleted in human medulloblastoma," *Proceedings of the National Academy of Sciences of the United States of America*, vol. 101, no. 29, pp. 10833–10838, 2004.

[21] M. M. Mancarelli, F. Zazzeroni, L. Ciccocioppo et al., "The tumor suppressor gene KCTD11REN is regulated by Sp1 and methylation and its expression is reduced in tumors," *Molecular Cancer*, vol. 9, article 172, 2010.

[22] G. Canettieri, L. di Marcotullio, A. Greco et al., "Histone deacetylase and Cullin3-REN KCTD11 ubiquitin ligase interplay regulates Hedgehog signalling through Gli acetylation," *Nature Cell Biology*, vol. 12, no. 2, pp. 132–142, 2010.

[23] J. W. Theunissen and F. J. de Sauvage, "Paracrine hedgehog signaling in cancer," *Cancer Research*, vol. 69, no. 15, pp. 6007–6010, 2009.

[24] M. Kasper, G. Regl, A.-M. Frischauf, and F. Aberger, "GLI transcription factors: Mediators of oncogenic Hedgehog signalling," *European Journal of Cancer*, vol. 42, no. 4, pp. 437–445, 2006.

[25] T. Sheng, C. Li, X. Zhang et al., "Activation of the hedgehog pathway in advanced prostate cancer," *Molecular Cancer*, vol. 3, article 29, 2004.

[26] P. Sanchez, A. M. Hernández, B. Stecca et al., "Inhibition of prostate cancer proliferation by interference with SONIC HEDGEHOG-GLI1 signaling," *Proceedings of the National Academy of Sciences of the United States of America*, vol. 101, no. 34, pp. 12561–12566, 2004.

[27] S. S. Karhadkar, G. S. Bova, N. Abdallah et al., "Hedgehog signalling in prostate regeneration, neoplasia and metastasis," *Nature*, vol. 431, no. 7009, pp. 707–712, 2004.

[28] B. Y. Chen, J. Y. Liu, H. H. Chang et al., "Hedgehog is involved in prostate basal cell hyperplasia formation and its progressing towards tumorigenesis," *Biochemical and Biophysical Research Communications*, vol. 357, no. 4, pp. 1084–1089, 2007.

[29] B. Y. Chen, D. P. Lin, J. Y. Liu et al., "A mouse prostate cancer model induced by Hedgehog overexpression," *Journal of Biomedical Science*, vol. 13, pp. 373–384, 2006.

[30] S. Azoulay, S. Terry, M. Chimingqi et al., "Comparative expression of Hedgehog ligands at different stages of prostate carcinoma progression," *Journal of Pathology*, vol. 216, no. 4, pp. 460–470, 2008.

[31] H. H. Chang, B. Y. Chen, C. Y. Wu et al., "Hedgehog overexpression leads to the formation of prostate cancer stem cells with metastatic property irrespective of androgen receptor expression in the mouse model," *Journal of Biomedical Science*, vol. 18, no. 1, article 6, 2011.

[32] A. Gonnissen, S. Isebaert, and K. Haustermans, "Hedgehog signaling in prostate cancer and its therapeutic implication," *International Journal of Molecular Sciences*, vol. 14, no. 7, pp. 13979–14007, 2013.

[33] F. Zazzeroni, S. Papa, A. Algeciras-Schimnich et al., "Gadd45β mediates the protective effects of CD40 costimulation against Fas-induced apoptosis," *Blood*, vol. 102, no. 9, pp. 3270–3279, 2003.

[34] H. Beltran and M. A. Rubin, "New strategies in prostate cancer: Translating genomics into the clinic," *Clinical Cancer Research*, vol. 19, no. 3, pp. 517–523, 2013.

[35] S. Roychowdhury and A. M. Chinnaiyan, "Advancing precision medicine for prostate cancer through genomics," *Journal of Clinical Oncology*, vol. 31, no. 15, pp. 1866–1873, 2013.

[36] S. A. Tomlins, S. M. J. Aubin, J. Siddiqui et al., "Urine TMPRSS2:ERG fusion transcript stratifies prostate cancer risk in men with elevated serum PSA," *Science Translational Medicine*, vol. 3, no. 94, Article ID 94ra72, 2011.

Hindawi Publishing Corporation
BioMed Research International
Volume 2014, Article ID 909623, 7 pages
http://dx.doi.org/10.1155/2014/909623

Review Article

Bioclinical Parameters Driving Decision-Making of Subsequent Lines of Treatment in Metastatic Castration-Resistant Prostate Cancer

A. Irelli,[1,2] G. Bruera,[1,2] K. Cannita,[1] E. Palluzzi,[1,2] G. L. Gravina,[3] C. Festuccia,[2] C. Ficorella,[1,2] and E. Ricevuto[1,2]

[1] *Medical Oncology, S. Salvatore Hospital, University of L'Aquila, 67100 L'Aquila, Italy*
[2] *Department of Biotechnological and Applied Clinical Sciences, University of L'Aquila, 67100 L'Aquila, Italy*
[3] *Radiotherapy, S. Salvatore Hospital, University of L'Aquila, 67100 L'Aquila, Italy*

Correspondence should be addressed to E. Ricevuto; enrico.ricevuto@univaq.it

Received 7 February 2014; Accepted 30 April 2014; Published 28 May 2014

Academic Editor: Andrea Maria Isidori

Different options are available as second-line treatment of metastatic castrate-resistant prostate cancer: cabazitaxel, abiraterone, and enzalutamide. Phase III studies evaluating cabazitaxel and the two hormonal agents have been shown to significantly prolong overall survival compared to mitoxantrone and placebo, respectively. Several studies have also demonstrated feasibility and activity of docetaxel rechallenge in case of a sufficient progression-free interval (3–6 months), good performance status, and previous acceptable safety profile, thus providing an additional treatment option in clinical practice. Clinical and biological parameters should be considered to tailor II line treatment. In clinical practice, we can primarily evaluate patients' fitness according to age, performance status, symptomatic disease, comorbidities, and expected safety profile of each drug. Different prognostic/predictive factors may be considered, such as presence of bone-limited or visceral metastases, length of androgen deprivation therapy (ADT) before chemotherapy, time to progression after docetaxel, Gleason score, PSA doubling time, and serum testosterone, even if their clinical relevance is still debated. This review will discuss current options of innovative drugs sequencing and selection according to bioclinical parameters.

1. Treatment Options in Clinical Practice after Progression to Docetaxel

In clinical practice, different treatment options are now available after progression to docetaxel in the management of castrate-resistant prostate cancer (CRPC) patients: cabazitaxel, abiraterone and enzalutamide, and other drugs are currently under evaluation for clinical recommendation, such as alpha emitter radium-223 [1–7].

1.1. Cabazitaxel. Cabazitaxel is a novel taxane that inhibits microtubule depolymerization and cell division by binding tubulin, resulting in cell cycle arrest. It showed antitumor activity in models resistant to docetaxel and is able to cross the blood-brain barrier [1].

In the phase III randomized Tropic trial, patients progressing during or after docetaxel were randomized to cabazitaxel 25 mg/m^2 or mitoxantrone 12 mg/m^2. At median follow-up 12.8 months, overall survival was 15.1 versus 12.7 months (HR 0.70, $P < 0.0001$) [1]. Treatment with cabazitaxel was prognostic for survival ≥2 years, 27% versus 16%, respectively [2]. Median progression-free survival was 2.8 months compared to 1.4 months (HR 0.74, $P < 0.0001$), with a significantly higher tumor response rate 14.4% compared with 4.4% ($P = 0.0005$) with cabazitaxel and mitoxantrone, respectively. More, median time to PSA progression was 6.4 months compared to 3.1 months, $P = 0.0010$; PSA response rate was 39.2% compared to 17.8%, $P = 0.0002$. No statistical differences were reported in progression of pain and response to pain. Grade 3-4 related adverse events significantly different in

the cabazitaxel and mitoxantrone arms were: neutropenia (82% versus 58%, febrile 8% versus 1%) and diarrhea (6% versus <1%). Thus, prophylactic use of granulocyte colony-stimulating growth factors are strongly recommended, and a lower dose of cabazitaxel (e.g. 20 mg/m^2) may be considered and is now under evaluation [1].

Overall survival benefit was reported in patients who received a cumulative dose of docetaxel <225 mg/m^2, who progressed during docetaxel (29%) and who progressed during and within 3 months after docetaxel (45%). The survival advantage of cabazitaxel also persisted in patients with measurable disease or pain, most pronounced in patients with performance status 0-1, and disease progression within <3 months from docetaxel. PSA immediate reduction or flare were associated with a OS benefit.

1.2. Abiraterone. Abiraterone is a selective inhibitor of cytochrome P450, CYPC17, and inhibits the residual amount of androgenic steroid predominantly produced in adrenal gland [3].

In phase III, randomized COU-AA-301 trial, patients were randomized to receive 1000 mg of abiraterone acetate or placebo, with 5 mg of prednisone twice daily. At median follow-up 12.8 months, abiraterone significantly increased overall survival, 14.8 versus 10.9 months, $P < 0.001$; and also time to PSA progression (10.2 versus 6.6 months, $P < 0.001$), progression-free survival (5.6 months versus 3.6 months, $P < 0.001$), and PSA response rate (29% versus 6%, $P < 0.001$). An attenuation of pain was significantly higher with abiraterone (44% versus 27%, $P = 0.002$), with progression of pain at 6 (22% versus 28%), 12 (30% versus 38%) and 18 months (35% versus 46%), and time until progression of pain was 7.4 months compared with 4.7 months, respectively [3].

Abiraterone produced similar improvement in median overall survival in patients with (4.6 months) and without (4.8 months) visceral disease, hazard ratios 0.79 and 0.69 ($P = 0.0001$), respectively; HRs for rPFS were 0.60 ($P = 0.0002$) and 0.68 ($P < 0.0001$); PSA response rates were 28% versus 7% and 30% versus 5% (both $P = 0.0001$), respectively; ORRs were 11% versus 0% ($P = 0.0058$) and 19% versus 5% ($P = 0.0010$), respectively [4].

A lower percentage of skeletal related events were reported with abiraterone at 6 months (18% versus 28%), 12 months (30% versus 40%), and 18 months (35% versus 40%), and the time at the first skeletal event was 9.9 months compared to 4.9 months. More common adverse events were hypokalemia, fluid retention, and hypertension, largely abrogated by low-dose glucocorticoids [3].

At an update follow-up 20.2 months, significantly increased clinical outcomes were confirmed in abiraterone arm: overall survival (15.8 versus 11.2 months, $P < 0.0001$), median time to PSA progression (8.5 versus 6.6 months, $P < 0.0001$), radiologic progression-free survival (5.6 versus 3.6 months, $P < 0.0001$), and PSA response rate (29.5% versus 5.5%; $P < 0.0001$) [5].

1.3. Enzalutamide. Enzalutamide is an androgen-receptor-signaling inhibitor that inhibits nuclear translocation of the androgen receptor, DNA binding, and coactivator recruitment. It also has a greater affinity for the receptor and has no known agonistic effects [6].

In the AFFIRM phase 3 randomized trial, at median follow-up 14.4 months, enzalutamide 160 mg significantly increased clinical outcome compared to placebo: median overall survival 18.4 and 13.6 months, with 37% reduction in the risk of death ($P < 0.001$); radiographic progression-free survival 8.3 and 2.9 months ($P < 0.001$); median time to PSA progression 8.3 and 3.0 months ($P < 0.001$); median time to first skeletal event 16.7 and 13.3 months ($P < 0.001$). More frequent adverse events were fatigue, diarrhea, hot flashes, musculoskeletal pain and headache [6].

1.4. Radium-223. Radium-223 dichloride (radium-223), an alpha emitter, selectively targets bone metastases with alpha particles. Alpha emitter radium-223 recently showed a significantly improved overall survival (14.9 versus 11.3 months, $P < 0.001$) in the phase III ALSYMPCA study [7].

2. Bioclinical Parameters to Tailor Treatment Strategies

2.1. Patients' Fitness. Prostate cancer is prevalently an elderly disease: median age at diagnosis 67 years [8]. Patient's distribution according to age is: young < 65 years, elderly ≥ 65 years, and specifically young-elderly (65–74 years), old-elderly (75–84 years), and oldest (≥85 years).

In the decision-making process different clinical parameters, such as age, functional, nutritional, and comorbidity status should be considered. Different geriatric assessment evaluations can be used to properly define patients' fitness and select tailored treatment options, with different schedules and drug dosages. In our clinical practice experience, Cumulative Illness Rating Scale (CIRS) is commonly used to objectively define comorbidity status in the individual patient [9]. CIRS evaluates the presence and the severity (absent, slight, moderate, severe, and very serious) of the coexisting disorders in the major organs (heart, vascular, respiratory, eye, ear nose and throat, upper digestive tract, lower digestive tract, liver, kidney, genitourinary, musculoskeletal, neurological, and endocrinological disorders). More, functional status is evaluated using instrumental activities of daily living measured by ADL [10] and IADL [11]. Patients are classified into different CIRS stages: primary, if absent comorbidities and functional independent; intermediate, <3 mild and/or moderate categories, and dependent IADL; secondary, ≥3 categories or severe comorbidity, and dependent ADL. In this decision-making process, young and young-elderly patients with primary and/or intermediate CIRS stage can be considered fit for standard treatments, while old-elderly and/or secondary CIRS stage patients are not eligible for conventional treatments and should be considered for treatment modifications (dose, schedule), to properly balance safety and efficacy.

Moreover, nutritional status can be estimated by the variation of weight during the previous 3 months: good

Table 1: Patients' features.

Clinical trial	Median age	Range	≥75 years	PS 2	Visceral metastases
TROPIC	68	62–73	18%	7%	25%
COU-AA-301	69	42–95	28%	10%	11% (liver metastases)
AFFIRM	69	41–92	25%	8.5%	23.2%

Table 2: Cumulative G3-4 toxicity according to age.

(a) Cabazitaxel

	<70 years	≥70 years
Diarrhea	3.3%	2.2%
Fatigue	4%	4.3%
Asthenia	1.4%	4.9%
Neutropenia	15%	19.7%
Febrile neutropenia	5.2%	5.5%
Anemia	5%	4.3%

(b) Enzalutamide

	≥75 years	<75 years
Fatigue	40%	32%
Nausea	32%	33%

nutritional status, weight loss <5%, risk of malnutrition, 5–10%, severe malnutrition, >10%. All these clinical features should be considered to define fitness and discriminate patients fit or unfit for specific drugs (Table 1).

2.1.1. Age. In the interim analysis of the European compassionate use program, cabazitaxel-related adverse events were manageable in clinical practice in elderly population (≥70 years). Dose intensity, dose delays and dose reductions were similar in ≥70 years and younger patients. Diarrhea was the most common adverse event, usually mild with grade ≥3 in 2.2%. Prophylactic G-CSF was more commonly administered in patients ≥70 years [12]. However, haematological toxicity of cabazitaxel appeared similar to younger patients. In multivariate analysis, advanced age (≥75 years), first cabazitaxel cycle and low neutrophil count before cabazitaxel ($<4000/mm^3$) were associated with an increased risk of grade ≥3 neutropenia and/or neutropenic complications [13]. In the cabazitaxel compassionate-use and early access programs, prevalently enrolling ≤75 years patients (81.6%), adverse events were more frequent in older patients (64.2% versus 54.8%), resulting in treatment discontinuation in 24.4% and 36.4%, respectively. Grade ≥3 neutropenia was observed in 25.8% and 17.0% of < and ≥75 years patients, respectively [14].

In the post hoc analysis of COU-AA-301, grade 3/4 adverse events with abiraterone occurred in 62% and 60% of elderly (≥75 years) and younger (<75 years) patients, respectively. Incidences of hypertension and hypokalemia were similar in both age subgroups [15].

In the AFFIRM trial, similar safety profiles were observed in elderly and younger patients [16] (Table 2).

2.1.2. Performance Status. About 20% prostate cancer patients show ECOG PS 2 at diagnosis. Among overall PS 2 population who progressed after docetaxel, experimental treatments decreased risk of death by 26% ($P = 0.035$); activity was similar in PS 0 or 1 with reduced risk of death of 31%. The significant reduction of risk of death was confirmed for hormonal therapies, abiraterone and enzalutamide (HR = 0.72; $P = 0.046$), but not for chemotherapy (HR = 0.81, $P = 0.43$) [17] (Table 3).

2.2. Symptomatic Disease. Almost 70% metastatic PC patients have a high incidence of bone lesions that correlate with skeletal-related events (SREs), defined as fracture (pathological vertebral and/or nonvertebral), bone radiation, bone surgery, and spinal cord compression, including or not hypercalcemia [18]. SRE rate can depend on: number of bone metastases, metastatic site, type of lesion, treatment especially preventive one. Several studies have attempted to correlate skeletal involvement with survival. Staging systems based on scintigraphic distribution (axial versus appendicular) or number of metastases showed a significant association with survival. Median survivals of patients with low, intermediate, or extensive skeletal involvement evaluated by the bone scan index, based on the percentage of tumor involvement multiplied by the weights of each of the 158 bones, were 18.3, 15.8, and 8.1 months, respectively [19]. SREs do not include pain, although persistent prostate cancer-induced bone pain (PCIBP) is one of the most distressing symptoms [20]. In clinical practice, treatment choice for metastatic CRPC patients is driven primarily by asymptomatic or minimally symptomatic, versus symptomatic disease [21].

3. Prognostic and Predictive Factors

Prognostic factor is any clinical and/or biological parameter that correlates with clinical outcome and that can therefore be used in clinical practice in the decision-making process; instead, predictive factor is any clinical or biological parameter that significantly correlate with activity and efficacy of a specific drug, and that can be used to select specific population suitable for a specific therapy or targeted agent. However, more frequently, most parameters show a prognostic and predictive relevance. In metastatic CRPC, prognostic factors usually evaluated in clinical trials are symptomatic disease, presence of visceral metastases, short duration of hormone therapy before chemotherapy (16–20 months), and baseline levels of serum testosterone. Predictive factors are disease progression during or <3 months after docetaxel, Gleason score, and PSA doubling time.

Table 3: Overall survival.

Experimental treatments	Control treatment	HR	95% CI	*P* value
Cabazitaxel	Mitoxantrone	0.81	0.48–1.37	0.43
Abiraterone and enzalutamide	Placebo	0.72	0.52–0.99	0.046
All treatments in PS 2 patients		0.74	0.56–0.98	0.035

3.1. Metastatic Sites. All phase 2 or 3 clinical trials showed a significant trend over time ($P = 0.001$) of increasing proportions of patients with non-osseous metastasis (lymph node, visceral, and soft tissue) (1.4% per year increase), with stable proportion of liver involvement [22]. The presence of visceral metastases is a negative prognostic factor and may confer less sensitivity to hormone therapy. In an updated analysis of COU-AA-301 trial, overall survival benefit of abiraterone was similarly improved in patients with visceral (liver or lung, but not nodal-only metastases) (4.6 months) and without visceral metastases (4.8 months), even if not significantly for visceral disease. Abiraterone conferred significant 40% and 32% reductions in the risk of radiographic progression or death in patients with or without visceral disease, respectively. Soft-tissue objective response rates were superior with abiraterone in both groups. PSA response rates were significantly improved by abiraterone in both groups [23].

3.2. Previous Duration of Hormonal Therapy. In the Institut Gustave Roussy clinical trials database, median duration of prostate cancer sensitivity to androgen deprivation therapy ≥16 months significantly and strongly predicted for both PSA response (58% versus 18%, $P = 0.01$) and PFS (5 and 3 months, $P < 0.043$), in >16 months and <16 months subgroups, respectively. So, it may represent a significant predictive factor for efficacy of subsequent endocrine manipulations [24].

3.3. Disease Progression during or <3 Months after Docetaxel. None of docetaxel refractory patients had PSA, radiological, or clinical response to abiraterone. In 16% metastatic CRPC patients treated with docetaxel followed by abiraterone PSA decline ≥50% was observed. There was no relationship between length of time on LHRH agonist and PSA response to abiraterone [25].

3.4. PSA Doubling Time. In a cohort of men with biochemical recurrence after prostatectomy, at a median follow-up 4 years, 29.3% developed metastases, and there was a statistically significant inverse correlation between PSA doubling time and PSA at metastasis ($P = 0.02$), but not for Gleason score [26].

3.5. Testosterone Serum Level. In 9 first line phase II-III trials, testosterone under castration level (<50 ng/dL) was prognostic for overall survival, and PSA response to salvage hormone-therapy differed depending on testosterone serum levels: median overall survival was 22.4 months compared to 32.7 months in patients with testosterone level under and higher median value (11.53 ng/dL) ($P = 0.0162$), and PSA response 21.74% and 55.6%, respectively [27]. In clinical practice, serum testosterone <20 ng/dL seems to represent an adequate castration level [28].

3.6. Gleason Score. Initial Gleason score between 8 and 10 may be predictive factor of a poor response to hormonal treatment including abiraterone [29].

4. Clinical Algorithm to Define the Sequence of Administration in Second and Subsequent Lines

After docetaxel, treatment options for metastatic CRPC include cabazitaxel, abiraterone acetate, and enzalutamide. Phase III studies evaluating cabazitaxel and abiraterone included patients with similar baseline features: median age 68 and 69 years, 18% and 28% patients > 75 years, PSA basal level 143.9 and 128.8 ng/mL, 46% and 44% symptomatic disease, respectively. In the TROPIC trial, 6% patients were treated for >2 lines. All outcomes were significantly increased in the experimental arms: median overall survival 15.1 and 14.8 months, with HR for risk of death 0.70 and 0.65, compared to mitoxantrone and placebo, in the TROPIC and COU-AA-301 trials, respectively. Thus, in second-line setting, overall survival was equivalently improved by cabazitaxel and abiraterone, even if survival of control arms were slightly different, 10.9 versus 12.7 months for prednisone and mitoxantrone, respectively (Table 4).

Optimal sequence of cabazitaxel and abiraterone after docetaxel was evaluated in 130 patients, significantly more frequently ($P < 0.001$) treated with docetaxel → cabazitaxel → abiraterone (67.7%) compared with docetaxel → abiraterone → cabazitaxel (32.3%). The sequence docetaxel-abiraterone was prevalent among patients not eligible to receive more than 2 lines of treatment, while the sequence docetaxel-cabazitaxel was preferable for patients suitable for 3 lines of treatment. Thus, the unbalance favoring the sequence docetaxel-cabazitaxel-abiraterone could be partially related to the clinical *a priori* selection [30]. A retrospective analysis was conducted on an American electronic database (iKnowMed Electronic Health Records). A total of 113 patients were treated with sequential docetaxel, cabazitaxel, and abiraterone: 77 with the sequence docetaxel-cabazitaxel-abiraterone and 36 with docetaxel-abiraterone-cabazitaxel. Overall survival was superior in the sequence docetaxel-cabazitaxel-abiraterone versus docetaxel-abiraterone-cabazitaxel, 18.2 versus 11.8 months, respectively (HR = 0,12) [31]. Cabazitaxel may be considered an option for patients refractory to first-line

Table 4: Clinical outcome.

	Cabazitaxel		Mitoxantrone	
OS (months)	15.1		12.7	$P < 0.0001$
Median followup (months)		12.8		HR 0.70 (0.59–0.83)
PFS (months)	2.8		1.4	$P < 0.0001$
PSA progression (months)	6.4		3.1	$P = 0.001$
PSA response rate (%)	39.2		17.8	$P = 0.0002$
ORR (%)	14.4		4.4	$P = 0.0005$
	Abiraterone		Placebo	
OS (months)	14.8		10.9	$P < 0.001$
Median followup (months)		12.8		HR 0.65 (0.54–0.77)
PFS (months)	5.6		3.6	$P < 0.001$
PSA progression (months)	10.2		6.6	$P < 0.001$
PSA response rate (%)	29		6	$P < 0.001$
ORR (%)	14		2.8	$P < 0.001$
	Enzalutamide		Placebo	
OS (months)	18.4		13.6	$P < 0.001$
Median followup (months)		14.4		HR 0.63 (0.53–0.75)
PFS (months)	8.3		2.9	$P < 0.001$
PSA progression (months)	8.3		3	$P < 0.001$
PSA response rate (%)	54		2	$P < 0.001$
ORR (%)	29		4	$P < 0.001$

docetaxel, with very early development of CRPC, visceral metastases and a very short PSA doubling time.

In the compassionate use of abiraterone after docetaxel, 18.4% subsequently received cabazitaxel, prevalently at 20 mg/m^2, and obtained 26% PSA control. Median survival from docetaxel was 32.0 months, from abiraterone 16.1 months, from cabazitaxel 8.2 months. Non progression to docetaxel was associated with longer survival with cabazitaxel, 43.1 versus 17.4 months ($P = 0.049$), while not to abiraterone [32]. Among patients treated with third-line cabazitaxel after abiraterone, 20% had a partial response [33].

In metastatic CRPC patients previously treated with abiraterone, docetaxel rechallenge resulted in PSA decline ≥50% in 26%, with partial responses 11%, time to PSA progression 4.6 months, and overall survival 12.5 months. No responses to docetaxel were observed in abiraterone-refractory patients. These data may support the hypothesis of cross-resistance between these agents and preclinical evidence that docetaxel antitumour activity may be related to its impact on androgen receptor signaling. The high intratumoral androgens in patients discontinuing abiraterone could reduce docetaxel antitumour activity, and androgen receptor overexpression or mutation may also contribute to docetaxel resistance. More, abiraterone activity seems to be different according to its sequencing with docetaxel [34].

PSA decrease ≥50% was reached in 41.3% patients treated with cabazitaxel, with median overall survival 13.3 months and median clinical and/or radiological progression-free survival 6.5 months. Abiraterone or enzalutamide were given before and after cabazitaxel in 33% and 16% patients, respectively. In patients treated with abiraterone or enzalutamide after and before cabazitaxel, median overall survival from docetaxel was 65 months versus 39 months, respectively. Overall survival was significantly reduced in patients with ECOG 2, alkaline phosphatase ≥1.5 upper limit of normal, lymph node involvement, and significantly prolonged in patients treated with ≥2 docetaxel lines, prior curative therapy, PSA decrease ≥30% with cabazitaxel and in patients treated with abiraterone/enzalutamide after cabazitaxel. Thus, patients treated with new hormonal agents after cabazitaxel seemed to experience a prolonged overall survival [35].

After failure of abiraterone, enzalutamide achieved response rate 2.9%, time to progression 4.0 months: PSA decline >50% in 45.7%, specifically 43.8% and 15.8% in abiraterone-sensitive and abiraterone-insensitive patients, respectively. 48.6% of patients were enzalutamide-resistant and showed a rising PSA as the best response [36].

In the enzalutamide expanded access program after progression to docetaxel and abiraterone, 39% of patients showed >50% PSA reduction, 60% and 23% in patients sensitive and insensitive to abiraterone, respectively [37].

In an indirect comparative effectiveness analysis between enzalutamide and abiraterone using the results of AFFIRM and COU-AA-301 trials, respectively, based on the assumption that the relative effects of each drug compared to placebo were the same, enzalutamide appears to be more effective than abiraterone in terms of time to PSA progression, radiologic progression-free survival and PSA response, and overall survival was not different: hazard ratios for overall survival were 0.63 (0.53–0.75) and 0.66 (0.56–0.79); indirect estimate for enzalutamide versus abiraterone 0.96 (0.75–1.22); HR for time to PSA progression 0.40 (0.35–0.47) and 0.67 (0.59–0.78); indirect estimate of HR for enzalutamide versus

abiraterone 0.60 (0.49–0.74); odds ratios for PSA response 77.08 (34.02–174.70) and 5.49 (3.84–7.84); indirect estimate for enzalutamide versus abiraterone 14.04 [38].

Several studies have demonstrated feasibility and activity of docetaxel rechallenge in metastatic CRPC patients in case of a sufficient progression-free interval (3–6 months), good ECOG PS, and previous acceptable safety profile, thus providing an additional treatment option in clinical practice: overall biochemical response rate (PSA reduction > 50%) 66%, overall survival 32 months with projected 2-year overall survival from first docetaxel administration 77.5%. Multivariate analysis showed that time slope-log PSA, time from the previous cycle, and response to the previous cycle were predictive of response to rechallenge [39].

Thus, in the complex management of metastatic CRPC different clinical and biological parameters should be considered in clinical practice to better define patients' fitness and select treatment strategy to optimize clinical outcome.

Conflict of Interests

The authors declare that there is no conflict of interests regarding the publication of this paper.

Authors' Contribution

A. Irelli and G. Bruera equally contributed to the present paper.

References

[1] J. S. de Bono, S. Oudard, M. Ozguroglu et al., "Prednisone plus cabazitaxel or mitoxantrone for metastatic castration-resistant prostate cancer progressing after docetaxel treatment: a randomised open-label trial," *The Lancet*, vol. 376, no. 9747, pp. 1147–1154, 2010.

[2] A. Bahl, S. Oudard, B. Tombal et al., "Impact of cabazitaxel on 2-years survival and palliation of tumor-related pain in men with metastatic castration-resistant prostate cancer treated in the Tropic trial," *Annals of Oncology*, vol. 24, pp. 2402–2408, 2013.

[3] J. S. de Bono, C. J. Logothetis, A. Molina et al., "Abiraterone and increased survival in metastatic prostate cancer," *The New England Journal of Medicine*, vol. 364, no. 21, pp. 1995–2005, 2011.

[4] O. B. Goodman Jr, T. W. Flaig, A. Molina et al., "Exploratory analysis of the visceral disease subgroup in a phase III study of abiraterone acetate in metastatic castration-resistant prostate cancer," *Prostate Cancer and Prostatic Diseases*, vol. 17, pp. 34–39, 2013.

[5] K. Fizazi, H. I. Scher, A. Molina et al., "Abiraterone acetate for treatment of metastatic castration-resistant prostate cancer: final overall survival analysis of the COU-AA-301 randomised, double-blind, placebo-controlled phase 3 study," *The Lancet Oncology*, vol. 13, no. 10, pp. 983–992, 2012.

[6] H. I. Scher, K. Fizazi, F. Saad et al., "Increased survival with enzalutamide in prostate cancer after chemotherapy," *The New England Journal of Medicine*, vol. 367, no. 13, pp. 1187–1197, 2012.

[7] C. Parker, S. Nilsson, D. Heinrich et al., "Alpha emitter radium-223 and survival in metastatic prostate cancer," *The New England Journal of Medicine*, vol. 369, no. 3, pp. 213–223, 2013.

[8] S. K. Bechis, P. R. Carroll, and M. R. Cooperberg, "Impact of age at diagnosis on prostate cancer treatment and survival," *Journal of Clinical Oncology*, vol. 29, no. 2, pp. 235–241, 2011.

[9] P. A. Parmelee, P. D. Thuras, I. R. Katz, and M. P. Lawton, "Validation of the cumulative illness rating scale in a geriatric residential population," *Journal of the American Geriatrics Society*, vol. 43, no. 2, pp. 130–137, 1995.

[10] S. Katz, T. D. Downs, H. R. Cash, and R. C. Grotz, "Progress in development of the index of ADL," *Gerontologist*, vol. 10, no. 1, pp. 20–30, 1970.

[11] M. P. Lawton and E. M. Brody, "Assessment of older people: self-maintaining and instrumental activities of daily living," *Gerontologist*, vol. 9, no. 3, pp. 179–186, 1969.

[12] M. S. Aapro, J. Bohlius, D. A. Cameron et al., "2010 update of EORTC guidelines for the use of granulocyte-colony stimulating factor to reduce the incidence of chemotherapy-induced febrile neutropenia in adult patients with lymphoproliferative disorders and solid tumours," *European Journal of Cancer*, vol. 47, no. 1, pp. 8–32, 2011.

[13] A. Heidenreich, S. Bracarda, M. Mason et al., "Tolerability of cabazitaxel in senior adults with metastatic castration-resistant prostate cancer (mCRPC) in Europe," in *Proceedings of the ESMO: Webcasts, Posters & Reports*, 2012.

[14] Z. Malik, G. di Lorenzo, S. Bracarda et al., "Cohort compassionate-use program (CUP) and early access program (EAP) with cabazitaxel (Cbz) plus prednisone (P, Cbz + P) in patients (pts) with metastatic castration-resistant prostate cancer (mCRPC) previously treated with docetaxel (D): analysis by age group," 109 General Poster Session A, (Board #G8), ASCO GU, 2014.

[15] P. F. Mulders, A. Molina, M. Marberger et al., "Efficacy and safety of abiraterone acetate in an elderly patient subgroup (aged 75 and older) with metastatic castration-resistant prostate cancer after docetaxel-based chemotherapy," *European Urology*, vol. 65, no. 5, pp. 875–83, 2013.

[16] C. N. Sternberg, J. S. de Bono, K. N. Chi et al., "Outcomes in elderly patients with metastatic castration-resistant prostate cancer (mCRPC) treated with the androgen receptor inhibitor enzalutamide: results from the phase III AFFIRM trial," in *Proceedings of the Genitourinary Cancer Symposium ASCO*, 2013.

[17] R. Iacovelli, A. Altavilla, G. Procopio et al., "Are post-docetaxel treatments effective in patients with castration-resistant prostate cancer and performance of 2? A meta-analysis of published trials," *Prostate Cancer and Prostatic Diseases*, vol. 16, no. 4, pp. 323–327, 2013.

[18] C. H. van Poznak, S. Temin, G. C. Yee et al., "American Society of Clinical Oncology executive summary of the clinical practice guideline update on the role of bone-modifying agents in metastatic breast cancer," *Journal of Clinical Oncology*, vol. 29, no. 9, pp. 1221–1227, 2011.

[19] R. E. Coleman, "Clinical features of metastatic bone disease and risk of skeletal morbidity," *Clinical Cancer Research*, vol. 12, pp. 6243s–6249s, 2006.

[20] P. W. Mantyh, "Cancer pain and its impact on diagnosis, survival and quality of life," *Nature Reviews Neuroscience*, vol. 7, no. 10, pp. 797–809, 2006.

[21] E. J. Small, D. F. Penson, and O. Sartor, "The relationship between symptomatology and treatment selection in metastatic

castrate-resistant prostate cancer," *Clinical Advances in Hematology and Oncology*, vol. 9, supplement 13, no. 7, pp. 1–15, 2011.

[22] W. K. Oh, S. Doctor, J. H. Godbold, M. D. Galsky, and C. K. Tsao, "Evolving patterns of metastatic disease in castration-resistant prostate cancer (CRPC) reported in clinical trials from 1990 to 2011," *Journal of Clinical Oncology*, vol. 31, supplement 6, abstract 195, 2013.

[23] O. B. Goodman, T. W. Flaig, A. Molina et al., "Exploratory analysis of the visceral disease (VD) patient subset in COU-AA-301, a phase III study of abiraterone acetate (AA) in metastatic castration-resistant prostate cancer (mCRPC)," *Journal of Clinical Oncology*, vol. 31, supplement 6, abstract 14, 2013.

[24] Y. Loriot, C. Massard, L. Albiges et al., "Personalizing treatment in patients with castrate-resistant prostate cancer: a study of predictive factors for endocrine therapies secondary activity," *Journal of Clinical Oncology*, vol. 30, supplement 5, abstract 213, 2012.

[25] D. Mukherji, C. Jo Pezaro, D. Bianchini, A. Zivi, and J. Sebastian de Bono, "Response to abiraterone acetate in the postchemotherapy setting in patients with castration-resistant prostate cancer whose disease progresses early on docetaxel," *Journal of Clinical Oncology*, vol. 30, supplement 5, abstract 17, 2012.

[26] E. S. Antonarakis, D. Keizman, M. A. Carducci, and M. A. Eisenberger, "The effect of PSA doubling time (PSADT) and Gleason score on the PSA at the time of initial metastasis in men with biochemical recurrence after prostatectomy," *Journal of Clinical Oncology*, vol. 29, supplement 7, abstract 16, 2011.

[27] A. Gomez de Liano Lista, Ó. Reig, B. Mellado et al., "Castrate-resistant prostate cancer (CRPC): prognostic and predictive value of testosterone levels in patients receiving chemotherapy," *Journal of Clinical Oncology*, vol. 31, abstract e16049, 2013.

[28] "EAU guidelines on prostate cancer," http://www.uroweb.org/.

[29] D. Azria, C. Massard, and D. Tosi, "An ambispective observational study in the safety and efficacy of abiraterone acetate in the French temporary authorizations for use (ATU): predictive parameters of response," *Journal of Clinical Oncology*, vol. 30, supplement 5, abstract 149, 2012.

[30] I. D. Schnadig, M. Bhor, and N. J. Vogelzang, "Sequencing of cabazitaxel and abiraterone acetate following docetaxel in metastatsic castration-resistant prostate cancer (mCRPC)," *Journal of Clinical Oncology*, vol. 31, supplement 6, abstract 79, 2013.

[31] G. Sonpavde, M. Bhor, D. Hennessy et al., " Outcomes with different sequence of cabazitaxel and abiraterone acetate following docetaxel in metastatic castration resistant prostate cancer," in *Proceedings of the European Society For Medical Oncology (ESMO '13)*, 2013, abstract 2905.

[32] A. Sella, T. Sella, A. Peer et al., "Activity of cabazitaxel following docetaxel and abiraterone acetate in patients with castration-resistant prostate cancer," *Journal of Clinical Oncology*, vol. 31, supplement 6, abstract 186, 2013.

[33] C. Jo Pezaro, S. le Moulec, L. Albiges et al., "Response to cabazitaxel in CRPC patients previously treated with docetaxel and abiraterone acetate," *Journal of Clinical Oncology*, vol. 31, supplement 6, abstract 155, 2013.

[34] J. Mezynski, C. Pezaro, D. Bianchini et al., "Antitumor activity of docetaxel following treatment with the CYP17A1 inhibitor abiraterone: clinical evidence for cross-resistance?" *Annals of Oncology*, vol. 23, no. 11, pp. 2943–2947, 2012.

[35] A. Angelergues, D. Maillet, A. Flechon et al., "Prognostic factors of survival in patients with metastatic castration resistant prostate cancer (mCRPC) treated with cabazitaxel: sequencing might matter," *Journal of Clinical Oncology*, vol. 31, supplement 6, abstract 5063, 2013.

[36] A. J. Schrader, M. Boegemann, C. H. Ohlmann et al., "Enzalutamide in castration-resistant prostate cancer patients progressing after docetaxel and abiraterone," *European Urology*, vol. 65, no. 1, pp. 30–36, 2014.

[37] D. Thomson, N. Charnley, and O. Parikh, "Enzalutamide after failure of docetaxel and abiraterone in metastatic castrate resistant prostate cancer (mCRPC): results from an expanded access program. 188 General Poster Session A," Board #L9), ASCO GU, 2014.

[38] A. Chopra, B. Haaland, and G. Lopes, "Comparative effective analysis between enzalutamide and abiraterone in the treatment of metastatic castration-resistant prostate cancer," *Journal of Clinical Oncology*, vol. 31, supplement 6, abstract 217, 2013.

[39] O. Caffo, G. Pappagallo, S. Brugnara et al., "Multiple rechallenges for castration-resistant prostate cancer patients responding to first-line docetaxel: assessment of clinical outcomes and predictive factors," *Urology*, vol. 79, no. 3, pp. 644–649, 2012.

Hindawi Publishing Corporation
BioMed Research International
Volume 2014, Article ID 135048, 12 pages
http://dx.doi.org/10.1155/2014/135048

Research Article

Antitumor Effects of Saffron-Derived Carotenoids in Prostate Cancer Cell Models

Claudio Festuccia,[1] Andrea Mancini,[1] Giovanni Luca Gravina,[1,2] Luca Scarsella,[1] Silvia Llorens,[3] Gonzalo L. Alonso,[4] Carla Tatone,[5] Ernesto Di Cesare,[6] Emmanuele A. Jannini,[7] Andrea Lenzi,[2] Anna M. D'Alessandro,[6] and Manuel Carmona[4,8]

[1] *Laboratory of Radiobiology, Department of Biotechnological and Applied Clinical Sciences, University of L'Aquila, 67100 L'Aquila, Italy*
[2] *Section of Medical Pathophysiology, Food Science and Endocrinology, Department of Experimental Medicine, University of Rome "La Sapienza", 00161 Rome, Italy*
[3] *Area of Physiology, Department of Medical Sciences, School of Medicine and Regional Centre for Biomedical Research (CRIB), University of Castilla-La Mancha, 02006 Albacete, Spain*
[4] *Cátedra Química Agricola, Universidad de Castilla-La Mancha, Avenida de España s/n., 02071 Albacete, Spain*
[5] *Department of Health Sciences, University of L'Aquila, 67100 L'Aquila, Italy*
[6] *Department of Biotechnological and Applied Clinical Sciences, Division of Radiotherapy, San Salvatore Hospital, University of L'Aquila, 67100 L'Aquila, Italy*
[7] *Department of Clinical and Applied Sciences and Biotechnologies, School of Sexology, University of L'Aquila, 67100 L'Aquila, Italy*
[8] *Albacete Science and Technology Park, Avenida de la Innovacion, 02006 Albacete, Spain*

Correspondence should be addressed to Claudio Festuccia; claudio.festuccia@univaq.it

Received 6 February 2014; Accepted 12 April 2014; Published 11 May 2014

Academic Editor: Andrea Maria Isidori

Crocus sativus L. extracts (saffron) are rich in carotenoids. Preclinical studies have shown that dietary intake of carotenoids has antitumor effects suggesting their potential preventive and/or therapeutic roles. We have recently reported that saffron (SE) and crocin (CR) exhibit anticancer activity by promoting cell cycle arrest in prostate cancer (PCa) cells. It has also been demonstrated that crocetin esters are produced after SE gastrointestinal digestion by CR hydrolysis. The aim of the present report was to investigate if SE, crocetin (CCT), and CR affected *in vivo* tumor growth of two aggressive PCa cell lines (PC3 and 22rv1) which were xenografted in male nude mice treated by oral gavage with SE, CR, and CCT. We demonstrated that the antitumor effects of CCT were higher when compared to CR and SE and treatments reverted the epithelial-mesenchymal transdifferentiation (EMT) as attested by the significant reduction of N-cadherin and beta-catenin expression and the increased expression of E-cadherin. Additionally, SE, CR, and CCT inhibited PCa cell invasion and migration through the downmodulation of metalloproteinase and urokinase expression/activity suggesting that these agents may affect metastatic processes. Our findings suggest that CR and CCT may be dietary phytochemicals with potential antitumor effects in biologically aggressive PCa cells.

1. Introduction

The need for anticancer drugs with high efficacy and low toxicity has led to studies evaluating putative antineoplastic factors in fruits, vegetables, herbs, and spices. Natural products are grouped into three main categories: phenylpropanoids, isoprenoids, and alkaloids, which are widely distributed in plant foods and medicinal herbs [1–3] and are crucial to human nutrition and health. Saffron, the dry stigmas of the plant *Crocus sativus* L., belongs to the Iridaceae family and is cultivated in Iran, Spain, Greece, and Italy [4–9]. This is widely known as a spice and its uses in traditional medicine are well established [10, 11]. Major constituents of saffron extracts (SE) belong to the category of carotenoids. The highly

water-soluble carotenoids, crocins, are responsible for the majority of its color and represent the major components of SE. The bitter taste of saffron is attributed to picrocrocin, a degradation product of the zeaxanthin carotenoid and also a monoterpene glycoside precursor of safranal. Safranal is an aromatic aldehyde that is the main component of plant volatile oil [12, 13]. Studies in animal models and with cultured human malignant cell lines have demonstrated antitumor and anticancer activities of SE [11, 14–19]. The mechanisms underlying cancer chemopreventive activities of SE include (i) inhibition of synthesis of DNA and RNA, but not protein [16]; (ii) ability to scavenge free radicals [20, 21]; (iii) involvement in the metabolic conversion of carotenoids to retinoids [22]; (iv) direct or indirect interactions with topoisomerase II [16]; (v) promotion of interactions mediated via lectins [23]; and (vi) downregulation of the expression of the catalytic subunit of the human telomerase, hTERT [24].

We have previously demonstrated that SE and CR possessed *in vitro* antiproliferative/cytostatic effects in prostate cancer cells [12] with low proapoptotic activity. Here, two aggressive prostate cancer cell lines, PC3 and 22rv1, were xenografted into nude mice and tumor-bearing animals were treated by oral gavage with saffron extract (300 mg/Kg/day), crocin (200 mg/Kg/day), and crocetin (30 mg/Kg/day) after the development of palpable tumors. The addition of CCT as an additional experimental group was due to the evidence that crocetin esters are produced after SE gastrointestinal CR hydrolysis [24, 25]. Interestingly, we observed that CCT showed the strongest antitumor effects when compared to CR and SE and this was in agreement with the data observed *in vitro*. The major potential mechanism that may explain the antitumor activity of SE and its components CR and CCT is the direct interference with topoisomerase II inducing DNA damage and apoptosis and the reversion of epithelial-mesenchymal transition (EMT), a critical event in the progression of cancer.

2. Material and Methods

2.1. Materials. All the materials for tissue culture were purchased from Hyclone (Cramlington, NE, USA). Plasticware was obtained from Nunc (Roskilde, Denmark). Antibodies were purchased from Santa Cruz (Santa Cruz, CA, USA) unless otherwise indicated.

2.2. Saffron Spice and Crocin Preparation. Saffron spice harvested from the Cooperativa Altopiano di Navelli company (Navelli, L'Aquila, Italy) during the 2011-2012 harvest was kindly provided by Agenzia per lo Sviluppo, Chamber of Commerce, L'Aquila, Italy [11]. Briefly, 1 g of dried and ground stigma was extracted with 20 mL of water or 85% (v/v) ethanol for 3 h in the dark. The extracts were filtered and concentrated under vacuum, and the extracts were kept at 4°C until use. Crocin was purified by the HPLC method. We used a Varian 9012 liquid chromatographic system equipped with a Varian 9050 UV detector (Walnut Creek, CA, USA). The separations were carried out on a Phenomenex Lichrosphere 5 RP C18 column (250 × 4.6 mm, 5 μm) (Torrance, CA, USA). The precolumn was a Phenomenex C18 column (30 × 4 mm). The detector was set at 442 nm with a spectral acquisition rate of 1.25 scans/s. For the mobile phase, solvent A (methanol) and solvent B (1% [v/v] aqueous acetic acid in water) were used. The mixing of the gradient solvent eluting system was as follows: initial 30% A and 70% B; 0–5 min, linear change to 40% A; 5–10 min, change to 55% A; 10–25 min, change to 68% A; 25–27 min, change to 90% A; 27–30 min, 90% A; 30–33 min, change to 30% A; 33–40 min, 30% A. The flow rate of the mobile phase was 0.8 mL/min, and the injection volume was 20 μL. All solutions were filtered through a 0.2 μm hydrophilic polypropylene membrane (Millipore, Richmond, USA) before use. Separation was accomplished at 25°C. Five different concentrations of crocin solutions were prepared to determine the calibration curve. The calibration curve was constructed with crocin content versus peak area ($y = 0.0002x + 1.0422$; $R^2 = 0.9993$; linear range: 0.01–0.2 mg/mL). The content of crocin in SE was calculated using the standard curve of crocin, and determinations were repeated three times.

2.3. Crocetin Preparation. Saffron spice samples were obtained from the Verdú Cantó Saffron Spain company (Novelda, Alicante, Spain) during the 2011-2012 harvest. The CCT isolation was performed by an internal protected method of the Verdú Cantó Saffron Spain company using the same saffron batch. Quality control of saffron spice was done by UV-vis spectrophotometry according to ISO 3632. Saffron spice aqueous extracts at 500 mg/L concentration were prepared with ultrahigh-purity water. They were magnetically stirred for 1 hour at room temperature in the dark and centrifuged at 4000 rpm for 5 min (Selecta, Barcelona, Spain). Their spectral characteristics were monitored by scanning from 190 to 700 nm using a Perkin-Elmer Lambda 25 spectrophotometer (Norwalk, CT, USA) with UV WinLab 2.85.04 software (Perkin-Elmer) and their coloring strengths ($E^{1\%}_{1\,cm}$ 440 nm, $E^{1\%}_{1\,cm}$ 257 nm, and $E^{1\%}_{1\,cm}$ 330 nm) were determined. Samples of saffron spice and CCT were analyzed by the reverse-phase HPLC technique. Twenty μL of aqueous extracts of saffron spice (500 mg/L) and CCT aqueous solutions (252 mg/L) was filtered through a 0.45 μm PTFE filter and injected into an Agilent 1200 chromatograph (Palo Alto, CA) operating with a 150 mm × 4.6 mm i.d., 5 μm Phenomenex (Le PecqCedex, France) Luna C18 chromatographic column, at 30°C. Eluents were water (A) and acetonitrile (B) with the following elution gradient: 20% B, 0–5 min; 20–80% B, 5–15 min; 80% B, 15–18 min; 20% B, 18–30 min. The flow rate was 0.8 mL min^{-1} and the DAD detector (Hewlett Packard, Waldbronn, Germany) was set at 440 nm for the detection of crocetin esters in saffron spice samples and cis/trans CCT in the samples of CCT isolated from saffron spice [25]. Crocetin esters quantification was estimated using the method based on the extinction coefficient and the related area calculated according to [26, 27].

2.4. Cell Cultures. PC3 [28] and 22rv1 [29] cells were obtained from ATCC and DSMZ cell bank, respectively. Cells were seeded at a density of 2×10^4 cells/mL in 24-well plates.

Cells were left to attach and grow in 5% FCS DMEM for 24 h. After this time, cells were maintained in the appropriate culture conditions. Morphological controls were performed every day with an inverted phase-contrast photomicroscope (Nikon Diaphot, Tokyo, Japan) before cell trypsinization and counting. Cells were trypsinized and resuspended in 1.0 mL of saline and counted using the NucleoCounter NC-100 (Chemotec, Cydevang, DK) as previously described [30]. NucleoCounter NC-100 also allows determination of the number of dead cells present in a cell sample and, therefore, we considered viable and dead cells to be separated entities. All experiments were conducted in triplicate. IC50 values were calculated by the GraFit method (Erithacus Software Limited, Staines, UK). The effect on cell proliferation was measured by taking the mean cell number with respect to controls over time for the different treatment groups. As a second method for determining the cytotoxicity of PCa cells, we used the crystal violet assay. They were allowed to attach overnight before treatments as described above. After washing with PBS, the cells were incubated and were slightly shaken at RT with 50 μL staining solution (0.5% crystal violet, 20% methanol) that stains DNA. The plate was washed twice with dH_2O and dried completely. The taken-up crystal violet was solubilized by addition of 200 μL of methanol and 15 min incubation on a shaker. Finally, the amount of dye taken up by the monolayer was quantified by measuring the absorbance at 570 nm in a microplate reader. All studies were performed in triplicate and independently repeated three times.

2.5. Mouse Fibroblast NI3T3-Conditioned Medium. Mouse NIH3T3 fibroblast (ATCC) were incubated at 37°C in a humidified atmosphere of 95% air 5% CO_2 with medium changes every 2 days. For collection of conditioned medium, subconfluent cell cultures were replaced with serum-free medium and left for additional 24 hr at 37°C. Next, medium was collected, centrifuged to eliminated cell debris, and stored at −20°C until use.

2.6. Migration and Invasion Assay. Cell migration and invasion assays were performed after appropriate treatments using Boyden chambers containing 8 μm PVPF polycarbonate filters (Nucleopore, Concorezzo, Milan, Italy) coated on one side with 10 μg/mL type I collagen or 25 μg/mL of Matrigel (Becton Dickinson Italia, Milan, Italy), respectively. Tests were performed as previously described [31].

2.7. Protease Expression. The expression and activation of gelatinase A (pro-MMP-2) and gelatinase B (pro-MMP-9) were analyzed by zymography performed using SDS-polyacrylamide gel copolymerized with 0.1 mg/mL gelatin [32]. For plasminogen activator analysis, gels were performed by copolymerizing SDS-polyacrylamide with 0.1 mg/mL of lactose-free casein and 15 mg/mL of human plasminogen B as previously described [32]. Routinely, conditioned media were obtained in cultures grown on 24-well plates coated with different substrates. After adhesion, cells were washed with PBS and incubated for different times according to experimental protocols. Following incubation, culture supernatants were collected, centrifuged at top speed in an Eppendorf Microcentrifuge (Hamburg, Germany) for 5 min to remove cell debris, and stored at −80°C until being assayed. Corresponding monolayers were trypsinized and the cells counted in a Neubauer chamber (Hausser, Blue Bell, PA, USA) to normalize the gelatinase activity of the conditioned media.

2.8. Western Blotting. Conditioned media from treated and untreated cells were electrophoresed under reducing conditions and transferred to nitrocellulose filter (Schleicher and Schuell GmbH, Dassel, Germany). Nonspecific binding sites were blocked for 1 h in 5% nonfat dried milk in a Tris buffer containing 20 mM Tris and 137 mM NaCl (pH 7.6). Blots were incubated with 1 μg/mL of primary antibody diluted in blocking solution for 1 h at room temperature, before being washed and then incubated for 1 h in secondary antibody diluted in blocking solution according to the manufacturer's protocol. Following a further wash, reactive bands were visualized by chemiluminescent detection (Supersignal, Perbio Science, Tattenhall, UK) using a Bio-Rad gel DocTM (Bio-Rad Laboratories S.r.l., Milan, Italy).

2.9. Animals and Therapeutic Regimes. Male CD1 athymic nude mice (Charles River, Calco, Milan, Italy) were maintained under the guidelines established by our institution (University of L'Aquila, Medical School and Science and Technology School Board Regulations, in compliance with the Italian government regulation number 116 on January 27, 1992 for the use of laboratory animals) as previously described [33]. Before any invasive manipulation, mice were anesthetized with a mixture of ketamine (25 mg/mL) and xylazine (5 mg/mL). PC3 or 22rv1 cells (1×10^6 cells/mouse) mixed with Matrigel (Becton Dickinson Labware, Bedford, MA, USA) were injected subcutaneously (s.c.) into the right hind limb of nude mice. At about 10 days after the tumor injection, 48 mice with tumor volume of 0.5–0.8 cm^3 were retained and randomly divided into four groups (8 mice per group): (1) control; (2) saffron extract (300 mg/kg administered po 5 days/week); (3) crocin (200 mg/kg administered po 5 days/week); (4) crocetin (100 mg/kg administered po 5 days/week).

2.10. Evaluation of In Vivo Treatment Response. The effects on tumor growth of different treatments were evaluated measuring the following: (1) tumor volume measured during and at the end of the experiment. Tumor volume was assessed by twice a week measurements of tumor diameters with a vernier caliper (length × width). The volume of the tumor was expressed in mm^3 according to the formula $4/3\pi r^3$; (2) weight measured at the end of experiment; (3) complete response (CR) defined as the disappearance of a measurable lesion; (4) partial response (PR) defined as a reduction of greater than 50% of tumor volume; (5) stable disease (SD) defined as a reduction of less than 50% or an increase of less than 50% of tumor volume; (6) tumor progression (TP) defined as an increase of greater than 50% of tumor volume; and (7) time to progression (TTP). Tumor growth delay (TGD) was determined as $\%TGD = ((T \times C)/C) \times 100$, where

T and C are the mean times in days required to reach the same fixed tumor volume in the treated group and control group, respectively [34].

2.11. In Vivo Toxicity. Serial bodyweight measurements were performed every 3-4 days during treatment. Changes in bodyweight were compared using the control groups and the three treatment groups in each xenograft model.

2.12. Manipulation of Tumor Tissue Samples. Animals were euthanized by CO_2 inhalation and tumors were subsequently removed surgically. Half of the tumor was directly frozen in liquid nitrogen for protein analysis and the other half was fixed in paraformaldehyde overnight for immunohistochemical analyses. Indirect immunoperoxidase staining of tumor xenograft samples was performed on paraffin-embedded tissue sections (4 μm). Briefly, sections were incubated with primary antibodies overnight at 4°C. Next, avidin-biotin assays were done using the Vectastain Elite kit obtained from Vector Laboratories. Mayer's hematoxylin was used as a nuclear counterstain. Negative controls were incubated only with universal negative-control antibodies under identical conditions, processed and mounted. Images of the stained blood vessels were taken using a Leitz photomicroscope. For immunohistochemical analyses we used the following antibodies: monoclonal mouse anti-human E-cadherin, clone NCH-38; monoclonal mouse anti-human N-cadherin, clone 6G11; monoclonal mouse anti-human cytokeratin, clone AE1/AE3; monoclonal mouse anti-human beta-catenin, clone β-catenin-1; monoclonal mouse anti-vimentin, clone V9; monoclonal mouse anti-human Ki-67 antigen, clone MIB-1; monoclonal mouse anti-human Ki-67 antigen, clone MIB-1 (Dako Italia, Cernusco sul Naviglio, MI); mouse CD31 (PECAM-1) antibody (Dianova GmbH, Hamburg, Germany); and APO-BrdU TUNEL Assay Kit, (Invitrogen Ltd., Paisley, UK).

2.13. Martius Yellow-Brilliant Crystal Scarlet Blue Technique. Stains for these techniques were purchased from HD Supplies (Aylesbury, UK). This technique was used to analyze the presence of red cells dispersed in tumor tissue and present in blood vessels as well as to better evaluate the presence of microthrombi and bleeding zones. Martius yellow, a small-molecule dye together with phosphotungstic acid in alcoholic solution stains red cells. Early fibrin deposits may be colored, but the phosphotungstic acid blocks the staining of muscle, collagen, and connective tissue fibers. Brilliant crystal scarlet, a medium-sized molecule, stains muscle and mature fibrin. Phosphotungstic acid removes any red stain from the collagen. The large-molecule dye aniline blue stains the collagen and old fibrin.

2.14. Statistics. Continuous variables were summarized as mean and standard deviation or as median and 95% CI for the median. For continuous variables, statistical comparisons between control and treated groups were established by carrying out the Kruskal-Wallis test. When the Kruskal-Wallis test revealed a statistical difference, pairwise comparisons were made by the Dwass-Steel-Chritchlow-Fligner method and the probability of each presumed "nondifference" was indicated. Dichotomous variables are summarized by absolute and/or relative frequencies. For dichotomous variables, statistical comparisons between control and treated groups were established by carrying out the exact Fisher's test. For multiple comparisons, the level of significance was corrected by multiplying the P value by the number of comparisons performed (n) according to the Bonferroni correction. TTP was analyzed by Kaplan-Meier curves and Gehan's generalized Wilcoxon test. When more than two survival curves were compared, the log-rank test for trend was used. This tests the probability that there is a trend in survival scores across the groups. All tests were two-sided and were determined by Monte Carlo significance. P values <0.05 were considered statistically significant. SPSS (statistical analysis software package) version 10.0 and StatDirect (version. 2.3.3, StatDirect Ltd.) were used for statistical analysis and graphic presentation.

3. Results

3.1. Effect of SE, CCT, and CR on Tumor Growth in Athymic Nude Mice. Tumors were measured twice per week. We observed that SE, CR, and CCT reduced tumor growth in both PC3 and 22rv1 (Figures 1 and 2) xenografts confirming our previous *in vitro* data [12]. In the PC3 *in vivo* model, the tumor mass (Figures 1(a)–1(c) and Table 1) was, respectively, reduced by 18% ($P > 0.05$), 38% ($P < 0.05$), and 75% ($P < 0.001$) after SE, CR, and CCT treatment with respect to controls. The comparative effect of treatment with extract (SE) versus crocin (CR) in terms of tumor growth did not reach statistical significance ($P > 0.05$) whereas crocetin (CCT) significantly affected tumor growth with respect to SE and CR ($P < 0.001$). TTP probability, as determined by Kaplan-Meier analyses, showed a delay of tumor progression with respect to control in all treatments except for SE (Figures 1(c)–1(e)). The analysis of hazard ratio (HR) values indicated that CR- and CCT-based treatments significantly improved the probability of delaying the tumor progression (Figure 1(d)), with the best performance observed for CCT. This evidence paralleled with data of panel E in which CR- and CCT-based treatments significantly increased the median time necessary to tumor progression. SE treatment significantly delayed the occurrence of tumor progression although to a lesser extent with respect to CR and CCT.

In the 22rv1 *in vivo* model, the tumor mass (Figures 2(a)–2(c) and Table 2) was, respectively, reduced by 33% ($P < 0.05$), 35% ($P < 0.05$), and 80% ($P < 0.001$) after SE, CR, and CCT treatment with respect to controls (Figure 2(b)). Therefore, when the two xenograft models were compared in terms of tumor growth reduction, all treatments were more effective in the 22rv1 tumor model. TTP probability, as determined by Kaplan-Meier analyses, showed a delay of tumor progression with respect to control in all treatments except for SE (Figures 2(c)–2(e)). The analysis of hazard ratio (HR) values indicated that CR- and CCT-based treatments significantly improved the probability

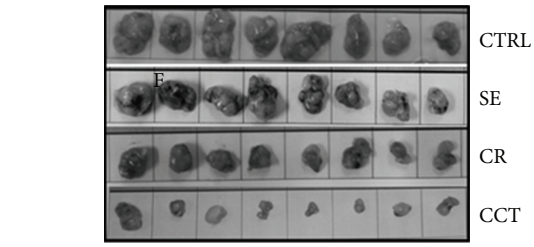

(a)

Comparisons	Hazard ratio	95% CI	Statistics
SE versus CTRL	1.9978	0.6031 to 6.6176	$P = 0.2574$ (NS)
CR versus CTRL	7.3321	2.0369 to 26.3926	$P = 0.0023$
CCT versus CTRL	16.7583	4.3901 to 63.9710	$P < 0.0001$
CR versus SE	5.5498	1.4995 to 20.5399	$P = 0.0103$
CCT versus SE	15.1028	3.9262 to 58.0951	$P = 0.0001$
CCT versus CR	13.7955	3.56791 to 53.3230	$P = 0.0001$

(d)

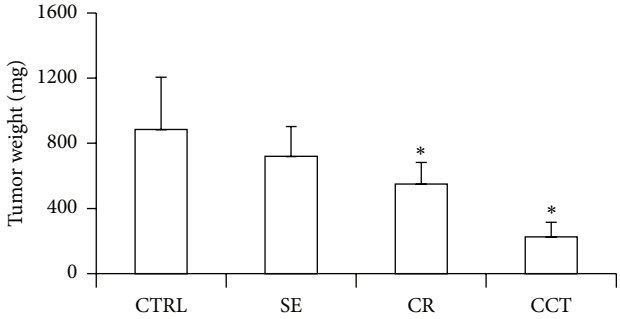

(b)

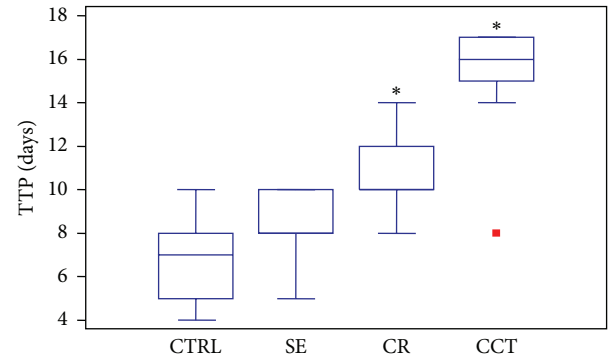

(e)

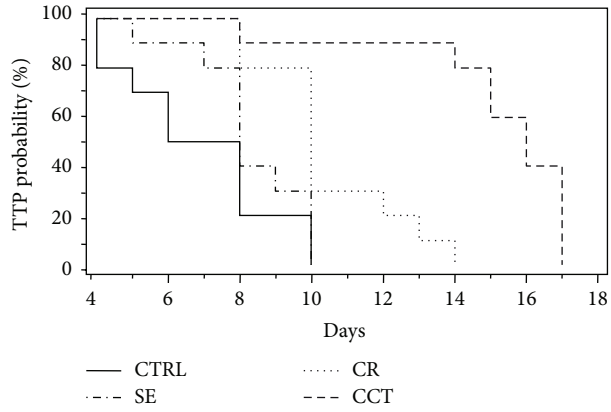

(c)

Figure 1: *In vivo* experiments using PC3-bearing male nude mice treated with saffron extract (SE, 300 mg/kg administered po 5 days/week), crocin (CR, 200 mg/kg administered po 5 days/week), and crocetin (CCT, 100 mg/kg administered po 5 days/week) administered by oral gavage when tumors reached 0.5–0.8 cm^3. After 30 days of treatment, animals were sacrificed and tumors harvested, weighed, and analyzed. Experiments were performed using 8 animals/group and were stopped at the indicated times. (a) Macroscopic appearance of PC3 tumors subjected to different treatments. (b) Tumor weight comparisons at the end of experiments. CR and CCT induced a significant reduction of tumor weight in the PC3 xenografts whereas SE resulted in only a 20% reduction. (c) Time to progression (TTP) probability determined by Kaplan-Meier analysis in PC3 xenografts. (d) Hazard ratio value with 95% CI and *P* values determined according to different treatments. (e) Comparisons of TTP expressed in days after treatments.

of delaying the tumor progression (Figure 2(d)), with the best performance observed for CCT. This evidence paralleled with data of panel E in which CR- and CCT-based treatments significantly increased the median time necessary to tumor progression (Figure 2(e)). SE treatment significantly delayed the occurrence of tumor progression although to a lesser extent with respect to CR and CCT (Figures 2(c)–2(e)).

Upon SE, CR, and CCT treatment (Table 1), the proliferation index (PI) of the PC3 tumor model, assessed by Ki67, was lower by 16% ($P > 0.05$), 30% ($P < 0.01$), and 59% ($P < 0.001$) with respect to controls. SE, CR, and CCT treatment (Table 2) decreased the percentage of Ki67 by 15% ($P > 0.05$), 27% ($P < 0.05$), and 60% ($P < 0.001$) with respect to control.

SE, CR, and CCT treatments (Table 1) decreased the vessel count (CD31-positive endothelial cells) by 2% ($P > 0.05$), 12% ($P > 0.05$), and 30% ($P < 0.01$) with respect to control, while in the 22rv1 tumor model the vessel count was reduced by 18% ($P > 0.05$), 29% ($P < 0.05$), and 44% ($P < 0.001$) (Table 2). Apoptosis, as assessed by TUNEL assay, significantly increased after CCT treatment ($P < 0.001$) in

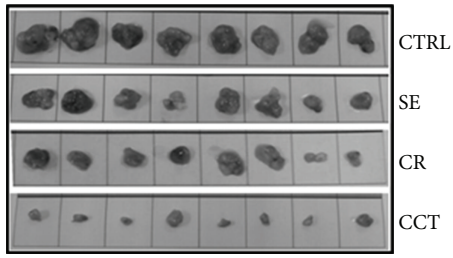

(a)

Comparisons	Hazard ratio	95% CI	Statistics
SE versus CTRL	8.9027	2.5539 to 31.0339	$P = 0.0006$
CR versus CTRL	23.9969	6.0361 to 95.4013	$P < 0.0001$
CCT versus CTRL	28.0011	6.8818 to 113.9327	$P < 0.0001$
CR versus SE	23.4146	5.8800 to 93.2382	$P < 0.0001$
CCT versus SE	29.4487	6.9445 to 110.944	$P < 0.0001$
CCT versus CR	14.1386	3.6635 to 54.4907	$P = 0.0001$

(d)

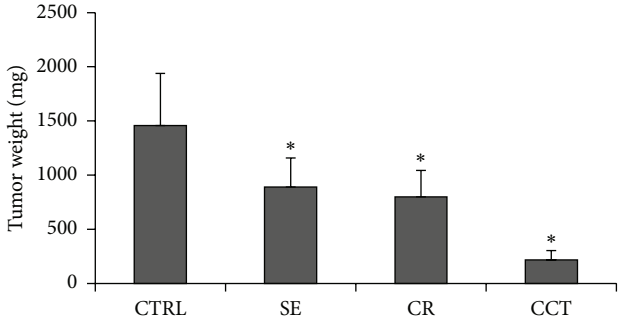

(b)

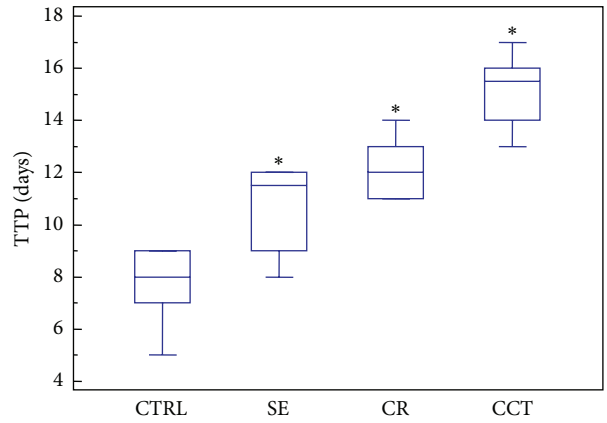

(e)

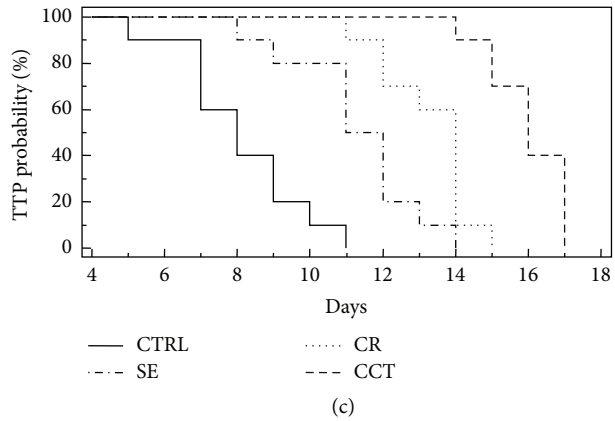

(c)

Figure 2: *In vivo* experiments using PC3-bearing male nude mice treated with saffron extract (SE, 300 mg/kg administered po 5 days/week), crocin (CR, 200 mg/kg administered po 5 days/week), and crocetin (CCT, 100 mg/kg administered po 5 days/week) administered by oral gavage when tumors reached 0.5–0.8 cm^3. After 30 days of treatment, animals were sacrificed and tumors harvested, weighed, and analyzed. Experiments were performed using 8 animals/group and were stopped at the indicated times. (a) Macroscopic appearance of PC3 tumors subjected to different treatments. (b) Tumor weight comparisons at the end of experiments. CR and CCT induced a significant reduction of tumor weight in the PC3 xenografts whereas SE resulted in only a 20% reduction. (c) Time to progression (TTP) probability determined by Kaplan-Meier analysis in PC3 xenografts. (d) Hazard ratio value with 95% CI and *P* values determined according to different treatments. (e) Comparisons of TTP expressed in days after treatments.

both tumor models while the SE and CR treatments did not significantly affect apoptosis (Tables 1 and 2).

Histochemical staining with hematoxylin/eosin, Masson trichrome, and Martius yellow-brillant crystal scarlet blue were used to analyze potential morphological changes treatments induced by treatments. Dense blue-stained collagen I deposits, suggestive of fibrosis, enveloped tumor cell nests in peripheral areas whereas PCa cells were arranged to form large cell masses surrounded by red-stained dilated blood vessels. Blue-stained collagen strands followed tumor cell growth but entrapped tumor nests in treated cells often in areas in which necrosis was also present. These behaviors were more evident in tissue sections derived from xenografts harvested from mice treated with CR and CCT. In these

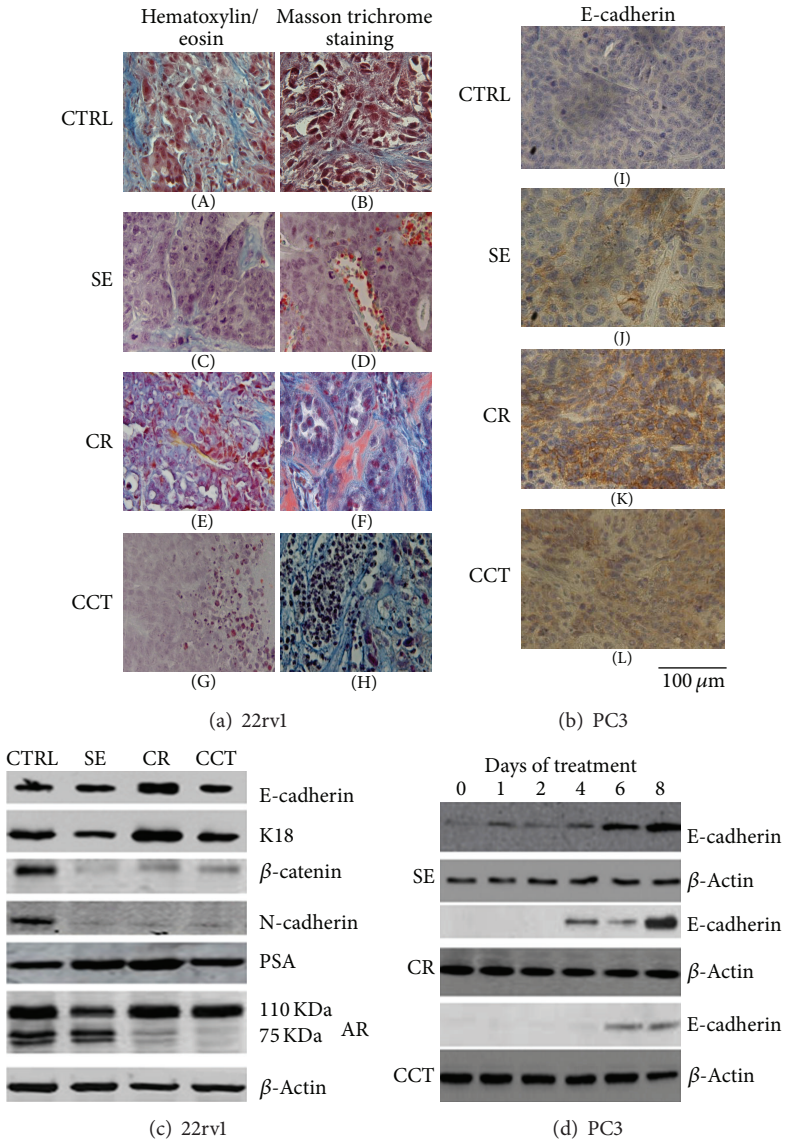

Figure 3: (a) Hematoxylin/eosin (A, C, E, G) and Masson trichrome (B, D, F, H) staining of 22rv1 tumors treated with SE (C, D), CR (E, F), and CCT (G, H). Untreated 22rv1 tumors show tumor cell nests enveloped by dense blue-stained collagen deposits that are abundant in the peripheral areas (A). Tumor cell nests show their undifferentiated characteristics (B). SE seem to induce a differentiated phenotype with large tumor cells and prominent nuclei organizing in structures similar to glands (C, D). Vessels (D) appear dilated with unstructured capillary bed dispersed in collagen I deposits (azure staining). The differentiated appearance was greater after CR treatment (E, F) with smaller blood pervious vessels that follow the fibrous strands of collagen and surrounding the pseudoglandular acini (E). CR treatment induces deposition of fibrin clots (pale pink/orange staining) dispersed in dense collagen I deposits (fibrosis), enveloping tumor cell nests, as evolution of massive blood pouring. This appearance was not associated with presence of thrombotic vessels. CCT treatments (G, H) show a histological structure poorly differentiated (G) and rich in necrotic areas with the presence of numerous phagocytes (neutrophils and monocytes) dispensed in collagen I deposit resulting from a colliquative necrosis. Scale bar is 100 μm. (b) Immunohistochemical evaluation of E-cadherin in PC3 xenografts (I, J, K, L) treated or not with SE (J), CR (K), or CCT (L). Indirect immunoperoxidase staining of tumor xenograft samples was performed on paraffin-embedded tissue sections (4 μm). It is opportune to note the strong E-cadherin staining after SE and CR treatments whereas controls (CTRL) tissues were negative and CCT showed low levels of this antigen. Scale bar is 100 μm. (c) Western blotting performed on 22rv1 cell extracts derived from cultures treated for 8 days with SE (0.4 mg/mL), CR (0.4 mM), and CCT (0.1 mM). EMT markers (vimentin, β-catenin, and N-cadherin) were significantly reduced whereas epithelial markers (E-cadherin, K18, and PSA) were upregulated in 22rv1 cells. Interestingly, the expression levels of the truncated form (ligand-independent) of AR were significantly reduced after CR and CCT treatments whereas no changes were showed for full-length AR levels. (d) Densitometric analysis performed on E-cadherin and K18 expression in PC3 and 22rv1 cells treated with SE, CR, and CCT. (d) Time-dependent modulation of E-cadherin after treatments with SE (0.4 mg/mL), CR (0.4 mM), and CCT (0.1 mM) in the PC3 cell model (an *in vitro* assay). Western blots are representative of three different analyses.

Table 1: Antitumor activity of SE, CR, and CCT in PC3 xenografts.

Drug	Dose mg/Kg	Tumors	Weight of mice mean ± SD	Tumor weight (mg ± SD)	PI (ki67 %) mean ± SD	Apoptosis mean ± SD	Vessels mean ± SD
Saline		8	24.0 ± 2.1	885 ± 321	37.3 ± 4.5	<2	30.0 ± 5.5
SE	300	8	26.1 ± 2.0	720 ± 183	31.4 ± 2.7	<2	29.4 ± 2.0
% versus baseline				18.0%	16%		2%
CR	200	8	23.0 ± 1.7	550 ± 132	26.0 ± 3.0	<2	26.4 ± 1.5
% versus baseline				38.0%	30%		12%
CCT	100	8	19.3 ± 1.5	225 ± 91	15.2 ± 1.2	24.0 ± 3.0	18.3 ± 2.5
% versus baseline				75.0%	59%		30%

Apoptosis was measured as the percentage of tunel positive cells ± SD mesured on five random fields (100X); tumor microvessels were counted in five arbitrary selected fields/tumor and the data are presented as number of CD31+ microvessels/microscopic field for each group (100X). Proliferation index (PI) was determined as percentage by counting on 500 cells at 100X the number of Ki67 stained cells.

Table 2: Antitumor activity of SE, CR, and CCT in 22rv1 xenografts.

Drug	Dose mg/Kg	Tumors	Weight of mice mean ± SD	Tumor weight (mg ± SD)	PI (ki67 %) mean ± SD	Apoptosis mean ± SD	Vessels mean ± SD
Saline		8	24.3 ± 1.8	1458 ± 481	45.5 ± 6.5	<2	32.7 ± 4.3
SE	300	8	26.1 ± 2.0	890 ± 267	38.7 ± 2.7	<2	26.2 ± 2.7
% versus baseline				39.0%	15%		18%
CR	200	8	23.0 ± 1.7	800 ± 244	32.2 ± 3.3	5.2 ± 2.7	23.2 ± 4.5
% versus baseline				45.1%	27%		29%
CCT	100	8	19.3 ± 1.5	217 ± 85	18.2 ± 1.4	21.5 ± 3.2	18.3 ± 2.5
% versus baseline				85.1%	60%		44%

Apoptosis was measured as the percentage of tunel positive cells ± SD mesured on five random fields (100X); tumor microvessels were counted in five arbitrary selected fields/tumor and the data are presented as number of CD31+ microvessels/microscopic field for each group (100X). Proliferation index (PI) was determined as percentage by counting on 500 cells at 100X the number of Ki67 stained cells.

mice, xenograft tumors had massive fibrosis and orange-stained fibrin strands, which appeared right where there were residues of blood vessels or blood pouring. In Figure 3(a), we show representative microscopic fields demonstrating histological effects of SE, CR, and CCT treatments in 22rv1 tumors.

3.2. Differentiation Effects of SE and Crocin. An important aspect of treatment with carotenoids is the potential for prodifferentiating effects. Literature data suggest that epithelial tumor cell aggressiveness is characterized by epithelial-mesenchymal transdifferentiation (EMT) with aggressive cancers characterized by loss of cell-cell adhesion, repression of E-cadherin and cytokeratin 18 (K18), and increased cell mobility. The major markers for EMT are N-cadherin and β-catenin. We analyzed the expression of these antigens by immunohistochemistry in tissues slides harvested from the mice bearing tumor xenografts and treated or untreated with SE, CR, and CCT. These *in vivo* data were coupled with *in vitro* experiments performed on the same tumor cells in the presence of the same treatments. We observed that SE and CR strongly induced E-cadherin and K18 expression with reduced expression of vimentin, N-cadherin, and β-catenin. In Figure 3(b), we show a representative staining of E-cadherin in PC3 xenografts upon SE, CR, or CCT treatment. K18 staining had a similar trend whereas vimentin, N-cadherin, and β-catenin expression was inverted with high levels in untreated tumors and low or absent expression in treated tumors (data not shown). To directly test the prodifferentiating effects of SE, CR, and CCT, an *in vitro* assessment of EMT markers was performed by using both 22rv1 and PC3 tumor models. Cells were treated with SE (0.4 mg/mL), CR (0.4 mM), and CCT (0.1 mM). After prolonged treatment with these pharmacological agents, a differentiated phenotype was observed in both cellular models. In Figure 3(c), we demonstrate that E-cadherin and K18, two well-known epithelial markers, were significantly increased after CR treatment whereas changes in the extent of these markers were lower after SE. In Figure 3(d), we show the results of densitometric analysis performed on E-cadherin and K18 expression in PC3 and 22rv1 cells treated with SE, CR and CCT. These effects were lower in PC3 cells when compared to those observed in 22rv1 cells. Western blots performed on PC3 cell extracts demonstrate that treatments induced E-cadherin expression in a time-dependent manner. Our results suggests that the induction of a differentiated phenotype may concur in inducing the antitumor properties especially after CCT treatment. The EMT was also investigated by analyzing

the expression of vimentin, K18, N-cadherin, β-catenin, prostate specific antigen (PSA), and androgen receptor (AR) after 8 days of treatment with SE, CT, and CCT treatments. Mesenchymal markers (β-catenin and N-cadherin) changes were of opposite tendency with marked reduced expression upon all treatments. The analyses of markers historically considered to be associated with more differentiated PCa (PSA and AR) showed that SE and CR upmodulated PSA whereas the expression levels of the ligand-independent truncated AR form were significantly reduced after CR and CCT treatment. No changes in the full length AR form were found after SE, CR, and CCT treatments.

3.3. Saffron Extract and Its Components Inhibit Cell Invasion through Modulation of Metalloproteinases and Urokinase Expression/Activity. An important aspect of EMT is acquisition of higher migration and invasion capacities of tumor cells coupled with increased expression of proteolytic enzymes of the extracellular matrix (ECM) such as gelatinases A and B, MMP-9, MMP-2, and urokinase-type plasminogen activator (uPA). Therefore, in order to reinforce the concept that saffron-derived compounds maintain a differentiated state of prostate cancer cells, we analyzed the immunohistochemistry expression of proteases involved in the migratory and invasive properties of PCa. PC3 and 22rv1 xenografts were studied after SE (0.4 mg/mL), CR (0.4 mM), and CCT (0.1 mM) treatment. In parallel, we verified the *in vitro* secretion of these metalloproteinases upon the same treatments. Basally, PC3 tumor xenografts are strongly positive for MMP-9, MMP-2, and uPA. Immunohistochemical analyses revealed that MMP-9, MMP-2, and uPA expression levels were markedly reduced after all treatments in both *in vivo* tumor models. In Figure 4(a), we show a representative immunohistochemistry performed on a PC3 xenograft. As for the experiments performed to detect EMT/epithelial marker changes, *in vitro* experiments on PC3 cells were performed by treating these cells for 8 days with SE (0.4 mg/mL), CR (0.4 mM), and CCT (0.1 mM). In order to collect conditioned medium on which we tested metalloproteinase and urokinase activities, cell cultures were allowed to grow in complete medium for 6 days in presence of SE, CR, and CCT. Next, medium was changed and serum-free medium containing SE, CR, and CCT was added for additional 24–48 hr. In Figure 4(b), we show that the active isoforms of MMP-9, MMP-2, the 80 kDa tissue-derived plasminogen activator (tPA), and uPA (47–52 kDa plasminogen activator isoforms) were markedly reduced after treatments. For migration/invasion tests (panels C, D) cells were cultured for 8 days in complete medium, then harvested by trypsinization, and used for the tests.

Interestingly, SE and CR significantly reduced the migratory and invasive properties of PC3 and 22rv1 tumor cells (Figures 4(c)-4(d)). No significant changes were found in either model when tumor cells were treated with CCT (Figures 4(c)-4(d)). These findings fit with the data concerning the protease expression suggesting that SE and CR significantly decrease some key aspects of the metastatic processes.

4. Discussion

Prostate cancer continues to be a leading cause of cancer death in European males [35]. Patients with localized prostate cancer possess a favorable 5-year survival rate, whereas patients with metastatic cancer have a median survival of only 12–15 months, which is an indication that PCa cell metastasis is the primary mediator of mortality for this disease [36]. A variety of therapeutic strategies are utilized for the treatment of advanced metastatic PCa [37]. However, despite advances in the understanding of PCa biology, these therapies rarely produce significant increases in survival time in metastatic PCa. Natural products have long been used to prevent and treat diseases including cancers and might be good candidates for the development of anticancer drugs. Many herbs and spices are the subject of scientific investigations related to antioxidant properties and health. Saffron, a commonly used spice and food additive, is known for its anticancer and antitumor properties [12–16, 38]. CR and CCT, two carotenoid compounds derived from saffron, have shown a significant inhibitory effect on the growth of cancer cells [4, 7, 11, 14, 38, 39].

Many mechanisms of action have been identified or supposed. Different hypotheses for antitumor effects of saffron and its ingredients have been proposed including (a) inhibition of DNA and RNA synthesis, but not protein [40]; (b) ability to scavenge free radicals [24]; (c) involvement in the metabolic conversion of carotenoids to retinoids [41]; (d) mediation of interactions of carotenoids with topoisomerase II (an enzyme involved in cellular DNA-protein interaction) [41]; and (e) downregulation of the expression of the catalytic subunit of the human telomerase (hTERT) [42].

Here, we demonstrate that, although different phytochemicals in saffron extracts could have additive and synergistic effects enhancing its anticarcinogenic properties [39], only CR and CCT showed higher antitumor effects with respect to SE. The *in vivo* effects of these compounds were evident in *in vivo* models. SE, CR, and CCT inhibited tumor cell proliferation of aggressive models of PCa as shown by the reduced proliferating cell nuclear antigens, mitotic figure counts, tumor vessels, and tumor growth rate and increased apoptosis especially in the CCT-treated animal group. CCT showed the strongest antitumor effects since it resulted in a tumor weight reduction of 75% and 85% in PC3 and 22rv1 xenografts, with respect to control while CR and SE resulted in tumor weight reduction of 38% and 18%, and 54% and 39%, in PC3 and 22rv1 xenografts Additionally, CCT tumor xenografts had a reduction of 50% and 69% of proliferating index (PI) in PC3 and 22rv1 xenografts, while CR and SE decreased PI by 30% and 16% and 27 and 15%, respectively The induction of apoptosis and the decrease of the vessel count were once again mainly affected by CCT. The changes in biologically relevant markers were parallel with the increase in the time to progression as shown by the data concerning the time trend of tumor growth. Conversely, SE and CR induced stronger epithelial differentiation with increased E-cadherin and K18 expression levels and a decrease in EMT markers such as N-cadherin, β-catenin, and vimentin.

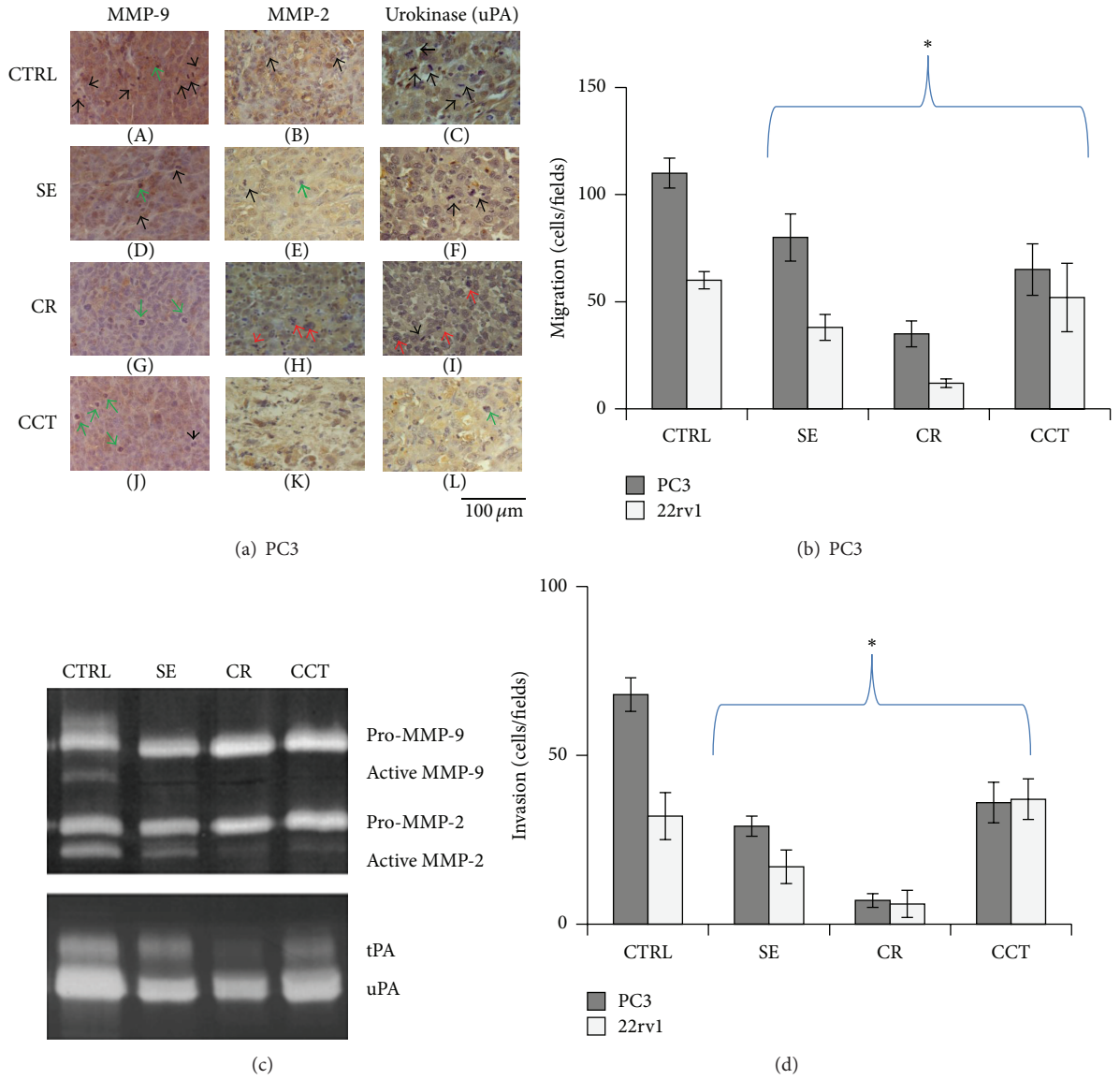

Figure 4: (a) Immunostaining for MMP-9 (A, D, G, J), MMP-2 (B, E, H, K), and uPA (C, F, I, L) performed in PC3 tumors treated or not with SE (D, E, F), CR (G, H, I), and CCT (J, K, L). Untreated PC3 tumors (A, B, C) show high expression of MMP-9, MMP2, and uPA. Indirect immunoperoxidase staining of tumor xenograft samples was performed on paraffin-embedded tissue sections (4 μm). SE, CR, and CCT significantly reduced the expression of these proteases. Black arrows show mitotic figures (mean 16 ± 4 mitotic figures/100x microscopic field), which are high in CTR and were reduced after SE (about 40% versus CTRL), CR (70% versus CTRL) or CCT (90% versus CTRL). Green arrows show condensed/pyknotic nuclei. This appearance is evident in SE- (1–4 pyknotic nuclei/100x microscopic field), CR- (2–8 pyknotic nuclei/100x microscopic field), or CCT-treated tumor bearing mice (>10 pyknotic nuclei/100x microscopic field). Red arrows show aberrant mitosis, which is more evident in CCT-treated tumors. Scale bar is 100 μm. (b) Zymography for gelatinases, (a) and (b), and plasminogen activator performed in PC3 cells treated with SE (0.4 mg/mL), CR (0.4 mM), and CCT (0.1 mM). Cell cultures were allowed to grow in complete medium for 8 days in presence of SE, CR, and CCT. Next, medium was changed and serum-free medium containing SE, CR, and CCT was added for additional 24–48 hr. (c) Migration assay performed by using filters with 8 μm pores coated with 0.1% gelatin and using as chemoattractant the NI3T3-conditioned medium. Cells were cultured for 8 days in complete medium with SE, CR, and CCT, then harvested by trypsinization, and added to the upper compartment of the Boyden chambers at the above-mentioned concentrations. Five 10x microscopic fields were counted for each replicate. Data (±SD) are representative of three different analyses. Treatment reduced significantly the migration of PC3 and 22rv1 cells ($^*P < 0.01$). (d) Invasion assay performed by using filters with 8 μm pores coated with 50 μL (12.5 μg/mL) Matrigel and using as a chemoattractant the mouse fibroblast NI3T3-conditioned medium. Cells cultured for 6 days with SE, CR, and CCT were added to the upper compartment of Boyden chambers at the above-mentioned concentrations. Five 10x microscopic fields were counted for each replicate. Data (±SD) are representative of three different analyses. We considered $P < 0.05$ as significant (*).

EMT phenotype is associated with the activation of the Wnt signaling pathway, in which its key component β-catenin plays critical roles in embryonic development as well as in human diseases, including cancer. The progression of carcinomas is associated with the loss of epithelial morphology and a concomitant acquisition of a more mesenchymal phenotype, which in turn is thought to contribute to the invasive and/or metastatic behavior of the malignant process. Loss of E-cadherin is reported to be associated with a poor prognosis [1–6]. It has been demonstrated that N-cadherin was not expressed in normal prostate tissue; however, in prostatic cancer, N-cadherin was expressed in the poorly differentiated areas, which showed negative E-cadherin staining. Accumulated evidence has demonstrated a significant role for the Wnt pathway in the development and progression of human prostate cancer. Clearly, the mere loss of cell-cell contact and communication cannot be the sole explanation for the observed relationship between loss of E-cadherin-mediated adhesion and poor clinical outcome. Recently, a number of papers have been published that describe the inappropriate expression of nonepithelial cadherins by epithelial cells as a putative novel mechanism for promoting the interaction with the stroma, thereby facilitating invasion and metastasis [13–16]. We showed that human prostate cancer cell lines, which lack expression of either E-cadherin or catenins and, therefore, lack an E-cadherin-mediated cell-cell adhesion, acquire cadherin expression [17].

In our previous report we noticed that SE and CR were effective *in vitro* in PCa tumor cells including PC3 cells used in the present report [12]. Androgen sensitive PCa cells seem to be more affected by treatments of androgen insensitive ones. The lower efficacy of SE observed *in vivo*, especially for PC3 cells, could be due to the reduced blood levels (and thus reduced tumor levels) of carotenoids that were achieved after the oral administration of SE. It has been demonstrated that CR was absorbed in the intestinal tract in a minimal amount whereas, when we administered SE *in vitro*, we provide to cultures mainly CR and not CCT which is the metabolic product of CR in gastrointestinal environment. CCT could be, indeed, the major compound which can be found in the blood. Crocin shows intrinsic antiproliferative effects but the oral administration shows only the effects of CCT. In addition, not all crocin turns into crocetin. However the relative blood amounts and blood peaks are unknown. Further experiments are necessary to establish the amount of carotenoids found in the blood after oral administration of SE, CR, and CCT (paper in preparation). In addition, although CCT is more effective of CR, its tumor levels were probably not sufficient to determine antiproliferative/proapoptotic effects in our PCa xenografts.

In addition, as widely described in this paper, CCT showed higher effects on proliferation/apoptosis when compared to differentiative ones; therefore, although MMPs was reduced (whereas uPA was not modified) overall Matrigel degradation (and invasion) seems to be not influenced.

To our knowledge, this is the first report showing that saffron-induced antitumor effects may affect EMT processes. Specifically, we observed that the induction of epithelial differentiation was a time-dependent event and was evident from 4 days of treatment with SE and CR. Based on the current data, saffron and its ingredients could be considered as a promising candidate for clinical anticancer trials in aggressive prostate cancer with a high risk of metastases.

Conflict of Interests

The authors declare that there is no conflict of interests regarding the publication of this paper.

Authors' Contribution

Claudio Festuccia, Andrea Mancini, and Giovanni Luca Gravina equally contributed to this paper.

References

[1] S. A. Holstein and R. J. Hohl, "Isoprenoids: remarkable diversity of form and function," *Lipids*, vol. 39, no. 4, pp. 293–309, 2004.

[2] F. I. Abdullaev and E. González De Mejía, "Antitumor activity of natural substances: lectins and saffron," *Archivos Latinoamericanos de Nutricion*, vol. 47, no. 3, pp. 195–202, 1997.

[3] M. Carmona, A. Zalacain, A. M. Sánchez, J. L. Novella, and G. L. Alonso, "Crocetin esters, picrocrocin and its related compounds present in *Crocus sativus* stigmas and Gardenia jasminoides fruits. Tentative identification of seven new compounds by LC-ESI-MS," *Journal of Agricultural and Food Chemistry*, vol. 54, no. 3, pp. 973–979, 2006.

[4] B. Deo, "Growing saffron—the world's most expensive spice," *Crop and Food Research*, vol. 20, no. 1, pp. 1–4, 2003.

[5] J. P. Melnyk, S. Wang, and M. F. Marcone, "Chemical and biological properties of the world's most expensive spice: saffron," *Food Research International*, vol. 43, no. 8, pp. 1981–1989, 2010.

[6] C. C. Licón, M. Carmona, A. Molina, and M. I. Berruga, "Chemical, microbiological, textural, color, and sensory characteristics of pressed ewe milk cheeses with saffron (*Crocus sativus* L.) during ripening," *Journal of Dairy Science*, vol. 95, no. 8, pp. 4263–4274, 2012.

[7] L. Cossignani, E. Urbani, M. S. Simonetti, A. Maurizi, C. Chiesi, and F. Blasi, "Characterisation of secondary metabolites in saffron from central Italy (Cascia, Umbria)," *Food Chemistry*, vol. 143, pp. 446–451, 2014.

[8] C. Ulbricht, J. Conquer, D. Costa et al., "An evidence-based systematic review of saffron (*Crocus sativus*) by the natural standard research collaboration," *Journal of Dietary Supplements*, vol. 8, no. 1, pp. 58–114, 2011.

[9] F. I. Abdullaev and J. J. Espinosa-Aguirre, "Biomedical properties of saffron and its potential use in cancer therapy and chemoprevention trials," *Cancer Detection and Prevention*, vol. 28, no. 6, pp. 426–432, 2004.

[10] Y. Deng, Z.-G. Guo, Z.-L. Zeng, and Z. Wang, "Studies on the pharmacological effects of saffron(*Crocus sativus* L.)—a review," *Zhongguo Zhongyao Zazhi*, vol. 27, no. 8, pp. 565–568, 2002.

[11] M. Carmona, A. Zalacain, M. R. Salinas, and G. L. Alonso, "A new approach to saffron aroma," *Critical Reviews in Food Science and Nutrition*, vol. 47, no. 2, pp. 145–159, 2007.

[12] A. M. D'Alessandro, A. Mancini, A. R. Lizzi et al., "*Crocus sativus* stigma extract and its major constituent crocin possess significant antiproliferative properties against human prostate cancer," *Nutrition and Cancer*, vol. 65, no. 6, pp. 930–942, 2013.

[13] J. Tavakkol-Afshari, A. Brook, and S. H. Mousavi, "Study of cytotoxic and apoptogenic properties of saffron extract in human cancer cell lines," *Food and Chemical Toxicology*, vol. 46, no. 11, pp. 3443–3447, 2008.

[14] S. C. Nair, B. Pannikar, and K. R. Panikkar, "Antitumour activity of saffron (*Crocus sativus*)," *Cancer Letters*, vol. 57, no. 2, pp. 109–114, 1991.

[15] S. H. Mousavi, J. Tavakkol-Afshari, A. Brook, and I. Jafari-Anarkooli, "Role of caspases and Bax protein in saffron-induced apoptosis in MCF-7 cells," *Food and Chemical Toxicology*, vol. 47, no. 8, pp. 1909–1913, 2009.

[16] D. G. Chryssanthi, P. G. Dedes, N. K. Karamanos, P. Cordopatis, and F. N. Lamari, "Crocetin inhibits invasiveness of MDA-MB-231 breast cancer cells via downregulation of matrix metalloproteinases," *Planta Medica*, vol. 77, no. 2, pp. 146–151, 2011.

[17] H. H. Aung, C. Z. Wang, M. Ni et al., "Crocin from *Crocus sativus* possesses significant anti-proliferation effects on human colorectal cancer cells," *Experimental Oncology*, vol. 29, no. 3, pp. 175–180, 2007.

[18] A. Bolhassani, A. Khavari, and S. Z. Bathaie, "Saffron and natural carotenoids: biochemical activities and anti-tumor effects," *Biochimica et Biophysica Acta*, vol. 1845, no. 1, pp. 20–30, 2014.

[19] I. Das, S. Das, and T. Saha, "Saffron suppresses oxidative stress in DMBA-induced skin carcinoma: a histopathological study," *Acta Histochemica*, vol. 112, no. 4, pp. 317–327, 2010.

[20] K. Premkumar, S. K. Abraham, S. T. Santhiya, and A. Ramesh, "Protective effects of saffron (*Crocus sativus* Linn.) on genotoxins-induced oxidative stress in Swiss albino mice," *Phytotherapy Research*, vol. 17, no. 6, pp. 614–617, 2003.

[21] F. I. Abdullaev and G. D. Frenkel, "The effect of saffron on intracellular DNA, RNA and protein synthesis in malignant and non-malignant human cells," *BioFactors*, vol. 4, no. 1, pp. 43–45, 1992.

[22] E. García-López, A. González-Gallardo, A. Antaramián et al., "In vitro conversion of β-carotene to retinal in bovine rumen fluid by a recombinant β-carotene- 15, 15′-monooxygenase," *International Journal for Vitamin and Nutrition Research*, vol. 82, no. 2, pp. 94–103, 2012.

[23] J. Molnár, M. D. Kars, U. Gündüz et al., "Interaction of tomato lectin with ABC transporter in cancer cells: glycosylation confers functional conformation of P-gp," *Acta Histochemica*, vol. 111, no. 4, pp. 329–333, 2009.

[24] S. K. . Noureini and M. Wink, "Antiproliferative effects of crocin in HepG2 cells by telomerase inhibition and hTERT down-regulation," *Asian Pacific Journal of Cancer Prevention*, vol. 13, no. 5, pp. 2305–2309, 2012.

[25] A. Kyriakoudi, M. Z. Tsimidou, Y. C. O'Callaghan, K. Galvin, and N. M. O'Brien, "Changes in total and individual crocetin esters upon in vitro gastrointestinal digestion of saffron aqueous extracts," *Journal of Agricultural and Food Chemistry*, vol. 61, no. 22, pp. 5318–5327, 2013.

[26] A. M. Sánchez, M. Carmona, S. A. Ordoudi, M. Z. Tsimidou, and G. L. Alonso, "Kinetics of individual crocetin ester degradation in aqueous extracts of saffron (*Crocus sativus* L.) upon thermal treatment in the dark," *Journal of Agricultural and Food Chemistry*, vol. 56, no. 5, pp. 1627–1637, 2008.

[27] A. M. Sánchez, M. Carmona, A. Zalacain, J. M. Carot, J. M. Jabaloyes, and G. L. Alonso, "Rapid determination of crocetin esters and picrocrocin from saffron spice (*Crocus sativus* L.) using UV-visible spectrophotometry for quality control," *Journal of Agricultural and Food Chemistry*, vol. 56, no. 9, pp. 3167–3175, 2008.

[28] M. E. Kaighn, J. F. Lechner, K. Shankar Narayan, and L. W. Jones, "Prostate carcinoma: tissue culture cell lines," *National Cancer Institute Monograph*, vol. 49, pp. 17–21, 1978.

[29] R. M. Sramkoski, T. G. Pretlow II, J. M. Giaconia et al., "A new human prostate carcinoma cell line, 22Rv1," *In Vitro Cellular and Developmental Biology—Animal*, vol. 35, no. 7, pp. 403–409, 1999.

[30] G. L. Gravina, F. Marampon, I. Giusti et al., "Differential effects of PXD101 (belinostat) on androgen-dependent and androgen-independent prostate cancer models," *International Journal of Oncology*, vol. 40, no. 3, pp. 711–720, 2012.

[31] C. Festuccia, P. Muzi, G. L. Gravina et al., "Tyrosine kinase inhibitor CEP-701 blocks the NTRK1/NGF receptor and limits the invasive capability of prostate cancer cells in vitro," *International Journal of Oncology*, vol. 30, no. 1, pp. 193–200, 2007.

[32] C. Festuccia, C. Vincentini, A. B. Di Pasquale et al., "Plasminogen activator activities in short-term tissue cultures of benign prostatic hyperplasia and prostatic carcinoma," *Oncology Research*, vol. 7, no. 3-4, pp. 131–138, 1995.

[33] C. Festuccia, G. L. Gravina, A. M. D'Alessandro et al., "Azacitidine improves antitumor effects of docetaxel and cisplatin in aggressive prostate cancer models," *Endocrine-Related Cancer*, vol. 16, no. 2, pp. 401–413, 2009.

[34] F. Bruzzese, E. Di Gennaro, A. Avallone et al., "Synergistic antitumor activity of epidermal growth factor receptor tyrosine kinase inhibitor gefitinib and IFN-α in head and neck cancer cells in vitro and in vivo," *Clinical Cancer Research*, vol. 12, no. 2, pp. 617–625, 2006.

[35] U. D. Kahlert, G. Nikkhah, and J. Maciaczyk, "Epithelial-to-mesenchymal(-like) transition as a relevant molecular event in malignant gliomas," *Cancer Letters*, vol. 331, no. 2, pp. 131–138, 2013.

[36] H. Li, J. Huang, B. Yang et al., "Mangiferin exerts antitumor activity in breast cancer cells by regulating matrix metalloproteinases, epithelial to mesenchymal transition, and β-catenin signaling pathway," *Toxicology and Applied Pharmacology*, vol. 272, no. 1, pp. 180–190, 2013.

[37] J. Ferlay, D. M. Parkin, and E. Steliarova-Foucher, "Estimates of cancer incidence and mortality in Europe in 2008," *European Journal of Cancer*, vol. 46, no. 4, pp. 765–781, 2010.

[38] E. F. Burgess and D. Raghavan, "Prostate cancer: what did we learn from the 2012 Annual Scientific Meeting of ASCO?" *Oncology (Williston Park)*, vol. 26, no. 12, pp. 1216–1221, 2012.

[39] B. A. Hadaschik, R. D. Sowery, and M. E. Gleave, "Novel targets and approaches in advanced prostate cancer," *Current Opinion in Urology*, vol. 17, no. 3, pp. 182–187, 2007.

[40] C. Y. Wu, Y. P. Tsai, M. Z. Wu, S. C. Teng, and K. J. Wu, "Epigenetic reprogramming and post-transcriptional regulation during the epithelial-mesenchymal transition," *Trends in Genetics*, vol. 28, no. 9, pp. 454–463, 2012.

[41] Q. Gao, W. Liu, J. Cai et al., "EphB2 promotes cervical cancer progression by inducing epithelial-mesenchymal transition," *Human Pathology*, vol. 45, no. 2, pp. 372–381, 2014.

[42] H. Whiteland, S. Spencer-Harty, D. H. Thomas et al., "Putative prognostic epithelial-to-mesenchymal transition biomarkers for aggressive prostate cancer," *Experimental and Molecular Pathology*, vol. 95, no. 2, pp. 220–226, 2013.

Hindawi Publishing Corporation
BioMed Research International
Volume 2014, Article ID 890697, 9 pages
http://dx.doi.org/10.1155/2014/890697

Review Article

Novel Tools for Prostate Cancer Prognosis, Diagnosis, and Follow-Up

Andreas Dimakakos, Athanasios Armakolas, and Michael Koutsilieris

Physiology Laboratory, Medical School, National and Kapodistrian University of Athens, Mikras Asias 75, 11527 Athens, Greece

Correspondence should be addressed to Michael Koutsilieris; mkoutsil@med.uoa.gr

Received 7 February 2014; Accepted 9 April 2014; Published 4 May 2014

Academic Editor: Giovanni Luca Gravina

Prostate-specific antigen (PSA) is the main diagnostic tool when it comes to prostate cancer but it possesses serious limitations. Therefore, there is an urgent need for more sensitive and specific biomarkers for prostate cancer prognosis and patient follow-up. Recent advances led to the discovery of many novel diagnostic/prognostic techniques and provided us with many worthwhile candidates. This paper briefly reviews the most promising biomarkers with respect to their implementation in screening, early detection, diagnostic confirmation, prognosis, and prediction of therapeutic response or monitoring disease and recurrence; and their use as possible therapeutic targets. This review also examines the possible future directions in the field of prostate cancer marker research.

1. Introduction

Prostate cancer is the sixth leading cause of cancer-related death in men (it is now the second in the United States and first in the UK) [1]. While there are exceptions, it is not a particularly aggressive form of cancer, and it tends to metastasize mainly to bones and lymph nodes [2]. Many factors have been proven to be implicated in the development of prostate cancer, including diet and genetics. Curative treatment generally involves surgery, various forms of radiation therapy, or, less commonly, cryosurgery. Hormonal therapy and chemotherapy are not usually implemented, unless the disease reaches advanced stages and there have been instances where hormonal therapy has been combined with radiation therapy [3].

Over the years, many markers have been used for the diagnosis and follow-up of prostate cancer. Prostate-specific antigen (PSA) is the most common marker used for prostate cancer detection and follow-up, and until recently, PSA was considered the most reliable marker to predict prostate cancer [4]. In 1994, the FDA approved the use of the PSA test in conjunction with a digital rectal exam (DRE) to test asymptomatic men for prostate cancer. Blood PSA levels higher than 4.0 ng/mL is an indication of prostate cancer. Studies have shown that the levels of free PSA in the serum act as a more accurate marker for BPH, while the levels of α1-antichymotrypsin-PSA complex more accurately predict prostate cancer [5].

Lately, however, PSA screening has fallen under controversy since it is detected in 30–50% of the cases of benign prostate hyperplasia [BPH] and in only 20% of the cases of prostate cancer. Recent evidence suggests that some prostate cancer patients may present PSA levels below 4.0 ng/mL, while PSA levels can be affected by various other factors, such as prostatitis, urinary tract infection, and benign prostate hyperplasia (BPH) [6–8]. Additionally, a variety of drugs (5α-reductase inhibitors, that is, finasteride and dutasteride) used to treat BPH reduce PSA in the blood [9].

Out of the men that display elevated PSA levels in the blood, only 25% are associated with prostate cancer. In order to get more accurate readings on the association between PSA levels and prostate cancer, other factors are taken into consideration, such as free versus total PSA, age (PSA increases with age), PSA velocity and doubling time, pro-PSA, and PSA density of the transition zone [6–8, 10]. Velocity refers to the rate of change in a man's PSA level over time, expressed in (ng/mL)/year, while doubling time refers to the period of time in which the concentration of

PSA in the blood doubles. Pro-PSA refers to several inactive PSA precursors that have been suggested to more strongly associate with prostate cancer, while PSA density refers to the blood level of PSA divided by the volume of the interior part of the prostate that surrounds the urethra transition zone.

The absence of a reliable marker for prostate cancer diagnosis and follow-up creates the demand for novel, specific, sensitive, and cost effective biological markers. In this review, we are going to focus on novel biological markers for prostate cancer prognosis and patient follow-up and the possibility to be targeted as markers for prostate cancer treatment.

2. The Ideal Marker

Only a few markers have managed to withstand the test of time and entered into clinical trials. The main characteristics of an ideal tumor marker are its specificity for a given tumor type and its sensitivity, and it should also provide advance warning before clinical diagnosis. The levels of the marker should accurately depict the progress or regression of the target tumor. A short half-life would allow for frequent serial measurements. Finally, the detection test should be cheap and noninvasive, so as to allow patient screening and also to be acceptable by the majority of the patients. Finally, tumor-associated markers should be able to predict the metastatic onset or, in advanced stages, determine the metastatic spread [11].

3. Current Prostate Cancer Markers

The rapid advancements in overall detection techniques have made it possible to identify a large number of new possible biomarkers; however, a recent study on prostate cancer tissue samples has shown that the equivalence between RNA transcripts and protein products ranges only between 48% and 64% [12]. Since proteins are the true functional molecules of the cell, much of the current research has shifted towards the definition of solely protein markers. The most promising prostate cancer markers among others are the prostate-specific membrane antigen (PSMA), prostate stem cell antigen (PSCA), early prostate cancer antigen (EPCA), enhancer of zeste homolog gene 2 (EZH2), and the urokinase plasminogen activator (uPA) [13, 14].

The PSMA is a type II integral membrane glycoprotein, originally identified in 1987 as being significantly overexpressed in the epithelial cells of prostate cancer patients. Since then, it has undergone multiple evaluations with mixed results. The sensitivity and specificity of PSMA in distinguishing prostate adenocarcinoma from any other type of malignancy are 65.9% and 94.5%, respectively. Some believe that it can be utilized to check the progress of the disease posttreatment. It can also take part in the radiologic imaging of prostate cancer and has been studied as a possible target for monoclonal antibodies to combat prostate cancer, due to its overexpression, despite the fact that its function in prostate cancer is still unclear [15–21].

The PSCA is a prostate-specific glycosyl phosphatidylinositol-anchored glycoprotein expressed on the cell surface. Several studies have shown correlation between increased levels of PSCA and prostate cancer presence, stage, progression, and metastases. Moreover, PSCA RNA is detectable in the peripheral blood through the use of real-time PCR (RT-PCR), an aspect that has been implemented in circulating tumor cell (CTC) detection, while the protein product can act as a target for monoclonal antibodies, as it is situated on the tumor cell surface. As a result, it is a very promising biological marker [22, 23].

The EPCA is a prostate cancer-associated nuclear structural protein. A blood test using an EPCA enzyme-linked immunosorbent assay has displayed 92% sensitivity and 94% specificity for prostate cancer, suggesting a possibly immensely useful biomarker [24].

The EZH2 is a member of the polycomb group of proteins, and it is involved in maintaining the transcriptional repressive state of genes over successive cell generations. EZH2 acts mainly as a gene silencer. EZH2 overexpression may promote cancer due to increase in histone methylation which silences the expression of tumor suppressor genes. Its expression is significantly increased in metastatic prostate cancer in comparison to localized prostate cancer and in localized prostate cancer in comparison to benign prostate tissue [25]. Currently, there is no blood test for EZH2, but it could prove to be a useful biological marker to identify patients at risk of metastasis [13].

The uPA axis is involved in various phases of tumor development and so could act as a potential treatment target. Results show that elevated circulating levels of uPA and uPA receptor (uPAR) are connected with prostate cancer stage and bone metastases. Additionally, uPA has been described as a strong predictor of recurrence after radical prostatectomy [26–28].

Transmembrane protease serine 2 (TMPRSS2) is an enzyme that in humans is encoded by the androgen-regulated TMPRSS2 gene. Its function in prostate cancer lies in the overexpression of E26 transformation-specific (ETS) transcription factors, such as ETS-related gene (ERG) and ETS translocation variant 1 (ETV1) through gene fusion [29]. TMPRSS2-ERG fusion gene is frequently present in human prostate cancer (50%) and it is not detected in normal prostate or BPH [30–33]. It has been suggested that ERG overexpression facilitates prostate cancer progression by promoting androgen independence through disruption of androgen-receptor signaling [29]. Noninvasive detection of TMPRSS2-ERG transcripts is possible in urinary sediments through real-time PCR, presenting a 93% specificity for prostate cancer. This technique is usually carried out in combination with and after digital rectal examination (DRE) [34]. Once combined with prostate cancer antigen 3 (PCA3), the sensitivity increases from 62% (PCA3 alone) to 72% (combined) without sacrificing any of the specificity [35, 36]. These facts constitute TMPRSS2-ERG, a powerful diagnostic tool on its own and a viable way to improve the efficiency of other promising biomarkers.

Studies with general cancer markers are also being performed to determine a possible connection with prostate cancer, aiming to provide accuracy in prostate cancer detection when used solely or in combination with one of the prostate

cancer specific markers. The most promising general cancer markers for prostate cancer detection are transforming growth factor-β1 (TGF-β1) and interleukin-6 (IL-6). TGF-β1 is involved in cellular proliferation, redifferentiation, angiogenesis, and epithelial to mesenchymal transition (EMT), the process by which epithelial cells lose cell polarity and cell-to-cell adhesion, gaining migratory and invasive properties, and it has been associated with metastasis in prostate cancer models [37–41]. However, the results are inconclusive regarding its correlation to prostate cancer progression [42, 43]. IL-6 is a cytokine with a large number of biological activities, including regulation of immune response. It has been shown to stimulate cell growth in androgen-independent prostate cancer cells but inhibit it in androgen-dependent prostate cancer cells [44, 45]. Recent studies have introduced the idea of the combined use of TGF-β1 and IL-6 to improve the chances of accurately predicting lymph node metastases [46, 47].

Studies have shown that E-cadherin loss correlates with prostate tumor progression, establishing E-cadherin as a prognosis factor for clinical disease progression [48]. On the other hand, the elevation of N-cadherin has been shown to be a significant predictor of prostate cancer recurrence following radical prostatectomy, making it one of the few biomarkers capable of providing information for prostate cancer treatment follow-up [40, 49]. Additional data has shown significant correlation between elevated ZEB1 expression, induced by androgens, and high Gleason scores in prostate cancer [50]. This means that ZEB1 could function as a possible biomarker for predicting the onset of metastatic spread in prostate cancer.

The cancer cells subjected to EMT develop stem-cell-like qualities, practically becoming circulating stem cells. These cells exhibit both tumor and mesenchymal markers [51]. The existence of malignant cells of epithelial origin in the blood, the CTCs, has been known for over a century and has been associated with metastasis. Circulating tumor cell (CTC) counts in the blood have been suggested to act as prostate cancer prognostic markers, especially in cases with bone metastases [52–55]. Over the past few years, different approaches have been developed prior to the detection of CTCs in different tumors. Each of these approaches has distinct advantages and disadvantages, with the most notable being sensitivity and specificity [21, 51, 56–58]. At the moment, there are diagnostic platforms designed to detect CTCs in order to ascertain, up to a point, whether chemotherapy was successful and if there is going to be a cancer recurrence [52, 56].

4. The IGF System

The insulin-like growth factor (IGF)/insulin family of growth factors is a system which plays a critical role in the development and growth of several tissues as well as the overall metabolism. It is comprised of three different receptors: the IGF-1 receptor (IGF-1R), IGF-2 receptor (IGF-2R), and the insulin receptor (IR), three different ligands (IGF-1, IGF-2, and insulin), and six types of circulating IGF-binding proteins (IGFBP1-6) [59, 60].

So far, the scientific community is convinced, without data to the contrary, that the IGF-1 system is not, by its nature, oncogenic. The activated receptors are not genotoxic nor do they cause DNA mutations or any other kind of DNA damage [61]. However, they do severely affect the progress of the cell cycle, pushing cells to proliferate at an alarming rate, once their regulation is influenced, like in cases of cancer.

There have been attempts in the past to ascertain whether any part of the IGF axis (ligands, receptors, or binding proteins) could be used as a reliable biological marker for prostate cancer and prostate cancer metastases with controversial results [62, 63]. Since elevated IGF-1 and IGF-1R levels have been associated with many types of cancer and metastases, they cannot be used as prostate cancer markers, at least individually, due to their lack of specificity [59, 60, 63–65]. Certain data showed that the PSA/IGF-1 ratio could differentiate between prostate cancer and BPH but was met with criticism [66]. So far, IGF-1, IGF-1R, and IGFBP3 levels have only been shown to be possible but deficient prostate cancer risk markers. However, there is data that supports the idea that IGF-1 and IGF-1R could be used as biomarkers for advanced stages of prostate cancer and prostate cancer metastases [63, 65, 67]. This could be significant, as compared to some of the other possible biomarkers mentioned.

The phosphorylation of the receptor through the binding of the ligands leads indirectly to the activation of the MAPK/ERK, AKT, and RAS/RAF pathways. This makes the IGF-1R an ideal target for several experimental treatments [59, 60, 68]. Anticancer strategies focusing on the IGF1 signaling system usually belong in one of two categories: neutralizing antibodies and small molecule inhibitors of the IGF-1R kinase activity. Some of them are now being tested at a clinical level, in tandem with standard chemotherapeutic or targeted agents in cancer patients.

Monoclonal antibodies targeting IGF-1R usually target its extracellular domain. Binding of these antibodies has the added effect of downregulating IGF-1R by promoting its internalization. Most antibodies that have been tested in clinical trials have shown no adverse reactions [69]. It was not known until recently that although these antibodies inhibit the binding of the IGF-1 to the IGF-1R, they also activate the IGF-1R (to a lesser extent) by binding to it [70, 71]. A solution to that suggests the use of these antibodies in combination with other antibodies or therapeutic factors targeting the IGF-1R intracellular pathways.

However, IGF-1R is not the only part of the IGF1 axis that has been targeted by neutralizing antibodies. There have been attempts in the past to construct anti-IGF-1 monoclonal antibodies with little success [72, 73]. Nowadays, the focus has shifted entirely towards the IGF-1R.

Along with advancements in analytical technology comes the progress in the characterization of IGF-1R structure [74]. This knowledge facilitates the design and use of small molecule inhibitors targeting IGF-1R. However, it is vitally important that there is no cross-reactivity between them and IR. At the moment, most of these small molecule inhibitors either display high levels of toxicity or they have not made it past stage II clinical trials [67, 75–78].

The anticancer strategies focusing on the IGF-1 system are still in the early stages of research, but their effects on prostate cancer were not associated with a spectacular success. The absence of an alternative, better than PSA, prostate cancer marker, leads to the consideration of other venues of research.

5. A Glimpse at the Future

The ideal prostate cancer marker has not been discovered yet. Sometimes, however, just one marker is not enough. This fact gave rise to the idea that the use of multiple markers at the same time could provide improved results. Tumor-associated antigens stimulate the production of autoantibodies (antibodies targeting an individual's own proteins) against cancer [79–82]. The measurement of different anti-tumor autoantibodies, through the use of protein microarrays, is expected to give us autoantibody signatures, that could prove to be a very accurate analytical tool for prostate cancer diagnosis, prognosis, and patient follow-up [83, 84].

Another promising approach towards the discovery of markers, more specific and sensitive than PSA, is the large-scale analysis of prostate cancer proteins, regarding their structures and functions, by proteomics [85]. Several biological sources, including tissues, urine, serum, plasma, and prostatic fluids, are currently under investigation using high-throughput proteomic platforms, such as nanoparticle capture based analysis, for that exact purpose [86]. Secretomics, a subfield of proteomics that studies secreted proteins and secretion pathways using proteomic approaches, has recently emerged as an important tool for the discovery of biomarkers of disease [87].

The prostate has been known for a long time to display unique metabolic profiles [88, 89]. Metabolomics is the study of chemical processes involving metabolites. It is the study of the unique chemical fingerprint that a specific cellular process leaves behind. More specifically, the prostate is unique among human organs due to the high levels of citrate in the prostatic fluid levels that can be 200–700 times higher than the ones in the blood plasma. However, when the prostate is subjected to neoplastic transformation, the prostate's reserves of citrate are depleted due to the increased energy consumption by the rapidly proliferating cancer cells [90, 91].

Quite recently, certain results showed not only that sarcosine, also known as N-methylglycine, an intermediate and byproduct in glycine synthesis and degradation, could be used as a dynamic new biomarker for prostate cancer metastasis, but also that sarcosine levels could control the invasiveness of the cancer. Since then, these results have been widely disputed, while there is doubt that sarcosine is actually an appropriate prostate cancer marker [92–95].

Another marker related to prostate cancer that has surfaced from the realm of metabolomics is choline, a water-soluble essential nutrient. Studies have shown that prostate cancer tissue displays elevated levels of choline and its component metabolites (free choline, phosphocholine, and glycerophosphocholine), in comparison with healthy prostate tissue. These changes reflect enhanced synthesis and degradation of phospholipid membranes. Additionally, levels of choline-containing metabolites are higher in metastatic tissues, when compared to the primary prostate cancer [89, 96–99], indicating the possible use of choline as a prostate cancer progression marker.

Recently, the field of epigenetic modifications has proven to be of interest when it comes to prostate cancer, as they have been connected with both disease initiation and progression [100, 101]. More specifically, DNA-methylation, histone modifications, and microRNA (miRNA) alterations occur at a much higher frequency than mutations and are present at premalignant stages of the disease, making them promising biomarkers [102].

Currently, the most extensively studied methylation-based markers in prostate cancer are the hypermethylated glutathione S-transferase P1 (GSTP1) and Ras-association domain family protein isoform A (RASSF1A). GSTP1 is involved in the cellular protection system against toxic effects and is especially promising as a biomarker because it is highly specific for prostate cancer (>90%); levels of GSTP1 methylation are associated with different stages of the disease; levels of GSTP1 promoter region methylation can differentiate between prostate cancer and BPH and they are detectable by noninvasive means in body fluids [103–106]. The methylation of RASSF1A, on the other hand, can potentially be used to distinguish aggressive tumors from indolent ones [107].

Histone modifications have not been researched to the same extent as methylation-based markers, mostly due to the absence of highly sensitive detection methods [108]. Currently, immunohistochemistry is the only method available for the study of histone modifications, with ELISA being an as of yet unproven alternative [109]. So far, the levels of specific histone modifications, such as H3K18Ac, H4K12Ac, H3K4Me2, and H4R3Me2, have been shown to correlate with prostate cancer tumor stage [110]; but without a reliable method to detect these modifications in biological fluids, progress has been slow. It is clear that this aspect of epigenetic modifications requires further research.

miRNA is also another promising candidate for prostate cancer prognosis and therapy. The mature miRNAs are short, noncoding, single-stranded RNA molecules that bind to complementary sequences in the 3′ UTR of target mRNAs, usually resulting in their silencing. They are detectable in body fluids, such as blood and serum, highly stable due to their placement within microvesicles, and thought to be, in most cases, tumor specific [111, 112]. While a large number of miRNAs have been shown to be altered in prostate cancer, the ones that have displayed the most promise are miR-141 and miR-375 [36]. Further studies have shown that increased expression of miR-141 and miR-375 is significantly associated with pathological stage and Gleason score [113]. Elevated plasma levels of miR-141 and miR-375 could potentially differentiate patients with metastases from those without [114]. Despite the promising results, miRNA implementation in prostate cancer detection is still in its infancy, mainly due to the difficulties in isolating miRNA from limited biological sources.

However, in our quest of discovering and defining new biomarkers, one must take into account the fact that every individual patient is different than the next. Tumors, most

commonly, tend to be comprised of multiple cellular clones and this fact may alter the marker expression. There are several lines of evidence in the literature suggesting that the patients' genetic profile could affect patients' response to treatments [64, 115–120]. Therefore it can be understood that identifying new biological markers is clearly not enough and a point of vital importance is to understand how different genetic alterations can influence cancer, so that the most effective course of treatment can be applied.

6. Discussion

Despite the fact that NCI does not have such guidelines that suggest the use of markers in cancer, the American Society of Oncology and the National Academy of Clinical Biochemistry have published clinical practice guidelines for markers on a variety of tumors. There are more than 20 tumor markers currently in use, and only the PSA is used in prostate cancer. For the past few years, PSA has raised quite a cloud when it comes to its effectiveness as a biological marker for the detection of prostate cancer. Its deficiencies have given rise to serious efforts to either improve its specificity by combining it with other existing biomarkers or discover and define new ones and also examine the possibility to use those markers as targets for a therapy influencing the balance between benefits (saved lives) and costs (unnecessary surgery).

There are a number of promising markers displayed here that can be used solely or in combination prior to obtaining the desirable result. Despite that, a recent study where 380 prostate cancer markers from the literature were examined in prostate cancer tissues by microarray analysis indicates that none of the markers examined can compete with PSA for tissue specificity. The markers proposed generally presented great variability of expression in normal and tumor tissue or they were expressed at similar levels in other tissues. Furthermore the evidence of this study suggests that the diagnostic and prognostic testing is more difficult in prostate cancer than in other neoplasms probably due to the fact that the individual genetic variability affects the tumor's outcome [121].

For that reason the research for better markers for prostate cancer has been turned towards different markers such as the autoantibodies raised against some tumor markers and/or different technologies proteomics and metabolomics.

Indeed, many of these markers are still in the realm of possibility; but if we take into account the fact that prostate cancer is globally the sixth cancer-associated cause of death in men, its early detection or proper stratification could really make a difference in the socioeconomic system. Therefore, it is imperative that the proper steps are taken to determine which of these markers, if any, would better suit our needs.

Conflict of Interests

The authors declare that they have no conflict of interests regarding the publication of this paper.

References

[1] P. D. Baade, D. R. Youlden, and L. J. Krnjacki, "International epidemiology of prostate cancer: geographical distribution and secular trends," *Molecular Nutrition and Food Research*, vol. 53, no. 2, pp. 171–184, 2009.

[2] G. N. Thalmann, P. E. Anezinis, S.-M. Chang et al., "Androgen-independent cancer progression and bone metastasis in the LNCaP model of human prostate cancer," *Cancer Research*, vol. 54, no. 10, pp. 2577–2581, 1994.

[3] E. A. Klein, "Opportunities for prevention of prostate cancer: genetics, chemoprevention, and dietary intervention," *Reviews in Urology*, vol. 5, supplement 4, pp. S18–S28, 2002.

[4] I. M. Thompson, "PSA: a biomarker for disease. A biomarker for clinical trials. How useful is it?" *Journal of Nutrition*, vol. 136, no. 10, p. 2704, 2006.

[5] U. H. Stenman, J. Leinonen, H. Alfthan, S. Rannikko, K. Tuhkanen, and O. Alfthan, "A complex between prostate-specific antigen and α1-antichymotrypsin is the major form of prostate-specific antigen in serum of patients with prostatic cancer: assay of the complex improves clinical sensitivity for cancer," *Cancer Research*, vol. 51, no. 1, pp. 222–226, 1991.

[6] G. L. Andriole Jr., "PSA screening and prostate cancer risk reduction," *Urologic Oncology*, vol. 30, no. 6, pp. 936–937, 2012.

[7] M. J. Barry, "Evaluation of symptoms and quality of life in men with benign prostatic hyperplasia," *Urology*, vol. 58, supplement 6, pp. 25–32, 2001.

[8] F. H. Schröder, "PSA screening—a review of recent studies," *European Journal of Cancer*, vol. 45, no. 1, pp. 402–404, 2009.

[9] I. M. Thompson, C. Chi, D. P. Ankerst et al., "Effect of finasteride on the sensitivity of PSA for detecting prostate cancer," *Journal of the National Cancer Institute*, vol. 98, no. 16, pp. 1128–1133, 2006.

[10] S. D. Mikolajczyk and H. G. Rittenhouse, "Pro PSA: A more cancer specific form of prostate specific antigen for the early detection of prostate cancer," *Keio Journal of Medicine*, vol. 52, no. 2, pp. 86–91, 2003.

[11] S. Sharma, ". Tumor markers in clinical practice: general principles and guidelines. Indian journal of medical and paediatric oncology," *Official Journal of Indian Society of Medical & Paediatric Oncology*, vol. 30, no. 1, pp. 1–8, 2009.

[12] S. Varambally, J. Yu, B. Laxman et al., "Integrative genomic and proteomic analysis of prostate cancer reveals signatures of metastatic progression," *Cancer Cell*, vol. 8, no. 5, pp. 393–406, 2005.

[13] T. J. Bradford, S. A. Tomlins, X. Wang, and A. M. Chinnaiyan, "Molecular markers of prostate cancer," *Urologic Oncology*, vol. 24, no. 6, pp. 538–551, 2006.

[14] S. F. Shariat, A. Semjonow, H. Lilja, C. Savage, A. J. Vickers, and A. Bjartell, "Tumor markers in prostate cancer I: blood-based markers," *Acta Oncologica*, vol. 50, supplement 1, pp. 61–75, 2011.

[15] J. K. Troyer, M. L. Beckett, and G. L. Wright Jr., "Detection and characterization of the prostate-specific membrane antigen (PSMA) in tissue extracts and body fluids," *International Journal of Cancer*, vol. 62, no. 5, pp. 552–558, 1995.

[16] J. Q. Ren, Z. Q. Chen, L. Zheng, Q. Chen, H. Li, and H. G. Zhu, "Correlation study of expression levels of prostate-specific membrane antigen and prostate-specific antigen with Gleason score of prostate carcinoma," *Zhonghua Zhong liu za zhi [Chinese journal of oncology]*, vol. 26, no. 12, pp. 735–738, 2004.

[17] G. P. Murphy, G. M. Kenny, H. Ragde et al., "Measurement of serum prostate-specific membrane antigen, a new prognostic marker for prostate cancer," *Urology*, vol. 51, supplement 5, pp. 89–97, 1998.

[18] P. Mhawech-Fauceglia, S. Zhang, L. Terracciano et al., "Prostate-specific membrane antigen (PSMA) protein expression in normal and neoplastic tissues and its sensitivity and specificity in prostate adenocarcinoma: An immunohistochemical study using mutiple tumour tissue microarray technique," *Histopathology*, vol. 50, no. 4, pp. 472–483, 2007.

[19] R. Kurek, G. Nunez, N. Tselis et al., "Prognostic value of combined "triple"-reverse transcription-PCR analysis for prostate-specific antigen, human kallikrein 2, and prostate-specific membrane antigen mRNA in peripheral blood and lymph nodes of prostate cancer patients," *Clinical Cancer Research*, vol. 10, no. 17, pp. 5808–5814, 2004.

[20] M. C. Gong, S. S. Chang, M. Sadelain, N. H. Bander, and W. D. W. Heston, "Prostate-specific membrane antigen (PSMA)-specific monoclonal antibodies in the treatment of prostate and other cancers," *Cancer and Metastasis Reviews*, vol. 18, no. 4, pp. 483–490, 1999.

[21] D. C. Chu, C. K. Chuang, Y. F. Liou, R. D. Tzou, H. C. Lee, and C. F. Sun, "The use of real-time quantitative PCR to detect circulating prostate-specific membrane antigen mRNA in patients with prostate carcinoma," *Annals of the New York Academy of Sciences*, vol. 1022, pp. 157–162, 2004.

[22] Z. Zhigang and S. Wenlv, "Prostate stem cell antigen (PSCA) expression in human prostate cancer tissues: implications for prostate carcinogenesis and progression of prostate cancer," *Japanese Journal of Clinical Oncology*, vol. 34, no. 7, pp. 414–419, 2004.

[23] Z. Gu, G. Thomas, J. Yamashiro et al., "Prostate stem cell antigen (PSCA) expression increases with high gleason score, advanced stage and bone metastasis in prostate cancer," *Oncogene*, vol. 19, no. 10, pp. 1288–1296, 2000.

[24] B. Paul, R. Dhir, D. Landsittel, M. R. Hitchens, and R. H. Getzenberg, "Detection of prostate cancer with a blood-based assay for early prostate cancer antigen," *Cancer Research*, vol. 65, no. 10, pp. 4097–4100, 2005.

[25] S. Varambally, S. M. Dhanasekaran, M. Zhou et al., "The polycomb group protein EZH2 is involved in progression of prostate cancer," *Nature*, vol. 419, no. 6907, pp. 624–629, 2002.

[26] G. Hienert, J. C. Kirchheimer, H. Pfluger, and B. R. Binder, "Urokinase-type plasminogen activator as a marker for the formation of distant metastases in prostatic carcinomas," *Journal of Urology*, vol. 140, no. 6, pp. 1466–1469, 1988.

[27] H. Miyake, I. Hara, K. Yamanaka, S. Arakawa, and S. Kamidono, "Elevation of urokinase-type plasminogen activator and its receptor densities as new predictors of disease progression and prognosis in men with prostate cancer," *International Journal of Oncology*, vol. 14, no. 3, pp. 535–541, 1999.

[28] S. F. Shariat, C. G. Roehrborn, J. D. McConnell et al., "Association of the circulating levels of the urokinase system of plasminogen activation with the presence of prostate cancer and invasion, progression, and metastasis," *Journal of Clinical Oncology*, vol. 25, no. 4, pp. 349–355, 2007.

[29] J. Yu, J. Yu, R.-S. Mani et al., "An integrated network of androgen receptor, polycomb, and TMPRSS2-ERG gene fusions in prostate cancer progression," *Cancer Cell*, vol. 17, no. 5, pp. 443–454, 2010.

[30] N. Cerveira, F. R. Ribeiro, A. Peixoto et al., "TMPRSS2-ERG gene fusion causing ERG overexpression precedes chromosome copy number changes in prostate carcinomas and paired HGPIN lesions," *Neoplasia*, vol. 8, no. 10, pp. 826–832, 2006.

[31] K. Park, S. A. Tomlins, K. M. Mudaliar et al., "Antibody-based detection of ERG rearrangement-positive prostate cancer," *Neoplasia*, vol. 12, no. 7, pp. 590–598, 2010.

[32] G. J. Van Leenders, J. L. Boormans, C. J. Vissers et al., "Antibody EPR3864 is specific for ERG genomic fusions in prostate cancer: implications for pathological practice," *Modern Pathology*, vol. 24, no. 8, pp. 1128–1138, 2011.

[33] D. Gasi Tandefelt, J. Boormans, K. Hermans, and J. Trapman, "ETS fusion genes in prostate cancer," *Endocrine-Related Cancer*, 2014.

[34] D. Hessels, F. P. Smit, G. W. Verhaegh, J. A. Witjes, E. B. Cornel, and J. A. Schalken, "Detection of TMPRSS2-ERG fusion transcripts and prostate cancer antigen 3 in urinary sediments may improve diagnosis of prostate cancer," *Clinical Cancer Research*, vol. 13, no. 17, pp. 5103–5108, 2007.

[35] S. S. Salami, F. Schmidt, B. Laxman et al., "Combining urinary detection of TMPRSS2:ERG and CaP3 with serum PSA to predict diagnosis of prostate cancer," *Urologic Oncology*, vol. 31, no. 5, pp. 566–571, 2013.

[36] D. Hessels and J. A. Schalken, "Urinary biomarkers for prostate cancer: a review," *Asian Journal of Andrology*, vol. 15, no. 3, pp. 333–339, 2013.

[37] L. D. Truong, D. Kadmon, B. K. McCune, K. C. Flanders, P. T. Scardino, and T. C. Thompson, "Association of transforming growth factor-β1 with prostate cancer: an immunohistochemical study," *Human Pathology*, vol. 24, no. 1, pp. 4–9, 1993.

[38] T. C. Thompson, L. D. Truong, T. L. Timme et al., "Transforming growth factor beta 1 as a biomarker for prostate cancer," *Journal of cellular biochemistry Supplement*, vol. 16, pp. 54–61, 1992.

[39] V. Ivanović, M. Demajo, K. Krtolica et al., "Elevated plasma TGF-β1 levels correlate with decreased survival of metastatic breast cancer patients," *Clinica Chimica Acta*, vol. 371, no. 1-2, pp. 191–193, 2006.

[40] C. M. Grant and N. Kyprianou, "Epithelial mesenchymal transition (EMT) in prostate growth and tumor progression," *Translational Andrology and Urology*, vol. 2, no. 3, pp. 202–211, 2013.

[41] T. R. Samatov, A. G. Tonevitsky, and U. Schumacher, "Epithelial-mesenchymal transition: focus on metastatic cascade, alternative splicing, non-coding RNAs and modulating compounds," *Molecular Cancer*, vol. 12, article 107, 2013.

[42] S. F. Shariat, M. Shalev, A. Menesses-Diaz et al., "Preoperative plasma levels of transforming growth factor beta1 (TGF-β1 strongly predict progression in patients undergoing radical prostatectomy," *Journal of Clinical Oncology*, vol. 19, no. 11, pp. 2856–2864, 2001.

[43] Y. Matuo, N. Nishi, H. Takasuka et al., "Production and significance of TGF-β in AT-3 metastatic cell line established from the Dunning rat prostatic adenocarcinoma," *Biochemical and Biophysical Research Communications*, vol. 166, no. 2, pp. 840–847, 1990.

[44] D. Tan, X. Wu, M. Hou et al., "Interleukin-6 polymorphism is associated with more aggressive prostate cancer," *Journal of Urology*, vol. 174, no. 2, pp. 753–756, 2005.

[45] D. Giri, M. Ozen, and M. Ittmann, "Interleukin-6 is an autocrine growth factor in human prostate cancer," *American Journal of Pathology*, vol. 159, no. 6, pp. 2159–2165, 2001.

[46] S. F. Shariat, M. W. Kattan, E. Traxel et al., "Association of pre- and postoperative plasma levels of transforming growth factor beta(1) and interleukin 6 and its soluble receptor with prostate cancer progression," *Clinical Cancer Research*, vol. 10, no. 6, pp. 1992–1999, 2004.

[47] A. Voulgari and A. Pintzas, "Epithelial-mesenchymal transition in cancer metastasis: Mechanisms, markers and strategies to overcome drug resistance in the clinic," *Biochimica et Biophysica Acta*, vol. 1796, no. 2, pp. 75–90, 2009.

[48] K. Gravdal, O. J. Halvorsen, S. A. Haukaas, and L. A. Akslen, "A switch from E-cadherin to N-cadherin expression indicates epithelial to mesenchymal transition and is of strong and independent importance for the progress of prostate cancer," *Clinical Cancer Research*, vol. 13, no. 23, pp. 7003–7011, 2007.

[49] S. Sethi, J. Macoska, W. Chen, and F. H. Sarkar, "Molecular signature of epithelial-mesenchymal transition (EMT) in human prostate cancer bone metastasis," *The American Journal of Translational Research*, vol. 3, no. 1, pp. 90–99, 2011.

[50] B. M. Anose, L. Lagoo, and J. Schwendinger, "Characterization of androgen regulation of ZEB-1 and PSA in 22RV1 prostate cancer cells," *Advances in Experimental Medicine and Biology*, vol. 617, pp. 541–546, 2008.

[51] A. J. Armstrong, M. S. Marengo, S. Oltean et al., "Circulating tumor cells from patients with advanced prostate and breast cancer display both epithelial and mesenchymal markers," *Molecular Cancer Research*, vol. 9, no. 8, pp. 997–1007, 2011.

[52] V. V. Lukyanchuk, H. Friess, J. Kleeff et al., "Detection of circulating tumor cells by cytokeratin 20 and prostate stem cell antigen RT-PCR in blood of patients with gastrointestinal cancers," *Anticancer Research*, vol. 23, no. 3, pp. 2711–2716, 2003.

[53] O. Camara, M. Rengsberger, A. Egbe et al., "The relevance of circulating epithelial tumor cells (CETC) for therapy monitoring during neoadjuvant (primary systemic) chemotherapy in breast cancer," *Annals of Oncology*, vol. 18, no. 9, pp. 1484–1492, 2007.

[54] A. Armakolas, Z. Panteleakou, A. Nezos et al., "Detection of the circulating tumor cells in cancer patients," *Future Oncology*, vol. 6, no. 12, pp. 1849–1856, 2010.

[55] Z. Panteleakou, P. Lembessis, A. Sourla et al., "Detection of circulating tumor cells in prostate cancer patients: methodological pitfalls and clinical relevance," *Molecular Medicine*, vol. 15, no. 3-4, pp. 101–114, 2009.

[56] M. Thalgott, B. Rack, T. Maurer et al., "Detection of circulating tumor cells in different stages of prostate cancer," *Journal of Cancer Research and Clinical Oncology*, vol. 139, no. 5, pp. 755–763, 2013.

[57] A. Rolle, R. Günzel, U. Pachmann, B. Willen, K. Höffken, and K. Pachmann, "Increase in number of circulating disseminated epithelial cells after surgery for non-small cell lung cancer monitored by MAINTRAC® is a predictor for relapse: a preliminary report," *World Journal of Surgical Oncology*, vol. 3, article 18, 2005.

[58] K. Pachmann, O. Camara, A. Kavallaris et al., "Monitoring the response of circulating epithelial tumor cells to adjuvant chemotherapy in breast cancer allows detection of patients at risk of early relapse," *Journal of Clinical Oncology*, vol. 26, no. 8, pp. 1208–1215, 2008.

[59] M. Pollak, "Insulin, insulin-like growth factors and neoplasia," *Best Practice and Research: Clinical Endocrinology and Metabolism*, vol. 22, no. 4, pp. 625–638, 2008.

[60] E. J. Gallagher and D. LeRoith, "The proliferating role of insulin and insulin-like growth factors in cancer," *Trends in Endocrinology and Metabolism*, vol. 21, no. 10, pp. 610–618, 2010.

[61] H. Werner and I. Bruchim, "IGF-1 and BRCA1 signalling pathways in familial cancer," *The Lancet Oncology*, vol. 13, no. 12, pp. e537–e544, 2012.

[62] J. M. Chan, M. J. Stampfer, J. Ma et al., "Insulin-like growth factor-I (IGF-I) and IGF binding protein-3 as predictors of advanced-stage prostate cancer," *Journal of the National Cancer Institute*, vol. 94, no. 14, pp. 1099–1106, 2002.

[63] G. O. Hellawell, G. D. H. Turner, D. R. Davies, R. Poulsom, S. F. Brewster, and V. M. Macaulay, "Expression of the type 1 insulin-like growth factor receptor is up-regulated in primary prostate cancer and commonly persists in metastatic disease," *Cancer Research*, vol. 62, no. 10, pp. 2942–2950, 2002.

[64] D. W. Voskuil, A. Bosma, A. Vrieling, M. A. Rookus, and L. J. Van 'T Veer, "Insulin-like growth factor (IGF)-system mRNA quantities in normal and tumor breast tissue of women with sporadic and familial breast cancer risk," *Breast Cancer Research and Treatment*, vol. 84, no. 3, pp. 225–233, 2004.

[65] C. J. Ryan, C. M. Haqq, J. Simko et al., "Expression of insulin-like growth factor-1 receptor in local and metastatic prostate cancer," *Urologic Oncology: Seminars and Original Investigations*, vol. 25, no. 2, pp. 134–140, 2007.

[66] G. Koliakos, D. Chatzivasiliou, T. Dimopoulos et al., "The significance of PSA/IGF-1 ratio in differentiating benign prostate hyperplasia from prostate cancer," *Disease Markers*, vol. 16, no. 3-4, pp. 143–146, 2000.

[67] J. M. Carboni, A. V. Lee, D. L. Hadsell et al., "Tumor development by transgenic expression of a constitutively active insulin-like growth factor I receptor," *Cancer Research*, vol. 65, no. 9, pp. 3781–3787, 2005.

[68] S. A. Rosenzweig and H. S. Atreya, "Defining the pathway to insulin-like growth factor system targeting in cancer," *Biochemical Pharmacology*, vol. 80, no. 8, pp. 1115–1124, 2010.

[69] E. R. King and K.-K. Wong, "Insulin-like growth factor: current concepts and new developments in cancer therapy," *Recent Patents on Anti-Cancer Drug Discovery*, vol. 7, no. 1, pp. 14–30, 2012.

[70] Y. Wang, J. Hailey, D. Williams et al., "Inhibition of insulin-like growth factor-I receptor (IGF-IR) signaling and tumor cell growth by a fully human neutralizing anti-IGF-IR antibody," *Molecular Cancer Therapeutics*, vol. 4, no. 8, pp. 1214–1221, 2005.

[71] F. J. Calzone, E. Cajulis, Y. A. Chung, M. M. Tsai, P. Mitchell, J. Lu et al., "Epitope-specific mechanisms of IGF1R inhibition by ganitumab," *PLoS ONE*, vol. 8, no. 2, Article ID e55135, 2013.

[72] A. G. Papatsoris, M. V. Karamouzis, and A. G. Papavassiliou, "Novel insights into the implication of the IGF-1 network in prostate cancer," *Trends in Molecular Medicine*, vol. 11, no. 2, pp. 52–55, 2005.

[73] M. N. Pollak, E. S. Schernhammer, and S. E. Hankinson, "Insulin-like growth factors and neoplasia," *Nature Reviews Cancer*, vol. 4, no. 7, pp. 505–518, 2004.

[74] P. De Meyts and J. Whittaker, "Structural biology of insulin and IGF1 receptors: implications for drug design," *Nature Reviews Drug Discovery*, vol. 1, no. 10, pp. 769–783, 2002.

[75] C. García-Echeverría, M. A. Pearson, A. Marti et al., "In vivo antitumor activity of NVP-AEW541—a novel, potent, and selective inhibitor of the IGF-IR kinase," *Cancer Cell*, vol. 5, no. 3, pp. 231–239, 2004.

[76] A. Bielen, L. Perryman, G. M. Box et al., "Enhanced efficacy of IGF1R inhibition in pediatric glioblastoma by combinatorial targeting of PDGFRα/β," *Molecular Cancer Therapeutics*, vol. 10, no. 8, pp. 1407–1418, 2011.

[77] A. Arcaro, "Targeting the insulin-like growth factor-1 receptor in human cancer," *Frontiers in Pharmacology*, vol. 4, p. 30, 2013.

[78] J. Abraham, S. I. Prajapati, K. Nishijo et al., "Evasion mechanisms to Igf1r inhibition in rhabdomyosarcoma," *Molecular Cancer Therapeutics*, vol. 10, no. 4, pp. 697–707, 2011.

[79] B. O. Nilsson, L. Carlsson, A. Larsson, and G. Ronquist, "Autoantibodies to prostasomes as new markers for prostate cancer," *Upsala Journal of Medical Sciences*, vol. 106, no. 1, pp. 43–50, 2001.

[80] S. V. Bradley, K. I. Oravecz-Wilson, G. Bougeard et al., "Serum antibodies to Huntingtin interacting protein-1: a new blood test for prostate cancer," *Cancer Research*, vol. 65, no. 10, pp. 4126–4133, 2005.

[81] O. J. Finn, "Immune response as a biomarker for cancer detection and a lot more," *The New England Journal of Medicine*, vol. 353, no. 12, pp. 1288–1290, 2005.

[82] J. E. Hansen, G. Chan, Y. Liu et al., "Targeting cancer with a lupus autoantibody," *Science Translational Medicine*, vol. 4, no. 157, Article ID 157ra42, 2012.

[83] X. Wang, J. Yu, A. Sreekumar et al., "Autoantibody signatures in prostate cancer," *The New England Journal of Medicine*, vol. 353, no. 12, pp. 1224–1235, 2005.

[84] B. S. Reis, A. A. Jungbluth, D. Frosina et al., "Prostate cancer progression correlates with increased humoral immune response to a human endogenous retrovirus GAG protein," *Clinical Cancer Research*, vol. 19, no. 22, pp. 6112–6125, 2013.

[85] H. Zhu, M. Bilgin, and M. Snyder, "Proteomics," *Annual Review of Biochemistry*, vol. 72, pp. 783–812, 2003.

[86] E. Pin, C. Fredolini, and E. F. Petricoin III, "The role of proteomics in prostate cancer research: biomarker discovery and validation. .," *Clinical Biochemistry*, vol. 46, no. 6, pp. 524–538, 2013.

[87] Y. Hathout, "Approaches to the study of the cell secretome," *Expert Review of Proteomics*, vol. 4, no. 2, pp. 239–248, 2007.

[88] B. J. Trock, "Application of metabolomics to prostate cancer," *Urologic Oncology*, vol. 29, no. 5, pp. 572–581, 2011.

[89] M. J. Roberts, H. J. Schirra, M. F. Lavin, and R. A. Gardiner, "Metabolomics: a novel approach to early and noninvasive prostate cancer detection," *Korean Journal of Urology*, vol. 52, no. 2, pp. 79–89, 2011.

[90] L. C. Costello and R. B. Franklin, "Concepts of citrate production and secretion by prostate 1. Metabolic relationships," *Prostate*, vol. 18, no. 1, pp. 25–46, 1991.

[91] V. Kumar, D. K. Dwivedi, and N. R. Jagannathan, "High-resolution NMR spectroscopy of human body fluids and tissues in relation to prostate cancer," *NMR in Biomedicine*, vol. 27, no. 1, pp. 80–89, 2014.

[92] E. A. Struys, A. C. Heijboer, J. van Moorselaar, C. Jakobs, and M. A. Blankenstein, "Serum sarcosine is not a marker for prostate cancer," *Annals of Clinical Biochemistry*, vol. 47, no. 3, p. 282, 2010.

[93] A. Sreekumar, L. M. Poisson, T. M. Rajendiran et al., "Metabolomic profiles delineate potential role for sarcosine in prostate cancer progression," *Nature*, vol. 457, no. 7231, pp. 910–914, 2009.

[94] M. Pavlou and E. P. Diamandis, "The search for new prostate cancer biomarkers continues," *Clinical Chemistry*, vol. 55, no. 7, pp. 1277–1279, 2009.

[95] J. Chen, J. Zhang, W. Zhang, and Z. Chen, "Sensitive determination of the potential biomarker sarcosine for prostate cancer by LC-MS with N, N′-dicyclohexylcarbodiimide derivatization," *Journal of Separation Science*, vol. 37, no. 1-2, pp. 14–19, 2014.

[96] M. G. Swanson, D. B. Vigneron, Z. L. Tabatabai et al., "Proton HR-MAS spectroscopy and quantitative pathologic analysis of MRI/3D-MRSI-targeted postsurgical prostate tissues," *Magnetic Resonance in Medicine*, vol. 50, no. 5, pp. 944–954, 2003.

[97] M. G. Swanson, K. R. Keshari, Z. L. Tabatabai et al., "Quantification of choline- and ethanolamine-containing metabolites in human prostate tissues using1H HR-MAS total correlation spectroscopy," *Magnetic Resonance in Medicine*, vol. 60, no. 1, pp. 33–40, 2008.

[98] T. Kobus, A. J. Wright, E. Weiland, A. Heerschap, and T. W. Scheenen, "Metabolite ratios in H MR spectroscopic imaging of the prostate," *Magnetic Resonance in Medicine*, 2014.

[99] T. Yoneyama, U. Tateishi, T. Terauchi, and T. Inoue, "Correlation of metabolic tumor volume and C-choline uptake with the pathology of prostate cancer: evaluation by use of simultaneously recorded MR and PET images," *Japanese Journal of Radiology*, vol. 32, no. 3, pp. 155–163, 2014.

[100] J. R. Dobosy, J. L. W. Roberts, V. X. Fu, and D. F. Jarrard, "The expanding role of epigenetics in the development, diagnosis and treatment of prostate cancer and benign prostatic hyperplasia," *Journal of Urology*, vol. 177, no. 3, pp. 822–831, 2007.

[101] C. Jerónimo, P. J. Bastian, A. Bjartell et al., "Epigenetics in prostate cancer: biologic and clinical relevance," *European Urology*, vol. 60, no. 4, pp. 753–766, 2011.

[102] T. A. Chan, S. Glockner, M. Y. Joo et al., "Convergence of mutation and epigenetic alterations identifies common genes in cancer that predict for poor prognosis," *PLoS Medicine*, vol. 5, no. 5, article e114, 2008.

[103] T. Wu, E. Giovannucci, J. Welge, P. Mallick, W.-Y. Tang, and S.-M. Ho, "Measurement of GSTP1 promoter methylation in body fluids may complement PSA screening: A meta-analysis," *British Journal of Cancer*, vol. 105, no. 1, pp. 65–73, 2011.

[104] M. Nakayama, C. J. Bennett, J. L. Hicks et al., "Hypermethylation of the human glutathione S-transferase-π gene (GSTP1) CpG island is present in a subset of proliferative inflammatory atrophy lesions but not in normal or hyperplastic epithelium of the prostate: a detailed study using laser-capture microdissection," *The American Journal of Pathology*, vol. 163, no. 3, pp. 923–933, 2003.

[105] L. C. Li, S. T. Okino, and R. Dahiya, "DNA methylation in prostate cancer," *Biochimica et Biophysica Acta*, vol. 1704, no. 2, pp. 87–102, 2004.

[106] H. Enokida, H. Shiina, S. Urakami et al., "Multigene methylation analysis for detection and staging of prostate cancer," *Clinical Cancer Research*, vol. 11, no. 18, pp. 6582–6588, 2005.

[107] K. Kawamoto, S. T. Okino, R. F. Place et al., "Epigenetic modifications of RASSF1A gene through chromatin remodeling in prostate cancer," *Clinical Cancer Research*, vol. 13, no. 9, pp. 2541–2548, 2007.

[108] K. Chiam, C. Ricciardelli, and T. Bianco-Miotto, "Epigenetic biomarkers in prostate cancer: current and future uses," *Cancer Letters*, vol. 342, no. 2, pp. 248–256, 2014.

[109] H. Schwarzenbach, D. S. B. Hoon, and K. Pantel, "Cell-free nucleic acids as biomarkers in cancer patients," *Nature Reviews Cancer*, vol. 11, no. 6, pp. 426–437, 2011.

[110] D. B. Seligson, S. Horvath, T. Shi et al., "Global histone modification patterns predict risk of prostate cancer recurrence," *Nature*, vol. 435, no. 7046, pp. 1262–1266, 2005.

[111] H. Valadi, K. Ekström, A. Bossios, M. Sjöstrand, J. J. Lee, and J. O. Lötvall, "Exosome-mediated transfer of mRNAs and microRNAs is a novel mechanism of genetic exchange between cells," *Nature Cell Biology*, vol. 9, no. 6, pp. 654–659, 2007.

[112] K. Wang, S. Zhang, J. Weber, D. Baxter, and D. J. Galas, "Export of microRNAs and microRNA-protective protein by mammalian cells," *Nucleic Acids Research*, vol. 38, no. 20, pp. 7248–7259, 2010.

[113] J. C. Brase, D. Wuttig, R. Kuner, and H. Sültmann, "Serum microRNAs as non-invasive biomarkers for cancer," *Molecular Cancer*, vol. 9, article 306, 2010.

[114] R. J. Bryant, T. Pawlowski, J. W. F. Catto et al., "Changes in circulating microRNA levels associated with prostate cancer," *British Journal of Cancer*, vol. 106, no. 4, pp. 768–774, 2012.

[115] P. P. Osin and S. R. Lakhani, "The pathology of familial breast cancer. Immunohistochemistry and molecular analysis," *Breast Cancer Research*, vol. 1, no. 1, pp. 36–40, 1999.

[116] L. M. Berstein, "Endocrinology of the wild and mutant BRCA1 gene and types of hormonal carcinogenesis," *Future Oncology*, vol. 4, no. 1, pp. 23–39, 2008.

[117] H. Eerola, P. Heikkilä, A. Tamminen, K. Aittomäki, C. Blomqvist, and H. Nevanlinna, "Relationship of patients' age to histopathological features of breast tumours in BRCA1 and BRCA2 and mutation-negative breast cancer families," *Breast Cancer Research*, vol. 7, no. 4, pp. R465–R469, 2005.

[118] C. M. Barnett, M. C. Heinrich, J. Lim, D. Nelson, C. Beadling, A. Warrick et al., "Genetic Profiling to Determine Risk of Relapse Free Survival in High-risk Localized Prostate Cancer," *Clinical Cancer Research*, vol. 20, no. 5, pp. 1306–1312, 2013.

[119] J. R. Schoenborn, P. Nelson, and M. Fang, "Genomic profiling defines subtypes of prostate cancer with the potential for therapeutic stratification," *Clinical Cancer Research*, vol. 19, no. 15, pp. 4058–4066, 2013.

[120] B. D. Hudson, K. S. Kulp, and G. G. Loots, "Prostate cancer invasion and metastasis: insights from mining genomic data," *Briefings in Functional Genomics*, vol. 12, no. 5, pp. 397–410, 2013.

[121] A. Amaro, A. I. Esposito, A. Gallina, M. Nees, G. Angelini, A. Albini et al., "Validation of proposed prostate cancer biomarkers with gene expression data: a long road to travel," *Cancer and Metastasis Reviews*, 2014.

Hindawi Publishing Corporation
BioMed Research International
Volume 2014, Article ID 781340, 8 pages
http://dx.doi.org/10.1155/2014/781340

Review Article

Hypofractionation in Prostate Cancer: Radiobiological Basis and Clinical Appliance

M. Mangoni,[1] I. Desideri,[1] B. Detti,[1] P. Bonomo,[1] D. Greto,[1] F. Paiar,[1] G. Simontacchi,[1] I. Meattini,[1] S. Scoccianti,[1] T. Masoni,[1] C. Ciabatti,[1] A. Turkaj,[1] S. Serni,[2] A. Minervini,[2] M. Gacci,[2] M. Carini,[2] and L. Livi[1]

[1] *Radiotherapy Unit, Department of Experimental and Clinical Biomedical Sciences, University of Florence, Largo Brambilla 3, 50134 Firenze, Italy*
[2] *Urology Unit, Department of Experimental and Clinical Medicine, University of Florence, 50134 Florence, Italy*

Correspondence should be addressed to M. Mangoni; m.mangoni@dfc.unifi.it

Received 1 March 2014; Accepted 6 April 2014; Published 30 April 2014

Academic Editor: Giovanni Luca Gravina

External beam radiation therapy with conventional fractionation to a total dose of 76–80 Gy represents the most adopted treatment modality for prostate cancer. Dose escalation in this setting has been demonstrated to improve biochemical control with acceptable toxicity using contemporary radiotherapy techniques. Hypofractionated radiotherapy and stereotactic body radiation therapy have gained an increasing interest in recent years and they have the potential to become the standard of care even if long-term data about their efficacy and safety are not well established. Strong radiobiological basis supports the use of high dose for fraction in prostate cancer, due to the demonstrated exceptionally low values of α/β. Clinical experiences with hypofractionated and stereotactic radiotherapy (with an adequate biologically equivalent dose) demonstrated good tolerance, a PSA control comparable to conventional fractionation, and the advantage of shorter time period of treatment. This paper reviews the radiobiological findings that have led to the increasing use of hypofractionation in the management of prostate cancer and briefly analyzes the clinical experience in this setting.

1. Introduction

Prostate cancer represents the most common male cancer diagnosed in Western countries after nonmelanomatous skin cancer [1]. Since in most cases the prostate cancer at diagnosis is organ confined [2], radical prostatectomy and definitive radiotherapy are the accepted standard for treating the vast majority of prostate cancer cases. External beam radiation therapy (EBRT) is the most diffused radiotherapy treatment modality for treating patients with prostate cancer. A conformal delivery of treatment is ideally adopted in order to spare as much as possible the amount of radiation received by the surrounding normal tissues. Nowadays, conventionally fractionated radiation therapy (CFRT, a single 1.8–2.0 Gy fraction lasting one hour per day, five days per week, for about eight weeks) to a total dose of 76–80 Gy represents the most adopted treatment modality. Dose escalation in this setting has been demonstrated to improve biochemical control with acceptable toxicity using contemporary radiotherapy techniques [3, 4]. CFRT schemes employing fraction sizes of 1.8–2.0 Gy are based upon the premise that tumors typically are less responsive to fraction size than are late responding normal tissues. The α/β ratio is a measure of fractionation response, with low ratios (high α/β's) associated with late responding normal tissues. A low α/β is consistent with a greater capacity for repair between fractions, with an accompanying greater relative sparing with small fraction sizes, than for tumors with their typically higher α/β ratios. Under these conditions, an improved therapeutic ratio is achieved with multiple small fractions for most types of tumors. The α/β ratios are thought to be associated with tumors; however, they are typically 8 or greater, whereas for late responding normal tissues, values on the order of 3 or 4 or somewhat less are suggested from the analyses of

numerous experimental and some clinical outcome studies. There appear to be exceptions to such typical tumor response to fractionation, however. Growth fraction (or effective cell cycle time) has often been associated with fractionation response, with slowly proliferating normal tissues (and some slowly proliferating tumors) generally displaying stronger than expected fraction size responses (low α/β ratios).

Hypofractionated radiotherapy (HFRT, a single 2.1–3.5 Gy fraction, five days per week, for around four weeks) has gained a considerable interest in recent years. Stereotactic body radiation therapy (SBRT, a single 3.5–15.0 Gy fraction, five days per week, for about two weeks) has been recently an object of increasing interest in the scientific community due to the technical improvements that have made possible the delivery of larger radiation fraction size; thus, it has the potential to become the standard of care even if long-term data about its efficacy and safety are not well established.

The aim of this paper is to review the radiobiological findings that have led to the increasing use of hypofractionation in the management of prostate cancer and briefly analyze the clinical experience in this setting.

2. Radiobiological Basis of Hypofractionation

Considerable efforts are being devoted at the present time to the improvement of radiotherapy and there is no doubt that radiobiology has been very fruitful in the generation of new ideas and in the identification of potentially exploitable mechanisms. In the last years improvements in biological knowledge have changed several aspects of radiobiology. About 40 years ago, Thames and Withers largely studied the influence of dose per fraction on response. In each study and for each chosen dose per fraction the total radiation dose (isoeffective dose) that produced some defined level of damage to the normal tissue or to the tumor was determined [5, 6]. The relationships between total dose and dose per fraction for acutely responding tissues (i.e., high-turnover tissues), late responding tissues (low or no turnover), and tumours provided the basic information required to optimize radiotherapy according to the dose per fraction and number of fractions. Those pioneering studies showed that the isoeffective total dose increased more rapidly with decreasing dose per fraction for late effect than for acute effect, which indicates a greater sensitivity of late responses to changes in dose per fraction (Figure 1). The relationship between total isoeffective dose and the dose per fraction in fractionated radiotherapy can be described using the linear-quadratic (LQ) cell survival model [LQ: $\ln S = \alpha d - \beta d^2$] [7], that is, the standard model for calculating isoeffects in the range of conventional dose per fraction [8]. The steepness and curvature of isoeffective lines are determined by α/β ratio. At the present time it is strongly recommended that the LQ model should always be used, with a correctly chosen α/β ratio, to describe isoeffect dose relationships at least over the range of doses per fraction between 1 and 5 Gy [9–11]. The renewed interest for hypofractionation has raised the problem of the need to adapt LQ model to higher dose per fraction because clinically the LQ model often underestimates tumor control observed at radiosurgical doses [12]. However, recent papers conclude that the available data do not support a need to change the LQ model at large dose per fraction, if α/β ratio is selected appropriately [8, 13]. A possible explanation for the difference in shape of dose-response relationships for early and late responding tissues is the different distribution of the cells through the cycle. The radiosensitivity of a population of cells varies with the distribution of cells through the cycle, with a greater radioresistance in the late phase S, in the early G_1, and in the quiescence phase G_0 [14]; likely many late responding normal tissues are resistant owing to the presence of many not-proliferating cells that are resting in G_0. Early responding tissues that proliferate quickly can have a part of cell in a radioresistant phase, but the redistribution through all the phases of the cell cycle allows the cells to be in more sensitive phases at the next fraction of radiation. At the same time, the fast proliferation itself is a form of resistance that increases the total number of cells to kill. Repopulation occurring during a protracted, fractionated regimen helps to spare normal tissues but is a potential danger for the control of tumor. If the overall duration of fractionated radiotherapy is increased, there will usually be greater repopulation of the irradiated tissues, both in the tumor and in early-reacting normal tissues. To counteract proliferation of tumor cells, an extra dose is needed. The proliferation is relevant in mouse skin about 2 weeks after the start of daily fractionation. The longer cell cycle of human cells makes proliferation evident after a longer period [15, 16]. As overall time increases, a greater total dose had been required to control tumors that show an accelerated repopulation of clonogenic tumor cells at some point during fractionated radiotherapy. In head and neck cancers, for treatment times longer than 4 weeks, the effect of proliferation is equivalent to a loss of radiation dose of about 0,48–0.6 Gy/day [17, 18]. Prolonging overall time within the normal radiotherapy range has a large sparing effect on early reactions but little sparing effect on late reactions, because the time at which extra dose is required to counteract proliferation in late responding tissues in humans is far beyond the overall time of any normal radiotherapy regimen [19]. Thus, in acute responding tissues fraction size and overall treatment time both determine the effect; instead for late responding tissues fraction size is the dominant factor in determining the radiation-induced effect. Acute and late responding tissues are usually differentiated on the basis of different alpha beta value, with high alpha beta (in the range of 7–20 Gy) for acute responding tissues and low alpha beta, generally in the range of 0.5–6 Gy, for late responding tissues. It is common practice to apply to tumors the same alpha beta of acute responding tissues of approximately 10 Gy [20, 21]. However there is evidence that some human tumor types exhibit low alpha beta ratios and also breast and early stage prostate cancer [22, 23], perhaps with alpha beta ratios even lower than for late normal tissue reaction. This can be due not only to different tumor characteristics but also to cell variability into the tumor or uncontrolled confounding factors, such as the presence of tumor hypoxia, repopulation, or patient-to-patient variability.

As Withers wrote in 1985 "conventional is commonly not universally correct, and so with dose fractionation in

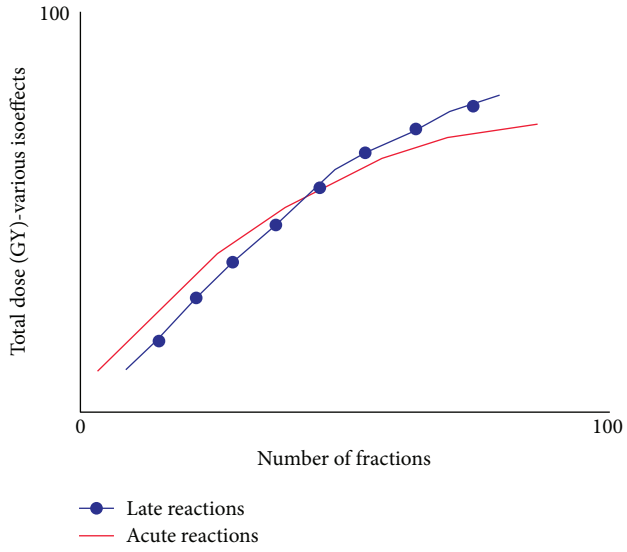

Figure 1: (Based on data from Withers and Thames [5, 6]) the steepness and curvature of these lines are determined by the α/β ratio. The graph indicates a greater sensitivity of late responses to changes in dose per fraction: using lower doses per fraction tends to spare late reactions.

radiotherapy" [5]. The heterogeneity of cancer cells and cancer types and the importance of overall treatment time make altered fractionation more useful in selected cases.

3. Brief History of Radiobiological Hypothesis Concerning α/β of Prostate Cancer

In radiobiology, the α/β ratio is used to estimate the effects of radiation on various tissues and compare various dose and fractionation schemes. The α/β ratio is estimated to be >10 Gy for early-responding tissues (e.g., skin, mucosa, and most tumors) and 3–5 Gy for late responding tissues (e.g., connective tissue, bladder/rectal mucosa, and muscles). In 1999 Brenner and Hall [10] promoted the hypothesis that prostate tumors have exceptionally low values of α/β. They derived an α/β ratio of 1.5 Gy with a 95% confidence interval of 0.8 to 2.2 Gy, based on 367 patients from two treatment centers. Their assumption stems from the documented result that similar biochemical long-term control is achieved using EBRT doses of about 70 Gy in 1.8–2.0 Gy fractions but using 145 Gy from permanent iodine-125 (I125) low-dose-rate (LDR) irradiation. In 2001, Fowler et al. [24] updated this analysis with 1020 patients from 11 centers and came to the same result of $\alpha/\beta = 1.5$ Gy, with a narrower confidence interval (1.25–1.75 Gy). These ranges of values were confirmed in a 2012 paper by Miralbell et al. [25] where a retrospective study was performed on nearly 6,000 prostate cancer patients from seven international institutional primary datasets treated with EBRT stratified by risk groups and androgen deprivation status. A direct analysis of 5-year biochemical relapse–free survival (bRFS) data with the linear-quadratic (LQ) model was implemented to estimate the dose fractionation sensitivity for this group of patients. Since the initial hypothesis about a low α/β for prostate cancer derived from brachytherapy data, a specific concern was expressed toward the fact that neither Brenner and Hall [10] nor Fowler et al. [24] assumed that repopulation in the tumors was significant during low-dose-rate treatment with I125. Wang et al. [26] and Kal and van Gellekom [27] took in account the effect of tumor repopulation in their work to derive LQ parameters for prostate cancer: all authors postulated that this effect is not negligible for the accurate description of the radiation therapy of prostate. This consideration caused a 23% reduction of I125 dose from 145 to 112 Gy and resulted in an estimate of α/β = 3-4 Gy instead of the previously derived 1.5 Gy. Furthermore, the work of Brenner and Hall [10] was questioned by King and Mayo [28] because of its extremely low radiosensitivity ($\alpha = 0.036\ \text{Gy}^{-1}$). Such a low α value leads to excessively low clonogenic cell numbers (in the range of 10 to 100); the authors proposed that a solid tumor would consist of a heterogeneous population of clonogens with a spectrum of radiosensitivities. Recently, Pedicini et al. [29] proposed a method to estimate intrinsic radiosensitivity (α), fractionation sensitivity (α/β), repopulation doubling time, number of clonogens, and kick-off time for accelerated repopulation of prostate cancer. They confirmed a low value of α/β, 2.96 Gy (95% CI 2.41–3.53 Gy), with a correspondingly high value of intrinsic radiosensitivity, $0.16\ \text{Gy}^{-1}$ (95% CI $0.14–0.18\ \text{Gy}^{-1}$), a realistic average number of clonogens, a long kick-off time for accelerated repopulation, and a surprisingly fast repopulation that suggests the involvement of subpopulations of specifically tumorigenic stem cells during continuing radiation therapy.

Finally it should be noted that all the above calculations agreed on a small value of α/β, providing an attracting rationale to utilize HFRT in prostate cancer.

4. Clinical Experiences Involving HFRT

Zaorsky et al. [30] recently published an extensive review concerning the history of HFRT. As stated by the authors, the first initial retrospective experience reported about the use of HFRT came from the UK. Over 200 patients were treated at St. Thomas Hospital in London with hypofractionated radiotherapy to a dose of 55 Gy in 12 fractions and later to doses of 36 Gy in 6 fractions with low rectal and urological complications [31, 32]. The trial included men with early (T1-T2) and advanced (T3-T4) disease that were treated by external beam radiotherapy. Depending on anatomy, patients were treated with 3-field, 4-field, or a double rotation technique from a cobalt-60 machine or linear accelerator.

One of the first phase III prospective randomized controlled trials (RCTs) comparing CFRT and HFRT was published by Lukka et al. [33] in 2005: in this trial a conventional dose of 66 Gy in 33 fractions was compared to a hypofractionated regimen of 52.5 Gy in 20 fractions (dose per fraction = 2.625 Gy) in more than 900 men with low and intermediate risk prostate cancer. Surprisingly, the 5-year rate of failure (both biochemical and clinical) was higher in the hypofractionated arm compared to the standard fractionation arm (60% versus 53%, $P < 0.05$). The worse outcome reported in

the hypofractionated arm may be explained by the fact that, for any α/β ratio >0.2, the biologically equivalent dose (BED) of 52.5 Gy in 20 fractions is expected to be lower than the BED of 66 Gy in 33 fractions. At a median followup of 5.7 years, no difference in 5-year actuarial rate of late grade 3 or higher gastrointestinal or genitourinary toxicity was observed between the two arms. Subsequently, Yeoh et al. [34, 35] reported that opposite results regarding 217 patients with T1-2 prostate carcinomas were randomized to either a CFRT or a HFRT arm between 1996 and 2006. Treatments were predominantly four-field box technique with customized blocks using 6–23 MV photons. Patient in the CFRT arm received a modest dose of 64 Gy in 32 fractions, while patients in the HFRT arm received a total dose of 55 Gy in 20 treatments. The study population was represented by men with favorable-risk prostate cancer. At a median followup of 90 months, biochemical relapse-free survival (bRFS) was significantly better with hypofractionation when Phoenix definition was used (53% versus 34%, $P < 0.5$). The contrary results reported by these two studies may be caused by a different number of reasons: first, no specific assumptions about the α/β ratio before the beginning of both trials. Second, the total dose of the CFRT arms was 66 Gy and 64 Gy, respectively, which is considerably lower than more contemporary conventional doses of 78–80 Gy utilized nowadays [3]. Finally, a different definition of biochemical failure (BF) was utilized in the two studies: while the Lukka et al. study [33] used mainly the ASTRO definition [18] (3 consecutive PSA rises), Yeoh et al.'s study [34, 35] used the ASTRO and Phoenix [36, 37] (nadir + 2 ng/mL) definitions.

After the publication of these initial RCTs comparing CFRT and HFRT, modern prospective phase III superiority trials were initiated based on the assumption that the α/β ratio for prostate cancer is 1.5 Gy. Dose escalation studies [38–45] have been utilized to determine the standard of care in determining the optimal CFRT schedule. Dearnaley et al. [38] conducted a pilot for a phase III trial randomising 64 Gy versus 74 Gy and reported 5-year biochemical control rates of 59% (standard dose) and 71% (escalated dose) (hazard ratio 0.64, 95% CI 0.38–1.10, $P = 0.10$) with acceptable acute and late toxicity [27]. The subsequent MRC RT01 trial [39] randomised 862 men to the same fractionation regimens and found that at 6 months after radiotherapy grade 2 or higher toxicity was low [28]. However almost all of this toxicity was seen in the group receiving 74 Gy. In both arms the radiotherapy was given in conjunction with androgen deprivation. This trial did also confirm an increase in biochemical progression-free survival (60% with the lower dose and 71% with the higher dose at 5-year followup, hazard ratio of 0.67 for clinical progression in the higher dose arm, CI 0.53–0.85, $P = 0.0007$) and metastasis-free survival, in addition to a reduction in need for salvage androgen suppression. Kupelian et al. [40] pooled the data from nine institutions totaling over 4800 men. Despite the higher dose cohort (>72 Gy) having worse prognostic features, their 5-year biochemical disease-free survival (bDFS) was significantly improved compared to the cohort who received <72 Gy [29]. Pollack et al. [41] conducted a phase 3 trial comparing 70 Gy to 78 Gy without androgen deprivation and found a significant improvement in freedom from failure (including biochemical failure) in the higher dose group (freedom from failure at 6 years: 64% versus 70%, $P = 0.03$ [30]. This included a reduction in the incidence of distant metastasis in the subgroup of patients with a PSA >10 ng/mL at 6 years of followup. However this trial also confirmed an increase in rectal side effects in the higher dose arm (grade 2 or higher toxicity: 26% versus 12%). This trial was conducted in the era before image-guided radiotherapy (IGRT) and intensity-modulated radiotherapy (IMRT) were standard and hence higher doses are likely to be deliverable with less toxicity today. Peeters et al. [42] also conducted a dose escalation trial randomizing 664 men 68 Gy or 78 Gy. The higher dose was associated with a 10% increase in freedom from failure at 5 years (HR 0.74, $P = 0.02$) [31]. Zelefsky et al. [43] reported their experience of treating over 2000 men between 1998 and 2004 in a nonrandomised observational study. They found that increasing dose was associated with better disease control for intermediate and high-risk patients but did not find a statistically significant association with the low-risk patients. Most patients in this study received neoadjuvant hormone therapy.

Arcangeli et al. [44–46] compared HFRT versus CFRT in patients with high-risk prostate cancer. The purpose of this study was to compare the toxicity and efficacy of hypofractionated (62 Gy/20 fractions/5 weeks, 4 fractions per week) versus conventional fractionation radiotherapy (80 Gy/40 fractions/8 weeks). From January 2003 to December 2007, 168 patients were randomized to receive either hypofractionated or conventional fractionated schedules of three-dimensional conformal radiotherapy to the prostate and seminal vesicles. All patients received a 9-month course of total androgen deprivation. There was no reported difference in late toxicity at five years between the two schedules. The 3-year freedom from biochemical failure (FFBF) rates was 87% and 79% in the hypofractionation and conventional fractionation groups, respectively ($P = 0.035$). The authors concluded that, with equivalent late toxicity between the two treatment groups, the hypofractionated treatment resulted in better PSA control. Kuban et al. [47] reported on the preliminary outcome and toxicity of a phase III RCT which based the treatment regimens on maintaining equivalent acute toxicities while delivering a higher BED to the prostate. They randomized 102 men to receive CFRT (BED at α/β of 3 = 121) to a dose of 75.6 Gy in 42 fractions and 102 men to receive HFRT (BED at α/β of 3 = 130) to a dose of 72 Gy in 30 fractions. The 5-year Phoenix FFBF rates were 92% and 96% (not statistically significant), respectively, and no patient had a clinical failure. Finally, Pollack et al. [48] recently reported the results of the RCT they conducted. Between June 2002 and May 2006, men with favorable- to high-risk prostate cancer were randomly allocated to receive 76 Gy in 38 fractions at 2.0 Gy per fraction (CFRT) versus 70.2 Gy in 26 fractions at 2.7 Gy per fraction (HFRT). High-risk patients received long-term androgen deprivation therapy (ADT), and some intermediate-risk patients received short-term ADT. There were no statistically significant differences in late toxicity between the arms; however, in subgroup analysis, patients with compromised urinary function before enrollment had significantly worse urinary function after

HFRT. No differences were observed in the two arms in terms of BF or any other type of failure. The authors concluded that even if HFRT did not result in a significant reduction in any type of failure (biochemical and clinical) it is delivered in 2.5 fewer weeks. Men with compromised urinary function before treatment may not be ideal candidates for HFRT. Other RCTs are currently ongoing. RTOG 0415 is a phase III RCT with fractionation schedules similar to the regimen of phase I/II trial by Kupelian et al. [49]. If the a/b ratio for prostate cancer is closer to 10, the trial will demonstrate equivalence between the fractionation regimens; if it is closer to 1.5, the HFRT schedule should produce better rates of biochemical control. While phase I and phase II portions of the CHHiP trial [50] have estimated toxicity, the UK Medical Research Council (MRC) phase III noninferiority study will include over 3000 patients in a 3-arm design to extrapolate the isoeffective dose for complications and address whether HFRT is equivalent to CFRT. The NCIC trial is a noninferiority trial that compares 78 Gy in 2 Gy fractions to 60 Gy in 3 Gy fractions. Its goal is to demonstrate the safety and efficacy of HFRT and evaluate it as a replacement for CFRT.

HDR brachytherapy has been historically used as a form of hypofractionation for treating men affected by prostate cancer. Using this technique, fractionation regimens of 48 Gy in 8 fractions or 54 Gy in 9 fractions over 5 days have demonstrated 70% PSA failure-free survival at 5 years, despite the majority of these patients having high-risk disease [51]. Relapse-free survival at 3 years was 100% for the low-risk patients included in this study. Five percent of patients had grade 3 acute GU toxicity and 21% had grade 2 acute GU toxicity. With regard to late toxicity, one patient had a grade 3 GI toxicity and 11% had grade 2 GU toxicity. Yoshioka et al. updated their results in 2010 and had treated 112 men with 54 Gy in 9 fractions with HDR brachytherapy [52]. The majority of these patients had high-risk disease and also received androgen deprivation therapy (ADT). Overall 5-year bRFS was 83%. This was achieved with 5% acute and 3% late grade 3 toxicity. Another cohort of 117 consecutive patients was treated with escalating doses of 6 fractions HDR from 36 Gy to 43.5 Gy, delivered in 2 insertions one week apart [53]. They report excellent 8-year bRFS of 94% for this group of low- and intermediate-risk prostate cancer patients. Four (3%) patients had grade 3 late urinary toxicity. Recently Demanes et al. have described their experience of treating 298 men with mostly low- and low-intermediate-risk prostate cancer [54]. Approximately half were treated with 36 Gy in six Gy fractions, and the others received 4 fractions of 9.5 Gy over 2 days. The 8-year bRFS was 97%. The grade 3 GU toxicity was 5% overall, 24% grade 2, but this was scored per event, not per patient, and hence the same patient with more than one symptom would be scored multiple times. Late GI toxicity was <1%. Mount Vernon Hospital has published outcomes for a group of men, some with locally advanced prostate cancer [55]. This was a dose escalation study so the first cohort received 34 Gy in 4 fractions over 3 days, the second cohort 36 Gy, and the third cohort 31.5 Gy in 3 fractions over 2 days. Only 25–31% patients had grade 1 or more toxicity at six months and two patients had grade 3 toxicity.

5. Clinical Experiences Involving the Use of SBRT for the Treatment of Prostate Cancer

SBRT in the management of prostate cancer constitutes a relatively new option. So far, only phases I-II studies have been published regarding its use, even if phase III trials are currently ongoing [56]. The first prospective trial of SBRT for prostate cancer was published by Madsen et al. [57], who treated 40 patients with SBRT using a daily dose of 6.7 Gy to a total dose of 33.5 Gy (6.7 Gy for 5 fractions). The fractionation schedule was calculated to be equivalent to 78 Gy in 2 Gy fractions using an estimated α/β ratio of 1.5. At the median followup of 41 months, there were no instances of grade 3 gastrointestinal toxicity and only a single episode of acute grade 3 genitourinary toxicity. There was no grade 3 or higher late toxicities. The PSA control rate was 90% by the Phoenix definition [37]. Tang et al. [58, 59] treated 30 men in a phase I/II study. The eligible men had low-risk prostate cancer and received 5 weekly doses of 7 Gy to a total dose of 35 Gy. The SBRT technique consisted of intensity-modulated radiotherapy (IMRT) with daily image guidance using implanted gold fiducials. All patients had at least 6 months of followup. The treatments were well tolerated and there was no grade 3 or 4 GI/GU toxicity. Although there were initial grade 2 toxicities (13% GU and 7% GI), these scores returned to or improved over baseline at 6 months. The biochemical control after 18 months was 100%. Katz et al. [60, 61] reported an experience of SBRT treatment given to 304 patients with clinically localized prostate cancer. Most received 5 fractions of 7.25 Gy (total dose 36.25 Gy). At a median followup of 40 months (range of 9–58 months), 10 patients died of other causes and 9 were lost to followup. The 4-year actuarial freedom from biochemical failure is 98.5%, 93.0%, and 75%, for the low-, intermediate-, and high-risk groups. Late toxicity included 4.2% RTOG grade 2 GI toxicity, 7.8% GU toxicity and 1.4% grade 3 GU toxicity. Freeman and King [62] report their experience of treating 41 low-risk prostate cancer patients with 35–36.25 Gy in 5 fractions [9]. None received adjuvant hormonal therapy. At a median followup of 5 years the biochemical relapse-free survival was 93%. There has been no grade 3 or higher rectal toxicity. One patient experienced grade 3 GU toxicity after repeated instrumentation. 32% and 16% experienced grade 1-2 late GU and GI toxicity, respectively. King et al. have also published their experience of treating 67 men with low-risk prostate cancer [63]. Patients were treated to a dose of 36.25 Gy in 5 fractions using CyberKnife and median followup was 2.7 years. The 4-year bRFS was 94%. Importantly, they clearly showed that alternate day treatment significantly reduces the chance of GU and GI toxicity compared with daily hypofractionated regimens and recommend that this should be the regimen of choice. Towsend et al. [64] reported an analysis of the first 50 patients treated with CyberKnife radiotherapy for prostate cancer. Most patients were affected with early to intermediate stage prostate cancer. Two patients had metastatic disease at presentation and were excluded. A total of 37 patients received irradiation at a dose of 35 to 37.5 Gy in 5 fractions of 7 to 7.5 Gy per fraction. Assuming an alpha/beta ratio of 1.5 Gy, this process delivered an equivalent dose of 85 to 96 Gy

Table 1: SBRT efficacy in selected experiences.

Study	Fractionation	Stage	Low risk	High risk	5 yr bRFS
Townsend et al. 2011 [64] 48 patients (37 monotherapy, 11 boost)	35–37.5 Gy in 5 fractions (boost 17.6–25 Gy in 2–5 fractions)	69% T1			Not reported
King et al. 2012 [63] 67 patients	36.25 Gy in 5 fractions	T1c or T2a/b	100%	None	4-year bRFS 94%
Freeman and King 2011 [62] 41 patients	35–36.35 Gy in 5 fractions	Low risk		None	93%
Katz et al. 2010 [61] 304 patients	35–36.25 Gy in 5 fractions	92% T1c	70%	4%	1.3% failed so far (17–30 month FU)
Madsen et al. 2007 [57] 40 patients	33.5 Gy in 5 fractions	T1c or T2a	100%	None	48 month bRFS 90%
Tang et al. 2008 [58] 124 patients	33.5 Gy in 5 fractions	T1c or T2a	100%	None	2 years: 90%

Abbreviations: bRFS: biochemical relapse-free survival.

in 2 Gy fractions (EQD2). A subset of patients ($n = 11$) received standard linear accelerator-based pelvic radiation treatment either by intensity-modulated radiation therapy or by tomotherapy and received a boost via the CyberKnife at a dose of 17.6 to 25 Gy in 2 to 5 fractions (EQD2 = 46.6–72 Gy). The mean pretreatment prostate specific antigen and Gleason scores were 9.16 ng/mL and 7, respectively. Grade 2 acute genitourinary toxicity was reported by 10% of patients ($n = 5$). Only 3 patients reported grade 3 acute genitourinary toxicity. No gastrointestinal grade 2 or grade 3 toxicities were reported. Table 1 summarizes the reported efficacy of SBRT in the abovementioned papers.

So far the results of SBRT studies are very encouraging and stress the potential of SBRT in the management of certain patients with prostate cancer. However all the toxicity data gathered so far come from single-centers experience and are often compared with older radiotherapy technique that did not use state-of-the-art technology such as IMRT or image-guided radiotherapy (IGRT). More solid evidences will be available with the currently ongoing phase III trials (NCT01584258—PACE Study, ISRCTN45905321—Scandinavian HYPO).

6. Conclusions

Nowadays EBRT constitutes an established treatment modality for almost all prostate cancer patients. Determining the optimal fractionation scheme has been one of the goals of radiation oncologists. Most of the evidence provided in the last decade by specialized literature about prostate cancer radiosensitivity supports the hypothesis that prostate tumor has an extremely low α/β ratio, thus encouraging the adoption of hypofractionated schedules in this setting. There is a growing body of compelling evidence supporting the safety and efficacy of abbreviated radiotherapy schedules for prostate cancer. So far results of RCTs comparing HFRT and CFRT have been puzzling due to a different number of factors (different doses, radiation techniques, and contouring policies). Results obtained from short-term SBRT have been promising so far, but longer followup and phase III trials are warranted.

Conflict of Interests

The authors declare that there is no conflict of interests regarding the publication of this paper.

References

[1] A. Jemal, F. Bray, M. M. Center, J. Ferlay, E. Ward, and D. Forman, "Global cancer statistics," *CA: A Cancer Journal for Clinicians*, vol. 61, no. 2, pp. 69–90, 2011.

[2] F. H. Schroder, J. Hugosson, M. J. Roobol et al., "Screening and prostate-cancer mortality in a randomized european study," *The New England Journal of Medicine*, vol. 360, no. 13, pp. 1320–1328, 2009.

[3] D. A. Kuban, S. L. Tucker, L. Dong et al., "Long-term results of the M. D. Anderson randomized dose-escalation trial for prostate cancer," *International Journal of Radiation, Oncology, Biology Physics*, vol. 70, no. 1, pp. 67–74, 2008.

[4] A. L. Zietman, K. Bae, J. D. Slater et al., "Randomized trial comparing conventional-dose with high-dose conformal radiation therapy in early-stage adenocarcinoma of the prostate: long-term results from Proton Radiation Oncology Group/American College Of Radiology 95-09," *Journal of Clinical Oncology*, vol. 28, no. 7, pp. 1106–1111, 2010.

[5] H. R. Withers, "Biologic basis for altered fractionation schemes," *Cancer*, vol. 55, supplement 9, pp. 2086–2095, 1985.

[6] H. D. Thames Jr., H. R. Withers, L. J. Peters, and G. H. Fletcher, "Changes in early and late radiation responses with altered dose fractionation: implications for dose-survival relationships," *International Journal of Radiation, Oncology, Biology Physics*, vol. 8, no. 2, pp. 219–226, 1982.

[7] J. F. Fowler, "The linear-quadratic formula and progress in fractionated radiotherapy," *British Journal of Radiology*, vol. 62, no. 740, pp. 679–694, 1989.

[8] F. McKenna and S. Ahmad, "Isoeffect calculations with the linear quadratic and its extensions: an examination of model-dependent estimates at doses relevant to hypofractionation," *Journal of Medical Physics*, vol. 36, no. 2, pp. 100–106, 2011.

[9] S. L. Tucker, H. D. Thames, J. M. Michalski et al., "Estimation of α/β for late rectal toxicity based on RTOG 94-06," *International Journal of Radiation, Oncology, Biology Physics*, vol. 81, no. 2, pp. 600–605, 2011.

[10] D. J. Brenner and E. J. Hall, "Fractionation and protraction for radiotherapy of prostate carcinoma," *International Journal of Radiation, Oncology, Biology Physics*, vol. 43, no. 5, pp. 1095–1101, 1999.

[11] D. J. Carlson, R. D. Stewart, X. A. Li, K. Jennings, J. Z. Wang, and M. Guerrero, "Comparison of *in vitro* and *in vivo* α/β ratios for prostate cancer," *Physics in Medicine and Biology*, vol. 49, no. 19, pp. 4477–4491, 2004.

[12] J. P. Kirkpatrick, J. J. Meyer, and L. B. Marks, "The linear-quadratic model is inappropriate to model high dose per fraction effects in radiosurgery," *Seminars in Radiation Oncology*, vol. 18, no. 4, pp. 240–243, 2008.

[13] J. M. Brown, D. J. Carlson, and D. J. Brenner, "The tumor radiobiology of SRS and SBRT: are more than the 5 Rs involved ?" *International Journal of Radiation, Oncology, Biology Physics*, vol. 88, no. 2, pp. 254–262, 2014.

[14] H. R. Withers, "The four R's of radiotherapy," in *Advances in Radiation Biology*, J. T. Lett and H. Adler, Eds., vol. 5, pp. 241–271, Academic Press, New York, NY, USA, 1975.

[15] J. Denekamp, "Changes in the rate of repopulation during multifraction irradiation of mouse skin," *British Journal of Radiology*, vol. 46, no. 545, pp. 381–387, 1973.

[16] J. F. Fowler, "Fractionated radiation therappy after Strandqvist," *Acta Radiologica Oncology*, vol. 23, no. 4, pp. 209–216, 1984.

[17] S. M. Bentzen and H. D. Thames, "Clinical evidence for tumor clonogen regeneration: interpretations of the data," *Radiotherapy & Oncology*, vol. 22, no. 3, pp. 161–166, 1991.

[18] H. R. Whithers, J. M. Taylor, and B. Maciejewski, "The hazard of accelerated tumor clonogen repopulation during radiotherapy," *Acta Oncologica*, vol. 27, no. 2, pp. 131–146, 1988.

[19] J. Denekamp, "Cell kinetics and radiation biology," *International Journal of Radiation Biology and Related Studies in Physics, Chemistry, and Medicine*, vol. 49, no. 2, pp. 357–380, 1986.

[20] H. R. Withers, H. D. Thames, L. J. Peters et al., "Normal tissue radioresistance in clinical radiotherapy," in *Biological Bases and Clinical Implications of Tumor Radioresistance*, G. H. Fletcher, C. Nervi, and H. R. Withers, Eds., Masson, New York, NY, USA, 1983.

[21] H. D. Thames Jr., H. R. Withers, L. J. Peters, and G. H. Fletcher, "Changes in early and late radiation responses with altered dose fractionation: implications for dose-survival relationships," *International Journal of Radiation, Oncology, Biology Physics*, vol. 8, no. 2, pp. 219–226, 1982.

[22] T. J. Whelan, D. H. Kim, and J. Sussman, "Clinical experience using hypofractionated radiation schedules in breast cancer," *Seminars in Radiation Oncology*, vol. 18, no. 4, pp. 257–264, 2008.

[23] J. R. Owen, A. Ashton, J. M. Bliss et al., "Effect of radiotherapy fraction size on tumour control in patients with early-stage breast cancer after local tumour excision: long-term results of a randomised trial," *The Lancet Oncology*, vol. 7, no. 6, pp. 467–471, 2006.

[24] J. F. Fowler, R. Chappell, and M. Ritter, "Is α/β for prostate tumors really low?" *International Journal of Radiation, Oncology, Biology Physics*, vol. 50, no. 4, pp. 1021–1031, 2001.

[25] R. Miralbell, S. A. Roberts, E. Zubizarreta, and J. H. Hendry, "Dose-fractionation sensitivity of prostate cancer deduced from radiotherapy outcomes of 5,969 patients in seven international institutional datasets: α/β = 1.4 (0.9–2.2) Gy," *International Journal of Radiation Oncology Biology Physics*, vol. 82, no. 1, pp. e17–e24, 2012.

[26] J. Z. Wang, M. Guerrero, and X. A. Li, "How low is the α/β ratio for prostate cancer?" *International Journal of Radiation Oncology Biology Physics*, vol. 55, no. 1, pp. 194–203, 2003.

[27] H. Kal and M. P. van Gellekom, "How low is the α/β ratio for prostate cancer?" *International Journal of Radiation, Oncology, Biology Physics*, vol. 57, no. 4, pp. 1116–1121, 2003.

[28] C. R. King and C. S. Mayo, "Is the prostate α/β ratio of 1.5 from Brenner and Hall a modeling artifact?" *International Journal of Radiation, Oncology, Biology Physics*, vol. 47, no. 2, pp. 536–539, 2000.

[29] P. Pedicini, L. Strigari, and M. Benassi, "Estimation of a self-consistent set of radiobiological parameters from hypofractionated versus standard radiation therapy of prostate cancer," *International Journal of Radiation, Oncology, Biology Physics*, vol. 85, no. 5, pp. e231–e237, 2013.

[30] N. G. Zaorsky, N. Ohri, T. N. Showalter, A. P. Dicker, and R. B. Den, "Systematic review of hypofractionated radiation therapy for prostate cancer," *Cancer Treatment Reviews*, vol. 39, no. 7, pp. 728–736, 2013.

[31] R. W. Lloyd-Davies, C. D. Collins, and A. V. Swan, "Carcinoma of prostate treated by radical external beam radiotherapy using hypofractionation. Twenty-two years' experience (1962–1984)," *Urology*, vol. 36, no. 2, pp. 107–111, 1990.

[32] C. D. Collins, R. W. Lloyd-Davies, and A. V. Swan, "Radical external beam radiotherapy for localised carcinoma of the prostate using a hypofractionation technique," *Clinical Oncology*, vol. 3, no. 3, pp. 127–132, 1991.

[33] H. Lukka, C. Hayter, J. A. Julian et al., "Randomized trial comparing two fractionation schedules for patients with localized prostate cancer," *Journal of Clinical Oncology*, vol. 23, no. 25, pp. 6132–6138, 2005.

[34] E. E. Yeoh, R. H. Holloway, R. J. Fraser et al., "Hypofractionated versus conventionally fractionated radiation therapy for prostate carcinoma: updated results of a phase III randomized trial," *International Journal of Radiation, Oncology, Biology Physics*, vol. 66, no. 4, pp. 1072–1083, 2006.

[35] E. E. Yeoh, R. J. Botten, J. Butters, A. C. di Matteo, R. H. Holloway, and J. Fowler, "Hypofractionated versus conventionally fractionated radiotherapy for prostate carcinoma: final results of phase III randomized trial," *International Journal of Radiation Oncology Biology Physics*, vol. 81, no. 5, pp. 1271–1278, 2011.

[36] American Society for Therapeutic Radiology and Oncology Consensus Panel, "Consensus statement: guidelines for PSA following radiation therapy," *International Journal of Radiation Oncology Biology Physics*, vol. 37, no. 5, pp. 1035–1041, 1997.

[37] M. C. Abramowitz, T. Li, M. K. Buyyounouski et al., "The phoenix definition of biochemical failure predicts for overall survival in patients with prostate cancer," *Cancer*, vol. 112, no. 1, pp. 55–60, 2008.

[38] D. P. Dearnaley, E. Hall, D. Lawrence et al., "Phase III pilot study of dose escalation using conformal radiotherapy in prostate cancer: PSA control and side effects," *British Journal of Cancer*, vol. 92, no. 3, pp. 488–498, 2005.

[39] D. P. Dearnaley, M. R. Sydes, R. E. Langley et al., "The early toxicity of escalated versus standard dose conformal radiotherapy with neo-adjuvant androgen suppression for patients with localised prostate cancer: results from the MRC RT01 trial

(ISRCTN47772397)," *Radiotherapy & Oncology*, vol. 83, no. 1, pp. 31–41, 2007.

[40] P. Kupelian, D. Kuban, H. Thames et al., "Improved biochemical relapse-free survival with increased external radiation doses in patients with localized prostate cancer: the combined experience of nine institutions in patients treated in 1994 and 1995," *International Journal of Radiation, Oncology, Biology Physics*, vol. 61, no. 2, pp. 415–419, 2005.

[41] A. Pollack, G. K. Zagars, G. Starkschall et al., "Prostate cancer radiation dose response: results of the M. D. Anderson phase III randomized trial," *International Journal of Radiation, Oncology, Biology Physics*, vol. 53, no. 5, pp. 1097–1105, 2002.

[42] S. T. Peeters, W. D. Heemsbergen, P. C. M. Koper et al., "Dose-response in radiotherapy for localized prostate cancer: results of the Dutch multicenter randomized phase III trial comparing 68 Gy of radiotherapy with 78 Gy," *Journal of Clinical Oncology*, vol. 24, no. 13, pp. 1990–1996, 2006.

[43] M. J. Zelefsky, Y. Yamada, Z. Fuks et al., "Long-term results of conformal radiotherapy for prostate cancer: impact of dose escalation on biochemical tumor control and distant metastases-free survival outcomes," *International Journal of Radiation, Oncology, Biology Physics*, vol. 71, no. 4, pp. 1028–1033, 2008.

[44] G. Arcangeli, B. Saracino, S. Gomellini et al., "A prospective phase III randomized trial of hypofractionation versus conventional fractionation in patients with high-risk prostate cancer," *International Journal of Radiation, Oncology, Biology Physics*, vol. 78, no. 1, pp. 11–18, 2010.

[45] G. Arcangeli, J. Fowler, S. Gomellini et al., "Acute and late toxicity in a randomized trial of conventional versus hypofractionated three-dimensional conformal radiotherapy for prostate cancer," *International Journal of Radiation, Oncology, Biology Physics*, vol. 79, no. 4, pp. 1013–1021, 2011.

[46] S. Arcangeli, L. Strigari, S. Gomellini et al., "Updated results and patterns of failure in a randomized hypofractionation trial for high-risk prostate cancer," *International Journal of Radiation Oncology, Biology, Physics*, vol. 84, no. 5, pp. 1172–1178, 2012.

[47] D. A. Kuban, G. M. Nogueras-Gonzalez, L. Hamblin et al., "Preliminary report of a randomized dose escalation trial for prostate cancer using hypofractionation," *International Journal of Radiation Oncology, Biology, Physics*, vol. 78, no. 3, supplement, pp. S58–S59, 2010.

[48] A. Pollack, G. Walker, E. M. Horwitz et al., "Randomized trial of hypofractionated external-beam radiotherapy for prostate cancer," *Journal of Clinical Oncology*, vol. 31, no. 31, pp. 3860–3868, 2013.

[49] P. A. Kupelian, T. R. Willoughby, C. A. Reddy, E. A. Klein, and A. Mahadevan, "Hypofractionated intensity-modulated radiotherapy (70 Gy at 2.5 Gy per fraction) for localized prostate cancer: cleveland clinic experience," *International Journal of Radiation, Oncology, Biology Physics*, vol. 68, no. 5, pp. 1424–1430, 2007.

[50] D. Dearnaley, I. Syndikus, G. Sumo et al., "Conventional versus hypofractionated high-dose intensity-modulated radiotherapy for prostate cancer: preliminary safety results from the CHHiP randomised controlled trial," *The Lancet Oncology*, vol. 13, no. 1, pp. 43–54, 2012.

[51] Y. Yoshioka, K. Konishi, R.-J. Oh et al., "High-dose-rate brachytherapy without external beam irradiation for locally advanced prostate cancer," *Radiotherapy & Oncology*, vol. 80, no. 1, pp. 62–68, 2006.

[52] Y. Yoshioka, K. Konishi, I. Sumida et al., "Monotherapeutic high-dose-rate brachytherapy for prostate cancer: five-year results of an extreme hypofractionation regimen with 54 Gy in nine fractions," *International Journal of Radiation, Oncology, Biology Physics*, vol. 80, no. 2, pp. 469–475, 2011.

[53] L. Schour, D. J. Demanes, G. A. Altieri, D. Brandt, M. Barnaba, and P. Skoolisariyaporn, "High dose rate monotherapy for prostate cancer," *International Journal of Radiation, Oncology, Biology Physics*, vol. 63, supplement 1, p. S315, 2005.

[54] D. J. Demanes, A. A. Martinez, M. Ghilezan et al., "High-dose-rate monotherapy: safe and effective brachytherapy for patients with localized prostate cancer," *International Journal of Radiation, Oncology, Biology Physics*, vol. 81, no. 5, pp. 1286–1292, 2011.

[55] C. Corner, A. M. Rojas, L. Bryant, P. Ostler, and P. Hoskin, "A phase II study of high-dose-rate afterloading brachytherapy as monotherapy for the treatment of localized prostate cancer," *International Journal of Radiation, Oncology, Biology Physics*, vol. 72, no. 2, pp. 441–446, 2008.

[56] N. G. Zaorsky, M. T. Studenski, A. P. Dicker et al., "Stereotactic body radiation therapy for prostate cancer: is the technology ready to be the standard of care?" *Cancer Treatment Reviews*, vol. 39, no. 3, pp. 212–218, 2013.

[57] B. L. Madsen, R. A. Hsi, H. T. Pham, J. F. Fowler, L. Esagui, and J. Corman, "Stereotactic hypofractionated accurate radiotherapy of the prostate (SHARP), 33.5 Gy in five fractions for localized disease: first clinical trial results," *International Journal of Radiation, Oncology, Biology Physics*, vol. 67, no. 4, pp. 1099–1105, 2007.

[58] C. I. Tang, D. A. Loblaw, P. Cheung et al., "Phase I/II study of a five-fraction hypofractionated accelerated radiotherapy treatment for low-risk localized prostate cancer: early results of pHART3," *Clinical Oncology*, vol. 20, no. 10, pp. 729–737, 2008.

[59] H. Quon, P. Cheung, A. Cesta et al., "Phase II study of a five-fraction hypofractionated accelerated radiotherapy treatment for low-risk localized prostate cancer: toxicity results of pHART3," in *Genitourinary Cancers Symposium*, Orlando, Fla, USA, 2010.

[60] A. J. Katz, M. Santoro, F. DiBlasio et al., "Stereotactic body radiation therapy for low-, intermediate- and high-risk prostate cancer: disease control and quality of life," *International Journal of Radiation, Oncology, Biology Physics*, vol. 81, no. 2, supplement, p. S100, 2011.

[61] A. J. Katz, M. Santoro, R. Ashley, F. Diblasio, and M. Witten, "Stereotactic body radiotherapy as boost for organ-confined prostate cancer," *Technology in Cancer Research and Treatment*, vol. 9, no. 6, pp. 575–582, 2010.

[62] D. E. Freeman and C. R. King, "Stereotactic body radiotherapy for low-risk prostate cancer: five-year outcomes," *Radiation Oncology*, vol. 6, no. 1, article 3, 2011.

[63] C. R. King, J. D. Brooks, H. Gill, and J. C. Presti Jr., "Long-term outcomes from a prospective trial of stereotactic body radiotherapy for low-risk prostate cancer," *International Journal of Radiation, Oncology, Biology Physics*, vol. 82, no. 2, pp. 877–882, 2012.

[64] N. C. Townsend, B. J. Huth, W. Ding et al., "Acute toxicity after cyberknife-delivered hypofractionated radiotherapy for treatment of prostate cancer," *American Journal of Clinical Oncology*, vol. 34, no. 1, pp. 6–10, 2011.

Hindawi Publishing Corporation
BioMed Research International
Volume 2014, Article ID 801473, 14 pages
http://dx.doi.org/10.1155/2014/801473

Research Article

In Vitro Chronic Administration of ERbeta Selective Ligands and Prostate Cancer Cell Growth: Hypotheses on the Selective Role of 3beta-Adiol in AR-Positive RV1 Cells

Alessandra Colciago,[1] Massimiliano Ruscica,[1] Ornella Mornati,[1] Margherita Piccolella,[1] Marina Montagnani-Marelli,[1] Ivano Eberini,[1] Claudio Festuccia,[2] Paolo Magni,[1] Marcella Motta,[1] and Paola Negri-Cesi[1]

[1] *Department of Pharmacological and Biomolecular Sciences, University of Milano, Via Balzaretti 9, 20133 Milano, Italy*
[2] *Department of Biotechnological and Applied Clinical Sciences, University of L'Aquila, Via Vetoio, Coppito 2, 67100 L'Aquila, Italy*

Correspondence should be addressed to Paola Negri-Cesi; paola.negricesi@unimi.it

Received 31 January 2014; Accepted 27 March 2014; Published 29 April 2014

Academic Editor: Giovanni Luca Gravina

Prostate cancer (PC) progression from androgen-dependent (AD) to castration-resistant (CR) disease is a process caused by modifications of different signal transduction pathways within tumor microenvironment. Reducing cell proliferation, estrogen receptor beta (ERbeta) is emerging as a potential target in PC chemoprevention. Among the known selective ERbeta ligands, 3beta-Adiol, the endogenous ligand in the prostate, has been proved to counteract PC progression. This study compares the effects of chronic exposure (1–12 weeks) to different ERbeta selective ligands (DPN, 8beta-VE2, 3beta-Adiol) on proliferation of human androgen-responsive CWR22Rv1 cells, representing an intermediate phenotype between the AD- and CR-PC. 3beta-Adiol (10 nM) is the sole ligand decreasing cell proliferation and increasing p21 levels. *In vitro* transcriptional activity assays were performed to elucidate different behavior between 3beta-Adiol and the other ligands; in these experiments the endogenous and the main ERbeta subtype activation were considered. It is concluded that ERbeta activation has positive effects also in androgen-responsive PC. The underlying mechanisms are still to be clarified and may include the interplay among different ERbeta subtypes and the specific PC microenvironment. ERbeta agonists might be useful in counteracting PC progression, although the final outcome may depend upon the molecular pattern specific to each PC lesion.

This paper is dedicated to the memory of our colleague and dear friend Donatella Dondi.

1. Introduction

Prostate cancer (PC) represents one of the main leading causes of death in men worldwide [1]. This is mainly due to a high rate recurrence and progression of the disease to a castration-resistant and disseminated stage (CR-PC), in which therapeutic options are few and often only palliative [1]. Thus, the discovery of drugs able to positively manage CR-PC and/or to delay its appearance still represents an important clinical challenge.

Estrogens, alone or along with androgens, are important players of prostate carcinogenesis and progression. Indeed, chronically high estrogenic levels are associated with increased risk to develop PC. However, anticancer activity has been observed in many instances by using synthetic or herbal-derived estrogens [2–5]. These conflicting observations are possibly due to the presence of two classes of estrogen receptors (ERalpha and ERbeta) [6, 7], which display differences in localization, expression levels, and functional roles in prostate biology and carcinogenesis. ERbeta, which is largely localized in the epithelial compartment, is linked to antiproliferative and differentiating effects [7–12]. *In vitro* data have shown how ERbeta-driven inhibitory activity on PC biology might be mediated by induction of apoptosis

[12], by enhanced synthesis of cell cycle inhibitor proteins [4, 13], or by a negative regulation of cell adhesion molecules [14]. Furthermore, the loss of ERbeta is associated with the progression from normal prostate epithelium to PC [15]. All these findings point to a major role of ERbeta to protect prostate cells from uncontrolled proliferation and malignant transformation. Thus, ERbeta activation by specific agonists may be a feasible option treatment for PC chemoprevention and CR-PC management. However, the mechanism of action of ERbeta is rather complex and still unclear due to the discovery of at least five ERbeta different isoforms resulting from alternative splicing of the same gene. Among them, ERbeta1, 2, and 5 are the most studied isoforms in human PC. ERbeta1, which is the one primarily lost during PC progression, is defined as the wild-type isoform and it is related to the antiproliferative and the proapoptotic activity [12, 16]. On the contrary, ERbeta2 and ERbeta5 bind estrogens with different affinity (none and low affinity, resp., [17]) and are associated to increased cell proliferation and enhanced cell migration, as well as to a PC poor prognosis [18, 19]. It is suggested that these isoforms, which are often coexpressed with ERbeta1 in many tissues, including the prostate [16, 17, 20, 21], bind as homo- or heterodimers to canonical ERE sequences and act as variable parameters with enhancer or dominant negative functions [17, 18, 20, 22]. Moreover, coexpression of ERbeta1 with ERbeta2 or ERbeta5 in HEK293 cells significantly enhances ERE-mediated transactivation when activated by estradiol or phytoestrogens [17]. To our knowledge, the ability of these complexes to activate transcription upon binding with ERbeta selective agonists has never been evaluated.

Thanks to the significant differences in the ligand binding domain between ERalpha and ERbeta, a series of ERbeta selective agonists have been developed in these last years [5, 23, 24], and most of them have been also tested for their biological activity in different experimental models [25–28]. The various ERbeta selective agonists have the same transcriptional activity on a battery of genes; however, it is demonstrated that they may also display gene-specific activation/repression resulting in distinct biological outcomes and possibly clinical effects [29]. The fact that different ERbeta-selective agonists might elicit different biological results points to the need of a careful evaluation of diverse structural classes of compounds in various disease models to identify the optimal ERbeta agonist in each condition.

Owing to the largely planar configuration of the phytoestrogens (the first ERbeta selective ligands discovered), nonsteroidal compounds retaining a similar topology have been synthesized; among these, diarylpropionitrile (DPN) is considered the prototype molecule of the group [5, 23]. However, compounds with nonplanar rigid configuration have shown a more robust and greater selectivity for ERbeta than the planar ones [5]. The prototype of this latter group is 8vinylestrane-1,3,5(10)-triene-3,17beta-diol (8beta-VE2) [5]. High affinity for ERbeta is also displayed by 5alpha-androstane-3beta,17beta-diol (3beta-Adiol), an endogenous metabolite of DHT which classically does not bind to the wild-type AR [30]. As the intraprostatic levels of 3beta-Adiol *in vivo* are about 100-folds higher than those of estradiol, this steroid is considered the natural ligand of ERbeta in the gland [11].

Among the different available *in vitro* PC models, the CWR22RV1 (Rv1) cells, which are derived from a primary androgen-dependent human PC tumor (CWR22) orthotopically transplanted in castrated nude mice, represent an intermediate phenotype between the AR-dependent and castration-resistant tumor. Rv1 cells are androgen ablation-resistant, but still androgen-responsive [31, 32]. They express ARs (both wild-type and mutated forms [33]), but conflicting results are reported on the expression levels of ERalpha and ERbeta [12, 34]. Due to the 35/40-h doubling time, they represent a suitable cell-based model, resembling the "*in vivo*" condition, to study the effect of a long-lasting treatment on cell proliferation [31].

The aim of the study was to evaluate in Rv1 cell line; (a) the expression of the different isoforms of androgen and estrogen receptors; (b) the effects driven by a chronic exposure to DPN, 8beta-VE2, and 3beta-Adiol on cell proliferation rate, on the expression of AR and ER gene levels and on the expression of some proteins involved in cell cycle arrest (PTEN, p21 and cyclin E). A series of *in vitro* transcriptional activity assessments were then performed to elucidate the different behavior between 3beta-Adiol and the other ERbeta selective ligands in Rv1 cell.

2. Material and Methods

2.1. Chemicals and Plasmids. 2,3-bis(4-hydroxyphenyl)-propionitrile (DPN, Tocris Cookson, Ellisville, MO, USA), 8vinylestrane-1,3,5(10)-triene-3,17beta-diol (8beta-VE2, kindly provided by Dr. K. Prelle, Bayer Schering Pharma AG), and 5alpha-androstane-3beta,17beta-diol (3beta-Adiol, Sigma-Aldrich, Milano, Italy) were used as ERbeta selective agonists. ICI 182,780 (Tocris Cookson, Ellisville, MO, USA) was used as estrogen receptor antagonist. All compounds were dissolved in ethanol.

pCMV5-ERbeta1, pCMV5-ERbeta2, pCMV5-ERbeta5, and pCMV5-EMPTY were kindly provided by Dr. P. G. V. Martini, Shire HGT, Boston, MA; pGL3-2ERE-pS2-luc was kindly provided by Dr. M. Marino, Rome, and pgL 4.0 hRLuc was from Promega (Milano, Italy).

2.2. Cell Cultures and Treatments. CWR22Rv1 (Rv1) cells were originally obtained from DSMZ (Frankfurt, Germany); HEK293 cell line was originally obtained by American Type Culture Collection (Rockville, MD) and currently used in our laboratory.

All cell culture reagents were purchased from Biochrom (Biochrom KG, Berlin, Germany). Rv1 cells were routinely grown at 37°C in a humidified atmosphere (5% CO_2—95% air) in 100 mm Petri dishes in phenol red free RPMI 1640 supplemented with 5% of heat inactivated fetal calf serum (FCS, GIBCO), glutamine (2 mM), penicillin (100 IU/mL), and streptomycin (100 microg/mL). Medium was changed biweekly. HEK293 were routinely maintained in the same culture conditions in 10% FCS phenol red free RPMI 1640.

Table 1

Target gene	Forward primer	Reverse primer
ERbeta1	GTCAGGCATGCGAGTAACAA	GGGAGCCCTCTTTGCTTTTA
ERbeta2	TCTCCTCCCAGCAGCAATCC	GGTCACTGCTCCATCGTTGC
ERbeta5	GATGCTTTGGTTTGGGTGAT	GGAGGAGTGGGTGTCGCTGT
Beta-actin	CCACCATGTACCCTGGC	CGGACTCGTCATACTCCTGC

Table 2

Target protein	Primary antibody	Secondary antibody
ERbeta (all)	Ab288 (Abcam, Cambridge, UK); 1 : 500 dilution	WesternDot 625 detection kits (Life Technologies Italia, Monza, Italy); 1 : 2000 dilution
AR	Sc816 (Santa Cruz Biotechnology, Santa Cruz, CA, USA); 1 : 400 dilution	HRP-conjugated anti-rabbit (Santa Cruz Biotechnology, Santa Cruz, CA, USA); 1 : 2000 dilution
PTEN	ab32199 (Abcam, Cambridge, UK); 1 : 1000 dilution	HRP-conjugated anti-rabbit (Santa Cruz Biotechnology, Santa Cruz, CA, USA); 1 : 8000 dilution
p21	05-345 (Millipore, Billerica, MA, USA); 1 : 1000 dilution	HRP-conjugated anti-mouse (Santa Cruz Biotechnology, Santa Cruz, CA, USA); 1 : 5000 dilution
Tubulin	T9026 (Sigma-Aldrich, Monza, Italy); 1 : 2000 dilution	HRP-conjugated anti-mouse (Santa Cruz Biotechnology, Santa Cruz, CA, USA); 1 : 8000 dilution
Beta-actin	Sc1616 (Santa Cruz Biotechnology, Santa Cruz, CA, USA); 1 : 4000 dilution	HRP-conjugated anti-goat (Santa Cruz Biotechnology, Santa Cruz, CA, USA); 1 : 4000 dilution

2.3. Experimental Schedule in Long-Term Experiments. Rv1 cells were seeded in 100 mm Petri dishes in phenol-red free RPMI 1640 supplemented with 5% charcoal stripped-FCS (FCS-CH) (2 independent samples/treatments/times) and chronically treated every 2 days with ethanol (control cells), DPN, 8beta-VE2, or 3beta-Adiol (all 10 nM) up to 12 weeks, on a weekly propagation schedule. At the beginning of the long-term exposure (T1) and after 5, 8, and 12 weeks (T5–T12) of chronic treatment, part of the cells from each group was harvested and utilized for RNA/protein extraction and for the growth rate evaluation. The schedule of chronic treatments is outlined in Figure 1.

2.4. Growth Rate Evaluation. Cells from the chronic exposure were seeded in 100 mm Petri dishes in 5% FCS-CH phenol-red free RPMI 1640 (3 independent samples/treatments/times) and the corresponding treatment went on every 2 days for 10 days. After 3, 5, 7, and 10 days, cells from some of the Petri dishes were harvested and counted by Tripan blue exclusion in a Burker chamber (see Figure 1).

2.5. Real-Time PCR. Total RNA from control and treated cells was extracted by the phenol-chloroform method according to standard protocols [35] and used for real-time PCR (qPCR). A mean of 2 independent RNA samples was used for each determination. Reverse transcription was performed on 1 μg of total RNA from each sample according to the manufacturer's protocol (iScript cDNA synthesis kit, BioRad, Segrate, Italy) using random primers. qPCR was done in singleplex in CFX96 Touch Real-Time PCR Detection System (BioRad, Segrate, Italy) using two different experimental protocols: ERalpha, ERbeta and AR genes were amplified using the SsoFast Probes supermix (BioRad, Segrate, Italy) and specific assays on demand (AoD, Life Technologies, Monza, Italy); ERbeta isoforms were amplified using the SsoAdvanced SYBR Green SuperMix (BioRad, Segrate, Italy) and the specific sets of primers listed in Table 1, designed using the Primer 3 software and purchased by Sigma Aldrich, Milano, Italy.

Each sample was analysed in triplicate. Relative mRNA levels were calculated using the comparative CT method ($2^{-\Delta\Delta Ct}$).

2.6. Western Blot Analysis. Constitutive proteins from control and treated cells were prepared by lysing in RIPA buffer with proteases inhibitors. Total proteins extracts (30 microgr/sample), determined with BCA assay (Pierce, Rockford, IL, USA), were resolved on SDS-PAGE followed by electrotransfer onto nitrocellulose membrane. The fluorescent qDot system (Life Technologies Italia, Monza, Italy) was used for ERbeta detection; the enhanced chemiluminescence (ECL) detection kit (GE Healthcare, Milano, Italy) was used for AR, PTEN, and p21 detection. Specific primary and secondary antibodies are listed in Table 2.

2.7. Transient Transfections and Transcriptional Activity Assay. Rv1 or HEK-293 cells, plated in 96-wells plate and maintained in RPMI 1640 without phenol-red and FCS, have been

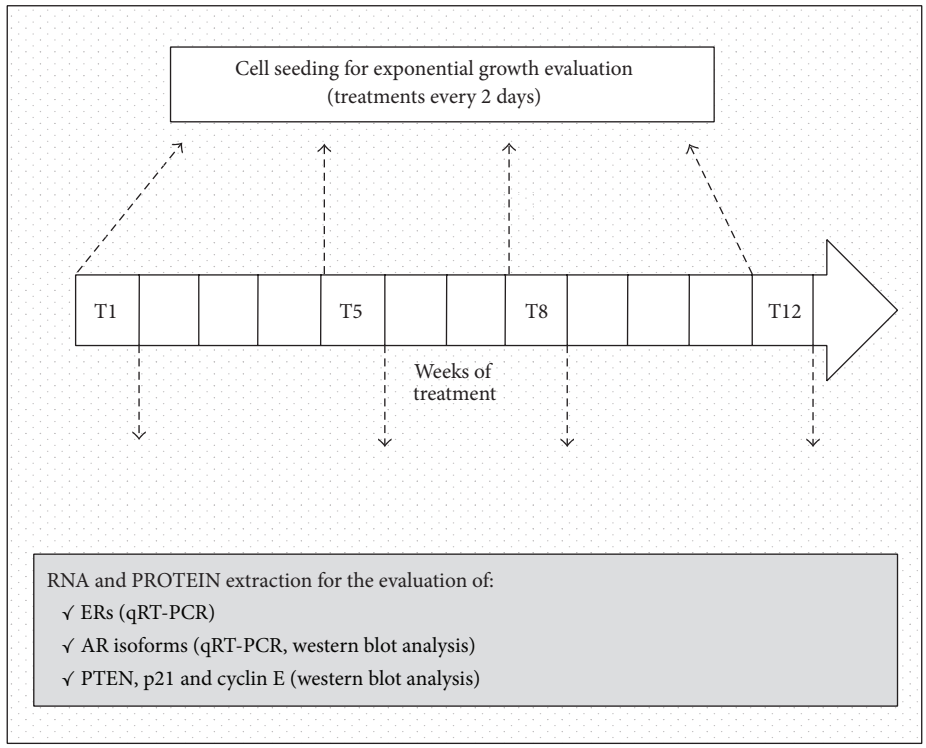

Figure 1: Experimental schedule of chronic treatment.

transfected by using Lipofectamine 2000 (Life Technologies Italia, Monza, Italy). Transfection was performed using a total of 0.2 microgr of plasmid DNAs/well, according to manufacturer's protocol. After 6 hours, the transfection medium was replaced with RPMI 1640 without phenol-red with 5% (Rv1) or 10% (HEK 293) FCS-CH containing the appropriate treatment. Transcriptional activity was evaluated 22 hours later by the luciferase assay (DUAL-GLO Luciferase Assay System kit, Promega, Milano, Italy), according to the manufacturer's protocol. The inducible firefly luciferase activity has been normalized by renilla luciferase. Each sample was assessed in duplicate.

2.8. Statistical Analysis. The statistical analysis of the row data was performed by one-way parametric ANOVA and expressed as mean ± SD; post hoc analyses were performed by Tukey's Multiple Comparison Test, using the Graph-Pad software for Macintosh (Evanston, IL). Only P values < 0.05 were considered statistically significant.

Cell growth rate was analyzed by an exponential curve fitting computer program (ESPSS) followed by the statistical analysis of the fitted curve parameters through parametric ANOVA and by the Student-Newman-Keuls post hoc Test for multiple comparisons. Only P values < 0.05 were considered statistically significant.

3. Results

3.1. Steroid Hormone Receptor Pattern in Rv1 Cells. Due to conflicting data on ERbeta expression in Rv1 cells, first of all we have assessed the presence of the endogenous ERs, along with that of ARs in our experimental model (Figure 2). Panel (a) shows the expression pattern of ERalpha, ERbeta and of the 110 kDa form of AR, evaluated by qPCR and expressed as % versus the 110 + 75 AR transcripts (AR total) after normalization for the housekeeping gene HPRT. It is apparent from the panel that this cell line expresses both ERalpha and ERbeta. Even though the levels of ERbeta are higher than those of ERalpha, taken as a whole, the expression of the two ER is very low in comparison to that of ARs; the 110 kDa AR represents roughly 20% of the totality of AR transcripts. In this qPCR experiment AR75 was not evaluated separately due to the impossibility to design a set of specific primers.

To confirm the presence of ERbeta also at protein level, Western blot analysis was performed on two independent RV1 samples using an antibody that maps to the N-terminus (common to all the ERbeta subtypes, see below). Figure 2(b) shows the presence of at least three immunoreactive bands with a MW within the 50–60 kDa range, which might correspond to the three main ERbeta subtypes present in CP cells [17]. AR75 and AR110 expression levels were evaluated separately by Western blot analysis. A representative Western blot carried out using a polyclonal antibody directed against the amino-terminus of the protein, which recognizes all the different AR forms, is shown in panel (c). It is evident that Rv1 cells contain both the AR form of 110 kDa (considered the wild type) and that of 75–80 kDa, corresponding to some forms truncated at the carbossi-terminal; panel (d) reports the mean ± SD of the densitometric analysis of a series of

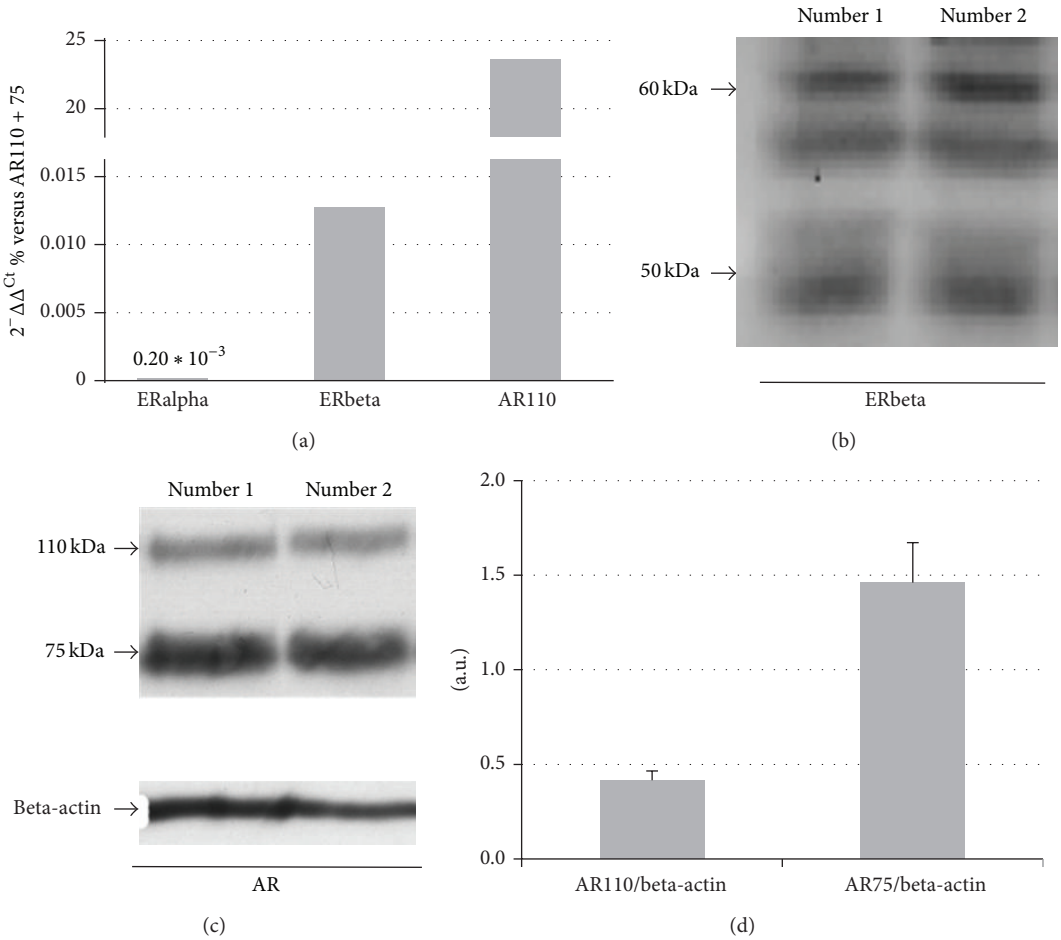

Figure 2: Relative expression of ERs and ARs by qPCR (a); Western blot analysis of ERbeta (b) and ARs (c); densitometric analysis of ARs (d).

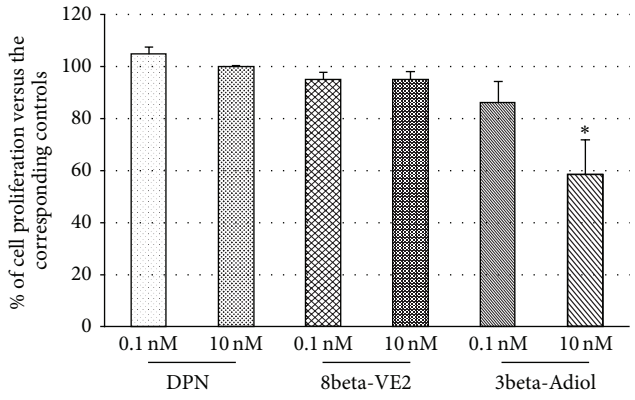

Figure 3: Dose-response effect of ERbeta selective agonists on short-term (9 days) proliferation of Rv1 cells. Data are mean ± SD and are expressed as percent of the corresponding controls. $^{*}P < 0.05$ versus 3beta-Adiol 0.1 nM.

samples after normalization with actin. As it appears from the figure, and in line with the qPCR results, the total amount of the truncated forms is about threefold higher than that of AR110, which represent the 20% of the total AR levels.

3.2. Determination of the Optimal Dose for the Chronic Studies. Previous preliminary experiments performed in our laboratory using other AR-PC cell lines showed that both DPN and 8beta-VE2 at the concentration of 10 nM were able to significantly reduce DU145 cell proliferation after 9 days of exposure (data not shown). Thus, to test the effect of DPN, 8beta-VE2, and 3beta-Adiol specifically on Rv1 cell proliferation, the same (10 nM) or a hundred times lower (0.1 nM) dose of each drug has been administered in a 9-day treatment schedule (Figure 3).

To compare experiments carried out in different times, the data in the figure are expressed as percent versus their own control. As shown, none of the three ligands is effective at the lower dose. Only 3beta-Adiol is able to significantly decrease cell proliferation at the dose of 10 nM, being the same dose of DPN and 8beta-VE2 ineffective in this cell line. Even though the two latter compounds are ineffective after a 9-day exposure, no higher doses have been tested because of the possibility of cross-activation of ERalpha [23, 36], or the achievement of the 100% of the transcriptional activity, as in the case of 8beta-VE2 [37].

3.3. Rv1 Proliferation Rate during Chronic Exposure. The proliferation rate of Rv1 chronically exposed to 10 nM DPN,

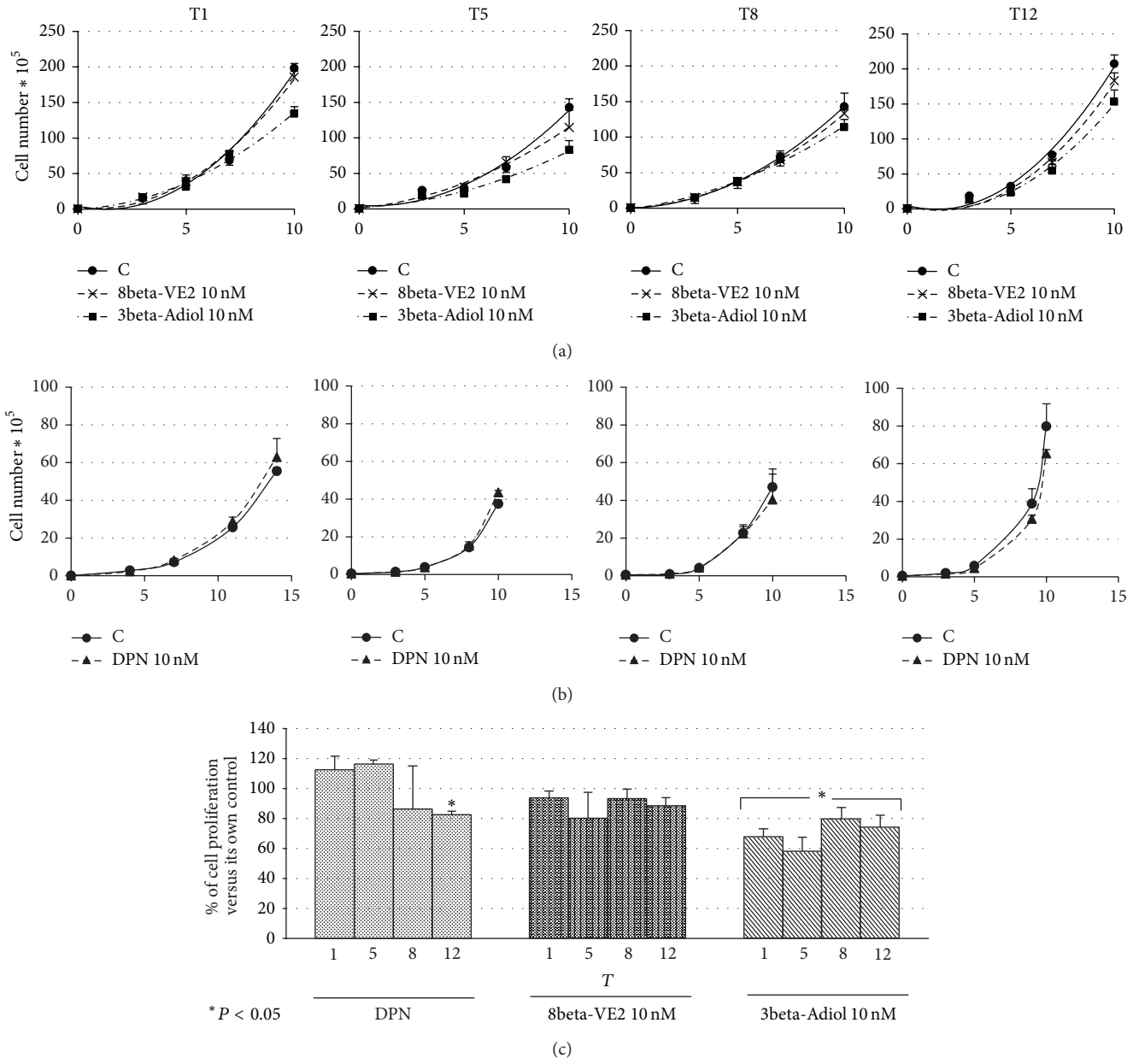

Figure 4: Effect of chronic exposure to ERbeta selective ligands on Rv1 cell proliferation: proliferation curves evaluated at T1-5-8-12 with vehicle (C), 8betaVE2, or 3beta-Adiol (a); with vehicle (C) and DPN (b). Cumulative data of the relative proliferation rate during the chronic treatments (c): data are mean ± SD and are expressed as percent of the corresponding controls. $^{*}P < 0.05$ versus the corresponding controls.

8beta-VE2, or 3beta-Adiol has been assessed in two separate sets of experiments. The corresponding exponential curves calculated at different weeks during the treatment are reported in Figures 4(a) and 4(b).

When tests for multiple comparisons have been applied to the fitted curve parameters, no statistically significant differences have been detected among the curves for all compounds at all the time points examined. However, in the case of cells exposed to 3beta-Adiol a constant decrement is apparent at all the time frames (Figure 4(a)). The statistical comparison of the last point of each curve only (10 days of exposure) for each treatment by a restricted ANOVA analysis shows statistically significant differences in comparison to control cells at all the time frames (from T1 to T12) for 3beta-Adiol, while the chronic treatment with 8beta-VE2 results in a slight but not significant decrease of cell proliferation (Figure 4(c)). The same figure shows that the 10 nM DPN is completely ineffective, but after 12 weeks of chronic exposure, when a significant antiproliferative effect is apparent (Figure 4(c)). In our experimental conditions, the efficacy of 3beta-Adiol to slow cell proliferation is also supported by the increase of the doubling time calculated for the proliferation curves at each time frame in comparison to the corresponding control cells (from 48–60 h of controls to 65–74 h of 3beta-Adiol treated cells).

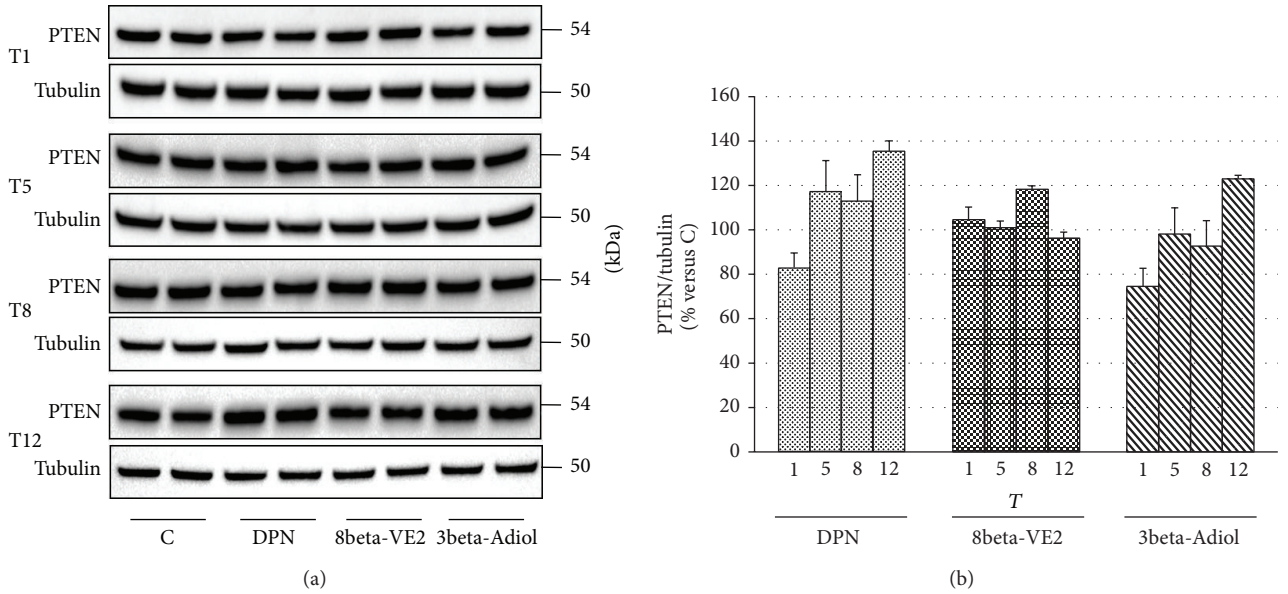

Figure 5: Effects of different chronic treatments with DPN, 8beta-VE2, and 3beta-Adiol on PTEN protein expression in Rv1 cells: immunoreactive bands (representative Western Blot) during chronic treatments (from T1 to T12) (a); histograms representing the time course of PTEN protein expression, normalized to the levels of tubulin, grouped by each treatment; values are expressed as mean ± SD (b).

3.4. Influence of the Chronic Exposure on Cell Cycle Regulators and on AR and ERbeta Levels. To clarify some of the molecular mechanisms at the basis of the antiproliferative action of the ERbeta selective agonists, we evaluated by Western blot analysis the modifications of PTEN (Figure 5) and of p21 (Figure 6) during the chronic treatment with DPN, 8beta-VE2, and 3beta-Adiol. In both figures, panels (a) show representative Western blots of PTEN and p21 levels in cells exposed to the three drugs from T1 to T12, respectively, while in panels (b) the cumulative results of different experiments have been pooled together as a function of the treatment and expressed as fold variation in comparison to the corresponding control samples. As far as PTEN is concerned, the results show a slight and not significant increase of PTEN levels in the DPN-treated cells (35% at T12), while neither 8beta-VE2 nor 3beta-Adiol is able to consistently enhance the expression of this cell cycle regulator (Figure 5(b)). On the contrary, as clearly appears from the Figure 6(b), only 3beta-Adiol leads to a progressive significant increase in p21 protein expression (+41%, $P < 0.05$; +47%, $P < 0.01$, and +78% $P < 0.01$ versus control, from T5 to T12). Treatments with DPN or 8beta-VE2 are completely ineffective. In parallel, only 3beta-Adiol induces a decrease of cyclin E expression levels (data not shown).

Neither 3beta-Adiol nor the other ERbeta selective agonists are able to influence the expression levels of AR and ERbeta, as revealed by qPCR experiments (data not shown).

3.5. Transcriptional Activity of Selective ERbeta Agonists. To elucidate the different behavior between 3beta-Adiol and the other ERbeta selective ligands on Rv1 cell growth, first of all we tested the ability of the compounds to activate transcription through the binding of ERbeta to ERE sequences (Figure 7). In this set of experiments, a reporter construct containing 2 estrogen response elements (EREs) coupled to luciferase has been transiently transfected into Rv1 cells. The stimulation of the transfected cells with 10 nM 3beta-Adiol (but not with the 0.1 nM dose) resulted in a huge increase of luciferase activity (about 35-fold, Figure 7(a), left panel). The transcriptional activity of 3beta-Adiol is dose-dependently inhibited by the addition of the pure antiestrogen ICI 182.780 (Figure 7(a), right panel), confirming that Rv1 cells possess an endogenous transcriptionally active ERbeta and that 3beta-Adiol, at the doses used in the proliferation studies, mediates the transcription through EREs. Surprisingly, neither DPN (not shown) nor 8beta-VE2, at the dose of 0.1 and 10 nM, was able to activate the endogenous ERbeta-mediated transcription in Rv1 cells (Figure 7(a), left panel). On the contrary, when the full length ERbeta (ERbeta1) was transiently expressed in HEK293 cells together with the 2ERE-containing gene reporter coupled to luciferase, the exposure to 8beta-VE2 at the doses of 0.1 and 10 nM results in a dose dependent increase of the transcriptional activity, while no response was elicited by the same amounts of 3beta-Adiol (Figure 7(b))

3.6. Have the Various ERbeta Isoforms a Role in Determining the Different Activity of 3beta-Adiol and 8beta-VE2? To answer this question, we first assess by qPCR the expression pattern of ERbeta subtypes in Rv1 cells in comparison to a mix of RNAs from different AD- and CR-PC cell lines (CWR22, Rv1, PC3, and DU145 cells). The results obtained, shown in Figure 8(a), indicate that Rv1 cells possess low but detectable levels of ERbeta1 and almost three times higher amounts of ERbeta2; ERbeta5 is the most expressed ERbeta subtype (about 5 times more than ERbeta1).

Figure 8(b) shows the results of cotransfection experiments in HEK293 cells, in which the ERE-mediated

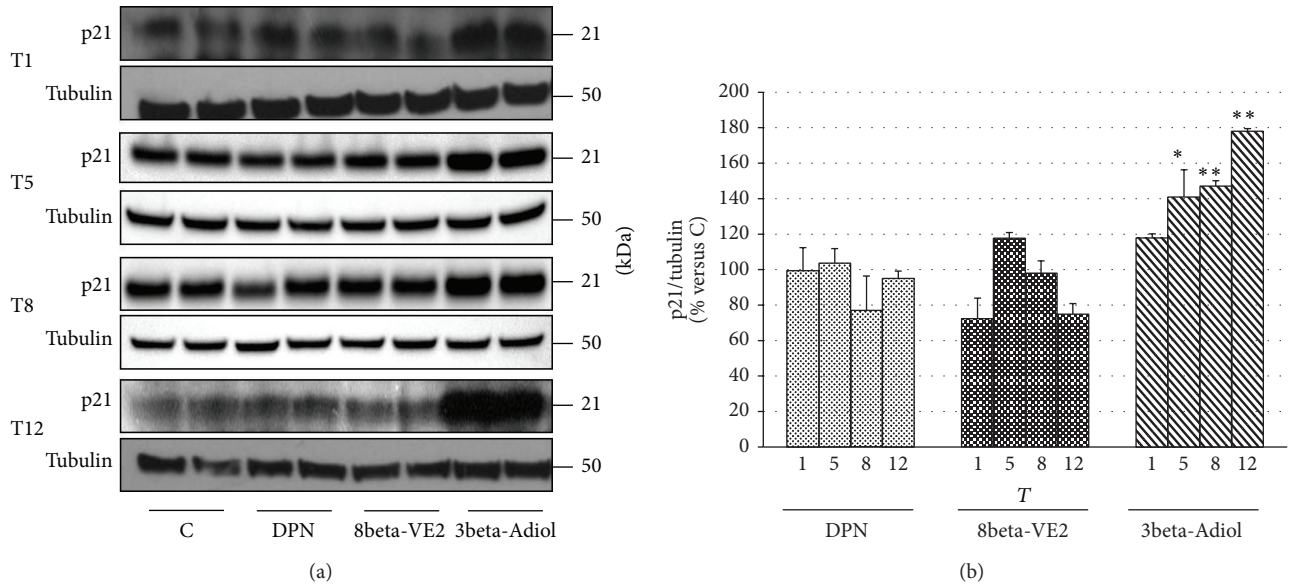

Figure 6: Effects of different chronic treatments with DPN, 8beta-VE2, and 3beta-Adiol on p21 protein expression in Rv1 cells: immunoreactive bands (representative Western Blot) during chronic treatments (from T1 to T12) (a); histograms showing the time course of p21 protein expression, normalized to the levels of tubulin, grouped by each treatment; data are expressed as mean ± SD; $^{*}P < 0.05$ versus corresponding controls; $^{**}P < 0.01$ versus corresponding controls (b).

transcriptional activity of ERbeta1 alone or along with ERbeta2 and ERbeta5 was assessed in presence of 3beta-Adiol or 8beta-VE2. Data are expressed as percent of variation versus control cells transfected with the same plasmids and treated with ethanol. First of all it is possible to note that, in agreement with the previous experiments, 10 nM 8beta-VE2 stimulates transcription both in presence of ERbeta1 alone and in presence of the two hetero-dimers (2- to 4-fold of control cells), while 3beta-Adiol is completely ineffective. Moreover, when activated by 8beta-VE2, the hetero-dimer beta1:beta5 induces a significant increase of the ERE-mediated transcription in comparison to both the homo-dimer beta1:beta1 and the hetero-dimer beta1:beta2. The presence of the ERbeta2 subtype in the hetero-dimer causes a slight but not significant reduction of the ERE-mediated transcriptional activity in comparison to the homo-dimer beta1:beta1.

4. Discussion

In the present study we analyzed whether a long-term activation of ERbeta by selective agonists was able to decrease the proliferation of Rv1 PC cells and, if so, which are the underlying molecular mechanisms. In particular, we assessed the effects of DPN [23] and 8beta-VE2 [5] in comparison to the natural ligand 3beta-Adiol [11]; DPN and 8beta-VE2 are two known synthetic selective ERbeta agonists, the biological activity of which have been tested in other mammalian cell models [25, 26], in comparison to the natural ligand 3beta-Adiol [11]. Rv1 cells were chosen as a model of primary androgen-responsive human PC; these cells have also the advantage to maintain an exponential growth up to 15 days *in vitro* and to display a steady doubling time for a long period [31].

As contrasting results are present in the literature on ERbeta expression in Rv1 cells [12, 33, 34], we assessed ERbeta gene and protein expression levels, which were shown to be low, but detectable. Interestingly, 3beta-Adiol at 10 nM, a dose that resembles endogenous intraprostatic levels [38], was found to be the sole ERbeta selective agonist active in decreasing cell proliferation both after short- (9 days) and long- (12 weeks) term intervals. Dose (10 nM) and antiproliferative effects of 3beta-Adiol appear similar to previously published data obtained in two commonly used CR-PC cells (DU145 and PC3 [39]) and in breast cancer cells [40].

This study shows for the first time that 3beta-Adiol efficacy persists over the time with a 20–40% reduction of cell proliferation during 12 weeks of administration. Although statistically significant at any time, such effect is particularly evident from 9 days to 5 weeks of administration and less pronounced over the following time frame (up to 12 weeks). This may be due to the possible development of some cell adaptive mechanisms, which, however, are not linked to drug resistance, as 3beta-Adiol is able to promote a progressive and significant increase of p21 protein expression.

The involvement of the endogenous ERbeta system in the mechanism of action of 3beta-Adiol in these cells is supported by the ability of the compound to activate ERE-mediated transcription, an effect that is dose-dependently counteracted by the presence of the pure antiestrogen ICI 182,780. Moreover, long-term administration of 3beta-Adiol and the consequent ERbeta activation are associated with a progressive increase of p21 expression levels and a slight decrease of the cyclin E (data not shown), suggesting a potential mechanistic relationship between these events. These findings appear to fit well with previous studies, demonstrating that activation of either the endogenous ERbeta in PC3 [41] and in DU145

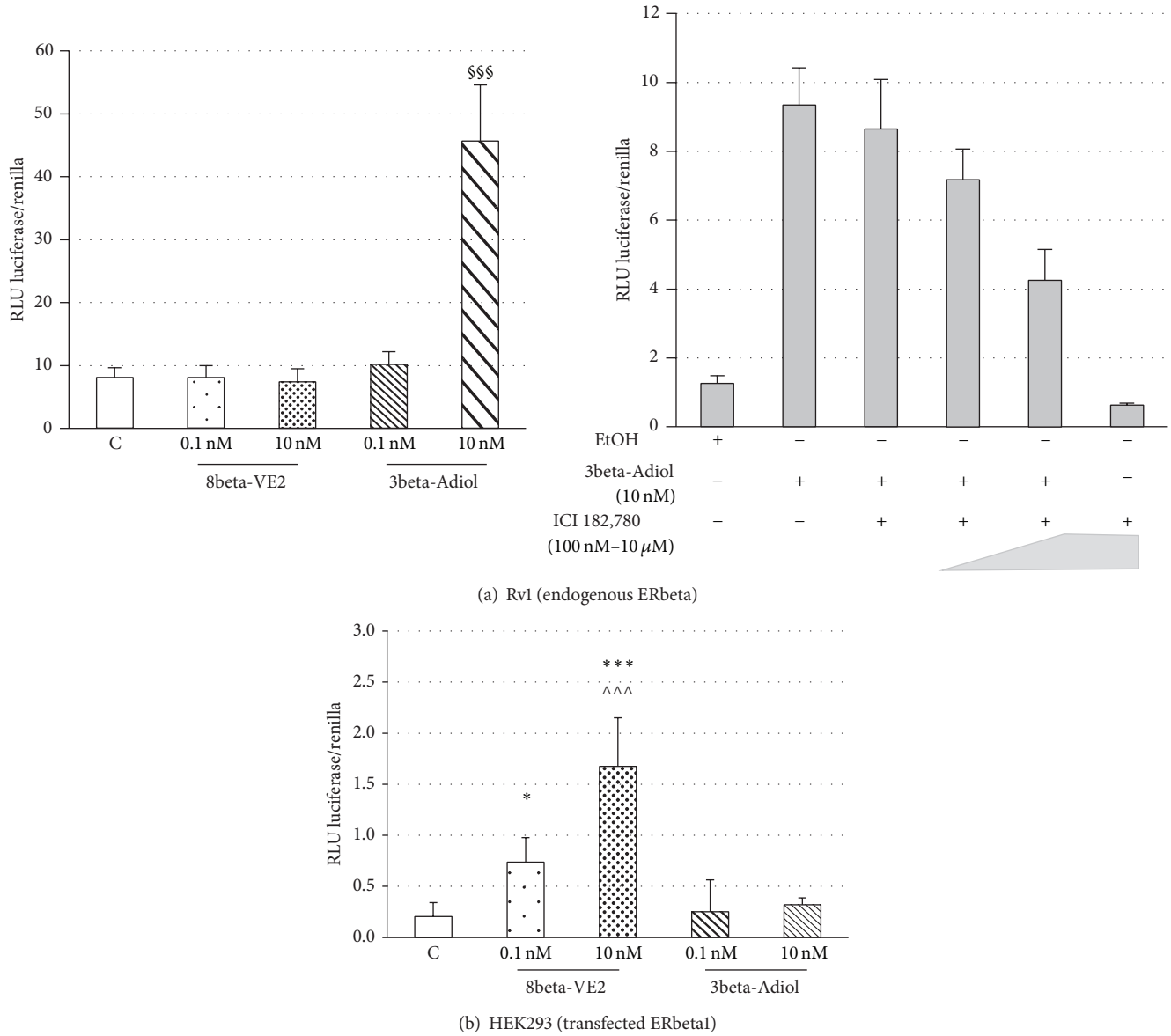

(a) Rv1 (endogenous ERbeta)

(b) HEK293 (transfected ERbeta1)

Figure 7: Transcriptional activity of ERbeta agonists in Rv1 (a) and in HEK 293 (b) cells: data are expressed as mean ± SD of the ratio between the luminescence (RLU) of the experimental over the control reporter; $^{*}P < 0.05$ versus C and 3beta-Adiol 1 and 10 nM; $^{***}P < 0.001$ versus C and 3beta-Adiol 1 and 10 nM; $^{§§§}P < 0.001$ versus C and 8beta-VE2 1 and 10 nM; $^{\wedge\wedge\wedge}P < 0.001$ versus 8beta-VE2 1 nM.

cells [13] or of the stably transfected ERbeta in AD- or CR-PC cell lines [42, 43] results in the increase of p21 expression and cell cycle arrest.

During PC progression, PTEN inactivation is an established key modification for the emergence of androgen refractoriness [44]. Moreover, a partial loss of PTEN is extremely frequent in human primary cancers, particularly in PC, making the possibility to increase or maintain appropriate PTEN levels, an important target for chemoprevention. The ability of ERbeta activation to increase PTEN expression in cancer cells has been demonstrated by some authors in PC [45] and in other cancer models [42, 46, 47], but, to our knowledge, such effect of ERbeta activation over a long time frame has never been evaluated. To this regard, our results demonstrated that PTEN expression levels are not influenced by the activation of the endogenous ERbeta by 3beta-Adiol, as well as by 8beta-VE2, whereas DPN seems to display a slight activity from 5 weeks of treatment onward, which however influences cell proliferation only at the end of the chronic treatment (T12). These results suggest that in Rv1 cells the main target of ERbeta in the control of proliferation seems to be the modulation of cell cycle progression rather than inhibition of cell survival.

The androgen sensitivity of this cell line [33] is suggested by our results, demonstrating that the main constitutive active AR subtype (75 kDa) is much more expressed than the wild-type AR (110 kDa subtype). One of the criticisms for the use of 3beta-Adiol in PC cure is its potential retro-conversion

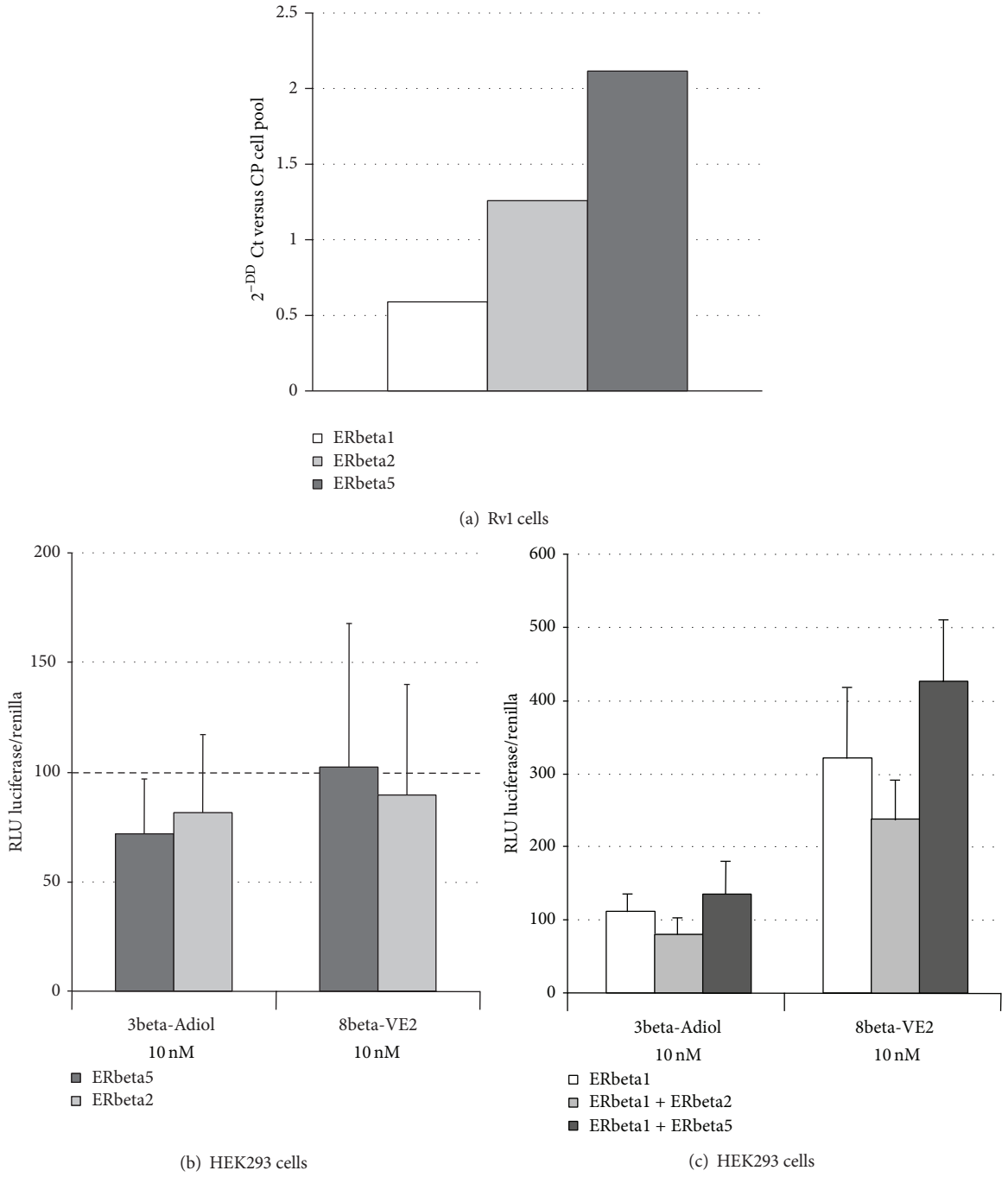

Figure 8: Relative expression of ERbeta isoforms by qPCR in Rv1 cells (a); ERbeta isoform-specific transcriptional activity induced by 3beta-Adiol and 8betaVE2 in HEK293 transfected cells ((b), (c)). ERbeta 2 and ERbeta5 were transfected separately (b) or together with ERbeta1 (c). Data are expressed as mean ± SD of the ratio between the luminescence (RLU) of the experimental over the control reporter. $^{**}P < 0.01$ versus beta1 + beta5 (8betaVE2); $^{***}P < 0.001$ versus the corresponding transfected cells in presence of 3beta-Adiol.

to DHT [48] and the very recently suggested ability of the compound to bind also to ARs in some particular conditions [49]. The results here presented, demonstrating that the antiproliferative effect of 3beta-Adiol is still present in a PC cell model expressing functional ARs, are particularly important, because they suggest a possible use of 3beta-Adiol (or its analogs) also in the androgen-dependent phase of PC progression. Interestingly, AR subtype expression in Rv1 cells is not affected by chronic exposure either to 3beta-Adiol or to the two other ERbeta selective agonists (data not shown), excluding a possible contribution of AR-mediated cell proliferation over time.

Chronic DPN administration does not influence cell proliferation with the exception of the last time point evaluated

(T12). As previously demonstrated in our laboratory, a 9-day exposure to DPN, at the same dose used in the present experiments, is able to significantly reduce DU145 cell proliferation [13]. Interestingly, the compound seems to be ineffective in LAPC-4 and in LNCaP cells, either in the absence or in the presence of DHT stimulation [50]. Notably, DU145 are CR-PC cells not expressing AR [51], while LAPC-4 and LNCaP cells are AD and express a 110 kDa AR [51]. Thus, it seems that, as opposed to 3beta-Adiol, the simultaneous presence of ERbeta and AR might interfere with DPN activity on PC cell proliferation. The possible interplay between the androgenic and estrogenic signaling pathways has apparently been evaluated only in breast cancer cells [52]. In this model, AR seems to target classical ERE sequences and it has been demonstrating an extensive interaction between AR and ERalpha in the control of target gene transcription, which results in a blunted proliferative action of ERalpha [52]. The possibility of a cross-talk between AR and ERbeta in controlling PC functions has never been studied yet but should be carefully examined in future studies to elucidate whether a similar mechanism could be active also in tumors where AR activation is the driving force for proliferation.

8beta-VE2 is as potent as estradiol in binding and activating ERbeta in prostate preparations [36, 37] and in inducing apoptosis in human prostatic basal cells [28]. However, the present study showed that this compound is completely unable to influence cell proliferation as well as p21 and PTEN expression in Rv1 cells. In a previously published study using different experimental conditions and cell models, 8beta-VE2, at a dose 60 times higher than that used in the present experiments and after a 12-h exposure, was able to activate the extrinsic pathway of apoptosis in another PC cell system, the PC3 cell line [27].

To get a better insight into the interactions of different ligands with the ERbeta pathway and the consequent biological effects (or lack of effect), we assessed the ability of 8beta-VE2 and 3beta-Adiol to induce ERE-mediated transcription upon binding either to the endogenous ERbeta in Rv1 cells or specifically to ERbeta1, transiently transfected into HEK293 cells (a cell line that lacks endogenous ERbeta proteins, [17]). 3beta-Adiol was able to activate ERE-mediated gene transcription in Rv1 cells, while 8beta-VE2 was completely inactive. On the contrary, 8beta-VE2 significantly and dose dependently stimulates ERE-mediated gene transcription through ERbeta1 in HEK293 cells, while 3beta-Adiol is completely ineffective in this experimental model.

One possible explanation of such opposite pattern of activation might be linked to a specific profile of expression of ERbeta subtypes in tumor cells and/or the different ability of the two compounds to bind to these subtypes and to activate transcription. It is indeed known that the alternative exon 8 present in the main ERbeta splice variants in humans (ERbeta2–ERbeta5) confers a conformational change in the second transactivation domain that alters the ability of the receptor to bind ligands and recruit cofactors [17]. However, all ERbeta subtypes can bind to canonical ERE-sequences on DNA as homo- or hetero-dimers [22]. It is also known that, during the development and progression of PC, ERbeta1 expression is gradually lost, while that of ERbeta2 and ERbeta5 increases [19]. Moreover, the relative expression between ERbeta2 and ERbeta5 differs among the different transformed prostate cell lines, since ERbeta2 is much higher than ERbeta5 in PC3 cells, while the opposite pattern is present in LNCaP cells [22].

The assessment of the relative mRNA expression levels of the three main ERbeta subtypes present in the human prostate (ERbeta1, -beta2, and -beta5) in Rv1 cells indicates that these cells possess low levels of ERbeta1 and higher levels of ERbeta2 and ERbeta5 (3- and 5-folds versus ERbeta1, resp.). In the Western blotting experiments, using an antibody able to recognize the N-terminus common to all the ERbeta subtypes (Figure 2(b), multiple bands within the 50–60 kDa range are shown: the presence of these bands is in agreement with the results obtained by qPCR and consistent with those reported by Leung et al. [17].

Differences in the cell response to ERbeta selective ligands among Rv1 (present results), DU145 [14], and PC3 cells [27] might be related to a different expression pattern of the ERbeta subtypes in the three cell lines. To test the possibility that 3beta-Adiol and 8beta-VE2 show a different transcriptional activity upon binding to ERbeta1, ERbeta2, or ERbeta5, we overexpressed the three ER subtypes alone or in combination in HEK293 cells and test the transcriptional activity of the two compounds by an ERE-coupled reporter gene. 8beta-VE2 was unable to stimulate transcription in the presence of ERbeta2 or ERbeta5 alone, confirming the inability of these ER subtypes to activate ERE-mediated transcription *per se*. On the contrary, the compound significantly stimulated gene transcription when ERbeta wild type was present, giving the possibility to form ERbeta1 homodimers or to heterodimerize with the other subtypes (ERbeta1:beta2 and ERbeta1:beta5). Analogous cotransfection experiments have demonstrated that, in comparison to ERbeta1, the coexpression of ER subtypes beta1:beta2 and of beta1:beta5 significantly increase the transcriptional activity of estradiol as well as other xenoestrogens [17]. In agreement with these findings, in our experiments, the transcriptional activity of 8beta-VE2 is significantly higher in the presence of the heterodimer beta1:beta5 in comparison to ERbeta1 alone. However, as opposed to what presented by these authors, we did not find significant difference between ERbeta1 alone and the dimer beta1:beta2. One possibility to explain the different behavior of 8beta-VE2 might be the propensity of the various ERbeta agonists to promote ERbeta homo- or heterodimerization. In line with this hypothesis, also phytoestrogens appear to favor only ERbeta1 homodimerization [17].

In agreement with the previous results, 3beta-Adiol appeared to lack any transcriptional activity in ERbeta transfected HEK293 cells in the presence either of a single or of different receptor subtypes. It should be underlined that in our experiments we cotransfected equimolar amounts of receptor subtypes, while, in normal or neoplastic prostate cells, the relative expression levels are widely variable ([19] and the data here presented). Thus, the possibility that 3beta-Adiol might stimulate ERE-mediated transcription only in the presence of a peculiar ratio among the different ER subtypes cannot be ruled out. As previously mentioned, the synergistic effect of ERbeta2 and ERbeta5 on ERbeta1-mediated transcription

depends on the ligand used. If ERbeta subtypes are expressed at different levels during the natural history of PC progression, this peculiar pattern, forming a wide and plastic array of homo or hetero-dimers, may contribute to the different pharmacology of the ERbeta selective agonists. The presence of a functional AR system in Rv1 cells adds a further level of complexity and might explain the different behavior between 3beta-Adiol and the other synthetic compounds. If part of the 3beta-Adiol, through its retro-conversion to DHT, binds to AR [48, 49], the effects observed on cell proliferation and p21 expression might imply a cross-talk between AR and ER signaling pathways and the recruitment of a particular set of coregulators. As previously mentioned, AR can also target classical ERE sequences and may interact with the ER systems, as already shown in breast cancer cells [52]. Studies are in progress in our laboratory to evaluate this hypothesis.

5. Conclusions

The results presented in this paper by using different ERbeta selective agonists demonstrate that the activation of the ERbeta pathway has an antiproliferative effect also in androgen-responsive primary PC tumors and that this activity is maintained for a long period of time. In addition, from our results it clearly appears that the mechanism of action through which ERbeta controls prostate cell proliferation is still obscure in some aspects because it possibly implies a complex interplay among ERbeta subtypes (which depends on their peculiar pattern of expression) and/or an interaction with the AR system. The high variability of ERbeta subtype levels in normal, preneoplastic, and cancerous prostatic cells, including Rv1 ([19] and the data shown here), coupled to the different behavior of selective ERbeta agonists on PC cell functions (as appears from our studies), strongly suggests that a careful assessment of the expression pattern of the ERbeta subtypes should not be disregarded, when considering ERbeta-targeted new drugs for PC chemoprevention.

Moreover, if different ERbeta selective agonists might produce distinct biological and clinical effects, it cannot be assumed that the lack of effect of one compound *in vitro* or in clinical trials may be extended to all the chemical classes of compounds that bind to ERbeta. In line with this concept, to prevent and/or slow down PC progression through ERbeta activation, it should be very important to identify the specific outcomes of the different ERbeta selective ligands in a PC specimen of each single patient. This strategy will be helpful to choose the appropriate drug for the therapy.

Conflict of Interests

The authors declare that there is no conflict of interests regarding the publication of this paper.

Authors' Contribution

Alessandra Colciago and Massimiliano Ruscica equally contributed to this work.

Acknowledgments

This study was supported by grants funded by the Italian Ministry of Education (PRIN 2007XLTPTK_001) and by the University of Milan (PUR). The authors are grateful to Dr. K. Prelle (Bayer Schering Pharma AG, Berlin, Germany) for providing 8beta-VE2 and to Dr. Paolo Martini (Shire Human genetic therapies, Cambridge, MA, USA) for providing ERbeta plasmids.

References

[1] J. Ferlay, D. M. Parkin, and E. Steliarova-Foucher, "Estimates of cancer incidence and mortality in Europe in 2008," *European Journal of Cancer*, vol. 46, no. 4, pp. 765–781, 2010.

[2] R. Geier, S. Adler, G. Rashid, and A. Klein, "The synthetic estrogen diethylstilbestrol (DES) inhibits the telomerase activity and gene expression of prostate cancer cells," *Prostate*, vol. 70, no. 12, pp. 1307–1312, 2010.

[3] L.-H. Chen, J. Fang, H. Li, W. Demark-Wahnefried, and X. Lin, "Enterolactone induces apoptosis in human prostate carcinoma LNCaP cells via a mitochondrial-mediated, caspase-dependent pathway," *Molecular Cancer Therapeutics*, vol. 6, no. 9, pp. 2581–2590, 2007.

[4] P. Mak, Y.-K. Leung, W.-Y. Tang, C. Harwood, and S.-M. Ho, "Apigenin suppresses cancer cell growth through ERβ," *Neoplasia*, vol. 8, no. 11, pp. 896–904, 2006.

[5] S. Nilsson, K. F. Koehler, and J.-A. Gustafsson, "Development of subtype-selective oestrogen receptor-based therapeutics," *Nature Reviews Drug Discovery*, vol. 10, no. 10, pp. 778–792, 2011.

[6] G. G. J. M. Kuiper, E. Enmark, M. Pelto-Huikko, S. Nilsson, and J.-A. Gustafsson, "Cloning of a novel estrogen receptor expressed in rat prostate and ovary," *Proceedings of the National Academy of Sciences of the United States of America*, vol. 93, no. 12, pp. 5925–5930, 1996.

[7] C. Thomas and J.-A. Gustafsson, "The different roles of ER subtypes in cancer biology and therapy," *Nature Reviews Cancer*, vol. 11, no. 8, pp. 597–608, 2011.

[8] H. Bonkhoff and R. Berges, "The evolving role of oestrogens and their receptors in the development and progression of prostate cancer," *European Urology*, vol. 55, no. 3, pp. 533–542, 2009.

[9] S.-M. Ho, M.-T. Lee, H.-M. Lam, and Y.-K. Leung, "Estrogens and Prostate Cancer: etiology, mediators, prevention, and management," *Endocrinology and Metabolism Clinics of North America*, vol. 40, no. 3, pp. 591–614, 2011.

[10] J. Hartman, A. Strom, and J. A. Gustafsson, "Current concepts and significance of estrogen receptor beta in prostate cancer," *Steroids*, vol. 77, no. 12, pp. 1262–1266, 2012.

[11] H. Kawashima and T. Nakatani, "Involvement of estrogen receptors in prostatic diseases," *International Journal of Urology*, vol. 19, no. 6, pp. 512–522, 2012.

[12] P. Dey, A. Strom, and J. A. Gustafsson, "Estrogen receptor beta upregulates FOXO3a and causes induction of apoptosis through PUMA in prostate cancer," *Oncogene*, 2013.

[13] A. Pravettoni, O. Mornati, P. G. V. Martini et al., "Estrogen receptor beta (ERbeta) and inhibition of prostate cancer cell proliferation: studies on the possible mechanism of action in DU145 cells," *Molecular and Cellular Endocrinology*, vol. 263, no. 1-2, pp. 46–54, 2007.

[14] V. Guerini, D. Sau, E. Scaccianoce et al., "The androgen derivative 5α-androstane-3β,17β-diol inhibits prostate cancer

cell migration through activation of the estrogen receptor β subtype," *Cancer Research*, vol. 65, no. 12, pp. 5445–5453, 2005.

[15] L. G. Horvath, S. M. Henshall, C.-S. Lee et al., "Frequent loss of estrogen receptor-β expression in prostate cancer," *Cancer Research*, vol. 61, no. 14, pp. 5331–5335, 2001.

[16] M. T. Lee, B. Ouyang, S. M. Ho, and Y. K. Leung, "Differential expression of estrogen receptor beta isoforms in prostate cancer through interplay between transcriptional and translational regulation," *Molecular and Cellular Endocrinology*, vol. 376, no. 1-2, pp. 125–135, 2013.

[17] Y.-K. Leung, P. Mak, S. Hassan, and S.-M. Ho, "Estrogen receptor (ER)-β isoforms: a key to understanding ER-β signaling," *Proceedings of the National Academy of Sciences of the United States of America*, vol. 103, no. 35, pp. 13162–13167, 2006.

[18] P. Dey, P. Jonsson, J. Hartman, C. Williams, A. Strom, and J. A. Gustafsson, "Estrogen receptors beta1 and beta2 have opposing roles in regulating proliferation and bone metastasis genes in the prostate cancer cell line PC3," *Molecular Endocrinology*, vol. 26, no. 12, pp. 1991–2003, 2012.

[19] Y.-K. Leung, H.-M. Lam, S. Wu et al., "Estrogen receptor β2 and β5 are associated with poor prognosis in prostate cancer, and promote cancer cell migration and invasion," *Endocrine-Related Cancer*, vol. 17, no. 3, pp. 675–689, 2010.

[20] C. Zhao, J. Matthews, M. Tujague et al., "Estrogen receptor β2 negatively regulates the transactivation of estrogen receptor α in human breast cancer cells," *Cancer Research*, vol. 67, no. 8, pp. 3955–3962, 2007.

[21] Z. Liu, Y. Liao, H. Tang, and G. Chen, "The expression of estrogen receptors beta2, 5 identifies and is associated with Prognosis in non-small cell lung cancer," *Endocrine*, 2013.

[22] J. T. Moore, D. D. McKee, K. Slentz-Kesler et al., "Cloning and characterization of human estrogen receptor β isoforms," *Biochemical and Biophysical Research Communications*, vol. 247, no. 1, pp. 75–78, 1998.

[23] W. R. Harrington, S. Sheng, D. H. Barnett, L. N. Petz, J. A. Katzenellenbogen, and B. S. Katzenellenbogen, "Activities of estrogen receptor alpha- and beta-selective ligands at diverse estrogen responsive gene sites mediating transactivation or transrepression," *Molecular and Cellular Endocrinology*, vol. 206, no. 1-2, pp. 13–22, 2003.

[24] A. Cvoro, S. Paruthiyil, J. O. Jones et al., "Selective activation of estrogen receptor-β transcriptional pathways by an herbal extract," *Endocrinology*, vol. 148, no. 2, pp. 538–547, 2007.

[25] L. A. Helguero, M. H. Faulds, J.-A. Gustafsson, and L.-A. Haldosén, "Estrogen receptors alfa (ERα) and beta (ERβ) differentially regulate proliferation and apoptosis of the normal murine mammary epithelial cell line HC11," *Oncogene*, vol. 24, no. 44, pp. 6605–6616, 2005.

[26] E. Motylewska, O. Stasikowska, and G. Mełeń-Mucha, "The inhibitory effect of diarylpropionitrile, a selective agonist of estrogen receptor beta, on the growth of MC38 colon cancer line," *Cancer Letters*, vol. 276, no. 1, pp. 68–73, 2009.

[27] S. J. McPherson, S. Hussain, P. Balanathan et al., "Estrogen receptor-β activated apoptosis in benign hyperplasia and cancer of the prostate is androgen independent and TNFα mediated," *Proceedings of the National Academy of Sciences of the United States of America*, vol. 107, no. 7, pp. 3123–3128, 2010.

[28] S. Hussain, M. G. Lawrence, R. A. Taylor et al., "Estrogen receptor beta activation impairs prostatic regeneration by inducing apoptosis in murine and human stem/progenitor enriched cell populations," *PLoS ONE*, vol. 7, no. 7, Article ID e40732, 2012.

[29] S. Paruthiyil, A. Cvoro, X. Zhao et al., "Drug and cell type-specific regulation of genes with different classes of estrogen receptor β-selective agonists," *PLoS ONE*, vol. 4, no. 7, Article ID e6271, 2009.

[30] G. G. J. M. Kuiper, P. J. Shughrue, I. Merchenthaler, and J.-A. Gustafsson, "The estrogen receptor β subtype: a novel mediator of estrogen action in neuroendocrine systems," *Frontiers in Neuroendocrinology*, vol. 19, no. 4, pp. 253–286, 1998.

[31] R. M. Sramkoski, T. G. Pretlow II, J. M. Giaconia et al., "A new human prostate carcinoma cell line, 22Rv1," *In Vitro Cellular and Developmental Biology: Animal*, vol. 35, no. 7, pp. 403–409, 1999.

[32] F.-M. Lin, C.-H. Tsai, Y.-C. Yang et al., "A novel diterpene suppresses CWR22Rv1 tumor growth in vivo through antiproliferation and proapoptosis," *Cancer Research*, vol. 68, no. 16, pp. 6634–6642, 2008.

[33] C. G. Tepper, D. L. Boucher, P. E. Ryan et al., "Characterization of a novel androgen receptor mutation in a relapsed CWR22 prostate cancer xenograft and cell line," *Cancer Research*, vol. 62, no. 22, pp. 6606–6614, 2002.

[34] M. J. Linja, K. J. Savinainen, T. L. J. Tammela, J. J. Isola, and T. Visakorpi, "Expression of ERα and ERβ in prostate cancer," *Prostate*, vol. 55, no. 3, pp. 180–186, 2003.

[35] P. Chomczynski and N. Sacchi, "Single-step method of RNA isolation by acid guanidinium thiocyanate-phenol-chloroform extraction," *Analytical Biochemistry*, vol. 162, no. 1, pp. 156–159, 1987.

[36] A. Hillisch, O. Peters, D. Kosemund et al., "Dissecting physiological roles of estrogen receptor α and β with potent selective ligands from structure-based design," *Molecular Endocrinology*, vol. 18, no. 7, pp. 1599–1609, 2004.

[37] A. Escande, A. Pillon, N. Servant et al., "Evaluation of ligand selectivity using reporter cell lines stably expressing estrogen receptor alpha or beta," *Biochemical Pharmacology*, vol. 71, no. 10, pp. 1459–1469, 2006.

[38] A. Belanger, J. Couture, S. Caron, and R. Roy, "Determination of nonconjugated and conjugated steroid levels in plasma and prostate after separation on C-18 columns," *Annals of the New York Academy of Sciences*, vol. 595, pp. 251–259, 1990.

[39] D. Dondi, M. Piccolella, A. Biserni et al., "Estrogen receptor β and the progression of prostate cancer: role of 5α-androstane-3β,17β-diol," *Endocrine-Related Cancer*, vol. 17, no. 3, pp. 731–742, 2010.

[40] C. Lattrich, A. Stegerer, J. Haring, S. Schuler, O. Ortmann, and O. Treeck, "Estrogen receptor beta agonists affect growth and gene expression of human breast cancer cell lines," *Steroids*, vol. 78, no. 2, pp. 195–202, 2013.

[41] K. Matsumura, T. Tanaka, H. Kawashima, and T. Nakatani, "Involvement of the estrogen receptor β in genistein-induced expression of p21waf1/cip1 in PC-3 prostate cancer cells," *Anticancer Research*, vol. 28, no. 2 A, pp. 709–714, 2008.

[42] P. Dey, R. P. Barros, M. Warner, A. Strom, and J. A. Gustafsson, "Insight into the mechanisms of action of estrogen receptor beta in the breast, prostate, colon, and CNS," *Journal of Molecular Endocrinology*, vol. 51, no. 3, pp. T61–T74, 2013.

[43] J. Cheng, E. J. Lee, L. D. Madison, and G. Lazennec, "Expression of estrogen receptor β in prostate carcinoma cells inhibits invasion and proliferation and triggers apoptosis," *FEBS Letters*, vol. 566, no. 1–3, pp. 169–172, 2004.

[44] M. M. Shen and C. Abate-Shen, "Pten inactivation and the emergence of androgen-independent prostate cancer," *Cancer Research*, vol. 67, no. 14, pp. 6535–6538, 2007.

[45] F. Cao, T.-Y. Jin, and Y.-F. Zhou, "Inhibitory effect of isoflavones on prostate cancer cells and PTEN gene," *Biomedical and Environmental Sciences*, vol. 19, no. 1, pp. 35–41, 2006.

[46] C. Guido, S. Panza, M. Santoro et al., "Estrogen receptor beta (ERbeta) produces autophagy and necroptosis in human seminoma cell line through the binding of the Sp1 on the phosphatase and tensin homolog deleted from chromosome 10 (PTEN) promoter gene," *Cell Cycle*, vol. 11, no. 15, pp. 2911–2921, 2012.

[47] P. Bulzomi, P. Galluzzo, A. Bolli, S. Leone, F. Acconcia, and M. Marino, "The pro-apoptotic effect of quercetin in cancer cell lines requires ERβ-dependent signals," *Journal of Cellular Physiology*, vol. 227, no. 5, pp. 1891–1898, 2012.

[48] J. L. Mohler, M. A. Titus, S. Bai et al., "Activation of the androgen receptor by intratumoral bioconversion of androstanediol to dihydrotestosterone in prostate cancer," *Cancer Research*, vol. 71, no. 4, pp. 1486–1496, 2011.

[49] J. Chen, W. Q. Wang, and S. X. Lin, "Interaction of Androst-5-ene-3beta, 17beta-diol and 5alpha-androstane-3beta, 17beta-diol with estrogen and androgen receptors: a combined binding and cell study," *The Journal of Steroid Biochemistry and Molecular Biology*, vol. 137, pp. 316–321, 2013.

[50] C. Weng, J. Cai, J. Wen et al., "Differential effects of estrogen receptor ligands on regulation of dihydrotestosterone-induced cell proliferation in endothelial and prostate cancer cells," *International Journal of Oncology*, vol. 42, no. 1, pp. 327–337, 2013.

[51] A. van Bokhoven, M. Varella-Garcia, C. Korch et al., "Molecular characterization of human prostate carcinoma cell lines," *Prostate*, vol. 57, no. 3, pp. 205–225, 2003.

[52] E. F. Need, L. A. Selth, T. J. Harris, S. N. Birrell, W. D. Tilley, and G. Buchanan, "Research resource: interplay between the genomic and transcriptional networks of androgen receptor and estrogen receptor alpha in luminal breast cancer cells," *Molecular Endocrinology*, vol. 26, no. 11, pp. 1941–1952, 2012.

Hindawi Publishing Corporation
BioMed Research International
Volume 2014, Article ID 465175, 6 pages
http://dx.doi.org/10.1155/2014/465175

Clinical Study

Image-Guided Hypofractionated Radiotherapy in Low-Risk Prostate Cancer Patients

Maurizio Valeriani, Alessia Carnevale, Linda Agolli, Paolo Bonome, Adelaide Montalto, Luca Nicosia, Mattia F. Osti, Vitaliana De Sanctis, Giuseppe Minniti, and Riccardo Maurizi Enrici

Department of Radiation Oncology, "La Sapienza" University, Sant'Andrea Hospital of Rome, Via di Grottarossa 1035-1039, 00189 Rome, Italy

Correspondence should be addressed to Maurizio Valeriani; mauval1@libero.it

Received 7 February 2014; Accepted 14 March 2014; Published 23 April 2014

Academic Editor: Giovanni Luca Gravina

Aim. To evaluate efficacy and toxicity of image-guided hypofractionated radiotherapy (HFRT) in the treatment of low-risk prostate cancer. Outcomes and toxicities of this series of patients were compared to another group of 32 low-risk patients treated with conventional fractionation (CFRT). *Methods*. Fifty-nine patients with low-risk prostate cancer were analysed. Total dose for the prostate and proximal seminal vesicles was 60 Gy delivered in 20 fractions. *Results*. The median follow-up was 30 months. The actuarial 4-year overall survival, biochemical free survival, and disease specific survival were 100%, 97.4%, and 97.4%, respectively. Acute grade 1-2 gastrointestinal (GI) and genitourinary (GU) toxicity rates were 11.9% and 40.7%, respectively. Grade 1 GI and GU late toxicity rates were 8.5% and 13.6%, respectively. No grade ≥2 late toxicities were recorded. Acute grade 2-3 GU toxicity resulted significantly lower ($P = 0.04$) in HFRT group compared to the CFRT group. The cumulative 4-year incidence of grade 1-2 GU toxicity was significantly higher ($P < 0.001$) for HFRT patients. *Conclusions*. Our study demonstrated that hypofractionated regimen provided excellent biochemical control in favorable risk prostate cancer patients. The incidence of GI and GU toxicity was low. However, HFRT presented higher cumulative incidence of low-grade late GU toxicity than CFRT.

1. Introduction

Hypofractionated radiation therapy (HFRT) has been suggested as an attractive strategy of treatment to improve results in localized prostate cancer. In contrast to other tumors, prostate cancer seems to have a low α/β ratio [1]. Thus, a therapeutic gain could be obtained by irradiating patients using schedules with larger dose per fraction and lower number of fractions. In addition to a possible radiobiological benefit, hypofractionated RT allows a shorter overall treatment time and reduction of treatment costs. Randomized trials have shown a better biochemical control when higher total doses of conventionally fractionated irradiation (CFRT) are delivered to the prostate [2].

In our study, we assessed the acute and late toxicity and the biochemical control in patients with low-risk prostate cancer receiving external beam radiation therapy (EBRT) using a hypofractionated schedule. Furthermore, toxicity rates were compared between this series and another group of patients who underwent standard fractionation regimen.

2. Materials and Methods

2.1. Patients' Characteristics. Between January 2007 and January 2013, 59 patients with biopsy proven, low-risk prostate cancer were treated with HFRT therapy associated with IGRT. Median age at diagnosis was 72 years (range 48–82 years). All patients presented cT1/2a N0 M0 clinical stage, a Gleason score of 6, and a pretreatment prostate-specific antigen (PSA) serum level <10 ng/mL.

Pretreatment evaluation included complete physical examination, PSA level, complete blood counts and standard biochemistry tests, bone scan, total body computed tomography (CT) with contrast medium, and prostate magnetic resonance image (MRI) with diffusion and perfusion sequences.

Table 1: Patients' characteristics.

Characteristics	HFRT ($n = 59$)		CFRT ($n = 32$)		Total ($n = 91$)	
	n	%	n	%	n	%
Age						
<70	19	32.2	4	12.5	23	25.3
≥70	40	67.8	28	87.5	68	74.7
PSA at diagnosis (ng/mL)						
0.1–5	19	32.2	9	28.1	28	30.8
5.1–9.9	40	67.8	23	71.9	63	69.2
Gleason score						
6	59	100	32	100	91	100
Clinical stage						
T1c	17	28.8	8	25.0	25	27.6
T2a	42	71.2	24	75.0	66	72.4

Median of PSA value at diagnosis was 5.94 ng/mL (range 2.6–9.4 ng/mL). Outcomes and toxicity profile of patients receiving HFRT were compared with a group of 32 low-risk patients treated with CFRT and image-guided radiotherapy (IGRT) that refused hypofractionated treatment. Median of PSA value at diagnosis for CFRT patients was 6.4 ng/mL (range 3.1–9.6 ng/mL). All patients provided written informed consent. Patient characteristics are summarized in Table 1.

2.2. Treatment. All patients underwent a pretreatment CT planning (2.5 mm slice thickness) in the supine position with feet rests for the implementation of treatment planning. The preparation for CT scan encompassed the administration to a mini enema for rectal emptying and then patients were invited to next urination. In addition, they were requested to drink 500 mL of water half an hour before the start of the procedure to fulfill the bladder. Planning CT images were fused with MRI images (diffusion ADC map, perfusion series, and axial high resolution T2-w) using point-to-point matching to help clinical target volume (CTV) delineation.

The CTV included the prostate and the first centimeter of the seminal vesicles. Planning target volume (PTV) was generated adding a 5 mm margin in all directions. The whole rectum from the anus to the sigmoid flexure, bladder, femoral heads, and penile bulb were delineated as organs at risk.

A 3D conformal plan on the Eclipse planning system (Varian, Palo Alto, CA) was performed using 5 coplanar fields. Treatment was delivered by a linear accelerator using 15 MV photons. Thus, the PTV received 60 Gy in 20 fractions (3 Gy per fraction) in the hypofractionated group and 76 Gy in 38 fractions (2 Gy per fraction) in the conventional group, five weekly times. According to the Linear Quadratic Model, the hypofractionated regimen is biologically equivalent to 77.1 Gy in 2 Gy fractions assuming an α/β ratio of 1.5 Gy. This regimen is also equivalent to 72 Gy in 2 Gy fractions assuming an α/β ratio of 3 Gy for late responding tissue. Dose-volume constraints were as follows: V50 < 35% and V58 < 25% for the rectum; V43 < 50% for the bladder.

Prior to each treatment, patients underwent a Kilovoltage cone-beam CT that was compared with the planning CT to verify the correct position. The patients' position was adjusted with an initial automatic bone alignment, followed by a soft tissue alignment using the prostate-rectum interface.

From the start of radiation therapy, all patients were advised to follow a low-fibre and low-fat diet and to assume a cranberry based integrator and lactic ferment once daily.

2.3. Toxicity and Follow-Up. Follow-up was performed every 3 months for the first year and every 6 months afterwards. Toxicities were assessed at each follow-up according to the Radiation Therapy Oncology Group (RTOG) scale for acute and late adverse effects [3]. Late toxicities were considerate after 90 days from the RT completion.

2.4. Statistical Analysis. The biochemical failure was defined as the PSA nadir + 2 ng/mL according to the Phoenix criteria [4]. Overall survival (OS), disease specific survival (DSS), and biochemical free survival (bNED) were calculated to the event using the Kaplan-Meier method. Difference in the cumulative incidence of ≥grade 2 late toxicities between the two groups (presence of toxicity at any time of follow-up was considered as event) was evaluated with log-rank test. In the subgroups analysis, acute toxicities between HFRT and CFRT groups were compared using the chi-square test. Statistical analysis was performed using SPSS statistical software package version 13.0 (SPSS, Inc., Chicago, IL). A P value lower than 0.05 was considered as statistically significant.

3. Results

3.1. Survivals and Relapse. The median follow-up for patients treated with HFRT was 30 months (range 12–76 months), whereas for patients treated with CFRT it was 52 months (range 7–79 months). The overall median follow-up was 40 months (range 7–76 months).

The median PSA value at last follow-up was 0.51 ng/mL (range 0.04–3.1 ng/mL) in the HFRT group. The median PSA value at last follow-up was 0.42 ng/mL (range 0.04–1.5 ng/mL) in the CFRT group.

The actuarial 4-year OS was 100% and 93.8% ($P = 0.053$) for the HFRT and CFRT groups, respectively. Two deaths occurred in the CFRT group at the time of the statistical analysis. The patients died after 7 and 10 months from RT completion, respectively, for cardiopulmonary disorders without any evidence of disease. The actuarial 4-year bNED and DSS were 97.4% for HFRT group. The actuarial 4-year bNED and DSS were 100% for the CFRT group. There was no statistical difference ($P = 0.374$) regarding survivals between the two groups. One patient developed biochemical failure with evidence of external iliac lymph nodes involvement confirmed by Choline TC-PET in the HFRT group.

3.2. Acute Toxicities. Toxicities occurred as follows during treatment: grade 1 and grade 2 gastrointestinal (GI) toxicity

Table 2: Comparison of acute GI and GU toxicities in the CFRT group versus HFRT group.

Toxicity	GI					GU				
	CFRT		HFRT		P value	CFRT		HFRT		P value
	n	%	n	%		n	%	n	%	
During RT										
G1	7/32	21.9	7/59	11.9	0.206	15/32	46.9	23/59	39.0	0.466
≥G2	2/32	6.3	0/59	0	0.052	6/32	18.8	1/59	1.7	0.04
3-month FU										
G1	2/32	6.3	3/59	5.1	0.816	3/32	9.4	6/59	10.2	0.904
≥G2	0	0	0	0		0	0	0	0	

in 14/91 (15.4%) and 2/91 patients (2.2%), respectively; grades 1, 2, and 3 genitourinary (GU) toxicity in 38/91 (41.8%), 6/91 (6.6%), and 1/91 patients (1.1%), respectively.

At 3 months after radiation treatment grade 1 GI toxicity was observed in 5/91 patients (5.5%), and grade 1 GU toxicity was observed in 9/91 patients (9.9%). No grade ≥2 GU or GI toxicities were recorded.

No statistically significant difference was calculated between the two groups treated with CFRT and HFRT at 3 months from the end of therapy. During treatment grade 2-3 GU toxicity resulted statistically higher ($P = 0.04$) in the group treated with CFRT. Toxicity rates are summarized in Table 2.

3.3. Late Toxicities. At 6 months from the end of therapy, 2 patients (3.4%) treated with HFRT and 4 (12.5%) treated with CFRT presented grade 1 GI toxicity. Grade 2 GI toxicity was observed in 1 patient (3.1%) that received CFRT treatment. Seven patients (11.9%) treated with HFRT and 3 (9.4%) treated with CFRT presented grade 1 GU toxicity. No grade ≥2 toxicities were recorded.

At the last follow-up, grade 1 GI and GU toxicities were observed in 5 (8.5%) and 8 (13.6%) patients treated with HFRT, respectively. Patients treated with CFRT experienced grade 1 GI and GU toxicity in 12.5% and 3.1% (1 patient), respectively. Only one patient (1.1%) developed grade 2 GI toxicity (CFRT group). No grade ≥3 toxicities were recorded.

The cumulative incidence of grade 1-2 GI toxicities at 4 years was 13.6%, for CFRT group was 7.2%, and for HFRT group was 24.5% ($P = 0.191$). The cumulative incidence of grade 1-2 GU toxicities at 4 years was 11.5%, for CFRT group was 4%, and for HFRT group was 49% ($P < 0.001$) (Figures 1 and 2).

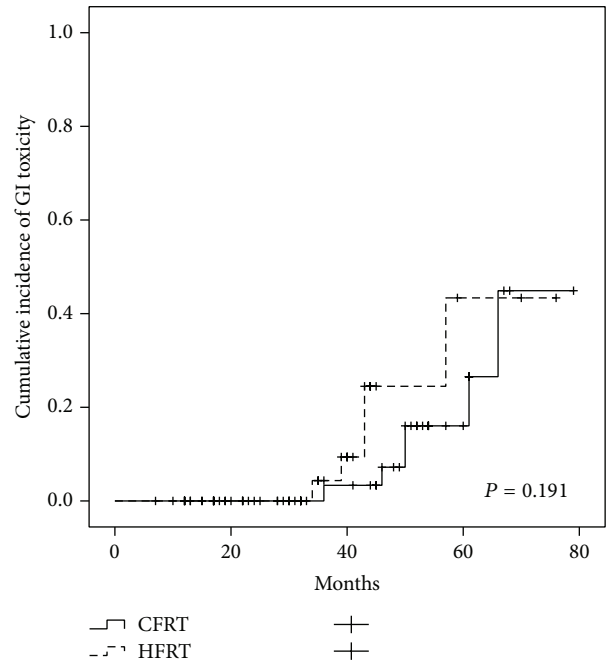

Figure 1: Comparison of grade 1-2 GI late toxicity in the CFRT and HFRT group.

4. Discussion

Early results from several hypofractionated trials [5, 6] indicate that HFRT is safe and provides good biochemical control. We reported our experience of favorable risk localized prostate carcinoma patients treated with hypofractionated radiotherapy schedule 60 Gy/20 fractions over 4 weeks associated with IGRT. This group of patients was compared with a group of 32 low-risk patients treated with conventional fractionation and IGRT that refused hypofractionated treatment.

The actuarial 4-year OS was 100% and 93.8% ($P = 0.053$) for the HFRT and CFRT groups, respectively. Two deaths occurred in the CFRT group at the time of analysis. The patients died after 7 and 10 months from RT completion, respectively, for cardiopulmonary disorders without any evidence of disease. The actuarial 4-year bNED and DSS were 97.4% for HFRT group. The actuarial 4-year bNED and DSS were 100% for the CFRT group. There was no significant difference ($P = 0.374$) between the two groups. One patient developed biochemical failure with evidence of external iliac lymph nodes involvement. Our results were favorable compared to other experiences of dose escalation using conventional fractionation regimens. In the literature, there are two randomized trials that reported long-term outcomes. Zietman et al. [7] had shown 5-year bNED rates of 91% and 10-year bNED rates of 84%. Kuban et al. [8] reported 5- and 8-year bNED rates of 100% and 88%, respectively, in low-risk prostate cancer patients.

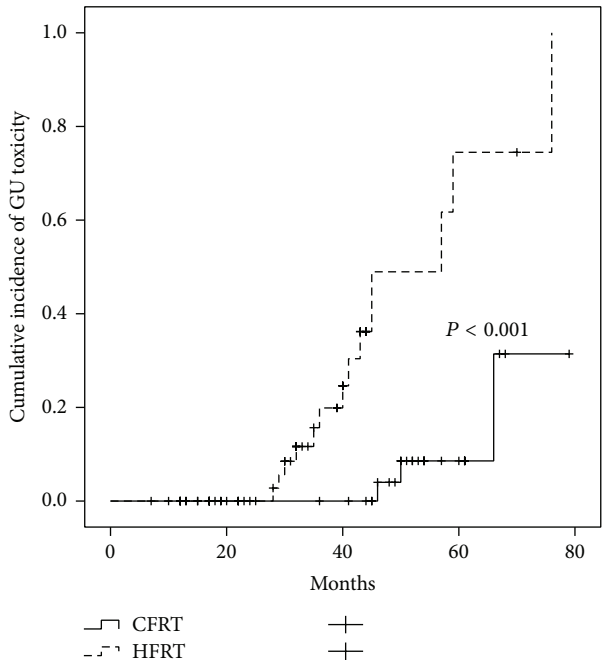

Figure 2: Comparison of grade 1-2 GU late toxicity in the CFRT and HFRT group.

A randomized study by Pollack et al. [9] reported no significant difference in terms of bNED between the two arms of patients treated with hypofractionated regimen versus standard fractionation, even though every type of prostate cancer risk was included in the study. Another study by Martin et al. [10] reported similar outcomes to our study: the 3-year bNED was 100% in low-risk patients who underwent IGRT-IMRT hypofractionated radiotherapy. Patel et al. [11] reported actuarial biochemical control rates and cancer-specific survival at 5 years of 97% and 100%, respectively, using 3-dimensional conformal radiotherapy with total dose of 66 Gy delivered in 22 fractions in low-intermediate-risk prostate cancer patients.

Treatment was well tolerated with more than 50% of patients presenting no acute urinary or gastrointestinal toxicity. The incidence of acute toxicity in our cohort was lower than other series. Martin et al. [10] reported 11% of grade 2 GI acute toxicity and 25% of grade 2 GU acute toxicity after HFRT with 60 Gy in 20 fractions in localized prostate cancer patients. Soete et al. [12] reported 5% of grade 2 acute GI toxicity with no grade 3 toxicity using 56 Gy/16 fractions regimen. In our study, toxicities during treatment occurred as follows: grade 1-2 acute GI toxicity in 17.6% patients; grade 1-2 and grade 3 acute GU toxicity in 48.4% and 1.1% patients, respectively. In a recent study by Patel et al. [11] the reported toxicity rates in patients with favourable risk prostate cancer who underwent 66 Gy/22 fractions were 17% of grades 1-2 GI toxicities and 33% of grade 1-2 GU toxicities; only 1% of patients experienced grade 3 GU toxicity. Pollack et al. [13] using 70.2 Gy in 26 fractions (2.7 Gy per fraction) found, at 3 months after RT, 6% grade 2 GU toxicity and no grade 2 GI toxicity. At 3 months after radiation treatment we observed grade 1 GI and GU toxicity in 5.1% and 10.2% of patients treated with HFRT, respectively. No grade ≥2 GU and GI toxicities were recorded. During the treatment grade 2-3 GU toxicity rates were low but resulted significantly higher ($P = 0.04$) in the group treated with CFRT. No statistically significant difference in acute toxicity was calculated between the two groups treated with CFRT and HFRT at 3 months from the end of therapy. As this comparison study is retrospective in nature, it is subject to the biases of this methodology.

One major concern about hypofractionation regimen with a high BED is the manifestation of potential late effects. Toxicity was prospectively scored in every patient at each follow-up visit. Our long-term results demonstrated that HFRT regimen was well tolerated. At 6 months from the end of therapy, 2 patients (3.4%) presented grade 1 GI toxicity and 7 patients (11.9%) presented grade 1 GU toxicity. No grade ≥2 toxicities were recorded.

Kupelian et al. [14] reported grade 1-2 of late GI toxicity in 9%, grade 3-4 in 1.4% of the patients, grade 1-2 of late GU toxicity in 9.4%, and grade 3 in 0.1% after conventional radiotherapy with 70 Gy in 28 fractions of 2.5 Gy with a 4 mm rectal margin. Pollack et al. [13] reported 5.9% of late grade ≥2 GI toxicity after 70.2 Gy in 26 fractions of 2.7 Gy. A recent update of the same trial described higher GU toxicities in the HFRT arm (18.3% versus 8.3%, $P = 0.028$) compared to the CFRT arm [9]. Martin et al. [10] described an incidence of 6.3% of late grade ≥2 GI toxicity and 4.3% of late grade ≥2 GU toxicity after hypofractionated regimen (60 Gy/20 fractions). After 2 and 5 years of follow-up, several studies reported grade ≥2 late GI side effects of 4% and 5.5% and late bladder side effects in 4.2% and 5.6%, respectively [15, 16]. Rene et al. [17] reported at the last follow-up persistent grade ≥2 late GU and GI toxicity of 2% and 1.5%, respectively. In the current study, at the last follow-up grade 1 GI and GU toxicities were observed in 5 patients (8.5%) and 8 patients (13.6%), respectively. No grade ≥2 toxicities were recorded. The actuarial incidence of grade 1-2 GI toxicities at 4 years was 13.6%, for CFRT group was 7.2%, and for HFRT group was 24.5% ($P = 0.191$). The actuarial incidence of grade 1-2 GU toxicities at 4 years was 11.5%, for CFRT group was 4%, and for HFRT group was 49% ($P < 0.001$). Patients treated with HFRT during the follow-up had more probability to develop transient event of grade 1-2 GU toxicity. In fact, most of these symptoms resolved over time and 84% of patients presented no GU symptoms at the last follow-up. The lower toxicity rates achieved in our study, especially GI, are likely a result of the advantage of reduced margins from CTV to PTV combined to daily IGRT. Although today IMRT has been widely adopted as the radiation technique of choice for prostate cancer according to better sparing of the bladder and rectum, our study demonstrated that hypofractionated radiation therapy can be safely delivered using IGRT-3D-CRT. In fact, we reported a toxicity rate similar to another study in which hypofractionated regimens were delivered with IMRT.

Men treated with 60 Gy/20 fractions in our study experienced acceptable toxicity rates. From our data, there appears to be no increase in late toxicity, using a 60 Gy

hypofractionated regimen for localized prostate cancer. There are three ongoing phase 3 randomized trials attempting to evaluate the effectiveness and tolerance of hypofractionated RT regimens compared with standard RT fractionation. The Canadian Prostate Fractionated Irradiation Trial (PROFIT) compared the Princess Margaret Hospital regimen of 60 Gy in 20 fractions [10] with standard regimen 78 Gy in 39 fractions in intermediate-risk patients. Up to 6 months of hormonal treatment before radiation therapy was allowed. The RTOG 0415 trial assessed HypoRT in low-risk patients without hormonal therapy. This study tested Kupelian's [14] regime of 70 Gy in 28 fractions versus 73.8 Gy in 41 fractions. Both trials are completed, but neither has reported preliminary results already. The British CHHiP (Conventional or Hypofractionated High Dose Intensity Modulated Radiotherapy for Prostate Cancer) [18] included a range of patients with localized prostate cancer even those with clinical stage T 1–3, PSA up to 30 ng/mL, and any Gleason score. This trial compared the standard fractionated schedule of 74 Gy in 37 fractions with 2 hypofractionated regimes (60 Gy/20 fractions and 57 Gy/19 fractions) in patients with low-, intermediate-, and high-risk disease. Short course hormonal therapy for 3–6 months was administered to the majority of patients. The interim analysis of this study has shown that grade ≥2 GI toxicity at 2 years in the conventional versus 60 Gy group versus 57 Gy group was 4.3%, 3.6%, and 1.4%, respectively, and grade ≥2 GU toxicity was 2.2%, 2.2%, and 0, respectively.

Further, technology has evolved dramatically since the publication of the earliest HFRT studies. Some retrospective studies show that such novel technologies may improve outcomes, but others show no effect in the context of HFRT [19, 20]. Image-guidance and prostate immobilization have become a critical component of stereotactic body radiation therapy (SBRT) because there is potential of large doses delivered to prostate cancer [21, 22]. SBRT and hadron therapy are acquiring acceptance as alternative to CFRT and HFRT schedules. No phase III data are available, although the current literature includes several phase I/II trials.

5. Conclusions

Our study demonstrated that hypofractionated regimen provided excellent biochemical control in favorable risk prostate cancer with the 4-year actuarial biochemical control rate of 97.4%. The incidence of acute and late GI and GU toxicity was low. However, in our study HFRT presented higher cumulative incidence of low-grade late GU toxicity than CFRT.

Results from completed randomized phase 3 trials will be necessary to allow us to define the α/β ratio of prostate cancer more accurately and confirm whether hypofractionation is a safe method of delivering dose-escalated curative radiation therapy.

Conflict of Interests

The authors declare that there is no conflict of interests regarding the publication of this paper.

References

[1] D. A. Loblaw and P. Cheung, "External beam irradiation for localized prostate cancer—the promise of hypofractionation," *The Canadian Journal of Urology*, vol. 13, supplement 1, pp. 62–66, 2006.

[2] M. Ritter, "Rationale, conduct, and outcome using hypofractionated radiotherapy in prostate cancer," *Seminars in Radiation Oncology*, vol. 18, no. 4, pp. 249–256, 2008.

[3] J. D. Cox, J. Stetz, and T. F. Pajak, "Toxicity criteria of the Radiation Therapy Oncology Group (RTOG) and the European Organization for Research and Treatment of Cancer (EORTC)," *International Journal of Radiation Oncology ∗ Biology ∗ Physics*, vol. 31, no. 5, pp. 1341–1346, 1995.

[4] M. Roach 3rd, G. Hanks, H. Thames Jr. et al., "Defining biochemical failure following radiotherapy with or without hormonal therapy in men with clinically localized prostate cancer. Recommendations of the RTOG-ASTRO Phoenix consensus conference," *International Journal of Radiation Oncology ∗ Biology ∗ Physics*, vol. 65, pp. 965–974, 2006.

[5] H. Lukka, C. Hayter, J. A. Julian et al., "Randomized trial comparing two fractionation schedules for patients with localized prostate cancer," *Journal of Clinical Oncology*, vol. 23, no. 25, pp. 6132–6138, 2005.

[6] E. E. Yeoh, R. H. Holloway, R. J. Fraser et al., "Hypofractionated versus conventionally fractionated radiation therapy for prostate carcinoma: updated results of a phase III randomized trial," *International Journal of Radiation Oncology ∗ Biology ∗ Physics*, vol. 66, no. 4, pp. 1072–1083, 2006.

[7] A. L. Zietman, K. Bae, J. D. Slater et al., "Randomized trial comparing conventional-dose with high-dose conformal radiation therapy in early-stage adenocarcinoma of the prostate: Long-term results from Proton Radiation Oncology Group/American College Of Radiology 95-09," *Journal of Clinical Oncology*, vol. 28, no. 7, pp. 1106–1111, 2010.

[8] D. A. Kuban, S. L. Tucker, L. Dong et al., "Long-term results of the M. D. Anderson randomized dose-escalation trial for prostate cancer," *International Journal of Radiation Oncology ∗ Biology ∗ Physics*, vol. 70, pp. 67–74, 2008.

[9] A. Pollack, G. Walker, E. M. Horwitz et al., "Randomized trial of hypofractionated external-beam radiotherapy for prostate cancer," *Journal of Clinical Oncology*, vol. 31, pp. 3860–3868, 2013.

[10] J. M. Martin, T. Rosewall, A. Bayley et al., "Phase II trial of hypofractionated image-guided intensity-modulated radiotherapy for localized prostate adenocarcinoma," *International Journal of Radiation Oncology ∗ Biology ∗ Physics*, vol. 69, no. 4, pp. 1084–1089, 2007.

[11] N. Patel, S. Faria, F. Cury et al., "Hypofractionated radiation therapy (66 Gy in 22 fractions at 3 Gy per fraction) for favorable-risk prostate cancer: long-term outcomes," *International Journal of Radiation Oncology ∗ Biology ∗ Physics*, vol. 86, pp. 534–539, 2013.

[12] G. Soete, S. Arcangeli, G. De Meerleer et al., "Phase II study of a four-week hypofractionated external beam radiotherapy regimen for prostate cancer: report on acute toxicity," *Radiotherapy and Oncology*, vol. 80, no. 1, pp. 78–81, 2006.

[13] A. Pollack, A. L. Hanlon, E. M. Horwitz et al., "Dosimetry and preliminary acute toxicity in the first 100 men treated for prostate cancer on a randomized hypofractionation dose escalation trial," *International Journal of Radiation Oncology ∗ Biology ∗ Physics*, vol. 64, no. 2, pp. 518–526, 2006.

[14] P. A. Kupelian, T. R. Willoughby, C. A. Reddy, E. A. Klein, and A. Mahadevan, "Hypofractionated intensity-modulated radiotherapy (70 Gy at 2.5 Gy per raction) for localized prostate cancer: Cleveland Clinic experience," *International Journal of Radiation Oncology ∗ Biology ∗ Physics*, vol. 68, no. 5, pp. 1424–1430, 2007.

[15] J. H. Coote, J. P. Wylie, R. A. Cowan, J. P. Logue, R. Swindell, and J. E. Livsey, "Hypofractionated intensity-modulated radiotherapy for carcinoma of the prostate: analysis of toxicity," *International Journal of Radiation Oncology ∗ Biology ∗ Physics*, vol. 74, no. 4, pp. 1121–1127, 2009.

[16] F. Leborgne and J. Fowler, "Late outcomes following hypofractionated conformal radiotherapy vs. standard fractionation for localized prostate cancer: a nonrandomized contemporary comparison," *International Journal of Radiation Oncology ∗ Biology ∗ Physics*, vol. 74, no. 5, pp. 1441–1446, 2009.

[17] N. Rene, S. Faria, F. Cury et al., "Hypofractionated radiotherapy for favorable risk prostate cancer," *International Journal of Radiation Oncology ∗ Biology ∗ Physics*, vol. 77, no. 3, pp. 805–810, 2010.

[18] D. Dearnaley, I. Syndikus, G. Sumo et al., "Conventional versus hypofractionated high-dose intensity-modulated radiotherapy for prostate cancer: preliminary safety results from the CHHiP randomised controlled trial," *The Lancet Oncology*, vol. 13, no. 1, pp. 43–54, 2012.

[19] W. Y. Song, B. Schaly, G. Bauman, J. J. Battista, and J. Van Dyk, "Evaluation of image-guided radiation therapy (IGRT) technologies and their impact on the outcomes of hypofractionated prostate cancer treatments: a radiobiologic analysis," *International Journal of Radiation Oncology ∗ Biology ∗ Physics*, vol. 64, no. 1, pp. 289–300, 2006.

[20] M. J. Zelefsky, M. Kollmeier, B. Cox et al., "Improved clinical outcomes with highdose image guided radiotherapy compared with non-IGRT for the treatment of clinically localized prostate cancer," *International Journal of Radiation Oncology ∗ Biology ∗ Physics*, vol. 84, no. 1, pp. 125–129, 2012.

[21] N. G. Zaorsky, M. T. Studenski, A. P. Dicker, L. Gomella, and R. B. Den, "Stereotactic body radiation therapy for prostate cancer: is the technology ready to be the standard of care?" *Cancer Treatment Reviews*, vol. 39, no. 3, pp. 212–218, 2013.

[22] M. R. Button and J. N. Staffurth, "Clinical application of image-guided radiotherapy in bladder and prostate cancer," *Clinical Oncology*, vol. 22, no. 8, pp. 698–706, 2010.

Hindawi Publishing Corporation
BioMed Research International
Volume 2014, Article ID 193635, 7 pages
http://dx.doi.org/10.1155/2014/193635

Research Article

Diverse Effects of ANXA7 and p53 on LNCaP Prostate Cancer Cells Are Associated with Regulation of SGK1 Transcription and Phosphorylation of the SGK1 Target FOXO3A

Meera Srivastava, Ximena Leighton, Joshua Starr, Ofer Eidelman, and Harvey B. Pollard

Department of Anatomy, Physiology and Genetics and Institute for Molecular Medicine, Uniformed Services University of Health Sciences (USUHS), School of Medicine, Bethesda, MD 20814, USA

Correspondence should be addressed to Meera Srivastava; meera.srivastava@usuhs.edu

Received 7 February 2014; Accepted 27 March 2014; Published 22 April 2014

Academic Editor: Giovanni Luca Gravina

Tumor suppressor function of the calcium/phospholipid-binding Annexin-A7 (ANXA7) has been shown in *Anxa7*-deficient mice and validated in human cancers. In the androgen-resistant prostate cancer cells, ANXA7 and p53 showed similar cytotoxicity levels. However, in the androgen-sensitive LNCaP, ANXA7 greatly exceeded the p53-induced cytotoxicity. We hypothesized that the p53 underperformance in LNCaP could be due to the involvement of p53-responsive SGK1 and FOXO3A. In this study, we show that p53 failed to match programmed cell death (PCD) and G1-arrest that were induced by ANXA7 in LNCaP. WT-ANXA7 preserved total FOXO3A expression with no hyperphosphorylation that could enable FOXO3A nuclear translocation and proapoptotic transcription. In contrast, in the p53-transfected LNCaP cells with maintained cell proliferation, the phosphorylated (but not total) FOXO3A fraction was increased implying a predominantly cytoplasmic localization and, subsequently, a lack of FOXO3A proapoptotic transcription. In addition, p53 reduced the expression of aberrant SGK1 protein form in LNCaP. Using Ingenuity Pathway Analysis and p53-signature genes, we elucidated the role of distinct SGK1/FOXO3A-associated regulation in p53 versus ANXA7 responses and proposed that aberrant SGK1 could affect reciprocal SGK1-FOXO3A-Akt regulation. Thus, the failure of the cell growth regulator p53 versus the phospholipid-binding ANXA7 could be potentially attributed to its diverse effects on SGK1-FOXO3A-Akt pathway in the PTEN-deficient LNCaP.

1. Introduction

The tumor suppressor gene (TSG) function of the Ca/phospholipid-binding Annexin-A7 (ANXA7, NP001147.1, NCBI) has been demonstrated in our previous studies, including *Anxa7(+/−)* murine model and ANXA7 tissue microarray profiling in normal versus tumor tissues [1, 2]. Loss of heterozygosity at the ANXA7-harboring 10q-locus [3] and a particular loss of ANXA7 expression in the hormone-refractory prostate tumors provided evidence for the hormone-related tumor suppressor role of ANXA7 in prostate cancer. ANXA7 matched cytotoxicity of a conventional tumor suppressor p53 in androgen-resistant DU145 and PC3, but greatly surpassed p53 effects in androgen-sensitive LNCaP [4]. We also showed that ANXA7 protected normal prostate cells and induced RB-associated cytotoxicity in prostate cancer cells *in vitro* [4]. The RB-associated ANXA7 effects in LNCaP included a reversal of the RB-dependent repression of the proapoptotic E2F-transcription. We undertook this study to understand the molecular mechanisms that caused p53 underperformance compared to ANXA7 and, subsequently, to elicit the beneficial tumor suppressor mechanisms of ANXA7 in LNCaP.

The PTEN-mutant LNCaP possess a constitutively active Akt which negatively regulates the forkhead transcription factor FOXO3A/FKHRL1. A FOXO3A decrease followed by the p53-downstream p27 promoter transactivation was reported in the LNCaP progression to androgen independence [5]. In a crosstalk between two transcription factors,

p53 and FOXO3A [6, 7], the activated FOXO3A impaired p53 transcriptional activity, while the activated p53 inhibited the FOXO3A-mediated transcription via FOXO3A phosphorylation and cytoplasmic retention. While a major FOXO3A-regulator Akt was not essential for the p53-dependent FOXO3A suppression, the serum/glucocorticoid regulated kinase 1, SGK1, was significantly induced in a p53-dependent manner. SGK1 is a target of p53 which can repress the glucocorticoid receptor (GR) transactivation and binding to SGK1-promoter [8]. The androgen-sensitive and PTEN-mutant LNCaP lack the SGK1-inducing GR [9] and TGF-beta [10, 11]. Consequently, the p53-responsive prosurvival SGK1, which facilitates androgen receptor- (AR-) dependent [12] and FOXO3A-mediated [13] cell survival, could be specifically involved in the p53 underperformance in LNCaP.

Hence, we studied the SGK1/FOXO3A-associated effects of p53 versus ANXA7 that were anticipated to reveal the alterations in canonical p53 cell survival control as well as beneficial ANXA7 tumor suppressor effects in the PTEN-deficient LNCaP.

2. Material and Methods

2.1. Cell Culturing and Infection. Normal prostate (PrEC) and androgen-sensitive LNCaP prostate cancer cells (ATCC) were cultured as suggested by the manufacturer and transfected with ANXA7 and p53 constructs. Adenoviral vector-based plasmids for infection (AdEasy System, Johns Hopkins Oncology Center) are "empty" vector, wild-type (WT) or dominant-negative (DN) ANXA7, and p53. WT-ANXA7 corresponded to a more abundant short ANXA7-isoform (NP 001147.1, NCBI). DN-ANXA7 (which is known to inhibit WT-ANXA7-induced phosphatidylserine liposome aggregation) contained triple mutations against calcium-binding site which was intended to affect COOH-terminal residues in annexin repeats 2, 3, and 4 (E277 → Q277, D360-E361 → N360-Q361, and D435-D436 → N435-N436, resp.).

2.2. Programmed Cell Death (PCD) and Cell Cycling Analysis. Programmed cell death (PCD) detection was performed in single GFP-positive cells. Early (phosphatidylserine exposure) and late (membrane permeabilization) PCD stages were studied by Annexin V-PE Apoptosis Detection Kit I (BD Pharmingen) and flow cytometry (EPICs XL-MCL, Beckman Coulter). DNA fragmentation was studied in the end-stage PCD by TUNEL- (terminal deoxynucleotidyl transferase dUTP nick end labeling-) based APO-BRDU Kit (BD Pharmingen) and flow cytometry (LSRII, BD Biosciences). To avoid the overlap with GFP-marker, FITC-labeled anti-BRDU mAb was substituted with the PE-conjugated anti-BRDU mAb (BD Pharmingen). Results were analyzed as the mean ± SE, and compared using an independent two-sample t-test at $P < 0.05$ level of significance. Cell cycle analysis was performed in parental and transfected (vector-, WT/DN-ANXA7-, or p53-) LNCaP cells (18 h), using propidium iodide staining (Sigma-Aldrich) and flow cytometry (ModFit LT, Verity Software House and EPICs XL-MCL, Beckman Coulter).

2.3. Western Blotting. Western blotting was performed using standard procedures, and equal amounts of total protein were electrophoresed on 4–20% Tris-Glycine gels and Magic-Mark (Invitrogen, Carlsbad, CA, USA). Antibodies used are FOXO3A and phospho-FOXO3A-Ser318/321 (numbers 9467 and 9465, resp., Cell Signaling Technology); SGK1 (number 3272, Cell Signaling Technology) and β-actin were used as control.

2.4. RNA Extraction and PCR. Confluent parental and vector-, WT/DN-ANXA7-, and p53-transfected LNCaP and DU145 cells were harvested, and total RNA was isolated with RNAqueous-4 PCR Kit (Ambion, Austin, TX, USA) and used for reverse transcription (SuperScript First-Strand Synthesis System for RT-PCR, Invitrogen, Carlsbad, CA, USA). SGK1 C-terminal fragments were amplified in duplex PCR using the following primers: SGK1 (forward—5′-CTCCTG-CAGAAGGACAGGA-3′; reverse—5′-GGACAGGCTCTT-CGGTAAACT-3′) and beta-actin (forward—5′ CTGGCC-GGGACCTGACTGACTACCTC-3′; reverse—5′ AAACAA-ATAAAGCCATGCCAATCTCA-3′ with the ratio to other primers 1 : 10). Full-length SGK1 was amplified using the following primers: 5′-TTTGAGCGCTAACGTCTTTCTGT-3′ and 5′-TTGCTAAGCTTCCAGAGATGTGC-3′. SGK1 cDNA was purified from agarose gels and sequenced (Veritas, Rockville, MD, USA).

2.5. Ingenuity Pathways Analysis. Ingenuity Pathways Analysis (IPA) (Ingenuity Systems, Redwood City, CA, USA) was used for the identification of SGK1/FOXO3A-associated molecular paths of p53 versus ANXA7 in LNCaP. The p53-signature genes (210) from Comparative Marker Selection (GenePattern) (data not shown) were mapped to corresponding genes/proteins in IPA's database. IPA yielded the p53-centered interactome network that was analyzed for significant alterations in major cancer-related cell survival pathways with a threshold of $P < 0.01$. The two identified canonical pathways, PI3K/Akt and PTEN signaling, were first enriched with p53, ANXA7, FOXO3A, and SGK1 relations from the IPA database. Next, the PI3K/Akt and PTEN pathways were modified using Path Designer, IPA, and were further customized by adding ANXA7 versus p53 connections (genes as nodes and relationships as edges) from the current report.

3. Results

3.1. WT-ANXA7 Eliminated Androgen-Sensitive LNCaP Prostate Cancer Cells and Inhibited Cell Cycle More Effectively Than the Canonical Tumor Suppressor p53. Programmed cell death (PCD) responses to WT/DN-ANXA7 and p53 (18 hr) were assessed by Annexin V-PE and APO-BRDU. In AnnexinV-PE assay (Figure 1(a)), WT-ANXA7 induced early apoptosis with phosphatidylserine exposure as well as late apoptosis with membrane permeabilization, whereas DN-ANXA7 failed to reach the same PCD rates ($P < 0.001$ for both comparisons) in LNCaP cells. In APO-BRDU assay (Figure 1(b)), WT-ANXA7 caused a 2-fold PCD

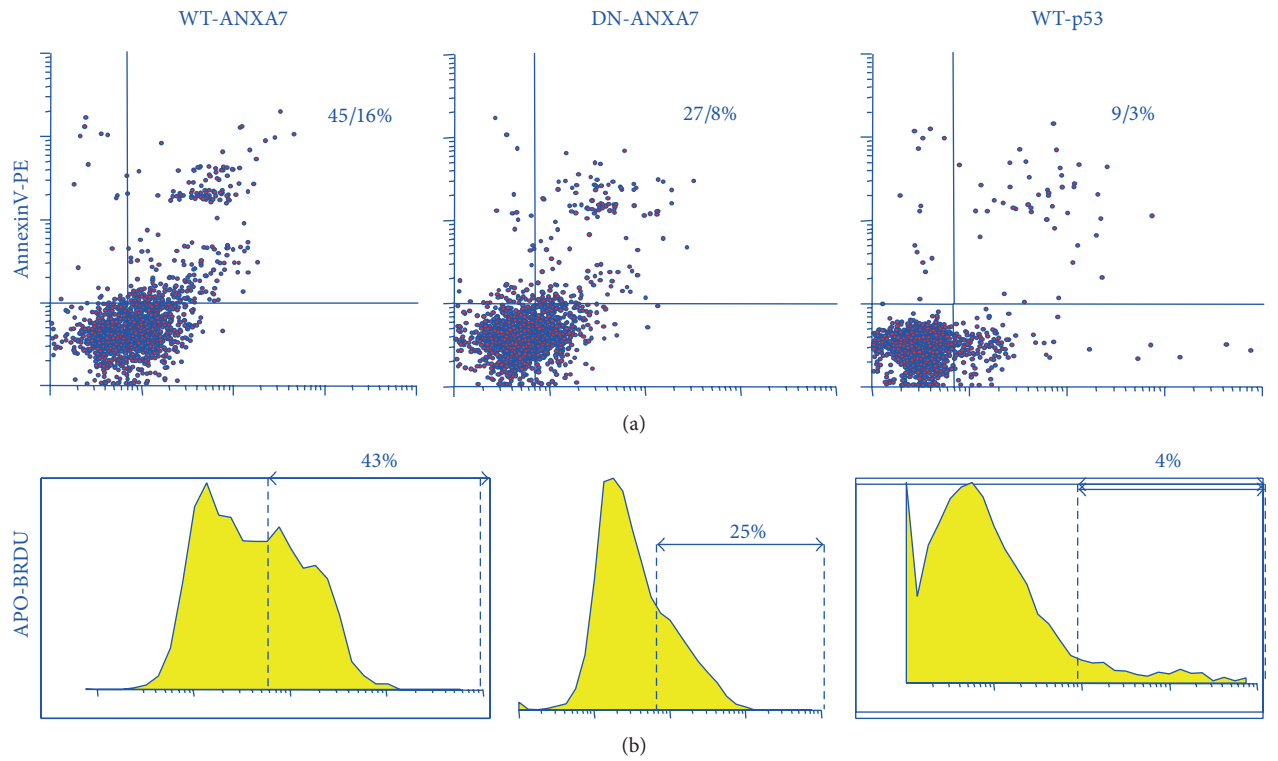

Figure 1: The WT/DN-ANXA7- and p53-induced cell death responses in LNCaP. PCD rates (18 h, AnnexinV-PE (a) and APO-BRDU (b)) were estimated in LNCaP cells transfected with vector alone, WT- or DN-ANXA7, and p53. Images represent typical results (%) from triplicate experiments.

increase compared to DN-ANXA7 ($P < 0.001$) inducing DNA fragmentation almost in half of LNCaP cells. In the meantime, p53 caused only a slight increase with the phosphatidylserine exposure causing a potentially reversible early apoptosis. In contrast, WT-ANXA7 and p53 induced comparable levels of PCD and cell growth inhibition in androgen-resistant DU145 and PC3 [4]. As shown in Figure 2, WT-ANXA7 caused a G1-arrest in LNCaP cells that was not matched by DN-ANXA7 ($P < 0.001$), whereas p53 failed to reach the cell growth inhibition effects of WT- as well as DN-ANXA7. These results along with DNA fragmentation (APO-BRDU) as well as by phosphatidylserine exposure and membrane permeabilization (AnnexinV-PE) suggest that wild-type- (WT-) ANXA7 surpassed the p53-induced PCD and cell cycle inhibition in androgen-sensitive LNCaP.

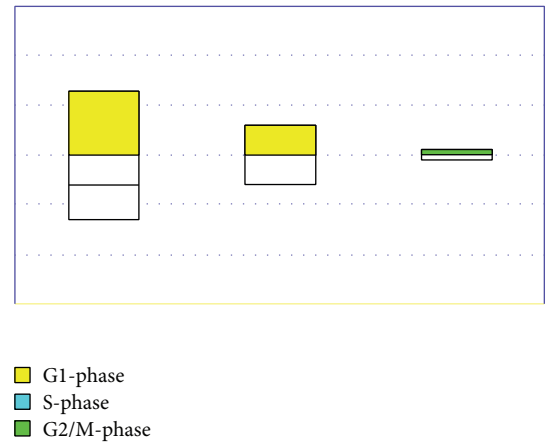

Figure 2: Graphs represent the differences (delta %) in cell numbers in different phases in response to WT/DN-ANXA7 and p53 (18 hr); mean values from replicates (%) are presented after the subtraction of control levels in corresponding vectors.

3.2. P53 Hyperphosphorylates FOXO3A and Reduces LMW SGK1 Products While ANXA7 Reduces FOXO3A Phosphorylation and Increases LMW SGK1. While similar tumor suppressor effects of WT-ANXA7 and p53 in DU145 were accompanied by similar RB-E2F profiles, the lack of RB1 dephosphorylation and *E2F* induction by p53 compared to WT-ANXA7 contributed to the p53 insufficiency in androgen-sensitive LNCaP [4]. In the PTEN-mutant LNCaP with a constitutively active Akt which is expected to phosphorylate FOXO3A [5], p53 activation can further hyperphosphorylate FOXO3A [6], thus preventing the proapoptotic FOXO3A transcription. Hence, we compared WT/DN-ANXA7 and p53 effects on the expression of FOXO3A in LNCaP. As shown in Figure 3, FOXO3A phosphorylation in LNCaP was distinctly affected by WT/DN-ANXA7 and p53 at the Ser318/321 site. Consistent with the lack of tumor suppressor effects, p53 drastically hyperphosphorylated FOXO3A-Ser318/321 in LNCaP, but not in other prostate cells (data not shown). In addition, p53 and DN- (but not WT-) ANXA7

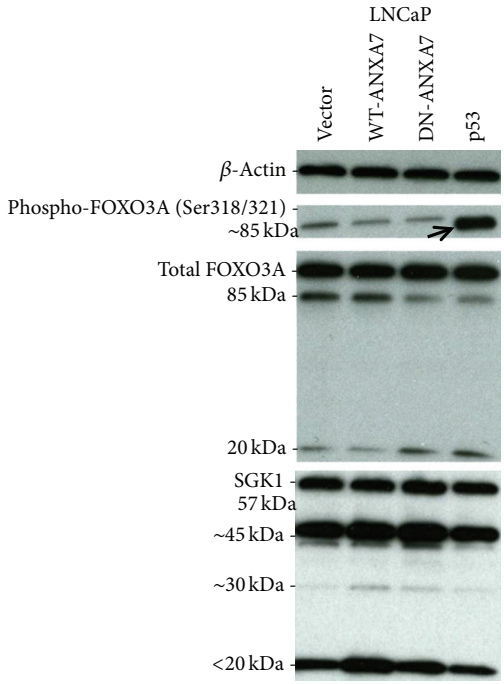

Figure 3: LNCaP cells transfected with vector, WT/DN-ANXA7, or p53. Protein synexpression was assessed by Western blotting. Arrows designate FOXO3A-S318/321 hyperphosphorylation in the p53-transfected LNCaP.

enhanced total FOXO3A degradation: 85 kDa was reduced and 20 kDa increased. In the meantime, the expression of full-length SGK1 was not changed, while LMW SGK1 products (including aberrant <45 kDa) were enhanced by WT-ANXA7 and reduced by p53. These results suggest that the LMW-SGK1 enhancement by ANXA7 in LNCaP was accompanied by the reduced FOXO3A-S318/321 phosphorylation which indicated a nuclear translocation of FOXO3A. In contrast, the p53-induced FOXO3A-S318/321 hyperphosphorylation indicated the enhancement of FOXO3A cytoplasmic retention and deactivation in LNCaP.

3.3. The p53-Regulated SGK1 Kinase Was Aberrantly Transcribed and Translated in LNCaP Prostate Cancer Cells. In order to further explore a possible role of aberrant SGK1 in FOXO3A hyperphosphorylation in LNCaP, we examined SGK1 cDNA in LNCaP versus DU145. Unlike DU145, LNCaP displayed a double-band for full-length *SGK1* cDNA, thereby validating a slightly smaller size of the extra-*SGK1*-transcript (not shown). cDNA sequence analysis verified that the *SGK1* sequences from LNCaP lacked the entire exon11 (90nt). In addition, *SGK1* from DU145 had a G/C-change (∗) in the same exon as compared to wild-type SGK1 reference (Figure 4(a)). Distinct SGK1 protein expression profiles in parental LNCaP and DU145 maintained their cell specificity in the ANXA7- and p53-transfected cells. LNCaP possessed a smaller extra-LMW-SGK1 protein form (marked by an arrow, Figure 4(b)) that was not found in DU145 cells. Most remarkably, both ANXA7s enhanced, while p53 abolished, the extra-45kDa-SGK1. In addition, WT-ANXA7 particularly induced ~15 kDa-SGK1 in LNCaP. In DU145, p53 reduced the LMW-SGK1-forms, while both ANXA7s did not cause detectable changes. These results suggest that the diverse LMW-SGK1 profiles in response to ANXA7 and p53 could distinctly affect the phosphorylation of SGK1-targets.

3.4. ANXA7 versus p53 in AKT/SGK and FOXO3A Associated Cell Survival Signaling (Ingenuity Pathways Analysis). A majority of putative FOXO3A-targeting kinases could be directly connected to p53 through various experimentally proven relations including phosphorylation. Particularly, the Akt-associated signaling could provide a clue for ANXA7 success versus p53 failure in LNCaP. Acting in concert with Akt, SGK1 could propagate PI3K survival that involves exporting FOXO3A from the nucleus and inhibiting transcription of the genes that promote apoptosis and cell growth arrest. Using Ingenuity Pathway Analysis and p53 regulated genes, we positioned the SGK1/FOXO3A-cascade in the overlapping Akt pathway. Furthermore, we elucidated the role of distinct SGK1/FOXO3A-associated regulation in p53 versus ANXA7 responses and proposed that aberrant SGK1 could affect reciprocal SGK1-FOXO3A-Akt regulation (Figure 5). While ANXA7 appeared to overcome PTEN-mutant status in LNCaP, the lack of dephosphorylation by this lipid phosphatase could further fuel the p53-induced FOXO3A phosphorylation.

4. Discussion

This study reveals the differential role of SGK1/FOXO3A-associated molecular mechanisms in contrasting TSG effects of ANXA7 and p53 in LNCaP, a model for the androgen-sensitive prostate cancer. The novel aberrant SGK1 form that was identified in this study appeared to modulate the FOXO3A phosphorylation and, subsequently, the p53 and ANXA7 tumor suppressor effects. Although known SGK1 protein isoforms differ in their N-terminals (SwissProt), almost all predicted SGK1 splice isoforms lack the C-terminal exon11 (ASAP II, data not shown). Compared to the longer splice variants overexpressed in tumors [14], the exon11-lacking aberrant SGK1 in LNCaP is likely to affect the SGK1 kinase function versus the N-terminal-associated subcellular localization. SGK1 has been hitherto postulated to enhance cell survival. However, the aberrant SGK1 was distinctly regulated by the p53 and WT-ANXA7 with opposite cell survival effects, thereby suggesting a more complex modulation of cell survival by SGK1 splice variants. Cell-specific insufficiency of p53 in LNCAP coincided with the presence of aberrant SGK1 transcript and protein form that could potentiate baseline FOXO3A phosphorylation at the SGK1-specific site (Ser315), thereby priming the 315-318-321 site for the catalyzed phosphorylation by other kinases such as Akt. Additionally, a loss of the Ser422-neighboring exon11 may particularly affect the SGK1 recruitment in Akt/mTOR signaling. Playing a critical role in SGK1 activation, SGK1

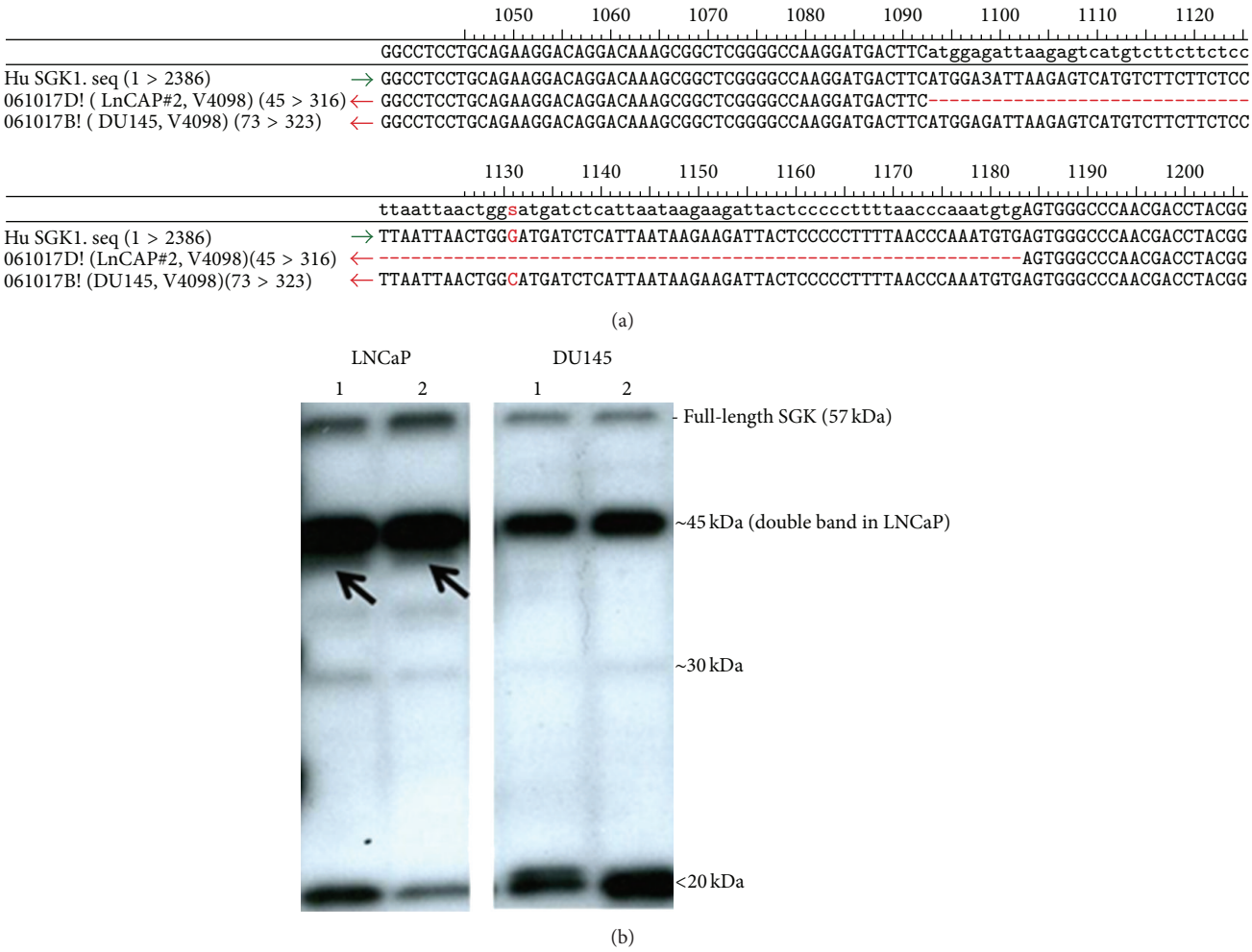

Figure 4: Aberrant SGK1 isoforms in LNCaP compared to DU145. (a) SGK1 cDNA from LNCaP and DU145 was sequenced and aligned with wild-type SGK1 reference. The alignment image shows the missing exon11 in LNCaP (red dotted line) and the G/C-change in DU145. (b) SGK1 isoform in LNCaP is designated by an arrow. Both cells are represented by controls only (parental and vector alone as 1 and 2, resp.).

catalytic domain is phosphorylated by PDK1 at Thr256, while Ser422 phosphorylation is catalyzed by mTORC2 which phosphorylates a similar site in Akt/PKB [15].

The opposing effects of WT- and DN-ANXA7 (the latter inhibits calcium-dependent phospholipid binding and aggregation) specifically underlined the role of annexin properties in the cell survival regulation by ANXA7. The lipid phosphatase PTEN and inositol-1,4,5-triphosphate receptor ITPR3 were reduced in our tumorigenesis-prone *Anxa7*-deficient mice that have defective nutrient response [1, 16]. On the contrary, the upregulation of PTEN by WT- (but not DN-) ANXA7 possibly restored the nutrient-sensing cell survival control in PI3K/Akt/mTOR-cascade including the serum-regulated SGK1. DN-ANXA7 (which lacks phospholipid-binding properties) failed to match the WT-ANXA7-induced PCD and G1-arrest, thereby emphasizing the importance of phospholipid-associated signaling in the LNCaP cells with mutant PTEN status and activated Akt prosurvival.

5. Conclusions

In conclusion, unlike p53 that was incapacitated in LNCaP, the Ca/phospholipid-binding WT-ANXA7 revived the PTEN/FOXO3A-associated cell survival control in these PTEN-deficient and androgen-sensitive prostate cancer cells. For the first time, we demonstrated that LNCaP possess aberrant *SGK1* transcript that lacks exon11. Consistent with that, SGK1 protein profile included the extra-low-molecular-weight-SGK1-form that was abolished by p53. The initially high SGK1-specific S318/321 phosphorylation of FOXO3A was further enhanced by p53 in LNCaP, but not in DU145, implied a cytoplasmic retention. In contrast, WT-ANXA7 dephosphorylated FOXO3A in the PTEN-deficient LNCaP. The SGK1-antagonists that block androgen effects on LNCaP growth are considered prostate cancer therapeutics [17]. While phospho-FOXO3A can be an adverse prognostic factor in cancer [18], the FOXO3A

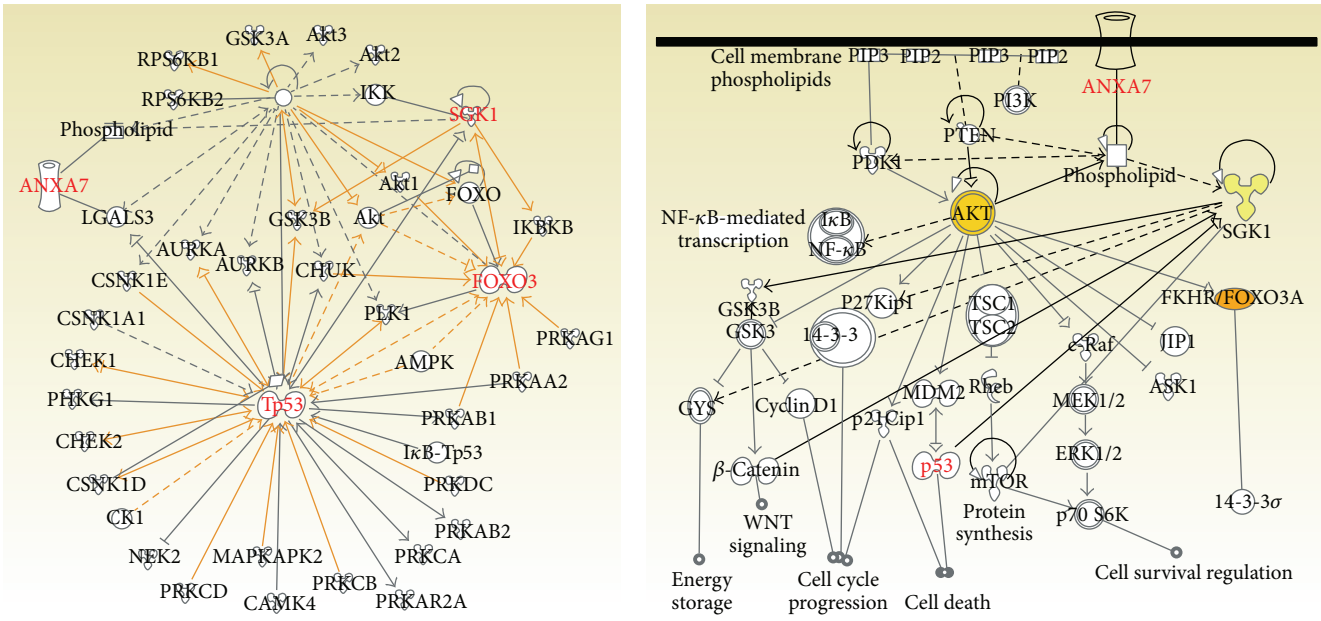

Figure 5: Both images were created using IPA. The left image shows ANXA7, p53, and PTEN connections to the network that involves FOXO3A and putative FOXO3A-phosphorylating kinases; the phosphorylation involving relationships are highlighted (yellow edges). The right image shows a schematic pathway that was created using PI3K/Akt canonical pathway as a template and was enriched by putative ANXA7 and SGK1 connections; FOXO3A and the FOXO3A-phosphorylating SGK1 and Akt are highlighted in yellow.

transactivation is employed by anticancer drugs [19]. We propose that aberrant SGK1 could affect reciprocal SGK1-FOXO3A-Akt regulation and, hence, further studies of ANXA7 TSG effects may lead to the compelling therapeutic modulation of SGK1/FOXO3A-mediated cell survival in cancer cells.

Conflict of Interests

The authors declare that there is no conflict of interests regarding the publication of this paper.

Acknowledgments

This work was supported by the DoD, CDMRP. The authors thank Shanmugam Naga and Wei Huang for excellent technical support.

References

[1] M. Srivastava, C. Montagna, X. Leighton et al., "Haploinsufficiency of Anx7 tumor suppressor gene and consequent genomic instability promotes tumorigenesis in the Anx7(+/-) mouse," *Proceedings of the National Academy of Sciences of the United States of America*, vol. 100, no. 2, pp. 14287–14292, 2003.

[2] M. Srivastava, Y. Torosyan, M. Raffeld, O. Eidelman, H. B. Pollard, and L. Bubendorf, "ANXA7 expression represents hormone-relevant tumor suppression in different cancers," *International Journal of Cancer*, vol. 121, no. 12, pp. 2628–2636, 2007.

[3] M. Srivastava, L. Bubendorf, V. Srikantan et al., "Anx7, a candidate tumor suppressor gene for prostate cancer," *Proceedings of the National Academy of Sciences of the United States of America*, vol. 98, no. 8, pp. 4575–4580, 2001.

[4] Y. Torosyan, O. Simakova, S. Naga et al., "Annexin-A7 protects normal prostate cells and induces distinct patterns of RB-associated cytotoxicity in androgen-sensitive and -resistant prostate cancer cells," *International Journal of Cancer*, vol. 125, no. 11, pp. 2528–2539, 2009.

[5] R. L. Lynch, B. W. Konicek, A. M. McNulty et al., "The progression of LNCaP human prostate cancer cells to androgen independence involves decreased FOXO3a expression and reduced $p27^{KIP1}$ promoter transactivation," *Molecular Cancer Research*, vol. 3, no. 3, pp. 163–169, 2005.

[6] H. You, Y. Jang, A. I. You-Ten et al., "p53-dependent inhibition of FKHRL1 in response to DNA damage through protein kinase SGK1," *Proceedings of the National Academy of Sciences of the United States of America*, vol. 101, no. 39, pp. 14057–14062, 2004.

[7] H. You, K. Yamamoto, and T. W. Mak, "Regulation of transactivation-independent proapoptotic activity of p53 by FOXO3a," *Proceedings of the National Academy of Sciences of the United States of America*, vol. 103, no. 24, pp. 9051–9056, 2006.

[8] G. L. Firestone, J. R. Giampaolo, and B. A. O'Keeffe, "Stimulus-dependent regulation of serum and glucocorticoid inducible protein kinase (SGK) transcription, subcellular localization and enzymatic activity," *Cellular Physiology and Biochemistry*, vol. 13, no. 1, pp. 1–12, 2003.

[9] A. Yemelyanov, J. Czwornog, D. Chebotaev et al., "Tumor suppressor activity of glucocorticoid receptor in the prostate," *Oncogene*, vol. 26, no. 13, pp. 1885–1896, 2007.

[10] L. Konrad, J. A. Scheiber, E. Völck-Badouin et al., "Alternative splicing of TGF-betas and their high-affinity receptors TβRI,

TβRII and TβRIII (betaglycan) reveal new variants in human prostatic cells," *BMC Genomics*, vol. 8, article 318, 2007.

[11] F. Lang, K. Klingel, C. A. Wagner et al., "Deranged transcriptional regulation of cell-volume-sensitive kinase hSGK in diabetic nephropathy," *Proceedings of the National Academy of Sciences of the United States of America*, vol. 97, no. 14, pp. 8157–8162, 2000.

[12] I. Shanmugam, G. Cheng, P. F. Terranova, J. B. Thrasher, C. P. Thomas, and B. Li, "Serum/glucocorticoid-induced protein kinase-1 facilitates androgen receptor-dependent cell survival," *Cell Death and Differentiation*, vol. 14, no. 12, pp. 2085–2094, 2007.

[13] A. Brunet, J. Park, H. Tran, L. S. Hu, B. A. Hemmings, and M. E. Greenberg, "Protein kinase SGK mediates survival signals by phosphorylating the forkhead transcription factor FKHRL1 (FOXO3a)," *Molecular and Cellular Biology*, vol. 21, no. 3, pp. 952–965, 2001.

[14] P. Simon, M. Schneck, T. Hochstetter et al., "Differential regulation of serum- and glucocorticoid-inducible kinase 1 (SGK1) splice variants based on alternative initiation of transcription," *Cellular Physiology and Biochemistry*, vol. 20, no. 6, pp. 715–728, 2007.

[15] J. M. García-Martínez and D. R. Alessi, "mTOR complex 2 (mTORC2) controls hydrophobic motif phosphorylation and activation of serum- and glucocorticoid-induced protein kinase 1 (SGK1)," *Biochemical Journal*, vol. 416, no. 3, pp. 375–385, 2008.

[16] M. Srivastava, I. Atwater, M. Glasman et al., "Defects in inositol 1,4,5-trisphosphate receptor expression, Ca^{2+} signaling, and insulin secretion in the anx7(+/-) knockout mouse," *Proceedings of the National Academy of Sciences of the United States of America*, vol. 96, no. 24, pp. 13783–13788, 1999.

[17] A. B. Sherk, D. E. Frigo, C. G. Schnackenberg et al., "Development of a small-molecule serum- and glucocorticoid-regulated kinase-1 antagonist and its evaluation as a prostate cancer therapeutic," *Cancer Research*, vol. 68, no. 18, pp. 7475–7483, 2008.

[18] S. M. Kornblau, N. Singh, Y. Qiu, W. Chen, N. Zhang, and K. R. Coombes, "Highly phosphorylated FOXO3A is an adverse prognostic factor in acute myeloid leukemia," *Clinical Cancer Research*, vol. 16, no. 6, pp. 1865–1874, 2010.

[19] J.-Y. Yang and M.-C. Hung, "A new fork for clinical application: targeting forkhead transcription factors in cancer," *Clinical Cancer Research*, vol. 15, no. 3, pp. 752–757, 2009.

Hindawi Publishing Corporation
BioMed Research International
Volume 2014, Article ID 102478, 7 pages
http://dx.doi.org/10.1155/2014/102478

Research Article

Evaluation of 12-Lipoxygenase (12-LOX) and Plasminogen Activator Inhibitor 1 (PAI-1) as Prognostic Markers in Prostate Cancer

Tomasz Gondek,[1,2] Mariusz Szajewski,[3,4] Jarosław Szefel,[3,4] Ewa Aleksandrowicz-Wrona,[5] Ewa Skrzypczak-Jankun,[6] Jerzy Jankun,[5,6,7] and Wieslawa Lysiak-Szydlowska[5,8]

[1] *Department of Urology, St' Vincent A Paulo Hospital, Wójta Radtkego 1, 81-348 Gdynia, Poland*
[2] *Department of Urology, Multidisciplinary Hospital Jantar, Rybacka 15, 82-103 Jantar, Poland*
[3] *Department of Surgical Oncology, Gdynia Oncology Center, PCK's Maritime Hospital in Gdynia, Powstania Styczniowego 1, 81-519 Gdynia, Poland*
[4] *Department of Propaedeutic Oncology, Faculty of Health Sciences, Medical University of Gdańsk, Powstania Styczniowego 9b, 81-519 Gdynia, Poland*
[5] *Department of Clinical Nutrition, Medical University of Gdańsk, Dębinki 7, 80-211 Gdańsk, Poland*
[6] *Urology Research Center, Department of Urology, The University of Toledo, Health Science Campus, Toledo, OH 43614, USA*
[7] *Protein Research Chair, Department of Biochemistry, College of Sciences, King Saud University, Riyadh 11451, Saudi Arabia*
[8] *Powiślanski College, Faculty of Health Science, 11 Listopada 13, 82-500 Kwidzyń, Poland*

Correspondence should be addressed to Jerzy Jankun; jerzy.jankun@utoledo.edu

Received 3 January 2014; Accepted 11 February 2014; Published 24 March 2014

Academic Editor: Giovanni Luca Gravina

In carcinoma of prostate, a causative role of platelet 12-lipoxygenase (12-LOX) and plasminogen activator inhibitor 1 (PAI-1) for tumor progression has been firmly established in tumor and/or adjacent tissue. Our goal was to investigate if 12-LOX and/or PAI-1 in patient's plasma could be used to predict outcome of the disease. The study comprised 149 patients (age 70 ± 9) divided into two groups: a study group with carcinoma confirmed by positive biopsy of prostate ($n = 116$) and a reference group ($n = 33$) with benign prostatic hyperplasia (BPH). The following parameters were determined by the laboratory test in plasma or platelet-rich plasma: protein level of 12-LOX, PAI-1, thromboglobulin (TGB), prostate specific antigen (PSA), C-reactive protein (CRP), hemoglobin (HGB), and hematocrit (HCT), as well as red (RBC) and white blood cells (WBC), number of platelets (PLT), international normalized ratio of blood clotting (INR), and activated partial thromboplastin time (APTT). The only difference of significance was noticed in the concentration of 12-LOX in platelet rich plasma, which was lower in cancer than in BPH group. Standardization to TGB and platelet count increases the sensitivity of the test that might be used as a biomarker to assess risk for prostate cancer in periodically monitored patients.

1. Introduction

The prostate cancer is the most common malignancy diagnosed in older men in the Western Hemisphere population. According to the European Association of Urology (EAU) Guidelines of 2012 mortality from prostate cancer is ranked second to lung cancer [1]. The diagnosis of prostate cancer at an early stage and ability to differentiate benign and aggressive form would improve the selection of the optimal method of treatment resulting in better outcome. Currently used diagnostic standards consist of determination of prostate specific antigen (PSA), clinical stage, and total Gleason grade. Unfortunately, they do not give sufficient justification for choosing the optimal therapy for a particular

patient. Hence, it is necessary to search for new biomarkers to allow for the prediction of disease dynamics and personalization of therapy [2, 3].

It has been shown that men who consume high-fat diet containing abundance of arachidonic acid (AA) have a high rate of incidence of prostate cancer [4, 5]. Availability of AA in combination with the overexpression of lipoxygenases (12-LOX, 5-LOX), cyclooxygenase (COX-2), and cytochrome P450 (CYP) excess leads to the synthesis of eicosanoids [6–8]. Eicosanoids trigger signals for transcription of genes that modulate the immune system, hemostasis, apoptosis, cell proliferation, and many other processes [9, 10]. This avalanche of signals results in the development of inflammation favoring carcinogenesis [11, 12]. Also, eicosanoids accelerate the rate of proliferation of glandular cells, inhibit their apoptosis, and further intensify angiogenesis [13–16]. Angiogenesis is a prerequisite for tumor development and plasminogen activation system (PAS) has a significant impact on that crucial step. PAS includes urokinase plasminogen activator (uPA), urokinase plasminogen activator receptor (uPAR), and plasminogen activator inhibitor type-1 (PAI-1) [17]. The increase in uPA activity and number of uPAR correlate with the ability of cancer to form angiogenic vasculature and increase cancer cells metastasis. Urokinase, both free and receptor bound, converts plasminogen to proteolytically active plasmin that is responsible for lysis of extracellular matrix, essential for angiogenesis and metastasis [18, 19]. Inhibition of both uPA and uPAR activity reduces angiogenesis and metastasis [20, 21]. Research indicates that inhibition of uPA by PAI-1 reduces the size of the tumor [22]. In the capillaries surrounding the tumor there are a large amount and activity of uPA and uPAR [23]. Taking into account the role of uPA, uPAR, and PAI-1 in angiogenesis, Pepper considers that normal vessel formation by angiogenesis depends on proteases and antiproteases balance [24]. However, role of PAI-1 in carcinogenesis is more complex than simple inhibition of proteolysis. PAI-1 overexpressed up to approximately ten times more than normal level increases motility of cancer cells by interacting with vitronectin and other proteins. However, PAI-1 in supramolecular levels significantly inhibits angiogenesis and metastasis reducing activity of uPA [18, 25, 26]. This phenomenon is called "PAI-paradox" [27]. Now, a high level of PAI-1 appears to inhibit angiogenesis, while slightly elevated level of PAI-1 is necessary for growth of angiogenic vessels.

A healthy body maintains a balance between activators and inhibitors of angiogenesis. The tumor microenvironment is different than normal tissue where the pro- and antiangiogenic factors are well balanced. Folkman and Hanahan introduced the concept of the angiogenic switch wherein it is stated that angiogenesis starts at a global disturbance of the expression of pro- and antiangiogenic factors [28]. The primary target of both of them is endothelial cell [29]. Among the others 12-LOX and PAI-1 are proteins governing these processes and can be secreted at high levels by tumor cells. While expression of these proteins by cancer cell was studied and documented, serum tests were not well investigated [30–32], albeit they might provide an easy laboratory test as a diagnostic tool. Therefore, we have studied expression of human platelet 12-LOX and PAI-1 in serum of patients to find whether any correlation exists between their concentration in blood and stage of the prostate disease.

2. Materials and Methods

2.1. Patients. The study involved 149 men (age 70 ± 9 years) qualified for diagnostic biopsy of the prostate. The criteria for inclusion in the study were a positive digital rectal examination (DRE) result, PSA level above the upper limit of the reference value of 4 ng/mL, and a positive transrectal ultrasound (TRUS) test result. The study excluded patients with previously diagnosed cancer, regardless of its location and nature. Patients taking aspirin, warfarin, COX inhibitors, and heparin were also excluded from study since these drugs may affect level or activity of 12-LOX and/or PAI-1 [33–37].

In all patients the entire volume of the prostate adenoma and cancer foci were determined by TRUS. Biopsy was done for all patients with a total of 12 samples taken in the following way: biopsies 1–4 taken from the suspected foci, biopsies 5–8 taken from the opposite lobe of the prostate, and biopsies 9–12 taken from the lobe where the suspected foci were present. Targeted biopsy was performed on patients suspected with pathological growth. Formaldehyde and paraffin embedded slides were examined by pathologist who determined the type of cancer (or lack of it), tumor grade and Gleason sum. Based on the results of the histopathological examination of biopsy material the patients were divided into two groups (group with cancer, $n = 116$, and without prostate cancer, $n = 33$). The study was approved by the Bioethical Committee for Scientific Research at the Medical University of Gdańsk. Each patient prior to study was informed of the objectives and principles and signed an informed consent to participate in it.

2.2. Blood. For all patients the following parameters were determined in hospital laboratory by the routine tests: hemoglobin (HGB), hematocrit (HCT), red blood cells (RBC), and white blood cells (WBC). Citrated blood samples were divided into two parts, one of them was centrifuged at 100 ×g for fifteen minutes to obtain platelet rich plasma, frozen, and stored at −20°C for the determination of PAI-1, 12-LOX, and thromboglobulin (TGB); the other was centrifuged at 1500×g for ten minutes for the determination of PSA, C-reactive protein (CRP), international normalized ratio of blood clotting (INR), and activated partial thromboplastin time (APTT).

2.3. ELISA Kits. Thromboglobulin was assayed by Asserachrom-TBG, product number REF 00950 from Diagnostic Stago Inc., Mount Olive, NJ, USA. PAI-1 was analyzed by active human PAI-1 functional assay ELISA kit, HPAIKIT from Molecular Innovation, Novi, MI 48377, USA. 12-LOX was analyzed by IMUBIND 12-Lipoxygenase ELISA product number ADG872 from American Diagnostica GmbH, Pfungstadt, Germany.

2.4. Statistical Analysis. Statistical analysis was done using Statistica 10 (StatSoft Polska Sp. z o.o., Kraków, Poland) for

Table 1: Characteristics of the study group.

	BPH Mean ± SD (median)	Prostate cancer Mean ± SD (median)	P
Age of patients (years)	67.3 ± 9.9 (65)	71.2 ± 8.5 (72)	0.02
Volume of prostate (mL)	64.4 ± 32.5 (55.7)	50.1 ± 24.4 (47.7)	0.01
Volume of adenoma (mL)	31.1 ± 20.8 (25.1)	22 ± 15.8 (18.3)	0.004
Volume of cancer foci (mL)	—	0.5 ± 0.9 (0.2)	
PSA (ng/mL)	6.6 ± 4.8 (5.0)	58.4 ± 302.0 (8.6)	0.0004
Gleason grade ≤ 6	—	63%	
Gleason grade > 6	—	37%	

Table 2: Normal expression of 12-LOX and PAI-1 and normalized expression to TBG and PLT in BPH and prostate cancer patients.

	BPH Mean ± SD (median)	Prostate cancer Mean ± SD (median)	P
12-LOX (ng/mL)	219.6 ± 209.3 (137)	144.6 ± 304.8 (56)	0.0001
PAI-1 (U/mL)	447.0 ± 345.8 (367)	610.8 ± 483.9 (441)	0.1
TBG (kU)	5.81 ± 6.02 (2.8)	6.21 ± 4.03 (6.7)	0.054
PLT (10^3/mm^3)	207 ± 55 (208)	219 ± 69 (211)	0.6
12-LOX/TBG	83.2 ± 111.2 (52.3)	34.1 ± 77.9 (9.3)	0.000005
PAI-1/TBG	217.5 ± 321.6 (120)	151.7 ± 180.9 (90)	0.2
TBG/PLT	0.02 ± 0.02 (0.01)	0.03 ± 0.02 (0.02)	0.13
12-LOX/PLT	1.07 ± 0.97 (0.8)	0.66 ± 1.40 (0.25)	0.00003
PAI-1/PLT	2.28 ± 1.68 (1.7)	2.98 ± 2.57 (2.2)	0.2

nonparametric Mann-Whitney U test, Chi square distribution, and analysis of the Pearson correlation coefficient. The level of significance was established as $P \leq 0.05$.

3. Results and Discussion

Enrolled patients in addition to BPH and prostate cancer were diagnosed with diabetes (12%), hypertension (42%), chronic obstructive pulmonary disease (6%), coronary disease (94%), diabetes (10.3%), and hypertension (50.8%). Patients in study were divided into two groups: with prostate cancer and with benign prostatic hyperplasia (BPH). No prevalence of any of these diseases was observed between BPH and prostate cancer patients. Blood work revealed also that there were no differences in test values of CRP, APTT, HGB, HCT, WBC, RBC, PLT, and TGB between these two groups (data not shown). As can be seen in Table 1 patients with BPH were younger and have had higher volume of prostate, volume of adenoma and, as expected, significantly lower PSA than these with prostate cancer.

Table 2 shows that expression of 12-LOX in platelet rich plasma was significantly lower in prostate cancer patients than in BPH population and normalization to PLT and TBG increases statistical significance (Figure 1). Differences between the groups in all other tested parameters were not statistically significant.

Also as it is shown in Table 3 there were no differences in tested parameters in prostate cancer patients divided for groups according to the Gleason grade <6 and >6, respectively.

This study includes only BPH and prostate cancer patients. Healthy individuals were excluded due to an ethical consideration. Defining a person as "healthy" would require verification by blood work, digital rectum examination, and biopsy which (especially biopsy) was considered unethical for the asymptomatic person.

Cancer markers indicate a high probability for the existence of cancer in the body. Most markers are assayed by analysis of blood plasma [38]. It is expected that the concentration of tumor markers in the plasma or urine of patients with cancer should considerably vary from the values typically observed in healthy subjects [39]. This assumption results from the positive relationship between the mass of cancer cells and the amount of the substance produced by them [40]. At this moment markers of prostate cancer cannot select precisely a group at risk for the disease progression [41, 42]. The 12-LOX and PAI-1 together with the products of the reactions catalyzed by them seem to point an interesting direction of research [30, 43]. In our initial studies we measured 12-LOX expression in serum and found that 12-LOX was lower in prostate cancer patients in comparison with healthy individuals and BPH patients. However limited number of individuals in each group did not allow us to establish statistical significant differences [44]. The other studies show promise but are difficult to compare due to the fact that some of them analyzed prostate tissue, while other were done in plasma [26, 45, 46]. Also, one study analyzed the expression of genes; the other reported levels of protein, and yet in some other the enzyme activity in plasma was determined for 12-LOX and PAI-1 [47, 48]. The disparities were also observed in the method of selecting groups of patients. Studies compared the results for patients without and with cancer, which could mean healthy, but also from cobenign prostatic hyperplasia [8, 14, 49, 50]. Moreover, laboratory tests for the determination of 12-LOX and PAI-1 used antibodies of different specificity. These diversities make the comparison of the results difficult and rather questionable.

Higher PSA depending on the severity of cancer, lower volume of cancerous prostate confirm not only the generally accepted and recognized standards of diagnosis and management in the field of prostate cancer, but also the proper

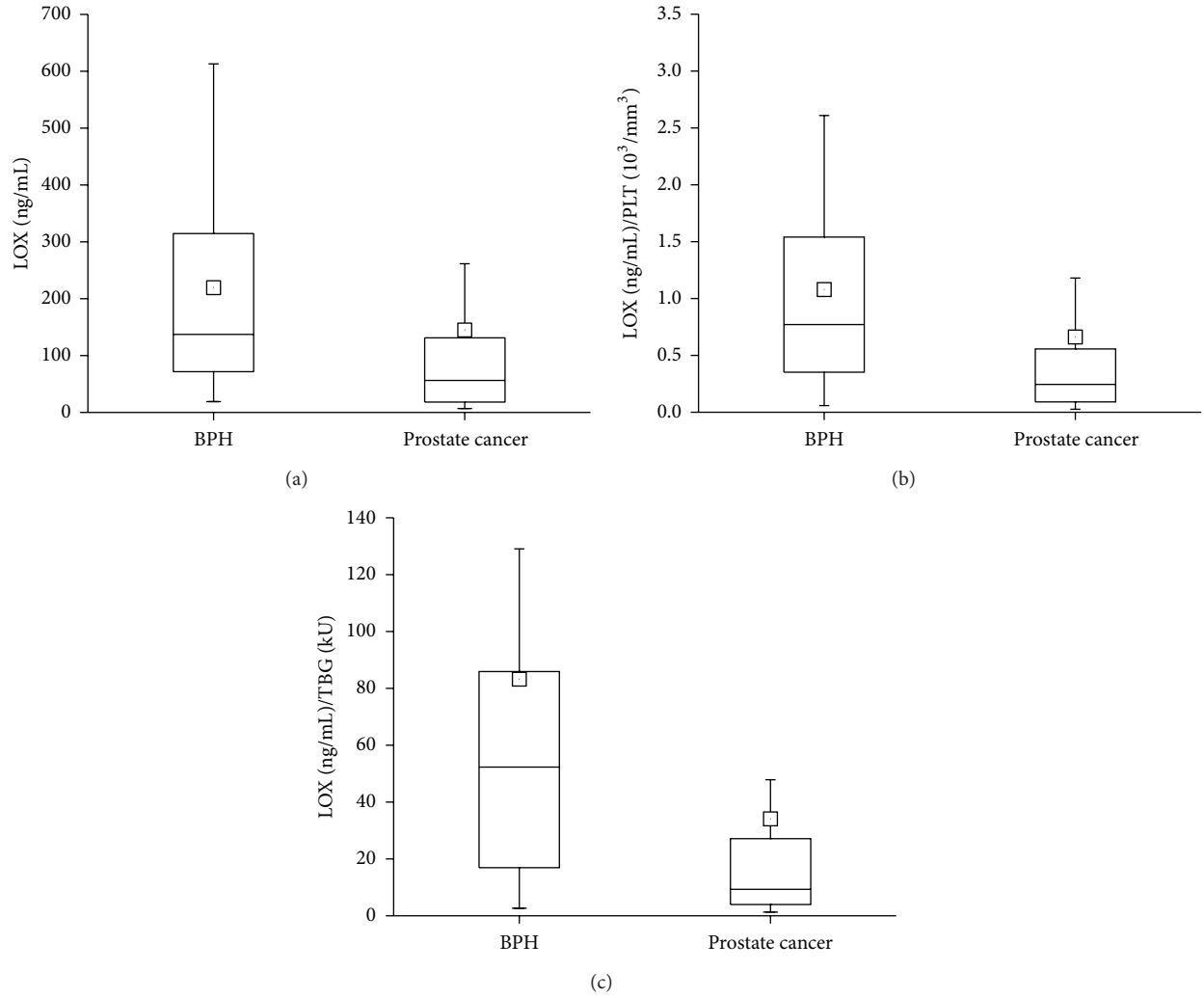

Figure 1: Expression of 12-LOX in platelet-rich plasma of BPH and prostate cancer patients. Normalization to PLT and TBG greatly increases sensitivity of correlation. Box and whisker plots of expression of 12-LOX ($P = 0.0001$) (a), 12-LOX normalized to PLT ($P = 0.00003$) (b), and 12-LOX normalized to TBG ($P = 0.000005$) (c) for BPH and prostate cancer. Solid, horizontal line inside box represents the median, position of the little square gives the average, box encompasses results within 25–75%, and wiskers mark values between 5–95%.

selection of patients in the study group. To improve the results in our study we normalized assayed parameters to the number of platelets and TBG in platelet rich plasma. Each platelet rich plasma sample was frozen for storage (not exceeding 12–16 weeks) and thaw immediately before the appropriate tests were performed to guarantee uniform conditions for releasing TBG and other proteins in the determination of platelet-rich plasma parameters studied [51].

Analyzing the results for the concentrations of TBG in the platelet-rich plasma, we have observed that the differences in the TBG levels of $P = 0.054$ (Table 2) where close to the chosen level of significance P less or equal 0.05, with the mean value of TBG higher in the cancer group. This somewhat diminished that statistical level of significance may be due to the fact that the control group consisted of patients with BPH and not prostate-trouble-free individuals.

The activity of the platelet 12-LOX in prostate cancer was investigated extensively and tied with angiogenesis. Nie et al. examined 12-LOX concentration in prostate cancer cell lines using antibodies and postulated that increase of 12-LOX expression stimulates prostate cancer tumor growth and activates angiogenesis [13]. Elevated levels or activity in cancer tissue has been reported before by others as well [30, 52–55]; thus, our finding of reduced amount of 12-LOX in platelet-rich plasma of prostate cancer patients was somewhat surprising. One of the explanations is that volume of prostate in BPH patients was larger than prostate cancer patients. So, if BPH and prostate cancer gland release steady amount of 12-LOX into blood, indeed this protein level can depend on gland volume. It is worthy to emphasize that a mean total volume of prostate in cancer patients was 65% of BPH prostate group of patients, and percentage of 12-LOX expression in platelet rich plasma was also 65% for

Table 3: Normal expression of 12-LOX and PAI-1 and normalized expression to TBG and PLT in prostate cancer patients with different Gleason grade.

	Gleason grade ≤ 6 Mean ± SD (median)	Gleason grade > 6 Mean ± SD (median)	P
12-LOX (ng/mL)	158.5 ± 354.0 (56)	112.8 ± 133.7 (63)	0.8
PAI-1 (U/mL)	577.3 ± 442.2 (428)	687.3 ± 568.6 (499)	0.3
TBG (kU)	6.5 ± 4.5 (7.75)	5.5 ± 2.7 (5.4)	0.4
PLT (10^3/mm^3)	209.9 ± 49.9 (210)	241.3 ± 97.1 (219)	0.2
12-LOX/TBG	35.6 ± 80.8 (8.8)	30.7 ± 71.7 (11.4)	0.5
PAI-1/TBG	135.8 ± 155.3 (80)	188.6 ± 227.9 (90)	0.6
TBG/PLT	0.03 ± 0.02 (0.03)	0.025 ± 0.01 (0.02)	0.3
12-LOX/PLT	0.75 ± 1.6 (0.25)	0.47 ± 0.53 (0.27)	0.9
PAI-1/PLT	2.95 ± 2.6 (2.1)	3.0 ± 2.6 (2.4)	0.7

cancer group versus patients with BPH. Moreover, the mean volume of cancer foci was only ~1% of prostate volume in prostate cancer patients so its impact on total secretion of 12-LOX in blood could be limited. The other possibility is that lower 12-LOX expression in cancer is intrinsic property of cancer. Observations from the cell lines are consistent with the results from human tissue in the fact that 12-LOX level is growing with the progression of cancer. However, Gohara et al. reported that expression of 12-LOX in normal kidney tissue is higher than in low grade and stage form of this cancer, to rise in terminal malignancy, approximating but not quite reaching the level of expression observed in the normal tissue samples [56]. Thus this mechanism requires more investigations.

Expression of 12-LOX also depends on type of cancer. For example it has been reported that significant increase in 12-LOX levels in serum was observed in breast cancer patients (40 ng/mL) as compared to healthy controls (13 ng/mL) ($P < 0.0001$) in study of 86 biopsy proven breast cancer patients. Moreover, serum 12-LOX levels were significantly higher ($P < 0.002$) in patients with metastasis to the lymph nodes and over 75% patients had shown significant ($P < 0.0001$) reduction of 12-LOX levels after chemotherapy [57].

We have not seen any significant differences in expression of PAI-1 in platelet rich plasma between BPH and prostate cancer patients, as well as in groups with different Gleason grade (Table 3), regardless of many reports stating that PAI-1 is overexpressed in prostate cancer [43, 58, 59], although uPA and its receptor are overexpressed on the surface of cancer cells. However, when PAI-1 binds to uPA-uPAR complexes it interacts with LPR leading to internalization of PAI-1/uPA-uPAR/LPR into the cancer cells. PAI-1 and uPA are degraded while uPAR and LPR are recycled to the cell surface [25, 60–63]. Thus PAI-1 might not be secreted into the blood stream. Although expression of 12-LOX and PAI-1 and normalized expression to TBG and PLT in prostate cancer patients clearly were not statistically different in patients with different Gleason grade (Table 3), but some trend was observed. Concentrations of 12-LOX were lower in group with Gleason >6, while PAI-1 was higher when compared with group of Gleason <6. Together with other parameters the Gleason grading system helps evaluate the prognosis of men with prostate cancer. Cancers with the higher Gleason score are more aggressive and have a worse prognosis but this score itself cannot predict outcome precisely [64]. Thus, it is possible that expressions of 12-LOX and PAI-1 are related to other parameters such as outcome of disease or survival which we are going to monitor in the future studies.

4. Conclusion

No significant difference in platelet-rich plasma was noted for PAI-1 levels or 12-LOX and PAI-1 ratio between patients with cancer and BPH. Therefore, PAI-1 results in this study do not meet the conditions expected for the prostate cancer marker.

The concentration of 12-LOX in platelet-rich plasma in patients with prostate cancer is significantly lower than in patients with BPH; thus, the low concentration of 12-LOX might indicate the increased risk of developing prostate cancer or the onset of the disease in periodically monitored patients. Standardization of the expression of 12-LOX in platelet-rich plasma to the concentration of TGB and the number of PLT significantly increases the sensitivity of the test and could be used as biomarker for the assessment of risk for the prostate cancer.

Conflict of Interests

The authors declare that there is no conflict of interests regarding the publication of this paper.

Acknowledgments

This study was supported in part by grants from the Frank Stranahan Endowed Chair and Children Miracle Network (Jerzy Jankun).

References

[1] A. Heidenreich, J. Bellmunt, M. Bolla et al., "EAU guidelines on prostate cancer—part 1: screening, diagnosis, and treatment of clinically localised disease," *European Urology*, vol. 59, no. 1, pp. 61–71, 2011.

[2] S. F. Shariat, J. A. Karam, J. Walz et al., "Improved prediction of disease relapse after radical prostatectomy through a panel of preoperative blood-based biomarkers," *Clinical Cancer Research*, vol. 14, no. 12, pp. 3785–3791, 2008.

[3] S. K. Martin, T. B. Vaughan, T. Atkinson, H. Zhu, and N. Kyprianou, "Emerging biomarkers of prostate cancer (Review)," *Oncology Reports*, vol. 28, no. 2, pp. 409–417, 2012.

[4] U. P. Kelavkar, W. Glasgow, S. J. Olson, B. A. Foster, and S. B. Shappell, "Overexpression of 12/15-lipoxygenase, an ortholog of human 15-lipoxygenase-1, in the prostate tumors of TRAMP mice," *Neoplasia*, vol. 6, no. 6, pp. 821–830, 2004.

[5] G. Mamalakis, A. Kafatos, N. Kalogeropoulos, N. Andrikopoulos, G. Daskalopulos, and A. Kranidis, "Prostate cancer versus hyperplasia: relationships with prostatic and adipose tissue fatty acid composition," *Prostaglandins, Leukotrienes and Essential Fatty Acids*, vol. 66, no. 5-6, pp. 467–477, 2002.

[6] J. Ghosh and C. E. Myers, "Arachidonic acid stimulates prostate cancer cell growth: critical role of 5-lipoxygenase," *Biochemical and Biophysical Research Communications*, vol. 235, no. 2, pp. 418–423, 1997.

[7] R. Jones, L.-A. Adel-Alvarez, O. R. Alvarez, R. Broaddus, and S. Das, "Arachidonic acid and colorectal carcinogenesis," *Molecular and Cellular Biochemistry*, vol. 253, no. 1-2, pp. 141–149, 2003.

[8] S. B. Shappell, S. J. Olson, S. E. Hannah et al., "Elevated expression of 12/15-lipoxygenase and cyclooxygenase-2 in a transgenic mouse model of prostate carcinoma," *Cancer Research*, vol. 63, no. 9, pp. 2256–2267, 2003.

[9] J. Szefel, M. Piotrowska, W. J. Kruszewski, J. Jankun, W. Łysiak-Szydłowska, and E. Skrzypczak-Jankun, "Eicosanoids in prevention and management of diseases," *Current Molecular Medicine*, vol. 11, no. 1, pp. 13–25, 2011.

[10] M. Azrad, C. Turgeon, and W. Demark-Wahnefried, "Current evidence linking polyunsaturated fatty acids with cancer risk and progression," *Frontiers in Oncology*, vol. 3, article 224, 2013.

[11] D. Nie and K. V. Honn, "Cyclooxygenase, lipoxygenase and tumor angiogenesis," *Cellular and Molecular Life Sciences*, vol. 59, no. 5, pp. 799–807, 2002.

[12] D. Nie, M. Che, D. Grignon, K. Tang, and K. V. Honn, "Role of eicosanoids in prostate cancer progression," *Cancer and Metastasis Reviews*, vol. 20, no. 3-4, pp. 195–206, 2001.

[13] D. Nie, G. G. Hillman, T. Geddes et al., "Platelet-type 12-lipoxygenase in a human prostate carcinoma stimulates angiogenesis and tumor growth," *Cancer Research*, vol. 58, no. 18, pp. 4047–4051, 1998.

[14] M. Matsuyama, R. Yoshimura, M. Mitsuhashi et al., "Expression of lipoxygenase in human prostate cancer and growth reduction by its inhibitors," *International Journal of Oncology*, vol. 24, no. 4, pp. 821–827, 2004.

[15] G. P. Pidgeon, M. Kandouz, A. Meram, and K. V. Honn, "Mechanisms controlling cell cycle arrest and induction of apoptosis after 12-lipoxygenase inhibition in prostate cancer cells," *Cancer Research*, vol. 62, no. 9, pp. 2721–2727, 2002.

[16] J. Timár, E. Rásó, B. Döme et al., "Expression, subcellular localization and putative function of platelet-type 12-lipoxygenase in human prostate cancer cell lines of different metastatic potential," *International Journal of Cancer*, vol. 87, no. 1, pp. 37–43, 2000.

[17] J. Zhang, S. Sud, K. Mizutani, M. R. Gyetko, and K. J. Pienta, "Activation of urokinase plasminogen activator and its receptor axis is essential for macrophage infiltration in a prostate cancer mouse model," *Neoplasia*, vol. 13, no. 1, pp. 23–30, 2011.

[18] M. J. Duffy, "The urokinase plasminogen activator system: role in malignancy," *Current Pharmaceutical Design*, vol. 10, no. 1, pp. 39–49, 2004.

[19] H. Noh, S. Hong, and S. Huang, "Role of urokinase receptor in tumor progression and development," *Theranostics*, vol. 3, no. 7, pp. 487–495, 2013.

[20] J. Jankun and E. Skrzypczak-Jankun, "Molecular basis of specific inhibition of urokinase plasminogen activator by amiloride," *Cancer Biochemistry Biophysics*, vol. 17, no. 1-2, pp. 109–123, 1999.

[21] E. M. Bekes, E. I. Deryugina, T. A. Kupriyanova et al., "Activation of pro-uPA is critical for initial escape from the primary tumor and hematogenous dissemination of human carcinoma cells," *Neoplasia*, vol. 13, no. 9, pp. 806–821, 2011.

[22] P. A. Andreasen, R. Egelund, and H. H. Petersen, "The plasminogen activation system in tumor growth, invasion, and metastasis," *Cellular and Molecular Life Sciences*, vol. 57, no. 1, pp. 25–40, 2000.

[23] R. Swiercz, J. D. Wolfe, A. Zaher, and J. Jankun, "Expression of the plasminogen activation system in kidney cancer correlates with its aggressive phenotype," *Clinical Cancer Research*, vol. 4, no. 4, pp. 869–877, 1998.

[24] M. S. Pepper, "Extracellular proteolysis and angiogenesis," *Thrombosis and Haemostasis*, vol. 86, no. 1, pp. 346–355, 2001.

[25] J. Jankun, "Antitumor activity of the type 1 plasminogen activator inhibitor and cytotoxic conjugate in vitro," *Cancer Research*, vol. 52, no. 20, pp. 5829–5832, 1992.

[26] J. Jankun, A. M. Aleem, Z. Specht et al., "PAI-1 induces cell detachment, downregulates nucleophosmin (B23) and fortilin (TCTP) in LnCAP prostate cancer cells," *International Journal of Molecular Medicine*, vol. 20, no. 1, pp. 11–20, 2007.

[27] B. R. Binder and J. Mihaly, "The plasminogen activator inhibitor "paradox" in cancer," *Immunology Letters*, vol. 118, no. 2, pp. 116–124, 2008.

[28] J. Folkman and D. Hanahan, "Switch to the angiogenic phenotype during tumorigenesis," *Princess Takamatsu Symposia*, vol. 22, pp. 339–347, 1991.

[29] E. K. O. Kruithof, "Regulation of plasminogen activator inhibitor type 1 gene expression by inflammatory mediators and statins," *Thrombosis and Haemostasis*, vol. 100, no. 6, pp. 969–975, 2008.

[30] M. Kandouz, D. Nie, G. P. Pidgeon, S. Krishnamoorthy, K. R. Maddipati, and K. V. Honn, "Platelet-type 12-lipoxygenase activates NF-κB in prostate cancer cells," *Prostaglandins and Other Lipid Mediators*, vol. 71, no. 3-4, pp. 189–204, 2003.

[31] M. Kumano, H. Miyake, M. Muramaki, J. Furukawa, A. Takenaka, and M. Fujisawa, "Expression of urokinase-type plasminogen activator system in prostate cancer: correlation with clinicopathological outcomes in patients undergoing radical prostatectomy," *Urologic Oncology*, vol. 27, no. 2, pp. 180–186, 2009.

[32] H. C. Kwaan, A. P. Mazar, and B. J. McMahon, "The apparent uPA/PAI-1 paradox in cancer: more than meets the eye," *Seminars in Thrombosis and Hemostasis*, vol. 39, no. 4, pp. 382–391, 2013.

[33] F. L. Li-Saw-Hee, A. D. Blann, and G. Y. H. Lip, "Effects of fixed low-dose warfarin, aspirin-warfarin combination therapy, and dose-adjusted warfarin on thrombogenesis in chronic atrial fibrillation," *Stroke*, vol. 31, no. 4, pp. 828–833, 2000.

[34] G. S. McMahon, C. I. Jones, P. D. Hayes, A. R. Naylor, and A. H. Goodall, "Transient heparin-induced platelet activation linked to generation of platelet 12-lipoxygenase. Findings from a randomised controlled trial," *Thrombosis and Haemostasis*, vol. 109, no. 6, pp. 1099–1107, 2013.

[35] J. L. Mehta, J. Chen, F. Yu, and D. Y. Li, "Aspirin inhibits ox-LDL-mediated LOX-1 expression and metalloproteinase-1 in human coronary endothelial cells," *Cardiovascular Research*, vol. 64, no. 2, pp. 243–249, 2004.

[36] T. Sadowski and J. Steinmeyer, "Differential effects of nonsteroidal antiinflammatory drugs on the IL-1 altered expression of plasminogen activators and plasminogen activator inhibitor-1 by articular chondrocytes," *Inflammation Research*, vol. 51, no. 8, pp. 427–433, 2002.

[37] Y.-F. Wang, W.-J. Wu, M. Zhang, M. Zhou, and B. Li, "Inhibiting cyclooxygenase and 5-lipoxygenase activities is an anti-inflammatory mechanism of Huzhang Gout Granule," *Journal of Chinese Integrative Medicine*, vol. 7, no. 10, pp. 963–968, 2009.

[38] S. F. Shariat, A. Semjonow, H. Lilja, C. Savage, A. J. Vickers, and A. Bjartell, "Tumor markers in prostate cancer I: blood-based markers," *Acta Oncologica*, vol. 50, supplement 1, pp. 61–75, 2011.

[39] S. Sharma, "Tumor markers in clinical practice: general principles and guidelines," *Indian Journal of Medical and Paediatric Oncology*, vol. 30, no. 1, pp. 1–8, 2009.

[40] M. Ohori, "Biomarkers for prostate cancer in predicting diagnosis, staging and prognosis," *Cancer & Chemotherapy*, vol. 36, no. 1, pp. 6–10, 2009.

[41] C. M. Sturgeon, M. J. Duffy, U.-H. Stenman et al., "National Academy of Clinical Biochemistry laboratory medicine practice guidelines for use of tumor markers in testicular, prostate, colorectal, breast, and ovarian cancers," *Clinical Chemistry*, vol. 54, no. 12, pp. e11–e79, 2008.

[42] A. C. P. Riddick, C. J. Shukla, C. J. Pennington et al., "Identification of degradome components associated with prostate cancer progression by expression analysis of human prostatic tissues," *British Journal of Cancer*, vol. 92, no. 12, pp. 2171–2180, 2005.

[43] L. Bohm, A. Serafin, J. Akudugu, P. Fernandez, A. van der Merwe, and N. A. Aziz, "uPA/PAI-1 ratios distinguish benign prostatic hyperplasia and prostate cancer," *Journal of Cancer Research and Clinical Oncology*, vol. 139, no. 7, pp. 1221–1228, 2013.

[44] M. Piotrowska, J. Szefel, E. Skrzypczak-Jankun et al., "The concentration of 12-lipoxygenase in platelet rich plasma as an indication of cancer of the prostate," *Contemporary Oncology*, vol. 17, no. 4, pp. 389–393, 2013.

[45] C. Festuccia, C. Vincentini, A. B. di Pasquale et al., "Plasminogen activator activities in short-term tissue cultures of benign prostatic hyperplasia and prostatic carcinoma," *Oncology Research*, vol. 7, no. 3-4, pp. 131–138, 1995.

[46] N. P. McCabe, F. F. Angwafo III, A. Zaher, S. H. Selman, A. Kouinche, and J. Jankun, "Expression of soluble urokinase plasminogen activator receptor may be related to outcome in prostate cancer patients," *Oncology Reports*, vol. 7, no. 4, pp. 879–882, 2000.

[47] P. A. Usher, O. F. Thomsen, P. Iversen et al., "Expression of urokinase plasminogen activator, its receptor and type-1 inhibitor in malignant and benign prostate tissue," *International Journal of Cancer*, vol. 113, no. 6, pp. 870–880, 2005.

[48] S.-J. Shih, M. A. Dall'Era, J. R. Westphal et al., "Elements regulating angiogenesis and correlative microvessel density in benign hyperplastic and malignant prostate tissue," *Prostate Cancer and Prostatic Diseases*, vol. 6, no. 2, pp. 131–137, 2003.

[49] M. F. McCarty, "Targeting multiple signaling pathways as a strategy for managing prostate cancer: multifocal signal modulation therapy," *Integrative Cancer Therapies*, vol. 3, no. 4, pp. 349–380, 2004.

[50] M. Kandouz and K. V. Honn, "Eicosanoids regulation of transcription factors in PC-3 prostate cancer cells," *Advances in Experimental Medicine and Biology*, vol. 507, pp. 563–568, 2002.

[51] H. Al-Mondhiry, "Beta-thromboglobulin and platelet-factor 4 in patients with cancer: correlation with the stage of disease and the effect of chemotherapy," *American Journal of Hematology*, vol. 14, no. 2, pp. 105–111, 1983.

[52] A. K. Dilly, P. Ekambaram, Y. Guo et al., "Platelet-type 12-lipoxygenase induces MMP9 expression and cellular invasion *via* activation of PI3K/Akt/NF-kappaB," *International Journal of Cancer*, vol. 133, no. 8, pp. 1784–1791, 2013.

[53] K. V. Honn, A. Aref, Y. Q. Chen et al., "Prostate cancer—old problems and new approaches—part II: diagnostic and prognostic markers, pathology and biological aspects," *Pathology & Oncology Research*, vol. 2, no. 3, pp. 191–211, 1996.

[54] K. Jaśkiewicz, E. Izycka-Świeszewska, M. Janiak et al., "Platelet 12-lipoxygenase and stem cells in Barrett's esophagus," *Oncology Letters*, vol. 1, no. 5, pp. 789–791, 2010.

[55] S. Krishnamoorthy, R. Jin, Y. Cai et al., "12-Lipoxygenase and the regulation of hypoxia-inducible factor in prostate cancer cells," *Experimental Cell Research*, vol. 316, no. 10, pp. 1706–1715, 2010.

[56] A. Gohara, N. Eltaki, D. Sabry et al., "Human 5-, 12- and 15-lipoxygenase-1 coexist in kidney but show opposite trends and their balance changes in cancer," *Oncology Reports*, vol. 28, no. 4, pp. 1275–1282, 2012.

[57] A. K. Singh, S. Kant, R. Parshad, N. Banerjee, and S. Dey, "Evaluation of human LOX-12 as a serum marker for breast cancer," *Biochemical and Biophysical Research Communications*, vol. 414, no. 2, pp. 304–308, 2011.

[58] Z. Dong, A. D. Saliganan, H. Meng et al., "Prostate cancer cell-derived urokinase-type plasminogen activator contributes to intraosseous tumor growth and bone turnover," *Neoplasia*, vol. 10, no. 5, pp. 439–449, 2008.

[59] C. Festuccia, V. Dolo, F. Guerra et al., "Plasminogen activator system modulates invasive capacity and proliferation in prostatic tumor cells," *Clinical and Experimental Metastasis*, vol. 16, no. 6, pp. 513–528, 1998.

[60] S. F. Shariat, S. Park, Q.-D. Trinh, C. G. Roehrborn, K. M. Slawin, and P. I. Karakiewicz, "Plasminogen activation inhibitor-1 improves the predictive accuracy of prostate cancer nomograms," *The Journal of Urology*, vol. 178, no. 4, part 1, pp. 1229–1237, 2007.

[61] D. Croucher, D. N. Saunders, and M. Ranson, "The urokinase/PAI-2 complex: a new high affinity ligand for the endocytosis receptor low density lipoprotein receptor-related protein," *The Journal of Biological Chemistry*, vol. 281, no. 15, pp. 10206–10213, 2006.

[62] D. Dondi, C. Festuccia, M. Piccolella, M. Bologna, and M. Motta, "GnRH agonists and antagonists decrease the metastatic progression of human prostate cancer cell lines by inhibiting the plasminogen activator system," *Oncology Reports*, vol. 15, no. 2, pp. 393–400, 2006.

[63] A. Nykjaer, M. Conese, E. I. Christensen et al., "Recycling of the urokinase receptor upon internalization of the uPA:serpin complexes," *The EMBO Journal*, vol. 16, no. 10, pp. 2610–2620, 1997.

[64] J. I. Epstein, W. C. Allsbrook Jr., M. B. Amin et al., "The 2005 International Society of Urological Pathology (ISUP) consensus conference on Gleason grading of prostatic carcinoma," *The American Journal of Surgical Pathology*, vol. 29, no. 9, pp. 1228–1242, 2005.

Hindawi Publishing Corporation
BioMed Research International
Volume 2014, Article ID 541847, 9 pages
http://dx.doi.org/10.1155/2014/541847

Clinical Study

Image Guided Hypofractionated Radiotherapy by Helical Tomotherapy for Prostate Carcinoma: Toxicity and Impact on Nadir PSA

Salvina Barra,[1] Stefano Vagge,[1] Michela Marcenaro,[1] Gladys Blandino,[2] Giorgia Timon,[2] Giulia Vidano,[2] Dario Agnese,[2] Marco Gusinu,[3] Francesca Cavagnetto,[3] and Renzo Corvò[1,2]

[1] *Department of Radiation Oncology, IRCCS San Martino-IST, National Cancer Research Institute, 16100 Genoa, Italy*
[2] *University of Genoa, DISSAL, 16100 Genoa, Italy*
[3] *Department of Medical Physics, IRCCS San Martino-IST, National Cancer Research Institute, Genova, Italy*

Correspondence should be addressed to Stefano Vagge; stefano.vagge@unige.it

Received 18 January 2014; Accepted 13 February 2014; Published 18 March 2014

Academic Editor: Giovanni Luca Gravina

Aim. To evaluate the toxicity of a hypofractionated schedule for primary radiotherapy (RT) of prostate cancer as well as the value of the nadir PSA (nPSA) and time to nadir PSA (tnPSA) as surrogate efficacy of treatment. *Material and Methods*. Eighty patients underwent hypofractionated schedule by Helical Tomotherapy (HT). A dose of 70.2 Gy was administered in 27 daily fractions of 2.6 Gy. Acute and late toxicities were graded on the RTOG/EORTC scales. The nPSA and the tnPSA for patients treated with exclusive RT were compared to an equal cohort of 20 patients treated with conventional fractionation and standard conformal radiotherapy. *Results*. Most of patients (83%) did not develop acute gastrointestinal (GI) toxicity and 50% did not present genitourinary (GU) toxicity. After a median follow-up of 36 months only grade 1 of GU and GI was reported in 6 and 3 patients as late toxicity. Average tnPSA was 30 months. The median value of nPSA after exclusive RT with HT was 0.28 ng/mL and was significantly lower than the median nPSA (0.67 ng/mL) of the conventionally treated cohort ($P = 0.02$). *Conclusions*. Hypofractionated RT schedule with HT for prostate cancer treatment reports very low toxicity and reaches a low level of nPSA that might correlate with good outcomes.

1. Introduction

Many publications suggested that the α/β ratio (recognized as the ratio of "intrinsic radiosensitivity" to the "repair capability") of prostate adenocarcinoma was comparable to that of late-responding normal tissues or even lower. If the estimated value for prostate α/β (1.5 Gy) [1] is reliably less than that for late-responding rectal damage (3 Gy), hypofractionation in the treatment of prostate cancer can offer an improved therapeutic ratio, due to a presumed higher sensitivity of prostate cancer tissues to higher fraction dose compared to the sensitivity of normal tissues damage. Randomized and prospective trials of hypofractionation treatment schedule for prostate cancer have confirmed excellent biochemical control rates and low toxicities [2–8]. These clinical studies used external beam hypofractionated regimens with dose-per-fraction ranging from 2.5 to 3.1 Gy delivered daily for 4–6 weeks. Concern remains over the use of such schedules with conformal radiotherapy technique (3D-CRT) because of the potential acute toxicity to normal organs close to the prostate. Today, with new technologies such as the use of image guided radiotherapy (IGRT) and dynamic intensity modulated radiotherapy (IMRT), it is possible to irradiate the target more accurately [9, 10] by reducing the volume of normal tissue irradiated, compared with conventional conformal (3D-CRT) techniques, while allowing to deliver higher doses to the clinical target. We present the results of a retrospective analysis of prostate cancer patients treated with hypofractionated IMRT by Helical Tomotherapy (HT)

(Accuray, Inc, Sunnyvale, CA, USA). This hypofractionated schedule is radiobiologically isoeffective to 82 Gy with a conventional 2 Gy per fraction treatment (considering a prostate cancer α/β ratio of 1.5). The aims of our analysis were to assess acute and late toxicities of a hypofractionation regimen delivered with HT and investigate the radiobiological effects of mild hypofractionation on the value of PSA nadir (nPSA) and the time to reach nPSA nadir (tnPSA).

2. Materials and Methods

2.1. Patient Eligibility. In our Department, 120 men were treated with HT for prostate cancer between 2009 and 2013. All patients had a histological confirmed diagnosis of prostate cancer. Radical radiotherapy was planned for 80 (66%) patients; 17 (14%) patients underwent postoperative adjuvant radiotherapy and 23 (19%) were treated as patients that need salvage radiotherapy after biochemical relapse and/or clinical symptoms. For this report we analyzed only 80 patients treated with radical "up-front" radiotherapy. All patients were staged with ultrasound-guided biopsy; median prostatic sampling number was 10 (range, 6–18 samples). Patients with intermediate and high-risk disease also underwent bone scan and MRI (magnetic resonance imaging); in the postoperative and salvage radiotherapy the most recent cases received an additional staging with choline PET-CT (positron emission tomography-computed tomography). The median age was 72 years old (range: 53–82) with an ECOG-performance status value of 0-1 [16]. As for their risk-category (D'Amico) [17], 14 (17.5%) patients were at low risk (PSA $\leq$ 10 ng/mL; Gleason Score $\leq$ 6, and tumor category T1c-T2a), 28 (35%) were at intermediate risk (PSA > 10–20 ng/mL or Gleason Score = 7 or T2c), and 38 (47.5%) were at high risk (PSA > 20 ng/mL or Gleason Score > 7 or two median risk factors). Androgen deprivation therapy (ADT) was administered to 54 (67.5%) patients before and after radiotherapy, for a mean duration of 22.5 months, range: 3–43. To evaluate the radiobiological effect of hypofraction on PSA kinetics, the nPSA and tnPSA of 26 patients treated with hypofractionation without ADT were retrospectively compared with those of a similar cohort of 20 prostate cancer patients treated by LINAC (linear accelerator) based conventional 3D-CRT with a standard dose of 76 Gy in 38 fractions. The clinical characteristics and initial PSA levels of all these patient populations are summarized in Tables 1 and 2. The two cohorts of patients, evaluated in this retrospective study, were treated during the same time lag between 2009 and 2013. The criterion of choice between hypofractionated and conventional fractionated schedule was due to the order of priority of patients' admission to our department and the availability of HT.

2.2. Treatment. Hypofractionated radiotherapy was delivered with HT. Setup and CT scan simulation were performed with the patient in supine position, placed in an appropriate fixation device (Combifix, Civco Medical Solutions, USA) using a 2.5 mm slice thickness, and covered the abdominal-pelvic area. Prior to CT simulation and each day before the treatment, patients followed instructions with a brochure on proper bowel and rectal preparation with partially full bladder and an empty rectum. CT data sets were sent for contouring on the Eclipse treatment planning system (Varian Medical System, Palo Alto, USA) and then exported using DICOM-RT (digital imaging and communication in medicine) format to Tomotherapy Planning System. For all patients Clinical Target Volume (CTV) consisted of the prostate and the seminal vesicles. The entire prostate was outlined as CTVp, seminal vesicles as CTVsv. Pelvic lymph nodes were outlined as CTVln following RTOG consensus guidelines [18] in all the patients at risk according to the Roach formula. To obtain the planning target volume of the prostate (PTVp) and the seminal vesicles (PTVsv), CTV was expanded isotropically with a 7 mm margin, except posteriorly where only a 3 mm margin was added. Rectum, bladder, femoral heads, large and small bowel, and penile bulb were outlined as organs at risk. The course of radiotherapy consisted of 27 fractions of 2.6 Gy daily for a total dose of 70.2 Gy. The dose was calculated with the formula NTD (normalized total dose) with a prostate α/β of 1.5 Gy. The volume of the seminal vesicles received a total dose of 60.75 Gy in 27 fractions, 2.25 Gy daily. If pelvic nodes were irradiated with adjuvant intent, a total dose of 50 Gy in 27 fractions with a single dose of 1.85 Gy per fraction was delivered. Dose was planned to cover the 95% of the PTV with at least the 95% of the prescription dose. Dose-volume histogram (DVH) goals for the rectum were such that the $V40 \leq 43\%$, $V50 \leq 32\%$, and $V65 \leq 10\%$ were obtained (Vx: the percentage of target volume that received the x dose). The bladder DVH goals were $V40 \leq 47\%$, $V55 \leq 27\%$, and $V60 \leq 14\%$. The femoral head DVH goal was $V20 < 50\%$; a constraint to the bowel placed out of the PTV was accepted with a mean dose of 19.8 Gy. Megavoltage computed tomography (MVCT) by HT was performed every day before treatment to correct patient setup according to bone and soft tissue anatomy and to take into account intrafraction variability (e.g., due to over distension of the rectum). Treatment times were typically of 15–20 min. If patients were found with unacceptable bladder or rectal filling; the treatment was deferred to obtain correct filling volumes. For the cohort of 20 patients treated with 3D-CRT by a linear accelerator (Clinac 2100 CD, Varian, Palo Alto, CA, USA) the treatment was delivered with 38 fractions of 2.0 Gy to a total dose of 76 Gy. CTV were the same as those of hypofractionated cohort. CTV expansion to PTV that was 13 mm isotropically with exception of posterior expansions that were only 8 mm was added. PTV coverage goals were the same as previously mentioned for the patients treated with HT. Dose constraints to the rectum were $V70 < 20\%$, $V60 < 40\%$, and $V50 < 55\%$. Bladder constraints were $V75 < 25\%$, $V70 < 35\%$, and $V65 < 50\%$. Clinical setup was assessed with weekly electronic portal imaging device (EPID).

2.3. Follow-Up, PSA Nadir Evaluation, Toxicity Scoring, and Statistical Analysis. Patients were assessed weekly during treatment, 4 weeks after the end of treatment, and then subsequently every three months. The follow-up was performed with medical examination, PSA assay, and filling out a form for the detection of toxicity; imaging studies were prescribed

Table 1: Patient characteristics.

	Hypofractionated group		Comparative 3D-CRT group
	RT 26 pts. (%)	RT + ADT 54 pts. (%)	RT 20 pts. (%)
Stage			
T1	7 (27)	14 (26)	13 (65)
T2	16 (62)	28 (52)	6 (30)
T3	3 (11)	12 (22)	1 (5)
N0	24 (92)	46 (85)	20 (100)
N1	2 (8)	8 (15)	0
Gleason score			
≤6	16 (62)	11 (20)	14 (70)
>6	10 (48)	43 (80)	6 (30)
Risk category			
Low	10 (38)	4 (7)	12 (60)
Intermediate	13 (50)	15 (28)	7 (35)
High	3 (12)	35 (65)	1 (5)

Table 2: Pretreatment PSA.

	Mean	Median	Range (ng/mL)
Hypofractionated group			
All patients	10.45	34.90	0.02–61.72
RT only	6.93	6.84	3.20–11.0
RT + ADT	12.10	7.50	0.02–61.72
Comparative 3D-CRT group			
RT only	7.74	7.39	3.80–12.77

only in those cases with abnormalities at diagnosis. Acute and late toxicity were assessed using the RTOG/EORTC (Radiation Therapy Oncology Group/European Organization for Research and Treatment of Cancer) radiation morbidity scoring criteria [18]; toxicity was defined to be acute or late if occurred within 3 months or after 3 months following the treatment, respectively. Adverse gastrointestinal (GI) and genitourinary (Gu) reactions were analyzed by incidence. The nPSA is defined as the lowest PSA value following radiotherapy. Biochemical failure (BF) was assessed using the nadir + 2 (Phoenix) definition [19, 20]. Statistical analyses were performed using JMP v 10.0 (SAS Institute, Cary, NC, USA). Cumulative incidence of biochemical failure (bF) and biochemical disease free survival (bDFS) was estimated by Kaplan-Meier method. An analysis between median nPSA of exclusive hypofractionated RT and exclusive 3D-CRT patients was carried out with Mann Whitney test for non-parametric data. Comparison of bDFS distribution between patients treated with or without ADT was calculated with Log-Rank Test.

3. Results

Data of eighty patients submitted to radical radiotherapy were eligible to be retrospectively analyzed for study. All patients completed the full treatment without any delays. No patients were lost for follow-up. The treatment plans provided excellent PTV coverage with an average of 98.4% of the PTV receiving 95% of the prescribed dose. With a median follow-up of 36 months (range 5–52) 79 patients were alive. A patient died from cancer unrelated cause at 24 months after radiotherapy. The 36-month bDFS was 88.9%. There was no significant difference in bDFS among patients treated with radiotherapy plus ADT and those treated with exclusive radiotherapy (95% versus 86.7%; $P = 0.9$). The cumulative incidence of biochemical failure at 36 months was 11% for the whole group of patients and, respectively, 5% in the RT group and 13.3 in the RT + ADT group (Figures 1 and 2).

3.1. Acute Toxicity. All patients were evaluable for acute toxicity. The treatment was well tolerated with 50% of patients with no GI toxicity and 83% no GU toxicity with no patient experiencing any grade 4 urinary or bowel toxicity; only one patient had a grade 3 GI toxicity. The results are reported in Tables 3 and 4 (or Figures 3 and 4). The most frequent symptoms during or soon after radiotherapy were urinary urgency, moderate increase of frequency, nicturia, and dysuria.

3.2. Late Toxicity. Median follow-up was 3 years (range 5–52 months); 74 (92.5%) patients were evaluable for late toxicity. 24/74 patients had been treated with radiotherapy alone and 50/74 with ADT also. No GU effects were reported in 65 (88%) patients (score 0) for RTOG-EORTC and 6 (8%)

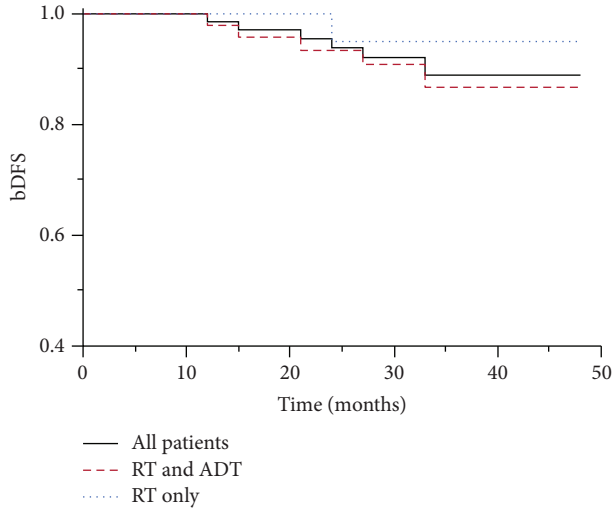

Figure 1: Biochemical disease-free survival (bDFS) in exclusive RT and ADT + RT.

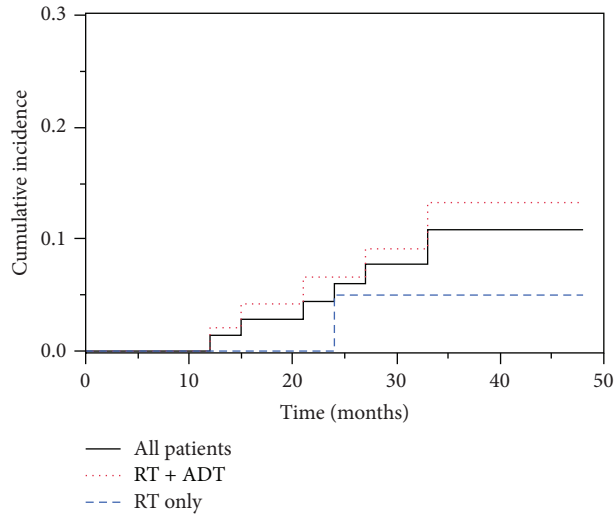

Figure 2: Incidence of biochemical disease failure (bDF) for exclusive RT and ADT + RT.

suffered minor effects (score 1). No GI problem was reported in 73 (99%) patients. A modest degree of toxicity (score 1) occurred in one patient. In Tables 1 and 2 we summarize the rates of urinary and rectal toxicity (incidence) observed at follow-up. As shown, there were no grades 3 and 4 toxicities. Grades 2 and 1 bladder toxicities were seen in 3% (4 patients) and 8% (6 patients), respectively. The only common factor between both patients with grade 2 genitourinary toxicity was frequency. None of the patients had urologic instrumentation procedures. Urinary incontinence, complete obstruction, or persistent hematuria was not observed. No patients had grade 3 GI toxicity; only one patient developed a grade 1. Persistent rectal bleeding was not observed. Toxicity rates compared between patients with or without hormone therapy showed no differences between the two groups. Erectile dysfunction evaluation was reported only in 63 cases. Erectile dysfunction before treatment was registered only by structured interview in 12 patients. During the follow-up 45 patients referred impotence, 30 were submitted to RT + ADT, and 15 to exclusive RT.

3.3. PSA Nadir and Time to PSA Nadir. The patterns of PSA response after completion of radiotherapy showed a gradual decline. For the entire group (±ADT) of patients the average nPSA was 0.37 ng/mL, median 0.08 (SD 0.8) (standard deviation). We examined separately the values of the nPSA in the group of patients after exclusive RT and after RT plus ADT. The RT group average nPSA to date was 0.32 ng/mL and median 0.28 ng/mL (SD 0.4—range 0.01–1.36). One of the objectives of the study was to evaluate the nPSA. For the cohort of 80 patients we found an average and median values of 30 months. For the exclusive RT group the mean and median time of the nPSA were 30 months. To study whether a radical radiotherapy treatment delivered in less than 6 weeks by a hypofractionation schedule impact on nPSA differently from a 2 Gy daily fractionation schedule we collected the nPSA value and the corresponding time to nadir between a group of 20 patients treated with standard fractionation. The reported results for this group were average nPSa 0.86 ng/mL, median nPSA 0.67 ng/mL (SD 0.7; range 0.05–3.44); average tnPSA 18 months, median 27 months. Comparing the tnPSA and the median nPSA between patients treated with exclusive radiotherapy with hypofractionation or conventional fractionation no significant differences were observed between the times to reach the nadir (30 versus 27 months, P = ns), while the values of the nPSA were significantly lower in the group treated with hypofractionated RT ($P = 0, 02$) (Figures 5 and 6).

4. Discussion

We report our experience of hypofractionation with HT for prostate cancer. The study aimed to report the registered toxicity of hypofractionation with volumetric IG-IMRT technique and investigate whether hypofractionated schedule could have an impact on the nadir PSA and the time required reaching it. Our study has several strengths including the numerous detection of PSA after radiotherapy (every 3 months) for all the cohort of patients analyzed. Moreover few data have been published yet about the slope of PSA and nPSA after hypofractionated radiotherapy compared with conventional one. On the other hand we are well aware of the limitation of our study as the low number of patients evaluated and the short follow-up time. The HT is a unit of treatment with intensity-modulated beams equipped with a system of image guided integrated (IGRT). The megavoltage (MV) CT images acquired with the HT can be recorded and matched with the CT planning, immediately before irradiation, to correct errors in the setup and interfraction organ motion. The use of IGRT allowed the reduction of the expansion of CTV to 7 mm from 13 mm in all directions except posteriorly, where we expanded only 3–5 mm. The importance of IGRT in prostate cancer treatment has been recently evaluated in the report of Zelefsky et al. [21], where

Table 3: Acute and late genitourinary toxicity.

Toxicity	Grade 0	Grade 1	Grade 2	Grade 3	Grade 4
Acute (80 pts.)					
All patients	40 (50%)	29 (36%)	10 (13%)	1 (4%)	0
RT (26 pts.)	19 (73%)	5 (19%)	1 (4%)	1 (4%)	0
RT + ADT (54 pts.)	21 (39%)	24 (44%)	9 (17%)	0	0
Late (74 pts.)					
All patients	65 (88%)	6 (8%)	3 (4%)	0	0
RT (25 pts.)	23 (92%)	2 (8%)	0	0	0
RT + ADT (49 pts.)	42 (86%)	4 (8%)	3 (6%)	0	0

Table 4: Acute and late gastrointestinal toxicity.

Toxicity	Grade 0	Grade 1	Grade 2	Grade 3	Grade 4
Acute (80 pts.)					
All patients	66 (83%)	13 (16%)	1 (4%)	0	0
RT (26 pts.)	21 (81%)	4 (15%)	1 (4%)	0	0
RT + ADT (54 pts.)	45 (83%)	9 (17%)	0	0	0
Late (74 pts.)					
All patients	73 (99%)	1 (4%)	0	0	0
RT (25 pts.)	24 (96%)	1 (4%)	0	0	0
RT + ADT (49 pts.)	49 (100%)	0	0	0	0

186 patients have been treated with IGRT to a dose of 86.4 Gy. The target of the patients was corrected daily based on kilo-voltage imaging of implanted prostatic fiducial markers. This group of patients were retrospectively compared with a similar cohort of 190 patients treated in the same period with IMRT and with the same prescription dose without, however, implanted fiducial markers (non-IGRT). At median follow-up time of 2.8 years (range, 2–6 years) the authors found a significant reduction in late urinary toxicity for IGRT patients compared with the non-IGRT patients. The 3-year likelihood of grade 2 and higher urinary toxicity for the IGRT and non-IGRT cohorts were 10.4% and 20.0%, respectively ($P < 0.02$). The incidence of grade 2 and higher rectal toxicity was low for both treatment groups (1.0% and 1.6%, resp., $P < 0.81$). This study, also, reported an improvement in prostate-specific antigen relapse-free survival for high-risk patients treated with IGRT compared with non-IGRT (97% versus 77.7%; $P = 0.05$). Another study investigating the role of IGRT in 367 patients was reported by Singh et al. [22]: in this trial the irradiation was delivered by 3D-CRT, with and without IGRT. Compared with the non-IGRT group, improvement was noted in all dysfunctional rectal symptoms using IGRT. In multivariable analyses, IGRT improved rectal pain ($P < 0.02$), urgency ($P < 0.01$), diarrhea ($P < 0.01$), and change in bowel habits ($P < 0.01$). The toxicities reported from our study confirm that a hypofractionated course using HT for prostate cancer is associated with infrequent rates of clinically significant urinary and rectal toxicity. Our results are similar to the ones reported by Kupelian et al. [23] that using IMRT with daily transabdominal ultrasound image guidance and with a fractionation of 70 Gy/2.5 Gy for fraction reported gastrointestinal late toxicity of G2, G3, and G4 of 3.1%, 1.3%, and 0,1%, respectively, while the urinary toxicities of G2, G3 were 5.1% and 0.1%. Also Martin et al. [24] reported results of 92 patients irradiated with single dose of 3 Gy, total dose of 60 Gy, using IMRT and daily electronic portal image (EPID) with implanted fiducial markers. The gastrointestinal late toxicity of G2 was 4% and urinary toxicity of G2 was 3%. Lock et al. [25] report the study of 66 patients who received 63.2 Gy in 20 fractions over 4 weeks. Fiducial markers and daily ultrasound were used for image guidance. At 36 months acute grades 2 and 3 toxicities were 34% and 9% for GU versus 25% and 10% for GI symptoms. Late grades 2 and 3 toxicity for GU were 14% and 5%, and GI toxicity was 25% and 3%. However, despite these good toxicity results, recently Pollack et al. [7] reported data from a randomized clinical trial of comparison between hypofractionationated and conventional external beam RT for prostate cancer and suggest that patients with compromised urinary function before RT may not be candidate to hypofractionation due to the higher incidence of late GU toxicity. Many studies have also shown that greater PSA nadir (nPSA) levels are associated with an increased risk of biochemical failure, local failure, distant failure, progression-free survival, and disease-specific survival [26–30]. These studies have proposed various nPSA cutoffs ranging from 0.2 to 4.0 ng/mL as being predictive for outcomes in patients treated with external beam RT, brachytherapy, or the combination with and without androgen suppression. Some studies have also suggested that the time duration of the nPSA after RT is related to the outcome [31, 32]. Ray at al. [33] reported the result of 4839 patients with median follow-up of 6.3 years. All patients were treated definitively with RT alone to doses higher than 60 Gy, without ADT; nPSA was the lowest PSA measurement during the entire follow-up period. In this study the tnPSA was defined as the time from completion

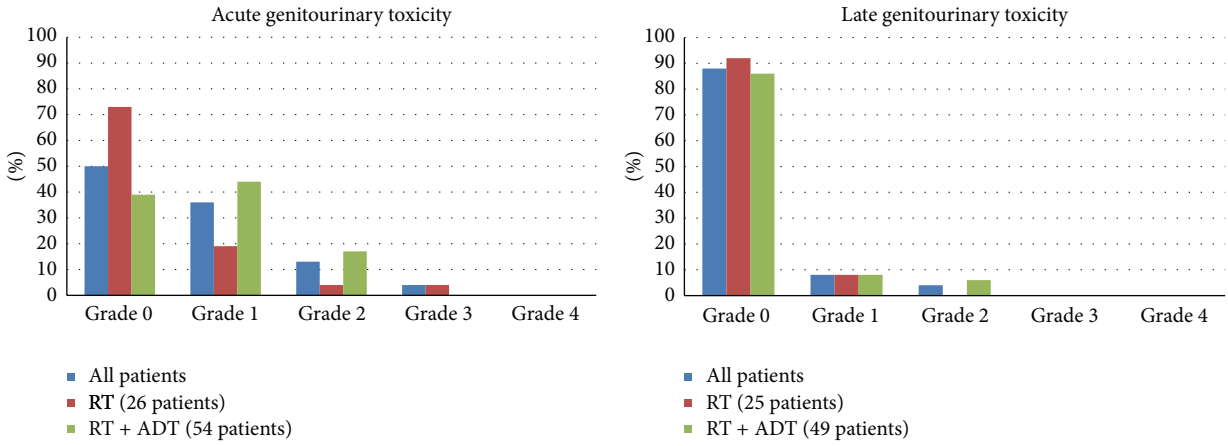

Figure 3: Genitourinary toxicity.

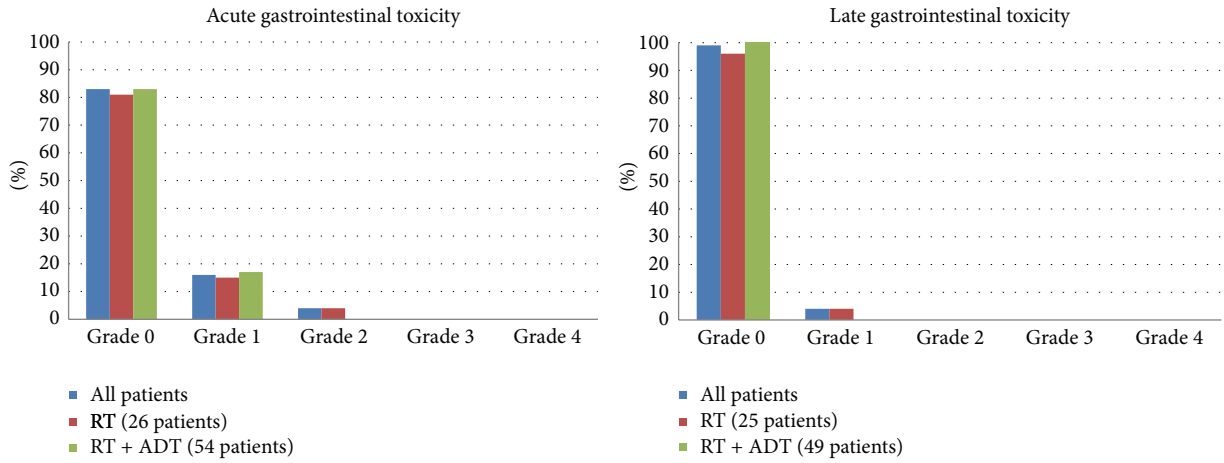

Figure 4: Gastrointestinal toxicity.

of RT to the nPSA date. Greater nPSA level and shorter tnPSA were associated with decreased biochemical or clinical disease-free survival (PSA-DFS) and distant metastasis-free survival (DMFS) in all patients and in all risk categories. The authors, also, correlated the total dose of irradiation with nPSA and tnPSA: the results suggest that a dose >70 Gy was associated with a lower nPSA level and longer TnPSA in all the patients. Johnson et al. have studied the nPSA and tnPSA for 410 patients after definitive high dose (>75 Gy) external beam radiotherapy without androgen deprivation. On univariate analysis both nPSA and tnPSA were predictive of freedom from biochemical failure, freedom from metastases, and prostate cancer specific survival ($P < 0.0001$). On Cox proportional hazards, a tnPSA <12 months did have worse prognosis as compared with longer tnPSA, but for those who achieved nPSA after 12 months the tnPSA was no longer prognostic [34]. In consideration of these crucial parameters able to predict the response to radiotherapy, we examined in our group of patients the value of the nPSA. Our findings achieved with hypofractionation appear to be interesting. The nPSA was very low (mean 0.37 ng/mL) in the whole group of patients treated with hypofractionation IG-IMRT. Twenty-five patients treated with RT alone were compared with a cohort of patients irradiated in the same period with conventional fractionation by 3-D CRT without IGRT. The median nPSA for patients with RT hypofractionated was 0.28 ng/mL after a mean time of 30 months versus 0.67 ng/mL after mean time of 27 months ($P < 0.01$) in the other group. This comparison, evaluated in a nonrandomized setting, remains of low scientific significance. However, the difference in the biological dose delivered in different treatment times (5.5 weeks versus 7.5 weeks) may have an impact on ultimate local control. Many literature data have evidenced the role of hypofractionation for the successful treatment of prostate cancer. Our results, although on a small series of patients treated with hypofractionated IMRT, are interesting since a very low nPSA was obtained after 30 months. Interestingly, with very short schedules where high doses per fraction (>7 Gy) are delivered for five fractions, the nPSA could be much more low. Recently some authors have published the first results after robotic radiotherapy with Cyberknife. In Table 5 we briefly report some preliminary results from the literature. With these new modalities the values of nPSA are very low being between 0.1 and 0.3 ng/mL while time to

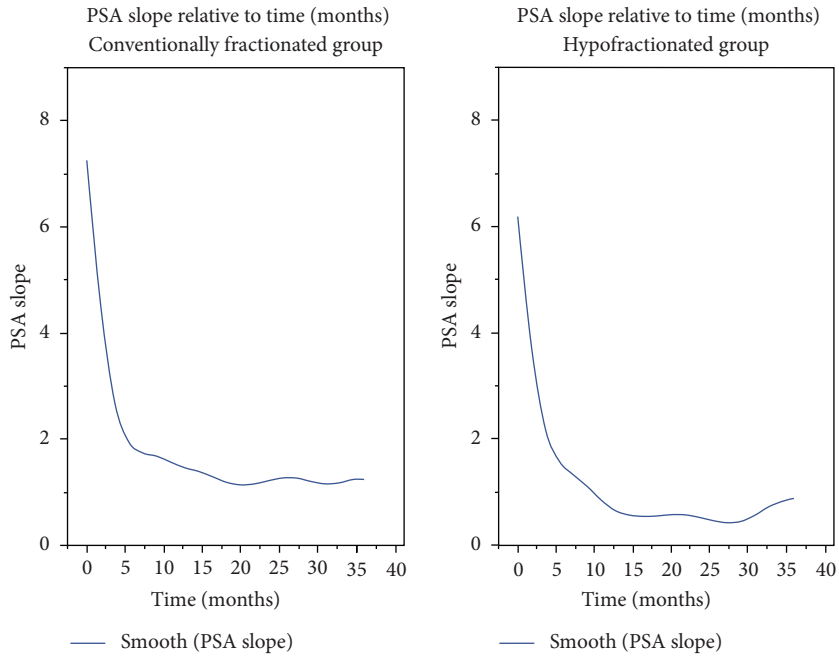

Figure 5: Trend of the PSA to achieve nadir.

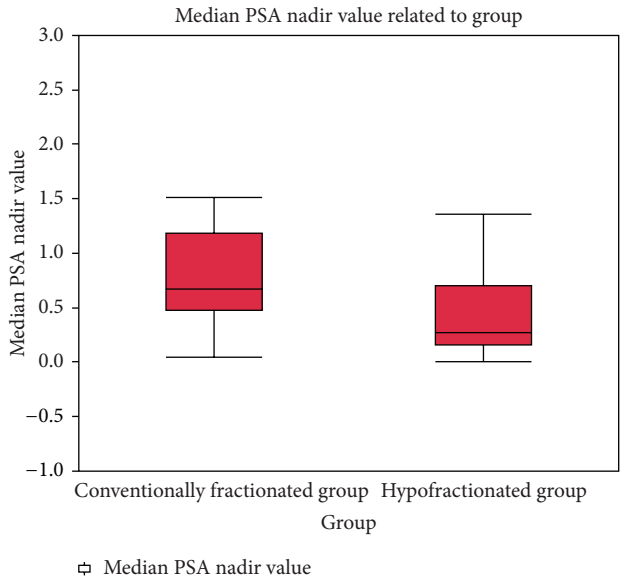

Figure 6: Boxplot of the median nadir PSA between patients treated with exclusive radiotherapy with a conventional fractionation and hypofractionation. The difference between the two groups of median PSA nadir is significative.

Table 5: Median nadir PSA after stereotactic series with extreme hypofractionation radiotherapy for prostate cancer.

Author	Median FU (months)	Median nPSA (ng/mL)
Katz et al. [11]	51	0.1
Mcbride et al. [12]	44	0.2
Freeman and King [13]	60	0.3
King et al. [14]	32	0.5
Bolzicco et al. [15]	36	0.6 (exclusive RT)
This report*	36	0.18 (ADT + RT)
	36	0.08 (ADT + RT)
	36	0.28 (exclusive RT)

*Mild hypofractionation.

nadir has not still been reported. Waiting for the mature data of these experiences we have recently started a prospective clinical trial delivering 36.25 Gy in 5 fractions, 7.25 Gy per fraction over 10 days with HT for patients with low-risk prostate cancer. In this new trial the nPSA and tnPSA are the main surrogate end-points of radiation tumor control. However, only a well-designed randomized trial comparing mild and ultrashort hypofractionation could demonstrate or not a detectable difference in toxicity and ultimate cure between these new fractionation schedules.

5. Conclusions

The hypofractionation by IG-IMRT, reported in this analysis, was confirmed to be effective for the treatment of prostate cancer in all category risks. The use of IMRT and IGRT limits acute and late toxicity. Moreover, the value of nPSA obtained with our fractionation is very low. This evidence has an important predictive value on the long-term efficacy of radiotherapy. However a greater number of patients and with adequate follow-up are warranted to confirm these

excellent findings; this mild hypofractionated schedule is now currently used at our Department for its safety and efficacy.

Conflict of Interests

The authors declare that there is no conflict of interests regarding the publishing of this paper.

References

[1] D. J. Brenner, A. A. Martinez, G. K. Edmundson, C. Mitchell, H. D. Thames, and E. P. Armour, "Direct evidence that prostate tumors show high sensitivity to fractionation (low α/β ratio), similar to late-responding normal tissue," *International Journal of Radiation Oncology. Biology. Physics*, vol. 52, no. 1, pp. 6–13, 2002.

[2] P. A. Kupelian, C. A. Reddy, E. A. Klein, and T. R. Willoughby, "Short-course intensity-modulated radiotherapy (70 GY at 2.5 GY per fraction) for localized prostate cancer: preliminary results on late toxicity and quality of life," *International Journal of Radiation Oncology. Biology. Physics*, vol. 51, no. 4, pp. 988–993, 2001.

[3] P. A. Kupelian, T. R. Willoughby, C. A. Reddy, E. A. Klein, and A. Mahadevan, "Hypofractionated intensity modulated radiotherapy (70 Gy at 2.5 Gy per fraction) for localized prostate cancer: Cleveland Clinic experience," *International Journal of Radiation Oncology. Biology. Physics*, vol. 68, no. 5, pp. 1424–1430, 2007.

[4] H. Lukka, C. Hayter, J. A. Julian et al., "Randomized trial comparing two fractionation schedules for patients with localized prostate cancer," *Journal of Clinical Oncology*, vol. 23, no. 25, pp. 6132–6138, 2005.

[5] G. Arcangeli, J. Fowler, S. Gomellini et al., "Acute and late toxicity in a randomized trial of conventional versus hypofractionated three-dimensional conformal radiotherapy for prostate cancer," *International Journal of Radiation Oncology. Biology. Physics*, vol. 79, no. 4, pp. 1013–1021, 2011.

[6] E. E. Yeoh, R. J. Botten, J. Butters, A. C. Di Matteo, R. H. Holloway, and J. Fowler, "Hypofractionated versus conventionally fractionated radiotherapy for prostate carcinoma: final results of phase III randomized trial," *International Journal of Radiation Oncology. Biology. Physics*, vol. 81, no. 5, pp. 1271–1278, 2011.

[7] A. Pollack, G. Walker, E. M. Horwitz et al., "Randomized trial of hypofractionated external-beam radiotherapy for prostate cancer," *Journal of Clinical Oncology*, vol. 31, pp. 3860–3867, 2013.

[8] D. Dearnaley, I. Syndikus, G. Sumo et al., "Conventional versus hypofractionated high-dose intensity-modulated radiotherapy for prostate cancer: preliminary safety results from the CHHiP randomised controlled trial," *The Lancet Oncology*, vol. 13, no. 1, pp. 43–54, 2012.

[9] A. M. Amer, J. Mott, R. I. Mackay et al., "Prediction of the benefits from dose-escalated hypofractionated intensity-modulated radiotherapy for prostate cancer," *International Journal of Radiation Oncology. Biology. Physics*, vol. 56, no. 1, pp. 199–207, 2003.

[10] E. Mayas, I. J. Chetty, M. Chetvertkov et al., "Evaluation of multiple image-based modalities for image-guided radiation therapy (IGRT) of prostate carcinoma: a prospective study," *Medical Physics*, vol. 40, article 4, 2013.

[11] A. J. Katz, M. Santoro, R. Ashley et al., "Stereotactic body radiotherapy for low- and low-intermediate risk prostate cancer: is there a dose effect," *Frontiers in Oncology*, vol. 1, article 49, 2011.

[12] S. M. Mcbride, D. S. Wong, J. J. Dombrowski et al., "Hypofractionated stereotactic body radiotherapy in low-risk prostate adenocarcinoma: preliminary results of a multi-institutional phase 1 feasibility trial," *Cancer*, vol. 118, pp. 3681–3690, 2012.

[13] D. E. Freeman and C. R. King, "Stereotactic body radiotherapy for low-risk prostate cancer: five-year outcomes," *Radiation Oncology*, vol. 6, no. 1, article 3, 2011.

[14] C. R. King, J. D. Brooks, H. Gill, and J. C. Presti Jr., "Long-term outcomes from a prospective trial of stereotactic body radiotherapy for low-risk prostate cancer," *International Journal of Radiation Oncology. Biology. Physics*, vol. 82, no. 2, pp. 877–882, 2012.

[15] G. Bolzicco, M. S. Favretto, and N. Satariano, "A single-centre study of 100 consecutive patients with localized prostate cancer treated with stereotactic body radiotherapy," *BMC Urology*, vol. 13, article 49, 2013.

[16] J. B. Sørensen, M. Klee, T. Palshof, and H. H. Hansen, "Performance status assessment in cancer patients. An inter-observer variability study," *British Journal of Cancer*, vol. 67, no. 4, pp. 773–775, 1993.

[17] D. J. Hernandez, M. E. Nielsen, M. Han, and A. W. Partin, "Contemporary evaluation of the d'amico risk classification of prostate cancer," *Urology*, vol. 70, no. 5, pp. 931–935, 2007.

[18] J. D. Cox, J. Stetz, and T. F. Pajak, "Toxicity criteria of the Radiation Therapy Oncology Group (RTOG) and the European Organization for research and treatment of cancer(EORTC)," *International Journal of Radiation Oncology. Biology. Physics*, vol. 31, no. 5, pp. 1341–1346, 1995.

[19] M. C. Abramowitz, T. Li, M. K. Buyyounouski et al., "The phoenix definition of biochemical failure predicts for overall survival in patients with prostate cancer," *Cancer*, vol. 112, no. 1, pp. 55–60, 2008.

[20] M. Roach, G. Hanks, H. Thames et al., "Defining biochemical failure following radiotherapy with or without hormonal therapy in men with clinically localized prostate cancer: recommendations of the RTOG-ASTRO Phoenix Consensus Conference," *International Journal of Radiation Oncology. Biology. Physics*, vol. 65, no. 4, pp. 965–974, 2006.

[21] M. J. Zelefsky, M. Kollmeier, B. Cox et al., "Improved clinical outcomes with high-dose image guided radiotherapy compared with non-IGRT for the treatment of clinically localized prostate cancer," *International Journal of Radiation Oncology. Biology. Physics*, vol. 84, pp. 125–129, 2012.

[22] J. Singh, P. B. Greer, M. A. White et al., "Treatment-related morbidity in prostate cancer: a comparison of 3-dimensional conformal radiation therapy with and without image guidance using implanted fiducial markers," *International Journal of Radiation Oncology. Biology. Physics*, vol. 8, pp. 1018–1023, 2013.

[23] P. A. Kupelian, T. R. Willoughby, C. A. Reddy, E. A. Klein, and A. Mahadevan, "Hypofractionated intensity-modulated radiotherapy (70 Gy at 2.5Gy per fraction) for localized prostate cancer: Cleveland Clinic experience," *International Journal of Radiation Oncology. Biology. Physics*, vol. 68, no. 5, pp. 1424–1430, 2007.

[24] J. M. Martin, T. Rosewall, A. Bayley et al., "Phase II trial of hypofractionated image-guided intensity modulated radiotherapyfor localized prostate adenocarcinoma," *International Journal of Radiation Oncology. Biology. Physics*, vol. 69, no. 4, pp. 1084–1089, 2007.

[25] M. Lock, L. Best, E. Wong et al., "A Phase II trial of arc-based hypofractionated intensity-modulated radiotherapy in localized prostate cancer," *International Journal of Radiation Oncology. Biology. Physics*, vol. 80, pp. 1306–1315, 2011.

[26] R. Vigna, E. G. Russi, A. Boriano et al., "Reliability of prostate specific antigen marker in determining biochemical failure during the first two years after external beam radiotherapy and hormone therapy in patients with non operated prostate cancer," *Urologic Oncology*, vol. 32, no. 1, pp. 30.e1–30.e7, 2014.

[27] S. X. Cavanaugh, P. A. Kupelian, C. D. Fuller et al., "Early prostate-specific antigen (PSA) kinetics following prostate carcinoma radiotherapy: prognostic value of a time-and-PSA threshold model," *Cancer*, vol. 101, no. 1, pp. 96–105, 2004.

[28] E. C. Ko, N. N. Stone, and R. G. Stock, "PSA Nadir of <0.5 ng/mL following brachytherapy for early-stage prostate adenocarcinoma is associated with freedom from prostate-specific antigen failure," *International Journal of Radiation Oncology. Biology. Physics*, vol. 83, pp. 600–607, 2012.

[29] D. Norkus, A. Karklelyte, and B. Engels, "A randomized hypofractionation dose escalation trial for high risk prostate cancer patients: interim analysis of acute toxicity and quality of life in 124 patients," *Radiation Oncology*, vol. 8, article 206, 2013.

[30] P. Nickers, A. Albert, D. Waltregny, and J.-M. Deneufbourg, "Prognostic value of PSA nadir ≤4 ng/mL within 4 months of high-dose radiotherapy for locally advanced prostate cancer," *International Journal of Radiation Oncology. Biology. Physics*, vol. 65, no. 1, pp. 73–77, 2006.

[31] F. A. Critz, "Time to achieve a prostate specific antigen nadir of 0.2 ng/ml after simultaneous irradiation for prostate cancer," *Journal of Urology*, vol. 168, no. 6, pp. 2434–2438, 2002.

[32] S. B. Johnson, W. C. Jackson, J. Murgic et al., "Time to nadir PSA: of popes and PSA—the immortality bias," *American Journal of Clinical Oncology*, 2013.

[33] M. E. Ray, H. D. Thames, L. B. Levy et al., "PSA nadir predicts biochemical and distant failures after external beam radiotherapy for prostate cancer: a multi-institutional analysis," *International Journal of Radiation Oncology. Biology. Physics*, vol. 64, no. 4, pp. 1140–1150, 2006.

[34] S. B. Johnson, W. C. Jackson, J. Murgic, F. Y. Feng, and D. A. Hamstra, "Time to nadir PSA: of popes and PSA—the immortality bias," *American Journal of Clinical Oncology*, 2013.

Hindawi Publishing Corporation
BioMed Research International
Volume 2014, Article ID 878319, 15 pages
http://dx.doi.org/10.1155/2014/878319

Review Article

Low Temperature Plasma: A Novel Focal Therapy for Localized Prostate Cancer?

Adam M. Hirst,[1] Fiona M. Frame,[2] Norman J. Maitland,[2] and Deborah O'Connell[1]

[1] *Department of Physics, York Plasma Institute, University of York, Heslington, York YO10 5DD, UK*
[2] *YCR Cancer Research Unit, Department of Biology, University of York, Heslington, York YO10 5DD, UK*

Correspondence should be addressed to Norman J. Maitland; njm9@york.ac.uk

Received 16 December 2013; Accepted 6 February 2014; Published 13 March 2014

Academic Editor: Giovanni Luca Gravina

Despite considerable advances in recent years for the focal treatment of localized prostate cancer, high recurrence rates and detrimental side effects are still a cause for concern. In this review, we compare current focal therapies to a potentially novel approach for the treatment of early onset prostate cancer: low temperature plasma. The rapidly evolving plasma technology has the potential to deliver a wide range of promising medical applications via the delivery of plasma-induced reactive oxygen and nitrogen species. Studies assessing the effect of low temperature plasma on cell lines and xenografts have demonstrated DNA damage leading to apoptosis and reduction in cell viability. However, there have been no studies on prostate cancer, which is an obvious candidate for this novel therapy. We present here the potential of low temperature plasma as a focal therapy for prostate cancer.

1. Introduction

Prostate cancer is now recognised as the second most diagnosed cancer overall and accounts for around a quarter of all cancers in males [1]. The risk of prostate cancer peaks in men over 60 years of age, yet high incidence rates are also found in younger aged groups [2]. In addition, benign enlargement of the prostate becomes increasingly common in men over the age of 40 and particularly so beyond 60 years of age [3].

Treatment for advanced prostate cancer is still unsatisfactory, with an almost inevitable development of hormone resistance [4]. Even new generation androgen ablation drugs fail to deliver a life extension beyond several months [5]. In addition, there is poor response to chemotherapy, alongside unpleasant side effects, and reduced quality of life [6]. Therefore, the emphasis remains to detect and treat prostate cancer at an early stage to have most hope of a cure. Indeed, early diagnosis has become more common with increased uptake of PSA testing [7, 8].

Once prostate cancer is diagnosed, the clinician is presented with a series of dilemmas; firstly, is the tumour localized or has it spread [9]; second, if localized is it potentially aggressive or indolent [10]; and the third, should the patient undergo active surveillance or be treated immediately [11]. If the latter is chosen in the context of a localized tumour, then the next decision is between radical surgery with the risk of incontinence and impotence, radiotherapy, or treatment with a focal therapy [12]. Radical surgery has the potential to be an overtreatment in early-onset or low-risk disease [13], where active surveillance or treatment with a focal therapy may be more suitable [14]. Ideally, focal therapy is targeted to maximize elimination of the tumour foci without treating the whole gland, while minimizing side effects [15, 16]. This review aims to evaluate several currently available focal therapies for prostate cancer and introduces a potential focal treatment in the form of low temperature plasma (LTP). Application of LTPs to internal organs such as the prostate may seem technically difficult but could offer many advantages over current treatments.

2. Approaches to Focal Therapy of Localized Prostate Cancer

For patients to be considered as candidates for focal therapy, their prostate cancer must be present in only one lobe, typically unifocal, and contained within the prostate capsule [17]. However, no absolute ideal patient selection criteria exist

for focal prostate treatment [18]. In the following subsections, some focal therapies for localized prostate cancer are briefly analyzed, with their respective advantages and pitfalls outlined for comparison. In addition, the importance of imaging techniques in the context of focal therapy treatments is also discussed.

2.1. High-Intensity Focused Ultrasound. The concept of high-intensity focused ultrasound (HIFU) was first applied in the 1980s to benign prostate hyperplasia (BPH) [19], with the first recorded application to localized prostate cancer in 1995 [20]. The physical mechanism of HIFU follows the same principles as diagnostic ultrasound, whereby ultrasonic waves pass through healthy tissues without causing harm. However, if the ultrasonic beam is sufficiently focused and the intensity increased, high levels of energy can be delivered to very localized regions [7]. These high levels of energy are capable of causing irreversible damage to the targeted tissue via hyperthermia mechanisms, either by heating or inertial cavitation [7, 21, 22]. In the case of thermal effects, energy delivered by the ultrasonic beam is absorbed by the treated area, leading to rapid heating effects, which can raise the temperature of the treated tissue to 80°C in a few seconds [23]. This instant heating leads to coagulative necrosis through protein denaturation [15, 24]. A recent study considered the treated area to have been successfully ablated once a minimum temperature of 65°C had been reached [25].

The typical devices used for HIFU treatment of the prostate are applied transrectally and so possess the advantage over other focal therapies in that an invasive surgical approach is not required. There are two devices currently available for HIFU: Sonablate and Ablatherm. Taking Sonablate as an example, the device utilizes a 4 MHz transducer which is capable of both treatment and imaging depending upon the intensity applied, with intensities of up to 2000 W cm^{-2} achievable at focal lengths as short as 3 cm [26]. Due to the extremely high intensities involved in the procedure, there is a need for accurate monitoring of the energy delivery to, and resulting temperature of, the target tissue. In recent years, the effectiveness of real-time magnetic resonance imaging (MRI) has improved, such that it constitutes an invaluable tool for the monitoring of the HIFU procedure [25, 27].

The difficulty with treating enlarged prostates lies mainly in limitations on the focal length of the ultrasound probe [22, 28]. A transurethral resection of the prostate (TURP) procedure is recommended prior to treatment to reduce organ volume, as post-HIFU swelling of the prostate is common [8, 29]. The effective treatment of anterior prostate tumours is also problematic using HIFU, as anterior perirectal fat tissue can prevent intended penetration depth of the ultrasound beam [30]. This occurs due to reflection of the signal and is a particular problem if the patient is overweight [31].

2.2. Photo-Dynamic Therapy. Photodynamic therapy (PDT) damages tissues in a highly localized fashion by exciting photosensitizing drugs with light. The drugs are administered either orally or intravenously, absorb energy from a light source, for example a laser, and transfer it to molecular oxygen residing in the surrounding tissues [32]. This in turn produces an activated form of molecular oxygen [33] known as singlet delta oxygen ($^1O_2$, SDO). It is believed that SDO is predominantly produced following the excitation of the sensitizing agent from its triplet ground state, upon irradiation from the light source [34]. SDO is highly toxic to cells and can interfere with cell signalling as well as inducing cellular stress [35–37]. Importantly, the photosensitizing process is recurrent, eliminating the need for repeated applications during delivery as a stream of SDO is produced [33]. In addition, PDT has the advantage of greater selectivity versus other cancer therapies, as only simultaneous exposure to the photosensitizing drug, light, and oxygen will result in a cytotoxic effect on the treated cells [34]. This selectivity can be further improved by the use of an antibody, applied in conjunction with the photosensitizer, which is specific to the tumour [38, 39].

PDT predominantly utilizes two approaches to damage cancerous tissue. Either tumour hypoxia can be induced following laser targeting of the blood supply to the tumour or an apoptotic/necrotic response can be initiated following direct targeting of the tumour surface itself [40]. It is necessary to protect the skin and eyes of the patient, even following treatment. Such protection may be required for a few hours up to several weeks, depending on the photosensitizer used [41], as the time each drug remains in the patient's bloodstream varies vastly. A transperineal approach allows treatment of tumours localized to anterior prostate [42], giving advantages over other treatment approaches such as HIFU (see Table 1), although this can still be problematic [7]. However, PDT has the advantage of being potentially applicable at the same treatment site multiple times [42], unlike for instance surgery or radiotherapy, in addition to being a potential salvage therapy following failure of these techniques [43].

2.3. Cryotherapy. Rapid freezing and thawing cycles are employed by cryotherapy techniques in order to cause localized cellular destruction due to either the extremely low temperature alone, the rapid rate of cooling, or the period of time for which the tissue stays frozen [21]. Either liquid nitrogen or argon gas is administered to the prostate transperineally via cryoprobes under transrectal ultrasound (TRUS) guidance. Argon gas probes are now favoured over liquid nitrogen based approaches due their thinner diameters, permitting the insertion of additional probes (in a brachytherapy-like manner) to improve the efficacy of treatment [44]. In addition, the use of argon gas dramatically improves the freeze-thaw effect by reducing the probe tip to a temperature of −187°C, before 67°C helium gas rapidly thaws the treated region [44, 45], causing rupturing and bursting of the cells. Two cycles, reaching at least −40°C are required for complete cell death, with cell shrinkage and protein denaturation occurring as the tissue temperature decreases beyond 0°C [21]. A urethral warming catheter and multiple thermosensors are typically used to prevent freezing of unwanted regions [45, 46].

Cryotherapy can be applied as a salvage therapy, for example, after the failure of or recurrence following radio- and

Table 1: Pros and cons of focal therapies currently available for prostate cancer.

Treatment	Summary of Pros	Summary of Cons
High-intensity focused ultrasound	(i) Transrectal application negates the need for surgical approach (ii) Improvements in MRI technology allow real-time procedure monitoring and improved targeting	(i) Difficulty treating enlarged prostates, especially in overweight patients (ii) Effective treatment of anterior tumours is not achievable
Photodynamic therapy	(i) More selective than other focal therapies due to conditions needed for SDO production (ii) Can be applied at the same treatment site multiple times	Photosensitizing agent remains in patient's bloodstream following treatment, requiring protection of the eyes and skin for potentially weeks after the procedure
Cryotherapy	(i) Double freeze-thaw cycle effectively destroys cells in targeted region (ii) Can be applied as a salvage following radiotherapy techniques	(i) Urinary infections and perineal discomfort posttreatment are common (ii) Relatively invasive treatment, with added needed for thermal protection of urethra, bladder and rectum
Radiotherapy	(i) Minimally invasive approach as radiation is usually applied externally (ii) Proton beam therapy and Cyberknife technologies give hope of improved targeting with fewer side effects	(i) Many side effects as a result of radiation at unintended sites, causing urinary incontinence, rectal pain, and erectile dysfunction (ii) A third of patients experience radiorecurrent disease
Brachytherapy	Image guided seed placement allows effective treatment of localized areas	Needle array application is a highly invasive process

brachytherapy [47, 48]. Common side effects following cryotherapy include rectal or perineal discomfort [49] and urinary infections [50]. Major complications can include rectourethral fistula, although this is rare [45].

2.4. Radiotherapy. Whilst radiotherapy is not considered a focal therapy, variants such as Cyberknife and brachytherapy have the potential to be applied to more localized cancers and are discussed later in this section. It has long been known that ionizing radiation (IR) can lead to adverse effects on cells. Using this principle, effects include, but are not limited to DNA damage, cell cycle arrest, and ultimately cell death can be achieved through radiotherapy [51]. This is due to reactive oxygen species (ROS) formed from interactions with free radicals, produced as a result of multiple ionizations via the Compton effect [52]. Radical formation is believed to take place in discrete regions [51], with so-called "clustered" DNA damage necessary in order to produce a potentially lethal cellular effect [53, 54]. However, it has been shown that cancer stem cells (CSCs), which are thought to instigate cancerous growth [55], can be resistant to radiological techniques, as well as promoting cancer recurrence following treatment [56, 57]. Indeed, prostate stem-like cells in epithelial cultures derived from patient samples are more radioresistant than more differentiated cells, due to increased levels of heterochromatin conferring a protective effect [58].

Some studies have suggested that at least 74 Gy, and indeed upwards of 80 Gy [59], should be applied in the case of localized prostate cancer, as patients treated with less than 72 Gy have shown higher cancer recurrence rates [60]. The total dose is usually delivered in multiple smaller fractions of, for example, 2 Gy per day for 60 days, not including weekends [61]. Following treatment, patients may often experience side effects including but not limited to urinary incontinence, diarrhoea, and rectal discomfort. Urinary problems can persist or present at longer time periods following initial treatment, as well as erectile dysfunction [62, 63]. In addition, and most worryingly, a third of patients experience radiorecurrent disease [64].

Different techniques are available, whereby the radiation is either deposited externally or internally. For the external treatment of tumours, the most applied therapy is external beam radiotherapy (EBRT), where the cancerous area is treated by a focused beam of IR. This relies on precise beam alignment with the targeted area, in order to maximize treatment efficacy and minimize collateral damage to surrounding healthy tissue. Several variants of EBRT are being pursued and constantly developed, including three-dimensional conformal radiotherapy (3D-CRT) and intensity-modulated radiation therapy (IMRT), which aim to utilize improvements in imaging technology to satisfy the aforementioned criteria for most effective treatment [65].

Other approaches for the radiological treatment of prostate cancer exist, which rely on the underlying principles of IR, including proton beam therapy. Proton beam therapy has the advantage that protons deliver their energy at the end of the particle's path in the tissue compared to photons which deliver radiation along their path in the tissue [66]. The focal nature of the energy delivery in proton beam therapy could in theory mean that untargeted areas are left unharmed [67]. However, a recent study indicated that damage to irradiated tissues outside of the target area is less severe following IMRT [68], in addition to being of lower cost than proton beam therapy. As such, questions still remain as to the efficacy and effectiveness of proton beam therapy as a focal technique.

Another recent development, which seeks to improve localization of radiotherapy compared to EBRT, is hypofractionated stereotactic body radiation therapy (SBRT) via the Cyberknife linear accelerator machine. A unique feature of prostate cancer is its low "α/β ratio," which represents nonrepairable versus repairable cellular damage,respectively, with the α-term linearly dependent on administered dose and the β-term to its square [69]. For this reason several studies have suggested that hypofractionated radiation doses may result in more effective treatment of localized tumours [69–72]. During Cyberknife SBRT movement of the prostate is detected and automatically corrected for during the procedure by the robotic arm [73], enabling delivery of the radiation to be directed within 2 mm of the target area [74]. This enables the Cyberknife to deliver a hypofractionated radiation dose more accurately and noninvasively to the tumour [73] than conventional EBRT. Another major advantage of SBRT over EBRT is that treatments are usually delivered over a few days rather than weeks, rendering posttreatment hospitalization unnecessary [73]. However, SBRT treatment results in similar side-effects to those experienced following conventional radiotherapy. Rectal and urinary complications have been reported, in addition to erectile dysfunction [70], although the levels of these have been proposed as within acceptable limits [75]. In addition, the cost of Cyberknife technology is more expensive than other radiological techniques, at least in terms of initial outlay [72], although this is yet to be thoroughly investigated.

An increasingly common approach for treating prostate cancer internally is brachytherapy, which uses radioisotopes such as ^{125}I, ^{103}Pd, and ^{131}Cs and is typically applied in order to ablate the whole prostate gland [76]. The radioisotopes, with half-lives ranging from ~10–60 days [76] are delivered to the prostate as seeds through a matrix of narrow diameter needles inserted transperineally. Brachytherapy can either be used as a stand-alone treatment, in conjunction with radiotherapy or radical prostatectomy, or as a salvage treatment following EBRT [77].

A more recent development of brachytherapy is known as high dose rate (HDR) brachytherapy with ^{192}Ir [76], which provides a boosted dose of radiation following EBRT [78]. If administered in conjunction with utilizing imaging tools such as MRI or TRUS, radioactive seeds may be delivered to the targeted area more accurately, providing a case for HDR brachytherapy as a focal therapy [79].

2.5. Imaging: An Integral Part of Focal Therapy. All focal therapies for prostate cancer rely on accurate imaging to have maximum effect [79]. Imaging techniques are constantly advancing and are used for initial detection, determination of tumour location, staging of tumour, assessment of tumour aggressiveness, and detection of recurrences as well as identifying metastases [80, 81]. In the context of administration of focal therapies, early detection is most critical. Since the widespread uptake of the PSA test, early detection has become more common [79].

The kinds of imaging used in prostate cancer detection, diagnosis, and treatment are TRUS to enable targeted biopsies; MRI for accurate imaging of soft tissue; positron emission tomography (PET) for detecting lymph node metastasis and bone scans; and X-rays and computerized tomography (CT) scans to assess bone metastases. To detect localized prostate cancer, TRUS and MRI are by far the most used and most useful scans.

TRUS was traditionally used to allow biopsies from predetermined sites in the prostate, following an abnormal digital rectal examination (DRE) and increased PSA, and not as a method to identify precise locations of tumour foci [82]. However, improvements to the technique, including contrast-enhanced ultrasound using microbubble contrast media, elastography to measure tissue stiffness, and Doppler ultrasound to measure blood flow, can result in more targeted biopsies, leading to improved detection and diagnosis [83, 84]. TRUS can distinguish between an outer and inner gland encompassing the central, peripheral, and transition zones, though not at the same resolution as MRI [82].

MRI is highly sensitive and is the dominant imaging modality used for focal treatment [85, 86]. To undertake standard MRI, endorectal and pelvic phase-arrayed coils are used in conjunction to improve positioning of the prostate and to receive MR signals, respectively, resulting in clearer images with optimal signal-to-noise ratio [79]. The prostate zones are clearly visualized using MRI [87]. However, standard MRI is not accurate enough to determine precise location and diagnosis, where multiparametric MRI is required [88]. This includes diffusion-weighted imaging (DWI-MRI) that measures water diffusivity, dynamic contrast enhanced (DCE-MRI), making use of a contrast agent, and proton magnetic resonance spectroscopic imaging (H MRSI) that measures metabolites (citrate, choline, creatine, and polyamines), the ratios of which change between normal and cancerous prostate [89]. The technology to allow real-time MRI-guided biopsy has also advanced, and it is conceivable that this would be the ultimate method used when administering any focal therapy, including low temperature plasma-based treatment [88, 90–92].

In order for the more sophisticated imaging procedures to become routine, there has to be access to specialized equipment and personnel (e.g., magnetic resonance physicists), which both contribute to the potentially prohibitive expense [93]. To confidently choose focal therapy as a treatment option, patients and clinicians alike have to be convinced of its effectiveness. Imaging technology and both present and future focal therapy procedures therefore need to evolve in tandem to assure focal tumour ablation.

3. Low-Temperature Plasmas and Their Use in Biomedicine

Low temperature plasmas are emerging as an exciting development for therapeutics. The unique properties of cold nonequilibrium plasmas have enormous potential in disease therapeutics and plasma pharmacology as drug alternatives. Applications of these plasmas range from surface sterilization and bacterial decontamination [94–99], biofilm inactivation [100–102], antimicrobial treatment in food preservation

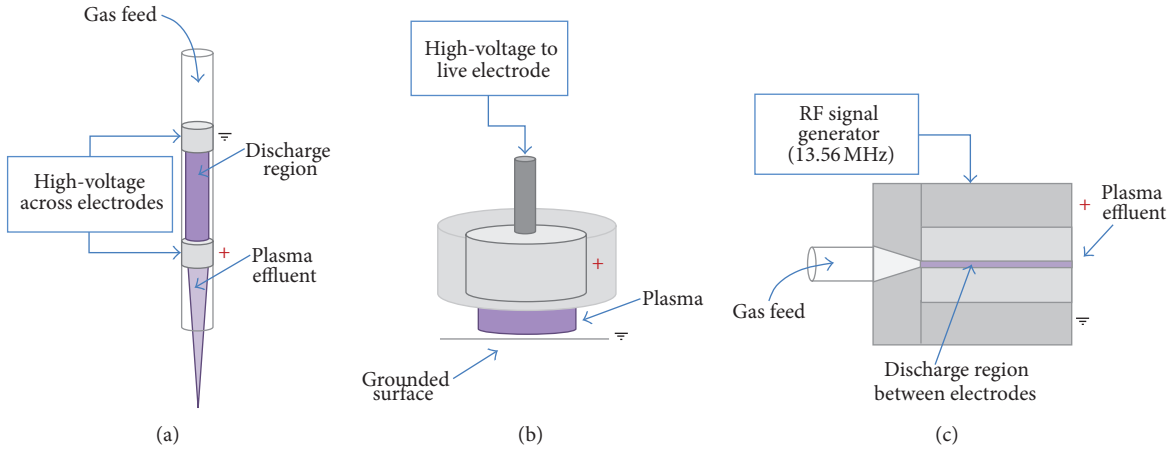

FIGURE 1: Examples of different plasma devices for medical applications. Linear-field plasma jets: (a) dielectric barrier discharge jet configuration (DBD), (b) floating-electrode DBD (FE-DBD), and cross-field plasma jets (c) radiofrequency (RF).

[103–105], and wound healing [106, 107], to cancer treatment [108–111]. This rapidly growing field of "plasma medicine" has emerged over the last 5–10 years and offers great potential, bringing together multidisciplinary branches of science and engineering.

Nonequilibrium plasmas, operated at ambient atmospheric pressure and temperature, are very efficient sources for the production of highly reactive neutral particles, for example, reactive oxygen and nitrogen species (RONS) (such as atomic oxygen [112–114], atomic nitrogen [115], hydroxyl radical, superoxide, singlet delta oxygen, and nitrogen oxides), charged particles, UV-radiation, and electromagnetic fields. Individually, many of these components have been implicated in therapeutics. RONS are known to play a crucial role in biological systems, such as signalling and generating oxidative damage to a variety of cellular components, which can ultimately lead to cell death [116–119]. Graves presents a comprehensive review summary on the role of RONS of relevance for plasma applications in biology [120]. Plasmas have the advantage of delivering these *simultaneously*, providing potentially superior processes. The role of these plasma components, even individually, is to date not fully known and is a topic of current research. It can be anticipated that, similar to low pressure plasma processes, in for example, plasma etching or plasma deposition, synergistic mechanisms govern the plasma surface interface rather than the individual species themselves.

3.1. Methods of Plasma Formation and Production of Reactive Species. The low temperature plasma environment is actually quite remarkable. Plasmas are formed by applying a sufficiently high electric field across a region of gas such that electrons are stripped off atoms and breakdown of the gas occurs. These free electrons in the background gas are accelerated by the applied field and collide with ions and neutral gas molecules through various processes, which are discussed below. An important feature is that the electrons are not in thermodynamic equilibrium with the background gas due to the largely different masses (light electrons, heavy atoms, and molecules). The background gas is the dominating constituent and is at room temperature, while the electrons are hotter and can drive a unique reactive environment. Ions and electrons can be created through ionization, and processes such as excitation and dissociation of the background gas result in, for example, formation of metastable particles, reactive species, radicals, and also radiation. These plasmas essentially create an otherwise impossible dry, chemically reactive environment at room temperature. Until recently, atmospheric pressure plasmas have been unstable and low temperature plasmas have conventionally been operated under lower gas pressure conditions. While this approach has proven extremely beneficial, for example, in the multibillion dollar semiconductor industry, it is limiting with regard to broader exploitation of nonvacuum compatible materials. Through the use of gas flow it is now possible to sustain stable, controllable plasmas at atmospheric pressure. Reactive species can be brought from the main plasma production region, transporting energy to a surface. Here, two distinctly different plasma sources, with varying degrees of reactivity will be discussed.

Various devices are available for the formation and delivery of plasma [120–124] which rely on broadly the same principles. One variant is the dielectric barrier discharge (DBD) configuration plasma jet (Figure 1(a)). Such plasmas are produced by feeding carrier gas (e.g., helium or argon) with small oxygen admixtures (around 0.5% is typical), across a high voltage kHz operated supply, typically 5–30 kV, generating a discharge between two electrodes of dielectric material. Using helium as a buffer gas provides a flexible parameter space for stable homogenous operation at cold gas temperatures. The resulting plasma plume self-propagates outwards, and as the dynamic high electric field is parallel to the direction of propagation, the jet contains reactive neutrals, charged particles, electric fields, and UV radiation (Figure 2). A variation of the DBD schematic is the floating electrode dielectric barrier discharge (FE-DBD) plasma (Figure 1(b)), which operates by using the surface

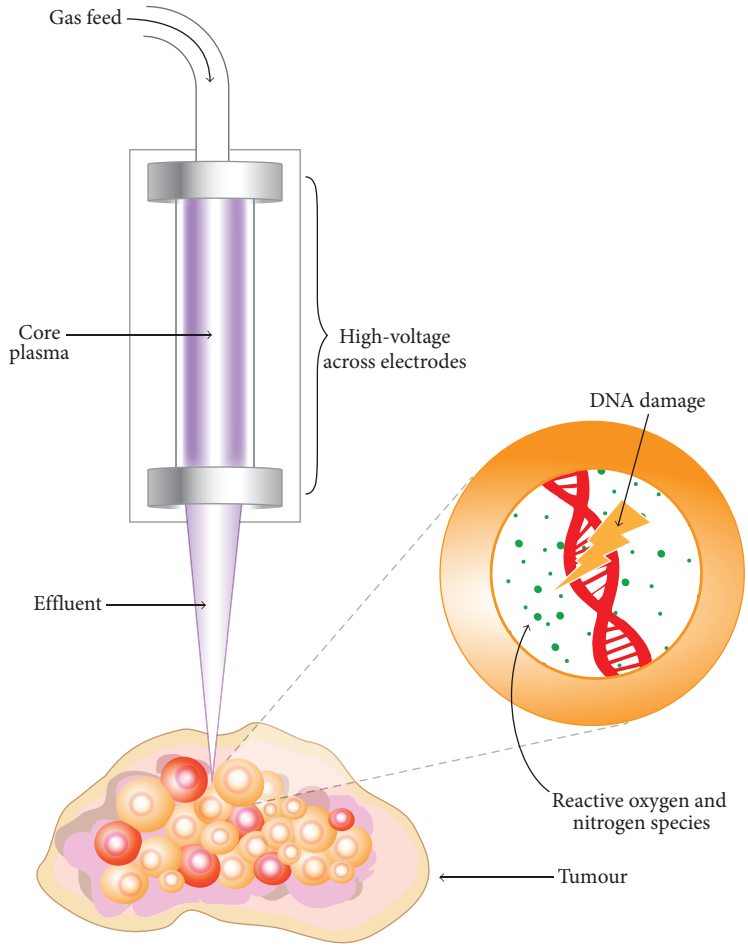

FIGURE 2: Illustrative diagram conveying the interaction of a DBD plasma jet with a cancerous tumour, leading to the induction of intracellular RONS, DNA damage, and resultant effects such as cell cycle arrest, cell death, and decreased viability.

to which it is applied as a floating counter electrode. This is possible provided that the surface has sufficient "charge storage" [94]. FE-DBD has even been applied to human skin without causing thermal damage or unwanted effects [125].

A third example of a plasma source arrangement is the radiofrequency (RF), or cross-field, plasma source (Figure 1(c)) which uses a 13.56 MHz RF signal as a means of gas excitation. This device utilizes plane-parallel electrodes, with a gas flow passing through the core plasma volume. This particular source, unlike the DBD plasma jet, possesses a charge-free effluent since the applied electric field is perpendicular to the direction of gas-travel, thus confining charged species to the core plasma region. Due to the high collision frequency at atmospheric pressure, the effluent is devoid of charge carriers and its characteristics are dominated by energy carrying reactive neutrals. The RF plasma jet is the most comprehensively studied LTP with respect to diagnostics and modelling [112, 115, 126–136] and is currently being developed into a reference source.

The transport of the plasma components to the targeted area is complex. In the core plasma region a large, but defined, number of species can be created (including O, N, NO, and O_2^-). As the plasma crosses the interface with ambient air, new reactions and components are formed. Upon interaction with either humidity or liquid layers on biological samples (Figure 2) new species with varying lifetimes can be created (OH, H, H_2O_2, and $ONOO^-$). Energy dissipation at these interfaces is important and to date unclear. Measurements and simulations under this atmospheric pressure environment are challenging, primarily due to the multiphase (solid, liquid, gas, and plasma), strongly nonequilibrium environment with large gradients (e.g., in electric field), high collisionality thus short-lived species and micron length scales. This requires the development of many new techniques for both measurements and models. The plasma chemistry can be deliberately manipulated or optimized for a desired result by fine alterations to gas admixtures or the electron energy distribution function (EEDF) [129, 137]. Despite the multitude of work that has been conducted to diagnose and characterize the RONS produced [126–128] in addition to the ionization processes and mechanisms that occur in LTPs, these are not yet comprehensively understood.

3.2. Supporting Evidence for LTP as a Therapeutic Medical Device. As already mentioned, the potential of LTPs has been explored in many different medical areas. One highly

active division of research is in the area of bacterial inactivation and surface sterilization. It has been shown that LTPs can damage the membranes of bacterial cells, through the interaction of reactive species, leading to the bactericidal effect [138]. Survival has been shown to be greatly reduced following LTP treatment, with a clearly defined voided region forming on the irradiated surface [139], suggesting that the interaction is mediated by short-lived reactive species [140, 141]. LTPs do not cause thermal or chemical damage to the treated surface, presenting an advantage over conventional sterilization techniques [140, 142]. Furthermore, LTPs have also been shown to be effective in the treatment of biofilms, minimizing bacterial formation posttreatment [101, 143] and greatly reducing cell viability even at short plasma-exposures [144]. These attributes give potential for applications in dentistry [145, 146].

Plasma-based bacterial inactivation has also been applied to the sterilization of chronic wounds in order to improve the rate of healing. This was shown in a recent phase II trial, which reported a significant reduction of bacterial load in the plasma treated area versus control [147, 148]. Crucially, plasma effects were localized, with no side effects (such as pain due to plasma application) reported. Another trial provided further agreement that LTP does not damage the surface of skin nor lead to dryness through exposure, with a view to antimicrobial applications [149]. It has also been found that when LTP was applied to surface wounds on the skin of mice, vastly improved blood coagulation and consequential accelerated healing resulted versus untreated wounds [106]. It was perceived that plasma-produced NO may be responsible for the improved wound response, which is in agreement with other work on NO as the key RONS in cell proliferation and wound healing [150–154]. Another study showed improved clotting of wounds on the surface of pig skin, in addition to establishing safe operating parameters for LTP exposure [107].

Despite LTPs being earmarked as a technology for future healthcare, plasmas have been used for a range of surgical applications in the field of electrosurgery since as long ago as 1991 [155, 156]. Though not technically a LTP, the argon plasma coagulator (APC) has been employed in various surgical disciplines for the purposes of tissue removal and wound cauterization [155] and is perceived as an improvement on existing laser-based techniques [157]. Recently, plasma vaporization has been applied to benign prostate hyperplasia (BPH), with the hope of reducing the common side effects of conventional transurethral resection of the prostate (TURP) procedures [158]. Early results show that the concept of plasma vaporization could prove to be a significant improvement over current TURP techniques [159] for BPH, with reduced complications [160].

In recent years, investigations have been performed into the interaction of LTPs with different types of cancer cells, including melanoma [161–163], ovarian [164], colorectal [165], liver [166], lung [110], breast [167], and brain [168] amongst others. The gold standard for LTP as a cancer therapy has to be the selective cytocidal targeting of cancerous tissue, whilst leaving healthy tissues unaffected. The effect of reactive species produced by plasma treatment has been extensively studied *in vitro*, with plasma induced DNA damage and apoptosis has been investigated [108, 169]. Another investigation showed the same response due to cellular detachment [170]. A considerable reduction in cell viability has been demonstrated using the MTT assay, as a result of high nitric NO and ROS concentrations [109]. It has also been suggested that immediate cell death can be caused by sufficiently high plasma doses, following minimal cell survival after extended plasma exposure [171]. LTP has also been applied *in vivo* to treat mice with tumours derived from glioma cell lines, where a preliminary study showed a reduction in tumour volume of over 50% at six days following initial plasma treatment [172]. Survival rates of plasma-treated mice increased by over half, compared with the control group who received no treatment [172]. In a follow-up study, ROS produced by the plasma were earmarked as the main antitumour agents, with evidence for cell cycle targeting [173] and apoptosis also presented [174–176]. LTP has also been recently applied to ablate tumours in mice subcutaneously injected with neuroblastoma cells, with a reduction in the rate of tumour growth observed versus control. In addition, survival time posttreatment almost doubled [177]. Another means of LTP-cellular interaction is the electric field that is generated at the effluent tip of DBD jet devices. This may lead to the phenomenon of irreversible cellular electroporation, which has been shown to cause tumour regression and cell death in its own right [178–180] and may aid the transport of RONS to the cell nucleus.

Despite LTP-based approaches demonstrating considerable promise in cancer treatment, further focussed work on the exact mechanisms of plasma-cellular interaction is required before such a technique could be used therapeutically. This includes primarily the quantification of which reactive species are causing adverse cellular effects, tailoring the plasma to deliver maximum damage to the cancer, before developing practical apparatus for patient treatment in the operating theatre. This process may be aided by the use of plasma in combination with radiological and chemotherapeutic techniques [181], in order to increase efficacy.

4. Low-Temperature Plasma as a Focal Therapy for Prostate Cancer

At the time of writing, no published study exists on the application of LTP to prostate cancer. The following section outlines how LTPs could be utilized as a focal therapy in practice, how LTPs might compare to other conventional focal therapies for prostate cancer in terms of efficacy, and what might be the upper limit of disease stage for treatment of localized cancer with LTP.

4.1. Methods of Treatment Delivery and Plasma "Dose". Application of LTP to a patient has been successfully applied clinically by treatment of the skin with the FE-DBD system mentioned earlier [125]. Clearly, delivery to the prostate represents a more complex technical challenge. Probably the most efficient means of application would be to follow the approach of PDT and brachytherapy by inserting the

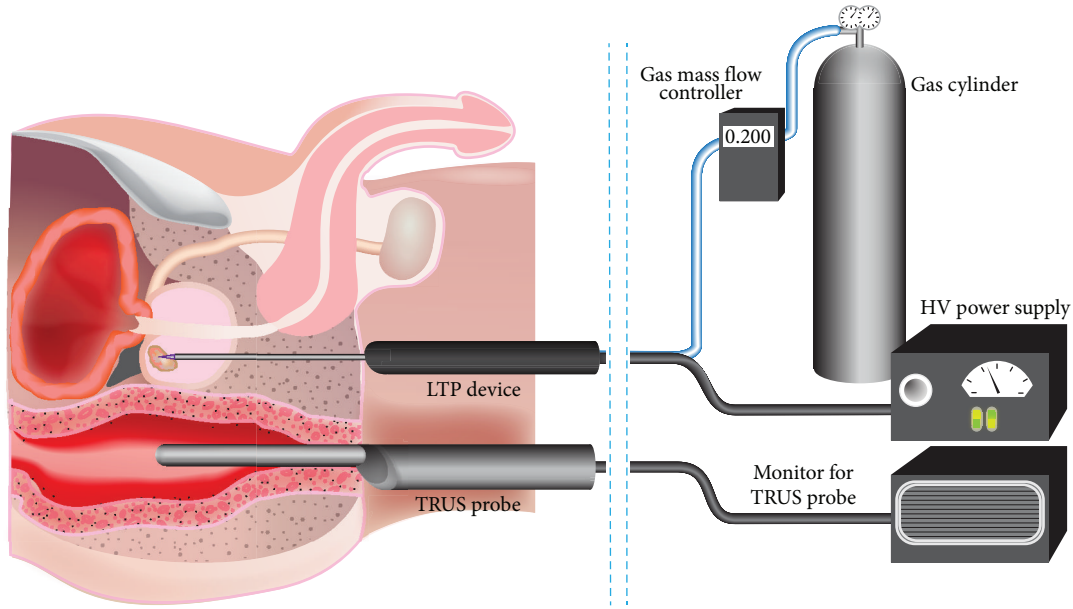

Figure 3: Proposed treatment approach for LTP treatment of localized prostate cancer. The LTP device is administered transperineally to an organ confined prostate cancer. Supporting image guidance from a TRUS probe, along with high-voltage (HV) power supply and gas flow-rate control are shown.

plasma transperineally to provide a focal treatment of organ confined cancers. In reality, whichever way LTP is applied, there is an obvious common dependence on accurate imaging techniques, as discussed in Section 2.5. With simultaneous image guidance by means of TRUS, following prior MRI scan, it is conceivable that LTP could be applied to localized tumours. A representation of one potential treatment delivery system is outlined in Figure 3.

DBD configuration plasma jet devices have already been fabricated and delivered via flexible optical fibres for the treatment of carcinoma, with outer diameters as fine as 60 μm [110].

One of the most important factors for LTP as a cancer therapy is a thorough understanding of the species produced and their concentration for each particular type of device. Correlating the concentration of produced species to a known plasma "dose" is crucial, as lower doses and exposures can stimulate a proliferative response in cells [182, 183]. For LTP therapy to be accepted clinically, there first needs to be agreement on what constitutes the units of plasma "dose." At present, independent research groups use different devices with different operating parameters (such as those outlined in Figure 1, amongst others), with varying exposure times. Such an agreement would lead to directly comparable data across institutions, which may accelerate the route to the clinic, and thus the patient.

4.2. Proposed Efficacy as Compared to Other Therapies. Given that plasma induces ROS, one obvious comparison to current cancer therapies is with radiotherapy, in that both are forms of ionizing radiation that produce reactive species. Besides the lack of a need for radioactive materials, another advantage that LTP possesses over radiotherapy is the production of reactive nitrogen species (RNS) in addition to ROS. As mentioned in Section 3.2, high concentrations of NO have been shown to have a considerable detrimental effect on cell viability, induce apoptosis [184], and have the potential to cause cytostasis in tumour cells [185]. In addition, the production of peroxynitrite ($ONOO^-$) formed as a result of reactions between superoxide (O_2^-) and NO has been shown to cause DNA damage and oxidation of proteins [186, 187]. Some recent diagnostic studies have demonstrated the production of the radical singlet-delta oxygen by LTPs [188–190], which suggests similarities between LTP treatment and PDT. LTP, however, has the advantage of SDO production in addition to a range of other reactive species with cytotoxic effects.

There is some evidence to suggest that LTP may offer a selective kill of cancerous cells [164, 191–193], which offers a potential advantage over conventional radiological techniques, where unwanted damage to surrounding tissues is the main concern. However, this selectivity is yet to be definitively proven. Furthermore, due to the ambient temperature of the plasma, there should be no requirement for the probes employed by cryoablation (which monitor and regulate the temperature of the urethra and bladder), as thermal effects to the neighbouring tissues should not be of concern. This could offer a more simplified treatment procedure, targeting the tumour bed preferentially.

4.3. When to Treat with LTP? In terms of patient selection for treatment with LTP, similar criteria to current focal therapies would be applied [194]. Patients with low risk cancer (Gleason 6) are likely to opt for active surveillance to avoid unnecessary invasive procedures [195]. Patients with metastatic or locally advanced prostate cancer (typically Gleason 8–10) are not generally considered for focal therapy, as stated in Section 2.

Therefore, the final group with intermediate risk prostate cancer would be candidates for LTP therapy. These patients are likely to have a predicted life expectancy of more than five years, with no detection of locally advanced disease using imaging technologies (clinical stage T2a or lower) [43, 196]. Their cancer is likely to be Gleason 7 (although some localized cancer could be Gleason 8) and their PSA should be low (less than 10–20 ng/mL). The other consideration for treatment is whether the tumour is unifocal or multifocal, thereby perhaps necessitating more than one treatment probe. 3D mapping of biopsies should assist in identification of the location, number, and size of tumour foci [197]. Fewer well-defined tumour foci would be logistically easier to treat than multiple foci. Ultimately, such focal therapy treatment is a good option for patients who do not like the uncertainty of watchful waiting but do not want to suffer the side effects of aggressive overtreatment for a low risk cancer.

5. Conclusions

In this review we have analysed some of the currently available focal therapies for localized prostate cancer and where their advantages and limitations lie. We propose that the emerging field of low temperature plasmas may offer an alternative and viable solution to the effective treatment of prostate cancer, with minimal side effects and improved treatment efficacy versus other focal therapies. However, for this promising concept to become a reality, further study must be undertaken in order to fully diagnose the cellular interaction mechanisms of the plasma, and also how surgical administration would occur, a means of which has been suggested here. In addition, there is a need for continued development of imaging diagnostics, upon which a plasma-based approach would rely for precise application.

Conflict of Interests

The authors declare that there is no conflict of interests regarding the publication of this paper.

Authors' Contribution

Norman J. Maitland and Deborah O'Connell contributed equally to this work.

Acknowledgments

This work was part-funded by the Wellcome Trust [ref: 097829/Z/11/A], the UK EPSRC through a Career Acceleration Fellowship (EP/H003797/1) and a Manufacturing Grant (EP/K018388/1). The authors wish to acknowledge funding from Yorkshire Cancer Research (YCR—Y257PA). Finally, the authors would like to thank Phil Roberts for his assistance with the diagrams presented in this paper.

References

[1] A. Jemal, F. Bray, M. M. Center, J. Ferlay, E. Ward, and D. Forman, "Global cancer statistics," *CA Cancer Journal for Clinicians*, vol. 61, no. 2, pp. 69–90, 2011.

[2] J. Li, J. A. Djenaba, A. Soman et al., "Recent trends in prostate cancer incidence by age, cancer stage, and grade, the United States, 2001–2007," *Prostate Cancer*, vol. 2012, Article ID 691380, 8 pages, 2012.

[3] H. Lepor, "Pathophysiology, epidemiology, and natural history of benign prostatic hyperplasia," *Reviews in Urology*, vol. 6, supplement 9, pp. S3–S10, 2004.

[4] J. Ansari, S. A. Hussain, A. Zarkar, J. S. Tanguay, J. Bliss, and J. Glaholm, "Docetaxel chemotherapy for metastatic hormone refractory prostate cancer as first-line palliative chemotherapy and subsequent re-treatment: birmingham experience," *Oncology Reports*, vol. 20, no. 4, pp. 891–896, 2008.

[5] P. Chris and O. Sartor, "Abiraterone and increased survival in metastatic prostate cancer," *The New England Journal of Medicine*, vol. 364, pp. 1995–2005, 2011.

[6] D. L. Berry, C. M. Moinpour, C. S. Jiang et al., "Quality of life and pain in advanced stage prostate cancer: results of a Southwest Oncology Group randomized trial comparing docetaxel and estramustine to mitoxantrone and prednisone," *Journal of Clinical Oncology*, vol. 24, no. 18, pp. 2828–2835, 2006.

[7] G. Bozzini, P. Colin, P. Nevoux et al., "Focal therapy of prostate cancer: energies and procedures," *Urologic Oncology*, vol. 31, no. 2, pp. 155–167, 2013.

[8] L. Mearini and M. Porena, "Transrectal high-intensity focused ultrasound for the treatment of prostate cancer: past, present, and future," *Indian Journal of Urology*, vol. 26, no. 1, pp. 4–11, 2010.

[9] G. Duchesne, "Localised prostate cancer: current treatment options," *Australian Family Physician*, vol. 40, no. 10, pp. 768–771, 2011.

[10] L. Klotz, "Active surveillance versus radical treatment for favorable-risk localized prostate cancer," *Current Treatment Options in Oncology*, vol. 7, no. 5, pp. 355–362, 2006.

[11] M. A. Kollmeier and M. J. Zelefsky, "How to select the optimal therapy for early-stage prostate cancer," *Critical Reviews in Oncology/Hematology*, vol. 83, no. 2, pp. 225–234, 2012.

[12] J. L. Stanford, Z. Feng, A. S. Hamilton et al., "Urinary and sexual function after radical prostatectomy for clinically localized prostate cancer: the prostate cancer outcomes study," *Journal of the American Medical Association*, vol. 283, no. 3, pp. 354–360, 2000.

[13] M. Bul, R. C. van den Bergh, X. Zhu et al., "Outcomes of initially expectantly managed patients with low or intermediate risk screen-detected localized prostate cancer," *BJU International*, vol. 110, no. 11, pp. 1672–1677, 2012.

[14] M. Bul, X. Zhu, R. Valdagni et al., "Active surveillance for low-risk prostate cancer worldwide: the PRIAS study," *European Urology*, vol. 63, no. 4, pp. 597–603, 2013.

[15] U. Lindner, J. Trachtenberg, and N. Lawrentschuk, "Focal therapy in prostate cancer: modalities, findings and future considerations," *Nature Reviews Urology*, vol. 7, no. 10, pp. 562–571, 2010.

[16] V. Kasivisvanathan, M. Emberton, and H. U. Ahmed, "Focal therapy for prostate cancer: rationale and treatment opportunities," *Clinical Oncology*, vol. 25, no. 8, pp. 461–473, 2013.

[17] S. Eggener, G. Salomon, P. T. Scardino, J. De la Rosette, T. J. Polascik, and S. Brewster, "Focal therapy for prostate cancer: possibilities and limitations," *European Urology*, vol. 58, no. 1, pp. 57–64, 2010.

[18] M. Valerio, H. U. Ahmed, M. Emberton et al., "The role of focal therapy in the management of localised prostate cancer: a systematic review," *European Urology*, 2013.

[19] R. Bihrle, R. S. Foster, N. T. Sanghvi, J. P. Donohue, and P. J. Hood, "High intensity focused ultrasound for the treatment of benign prostatic hyperplasia: early United States clinical experience," *Journal of Urology*, vol. 151, no. 5, pp. 1271–1275, 1994.

[20] S. Madersbacher, M. Pedevilla, L. Vingers, M. Susani, and M. Marberger, "Effect of high-intensity focused ultrasound on human prostate cancer in vivo," *Cancer Research*, vol. 55, no. 15, pp. 3346–3351, 1995.

[21] T. Nomura and H. Mimata, "Focal therapy in the management of prostate cancer: an emerging approach for localized prostate cancer," *Advances in Urology*, vol. 2012, Article ID 391437, 8 pages, 2012.

[22] E. R. Cordeiro, X. Cathelineau, S. Thüroff et al., "High-intensity focused ultrasound (HIFU) for definitive treatment of prostate cancer," *BJU International*, vol. 110, no. 9, pp. 1228–1242, 2012.

[23] G. R. Ter Haar, R. L. Clarke, M. G. Vaughan, and C. R. Hill, "Trackless surgery using focused ultrasound: technique and case report," *Minimally Invasive Therapy*, vol. 1, no. 1, pp. 13–19, 1991.

[24] F. Orsi, P. Arnone, W. Chen, and L. Zhang, "High intensity focused ultrasound ablation: a new therapeutic option for solid tumors," *Journal of Cancer Research and Therapeutics*, vol. 6, no. 4, pp. 414–420, 2010.

[25] A. Napoli, M. Anzidei, C. De Nunzio et al., "Real-time magnetic resonance-guided high-intensity focused ultrasound focal therapy for localised prostate cancer: preliminary experience," *European Urology*, vol. 63, no. 2, pp. 395–398, 2013.

[26] S. Madersbacher, C. Kratzik, N. Szabo, M. Susani, L. Vingers, and M. Marberger, "Tissue ablation in benign prostatic hyperplasia with high-intensity focused ultrasound," *European Urology*, vol. 23, no. 1, pp. 39–43, 1993.

[27] J. G. Bomers, J. P. Sedelaar, J. O. Barentsz et al., "MRI-guided interventions for the treatment of prostate cancer," *American Journal of Roentgenology*, vol. 199, no. 4, pp. 714–720, 2012.

[28] A. B. El Fegoun, E. Barret, D. Prapotnich et al., "Focal therapy with high-intensity focused ultrasound for prostate cancer in the elderly. A feasibility study with 10 years follow-up," *International Brazilian Journal of Urology*, vol. 37, no. 2, pp. 213–222, 2011.

[29] C. Chaussy and S. Thüroff, "The status of high-intensity focused ultrasound in the treatment of localized prostate cancer and the impact of a combined resection," *Current Urology Reports*, vol. 4, no. 3, pp. 248–252, 2003.

[30] G. M. Spencer, D. J. Rubens, and D. J. Roach, "Hypoechoic fat: a sonographic pitfall," *American Journal of Roentgenology*, vol. 164, no. 5, pp. 1277–1280, 1995.

[31] M. Sumitomo, J. Asakuma, H. Yoshii et al., "Anterior perirectal fat tissue thickness is a strong predictor of recurrence after high-intensity focused ultrasound for prostate cancer," *International Journal of Urology*, vol. 17, no. 9, pp. 776–782, 2010.

[32] T. Liu, L. Y. Wu, J. K. Choi, and C. E. Berkman, "Targeted photodynamic therapy for prostate cancer: inducing apoptosis via activation of the caspase-8/-3 cascade pathway," *International Journal of Oncology*, vol. 36, no. 4, pp. 777–784, 2010.

[33] S. B. Brown, E. A. Brown, and I. Walker, "The present and future role of photodynamic therapy in cancer treatment," *The Lancet Oncology*, vol. 5, no. 8, pp. 497–508, 2004.

[34] W. M. Sharman, C. M. Allen, and J. E. Van Lier, "Photodynamic therapeutics: basic principles and clinical applications," *Drug Discovery Today*, vol. 4, no. 11, pp. 507–517, 1999.

[35] L.-O. Klotz, K.-D. Kröncke, and H. Sies, "Singlet oxygen-induced signaling effects in mammalian cells," *Photochemical and Photobiological Sciences*, vol. 2, no. 2, pp. 88–94, 2003.

[36] L. J. Schiff, W. C. Eisenberg, J. Dziuba, K. Taylor, and S. J. Moore, "Cytotoxic effects of singlet oxygen," *Environmental Health Perspectives*, vol. 76, pp. 199–203, 1987.

[37] K. Briviba, L.-O. Klotz, and H. Sies, "Toxic and signaling effects of photochemically or chemically generated singlet oxygen in biological systems," *Biological Chemistry*, vol. 378, no. 11, pp. 1259–1265, 1997.

[38] W. M. Sharman, J. E. Van Lier, and C. M. Allen, "Targeted photodynamic therapy via receptor mediated delivery systems," *Advanced Drug Delivery Reviews*, vol. 56, no. 1, pp. 53–76, 2004.

[39] A. J. Bullous, C. M. A. Alonso, and R. W. Boyle, "Photosensitiser-antibody conjugates for photodynamic therapy," *Photochemical and Photobiological Sciences*, vol. 10, no. 5, pp. 721–750, 2011.

[40] N. L. Oleinick, R. L. Morris, and I. Belichenko, "The role of apoptosis in response to photodynamic therapy: what, where, why, and how," *Photochemical and Photobiological Sciences*, vol. 1, no. 1, pp. 1–21, 2002.

[41] C. M. Moore, M. Emberton, and S. G. Bown, "Photodynamic therapy for prostate cancer—an emerging approach for organ-confined disease," *Lasers in Surgery and Medicine*, vol. 43, no. 7, pp. 768–775, 2011.

[42] N. Arumainayagam, C. M. Moore, H. U. Ahmed, and M. Emberton, "Photodynamic therapy for focal ablation of the prostate," *World Journal of Urology*, vol. 28, no. 5, pp. 571–576, 2010.

[43] H. Lepor, "Vascular targeted photodynamic therapy for localized prostate cancer," *Reviews in Urology*, vol. 10, no. 4, pp. 254–261, 2008.

[44] A. Zisman, A. J. Pantuck, J. K. Cohen, and A. S. Belldegrun, "Prostate cryoablation using direct transperineal placement of ultrathin probes through a 17-gauge brachytherapy template—technique and preliminary results," *Urology*, vol. 58, no. 6, pp. 988–993, 2001.

[45] A. De La Taille, M. C. Benson, E. Bagiella et al., "Cryoablation for clinically localized prostate cancer using an argon-based system: complication rates and biochemical recurrence," *BJU International*, vol. 85, no. 3, pp. 281–286, 2000.

[46] J. K. Cohen and R. J. Miller, "Thermal protection of urethra during cryosurgery of prostate," *Cryobiology*, vol. 31, no. 3, pp. 313–316, 1994.

[47] P. Derakhshani, S. Neubauer, M. Braun, J. Zumbe, A. Heidenreich, and U. Engelmann, "Cryoablation of localized prostate cancer. Experience in 48 cases, PSA and biopsy results," *European Urology*, vol. 34, no. 3, pp. 181–187, 1998.

[48] J. L. Chin, D. Lim, and M. Abdelhady, "Review of primary and salvage cryoablation for prostate cancer," *Cancer Control*, vol. 14, no. 3, pp. 231–237, 2007.

[49] J. I. Izawa, K. Ajam, E. McGuire et al., "Major surgery to manage definitively severe complications of salvage cryotherapy for prostate cancer," *Journal of Urology*, vol. 164, no. 6, pp. 1978–1981, 2000.

[50] A. Gangi, G. Tsoumakidou, O. Abdelli et al., "Percutaneous MR-guided cryoablation of prostate cancer: initial experience," *European Radiology*, vol. 22, no. 8, pp. 1829–1835, 2012.

[51] D. A. Palacios, M. Miyake, and C. J. Rosser, "Radiosensitization in prostate cancer: mechanisms and targets," *BMC Urology*, vol. 13, no. 1, article 4, 2013.

[52] H. E. Johns, "The physicist in cancer treatment and detection," *International Journal of Radiation Oncology Biology Physics*, vol. 7, no. 6, pp. 801–808, 1981.

[53] I. R. Radford, "Evidence for a general relationship between the induced level of DNA double-strand breakage and cell-killing after X-irradiation of mammalian cells," *International Journal of Radiation Biology*, vol. 49, no. 4, pp. 611–620, 1986.

[54] J. F. Ward, "Biochemistry of DNA lesions," *Radiation Research. Supplement*, vol. 8, pp. S103–S111, 1985.

[55] Y. M. Cho, Y. S. Kim, M. J. Kang, W. L. Farrar, and E. M. Hurt, "Long-term recovery of irradiated prostate cancer increases cancer stem cells," *Prostate*, vol. 72, no. 16, pp. 1746–1756, 2012.

[56] K. Ogawa, Y. Yoshioka, F. Isohashi et al., "Radiotherapy targeting cancer stem cells: current views and future perspectives," *Anticancer Research*, vol. 33, no. 3, pp. 747–754, 2013.

[57] C. Chargari, C. Moncharmont, A. Lévy et al., "Cancer stem cells, cornerstone of radioresistance and perspectives for radiosensitization: glioblastoma as an example," *Bulletin du Cancerr*, vol. 99, no. 12, pp. 1153–1160, 2012.

[58] F. M. Frame, D. Pellacani, A. T. Collins et al., "HDAC inhibitor confers radiosensitivity to prostate stem-like cells," *British Journal of Cancer*, vol. 109, pp. 3023–3033, 2013.

[59] S. Hummel, E. Simpson, P. Hemingway, M. D. Stevenson, and A. Rees, "Intensity-modulated radiotherapy for the treatment of prostate cancer: a systematic review and economic evaluation," *Health Technology Assessment*, vol. 14, no. 47, pp. 1–108, 2010.

[60] P. Kupelian, D. Kuban, H. Thames et al., "Improved biochemical relapse-free survival with increased external radiation doses in patients with localized prostate cancer: the combined experience of nine institutions in patients treated in 1994 and 1995," *International Journal of Radiation Oncology Biology Physics*, vol. 61, no. 2, pp. 415–419, 2005.

[61] Y. Trada, A. Plank, and J. Martin, "Defining a dose-response relationship for prostate external beam radiotherapy," *Journal of Medical Imaging and Radiation Oncology*, vol. 57, no. 2, pp. 237–246, 2013.

[62] M. J. Chen, E. Weltman, R. M. Hanriot et al., "Intensity modulated radiotherapy for localized prostate cancer: rigid compliance to dose-volume constraints as a warranty of acceptable toxicity?" *Radiation Oncology*, vol. 2, no. 1, article 6, 2007.

[63] I. M. Lips, H. Dehnad, C. H. van Gils, A. E. Boeken Kruger, U. A. van der Heide, and M. van Vulpen, "High-dose intensity-modulated radiotherapy for prostate cancer using daily fiducial marker-based position verification: acute and late toxicity in 331 patients," *Radiation Oncology*, vol. 3, no. 1, article 15, 2008.

[64] J. S. Jones, "Radiorecurrent prostate cancer: an emerging and largely mismanaged epidemic," *European Urology*, vol. 60, no. 3, pp. 411–412, 2011.

[65] B. S. Chera, C. Rodriguez, C. G. Morris et al., "Dosimetric comparison of three different involved nodal irradiation techniques for stage ii hodgkin's lymphoma patients: conventional radiotherapy, intensity-modulated radiotherapy, and three-dimensional proton radiotherapy," *International Journal of Radiation Oncology Biology Physics*, vol. 75, no. 4, pp. 1173–1180, 2009.

[66] J. A. Efstathiou, P. J. Gray, and A. L. Zietman, "Proton beam therapy and localised prostate cancer: current status and controversies," *British Journal of Cancer*, vol. 108, no. 6, pp. 1225–1230, 2013.

[67] P. J. Gray and J. A. Efstathiou, "Proton beam radiation therapy for prostate cancer-is the hype (and the cost) justified?" *Current Urology Reports*, vol. 14, no. 3, pp. 199–208, 2013.

[68] N. C. Sheets, G. H. Goldin, A.-M. Meyer et al., "Intensity-modulated radiation therapy, proton therapy, or conformal radiation therapy and morbidity and disease control in localized prostate cancer," *Journal of the American Medical Association*, vol. 307, no. 15, pp. 1611–1620, 2012.

[69] J. F. Fowler, "The radiobiology of prostate cancer including new aspects of fractionated radiotherapy," *Acta Oncologica*, vol. 44, no. 3, pp. 265–276, 2005.

[70] C. Oliai, R. Lanciano, B. Sprandio et al., "Stereotactic body radiation therapy for the primary treatment of localized prostate cancer," *Journal of Radiation Oncology*, vol. 2, no. 1, pp. 63–70, 2013.

[71] D. J. Brenner and E. J. Hall, "Fractionation and protraction for radiotherapy of prostate carcinoma," *International Journal of Radiation Oncology Biology Physics*, vol. 43, no. 5, pp. 1095–1101, 1999.

[72] T. Seisen, S. J. Drouin, V. Phé et al., "Current role of image-guided robotic radiosurgery (Cyberknife) for prostate cancer treatment," *BJU International*, vol. 111, no. 5, pp. 761–766, 2013.

[73] D. E. Freeman and C. R. King, "Stereotactic body radiotherapy for low-risk prostate cancer: five-year outcomes," *Radiation Oncology*, vol. 6, no. 1, article 3, 2011.

[74] Y. Xie, D. Djajaputra, C. R. King, S. Hossain, L. Ma, and L. Xing, "Intrafractional motion of the prostate during hypofractionated radiotherapy," *International Journal of Radiation Oncology Biology Physics*, vol. 72, no. 1, pp. 236–246, 2008.

[75] N. C. Townsend, B. J. Huth, W. Ding et al., "Acute toxicity after CyberKnife-delivered hypofractionated radiotherapy for treatment of prostate cancer," *American Journal of Clinical Oncology*, vol. 34, no. 1, pp. 6–10, 2011.

[76] D. S. Park, "Current status of brachytherapy for prostate cancer," *Korean Journal of Urology*, vol. 53, no. 11, pp. 743–749, 2012.

[77] P. L. Nguyen, A. V. D'Amico, A. K. Lee, and W. W. Suh, "Patient selection, cancer control, and complications after salvage local therapy for postradiation prostate-specific antigen failure: a systematic review of the literature," *Cancer*, vol. 110, no. 7, pp. 1417–1428, 2007.

[78] M. I. Koukourakis and S. Touloupidis, "External beam radiotherapy for prostate cancer: current position and trends," *Anticancer Research*, vol. 26, no. 1B, pp. 485–494, 2006.

[79] B. Turkbey, P. A. Pinto, and P. L. Choyke, "Imaging techniques for prostate cancer: implications for focal therapy," *Nature Reviews Urology*, vol. 6, no. 4, pp. 191–203, 2009.

[80] A. H. Hou, D. Swanson, and A. B. Barqawi, "Modalities for imaging of prostate cancer," *Advances in Urology*, vol. 2009, Article ID 818065, 12 pages, 2009.

[81] H. Hricak, P. L. Choyke, S. C. Eberhardt, S. A. Leibel, and P. T. Scardino, "Imaging prostate cancer: a multidisciplinary perspective," *Radiology*, vol. 243, no. 1, pp. 28–53, 2007.

[82] A. Abdellaoui, S. Iyengar, and S. Freeman, "Imaging in prostate cancer," *Future Oncology*, vol. 7, no. 5, pp. 679–691, 2011.

[83] E. J. Halpern, "Contrast-enhanced ultrasound imaging of prostate cancer," *Reviews in Urology*, vol. 8, supplement 1, pp. S29–S37, 2006.

[84] M. Mitterberger, W. Horninger, F. Aigner et al., "Ultrasound of the prostate," *Cancer Imaging*, vol. 10, pp. 40–48, 2010.

[85] J. G. Bomers, D. Yakar, C. G. Overduin et al., "MR imaging-guided focal cryoablation in patients with recurrent prostate cancer," *Radiology*, vol. 268, no. 2, pp. 451–460, 2013.

[86] A. Oto, I. Sethi, G. Karczmar et al., "MR imaging-guided focal laser ablation for prostate cancer: phase I trial," *Radiology*, vol. 267, no. 3, pp. 932–940, 2013.

[87] M. Seitz, A. Shukla-Dave, A. Bjartell et al., "Functional magnetic resonance imaging in prostate cancer," *European Urology*, vol. 55, no. 4, pp. 801–814, 2009.

[88] F. Cornud, N. B. Delongchamps, P. Mozer et al., "Value of multiparametric MRI in the work-up of prostate cancer," *Current Urology Reports*, vol. 13, no. 1, pp. 82–92, 2012.

[89] A. Shukla-Dave and H. Hricak, "Role of MRI in prostate cancer detection," *NMR in Biomedicine*, vol. 27, no. 1, pp. 16–24, 2014.

[90] D. G. Engehausen, K. Engelhard, S. A. Schwab et al., "Magnetic resonance image-guided biopsies with a high detection rate of prostate cancer," *The Scientific World Journal*, vol. 2012, Article ID 975971, 6 pages, 2012.

[91] G. Fiard, N. Hohn, J. L. Descotes et al., "Targeted MRI-guided prostate biopsies for the detection of prostate cancer: initial clinical experience with real-time 3-dimensional transrectal ultrasound guidance and magnetic resonance/transrectal ultrasound image fusion," *Urology*, vol. 81, no. 6, pp. 1372–1378, 2013.

[92] A. Krieger, S.-E. Song, N. Bongjoon Cho et al., "Development and evaluation of an actuated MRI-compatible robotic system for MRI-guided prostate intervention," *IEEE/ASME Transactions on Mechatronics*, vol. 18, no. 1, pp. 273–284, 2013.

[93] F. Pinto, A. Totaro, A. Calarco et al., "Imaging in prostate cancer diagnosis: present role and future perspectives," *Urologia Internationalis*, vol. 86, no. 4, pp. 373–382, 2011.

[94] G. Fridman, M. Peddinghaus, H. Ayan et al., "Blood coagulation and living tissue sterilization by floating-electrode dielectric barrier discharge in air," *Plasma Chemistry and Plasma Processing*, vol. 26, no. 4, pp. 425–442, 2006.

[95] G. Daeschlein, S. Scholz, R. Ahmed et al., "Skin decontamination by low-temperature atmospheric pressure plasma jet and dielectric barrier discharge plasma," *Journal of Hospital Infection*, vol. 81, no. 3, pp. 177–183, 2012.

[96] M. G. Kong, "A complementary sterilisation strategy using cold atmospheric plasmas," *Medical Device Technology*, vol. 17, no. 3, pp. 26–28, 2006.

[97] M. G. Kong, "Cold atmospheric plasma destruction of solid proteins on stainless-steel surface and on real surgical instruments," *GMS Krankenhaushygiene Interdisziplinär*, vol. 3, no. 1, Article ID Doc07, 2008.

[98] K. Y. Baik, Y. H. Kim, Y. Hyo et al., "Feeding-gas effects of plasma jets on escherichia coli in physiological solutions," *Plasma Processes and Polymers*, vol. 10, no. 3, pp. 235–242, 2013.

[99] M. Laroussi, C. Tendero, X. Lu, S. Alla, and W. L. Hynes, "Inactivation of bacteria by the plasma pencil," *Plasma Processes and Polymers*, vol. 3, no. 6-7, pp. 470–473, 2006.

[100] K. Fricke, I. Koban, H. Tresp et al., "Atmospheric pressure plasma: a high-performance tool for the efficient removal of biofilms," *PLoS ONE*, vol. 7, no. 8, Article ID e42539, 2012.

[101] M. Y. Alkawareek, Q. T. Algwari, S. P. Gorman et al., "Application of atmospheric pressure nonthermal plasma for the in vitro eradication of bacterial biofilms," *Fems Immunology and Medical Microbiology*, vol. 65, no. 2, pp. 381–384, 2012.

[102] J. J. Cotter, P. Maguire, F. Soberon, S. Daniels, J. P. O'Gara, and E. Casey, "Disinfection of meticillin-resistant Staphylococcus aureus and Staphylococcus epidermidis biofilms using a remote non-thermal gas plasma," *Journal of Hospital Infection*, vol. 78, no. 3, pp. 204–207, 2011.

[103] D. Ziuzina, S. Patil, P. J. Cullen et al., "Atmospheric cold plasma inactivation of Escherichia coli in liquid media inside a sealed package," *Journal of Applied Microbiology*, vol. 114, no. 3, pp. 778–787, 2013.

[104] A. Fernandez, E. Noriega, and A. Thompson, "Inactivation of Salmonella enterica serovar Typhimurium on fresh produce by cold atmospheric gas plasma technology," *Food Microbiology*, vol. 33, no. 1, pp. 24–29, 2013.

[105] M. Laroussi, "Nonthermal decontamination of biological media by atmospheric-pressure plasmas: review, analysis, and prospects," *IEEE Transactions on Plasma Science*, vol. 30, no. 4, pp. 1409–1415, 2002.

[106] E. Garcia-Alcantara, R. López-Callejas, P. R. Morales-Ramírez et al., "In vivo accelerated acute wound healing in mouse skin using combined treatment of argon and helium plasma needle," *Archives of Medical Research*, vol. 44, no. 3, pp. 169–177, 2013.

[107] A. S. Wu, S. Kalghatgi, D. Dobrynin et al., "Porcine intact and wounded skin responses to atmospheric nonthermal plasma," *Journal of Surgical Research*, vol. 179, no. 1, pp. e1–e12, 2013.

[108] R. Sensenig, S. Kalghatgi, E. Cerchar et al., "Non-thermal plasma induces apoptosis in melanoma cells via production of intracellular reactive oxygen species," *Annals of Biomedical Engineering*, vol. 39, no. 2, pp. 674–687, 2011.

[109] X. Yan, Z. Xiong, F. Zou et al., "Plasma-induced death of HepG2 cancer cells: intracellular effects of reactive species," *Plasma Processes and Polymers*, vol. 9, no. 1, pp. 59–66, 2012.

[110] J. Y. Kim, J. Ballato, P. Foy et al., "Apoptosis of lung carcinoma cells induced by a flexible optical fiber-based cold microplasma," *Biosensors and Bioelectronics*, vol. 28, no. 1, pp. 333–338, 2011.

[111] N. K. Kaushik, Y. H. Kim, Y. G. Han et al., "Effect of jet plasma on T98G human brain cancer cells," *Current Applied Physics*, vol. 13, no. 1, pp. 176–180, 2013.

[112] J. Waskoenig, K. Niemi, N. Knake et al., "Atomic oxygen formation in a radio-frequency driven micro-atmospheric pressure plasma jet," *Plasma Sources Science and Technology*, vol. 19, no. 4, Article ID 045018, 2010.

[113] N. Knake, K. Niemi, S. Reuter, V. Schulz-von der Gathen, and J. Winter, "Absolute atomic oxygen density profiles in the discharge core of a microscale atmospheric pressure plasma jet," *Applied Physics Letters*, vol. 93, no. 13, Article ID 131503, 2008.

[114] N. Knake and V. Schulz-von der Gathen, "Investigations of the spatio-temporal build-up of atomic oxygen inside the microscaled atmospheric pressure plasma jet," *European Physical Journal D*, vol. 60, no. 3, pp. 645–652, 2010.

[115] D. Maletic, N. Puac, S. Lazović et al., "Detection of atomic oxygen and nitrogen created in a radio-frequency-driven microscale atmospheric pressure plasma jet using mass spectrometry," *Plasma Physics and Controlled Fusion*, vol. 54, no. 12, 2012.

[116] L. Packer and H. Sies, Eds., *Methods in Enzymology, Singlet Oxygen, UV-A and Ozone*, vol. 319, Academic Press, New York, NY, USA, 2000.

[117] H. Wiseman and B. Halliwell, "Damage to DNA by reactive oxygen and nitrogen species: role in inflammatory disease and progression to cancer," *Biochemical Journal*, vol. 313, no. 1, pp. 17–29, 1996.

[118] H. Sies, "Oxidative stress: oxidants and antioxidants," *Experimental Physiology*, vol. 82, no. 2, pp. 291–295, 1997.

[119] U. Bandyopadhyay, D. Das, and R. K. Banerjee, "Reactive oxygen species: oxidative damage and pathogenesis," *Current Science*, vol. 77, no. 5, pp. 658–666, 1999.

[120] D. B. Graves, "The emerging role of reactive oxygen and nitrogen species in redox biology and some implications for plasma applications to medicine and biology," *Journal of Physics D*, vol. 45, no. 26, 2012.

[121] M. Laroussi, *Plasma Medicine: Applications of Low-Temperature Gas Plasmas in Medicine and Biology*, Cambridge University Press, Cambridge, UK, 2012.

[122] J. Jaroslav, Q. T. Algwari, D. O'Connell et al., "Experimental-modeling study of an atmospheric-pressure helium discharge propagating in a thin dielectric tube," *Ieee Transactions on Plasma Science*, vol. 40, no. 11, pp. 2912–2919, 2012.

[123] Q. T. Algwari and D. O'Connell, "Electron dynamics and plasma jet formation in a helium atmospheric pressure dielectric barrier discharge jet," *Applied Physics Letters*, vol. 99, no. 12, Article ID 121501, 2011.

[124] J. L. Walsh and M. G. Kong, "Contrasting characteristics of linear-field and cross-field atmospheric plasma jets," *Applied Physics Letters*, vol. 93, no. 11, Article ID 111501, 2008.

[125] D. U. Silverthorn and B. R. Johnson, *HumAn Physiology: An Integrated Approach*, Pearson Education, San Francisco, Calif, USA, 3rd edition, 2004, contributions by Bruce R. Johnson.

[126] T. Murakami, K. Niemi, T. Gans et al., "Chemical kinetics and reactive species in atmospheric pressure helium-oxygen plasmas with humid-air impurities," *Plasma Sources Science & Technology*, vol. 22, no. 1, 2013.

[127] E. Wagenaars, T. Gans, D. O'Connell, and K. Niemi, "Two-photon absorption laser-induced fluorescence measurements of atomic nitrogen in a radio-frequency atmospheric-pressure plasma jet," *Plasma Sources Science & Technology*, vol. 21, no. 4, 2012.

[128] K. Niemi, J. Waskoenig, N. Sadeghi, T. Gans, and D. O'Connell, "The role of helium metastable states in radio-frequency driven helium-oxygen atmospheric pressure plasma jets: measurement and numerical simulation," *Plasma Sources Science and Technology*, vol. 20, no. 5, Article ID 055005, 2011.

[129] C. O'Neill, J. Waskoenig, and T. Gans, "Tailoring electron energy distribution functions through energy confinement in dual radio-frequency driven atmospheric pressure plasmas," *Applied Physics Letters*, vol. 101, no. 15, pp. 154107–154104, 2012.

[130] T. Murakami, K. Niemi, T. Gans, D. O'Connell, and W. G. Graham, "Afterglow chemistry of atmospheric-pressure helium-oxygen plasmas with humid air impurity," *Plasma Sources Science and Technology*, vol. 23, no. 2, Article ID 025005, 2014.

[131] K. Niemi, D. O'Connell, N. de Oliveira et al., "Absolute atomic oxygen and nitrogen densities in radio-frequency driven atmospheric pressure cold plasmas: synchrotron vacuum ultra-violet high-resolution Fourier-transform absorption measurements," *Applied Physics Letters*, vol. 103, no. 3, Article ID 034102, 2013.

[132] J. Waskoenig and T. Gans, "Nonlinear frequency coupling in dual radio-frequency driven atmospheric pressure plasmas," *Applied Physics Letters*, vol. 96, no. 18, Article ID 181501, 2010.

[133] K. Niemi, S. Reuter, L. M. Graham et al., "Diagnostic based modelling of radio-frequency driven atmospheric pressure plasmas," *Journal of Physics D*, vol. 43, no. 12, Article ID 124006, 2010.

[134] K. Niemi, S. Reuter, L. M. Graham, J. Waskoenig, and T. Gans, "Diagnostic based modeling for determining absolute atomic oxygen densities in atmospheric pressure helium-oxygen plasmas," *Applied Physics Letters*, vol. 95, no. 15, Article ID 151504, 2009.

[135] V. Schulz-von der Gathen, L. Schaper, N. Knake et al., "Spatially resolved diagnostics on a microscale atmospheric pressure plasma jet," *Journal of Physics D*, vol. 41, no. 19, Article ID 194004, 2008.

[136] D. Ellerweg, J. Benedikt, A. Von Keudell, N. Knake, and V. Schulz-von der Gathen, "Characterization of the effluent of a He/O_2 microscale atmospheric pressure plasma jet by quantitative molecular beam mass spectrometry," *New Journal of Physics*, vol. 12, Article ID 013021, 2010.

[137] G. E. Morfill, M. G. Kong, and J. L. Zimmermann, "Focus on plasma medicine," *New Journal of Physics*, vol. 11, Article ID 115011, 2009.

[138] M. Laroussi and F. Leipold, "Evaluation of the roles of reactive species, heat, and UV radiation in the inactivation of bacterial cells by air plasmas at atmospheric pressure," *International Journal of Mass Spectrometry*, vol. 233, no. 1–3, pp. 81–86, 2004.

[139] G. Fridman, A. D. Brooks, M. Balasubramanian et al., "Comparison of direct and indirect effects of non-thermal atmospheric-pressure plasma on bacteria," *Plasma Processes and Polymers*, vol. 4, no. 4, pp. 370–375, 2007.

[140] R. E. J. Sladek and E. Stoffels, "Deactivation of Escherichia coli by the plasma needle," *Journal of Physics D*, vol. 38, no. 11, pp. 1716–1721, 2005.

[141] S. Perni, G. Shama, J. L. Hobman et al., "Probing bactericidal mechanisms induced by cold atmospheric plasmas with Escherichia coli mutants," *Applied Physics Letters*, vol. 90, no. 7, Article ID 073902, 2007.

[142] M. Moisan, J. Barbeau, S. Moreau, J. Pelletier, M. Tabrizian, and L. Yahia, "Low-temperature sterilization using gas plasmas: a review of the experiments and an analysis of the inactivation mechanisms," *International Journal of Pharmaceutics*, vol. 226, no. 1-2, pp. 1–21, 2001.

[143] Z. L. Petrović, S. Puač, N. Lazović et al., "Biomedical applications and diagnostics of atmospheric pressure plasma," *Journal of Physics*, vol. 356, no. 1, Article ID 012001, 2012.

[144] M. Y. Alkawareek, Q. Th. Algwari, G. Laverty et al., "Eradication of Pseudomonas aeruginosa biofilms by atmospheric pressure non-thermal plasma," *PLoS ONE*, vol. 7, no. 8, Article ID e44289, 2012.

[145] E. Stoffels, R. E. J. Sladek, and I. E. Kieft, "Gas plasma effects on living cells," *Physica Scripta*, vol. 2004, article 79, 2004.

[146] C. Jiang, M.-T. Chen, A. Gorur et al., "Nanosecond pulsed plasma dental probe," *Plasma Processes and Polymers*, vol. 6, no. 8, pp. 479–483, 2009.

[147] G. Isbary, G. Morfill, H. U. Schmidt et al., "A first prospective randomized controlled trial to decrease bacterial load using cold atmospheric argon plasma on chronic wounds in patients," *British Journal of Dermatology*, vol. 163, no. 1, pp. 78–82, 2010.

[148] G. Isbary, J. Heinlin, T. Shimizu et al., "Successful and safe use of 2 min cold atmospheric argon plasma in chronic wounds: results of a randomized controlled trial," *British Journal of Dermatology*, vol. 167, no. 2, pp. 404–410, 2012.

[149] G. Daeschlein, S. Scholz, R. Ahmed et al., "Cold plasma is well-tolerated and does not disturb skin barrier or reduce skin moisture," *Journal der Deutschen Dermatologischen Gesellschaft*, vol. 10, no. 7, pp. 509–515, 2012.

[150] M. B. Witte and A. Barbul, "Role of nitric oxide in wound repair," *American Journal of Surgery*, vol. 183, no. 4, pp. 406–412, 2002.

[151] A. Soneja, M. Drews, and T. Malinski, "Role of nitric oxide, nitroxidative and oxidative stress in wound healing," *Pharmacological Reports*, vol. 57, pp. 108–119, 2005.

[152] G. Fridman, G. Friedman, A. Gutsol, A. B. Shekhter, V. N. Vasilets, and A. Fridman, "Applied plasma medicine," *Plasma Processes and Polymers*, vol. 5, no. 6, pp. 503–533, 2008.

[153] G. Lloyd, G. Friedman, S. Jafri, G. Schultz, A. Fridman, and K. Harding, "Gas plasma: medical uses and developments in

wound care," *Plasma Processes and Polymers*, vol. 7, no. 3-4, pp. 194–211, 2010.

[154] J. Heinlin, G. Morfill, M. Landthaler et al., "Plasma medicine: possible applications in dermatology," *Journal der Deutschen Dermatologischen Gesellschaft*, vol. 8, no. 12, pp. 968–976, 2010.

[155] K. R. Stalder, D. F. McMillen, and J. Woloszko, "Electrosurgical plasmas," *Journal of Physics D*, vol. 38, no. 11, pp. 1728–1738, 2005.

[156] J. Raiser and M. Zenker, "Argon plasma coagulation for open surgical and endoscopic applications: state of the art," *Journal of Physics D*, vol. 39, no. 16, Article ID 3520, 2006.

[157] J. M. Canard and B. Védrenne, "Clinical application of argon plasma coagulation in gastrointestinal endoscopy: has the time come to replace the laser?" *Endoscopy*, vol. 33, no. 4, pp. 353–357, 2001.

[158] B. Geavlete, R. Multescu, M. Dragutescu, M. Jecu, D. Georgescu, and P. Geavlete, "Transurethral resection (TUR) in saline plasma vaporization of the prostate vs standard TUR of the prostate: "The better choice" in benign prostatic hyperplasia?" *BJU International*, vol. 106, no. 11, pp. 1695–1699, 2010.

[159] L. P. Xie, J. Qin, X. Y. Zheng et al., "Transurethral vapor enucleation and resection of prostate with TURis button electrode," *Zhonghua Yi Xue Za Zhi*, vol. 92, no. 22, pp. 1558–1559, 2012.

[160] S. Y. Zhang, H. Hu, X. P. Zhang et al., "Efficacy and safety of bipolar plasma vaporization of the prostate with, "button-type" electrode compared with transurethral resection of prostate for benign prostatic hyperplasia," *Chinese Medical Journal*, vol. 125, no. 21, pp. 3811–3814, 2012.

[161] G. Fridman, A. Shereshevsky, M. M. Jost et al., "Floating electrode dielectric barrier discharge plasma in air promoting apoptotic behavior in Melanoma skin cancer cell lines," *Plasma Chemistry and Plasma Processing*, vol. 27, no. 2, pp. 163–176, 2007.

[162] G.-C. Kim, H. J. Lee, and C.-H. Shon, "The effects of a micro plasma on melanoma (G361) cancer cells," *Journal of the Korean Physical Society*, vol. 54, no. 2, pp. 628–632, 2009.

[163] S. Arndt, E. Wacker, Y. F. Li et al., "Cold atmospheric plasma, a new strategy to induce senescence in melanoma cells," *Experimental Dermatology*, vol. 22, no. 4, pp. 284–289, 2013.

[164] S. Iseki, K. Nakamura, M. Hayashi et al., "Selective killing of ovarian cancer cells through induction of apoptosis by nonequilibrium atmospheric pressure plasma," *Applied Physics Letters*, vol. 100, no. 11, Article ID 113702, 2012.

[165] C.-H. Kim, S. Kwon, J. H. Bahn et al., "Effects of atmospheric nonthermal plasma on invasion of colorectal cancer cells," *Applied Physics Letters*, vol. 96, no. 24, Article ID 243701, 2010.

[166] X. Zhang, M. Li, R. Zhou, K. Feng, and S. Yang, "Ablation of liver cancer cells in vitro by a plasma needle," *Applied Physics Letters*, vol. 93, no. 2, Article ID 021502, 2008.

[167] M. Wang, B. Holmes, X. Cheng et al., "Cold atmospheric plasma for selectively ablating metastatic breast cancer cells," *PLoS ONE*, vol. 8, no. 9, Article ID e73741, 2013.

[168] N. K. Kaushik, P. Attriemail, N. Kaushikemail et al., "A preliminary study of the effect of DBD plasma and osmolytes on T98G brain cancer and HEK non-malignant cells," *Molecules*, vol. 18, no. 5, pp. 4917–4928, 2013.

[169] D. O'Connell, L. J. Cox, W. B. Hyland et al., "Cold atmospheric pressure plasma jet interactions with plasmid DNA," *Applied Physics Letters*, vol. 98, no. 4, Article ID 043701, 2011.

[170] I. E. Kieft, M. Kurdi, and E. Stoffels, "Reattachment and apoptosis after plasma-needle treatment of cultured cells," *IEEE Transactions on Plasma Science*, vol. 34, no. 4, pp. 1331–1336, 2006.

[171] N. Barekzi and M. Laroussi, "Dose-dependent killing of leukemia cells by low-temperature plasma," *Journal of Physics D*, vol. 45, no. 42, 2012.

[172] M. Vandamme, E. Robert, S. Dozias et al., "Response of human glioma U87 xenografted on mice to non thermal plasma treatment," *Plasma Medicine*, vol. 1, no. 1, pp. 27–43, 2011.

[173] O. Volotskova, T. S. Hawley, M. A. Stepp et al., "Targeting the cancer cell cycle by cold atmospheric plasma," *Scientific Reports*, vol. 2, article 636, 2012.

[174] M. Vandamme, E. Robert, S. Lerondel et al., "ROS implication in a new antitumor strategy based on non-thermal plasma," *International Journal of Cancer*, vol. 130, no. 9, pp. 2185–2194, 2012.

[175] G. J. Kim, W. Kim, K. T. Kim, and J. K. Lee, "DNA damage and mitochondria dysfunction in cell apoptosis induced by nonthermal air plasma," *Applied Physics Letters*, vol. 96, no. 2, Article ID 021502, 2010.

[176] M. Thiyagarajan, X. F. Gonzales, and H. Anderson, "Regulated cellular exposure to non-thermal plasma allows preferentially directed apoptosis in acute monocytic leukemia cells," *Studies in Health Technology and Informatics*, vol. 184, pp. 436–442, 2013.

[177] R. M. Walk, J. A. Snyder, P. Srinivasan et al., "Cold atmospheric plasma for the ablative treatment of neuroblastoma," *Journal of Pediatric Surgery*, vol. 48, no. 1, pp. 67–73, 2013.

[178] J. T. Au, T. P. Kingham, K. Jun et al., "Irreversible electroporation ablation of the liver can be detected with ultrasound B-mode and elastography," *Surgery*, vol. 153, no. 6, pp. 787–793, 2013.

[179] J. Fanta, P. Hora'k, J. Marvan et al., "The NanoKnife and two successful cases of intracavitary irreversible electroporation of main bronchus tumours," *Rozhledy v Chirurgii*, vol. 91, no. 11, pp. 625–630, 2012.

[180] G. Onik, P. Mikus, and B. Rubinsky, "Irreversible electroporation: implications for prostate ablation," *Technology in Cancer Research and Treatment*, vol. 6, no. 4, pp. 295–300, 2007.

[181] L. Brulle, M. Vandamme, D. Riès et al., "Effects of a non thermal plasma treatment alone or in combination with gemcitabine in a MIA PaCa2-luc orthotopic pancreatic carcinoma model," *PLoS ONE*, vol. 7, no. 12, Article ID e52653, 2012.

[182] D. Dobrynin, G. Fridman, G. Friedman, and A. Fridman, "Physical and biological mechanisms of direct plasma interaction with living tissue," *New Journal of Physics*, vol. 11, Article ID 115020, 2009.

[183] S. Kalghatgi, G. Friedman, A. Fridman, and A. M. Clyne, "Endothelial cell proliferation is enhanced by low dose non-thermal plasma through fibroblast growth factor-2 release," *Annals of Biomedical Engineering*, vol. 38, no. 3, pp. 748–757, 2010.

[184] D. Hirst and T. Robson, "Targeting nitric oxide for cancer therapy," *Journal of Pharmacy and Pharmacology*, vol. 59, no. 1, pp. 3–13, 2007.

[185] D. J. Stuehr and C. F. Nathan, "Nitric oxide: a macrophage product responsible for cytostasis and respiratory inhibition in tumor target cells," *Journal of Experimental Medicine*, vol. 169, no. 5, pp. 1543–1555, 1989.

[186] A. Korkmaz, S. Oter, M. Seyrek et al., "Molecular, genetic and epigenetic pathways of peroxynitrite-induced cellular toxicity," *Interdisciplinary Toxicology*, vol. 2, no. 4, pp. 219–228, 2009.

[187] J. Fraszczak, M. Trad, N. Janikashvili et al., "Peroxynitrite-dependent killing of cancer cells and presentation of released

tumor antigens by activated dendritic cells," *Journal of Immunology*, vol. 184, no. 4, pp. 1876–1884, 2010.

[188] J. S. Sousa, K. Niemi, L. J. Cox, Q. T. Algwari, T. Gans, and D. O'Connell, "Cold atmospheric pressure plasma jets as sources of singlet delta oxygen for biomedical applications," *Journal of Applied Physics*, vol. 109, no. 12, Article ID 123302, 2011.

[189] V. Puech, G. Bauville, B. Lacour et al., "Micro-plasmas as efficient generators of singlet delta oxygen—art. no. 700527," *High-Power Laser Ablation Vii, Pts 1-2*, vol. 7005, article 527, 2008.

[190] A. A. Ionin, I. V. Kochetov, A. P. Napartovich, and N. N. Yuryshev, "Physics and engineering of singlet delta oxygen production in low-temperature plasma," *Journal of Physics D*, vol. 40, no. 2, article R01, pp. R25–R61, 2007.

[191] M. Keidar, R. Walk, A. Shashurin et al., "Cold plasma selectivity and the possibility of a paradigm shift in cancer therapy," *British Journal of Cancer*, vol. 105, no. 9, pp. 1295–1301, 2011.

[192] G. J. Kim, S. R. Park, G. C. Kim, and J. K. Lee, "Targeted cancer treatment using anti-EGFR and -TFR antibody-conjugated gold nanoparticles stimulated by nonthermal air plasma," *Plasma Medicine*, vol. 1, no. 1, pp. 45–54, 2011.

[193] M. Keidar, A. Shashurin, O. Volotskova et al., "Cold atmospheric plasma in cancer therapy," *Physics of Plasmas*, vol. 20, no. 5, Article ID 057101, 8 pages, 2013.

[194] H. U. Ahmed, R. G. Hindley, L. Dickinson et al., "Focal therapy for localised unifocal and multifocal prostate cancer: a prospective development study," *The Lancet Oncology*, vol. 13, no. 6, pp. 622–632, 2012.

[195] L. Klotz, "Active surveillance: patient selection," *Current Opinion in Urology*, vol. 23, no. 3, pp. 239–244, 2013.

[196] B. Tareen, G. Godoy, and S. S. Taneja, "Focal therapy: a new paradigm for the treatment of prostate cancer," *Reviews in Urology*, vol. 11, no. 4, pp. 203–212, 2009.

[197] K. F. Sullivan and E. D. Crawford, "Targeted focal therapy for prostate cancer: a review of the literature," *Therapeutic Advances in Urology*, vol. 1, no. 3, pp. 149–159, 2009.

Hindawi Publishing Corporation
BioMed Research International
Volume 2014, Article ID 827265, 12 pages
http://dx.doi.org/10.1155/2014/827265

Review Article

Advanced Imaging for the Early Diagnosis of Local Recurrence Prostate Cancer after Radical Prostatectomy

Valeria Panebianco,[1] Flavio Barchetti,[1] Daniela Musio,[1] Francesca De Felice,[1] Camilla Proietti,[1] Elena Lucia Indino,[1] Valentina Megna,[1] Orazio Schillaci,[2] Carlo Catalano,[1] and Vincenzo Tombolini[3]

[1] *Department of Radiological Sciences, Oncology and Pathology, Sapienza University of Rome, 00161 Rome, Italy*
[2] *Department of Diagnostic and Molecular Imaging, Interventional Radiology, Nuclear Medicine and Radiation Therapy, University Hospital "Tor Vergata", 00133 Rome, Italy*
[3] *Department of Radiological Sciences, Oncology and Pathology, Spencer-Lorillard Foundation, Sapienza University of Rome, 00161 Rome, Italy*

Correspondence should be addressed to Valeria Panebianco; valeria.panebianco@uniroma1.it

Received 19 December 2013; Accepted 6 February 2014; Published 13 March 2014

Academic Editor: Giovanni Luca Gravina

Currently the diagnosis of local recurrence of prostate cancer (PCa) after radical prostatectomy (RT) is based on the onset of biochemical failure which is defined by two consecutive values of prostate-specific antigen (PSA) higher than 0.2 ng/mL. The aim of this paper was to review the current roles of advanced imaging in the detection of locoregional recurrence. A nonsystematic literature search using the Medline and Cochrane Library databases was performed up to November 2013. Bibliographies of retrieved and review articles were also examined. Only those articles reporting complete data with clinical relevance for the present review were selected. This review article is divided into two major parts: the first one considers the role of PET/CT in the restaging of PCa after RP; the second part is intended to provide the impact of multiparametric-MRI (mp-MRI) in the depiction of locoregional recurrence. Published data indicate an emerging role for mp-MRI in the depiction of locoregional recurrence, while the performance of PET/CT still remains unclear. Moreover Mp-MRI, thanks to functional techniques, allows to distinguish between residual glandular healthy tissue, scar/fibrotic tissue, granulation tissue, and tumour recurrence and it may also be able to assess the aggressiveness of nodule recurrence.

1. Introduction

Currently most of the patients (about 50%) affected by prostate cancer (PCa) are treated with radical prostatectomy (RP) [1]. This is due to good functional results regarding oncological radical criteria that can be achieved thanks to modern surgical techniques. Nevertheless, local relapse after RP is a crucial point due to its high frequency. Generally, PSA is a nonspecific tumor marker but, after RP, the rise of PSA serum levels means that PSA producing tissue remained and it suggests the presence of persistent or recurrent disease in the pelvis or distant metastases. Moreover, a persistently elevated PSA serum level could be also due to residual glandular healthy tissue [2]. Tumor recurrence is usually preceded by the rise of PSA serum values and occurs in 20–50% of patients after RP during a 10-year follow-up, often without clinical or radiological evidence of disease [3]. It is well known that in 16–35% of cases the patients will receive second line treatments within 5 years from the initial therapy [4]. Freedland et al. found that biochemical recurrence precedes clinical relapse of a median of 5 years and that the time between the end of the therapy and the start of the biochemical failure represents a predictive value for cancer specific survival [5].

At present, according to EAU-guidelines, treatment failure after RP is defined by two consecutive values of PSA higher than 0.2 ng/mL [6]. Once biochemical failure has been diagnosed, it is essential to distinguish between local

recurrence and systemic metastases in order to plan the best therapeutic approach. For this reason the clinicians use some parameters that can help to differentiate between local and distant relapse. According to EAU-guidelines there are two specific criteria to theoretically assess the site of tumor recurrence: the rise of PSA over than 0.2 ng/mL within 6–12 months after RP suggests a high risk of local relapse, whereas a PSA increase within a shorter period of time suggests distant metastases. The second criterion used is PSA doubling time (PSAdt) [7]. Several values of PSAdt have been proposed as cut-off to discriminate between local recurrence and systemic metastases. Some authors state that a PSAdt cut-off value lower than 4 months may be more frequently associated with distant metastases, whereas a median PSAdt greater than 12 months predicts local failure [8]. Other papers showed that patients with a PSAdt less than 6 months most probably have systemic metastases, while those with a PSAdt greater than 12 months are more likely to experience local relapse [9].

Other information can be obtained from the pathological examination after RP. The TNM staging system of the International Union Against Cancer recommends to report not only the location but also the extension of extraprostatic invasion because extension is related to the risk of recurrence [10]. For what concerns the surgical margin status, even if there is insufficient evidence to prove a relationship between the extension of positive surgical margins and the risk of relapse [10, 11], surgical margin status is considered an independent risk factor for biochemical failure, particularly for local recurrence.

Treatment of PCa recurrence after RP remains a controversial area and different therapeutic options are available: in the absence of systemic metastases an increase of PSA serum values is supposed to be a locoregional persistent or recurrent disease and salvage radiation treatment could theoretically be the first line treatment. However, if metastatic disease is diagnosed, radiation treatment on the postprostatectomy bed would be unnecessary, with a high risk of morbidity for the patient, and the proper treatment is hormone deprivation therapy [12].

For all the aforementioned reasons there is a strong need for imaging techniques which may be able to recognize small lesions and to identify their nature (persistent or recurrent neoplastic tissue, healthy residual glandular tissue, and granulation tissue or fibrosis). These techniques should be able to detect residual or recurrent disease when the PSA serum level is very low (less than 1 ng/mL) in order to deliver the more relevant therapeutic option as early as possible.

Currently, transrectal ultrasound (TRUS) has neither good sensitivity (Se) nor good specificity (Spe) in detecting early recurrent cancer [13] and TRUS-guided biopsy of the postprostatectomy fossa is not recommended by EAU-guidelines in patients with PSA serum level less than 1 ng/mL. Scattoni et al. showed that TRUS-guided biopsy to detect local relapse after RP has a limited Se (25–54%) when the PSA serum value is less than 1.0 ng/mL [14].

Over the last few years new technological innovations have allowed the development of imaging techniques which link anatomic, functional, and biological information together. Multiparametric Magnetic Resonance Imaging (mp-MRI) and Positron Emission Tomography/Computed Tomography (PET/CT) have proven to be a useful tool in the early diagnosis of PCa recurrence. Both MRI and PET/CT are able to detect subtle changing in cellular metabolism. The spectroscopic imaging shows the relative concentrations of metabolites in the prostatic tissue which are choline, citrate, and creatine. PET/CT is able to highlight cellular metabolism by means of different radiopharmaceuticals: 18F-Fluorodeoxyglucose (18F-FDG), choline (Ch) labeled with 11C or 18F, acetate, and methionine labeled with 11C. The literature shows that Ch is the most useful radiotracer for the detection of PCa cells. The target of metabolic imaging should be to have a good spatial resolution in order to detect very small locoregional recurrences in patients with biochemical relapse and very low values of PSA.

To the best of our knowledge, both PET/CT and mp-MRI have provided promising results in the detection and localization of local PCa recurrence after RP.

2. Hybrid Imaging: PET/CT

PET is a molecular imaging that is able to create images from physiological and metabolic processes. PET uses positron emitters to create quantitative tomographic images. PET images are volumetric set of data that can be displayed as tomographic images in the transaxial, coronal, or sagittal planes. At the same time PET has a limitation: the lack of an anatomical reference frame. For this reason the combination of PET with CT offers optimal fusion of images with an excellent morphological imaging with anatomical resolution.

PET/CT is a molecular imaging hybrid technique that combines, in a single whole body session, metabolic and functional information of oncologic diseases with anatomic information provided by CT component of the exam. Fused PET/CT images can be assessed in multiparametric modality in axial, sagittal, or coronal planes, thanks to dedicated soft wares.

Malignant cells are usually characterized by a higher glucose metabolism compared with benign ones. Increased 18F-FDG uptake is correlated with increased cellular proliferation. For this reason the most used radiotracer is the 18F-FDG, an analogue of glucose.

In the case of PCa, 18F-FDG tracer, however, is of a limited use in the diagnosis, staging, and follow-up because of urinary excretion and low uptake by prostatic parenchyma. The physiological concentration in the bladder implies a difficult evaluation of the prostate bed. It has also been documented that the uptake of the 18F-FDG in the primary tumor of the prostate gland and in bone metastases may be reduced: the diagnostic Se of 18F-FDG PET in detecting skeletal metastases ranges between 18 and 65%, significantly lower than the sensitivity of bone scan. This fact is probably attributable to the slow proliferation of PCa [15, 16]. Sanz et al. reported similar findings in 1999, with 18F-FDG PET unable to reliably detect lymph node metastases [17]. 18F-FDG has

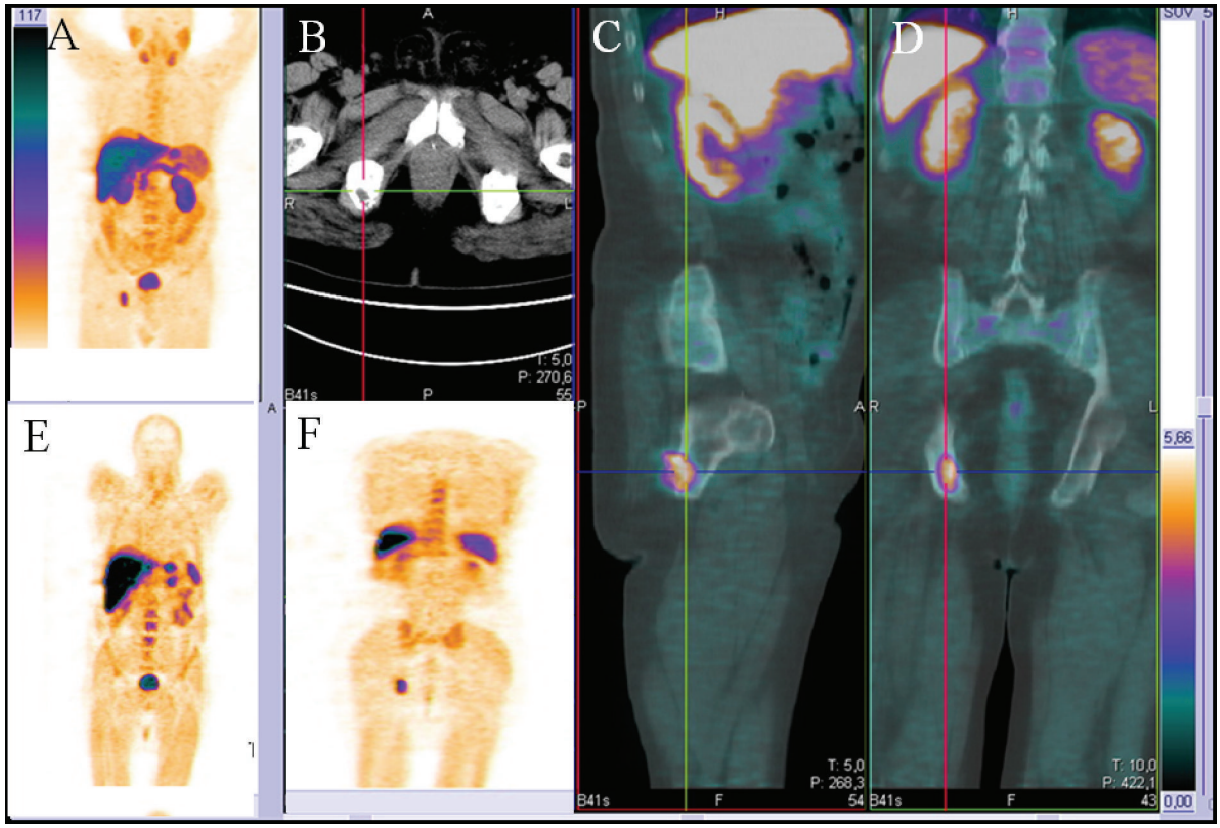

Figure 1: Ch-PET/CT images of a 73-year-old patient with biochemical failure (PSA serum value 2.1 ng/mL) after radical prostatectomy for prostate cancer with a metastatic lesion at the right ischiopubic branch. (A, E, and F) Whole body coronal PET images showing an uptake of the radiotracer at the level of the right ischiopubic branch. No uptake at the lymph node stations and at the level of the postprostatectomy bed was found. (B) Axial morphological CT image of the pelvis displaying a hypodense nodular lesion at the level of the right ischiopubic branch. (C) Sagittal and (E) coronal fused PET-CT images showing the uptake of the radiotracer at the level of the right ischiopubic branch.

been estimated to detect nodal metastases with a Se ranging from 0 to 50% and a Spe ranging from 72 to 90% [18].

Carcinogenesis is characterized by an increase of cell proliferation and, therefore, by means of induction of Ch kinase activity and by an increase of phospholipids in the neoplastic tissue. Hara et al. [19] on the basis of these observations introduced a new radioactive tracer in diagnosing of cancer: the methyl-Ch labeled with carbon-11 (11C-Ch), a substrate for the synthesis of phosphatidylcholine.

This radiotracer has been employed in various tumours, such as cerebral [20], lung [21], and bladder [22] tumors. As demonstrated by numerous studies published in recent years, its main clinical use is, however, the study of PCa, since PCa is a malignant neoplasia but characterized by very low glucose metabolism. The 11C-Ch, in fact, is taken up in the pelvis exclusively by prostatic tissue and this property is retained by the neoplastic tissue. In addition, this radiopharmaceutical has a negligible clearance through the urinary system.

The accuracy of Ch-PET/CT in staging and restaging of PCa has been evaluated by several studies [23, 24].

As regards 18F-FDG, some studies showed that Ch-PET/CT can detect a larger number of metastatic lymph nodes and bony metastatic lesions than 18F-FDG PET/CT in patients with PCa [25]. Furthermore, Picchio et al. found that Ch-PET/CT, compared to 18F-FDG PET/CT, can identify a greater number of local recurrences (42% versus 27%) and showed that Ch-PET is more accurate in identifying both local and distant relapses [26].

There are several papers about the role of Ch-PET in primary PCa detection [27, 28] and its role in staging prostatic disease before treatment [29–32]. However, since the Ch uptake can occur in some benignant conditions, such as prostatitis or prostatic hyperplasia, the role of this technique in this field is still not well clear. Restaging of PCa is, therefore, the main field of Ch-PET/CT imaging. In particular, its main role is in identifying the site of recurrent disease in patients who present with biochemical failure after RP (Figure 1).

The 11C-Ch is characterized by a short half-life (approximately 20.4 minutes), and for this reason its use is allowed only in centers provided with a cyclotron. In consideration of the logistical limitations of the use of 11C-Ch, Ch was subsequently labeled with 18F, which, thanks to the increased half-life (109.8 min), allows storage and transport. However, 18F-Ch radiotracer is characterized by an increased urinary excretion compared to 11C-Ch.

Heinisch et al., in a single-centre retrospective study, analyzed 31 men after RP and found that 8/17 patients (47%) with biochemical failure and with a PSA serum value

less than 5 ng/mL had positive results at 18F-Ch PET-CT examination. Furthermore they found malignancy in 7/8 patients confirmed by either biopsy or by the subsequent course of the disease [33].

Rinnab et al., in a single-centre retrospective study, analyzed 50 men with biochemical relapse after RP for PCa (average PSA serum value: 3.62 ng/mL; range 0.5–13.1 ng/mL); the authors considered the Se and Spe of 11C-Ch PET-CT only in patients with PSA serum level lower than 2.5 ng/mL, reporting 91% and 50%, respectively [34]. In another single-centre retrospective study Rinnab et al. enrolled 41 patients with biochemical recurrence following RP (average PSA value was 2.8 ng/mL; range 0.41–11.6 ng/mL): overall the Se of 11C-Ch PET-CT was 93%, Spe 36%, positive predictive value (PPV) 80%, and negative predictive value (NPV) 67% [35].

Castellucci et al. enrolled 190 men with biochemical failure after RP (mean PSA serum level 4.2 ng/mL; range 0.2–25.4 ng/mL) and found an overall Se of 11C-Ch PET-CT of 73% and Spe of 69% [36]. The same authors, in another single-centre retrospective study, analysed 102 patients with biochemical recurrence after RP (PSA serum level ranging from 0.2–1.5 ng/mL) who underwent 11C-Ch PET-CT scan; all suspected local recurrences at PET-CT exam were confirmed afterwards by TRUS-guided biopsy [37]. Regarding local recurrence the Se of 11C-Ch PET-CT was 53.8% and Spe was 100% (no false positive was recorded). Giovacchini et al. in a single-centre retrospective study analysed 170 patients (presenting with biochemical relapse after RP) with Ch-PET-CT; the average PSA serum value at the time of the exam was 3.24 ng/mL (range 0.23–48.6 ng/mL) and mean PSAdt was 9.37 months [38]. Ch-PET-CT showed a Se of 87%, Spe of 89%, PPV of 87%, NPV of 89%, and accuracy of 88%. In this work, Ch-PET-CT positive findings were confirmed using one of the following methods: histological analysis of lymph node specimen, biopsy of the urethra/bladder neck anastomosis, progression on PET-CT follow-up studies associated with increased PSA serum level, confirmation with conventional imaging, disappearance or sizable reduction of Ch uptake after local or systemic treatment, and PSA decrease greater than 50% after selective irradiation of the unique site of pathological Ch uptake.

In another second single-centre retrospective study, Giovacchini et al. enrolled 358 men with biochemical failure after RP: the average PSA serum value was 3.77 ng/mL (range 0.23–45.2 ng/mL). 11C-Ch PET-CT was performed in all patients and results were validated by histological analysis. The authors concluded that 11C-Ch PET-CT had an overall Se of 85%, Spe 93%, PPV 91%, NPV 87%, and accuracy 89% [39].

In a third single-center retrospective study Giovacchini et al. from a database of 2124 patients retrospectively analysed 109 men with biochemical relapse (average PSA before imaging of 1.31 ng/mL, range 0.22–16.76 ng/mL) who underwent 11C-Ch PET-CT. They reported positive findings at 11C-Ch PET-CT in 12/109 patients, which were confirmed subsequently to be local recurrence in 4 patients and pelvic nodal metastases in 8 cases [40].

A considerable limit of all these studies is the lack of information on the dimensions of local recurrence.

Reske et al. in a single-centre retrospective study, analysed 49 men with average PSA serum level of 2 ng/mL and median maximal diameter of the lesions of 1.7 cm (range 0.9–3.7 cm), who underwent 11C-Ch PET-CT scan. TRUS-guided biopsy was used to validate the results. They found a Se of 73%, Spe 88%, PPV 92%, NPV 61%, and an accuracy of 78% [41].

For the study of PCa the acetate labeled with 11C has also been proposed, which appears promising as it accumulates in the cells proportionally to the biosynthesis of fatty acids (in particular phospholipids), which is increased in neoplastic tissue. 11C-acetate has been proposed by some authors to be more sensitive for the detection of local nodal metastases and has had mixed results when compared with 18F-FDG for the detection of bone metastases [42–44]. Albrecht et al. demonstrated that this radiotracer could detect local recurrence in five of six patients [45]. Vees et al. [46] in a multicentre retrospective study, evaluated 20 patients divided into two different groups with biochemical recurrence or suspected residual tumour after RP with a PSA serum level less than 1.0 ng/mL (range 0.11–0.73 ng/mL): in the first group they used 18F-Ch PET-CT to detect local recurrence whereas in the second group they used 11C-acetate PET-CT. They reported a Se of 60% and 66% for 18F-Ch PET-CT and 11C-acetate PET-CT, respectively, in detecting local relapse. Sandblom and coworkers have also demonstrated the ability of 11C-acetate to detect local recurrence rate with 75% Se and a false-positive rate of 15% [47]. Other PET tracers under study are the 18F-dihydrotestosterone (18F-DHT) that binds to androgen receptors, the 11C-methionine, a marker of protein synthesis, and the 18F-fluoride that accumulates in areas of increased bone turnover are used for the depiction of skeletal metastases and demonstrate improved sensitivity and specificity compared with planar and single-photon emission computed tomography (SPECT) for the detection of osseous metastases [48]. It remains to be seen if this tracer will gain cost effectiveness and widespread use.

Up to now the overall Ch-PET/CT Se in detecting sites of PCa locoregional recurrence ranges between 38% and 98%. Moreover it has been demonstrated that Ch-PET/TC positive detection rate improves with increasing PSA serum values.

The most significant information provided by all the cited studies on this topic is about the apparently very tight relationship between Ch-PET/CT detection rate and PSA serum level in restaging patients with PCa. In the last decade, several authors proposed some cut-off values of PSA serum level to help in identifying those patients who can potentially derive a benefit by a Ch-PET/CT examination. Cimitan et al. proposed that a PSA cut-off value higher than 4 ng/mL is more likely to be associated with a greater chance to detect systemic metastases [49].

It has been found that the higher the value of PSA at the time of the Ch-PET/CT examination is, the greater the detection rate of Ch-PET/CT: 36% for values of PSA less than 1 ng/mL; 43% for PSA values between 1 and 2 ng/mL; and 62% for PSA values between 2 and 3 ng/mL and 73% if the PSA is higher than 3 ng/mL [50].

More recently, several authors proposed lower PSA cut-off values to individuate patients that could benefit from a Ch-PET/CT scan. Rinnab et al. proposed a cut-off value of

1.5 ng/mL but, generally, various authors agree that the exam has better Se when performed in patients with PSA serum level higher or equal to 2 ng/mL [34, 35, 38].

Krause et al. have demonstrated that the Ch-PET-CT examination is a very useful tool, even when the value of PSA is less 1 ng/mL, in differentiating only locally confined disease by metastatic disease, with significant implications for the clinical management of the patient: (1) local therapy is not appropriate if distant locations are proved, (2) the local treatment of second line has greater success in the case of low PSA values, and (3) the choice of therapeutic strategy can be customized in case of abdominal and pelvic lymph nodes involvement (radiation therapy and/or systemic therapy) [50].

More recently, many investigators have focused their attention on the potential role of PSA kinetics such as PSAdt and PSA velocity (PSAvel), which is a PSA derivative determined as linear regression of the PSA values over time [9].

In particular, as reported by the literature data, PSAdt and PSAvel values are correlated with specific mortality risk of PCa [51]. In addition, it has been well demonstrated that the risk of systemic metastases in patients with biochemical relapse after RP depends on PSA serum levels and PSAdt values. Notably, it has been shown that, when PSAdt is longer than 6 months, the risk of metastasis is less than 3%, even if absolute PSA values are more than 30 ng/mL. If PSAdt is shorter than 6 months and PSA is more than 10 ng/mL, the risk of metastasis is about 50% [52].

Partin et al. evaluated the capability of PSAvel in predicting relapse after RP and found that it turns out to be of some help to combine data relative to PSAvel, Gleason score, and pathological staging in differentiating locoregional recurrence from distant metastases [53].

Generally, the Se of Ch-PET/CT is significantly higher in patients with a PSAvel higher than 2 ng/mL/year or a PSAdt lower than 6 months [54]. The proposed PSAvel cut-off of 2 ng/mL/year seems to be the more reliable value to distinguish patients with a positive Ch-PET/CT examination from those with a negative scan in a more accurate way, even if there are some authors who suggest that patients with a PSAvel higher than 1 ng/mL/year could benefit by a Ch-PET/CT scan [55].

Rybalov et al. found a detection rate of 11C-Ch PET/CT lower than 50% in patients with total PSA lower than 2 ng/mL and/or PSAvel lower than 1 ng/mL/year. Marzola et al. in a patient population of 233 men with biochemical recurrence after RP found a detection rate of 18F-Ch PET/CT of 54%, which significantly increases with the increase in trigger PSA [56, 57].

In a recent meta-analysis Treglia et al. reported that the pooled detection rate of radiolabelled Ch-PET/CT in restaging PCa was 58% [95% confidence interval (CI) 55–60] and they found that it increased to 65% (95% CI 58–71) when PSAdt was lower than 6 months and to 71% (95% CI 66–76) and 77% (95% CI 71–82) when PSAvel was greater than 1 or 2 ng/mL/year, respectively [58]. PSAdt lower than 6 months and PSAvel more than 1 or 2 ng/mL/year proved to be relevant factors in predicting the positive result of radiolabelled Ch-PET/CT.

In all cited studies the very good detection rate and the Se of Ch-PET/CT scan are often associated with distant metastases (both bone metastases or lymph nodes) while the available data about the depiction of locoregional recurrence are still discordant. In particular, in the studies where the mean PSA serum level is lower than 1.5 ng/mL, the detection rate of Ch-PET/CT for local relapse is doubtless poor, probably because of low PET spatial resolution (5-6 mm) which limits the detection of small lesions. In a recent study Hausmann et al. assessed the possibility of using time-of-flight (TOF) reconstruction algorithm to obtain an increase of spatial resolution to detect small metastatic lesions and local recurrence. They concluded that TOF seems to be of additional value to detect small metastatic lesions in patients with PCa and biochemical recurrence, which may have further clinical implications for secondary treatment [59].

Another limitation of 11C-Ch PET/CT is represented from any finding of false-positive results due to the presence of accumulation of tracer in some benign prostate disease and in case of reactive lymph nodes (where it accumulates in granulocytes and macrophages).

Most studies state that the routine use of Ch-PET/CT for localization of locoregional recurrence of PCa cannot be recommended for PSA serum values less than 1 ng/mL [60, 61]. However in a more recent study Mamede et al. investigated the role of Ch-PET/CT in patients with biochemical relapse after RP showing PSA values lower than 0.5 ng/mL and found that Ch-PET/CT can be used even if PSA values are very low, preferentially in hormonal resistant patients showing fast PSA kinetics [62].

An early detection of the site of relapse could lead to a personalized and tailored treatment; for example, PET/CT fused images might be useful for delineating local sites of recurrence within the prostatic resection bed allowing a boost to PET positive sites (in addition to conventional local irradiation of the prostatic fossa) [63].

In summary, in agreement with the literature data, Ch-PET/CT could play a role in managing patients with PCa, in particular during the restaging phase, thanks to its good Se with regard to systemic metastases and good detection rate in relationship with PSA serum value higher than 1 ng/mL, PSAdt lower than 6 months, and PSAvel higher than 2 ng/mL/year. To date, its role in detecting locoregional recurrence in postprostatectomy fossa after radical surgical treatment still remains unclear in patients with biochemical failure and low PSA values.

3. Multiparametric MRI

Over the last 20 years substantial progress has been made in MRI clinical employment. High-field strength endorectal coil MRI is able to produce morphological T2-weighted imaging of the prostate gland. Among the other recent complementary functional techniques that improve both staging and detection of PCa there are dynamic contrast-enhanced MRI (DCE-MRI), 1H-spectroscopic imaging (1H-MRSI), and

diffusion-weighted imaging (DWI) [64, 65]. DCE-MRI is a technique that can detect those tumors in which an angiogenic pathway has been turned on, as it is based on Gradient-echo T1-weighted sequences which can assess neoangiogenesis during the passage of a gadolinium contrast agent [66].

DWI provides qualitative and quantitative information about cellularity density of the tissue and cell membrane integrity. Intracellular and extracellular water molecules move freely in all directions. In neoplastic prostatic tissue extracellular space is decreased; therefore the movement of water molecules is restricted and the so-called apparent diffusion coefficient values are low compared to healthy prostatic tissue. DWI can be performed without the administration of exogenous contrast medium and it does not require long acquisition times and therefore it can be considered the functional technique more practical and simple to use. MRSI provides three-dimensional data set of the prostate gland, with volume voxels ranging from 0.24 cm to 0.34 cm [67]. This functional technique evaluates the relative concentration of metabolites within voxels, such as citrate, choline, and creatine. Previous studies demonstrated that citrate levels are reduced in PCa tissue; on the contrary creatine and particularly choline are increased. The peak integral ratio of choline plus creatine to citrate can distinguish PCa tissue from healthy glandular tissue [67]. Conforming to the literature each voxel can be defined as follows: fibrotic or scar tissue when the ratio is less than 0.2, residual healthy prostatic glandular tissue when the ratio is between 0.2 and 0.5, probably recurrent PCa when the ratio is between 0.5 and 1, and definitely recurrent PCa tissue when the ratio is higher than 1 [68]. Compared with DWI or DCE-MRI, MRSI is a more complex functional technique and it also requires longer acquisition times.

The main advantage of Mp-MRI is its very good spatial resolution which allows the localization and characterization of PCa tissue and the detection of very small lesions and it is also able to better differentiate healthy glandular tissue from neoplastic zones. It is a complex exam and it needs therefore experienced and trained radiologists, in particular if MRSI is performed.

Recently, mp-MRI more than other imaging techniques (Figure 2) has been proposed as a useful tool in the diagnostic process of local recurrence of PCa after RP [69].

Once biochemical progression of PSA serum values occurs after RP; it is essential—for treatment planning—to determine whether the relapse is at local or distant sites; moreover the possibility of residual glandular healthy tissue should be taken into account as well. Given this scenario, diagnostic imaging techniques are very useful to distinguish locoregional cancer recurrence from systemic relapse and therefore to refer patients to the best therapeutic approach (i.e., radiation therapy for local recurrence and hormone deprivation therapy for systemic disease) [12]. Moreover, it is very important for radiation oncologists to differentiate a residual glandular healthy tissue from a locoregional neoplastic recurrence because the dose of radiation therapy delivered in the postprostatectomy fossa is quite different [70].

Currently Ch-PET/CT is recommended when PSA serum level is higher than 1 ng/mL because this technique has good Se and Spe in detecting metastatic lymph nodes, distant metastases, and local neoplastic recurrences after RP only in patients with high PSA serum values. In addition, the accuracy of Ch-PET/CT to detect locoregional PCa recurrences relies on the size of the lesion, being usually higher if the lesion is more than 1 cm in diameter [40, 41].

Although Ch-PET/CT is recommended in patients with high PSA serum values, in patients who experience low biochemical alterations after RP (PSA serum value between 0.2 and 1 ng/mL) it is very important to exclude the presence of locoregional recurrence, with this information being essential for radiation oncologists.

Up to now within mp-MRI DCE-MRI is assumed as the most reliable technique in detecting locoregional neoplastic recurrence [68, 71].

Presently there are several studies which demonstrate the usefulness of mp-MRI in depicting locoregional cancer relapse. Mp-MRI after RP is currently indicated to detect small locoregional relapse and also to discriminate between residual glandular healthy tissue, fibrotic tissue, granulation tissue, and nodule recurrence. It may also be able to assess the aggressiveness of nodule recurrence. Panebianco et al. compared ADC values of locoregional recurrences with the histological results [72]. The average and standard deviation of ADC values were $0.5 \pm 0.23\ mm^2/s$ for high-grade aggressiveness relapse, $0.8 \pm 0.09\ mm^2/s$ for intermediate-grade aggressiveness relapse, and $1.1 \pm 1.17\ mm^2/s$ for low-grade aggressiveness recurrence; ADC values higher than $1.3\ mm^2/s$ (mean ADC values 1.4; range 1.3–1.7) were found in patients with a histological finding of residual glandular healthy tissue.

Perianastomotic scar/fibrotic changings appear hypointense on T2-weighted images without enhancement on DCE-MRI. On the other hand both benign and recurrence nodules appear as tissues with intermediate to high signal intensity on T2-weighted morphological images compared to pelvic muscles and show enhancement after intravenous injection of contrast medium. On DCE-MRI images all benign nodules show signal enhancement less than 50% in the early phases, whereas neoplastic recurrence tissues display fast and avid signal enhancement in the early phases followed by a plateau or washout on the signal/intensity curve.

Sella et al. in a single-centre retrospective study analyzed 48 men with biochemical failure after RP with an average lesion size of 1.4 cm (maximum diameter ranging from 0.8 to 4.5 cm) and a mean PSA serum value of 2.18 ng/mL (range 0–10 ng/mL); the Se and Spe of mp-MRI were, respectively, 95% and 100%, but they were reached with a small group of patients and with a very large size of local relapse and a very high PSA serum value [73].

Further studies confirmed the importance of mp-MRI in detecting local PCa recurrence in patients with biochemical relapse after RP.

Cirillo et al. in a patient population of 72 men (local recurrence maximum diameter ranging from 0.8 to 3.5 cm, mean maximum diameter 1.7 cm, average PSA serum value

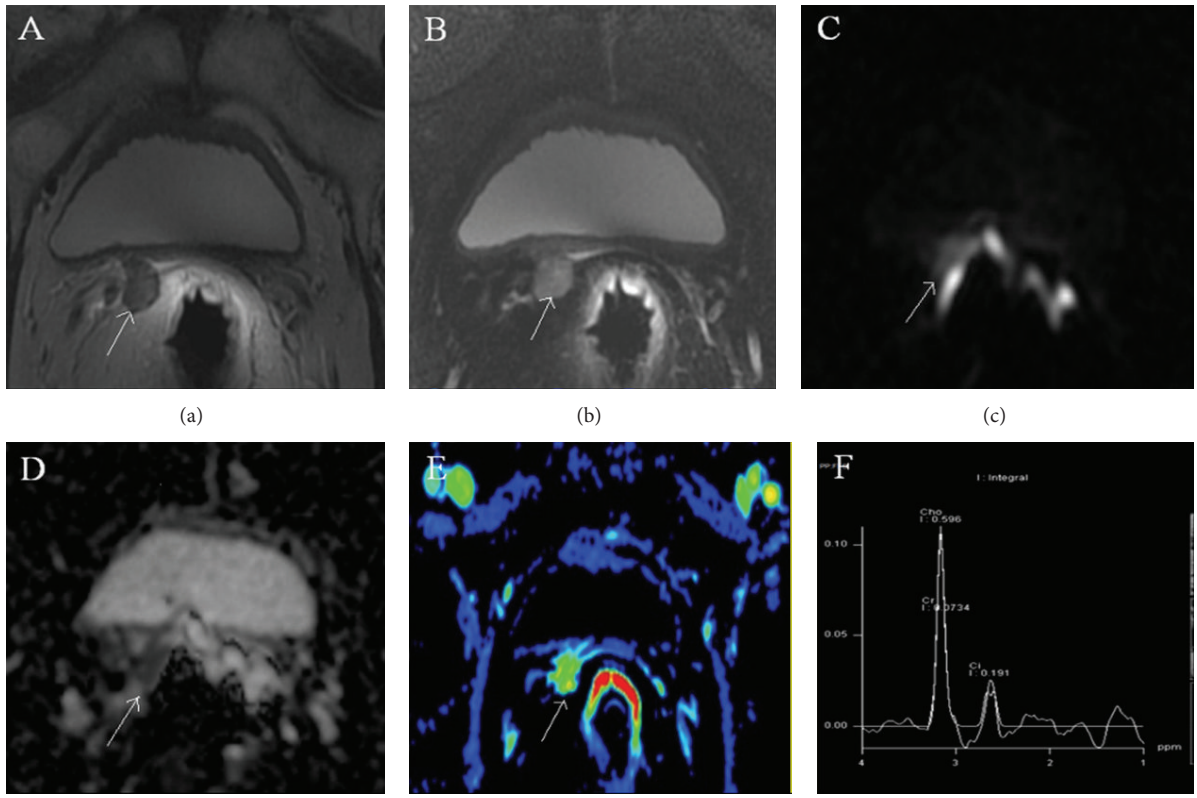

Figure 2: Multiparametric-MR images of a 71-year-old man with prostate-specific antigen progression (PSA serum level 0.47 ng/mL) after radical retropubic prostatectomy, with suspected local recurrence. (a) Axial T2-weighted fast spin-echo and (b) axial T2-weighted fat saturated fast spin-echo images show, on the zone previously occupied by the right seminal vesicle, a slightly hyperintense lobulated tissue (white arrow). (c) Axial native DWI image with *b* value of 1000 s/mm^{2}and (d) ADC map reconstructed from images obtained at *b* values of 0, 500, and 1000 s/mm^2 show a dark area corresponding to the abnormal hyperintense tissue seen on T2-weighted images. (e) Gradient-echo T1-weighted color map image shows a well-defined area of marked enhancement (white arrow) on the same location as the nodular tissue seen on T2-weighted images. (f) 1H-magnetic resonance spectroscopic imaging reveals a high choline peak with a choline-plus-creatine-to-citrate ratio greater than 1. All these findings are consistent with local recurrence.

1.23 ± 1.3 ng/mL, and range 0.2–8.8 ng/mL) compared T2-weighted to DCE-MRI images and they found a sensitivity, specificity, and accuracy of 61.4%, 82.1%, and 69.4% for T2-weighted images and 84.1%, 89.3%, and 86.1% for DCE-MRI images [74].

Casciani et al. in a single-centre retrospective study evaluated the role of mp-MRI with DCE in 46 men who previously underwent RP (average maximum diameter of the local recurrence 1.5 cm, ranging from 0.4 to 4.0 cm, and mean PSA serum value 1.9 ng/mL, ranging from 0.1 to 6.0 ng/mL) and they obtained a Se, Spe, and accuracy of 88%, 100%, and 94%, respectively [71].

Although these studies were based on a sizeable number of patients and the average PSA serum value was not very high, their accuracy is partially limited by the mean size of locoregional relapse which is always higher than 1.5 cm.

Sciarra et al., in a population of 70 patients (average PSA serum value in group A 1.26 ng/mL and in group B 0.8 ng/mL; mean size of the lesions 13.3 mm in group A and 6 mm in group B), compared 1H-MRSI and DCE-MRI and they found a sensitivity of 71–84% and a specificity of 83%–88% for 1H-MRSI alone, a sensitivity of 71–79% and a specificity of 94–100% for DCE-MRI alone, and for the two combined techniques a sensitivity of 86–87% and specificity of 94–100% [68].

In a recent study Panebianco et al., in a population of 84 men (average PSA serum level 1.1 ng/mL in group A and 1.9 ng/mL in group B; mean size of the lesions 6 mm in group B and 13.3 mm in group B), found that a combined technique of 1H-MRSI and DCE-MRI at 3 Tesla magnet is a valid tool to detect locoregional PCa relapse and it is more accurate than Ch-PET/CT in the identification of small lesions in patients with low biochemical progression after RP (PSA serum values ranging from 0.2 to 2 ng/mL) [75].

These last two recent studies were based on a considerable number of patients and detected tumor relapses less than 1.5 cm in maximum diameter, but they did not compare DCE-MRI with DWI technique.

Nowadays there is an increasingly growing interest in the use of DWI because it is an emergent, noninvasive technique that can be acquired without the intravenous injection of contrast medium, and it does not require long acquisition times

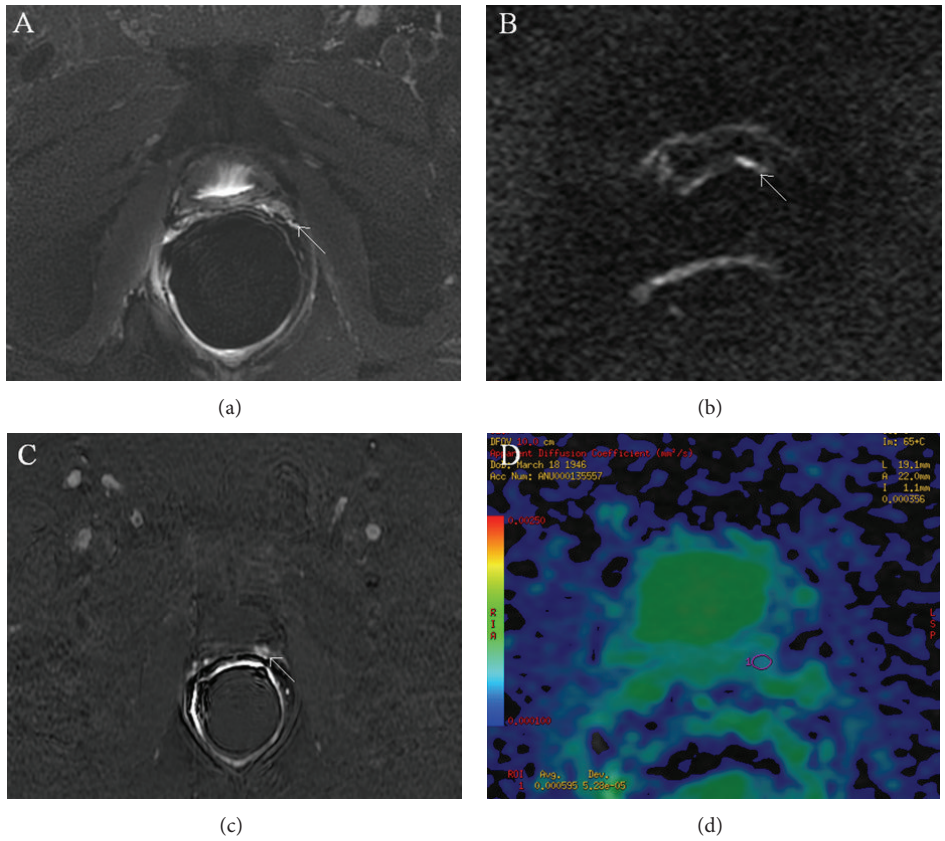

Figure 3: Multiparametric-MR images of a 71-year-old man with prostate-specific antigen progression (PSA serum value 0.6 ng/mL) after radical retropubic prostatectomy, with suspected local recurrence. (a) Axial T2-weighted fat saturated fast spin-echo image shows, on the zone previously occupied by the left seminal vesicle, a hyperintense solid nodular tissue (white arrow) compared to pelvic muscles, of about 7 mm in size. (b) Axial DWI image with a b value of 1000 s/mm^2 shows a focal area of restricted diffusion (white arrow) corresponding to the solid nodular tissue detected on T2-weighted image. (c) Axial Gradient-echo T1-weighted subtracted image showing a remarkable enhancement of the pathological tissue. All these findings are consistent with locoregional relapse. (d) ADC map reconstructed from images obtained at b values of 0, 500, and 1000, where the ROI was plotted for the measurement of ADC values in order to assess the aggressiveness of the nodule.

and therefore it can be considered the functional technique more practical and simple to use [76]. It is a powerful tool in detecting and localizing PCa recurrence in patients with biochemical progression after definitive radiation therapy [77, 78]. In a recent study Giannarini et al. described five patients with biochemical failure after RP and pelvic lymph node dissection in whom locoregional relapse could only be depicted with DWI [79]. Recent studies demonstrate the usefulness of DWI technique as a valid toot in detecting local cancer recurrence after external beam radiation therapy [77] and after RP [78], even though these early experiences were based on a small number of patients.

Panebianco et al. in a single-centre prospective study analyzed a large number of men (262 consecutive male patients) in order to validate the role of 3 Tesla DWI in mp-MRI in the detection of local PCa relapse in patients with biochemical failure after RP [72]. All in all the accuracy of DWI was slightly lower than DCE (92% versus 93% in group A and 89% versus 91% in group B). The authors suggested that the overall accuracy of DCE imaging is superior to that of DWI because DW images are more affected by intrinsic distortion artifacts and background noise than DCE images are, though there are some cases in which DCE is quite doubtful and DWI is needful for PCa local recurrence detection. As an example, sometimes it is very difficult to distinguish between a prominent periprostatic venous plexus and an enhancing recurrent nodule on the basis of DCE alone [80]; therefore when there is this potential pitfall DWI is a very useful technique to exclude the presence of pathological tissue in postprostatectomy fossa (Figure 3). This experience points out to the diagnostic power of DWI which is a functional technique nearly comparable to DCE-MRI, therefore justifying a MRI protocol of postprostatectomy bed composed only of morphological T2-weighted images and DWI images in patients with renal failure. Moreover, these results could pave the way to the possibility of using DWI as an alternative functional technique to DCE-MRI for follow-up of patients with biochemical progression after RP, with a Se, Spe, and accuracy in depicting local relapse almost comparable to those of DCE-MRI. In addition, the possibility of using DWI as an alternative functional technique to DCE is considered thanks to its short acquisition time and repeatability, which

are superior to those of DCE, and also because DWI, given the absence of intravenous administration of contrast medium, is free from complications and danger.

The depicting of local recurrence nodule by means of Mp-MRI is, moreover, of primary importance if external beam salvage radiation therapy is scheduled and feasible. Salvage external beam radiation therapy consists, typically, in the irradiation of the whole postprostatectomy bed with a delivered dose of 64/68 Gy in 2 Gy per daily fraction 5/week [81].

In this setting whenever Mp-MRI examination displays the locoregional relapse, it is possible to deliver to the pathological tissue discovered a radiation boost above 70 Gy with a shrinked field or with simultaneous integrated boost or even with SRT (stereotaxis radiation therapy) approach [82].

This specific treatment, that is a dose adapted MRI based approach treating the prostate bed with a boost to local recurrence, may also potentially improve the therapeutic ratio by selecting patients that are most likely expected to benefit from higher radiation doses. This kind of approach can furthermore improve the control of local disease avoiding further locoregional relapses over time. Moreover, the most recent radiation therapy techniques such as Intensity-Modulated Radiation Therapy with IGRT (image-guided radiation therapy) and Volumetric Modulated Arc Therapy allow both a lower toxicity to normal surrounding tissues (bladder, rectum, anal canal and penile bulb, and head of the femoris) and a more focused irradiation of the recurrence nodule without possibility of geographic miss and give us also the chance of utilization of ipofractionated radiation therapy regimen and dose escalation [83].

The new hybrid PET/MRI scanners, with simultaneous acquisition of mp-MRI and PET images, can provide combined structural, metabolic, and functional imaging information that can potentially be of some important benefit for patient management and outcome [84]. In a recent review by Thorwarth and Leibfarth on the potential role of PET/MRI in radiation therapy, the authors found that Ch-PET/MRI might be of value for target volume delineation of primary and recurrent prostate cancer as well as in the identification of prostate cancer lymph node involvement. The authors concluded that hybrid PET/MRI might improve radiation treatment planning by enabling more precise target volume delineation and also might provide a basis for dose painting [85].

4. Final Considerations

Currently, Ch-PET/CT is the most promising whole body imaging modality in detecting distant metastases of PCa, because of its ability to depict small pathological lymph nodes and bone metastases with a high sensitivity, specificity, and accuracy. This feature is of primary importance on management of patients with PCa and for evaluating their prognosis, thanks to the possibility to assess in a single session both anatomic and metabolic information about the disease.

This role can be heightened by the relevant selection of the patients treated with surgical curative intent by means of biochemical markers such as PSA serum values and PSA kinetics (PSAdt and PSAvel). Furthermore, the concurrent hormonal deprivation therapy has to be taken into account because it could negatively affect the Se of the exam. To date, the role of this diagnostic tool in detecting local recurrence in postprostatectomy bed after RP in patients with biochemical failure and low PSa values still remains unclear. The detection rate of Ch-PET-CT for locoregional relapse seems to be poor, probably because of limited spatial resolution (5-6 mm) of PET scanners which does not allow the depiction of small lesions.

Recently, mp-MRI has been proposed, more than other imaging procedures, as a useful tool in the diagnostic process of local recurrence of PCa after RP. Currently mp-MRI after RP is indicated to diagnose small local cancer recurrence in a range of PSA serum values between 0.2 and 1 ng/mL when Ch-PET/CT is not eligible. Moreover Mp-MRI, thanks to functional techniques, allows distinguishing between residual glandular healthy tissue, scar/fibrotic tissue, granulation tissue, and tumour recurrence and it may also be able to assess the aggressiveness of nodule recurrence. In addition an MRI based radiation therapy approach treating the prostatic fossa with a boost to local recurrence improves the treatment therapeutic ratio and allows a decrease of locoregional relapses.

Further studies are needed to evaluate the ability of Ch-PET/CT in the detection of locoregional PCa recurrence. Moreover, the recent development of hybrid PET/MRI scanners could improve the diagnostic accuracy in depicting local PCa relapses in postprostatectomy fossa.

Conflict of Interests

The authors declare that there is no conflict of interests regarding the publication of this paper.

References

[1] M. R. Cooperberg, J. M. Broering, and P. R. Carroll, "Time trends and local variation in primary treatment of localized prostate cancer," *Journal of Clinical Oncology*, vol. 28, no. 7, pp. 1117–1123, 2010.

[2] A. Bill-Axelson, L. Holmberg, F. Filén et al., "Radical prostatectomy versus watchful waiting in localized prostate cancer: the Scandinavian prostate cancer group-4 randomized trial," *Journal of the National Cancer Institute*, vol. 100, no. 16, pp. 1144–1154, 2008.

[3] M. Han, A. W. Partin, M. Zahurak, S. Piantadosi, J. I. Epstein, and P. C. Walsh, "Biochemical (prostate specific antigen) recurrence probability following radical prostatectomy for clinically localized prostate cancer," *Journal of Urology*, vol. 169, no. 2, pp. 517–523, 2003.

[4] G. D. Grossfeld, D. M. Stier, S. C. Flanders et al., "Use of second treatment following definitive local therapy for prostate cancer: data from the capsure database," *Journal of Urology*, vol. 160, no. 4, pp. 1398–1404, 1998.

[5] S. J. Freedland, E. B. Humphreys, L. A. Mangold, M. Eisenberger, and A. W. Partin, "Time to prostate specific antigen recurrence after radical prostatectomy and risk of prostate

cancer specific mortality," *Journal of Urology*, vol. 176, no. 4, pp. 1404–1408, 2006.

[6] A. Heidenreich, G. Aus, M. Bolla et al., "EAU guidelines on prostate cancer," *European Urology*, vol. 53, no. 1, pp. 68–80, 2008.

[7] R. Svatek, P. I. Karakiewicz, M. Shulman, J. Karam, P. Perrotte, and E. Benaim, "Pre-treatment nomogram for disease-specific survival of patients with chemotherapy-naive androgen independent prostate cancer," *European Urology*, vol. 49, no. 4, pp. 666–674, 2006.

[8] Association of Urology, *Guidelines on Prostate Cancer*, European Association of Urology, Arnhem, The Netherlands, 2012.

[9] S. G. Roberts, M. L. Blute, E. J. Bergstralh, J. M. Slezak, and H. Zincke, "PSA doubling time as a predictor of clinical progression after biochemical failure following radical prostatectomy for prostate cancer," *Mayo Clinic Proceedings*, vol. 76, no. 6, pp. 576–581, 2001.

[10] R. A. Marks, M. O. Koch, A. Lopez-Beltran, R. Montironi, B. E. Juliar, and L. Cheng, "The relationship between the extent of surgical margin positivity and prostate specific antigen recurrence in radical prostatectomy specimens," *Human Pathology*, vol. 38, no. 8, pp. 1207–1211, 2007.

[11] A. J. Stephenson, P. T. Scardino, M. W. Kattan et al., "Predicting the outcome of salvage radiation therapy for recurrent prostate cancer after radical prostatectomy," *Journal of Clinical Oncology*, vol. 25, no. 15, pp. 2035–2041, 2007.

[12] D. Loblaw, D. S. Mendelson, J. A. Talcott et al., "American society of clinical oncology recommendations for the initial hormonal management of androgen sensitive metastatic, recurrent, or progressive prostate cancer," *Journal of Clinical Oncology*, vol. 22, no. 14, pp. 2927–2941, 2004.

[13] A. K. Leventis, S. F. Shariat, and K. M. Slawin, "Local recurrence after radical prostatectomy: correlation of US features with prostatic fossa biopsy findings," *Radiology*, vol. 219, no. 2, pp. 432–439, 2001.

[14] V. Scattoni, F. Montorsi, M. Picchio et al., "Diagnosis of local recurrence after radical prostatectomy," *BJU International*, vol. 93, no. 5, pp. 680–688, 2004.

[15] S. D. Yeh, M. Imbriaco, S. M. Larson et al., "Detection of bony metastases of androgen-independent prostate cancer by PET-FDG," *Nuclear Medicine and Biology*, vol. 23, no. 6, pp. 693–697, 1996.

[16] P. D. Shreve, H. B. Grossman, M. D. Gross, and R. L. Wahl, "Metastatic prostate cancer: initial findings of PET with 2-deoxy-2-[F-18]fluoro-D-glucose," *Radiology*, vol. 199, no. 3, pp. 751–756, 1996.

[17] G. Sanz, J. E. Robles, M. Giménez et al., "Positron emission tomography with 18fluorine-labelled deoxyglucose: utility in localized and advanced prostate cancer," *BJU International*, vol. 84, no. 9, pp. 1028–1031, 1999.

[18] S. Jana and M. D. Blaufox, "Nuclear medicine studies of the prostate, testes, and bladder," *Seminars in Nuclear Medicine*, vol. 36, no. 1, pp. 51–72, 2006.

[19] T. Hara, N. Kosaka, and H. Kishi, "PET imaging of prostate cancer using carbon-11-choline," *Journal of Nuclear Medicine*, vol. 39, no. 6, pp. 990–995, 1998.

[20] T. Hara, N. Kosaka, N. Shinoura, and T. Kondo, "PET imaging of brain tumor with [methyl-11C]choline," *Journal of Nuclear Medicine*, vol. 38, no. 6, pp. 842–847, 1997.

[21] N. Khan, N. Oriuchi, H. Zhang et al., "A comparative study of 11C-choline PET and [18F]fluorodeoxyglucose PET in the evaluation of lung cancer," *Nuclear Medicine Communications*, vol. 24, no. 4, pp. 359–366, 2003.

[22] M. Picchio, U. Treiber, A. J. Beer et al., "Value of 11C-choline PET and contrast-enhanced CT for staging of bladder cancer: correlation with histopathologic findings," *Journal of Nuclear Medicine*, vol. 47, no. 6, pp. 938–944, 2006.

[23] M. Picchio, C. Crivellaro, G. Giovacchini, L. Gianolu, and C. Messa, "PET-CT for treatment planning in prostate cancer," *Quarterly Journal of Nuclear Medicine and Molecular Imaging*, vol. 53, no. 2, pp. 245–268, 2009.

[24] C. Fuccio, D. Rubello, P. Castellucci, M. C. Marzola, and S. Fanti, "Choline PET/CT for prostate cancer: main clinical applications," *European Journal of Radiology*, vol. 80, no. 2, pp. e50–e56, 2011.

[25] J. R. García, M. Soler, M. A. Blanch et al., "PET/CT with11C-choline and18F-FDG in patients with elevated PSA after radical treatment of a prostate cancer," *Revista Espanola de Medicina Nuclear*, vol. 28, no. 3, pp. 95–100, 2009.

[26] M. Picchio, C. Messa, C. Landoni et al., "Value of [11C]choline-positron emission tomography for re-staging prostate cancer: a comparison with [18F]fluorodeoxyglucose-positron emission tomography," *Journal of Urology*, vol. 169, no. 4, pp. 1337–1340, 2003.

[27] B. Scher, M. Seitz, W. Albinger et al., "Value of11C-choline PET and PET/CT in patients with suspected prostate cancer," *European Journal of Nuclear Medicine and Molecular Imaging*, vol. 34, no. 1, pp. 45–53, 2007.

[28] G. Giovacchini, M. Picchio, E. Coradeschi et al., "Choline uptake with PET/CT for the initial diagnosis of prostate cancer: relation to PSA levels, tumour stage and anti-androgenic therapy," *European Journal of Nuclear Medicine and Molecular Imaging*, vol. 35, no. 6, pp. 1065–1073, 2008.

[29] L. Rinnab, N. M. Blumstein, F. M. Mottaghy et al., "11C-choline positron-emission tomography/computed tomography and transrectal ultrasonography for staging localized prostate cancer," *BJU International*, vol. 99, no. 6, pp. 1421–1426, 2007.

[30] R. Schiavina, V. Scattoni, P. Castellucci et al., "11C-Choline positron emission tomography/computerized tomography for preoperative lymph-node staging in intermediate-risk and high-risk prostate cancer: comparison with clinical staging nomograms," *European Urology*, vol. 54, no. 2, pp. 392–401, 2008.

[31] F. Calabria, A. Chiaravalloti, M. Tavolozza, C. Ragano-Caracciolo, and O. Schillaci, "Evaluation of extraprostatic disease in the staging of prostate cancer by F-18 choline PET/CT: can PSA and PSA density help in patient selection?" *Nuclear Medicine Communications*, vol. 34, no. 8, pp. 733–740, 2013.

[32] F. Fazio, M. Picchio, and C. Messa, "Is 11C-choline the most appropriate tracer for prostate cancer?: for," *European Journal of Nuclear Medicine and Molecular Imaging*, vol. 31, no. 5, pp. 753–756, 2004.

[33] M. Heinisch, A. Dirisamer, W. Loidl et al., "Positron emission tomography/computed tomography with F-18-fluorocholine for restaging of prostate cancer patients: meaningful at PSA < 5 ng/ml?" *Molecular Imaging and Biology*, vol. 8, no. 1, pp. 43–48, 2006.

[34] L. Rinnab, F. M. Mottaghy, N. M. Blumstein et al., "Evaluation of [11C]-choline positron-emission/computed tomography in patients with increasing prostate-specific antigen levels after primary treatment for prostate cancer," *BJU International*, vol. 100, no. 4, pp. 786–793, 2007.

[35] L. Rinnab, J. Simon, R. E. Hautmann et al., "[11C]choline PET/CT in prostate cancer patients with biochemical recurrence after radical prostatectomy," *World Journal of Urology*, vol. 27, no. 5, pp. 619–625, 2009.

[36] P. Castellucci, C. Fuccio, C. Nanni et al., "Influence of trigger PSA and PSA kinetics on 11C-choline PET/CT detection rate in patients with biochemical relapse after radical prostatectomy," *Journal of Nuclear Medicine*, vol. 50, no. 9, pp. 1394–1400, 2009.

[37] P. Castellucci, C. Fuccio, D. Rubello et al., "Is there a role for11C-choline PET/CT in the early detection of metastatic disease in surgically treated prostate cancer patients with a mild PSA increase < 1.5 ng/ml?" *European Journal of Nuclear Medicine and Molecular Imaging*, vol. 38, no. 1, pp. 55–63, 2011.

[38] G. Giovacchini, M. Picchio, V. Scattoni et al., "PSA doubling time for prediction of [11C]choline PET/CT findings in prostate cancer patients with biochemical failure after radical prostatectomy," *European Journal of Nuclear Medicine and Molecular Imaging*, vol. 37, no. 6, pp. 1106–1116, 2010.

[39] G. Giovacchini, M. Picchio, A. Briganti et al., "[11C]Choline positron emission tomography/computerized tomography to restage prostate cancer cases with biochemical failure after radical prostatectomy and no disease evidence on conventional imaging," *Journal of Urology*, vol. 184, no. 3, pp. 938–943, 2010.

[40] G. Giovacchini, M. Picchio, E. Coradeschi et al., "Predictive factors of [11C]choline PET/CT in patients with biochemical failure after radical prostatectomy," *European Journal of Nuclear Medicine and Molecular Imaging*, vol. 37, no. 2, pp. 301–309, 2010.

[41] S. N. Reske, N. M. Blumstein, and G. Glatting, "[11C]choline PET/CT imaging in occult local relapse of prostate cancer after radical prostatectomy," *European Journal of Nuclear Medicine and Molecular Imaging*, vol. 35, no. 1, pp. 9–17, 2008.

[42] N. Oyama, T. R. Miller, F. Dehdashti et al., "11C-acetate PET imaging of prostate cancer: detection of recurrent disease at PSA relapse," *Journal of Nuclear Medicine*, vol. 44, no. 4, pp. 549–555, 2003.

[43] E. Fricke, S. Machtens, M. Hofmann et al., "Positron emission tomography with11C-acetate and18F-FDG in prostate cancer patients," *European Journal of Nuclear Medicine and Molecular Imaging*, vol. 30, no. 4, pp. 607–611, 2003.

[44] J. Kotzerke, B. G. Volkmer, B. Neumaier, J. E. Gschwend, R. E. Hautmann, and S. N. Reske, "Carbon-11 acetate positron emission tomography can detect local recurrence of prostate cancer," *European Journal of Nuclear Medicine*, vol. 29, no. 10, pp. 1380–1384, 2002.

[45] S. Albrecht, F. Buchegger, D. Soloviev et al., "11C-acetate PET in the early evaluation of prostate cancer recurrence," *European Journal of Nuclear Medicine and Molecular Imaging*, vol. 34, no. 2, pp. 185–196, 2007.

[46] H. Vees, F. Buchegger, S. Albrecht et al., "18F-choline and/or11C-acetate positron emission tomography: detection of residual or progressive subclinical disease at very low prostate-specific antigen values (< 1 ng/mL) after radical prostatectomy," *BJU International*, vol. 99, no. 6, pp. 1415–1420, 2007.

[47] G. Sandblom, J. Sörensen, N. Lundin, M. Häggman, and P. Malmström, "Positron emission tomography with c11-acetate for tumor detection and localization in patients with prostate-specific antigen relapse after radical prostatectomy," *Urology*, vol. 67, no. 5, pp. 996–1000, 2006.

[48] E. Even-Sapir, U. Metser, E. Mishani, G. Lievshitz, H. Lerman, and I. Leibovitch, "The detection of bone metastases in patients with high-risk prostate cancer: 99 mTc-MDP planar bone scintigraphy, single- and multi-field-of-view SPECT, 18F-fluoride PET, and 18F- Fluoride PET/CT," *Journal of Nuclear Medicine*, vol. 47, no. 2, pp. 287–297, 2006.

[49] M. Cimitan, R. Bortolus, S. Morassut et al., "[18F]fluorocholine PET/CT imaging for the detection of recurrent prostate cancer at PSA relapse: experience in 100 consecutive patients," *European Journal of Nuclear Medicine and Molecular Imaging*, vol. 33, no. 12, pp. 1387–1398, 2006.

[50] B. J. Krause, M. Souvatzoglou, M. Tuncel et al., "The detection rate of [11C]Choline-PET/CT depends on the serum PSA-value in patients with biochemical recurrence of prostate cancer," *European Journal of Nuclear Medicine and Molecular Imaging*, vol. 35, no. 1, pp. 18–23, 2008.

[51] A. Winter, J. Uphoff, R. Henke, and F. Wawroschek, "First results of [C]choline PET/CT-guided secondary lymph node surgery in patients with PSA failure and single lymph node recurrence after radical retropubic prostatectomy," *Urologia Internationalis*, vol. 84, no. 4, pp. 418–423, 2010.

[52] J. Y. Wo, M. Chen, P. L. Nguyen et al., "Evaluating the combined effect of comorbidity and prostate-specific antigen kinetics on the risk of death in men after prostate-specific antigen recurrence," *Journal of Clinical Oncology*, vol. 27, no. 35, pp. 6000–6005, 2009.

[53] A. W. Partin, C. R. Pound, J. D. Pearson et al., "Evaluation of serum prostate-specific antigen velocity after radical prostatectomy to distinguish local recurrence from distant metastases," *Urology*, vol. 43, no. 5, pp. 649–659, 1994.

[54] E. I. Benchikh, A. Fegoun, A. Villers et al., "PSA and follow-up after treatment of prostate cancer," *Progres en Urologie*, vol. 18, no. 3, pp. 137–144, 2008.

[55] O. Schillaci, F. Calabria, M. Tavolozza et al., "Influence of PSA, PSA velocity and PSA doubling time on contrast-enhanced18F-choline PET/CT detection rate in patients with rising PSA after radical prostatectomy," *European Journal of Nuclear Medicine and Molecular Imaging*, vol. 39, no. 4, pp. 589–596, 2012.

[56] M. Rybalov, A. J. Breeuwsma, A. M. Leliveld, J. Pruim, R. A. Dierckx, and I. J. de Jong, "Impact of total PSA, PSA doubling time and PSA velocity on detection rates of 11C-Choline positron emission tomography in recurrent prostate cancer," *World Journal of Urology*, vol. 31, no. 2, pp. 319–323, 2013.

[57] M. C. Marzola, S. Chondrogiannis, A. Ferretti et al., "Role of 18F-choline PET/CT in biochemically relapsed prostate cancer after radical prostatectomy: correlation with trigger PSA, PSA velocity, PSA doubling time, and metastatic distribution," *Clinical Nuclear Medicine*, vol. 38, no. 1, pp. e26–e32, 2013.

[58] G. Treglia, L. Ceriani, R. Sadeghi, G. Giovacchini, and L. Giovanella, "Relationship between prostate-specific antigen kinetics and detection rate of radiolabelled choline PET/CT in restaging prostate cancer patients: a meta-analysis," *Clinical Chemistry and Laboratory Medicine*, 2013.

[59] D. Hausmann, L. K. Bittencourt, U. I. Attenberger et al., "Diagnostic accuracy of 18F choline PET/CT using time-of-flight reconstruction algorithm in prostate cancer patients with biochemical recurrence," *Clinical Nuclear Medicine*, vol. 39, no. 3, pp. e197–e201, 2014.

[60] G. Giovacchini, M. Picchio, R. G. Parra et al., "Prostate-specific antigen velocity versus prostate-specific antigen doubling time for prediction of11C choline PET/CT in prostate cancer patients with biochemical failure after radical prostatectomy," *Clinical Nuclear Medicine*, vol. 37, no. 4, pp. 325–331, 2012.

[61] M. Picchio, A. Briganti, S. Fanti et al., "The role of choline positron emission tomography/computed tomography in the management of patients with prostate-specific antigen progression after radical treatment of prostate cancer," *European Urology*, vol. 59, no. 1, pp. 51–60, 2011.

[62] M. Mamede, F. Ceci, P. Castellucci et al., "The role of 11C-choline PET imaging in the early detection of recurrence in surgically treated prostate cancer patients with very low PSA level < 0.5 ng/mL," *Clinical Nuclear Medicine*, vol. 38, no. 9, pp. e342–e345, 2013.

[63] S. M. Schwarzenböck, J. Kurth, Ch. Gocke, T. Kuhnt, G. Hildebrandt, and B. J. Krause, "Role of choline PET/CT in guiding target volume delineation for irradiation of prostate cancer," *European Journal of Nuclear Medicine and Molecular Imaging*, vol. 40, supplement 1, pp. S28–S35, 2013.

[64] D. M. Somford, J. J. Fütterer, T. Hambrock, and J. O. Barentsz, "Diffusion and perfusion MR imaging of the prostate," *Magnetic Resonance Imaging Clinics of North America*, vol. 16, no. 4, pp. 685–695, 2008.

[65] M. Seitz, A. Shukla-Dave, A. Bjartell et al., "Functional magnetic resonance imaging in prostate cancer," *European Urology*, vol. 55, no. 4, pp. 801–814, 2009.

[66] M. V. Knopp, F. L. Giesel, H. Marcos, H. Von Tengg-Kobligk, and P. Choyke, "Dynamic contrast-enhanced magnetic resonance imaging in oncology," *Topics in Magnetic Resonance Imaging*, vol. 12, no. 4, pp. 301–308, 2001.

[67] M. Fuchsjäger, O. Akin, A. Shukla-Dave, D. Pucar, and H. Hricak, "The role of MRI and MRSI in diagnosis, treatment selection, and post-treatment follow-up for prostate cancer," *Clinical Advances in Hematology and Oncology*, vol. 7, no. 3, pp. 193–202, 2009.

[68] A. Sciarra, V. Panebianco, S. Salciccia et al., "Role of dynamic contrast-enhanced magnetic resonance (MR) imaging and proton MR spectroscopic imaging in the detection of local recurrence after radical prostatectomy for prostate cancer," *European Urology*, vol. 54, no. 3, pp. 589–600, 2008.

[69] A. Alfarone, V. Panebianco, O. Schillaci et al., "Comparative analysis of multiparametric magnetic resonance and PET-CT in the management of local recurrence after radical prostatectomy for prostate cancer," *Critical Reviews in Oncology/Hematology*, vol. 84, no. 1, pp. 109–121, 2012.

[70] W. Kluwer, *Perez and Brady's Principles and Practice of Radiation Oncology*, Lippincott Williams & Wilkins, Philadelphia, Pa, USA, 5th edition, 2007.

[71] E. Casciani, E. Polettini, E. Carmenini et al., "Endorectal and dynamic contrast-enhanced MRI for detection of local recurrence after radical prostatectomy," *American Journal of Roentgenology*, vol. 190, no. 5, pp. 1187–1192, 2008.

[72] V. Panebianco, F. Barchetti, A. Sciarra et al., "Prostate cancer recurrence after radical prostatectomy: the role of 3-T diffusion imaging in multi-parametric magnetic resonance imaging," *European Radiology*, vol. 23, no. 6, pp. 1745–1752, 2013.

[73] T. Sella, L. H. Schwartz, P. W. Swindle et al., "Suspected local recurrence after radical prostatectomy: endorectal coil MR imaging," *Radiology*, vol. 231, no. 2, pp. 379–385, 2004.

[74] S. Cirillo, M. Petracchini, L. Scotti et al., "Endorectal magnetic resonance imaging at 1.5 Tesla to assess local recurrence following radical prostatectomy using T2-weighted and contrast-enhanced imaging," *European Radiology*, vol. 19, no. 3, pp. 761–769, 2009.

[75] V. Panebianco, A. Sciarra, D. Lisi et al., "Prostate cancer: 1HMRS-DCEMR at 3 T versus [(18)F]choline PET/CT in the detection of local prostate cancer recurrence in men with biochemical progression after radical retropubic prostatectomy (RRP)," *European Journal of Radiology*, vol. 81, no. 4, pp. 700–708, 2012.

[76] D. M. Somford, J. J. Fütterer, T. Hambrock, and J. O. Barentsz, "Diffusion and perfusion MR imaging of the prostate," *Magnetic Resonance Imaging Clinics of North America*, vol. 16, no. 4, pp. 685–695, 2008.

[77] V. A. Morgan, S. F. Riches, S. Giles, D. Dearnaley, and N. M. DeSouza, "Diffusion-weighted MRI for locally recurrent prostate cancer after external beam radiotherapy," *American Journal of Roentgenology*, vol. 198, no. 3, pp. 596–602, 2012.

[78] R. Kilinç, O. G. Doluoglu, B. Sakman et al., "The correlation between diffusion-weighted imaging an histopathological evaluation of 356 prostate biopsy sites in patients with prostatic diseases," *ISRN Urology*, vol. 2012, Article ID 252846, 5 pages, 2012.

[79] G. Giannarini, D. P. Nguyen, G. N. Thalmann, and H. C. Thoeny, "Diffusion-weighted magnetic resonance imaging detects local recurrence after radical prostatectomy: initial experience," *European Urology*, vol. 61, no. 3, pp. 616–620, 2012.

[80] H. A. Vargas, C. Wassberg, O. Akin, and H. Hricak, "MR imaging of treated prostate cancer," *Radiology*, vol. 262, no. 1, pp. 26–42, 2012.

[81] NCCN guidelines version 4 2013.

[82] T. Zilli, S. Jorcano, N. Peguret et al., "Dose-adapted salvage radiotherapy after radical prostatectomy based on an erMRI target definition model: toxicity analysis," *Acta Oncologica*, vol. 53, no. 1, pp. 96–102, 2014.

[83] G. Bauman, M. Haider, U. A. Van der Heide, and M. Ménard, "Boosting imaging defined dominant prostatic tumors: a systematic review," *Radiotherapy & Oncology*, vol. 107, no. 3, pp. 274–281, 2013.

[84] V. Panebianco, F. Giove, F. Barchetti, F. Podo, and R. Passariello, "High-field PET/MRI and MRS: potential clinical and research applications," *Clinical and Translational Imaging*, vol. 1, no. 1, pp. 17–29, 2013.

[85] D. Thorwarth and S. Leibfarth, "Potential role of PET/MRI in radiotherapy treatment planning," *Clinical and Translational Imaging*, vol. 1, no. 1, pp. 45–51, 2013.

Hindawi Publishing Corporation
BioMed Research International
Volume 2014, Article ID 486798, 6 pages
http://dx.doi.org/10.1155/2014/486798

Research Article

The Role of M1 and M2 Macrophages in Prostate Cancer in relation to Extracapsular Tumor Extension and Biochemical Recurrence after Radical Prostatectomy

M. Lanciotti,[1] L. Masieri,[1] M. R. Raspollini,[2] A. Minervini,[1] A. Mari,[1] G. Comito,[3] E. Giannoni,[3] M. Carini,[1] P. Chiarugi,[3] and S. Serni[1]

[1] *Department of Urology, University of Florence, Careggi Hospital, Viale San Luca, 50134 Florence, Italy*
[2] *Department of Pathology, University of Florence, Careggi Hospital, Florence, Italy*
[3] *Department of Biomedical, Experimental and Clinical Sciences, University of Florence, Viale Morgagni 50, 50134 Florence, Italy*

Correspondence should be addressed to M. Lanciotti; m-lanciotti@libero.it

Received 29 November 2013; Revised 3 February 2014; Accepted 5 February 2014; Published 11 March 2014

Academic Editor: Lorenzo Livi

Introduction. The aim of our work was to investigate the causal connection between M1 and M2 macrophage phenotypes occurrence and prostate cancer, their correlation with tumor extension (ECE), and biochemical recurrence (BR). *Patient and Methods*. Clinical and pathological data were prospectively gathered from 93 patients treated with radical prostatectomy. Correlations of commonly used variables were evaluated with uni- and multivariate analysis. The relationship between M1 and M2 occurrence and BR was also assessed with Kaplan-Meier survival analysis. *Results*. Above all in 63.4% there was a M2 prevalence. M1 occurred more frequently in OC disease, while M2 was more represented in ECE. At univariate analysis biopsy and pathologic GS and M2 were statistically correlated with ECE. Only pathologic GS and M2 confirmed to be correlated with ECE. According to macrophage density BCR free survival curves presented a statistically significant difference. When we stratified our population for M1 and M2,we did not find any statistical difference among curves. At univariate analysis GS, pTNM, and positive margins resulted to be significant predictors of BCR, while M1 and M2 did not achieve the statistical significance. At multivariate analysis, only GS and pathologic stage were independent predictors of BR. *Conclusion*. In our study patients with higher density of M count were associated with poor prognosis; M2 phenotype was significantly associated with ECE.

1. Introduction

Several epidemiologic studies support the opinion that chronic inflammatory diseases are frequently associated with increased risk of various human cancers, even up to 25% of them [1, 2].

Prostate cancer (PCa) represents one of the most common cancers and the second leading cause of cancer-related death in men in the United States [3]. Actually there is a substantial epidemiological evidence that chronic inflammation is associated with PCa [4] and many studies aimed to investigate the causal connection between inflammation and PCa.

It has been recently observed that proliferative inflammatory atrophy (PIA) lesions are strictly related to chronic prostatic inflammation, and histological cellular transitions have been noted between areas of PIA and high-grade prostate intraepithelial neoplasia (HGPIN), and furthermore between PIA and PCa [5]. A key role of the PIA lesion is the presence of leukocyte infiltration, with the majority of cells belonging to the monocyte-macrophages lineage. Tumor-associated macrophages (TAMs) are a significant component of the inflammatory cell infiltrates in prostate cancer. Mononuclear cells and/or polymorphonuclear cells in both epithelial and stromal compartments promote carcinogenesis with their ability to communicate via a complex network of intercellular signalling pathways mediated by proinflammatory cytokines, their receptors, and cell surface adhesion molecules. TAMs may have both tumor stimulatory and/or -inhibitory properties, probably because they can,

by mechanisms largely unknown, differentiate into either cytotoxic (M1) or tumor growth promoting (M2) states. In several murine cancer models including chemically and genetically induced primary lung tumors, prostate tumors, colon xenografts, and lung metastases, TAMs expressed M2 early during tumorigenesis [6].

The aim of our work was to investigate the causal connection between M1 and M2 phenotype macrophages occurrence with PCa and to evaluate their correlation with clinic-pathological commonly used variables and survival.

2. Material and Methods

In our tertially referral center we routinely store in a specific database clinical and pathological data of patient undergoing radical prostatectomy (RP). In order to study a greater amount of neoplastic tissue and to better locate prostate inflammation at the pathological examination, we decided to prospectively select 93 consecutive patients with stage cT2b-c PCa undergoing RP from January 2000 to December 2011. Clinical stage assessment was routinely made by digital rectal examination at the visit, transrectal ultrasound at the time of the biopsy, and endorectal coil magnetic resonance for evaluating local extension. CT scan and bone scintigraphy were required for patients with PSA $\geq$ 20 ng/mL and GS $\geq$ 7.

All patients received anterograde RP according to our previously published technique [7]. The follow-up schedule included serum PSA assay every 3 months for the first year, then every 6 months for the following 2 years, and yearly thereafter. Biochemical recurrence (BCR) was defined as evidence of PSA > 0.2 ng/mL on two consecutive measurements.

2.1. Statistical Analysis. Statistical analysis was performed using StatView software. Univariate analysis was carried out as follows: Student's t-test was used comparing continuous parametric variables, Mann Whitney test was used comparing continuous nonparametric variables, and Pearson chi square test was used comparing nominal variables.

The risk of ECE, related to the preoperative variables analyzed, was evaluated using the logistic regression model, and odds ratios and risk ratios were calculated.

In order to establish the correlation between macrophages phenotype and prognosis, the BCR-free survival rate was estimated by the Kaplan-Meier method. Statistical significance was verified by the log-rank test.

2.2. Tissue Specimens and Immunohistochemistry. All specimens were obtained from the archives of formalin-fixed, paraffin-embedded tissue blocks. Haematoxylin-eosin stained sections from each histological specimen were reevaluated to confirm the histological diagnosis of PCa, for the Gleason grade [8] for detecting perineural invasion, and for surgical margin status. All cases were also reevaluated regarding the World Health Organization (WHO) 2004 classification [9] and pathological T staging was performed [10]. In addition, a representative tissue block was selected for further analysis. The following immunohistochemical markers were evaluated: CD68 and CD163. The stains for CD68 and CD163 were considered positive when there was a strong granular cytoplasmic or cytoplasmic and membrane staining patterns in cells of monocyte/macrophages lineage.

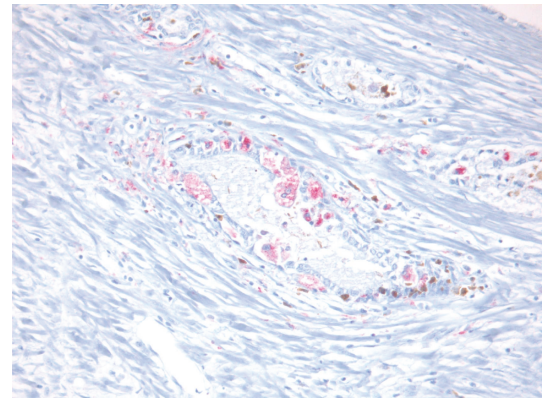

Figure 1: Presence of both M1 and M2 that were characterized by a red cytoplasm due to chromogen FAST RED for CD68 (M1) or with a brown cytoplasm due to chromogen diaminobenzidine (DAB) for CD163 (M2).

2.3. Slide Grading. Macrophages were quantified by systematically screening the entire carcinoma area at low magnification using a 2,5x or 5x lens and selecting the areas with the highest density of macrophages and by counting them. M1 and M2 are distinguished by two different primary antibodies: anti-CD163 (for M2) and anti-CD68 (for M1) and two different chromogens: chromogen diaminobenzidine (DAB) for CD163 (M2, color brown) and chromogen FAST RED for CD68 (M1, color red). Therefore, we were able to recognize easily the two types of macrophages due to this double coloration (brown macrophages or M2 versus red macrophages or M1), and consequently we were able to count separately M1 and M2. We systematically screened the entire carcinoma area at low magnification, and in this way we selected the areas rich with macrophages (called: hot spot). After that, both M1 and M2 macrophages were manually counted at high magnification (Figure 1). Finally, the mean of both the number of M1 macrophages and M2 macrophages in these three hot spots was obtained. All counting was performed by one investigator (MRR) unaware of clinical data.

3. Results

Clinical and pathological characteristics of 93 patients included in our study are listed in Table 1.

Our patients presented median (IQR) preoperative PSA of 7.6 (1.01–86.8) and a prevalence of biopsy GS 6 (53.8%). Mean (SD) follow-up time after radical prostatectomy was 50.4 months (19.2). BCR occurred in 23 patients (24.7%) with a mean (SD) follow-up period of 26.3 (25.2) months. Among them 11 patients underwent delayed radiotherapy and 12 patients underwent palliative hormone therapy during follow-up period.

Table 1: Clinical presentation, pathologic findings, and follow-up of the 93 patients.

Macrophages population	Total of patients	M1	M2
n (%)	93	34 (36.6)	59 (63.4)
Count in three hot spots	Mean (median)	12.06 (6)	17.18 (10)
Density of macrophages M1 and M2 in three hot spots according to median number	43 below median number 50 above median number		
	Preoperative variables		
Age (yy) median (IQR)	67 (45–75)	64 (55–74)	67 (45–75)
Total PSA (ng/mL) median (IQR)	7.6 (1.0–86.8)	8.3 (2.5–47.7)	7.0 (1–76.8)
Biopsy Gleason score *n* (%)			
6	50 (53.8)	19 (55.9)	31 (52.6)
7	28 (30.1)	12 (35.3)	16 (27.1)
8–10	15 (16.1)	3 (8.8)	12 (20.3)
	Postoperative variables		
Organ confine disease (OC) *n* (%)	33 (35.5)	19 (55.9)	14 (23.8)
Extracapsular extension (ECE) *n* (%)	60 (64.5)	15 (44.1)	45 (76.2)
TNM stage *n* (%)			
T2	33 (35.5)	19 (55.9)	14 (23.8)
T3a	35 (37.6)	7 (20.6)	28 (47.4)
T3b	23 (24.8)	8 (23.5)	15 (25.4)
T4	2 (2.1)	0	2 (3.4)
Pathologic Gleason score *n* (%)			
6	30 (32.2)	13 (38.2)	17 (28.8)
7	40 (43)	16 (47.1)	24 (40.7)
8–10	23 (24.8)	5 (14.7)	18 (30.5)
Lymph node involvement *n* (%)	5 (5.3)	2 (5.9)	3 (5.1)
Positive surgical margin *n* (%)	11 (11.8)	2 (5.9)	9 (15.2)
Follow-up (months) mean (SD)	50.4 (19.2)	55.5 (21.2)	47.6 (16.3)
Biochemical recurrence *n* (%)	23 (24.7)	7 (20.6)	16 (27.1)

At the final anatomopathological evaluation 33 patients (35.5%) presented organ confined disease (OC), while in 60 pts (64.5%) there was ECE and positive surgical margins were found in 11 patients (11.8%). Patients with ECE presented higher prevalence of GS 7 to 8–10 and higher prevalence of PSA > 10 ng/mL with respect to the OC disease patients.

The macrophages prevalence is reported in Table 1 as follow: in 34 (36.6%) patients a higher prevalence of M1 was found, while in 59 (63.4%) patients there was a higher prevalence of M2. Mean (median) macrophage count of M1 and M2 in the three hot spots was 12.06 (6.0) and 17.18 (10.0), respectively.

M1 occurred more frequently in OC PCa, especially with GS 6 to 7 (mean number 18.6, median 11.6), while M2 resulted to be more represented in PCa with ECE and GS 7 to 8-10 (mean number 20.2, median 10).

When we correlated M1-M2 ratio to GS, biopsy cores, stage, and BCR at Student's t-test and Pearson χ^2 test, we found statistical correlation only with stage ($P = 0.004$). Moreover, at univariate analysis for ECE, pathological GS and M2 phenotype were statistically correlated with extracapsular extension (0.029, 0.0001, and 0.0079, resp.).

On the contrary, we did not find any statistical correlation between BCR and M1-M2 ratio, even if patients with higher prevalence of M1 phenotype presented better results.

At logistic regression analysis only specimen GS and M1-M2 ratio confirmed to be statistically correlated with ECE ($P = 0.05$, RR 10.65, and 95% CI 1.11–102.26 and $P = 0.03$, RR 0.295, and 95% CI 0.09–0.89, resp.) (see Table 2).

Moreover, at univariate analysis biopsy GS, pathological GS, pTNM, positive surgical margins, and high density of macrophages in three hot spots resulted to be independently predictive of BCR ($P = 0.0009$, 0.0006, and 0.0147, resp.), while substratification in M1 and M2 did not achieve the statistical significance. At Cox multivariable analysis only pathologic GS and stage resulted to be independent predictors of BCR ($r = 19.146$, $P = 0.02$ and $r = 3.43$, $P = 0.05$, resp.) (see Table 3).

At the Kaplan-Meier survival analysis, the 36 and 60 months BR free survival rate for the global population

Table 2: Univariate (Pearson χ^2 test, t-test, and Mann Whitney test) and multivariate (logistic regression) analysis of common variables to predict extracapsular extension (ECE) of PCa.

Variables	Univariate analysis P value	Multivariate analysis		
		P value	Risk ratio	95% CI
Preoperative PSA	Ns	Not included in analysis		
Biopsy GS > 7	**0.029**	0.07	4.21	1.10–19.62
Anatomopathological GS > 7	**0.0001**	**0.05**	10.65	1.11–102.26
Lymphnode invasion	Ns	Not included in analysis		
M1/M2	**0.0079**	**0.03**	**0.295**	**0.09–0.89**

Table 3: Univariate (Pearson χ^2 test, Mann Whitney Test, and t-test) and multivariate (Cox proportional hazard model) analysis of common variables to predict BCR.

Variables	Univariate analysis P value	Multivariate analysis		
		P value	Risk ratio	95% CI
Preoperative PSA	Ns		—	
Biopsy GS > 7	**0.0009**	0.07	2.26	1.1–10.47
Anatomopathological GS > 7	**0.0006**	**0.02**	**16.04**	**1.44–177.9**
Pathological stage	**0.0147**	**0.03**	**3.43**	**1.09–11.8**
Lymphnode invasion	Ns		—	
Status	Ns		—	
Surgical margin status	Ns		—	
High density of macrophages M1 and M2 in three hot spots (above median value)	**0.05**	0.09	2.53	1.6–9.67
M1-2 phenotype	Ns		—	

resulted to be 84.6% and 72.5%, respectively. According to macrophage density, BCR free survival curves at the Kaplan-Meier analysis were 94.4 versus 74.0 and 85.1 versus 62.2 at 36 and 60 months, respectively, with a statistically significant difference among the curves ($P = 0.05$) (Figure 2).

Moreover, when we stratified our patients for M1 and M2 macrophage phenotypes, we did not find any statistical difference among BCR free survival curves (log rank $P = ns$), although we observed that patients with prevalence of M2 macrophages showed a trend toward worst BCR free survival rates at 36 and 60 months compared to patients with M1 prevalence (78.2 versus 94.1 and 71.0 versus 77.4, resp.) (see Figure 3). When we analyzed survival curves for the category of patients with only ECE, among them, stratification for M1 and M2 macrophage phenotype did not allow us to establish a significant correlation with prognosis, although even in this instance patients with M2 phenotype prevalence confirmed to have a slightly worse prognosis.

4. Discussion

To date several clinicopathological factors have been reported as prognostic factors, but few studies have been reported on anticancer immune response by the host.

Prostate is constituted by epithelium and surrounding stroma, which itself consists of smooth muscle, extracellular matrix, and inflammatory cells. Inflammation has been thoroughly described as a key player in PCa, and among various inflammatory cell population, macrophages have been recognized as one of the major components. Chronic inflammation characterized by sustained tissue damage, damage induced cellular proliferation, and tissue repair have been analyzed in order to explain prostatic carcinogenesis, demonstrating a strong association between chronic prostatic inflammation, premalignant, and malignant changes in the prostatic epithelium in a prospective five years follow-up study on needle biopsy specimens [4]. Moreover, Nonomura et al. noticed that TAM infiltration was significantly correlated with serum PSA level, GS, or stage among the clinicopathological factors in prostate needle biopsy specimens [11].

Shimura et al. studied the association between TAM infiltration and disease-free survival after RP using whole mount sections, demonstrating that disease-free survival is significantly shorter for patients with a high level of TAMs than for those with a low level [12].

Macrophages are likely to encounter factors that most frequently polarise them toward M1 and M2 subtype macrophages, especially TAMs that express selected M2

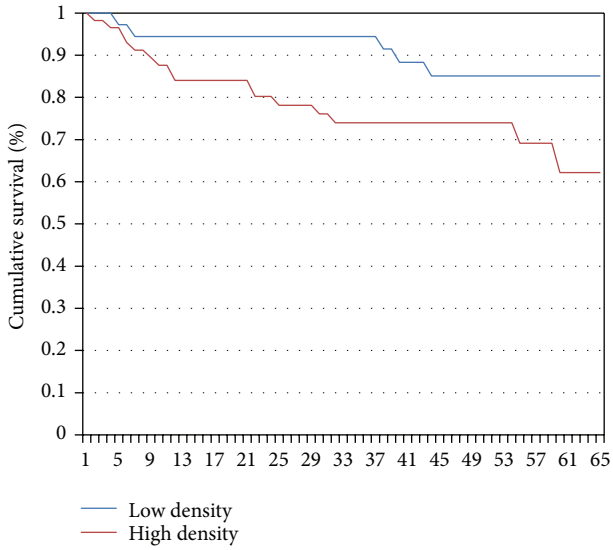

Figure 2: Biochemical recurrence (BCR) free survival curves at the Kaplan-Meier analysis of our 93 patients study population based on median number of macrophages. The blue line represents BCR free survival curve of patients with low density of macrophages M1 and M2 in three hot spots (n° of macrophages < median number), while the red line represents those with high density of M1 and M2 in three hot spots (>median number). BCR free survival rates at 36 and 60 months were 94.4 versus 74.0 and 85.1 versus 62.2, respectively, $P = 0.05$.

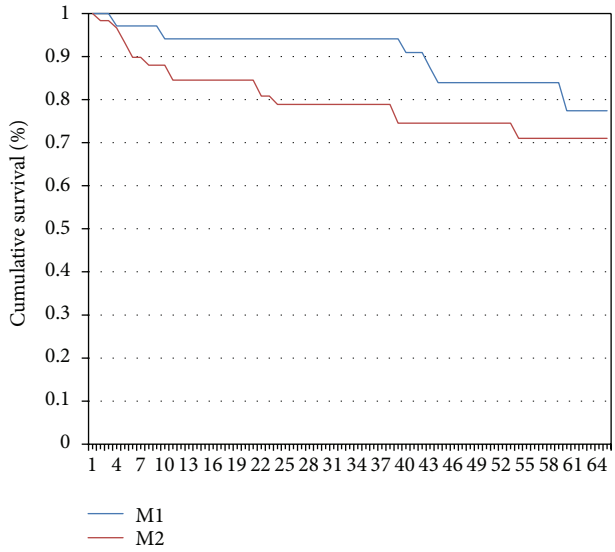

Figure 3: Biochemical recurrence (BCR) free survival curves at the Kaplan-Meier analysis of our 93 patients study population stratified for M1 and M2 macrophages prevalence. The blue line represents BCR free survival curve of patients with M1 macrophage prevalence, while the red line represents those with M2 macrophage prevalence. BCR free survival rates at 36 and 60 months were 94.1 versus 78.2 and 77.4 versus 71.0, respectively.

protumoural functions, tumor progression, and metastasis [13].

In our study we observed that higher density of macrophage was statistically associated to poorer prognosis ($P = 0.05$, Figure 2). Moreover we found higher prevalence of M2 macrophage phenotype, which resulted more represented in PCa with ECE ($P = 0.0079$) and GS 7 to 8–10 and pT3a stage ($P = ns$). Our patients expressing more M2 phenotype frequently presented ECE and BCR, even if it was not confirmed at our statistical analysis. According to previous data published in the literature, TAMs generally exhibit an M2 phenotype known to promote angiogenesis, tumor growth, and metastasis [14]. To corroborate our preliminary results, in male mice TAM polarization in primary tumors at four distinct stages including PIN, well-differentiated, moderately differentiated, and poorly differentiated PCa has been examined [15].

In comparison to our global series of prostatectomies performed in our referral center as previously reported [7], we noticed in these 93 patient a slight higher incidence of extracapsular disease and GS 7. This was certainly due to our necessity to definitely locate macrophages in the prostate specimen at the final pathological evaluation. Indeed even in the literature high TAM count is statistically found in patients with higher stages (extracapsular extension) and grades (GS > 7) [11]. Even if it could be a limit of the study, our study population on the border between OC and ECE disease may be anyway extremely indicative for macrophage evaluation.

In addition to our preliminary results, further analysis on larger series of patients will allow us to better define M1-2 phenotype role in tumour aggressiveness and outcome.

5. Conclusion

It has become increasingly clear that TAMs are active players in the tumor aggressiveness. This is a preliminary study in which we laid down groundwork for further studies. In our study population with clinically localized PCa with stage cT2b-c, we found correlation between high macrophage infiltration and unfavorable items after RP. Moreover, M2 macrophage phenotype was significantly associated with extracapsular extension, even if this phenotype prevalence was not capable at the moment to predict BCR. Macrophage phenotype has demonstrated to be fascinating and valuable to rationalize a more aggressive adjuvant approach, even if further studies are needed to verify it.

Conflict of Interests

The authors declare that there is no conflict of interests regarding the publication of this paper.

References

[1] M. Philip, D. A. Rowley, and H. Schreiber, "Inflammation as a tumor promoter in cancer induction," *Seminars in Cancer Biology*, vol. 14, no. 6, pp. 433–439, 2004.

[2] H. Lu, W. Ouyang, and C. Huang, "Inflammation, a key event in cancer development," *Molecular Cancer Research*, vol. 4, no. 4, pp. 221–233, 2006.

[3] A. Jemal, R. Siegel, E. Ward, Y. Hao, J. Xu, and M. J. Thun, "Cancer statistics, 2009," *CA Cancer Journal for Clinicians*, vol. 59, no. 4, pp. 225–249, 2009.

[4] G. T. MacLennan, R. Eisenberg, R. L. Fleshman et al., "The influence of chronic inflammation in prostatic carcinogenesis: a 5-year followup study," *Journal of Urology*, vol. 176, no. 3, pp. 1012–1016, 2006.

[5] A. M. De Marzo, V. L. Marchi, J. I. Epstein, and W. G. Nelson, "Proliferative inflammatory atrophy of the prostate: implications for prostatic carcinogenesis," *American Journal of Pathology*, vol. 155, no. 6, pp. 1985–1992, 1999.

[6] E. F. Redente, L. D. Dwyer-Nield, D. T. Merrick et al., "Tumor progression stage and anatomical site regulate tumor-associated macrophage and bone marrow-derived monocyte polarization," *American Journal of Pathology*, vol. 176, no. 6, pp. 2972–2985, 2010.

[7] M. Carini, L. Masieri, A. Minervini, A. Lapini, and S. Serni, "Oncological and functional results of antegrade radical retropubic prostatectomy for the treatment of clinically localized prostate cancer," *European Urology*, vol. 53, no. 3, pp. 554–563, 2008.

[8] J. I. Epstein, W. C. Allsbrook Jr., M. B. Amin et al., "The 2005 International Society of Urological Pathology (ISUP) consensus conference on Gleason grading of prostatic carcinoma," *American Journal of Surgical Pathology*, vol. 29, no. 9, pp. 1228–1242, 2005.

[9] J. N. Eble, G. Sauter, J. I. Epstein, and I. A. Sesterhenn, *World Health Organization Classification of Tumours. Pathology and Genetics of Tumours of the Urinary System and Male Genital Organs*, IARC Press, Lyon, France, 2004.

[10] AJCC, *Cancer Staging Manual*, Springer, New York, NY, USA, 7th edition, 2010.

[11] N. Nonomura, H. Takayama, M. Nakayama et al., "Infiltration of tumour-associated macrophages in prostate biopsy specimens is predictive of disease progression after hormonal therapy for prostate cancer," *BJU International*, vol. 107, no. 12, pp. 1918–1922, 2011.

[12] S. Shimura, G. Yang, S. Ebara, T. M. Wheeler, A. Frolov, and T. C. Thompson, "Reduced infiltration of tumor-associated macrophages in human prostate cancer: association with cancer progression," *Cancer Research*, vol. 60, no. 20, pp. 5857–5861, 2000.

[13] A. Sica, T. Schioppa, A. Mantovani, and P. Allavena, "Tumour-associated macrophages are a distinct M2 polarised population promoting tumour progression: potential targets of anti-cancer therapy," *European Journal of Cancer*, vol. 42, no. 6, pp. 717–727, 2006.

[14] A. Sica, P. Larghi, A. Mancino et al., "Macrophage polarization in tumour progression," *Seminars in Cancer Biology*, vol. 18, no. 5, pp. 349–355, 2008.

[15] K. Raina, R. P. Singh, R. Agarwal, and C. Agarwal, "Oral grape seed extract inhibits prostate tumor growth and progression in TRAMP mice," *Cancer Research*, vol. 67, no. 12, pp. 5976–5982, 2007.

Hindawi Publishing Corporation
BioMed Research International
Volume 2014, Article ID 437910, 1 page
http://dx.doi.org/10.1155/2014/437910

Erratum

Erratum to "Strategies for Imaging Androgen Receptor Signaling Pathway in Prostate Cancer: Implications for Hormonal Manipulation and Radiation Treatment"

Giovanni L. Gravina,[1,2,3] Claudio Festuccia,[1] Pierluigi Bonfili,[1] Mario Di Staso,[1] Pietro Franzese,[1] Valeria Ruggieri,[1] Vladimir M. Popov,[3] Vincenzo Tombolini,[4,5] Carlo Masciocchi,[6] Eleonora Carosa,[7] Andrea Lenzi,[2] Emmanuele A. Jannini,[7] and Ernesto Di Cesare[1]

[1] *Laboratory of Radiobiology and Division of Radiotherapy, Department of Applied, Clinical and Biotechnological Sciences, University of L'Aquila, Via Vetoio, Coppito 2, L'Aquila, Italy*
[2] *Section of Medical Pathophysiology, Food Science and Endocrinology, Department of Experimental Medicine, Sapienza University of Rome, Italy*
[3] *LIPOGEN LLC, Mount Laurel, NJ, USA*
[4] *Division of Radiotherapy, University of Rome, University Hospital "Policlinico Umberto I", Italy*
[5] *Division of Radiotherapy, Department of Radiological Sciences, University of Rome "La Sapienza", Spencer-Lorillard Foundation, Rome, Italy*
[6] *Division of Radiology, Department of Applied, Clinical and Biotechnological Sciences, University of L'Aquila, L'Aquila, Italy*
[7] *Course of Endocrinology and Medical Sexology, Department of Applied, Clinical and Biotechnological Sciences, University of L'Aquila, L'Aquila, Italy*

Correspondence should be addressed to Giovanni L. Gravina; giovanniluca.gravina@libero.it

Received 3 February 2014; Accepted 6 February 2014; Published 9 March 2014

The name of the first author (Gravina Giovanni Luca) was incorrect and is corrected here as Giovanni L. Gravina.

Hindawi Publishing Corporation
BioMed Research International
Volume 2014, Article ID 561571, 14 pages
http://dx.doi.org/10.1155/2014/561571

Review Article

Extracellular Vesicles in Prostate Cancer: New Future Clinical Strategies?

Ilaria Giusti and Vincenza Dolo

Department of Life, Health and Environmental Sciences, University of L'Aquila, Via Vetoio-Coppito 2, I-67100 L'Aquila, Italy

Correspondence should be addressed to Vincenza Dolo; vincenza.dolo@univaq.it

Received 2 December 2013; Accepted 9 January 2014; Published 23 February 2014

Academic Editor: Giovanni Luca Gravina

Prostate cancer (PCa) is the most common cancer—excluding skin tumors—in men older than 50 years of age. Over time, the ability to diagnose PCa has improved considerably, mainly due to the introduction of prostate-specific antigen (PSA) in the clinical routine. However, it is important to take into account that although PSA is a highly organ-specific marker, it is not cancer-specific. This shortcoming suggests the need to find new and more specific molecular markers. Several emerging PCa biomarkers have been evaluated or are being assessed for their potential use. There is increasing interest in the prospective use of extracellular vesicles as specific markers; it is well known that the content of vesicles is dependent on their cellular origin and is strongly related to the stimulus that triggers the release of the vesicles. Consequently, the identification of a disease-specific molecule (protein, lipid or RNA) associated with vesicles could facilitate their use as novel biological markers. The present review describes several *in vitro* studies that demonstrate the role of vesicles in PCa progression and several *in vivo* studies that highlight the potential use of vesicles as PCa biomarkers.

1. Prostate Cancer

The prostate is an exocrine gland in the male reproductive system that is responsible for the production of seminal/prostatic fluid, a liquid that usually constitutes 50–70% of the semen volume (along with seminal vesicle fluid and, of course, spermatozoa) [1]. The mature prostate gland is composed of columnar and polarized cells lining the prostatic lumen and more elongated basal epithelial cells that separate the lumen from the stroma [2, 3]; both basal and luminal epithelial cells can mutate, thus causing prostate cancer (PCa) [2].

As with all types of cancer, PCa is the result of genetic and epigenetic alterations that induce transformations of normal glandular epithelia [4]. The dysregulation of many molecules and genes has been implicated in PCa; some of these molecules (e.g., NKX3.1, FOXA1, and Myc) seem to be relevant for cancer initiation because their expression is altered during the early stages; other pathways (*TMPRSS2-ERG* and *RB*) seem to be involved in the transition from PCa to CRPC. The PI3 K, Akt, *PTEN,* and mTOR are always dysregulated in PCa [2].

With regard to epigenetic alterations, both hypo- and hypermethylation are well documented. Hypermethylation is common in PCa and is believed to play a role in PCa initiation and progression; hypermethylation of the *GSTP1* gene promoter (which can involve the 5V region or CpG islands) is a highly specific marker for PCa, but it lacks sensitivity [5]. The dysregulation of gene expression in PCa appears to be due to changes in chromatin remodeling as well as posttranslational modifications of histones, with several histone-modifying enzymes (namely, HDACs, HMTs, and HDMs) being altered. Changes in miRNA levels are also important in PCa progression, as demonstrated by the role of miRNAs in blocking apoptosis, cell-cycle promotion, migration, invasion, and the maintenance of androgen-independent growth [6, 7].

Among nonskin cancers, PCa is the most common cancer in men older than 50 years of age [8, 9]. The etiology of PCa has not been fully elucidated; however, its risk factors are well-established and include age (incidence and mortality rates increase exponentially after 50 years of age), ethnicity (African Americans have the highest rates), and a family history of PCa (men with fathers or brothers affected by

PCa have double the risk of developing this form of cancer) [8, 10, 11]. Other risk factors are likely involved, such as genetic susceptibility, and there is strong evidence from migrant studies that hormones, smoking, diet, sexual factors, and other lifestyle factors also play roles in the development of PCa [8, 10, 12, 13]; among all of these risk factors, diet seems to play a major role in the initiation, promotion, and progression of prostate cancer [13].

PCa incidence rates are generally higher in North America when compared to Western Europe, Oceania, and Asia, but the rates have increased considerably worldwide during the past half century, largely due to the advent of prostatic specific antigen (PSA) testing and its increased use, which has greatly improved diagnosis of this pathology and has highlighted an increased number of cases [14, 15]. At the same time, the extensive use of PSA screening accounts for a great reduction in the proportion of men who present with metastatic disease at the time of diagnosis and the lower mortality rate in some populations [16].

PSA is a serine protease that was first identified in 1966 in seminal fluid; in 1979, its role as tumor marker was first described. Some years later, it was approved by the U.S. Food and Drug Administration for monitoring the disease status of recurrence after definitive treatment in men with PCa, and it is now used to identify men with PCa. It seems, moreover, that PSA can even identify men who are at risk of developing PCa [17, 18]. PSA exists in the bloodstream in several specific forms, including free and complexed (e.g., α-1-antichymotrypsin) forms; free PSA is composed of three isoforms: i-PSA (inactive PSA), pro-PSA (proenzyme PSA), and BPH-PSA (benign prostatic hyperplasia-PSA). The measurement of total PSA and its specific forms can help to differentiate between malign (PCa) and benign conditions [17, 18].

In the blood of patients with either benign prostatic hyperplasia (BPH) or PCa, the prevailing form is the complexed form, whereas the ratio of free/total PSA is lower in PCa than in BPH. BPH-PSA and i-PSA are relatively more abundant than pro-PSA in BPH, whereas in PCa, the reverse is observed [17, 18]. It seems that higher levels of pro-PSA are associated with a higher risk for PCa in men with total PSA levels of 4–10 ng/mL [19] and with more aggressive forms of PCa, as characterized by Gleason scores ≥ 7 or extracapsular tumor extension [20]. The Gleason score is used to grade PCa, and it is based on the microscopic appearance of cancer tissue, which takes into account the differentiation grade of the tissue. Cancers with higher Gleason scores are more aggressive and have worse prognoses than cancers with lower scores [21].

PSA analysis in serum accompanied by digital rectal examination has been the standard method for PCa screening. Although PSA is highly organ-specific, it is not a cancer-specific marker because it cannot distinguish among indolent PCa, aggressive PCa, and benign conditions (e.g., prostate inflammation is characterized by increased levels of PSA) [18, 22]. PSA levels can even be altered by ejaculation, drugs, or prostate manipulation (particularly by catheterization or prostatic massage), thus contributing to false positives that lead to unnecessary biopsies or other clinical interventions [17, 23].

Nevertheless, in the last few years, mortality specifically attributable to PCa decreased in some countries (such as the US, Canada, Germany, Italy, Switzerland, France, and Spain). As already stated, this decrease is likely due to the introduction of PSA screening, which allows the detection of PCa at an early stage, allowing early curative treatments and improving clinical outcomes. At the same time, new surgical approaches, improved irradiation protocols, and antiandrogenic therapies likely have contributed to mortality decrease as well [24]. Antiandrogenic therapy is important because PCa depends on androgen receptor activity at all stages; standard treatment strategies for disseminated cancer are based on targeting this pathway using androgen deprivation therapy (ADT) or androgen receptor antagonists. Despite such interventions, a successful treatment effect is often followed by reactivation of the androgen receptors, leading to a recurrence of PCa (so-called "castrate-resistant PCa" or CRPC) [2].

2. Extracellular Vesicles

It is now widely known that cells are able to release several types of extracellular vesicles [25–28] that are not merely a form of waste elimination, as it was thought when they were discovered; instead, they act as signaling packages and are able to affect neighboring cells and the surrounding microenvironment with the messages they convey [29]. The involvement of extracellular vesicles in various physiological and pathological events, such as the immune response, cellular differentiation, and vascular and cancer pathologies, is also clear [30]. How extracellular vesicles interact with target cells remains to be fully elucidated, even if several hypotheses have been proposed—for example, direct cellular contact mediated by the interaction of membranes with target cell receptors, fusion with the plasma membrane, or encapsulation by endocytosis [26, 31].

Usually, extracellular vesicles can be isolated *in vivo* from all bodily fluids (e.g., blood, urine, semen, amniotic fluid, saliva, synovial and bronchoalveolar fluids, breast milk, spinal fluid, ascites, and malignant pleural effusion) [22, 32], particularly if they are exposed to primary tumors [33, 34].

The most important extracellular vesicles released from cells are apoptotic bodies, exosomes, and shed microvesicles (MVs) (Figure 1) [25–27]. Extracellular vesicles differ mainly in their cellular origins and sizes. Apoptotic bodies are released from the cell membrane as the final consequence of cell fragmentation during apoptosis, and they have irregular shapes with a range of 1–5 μm in size [26, 27]. Exosomes are released by the fusion of multivesicular bodies (MVB) with the plasma membrane and are 30–100 nm in size [26, 27]. Shed MVs are released through regulated outward budding or blebbing of the plasma membrane; they are heterogeneous in shape and are 100–1,000 nm in size [26, 27].

In addition to the well-defined differences in cell origin and size, extracellular vesicles can also exhibit differences or show overlapping features in their molecular compositions and functions. We will further discuss exosomes and

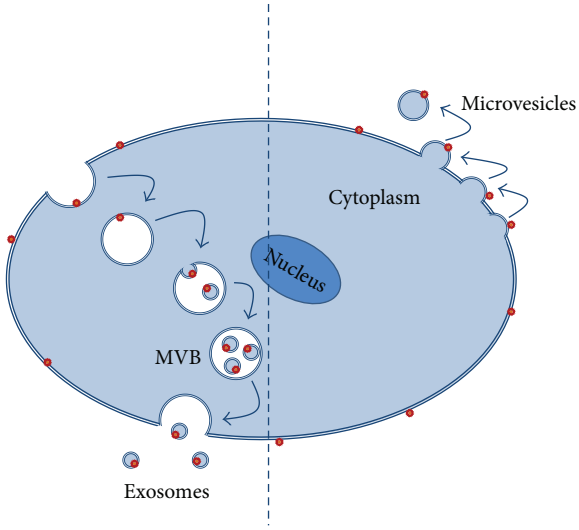

Figure 1: Schematic view of exosomes and microvesicles being released from a cell.

MVs, which are released from viable cells and are primarily involved in cell-to-cell communication.

The membranes of exosomes are composed of several lipids, including cholesterol, ceramide, and sphingomyelin, and they are specifically characterized by low levels of phosphatidylserine exposure [26]. The contents of exosomes include mRNA, microRNA (miRNA), and several proteins (ranging from cytoskeletal proteins and adhesion molecules to proteins involved in signal transduction, transcription regulation, and antigen presentation) [35, 36].

Exosomes, secreted both *in vitro* and *in vivo,* are involved in intercellular communication in both physiological as well as pathological processes (i.e., cancer) [27, 37] with the following effects.

(i) Immune system modulation. Exosomes are variously involved in immune system functions and show either stimulatory or inhibitory effects, acting in antigen presentation or mediating immune tolerance [38, 39]. Exosomes constitutively released from syncytiotrophoblasts, for example, play a role in promoting fetal survival, contributing to other mechanisms that provide maternal immune tolerance of a fetus [40].

(ii) Regulation of neuronal cell functions. Some authors have suggested that exosomes from microglia may provide an effective means of intercellular neural communication, which would be very useful considering the limited motility of such cells [41]. It has also been shown that exosomes released from oligodendroglial cells seem to be involved in the trophic support of axons and to contribute to a balanced production of proteins and lipids for myelin [42].

(iii) Cancer progression. Tumor cells release exosomes, which can contribute to metastasis and cancer progression. Exosomes are involved in adhesion to the substratum, an important feature for metastatic cells [43], and in angiogenesis induction [44]; moreover, they contain and deliver prooncogenic miRNA to target cells [45]. Adipose tissue-derived mesenchymal stem cells treated with tumor-derived exosomes adopt a myofibroblast phenotype, and myofibroblasts are important tumor-supporting cells [46]; Fas-L-expressing exosomes induce apoptosis in T cells, playing a role in tumor immune evasion [39]. Exosomes are also involved in drug resistance: in drug-resistant human ovarian carcinoma cells, higher cisplatin export via exosomes has been observed [47].

MVs' membranes are characterized by high levels of phosphatidylserine, which is translocated from the inner to the outer surface leaflet [25], and their cargo includes proteins (e.g., enzymes, growth factors, growth factor receptors, cytokines, and chemokines), lipids, and nucleic acids (mRNA, miRNA, ncRNA, and genomic DNA) [48, 49]. Several studies of the molecular characterization of MVs have suggested that MVs are not simply miniature versions of the parental cells; instead, they show both similarities and differences with respect to the molecular composition of their cells of origin [25, 50]. For example, MVs from human gliomas contain a multitude of molecules that are not detectable or are expressed in different amounts in the parental cells from which they originate [49]. MVs have been widely studied both in normal cell types (including platelets, red blood cells, and endothelial cells) and, more frequently, in cancer cells [27, 51–53] for their well-established role in cancer progression. Indeed, MVs contribute to cancer progression in different ways [28], as described below.

(i) Contribution to the proinvasive characteristics of cancer cells. Tumor progression and invasion depend on the ability to modify the extracellular matrix. MVs appear to promote the proteolytic cascade required for the localized degradation of the extracellular matrix through the involvement of lytic enzymes, such as uPA, MMPs, and cathepsins, which are contained in MVs [53–57].

(ii) Apoptosis evasion. Since MVs contain caspase 3, one of the main apoptotic enzymes, it has been suggested that tumor cells may escape apoptosis by releasing MVs enriched with caspase 3, thus preventing its intracellular accumulation [58].

(iii) Induction of transformation. MVs derived from human cancer cells (e.g., breast carcinoma and glioma cells) are able to transform normal fibroblasts and epithelial cells to adopt typical cancer cell characteristics (e.g., anchorage-independent growth and enhanced survival capability) through the transfer of the tissue-transglutaminase enzyme [59].

(iv) Drug resistance. Some antitumoral drugs accumulate in MVs and are expelled through them [60].

(v) Contribution to immunoescape. MVs mediate interactions between cancer and immune cells to modulate the immune response. MVs can carry Fas ligand, resulting in T-cell apoptosis and consequently preventing their cytotoxic effects on tumor cells [61].

The fusion of MVs from human melanomas and colorectal carcinomas with monocytes inhibits differentiation and promotes immunosuppressive cytokine release [62]. MV-associated CD46, a membrane complement inhibitor, helps cancer cells to escape from complement-induced lysis [63].

(vi) Induction of angiogenesis. It is well known that tumor growth and survival depend on the formation of new blood vessels (i.e., angiogenesis) that infiltrate the tumor mass [64]. MV-associated EGFR can activate the VEGF/VEGFR pathway in endothelial cells [65]; MVs are a rich source of proangiogenic growth factors, such as VEGF, FGF-2, and proteases (e.g., uPA, MMPs, and cathepsin B) [52, 53, 66–69], and of the MMP stimulant EMMPRIN [70]. Lytic enzymes can favor angiogenesis and new vessel formation by carrying out degradation of the basal membrane and the extracellular matrix.

Therefore, despite clear differences in cell origins and size ranges, the specific functions and features of the different extracellular vesicle subpopulations are often overlapping and ambiguous; moreover, difficulties related to the available isolation techniques make it difficult to precisely separate the subpopulations of MVs, thereby preventing the investigation of their specific characteristics.

To further amplify the confusion about the identity of the vesicle subpopulations, in seminal/prostatic fluid, another population of vesicles called prostasomes is present [22]. Prostasomes are derived from the prostate gland and are present in high concentrations in seminal/prostatic fluid; they range in size from 50 to 500 nm (with a mean diameter of 150 nm) [22]. Prostasomes share origins with exosomes because they are stored in the MVBs of epithelial cells lining the acinar ducts of the prostate gland and are released after MVB fusion with the cell membrane [71]. Despite their overlapping origins, exosomes and prostasomes differ not only in size (as already mentioned) but also in composition: the membrane surrounding prostasomes has a specific composition with a higher concentration of cholesterol and sphingomyelin and a substantially high cholesterol/phospholipid ratio when compared to exosomes [22, 72, 73]. Furthermore, exosomes are usually characterized by a bilayer of membranes, whereas prostasomes can have a multilayer membrane [74]. Moreover, in prostasomes, chromosomal DNA, which appears to be absent in exosomes, has been reported [71, 75]. In addition to lipids and DNA, the cargo of prostasomes could also consist of proteins, such as enzymes, transport proteins, structural proteins, signal transduction proteins, and GTP-binding proteins [76].

It is not clear, however, whether prostasomes isolated *in vivo* from seminal/prostatic fluid correspond to vesicles that are isolated *in vitro*. Some authors state that in prostate secretion, only exosomes and prostasomes are present [77], whereas others have hypothesized that prostasomes are exosomes derived from prostate cells in biological conditions [22], and others consider them as belonging to the "exosome family" [71]. Like exosomes and MVs, prostasomes are involved in the exchange of information, specifically from prostate cells to other cells (in physiological conditions, recipient cells are mainly spermatozoa) [78]. Transfers of messages can involve several mechanisms, such as fusion or direct contact between the prostasome and the sperm cell membrane, initiating the internalization of prostasomes by the sperm cell [78]. Regarding their biological function, prostasomes seem to be involved mainly in human reproduction; they have a stimulatory effect on spermatozoa motility (showing a promotional effect), capacitation, and the acrosome reaction (i.e., having a regulatory role involving cholesterol transfer) as well as modulation of immunologic attacks (i.e., protecting spermatozoa from phagocytosis performed by the female's immune cells); they also show antioxidant capacities (reducing reactive oxygen species production, to which human spermatozoa are very sensitive) and antibacterial properties (inducing bacterial membrane deformation) [78–81]. In addition to their physiological role in reproduction, prostasomes also appear to be involved in PCa progression [78].

In fact, prostasomes are released not only from normal prostate cells but also from benign prostate tissue, prostate cancer cells, and poorly differentiated cells of prostate cancer metastases [81, 82]. It was suggested that prostasomes contributed to the development of PCa because they were observed in secretions from the prostate (a cancer with a very high incidence) but not in seminal vesicle secretion (which is, indeed, a cancer extremely rare) [78].

Several authors have suggested that some features of prostasomes that may have developed to sustain their physiological role in reproduction could also promote cancer cell survival and proliferation [83]. The following are several roles that have been proposed for prostasomes in cancer progression.

(i) Inhibition of the immune system. Prostasomes inhibit mitogen-induced proliferation in a dose-dependent manner in cytotoxic T lymphocytes; therefore, they could most likely interfere with their role (i.e., the recognition of antigens expressed on tumor cells) [84].

(ii) Inhibition of the complement system. The complement system is involved in immune surveillance against tumor development. If cancer cells are unable to protect themselves against complement attack, they will be eliminated very early during the development of cancer. The phosphorylation of C3, a component of the complement system, results in the inhibition of both the classical and alternative pathways of complement activation [85]. PCa prostasomes are characterized by higher activities of protein kinases A and C and casein kinase II when compared to prostasomes isolated from seminal plasma. Consequently, they are able to phosphorylate the C3 component, thus inhibiting the complement [86]. Cancer prostasomes also may inhibit complement through an alternative mechanism: by expressing CD59, a glycosylphosphatidylinositol-anchored protein that prevents the full assembly of the membrane-attack complex of complements, they inhibit complement-mediated lysis [87]. Again, prostasomes from cancer

cells express higher CD59 levels than those from normal cells [87].

(iii) Induction of migration. Protein kinases A and C and casein kinase contained in prostasomes from PCa are able to perform fibrinogen phosphorylation. Fibrinogen phosphorylation inhibits fibrinolysis, making fibrinogen more resistant to cleavage and thereby more available as a substrate for cancer cells, easing their migration [78]. Additionally, prostasomes from PCa express high levels of tissue factor (TF) [88], which is known for its ability to promote cell migration [89] and is also involved in cancer progression due to its ability to induce tumor angiogenesis, cell adhesion, and invasion. Consequently, prostasome-associated TF may further contribute to tumor growth [78].

(iv) Induction of invasion. Dipeptidyl peptidase IV is associated with prostasomes and is involved in the proteolytic cascade required for cancer progression through the ECM because the activation of plasminogen and expression of MMP-9 seem to depend on the activity of dipeptidyl peptidase IV [83].

(v) Induction of angiogenesis. As has already been mentioned, tissue factor is able to promote angiogenesis through FVIIa-induced VEGF expression. VEGF is a key regulator of angiogenesis due to its ability to stimulate proliferation and migration in endothelial cells [90]. Another important molecule in inducing angiogenesis is angiotensin II, which is produced from the precursor angiotensin I by the action of the angiotensin-1 converting enzyme (ACE) [91]; ACE activity is very high in seminal fluid, and it is mainly associated with the prostasomal membrane [83].

So, prostasomes, which normally have a fundamental role in physiological processes related to fertilization, might turn against the host, favoring the transition of normal cells to cancer cells. The transition from positive to negative action seems to take place at approximately 50 years of age. This is likely why a higher prevalence of PCa is observed in men over 50 years [83].

3. Extracellular Vesicles in Prostate Cancers

Similarly to other cell types, PCa cells are able to release extracellular vesicles (Figures 2 and 3). Nevertheless, only a few *in vitro* studies in the literature refer to the role played by vesicles released from the PCa cells, highlighting their roles in cell-to-cell communication in cancer progression.

A deep proteomic analysis performed on vesicles from the PC3 cell line revealed that vesicles contain numerous proteins involved in the regulation of several biological processes, ranging from transport to metabolic process, response to stimuli, and cell differentiation and communication. Many were nuclear and cytosol proteins, but numerous cytoskeleton proteins were also present. Among these proteins, CDCP1 and CD151, whose involvement in PCa has already been described, stand out as possible biomarkers considering that they were more concentrated in vesicles released by prostate cancer cells than in those released by normal epithelial prostate cells [92].

PCa-derived vesicles stimulate fibroblast activation, a fundamental requirement for the induction of a favorable niche for cancer development, by increasing their motility and protecting them from apoptosis—events that are partially due to an increase in ERK1/2 phosphorylation. Vesicles from fibroblasts thus activated are, in turn, able to induce migration and invasion in the PC3 cell line, supporting cancer pathogenicity. It seems that the chemokine receptor CX3CR1 also plays a role in this process [93].

PCa tissue releases MVs capable of degrading collagen IV and the reconstituted basal membrane Matrigel. MVs released from PC3 cells (a highly metastatic PCa cell line) have been found to enhance the adhesive and invasive capabilities of LnCaP (a poorly invasive PCa cell line) [67].

It was also suggested that vesicles from hormone-refractory PCa cells are able to induce mouse osteoblast differentiation via Ets1 contained in them, suggesting a role for vesicles in cell-to-cell communication during the osteoblastic metastasis process [94]. It is well known that in osteoblastic metastasis, a vicious circle develops between PCa cells and osteoblasts/osteoclasts, with PCa cells providing growth factors to osteoblasts and osteolytic factors (e.g., BMPs, TGF-β, IGF, FGF, PDGF, ET1, VEGF, and MMPs) that activate these cells and allow them to produce bone-derived growth factors (e.g., PDGF, BMPs, TGFβ, IGFs, and FGFs) that further induce cancer-cell stimulation [94, 95]. Moreover, the release of vesicles from PCa cells is induced from osteoblast-conditioned media, further suggesting that vesicles contribute to communication between cells in the course of this vicious circle [96].

A recent study highlights the role of vesicles in tumor microenvironment cell-to-cell communication, showing that vesicles released from the human prostate carcinoma cell line DU145 are able to induce transformation in the non-malignant human prostate epithelial cell line, as evidenced by anchorage-independent growth in soft agar which is a typical feature of malignant cells. Additionally, vesicles isolated from PCa patients with a Gleason grade of 2 have similarly been used to treat nonmalignant prostate cells and have induced soft agar colony formation. The same study, however, suggested that vesicles could potentially be used to reverse the cancer phenotype because vesicles isolated from nonmalignant cells inhibited the growth of carcinoma cells in soft agar.

PCa vesicles are also involved in drug resistance: DU145 cells, which are normally sensitive to camptothecin treatment, became resistant to camptothecin-induced apoptosis after being cocultured with vesicles isolated from the camptothecin-resistant cell line RC1. Conversely, RC1 cells, cocultured with vesicles isolated from DU145, underwent apoptosis when treated with camptothecin, suggesting the role of vesicles in mediating drug resistance. Several molecules seem to be involved in these processes, including SOCS3 and STAT3 [97].

In addition to the *in vitro* studies that have tried to understand the roles played by vesicles in cancer progression, several *in vivo* studies have been performed to understand

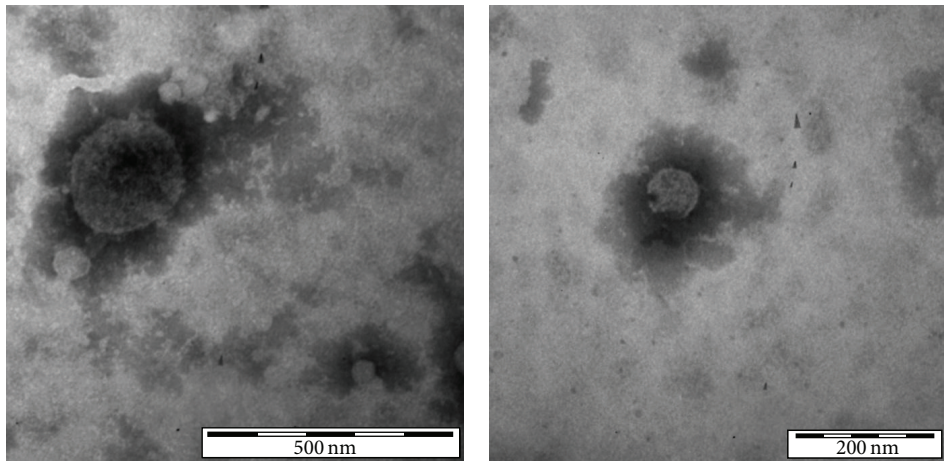

(a) (b)

Figure 2: Transmission electron micrograph of extracellular vesicles released from PC3 cells. (a) Vesicle sized 248 nm (microvesicle). (b) Vesicle sized 79 nm (exosome) (personal original unpublished data).

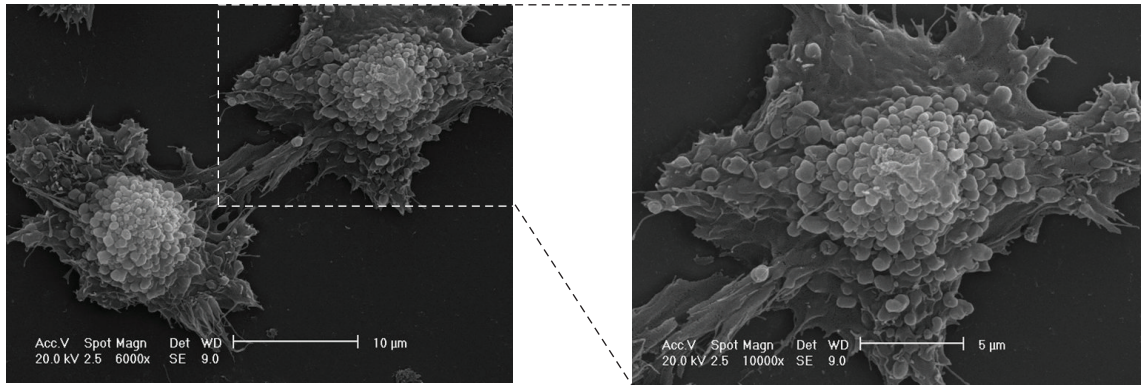

Figure 3: Scanning electron micrograph of PC3, a human prostate cancer cell line. Note the enormous release of microvesicles of heterogeneous dimensions ranging between 300 and 1,000 nm. Microvesicle shedding is visible over the entire cell body (personal original unpublished data).

whether vesicle number or some vesicle-associated molecules could be used for diagnosis and prognosis. Although PSA is currently considered the gold standard for the detection of PCa, it is important to take into account not only PSA's high organ specificity but also its lack of cancer specificity. PSA also gives no indication about the proliferation and metastatic potential of prostate cancer cells [78], hence the need to find new and more specific molecular markers to assist or replace PSA.

To this end, PCa was studied indirectly by analyzing biological fluids in a search for useful protein, DNA, and RNA markers [5]. Several emerging biomarkers have been evaluated or are being assessed for their potential use. Biomarker research looks at all useful specimens, as identified below.

(i) Prostate tissue. Tissues from PCa have been studied not only to understand PCa pathophysiology but also to find new biomarkers. The reliability of this strategy, however, is based on the correct tissue sampling: if the biopsy misses the tumor, even an optimal biomarker will fail to detect cancer [98]. Several molecules from prostate tissue are possible candidates, such as Ki-67, p53, Bcl-2, AMACR, PSMA, BMP-6, PTEN, NF-κB, CYCS, ICK, IKBKB, GAD1, CD10, and syndecan-1 [5].

(ii) Blood. Several useful techniques, ranging from ELISA to capillary electrophoresis coupled to mass spectrometry, are being studied to facilitate the accurate evaluation of plausible markers. Such studies have shown, however, that blood may present some technical problems in tissue sampling that may make it an unreliable source of biomarkers—this point follows from the fact that the amount of proteins being studied may depend on several factors (such as clotting time). Consequently, the use of serum or plasma may be more advisable [98]. Some blood markers are EPCA and PSCA; serum markers include

Crisp-3, hK2, OPG, CGA, TGF-β, hK2, IL-6, Cav-1, E-cadherin, EGFR, VEGF, von Willebrand factor, alpha-1 chymotrypsin, vilin, hepsin, neuron-specific enolase, β-catenin, and hK11 [5].

(iii) Urine. The use of urine for sampling has several obvious advantages. Samples are abundant, they are obtainable in a noninvasive way, and they have greater stability than tissue or blood samples; moreover, there are no difficulties related to sampling. Because urine can contain both exfoliated PCa cells and PCa-secreted products, it could be considered a potential source of markers for early detection [98]. Useful markers are TMPRSS2-ERG oncogenic gene fusion rearrangement, PCA3/DD3, Survivin, telomerase, Tb15, Bradeion, MCM-5, hepsin, δ-catenin, Lgals3, CFB, Apo-D, RECK, PECAM1, and others [5, 23, 99].

(iv) Seminal plasma. As with urine, seminal plasma has the advantage of being easily accessible and highly stable. Several biomarker candidates (N-acetyllactosaminide beta-1,3-N-acetylglucosaminyltransferase, prostatic acid phosphatase, stabilin-2, GTPase IMAP family member 6, and semenogelins-1 and -2) have been identified based on differential expression between PCa patients and controls [100].

The possibility of using extracellular vesicles as PCa biomarkers has generated considerable interest. Because the contents of these vesicles include a tumor-enriched repertoire of biomolecules dependent on their cellular origin, strongly related to the stimulus that triggers their release, the discovery of a disease-specific protein, lipid, or RNA associated with the vesicles could make it possible to use them as novel biological markers for prognostic and diagnostic purpose and for monitoring of the disease, not only in PCa but virtually in all types of cancers [22, 50]; indeed, several studies in this direction have been already conducted in several cancer diseases (Table 1). The findings that urine from cancer patient is characterized by elevated exosome secretion [101] and that prostasomes can be detected at higher levels in plasma from PCa patients if compared to patients with nonmalignant prostate pathologies or indolent PCa [71] further support this hypothesis. For the moment, the focus is primarily on vesicle-associated miRNA, which shows great potential in urologic cancers under diagnostic and prognostic profile [102].

miRNAs are short (19–26 nucleotides long), single-stranded, noncoding RNAs that are responsible for the regulation of gene expression at the posttranscriptional level because they inhibit mRNA translation at the initiation or elongation step, thereby blocking the translation of mRNAs into corresponding proteins [109]. Changes in miRNA expression mainly affect cell proliferation, apoptosis, differentiation, and cell-cycle regulation, thus explaining the role that miRNA plays in tumor cell survival and growth, which are undoubtedly involved in cancer development and progression [110, 111]. The consequences of changes in miRNA levels include the altered expression of target oncogenes and tumor suppressor genes. Indeed, it has been widely shown that a substantial number of miRNAs that normally act as tumor suppressors are downregulated in cancer cells, whereas miRNAs normally acting as oncogenes are expressed at higher levels in cancer cells [32, 112]. It was also demonstrated *in vitro* that associated exosomal miRNAs can downregulate their target genes in recipient cells [113].

Over the years, several miRNAs have been studied for their biological role in PCa. For example, miR-20a and miR-125b are oncogenic miRNAs that have antiapoptotic and pro-survival effects, respectively, in PCa cells. miR-221 and miR-222 contribute to cancer growth; miR-126 acts as tumor suppressor, and its loss could contribute to PCa progression. Additionally, miR-146a is a tumor suppressor [111].

Because miRNAs are attractive as potential diagnostic/prognostic PCa biomarkers and may potentially be used to monitor treatment response, their levels and profiles have been studied in PCa tissue and compared with healthy tissue [32, 102, 114]. Fifteen miRNAs have been observed to be differentially expressed in PCa and benign tissue and demonstrate up to 84% accuracy for discrimination between these categories; 10 of these 15 miRNAs (namely, miR-16, miR-31, miR-125b, miR-145, miR-149, miR-181b, miR-184, miR-205, miR-221, and miR-222) exhibit downregulation, whereas the remaining 5 (namely, miR-96, miR-182, miR-182$*$, miR-183, and miR-375) exhibit upregulation. miR-96 expression, moreover, has been associated with cancer recurrence after radical prostatectomy [115].

It is important to keep in mind that miRNAs are not only present within cells but they can also be released *in vitro* into cell culture media. Moreover, miRNAs have been identified *in vivo* in several biological fluids, such as blood, urine, breast milk, and seminal plasma [32, 116]. Although controversy has existed over whether miRNAs circulate freely or are encapsulated in vesicles, some studies have demonstrated that in biological fluids (specifically saliva and urine), the concentration of miRNAs was consistently higher in vesicles (especially exosomes) compared to the vesicle-depleted supernatant [117]. miRNAs can also be contained in apoptotic bodies and high-density lipoproteins or associated with Ago1 and Ago2 proteins; all of these forms of association are likely responsible for protecting the molecules from degradation secondary to RNase treatment [32, 102].

A large number of studies have evaluated the presence of miRNAs in serum or plasma, assessing the differences between PCa patients and healthy controls [32]. miR-375 and miR-141 have been demonstrated to be the most consistently associated with the pathological stage and Gleason score [102, 116]; their levels are higher in the serum of patients with castration-resistant prostate cancer than in the serum of low-risk, localized patients [118]. Additionally, miR-141 levels have been able to distinguish patients with prostate cancer from healthy controls [119].

Some of these studies specifically considered miRNA associated with serum-derived vesicles. Twelve miRNAs were differentially expressed in prostate cancer patients compared with controls, and the levels of 11 miRNAs were significantly increased in PCa patients with metastases compared to patients without metastases (vesicle-associated miRNA-141 and miRNA-375 were confirmed to be associated with

Table 1: Summary of some studies in which tumor EVs have been assessed for their potential clinical use in disease monitoring and diagnosis of cancer patients.

Cancer type	Evidences reported in the paper	Reference
Ovarian cancer	32 of 63 plasma samples from ovarian cancer patients contained exosomes containing claudin-4, a protein that is frequently overexpressed in ovarian cancers. Only 1 of 50 samples from control patients, instead, contained claudin-4-positive exosomes. The assay of exosomes-associated claudin-4 in blood could be useful, alone or in combination with other screening methods, for the detection of ovarian cancer.	[103]
Ovarian cancer	Exosomes purified from plasma of patients with ovarian cancer carried cancer-specific miRNAs; women with early or advanced cancer showed similar miRNAs profiles, whereas healthy women or patients with benign ovarian disease expressed very different profiles. Thus, miRNA profiles of circulating exosomes could be used as diagnostic marker.	[104]
Glioblastoma	Mutant mRNAs and miRNAs specific for gliomas can be detected in microvesicles from serum of glioblastoma patients. In 7 of 25 samples, for example, EGFRvIII was detected (the tumor-specific mutant splice variant of EGFR mRNA typical of many gliomas), but it was not found in serum exosomes from 30 control patients. Moreover, levels of miRNA-21, usually overexpressed in glioblastoma tumors, were higher in serum microvesicles from glioblastoma patients than in control patients. So, tumor-derived microvesicles could be used to obtain diagnostic information.	[49]
Bladder cancer	This pilot study showed that microvesicles from urine of cancer patients contained 8 proteins whose levels were elevated, suggesting that protein composition of microvesicles could be used in early detection of bladder cancer.	[105]
Gastric cancer	Platelet microparticles plasma levels were assessed in patient with gastric cancer. Levels were significantly higher in the patients than in the healthy controls and higher in patients with stage IV disease than those in patients with lower stages (I/II/III). Plasma levels of platelet microparticles had a high diagnostic accuracy and might be useful to identify metastatic gastric patients.	[106]
Mucinous adenocarcinomas	Microparticles from blood of patients with breast and pancreatic cancer had significantly increased levels of tissue factor (TF) compared with healthy controls. Patients with higher levels of TF and MUC1 (epithelial mucin) in MVs were associated with a lower survival rate at 3–9 month followup compared to those with low TF-activity and no MUC1 expression, suggesting the possible use of plasma vesicles in prognosis of disease.	[107]
Hormone refractory prostate cancer	In patients with hormone-refractory prostate cancer, platelet MVs levels were predictive of outcome; overall survival was significantly shorter in those patients with MVs level above the cut-off compared to those patients whose level was below it.	[108]

metastatic PCa), suggesting that circulating miRNAs could be used to diagnose and stage prostate cancer [120].

Using exosomes as biomarkers contained in urine would be even more preferable. Because urine passes through the prostate before being discharged, miRNA features in urine would reflect the status of tumor cells [102]. When compared to blood, urine offers several advantages. Particularly, the samples can be obtained in a noninvasive way and in large quantities; moreover, the composition of urine is undoubtedly less complex than that of blood, leading to easier sample analyses [32].

Apart from studies on exosome-associated miRNAs, the exosomal content from PCa patient samples has been variably evaluated.

The amount of urinary exosomes decreases after androgen deprivation therapy, and some PCa markers (specifically, PSA, PSMA, and tumor-associated marker T54) have sometimes been detected in urinary exosomes but never in healthy donor samples; in one patient, the decrease of exosomal PSA was clearly related to treatment [101]. Even if the authors admit that the future of urine-exosome analysis in PCa remains uncertain, the use of urinary exosomes could eventually be a noninvasive approach that provides clinically useful information.

RNA expression analyses in urine-derived exosomes from patients with PCa have further confirmed the possibility of using such vesicles for new methods of diagnosis. For example, exosomes from patients with high PSA levels and high Gleason scores expressed the mRNA transcript for the fusion gene TMPRSS2:ERG, whereas PCA3 was detectable in exosomes from all patients (mRNA of TMPRSS2:ERG and PCA3 being PCa biomarkers). TMPRSS2:ERG and PCA3 were not detectable in patients treated with ADT nor in medically castrated or prostatectomized patients with verified bone metastases [77]. The Nilsson study established the potential use of urine-derived exosomal mRNA to obtain

Table 2: Summary of clinical trials that assessed or are evaluating the application of EVs in anticancer therapy.

Cancer type	Phase of study	State	Purpose of clinical trials and outcome	References
Non-small-cell lung carcinoma (NSCLC)	Phase I	USA	The study intended to use exosomes carrying specific antigens to activate immune response against established tumours. Exosomes from dendritic cells (DCs) obtained through leukophoresis were collected from patients with advanced NSCLC with tumor expression of MAGE-A3 or -A4 antigens. These exosomes, loaded with specific MAGE peptides, were administrated to patients to induce immune response. This form of immunotherapy was well tolerated; in 3 of 9 patients, who had no reactivity to MAGE before immunization, an increased systemic immune response against MAGE, an increased NK cells lytic activity, and a long term stabilization of disease in some patients were observed.	[126]
Melanoma	Phase I	France	The study was intended to asses a DCs-derived exosomes based vaccination in melanoma patients; autologous exosomes pulsed with MAGE 3 peptides were used to induce the immunization in patients with melanoma at stages III and IV. The study confirmed the feasibility of exosomes production in large scale, the safety of their administration to patients, and the good tolerance in cancer patients; nevertheless, even if treatment induced minor or partial responses in some patients, no MAGE3 specific T-cell immune responses were detected in peripheral blood of the same patients.	[127]
Colorectal cancer	Phase I	China	The study wanted to assess the possibility to use exosomes in immunotherapy and reported that exosomes derived from ascites, if subcutaneously administrated with GM-CFS (granulocyte macrophage colony-stimulating factor) in patients with colorectal cancer, were able to induce an antigen-specific anticancer cytotoxic T lymphocyte response. Toxicity of exosomes was minimal and patients tolerated very well the administration.	[128]
NSCLC	Ongoing phase II	France	The study aims to assess the efficacy of a therapeutic vaccine constituted by autologous DC-derived exosomes in nonoperable and advanced NSCLC patients (stages IIIB and IV), to verify if they are able to stimulate the patients' natural defenses in order to obtain the stop of tumor progression or tumor regression.	[129]

information on tumor status. The presence of tumor-specific transcripts in vesicles, moreover, is not limited to PCa but it is also present in other cancers suggesting that tumor-specific transcripts contained in vesicles could serve for diagnostic of cancer diseases; in Ewing's sarcoma (ES), for example, it has been found that both exosomes and microvesicles contained the ES specific transcript EWS-FLI1, which is not present in healthy donors and might be useful as a noninvasive diagnostic ES marker in peripheral blood [121, 122].

The circulating levels of survivin (a member of the "inhibitor of apoptosis" family), either free or contained in serum/plasma-derived exosomes, have been found to be lower in patients with benign prostatic hyperplasia and in healthy controls when compared to PCa patients. Circulating survivin levels remain high both in subjects with low and high Gleason scores, suggesting that it may be useful as a biomarker even for the earlier detection of PCa [123].

Some studies on prostasomes have shown that they could be used as potential PCa biomarkers. Using a method called 4PLA, which is a variant of the proximity ligand assay and has high sensitivity and specificity for prostasomes, the researchers demonstrated that plasma from PCa patients contains high levels of prostasomes. Moreover, the assay seemed to be able to discriminate between patients with medium and high Gleason score from those with low Gleason score. The authors suggested that the loss of prostate epithelial cell polarity, typical of PCa, could be involved in the modification of prostasome features. This method could potentially be used for early diagnosis or for monitoring responses to treatment [34].

4. Conclusions

Over the years, many studies have been conducted to better understand the role of extracellular vesicles circulating in biological fluids in various clinical tumor conditions and their potential use as biomarkers for prognostic or diagnostic purpose or as vaccine to induce immune response [124, 125]; some clinical studies have been already conducted to evaluate the use of vesicles in this form of immunotherapy (Table 2). The other forms of clinical

application of extracellular vesicles need, instead, a further evaluation. Thus, a deeper understanding of the roles of extracellular vesicles in cell-to-cell communication and in prostate cancer biology, as well as continued expansion of the field of vesicle research, may lead to the development of extremely useful vesicular biomarkers for determining the diagnosis or prognosis of cancer. Such biomarkers may serve as valid instruments with which to assess the responses to clinical treatments. However, many questions remain about the effective role of extracellular vesicles in prostate physiological and pathological processes, and further studies are needed to clarify their usefulness as biomarkers. Furthermore, it is necessary to refine the techniques used to isolate and quantify, in blood or other biological fluids, vesicles specifically derived from tumor tissues as well as to standardize sample collection and analytical methodologies.

Abbreviations

ACE: Angiotensin-1 converting enzyme
ADT: Androgen deprivation therapy
Akt: Protein kinase B
AMACR: Alpha-methylacyl CoA racemase
Apo-D: Apolipoprotein D
Bcl-2: B-cell lymphoma 2
BMP: Bone morphogenetic protein
BPH: Benign prostatic hyperplasia
Cav-1: Caveolin 1
CFB: Complement factor B
CGA: Chromogranin A
Crisp-3: Cysteine-rich secretory protein 3
CRPC: Castrate-resistant PCa
CX3CR1: Chemokine (C-X3-C motif) receptor 1
CYCS: Cytochrome c, somatic
DCs: Dendritic cells
EGFR: Epithelial growth factor receptor
EMMPRIN: Extracellular matrix metalloproteinase inducer
EPCA: Early prostate cancer antigen
ERK-1: Extracellular regulated kinase 1
ES: Ewing's sarcoma
ET1: Endothelin 1
EWS/FLI1: Ewing's sarcoma/Friend leukemia integration 1
FGF: Fibroblast growth factor
GAD1: Glutamate decarboxylase 1
GM-CFS: Granulocyte macrophage colony-stimulating factor
GSTP1: Glutathione S-transferase p1
HDACs: Histone deacetylases
HDM: Histone demethylases
hK11: Human tissue kallikrein 11
hK2: Human kallikrein 2
HMTs: Histone methyltransferases
ICK: Intestinal cell kinase
IGF: Insulin-like growth factor
IKBKB: Inhibitor of NF-κB kinase subunit beta
IL-6: Interleukin 6
LGALS3: Lectin, galactoside-binding, soluble, 3
MAGE: Melanoma-associated antigen
MCM-5: Mini-chromosome maintenance 5
miRNA: Micro-RNA
MMPs: Matrix metalloproteinases
mTOR: Mammalian target of rapamycin
MVB: Multivesicular bodies
MVs: Microvesicles
ncRNA: Noncoding RNA
NF-κB: Nuclear factor-κB
NK: Natural killers
NSCLC: Non-small-cell lung carcinoma
OPG: Osteoprotegerin
PCa: Prostate cancer
PCA3/DD3: Prostate cancer antigen 3/differential display code 3
PDGF: Platelet-derived growth factor
PECAM1: Platelet endothelial cell adhesion molecule
PI3 K: Phosphatidylinositide 3-kinases
PSA: Prostate-specific antigen
PSCA: Prostate stem cell antigen
PSMA: Prostate-specific membrane antigen
PTEN: Phosphatase and tensin homolog
RB: Retinoblastoma
RECK: Reversion-inducing-cysteine-rich protein with kazal motifs
SOCS3: Suppressor of cytokine signaling 3
STAT3: Signal transducer and activator of transcription 3
Tb15: Thymosin beta 15
TF: Tissue factor
TGF-β: Transforming growth factor-beta
TMPRSS2-ERG: Transmembrane protease serine 2/ETS-related gene
uPA: Urokinase-type plasminogen activator
VEGF: Vascular endothelial growth factor

Conflict of Interests

The authors declare that there is no conflict of interests regarding the publication of this paper.

Acknowledgments

The authors are grateful to Dr. Marianna Di Francesco (University of L'Aquila) for performing electron microscopy on PC3 cells (scanning electron microscopy) and extracellular vesicles (transmission electron microscopy). The authors also thank Dr. Enzo Emanuele, a holder of both the M.D. and Ph.D. degrees (Living Research s.a.s., Robbio, Pavia, Italy), for his expert editorial assistance.

References

[1] C. Huggins, W. W. Scott, and J. H. Heinen, "Chemical composition of human semen and of the secretions of the prostate and

seminal vehicles," *American Journal of Physiology*, vol. 136, no. 3, pp. 467–473, 1942.

[2] R. Schrecengost and K. E. Knudsen, "Molecular pathogenesis and progression of prostate cancer," *Seminars in Oncology*, vol. 40, no. 3, pp. 244–258, 2013.

[3] W. G. Nelson, A. M. De Marzo, and W. B. Isaacs, "Prostate cancer," *The New England Journal of Medicine*, vol. 349, no. 4, pp. 366–381, 2003.

[4] N. Konishi, K. Shimada, E. Ishida, and M. Nakamura, "Molecular pathology of prostate cancer," *Pathology International*, vol. 55, no. 9, pp. 531–539, 2005.

[5] T. Bhavsar, P. McCue, and R. Birbe, "Molecular diagnosis of prostate cancer: are we up to age?" *Seminars in Oncology*, vol. 40, no. 3, pp. 259–275, 2013.

[6] V. Coppola, R. De Maria, and D. Bonci, "MicroRNAs and prostate cancer," *Endocrine-Related Cancer*, vol. 17, no. 1, pp. F1–F17, 2010.

[7] C. Jerónimo, P. J. Bastian, A. Bjartell et al., "Epigenetics in prostate cancer: biologic and clinical relevance," *European Urology*, vol. 60, no. 4, pp. 753–766, 2011.

[8] A. W. Hsing and A. P. Chokkalingam, "Prostate cancer epidemiology," *Frontiers in Bioscience*, vol. 11, no. 2, pp. 1388–1413, 2006.

[9] L. G. Gomella, J. Johannes, and E. J. Trabulsi, "Current prostate cancer treatments: effect on quality of life," *Urology*, vol. 73, no. 5, pp. S28–S35, 2009.

[10] A. W. Hsing and S. S. Devesa, "Trends and patterns of prostate cancer: what do they suggest?" *Epidemiologic Reviews*, vol. 23, no. 1, pp. 3–13, 2001.

[11] E. D. Crawford, "Epidemiology of prostate cancer," *Urology*, vol. 62, no. 6, pp. 3–12, 2003.

[12] K. Hemminki, R. Rawal, and J. L. Bermejo, "Prostate cancer screening, changing age-specific incidence trends and implications on familial risk," *International Journal of Cancer*, vol. 113, no. 2, pp. 312–315, 2005.

[13] A. Wolk, "Diet, lifestyle and risk of prostate cancer," *Acta Oncologica*, vol. 44, no. 3, pp. 277–281, 2005.

[14] A. L. Potosky, B. A. Miller, P. C. Albertsen, and B. S. Kramer, "The role of increasing detection in the rising incidence of prostate cancer," *Journal of the American Medical Association*, vol. 273, no. 7, pp. 548–552, 1995.

[15] K. McDavid, J. Lee, J. P. Fulton, J. Tonita, and T. D. Thompson, "Prostate cancer incidence and mortality rates and trends in the United States and Canada," *Public Health Reports*, vol. 119, no. 2, pp. 174–186, 2004.

[16] A. Jemal, E. Ward, X. Wu, H. J. Martin, C. C. McLaughlin, and M. J. Thun, "Geographic patterns of prostate cancer mortality and variations in access to medical care in the United States," *Cancer Epidemiology Biomarkers and Prevention*, vol. 14, no. 3, pp. 590–595, 2005.

[17] S. Loeb and W. J. Catalona, "What to do with an abnormal PSA test," *Oncologist*, vol. 13, no. 3, pp. 299–305, 2008.

[18] K. J. Pienta, "Critical appraisal of prostate-specific antigen in prostate cancer screening: 20 years later," *Urology*, vol. 73, no. 5, pp. S11–S20, 2009.

[19] M. A. Khan, A. W. Partin, H. G. Rittenhouse et al., "Evaluation of proprostate specific antigen for early detection of prostate cancer in men with a total prostate specific antigen range of 4.0 To 10.0 ng/ml," *Journal of Urology*, vol. 170, no. 3, pp. 723–726, 2003.

[20] W. J. Catalona, G. Bartsch, H. G. Rittenhouse et al., "Serum pro-prostate specific antigen preferentially detects aggressive prostate cancers in men with 2 to 4 ng/ml prostate specific antigen," *Journal of Urology*, vol. 171, no. 6, part 1, pp. 2239–2244, 2004.

[21] F. Brimo, R. Montironi, L. Egevad et al., "Contemporary grading for prostate cancer: implications for patient care," *European Urology*, vol. 63, no. 5, pp. 892–901, 2013.

[22] D. Duijvesz, T. Luider, C. H. Bangma, and G. Jenster, "Exosomes as biomarker treasure chests for prostate cancer," *European Urology*, vol. 59, no. 5, pp. 823–831, 2011.

[23] Q. Lu, J. Zhang, R. Allison et al., "Identification of extracellular δ-catenin accumulation for prostate cancer detection," *Prostate*, vol. 69, no. 4, pp. 411–418, 2009.

[24] C. Bouchardy, G. Fioretta, E. Rapiti et al., "Recent trends in prostate cancer mortality show a continuous decrease in several countries," *International Journal of Cancer*, vol. 123, no. 2, pp. 421–429, 2008.

[25] J. Rak, "Microparticles in cancer," *Seminars in Thrombosis and Hemostasis*, vol. 36, no. 8, pp. 888–906, 2010.

[26] S. Mathivanan, H. Ji, and R. J. Simpson, "Exosomes: extracellular organelles important in intercellular communication," *Journal of Proteomics*, vol. 73, no. 10, pp. 1907–1920, 2010.

[27] B. György, K. Módos, É. Pállinger et al., "Detection and isolation of cell-derived microparticles are compromised by protein complexes resulting from shared biophysical parameters," *Blood*, vol. 117, no. 4, pp. e39–e48, 2011.

[28] I. Giusti, S. D'Ascenzo, and V. Dolo, "Microvesicles as potential ovarian cancer biomarkers," *Biomed Research International*, vol. 2013, Article ID 703048, 12 pages, 2013.

[29] J. A. Schifferli, "Microvesicles are messengers," *Seminars in Immunopathology*, vol. 33, no. 5, pp. 393–394, 2011.

[30] A. K. Enjeti, L. F. Lincz, and M. Seldon, "Microparticles in health and disease," *Seminars in Thrombosis and Hemostasis*, vol. 34, no. 7, pp. 683–691, 2008.

[31] C. Théry, M. Ostrowski, and E. Segura, "Membrane vesicles as conveyors of immune responses," *Nature Reviews Immunology*, vol. 9, no. 8, pp. 581–593, 2009.

[32] N. P. Hessvik, K. Sandvig, and A. Llorente, "Exosomal miRNAs as biomarkers for prostate cancer," *Frontiers in Genetics*, vol. 4, p. 36, 2013.

[33] G. Rabinowits, C. Gerçel-Taylor, J. M. Day, D. D. Taylor, and G. H. Kloecker, "Exosomal microRNA: a diagnostic marker for lung cancer," *Clinical Lung Cancer*, vol. 10, no. 1, pp. 42–46, 2009.

[34] G. Tavoosidana, G. Ronquist, S. Darmanis et al., "Multiple recognition assay reveals prostasomes as promising plasma biomarkers for prostate cancer," *Proceedings of the National Academy of Sciences of the United States of America*, vol. 108, no. 21, pp. 8809–8814, 2011.

[35] K. Al-Nedawi, B. Meehan, J. Micallef et al., "Intercellular transfer of the oncogenic receptor EGFRvIII by microvesicles derived from tumour cells," *Nature Cell Biology*, vol. 10, no. 5, pp. 619–624, 2008.

[36] H. Valadi, K. Ekström, A. Bossios, M. Sjöstrand, J. J. Lee, and J. O. Lötvall, "Exosome-mediated transfer of mRNAs and microRNAs is a novel mechanism of genetic exchange between cells," *Nature Cell Biology*, vol. 9, no. 6, pp. 654–659, 2007.

[37] A. V. Vlassov, S. Magdaleno, R. Setterquist, and R. Conrad, "Exosomes: current knowledge of their composition, biological functions, and diagnostic and therapeuticpotentials," *Biochimica and Biophysica Acta*, vol. 1820, no. 7, pp. 940–948, 2012.

[38] A. Tan, J. Rajadas, and A. M. Seifalian, "Exosomes as a nanotheranostic delivery platforms for gene therapy," *Advanced Drug Delivery Reviews*, vol. 65, no. 3, pp. 357–367, 2013.

[39] A. J. Abusamra, Z. Zhong, X. Zheng et al., "Tumor exosomes expressing Fas ligand mediate $CD8^+$ T-cell apoptosis," *Blood Cells, Molecules, and Diseases*, vol. 35, no. 2, pp. 169–173, 2005.

[40] L. Mincheva-Nilsson and V. Baranov, "The role of placental exosomes in reproduction," *American Journal of Reproductive Immunology*, vol. 63, no. 6, pp. 520–533, 2010.

[41] I. Potolicchio, G. J. Carven, X. Xu et al., "Proteomic analysis of microglia-derived exosomes: metabolic role of the aminopeptidase CD13 in neuropeptide catabolism," *Journal of Immunology*, vol. 175, no. 4, pp. 2237–2243, 2005.

[42] E.-M. Krämer-Albers, N. Bretz, S. Tenzer et al., "Oligodendrocytes secrete exosomes containing major myelin and stress-protective proteins: trophic support for axons?" *Proteomics. Clinical Applications*, vol. 1, no. 11, pp. 1446–1461, 2007.

[43] R. B. Koumangoye, A. M. Sakwe, J. S. Goodwin, T. Patel, and J. Ochieng, "Detachment of breast tumor cells induces rapid secretion of exosomes which subsequently mediate cellular adhesion and spreading," *PLoS ONE*, vol. 6, no. 9, Article ID e24234, 2011.

[44] I. Nazarenko, S. Rana, A. Baumann et al., "Cell surface tetraspanin Tspan8 contributes to molecular pathways of exosome-induced endothelial cell activation," *Cancer Research*, vol. 70, no. 4, pp. 1668–1678, 2010.

[45] T. Kogure, W.-L. Lin, I. K. Yan, C. Braconi, and T. Patel, "Intercellular nanovesicle-mediated microRNA transfer: a mechanism of environmental modulation of hepatocellular cancer cell growth," *Hepatology*, vol. 54, no. 4, pp. 1237–1248, 2011.

[46] J. A. Cho, H. Park, E. H. Lim, and K. W. Lee, "Exosomes from breast cancer cells can convert adipose tissue-derived mesenchymal stem cells into myofibroblast-like cells," *International Journal of Oncology*, vol. 40, no. 1, pp. 130–138, 2012.

[47] R. Safaei, B. J. Larson, T. C. Cheng et al., "Abnormal lysosomal trafficking and enhanced exosomal export of cisplatin in drug-resistant human ovarian carcinoma cells," *Molecular Cancer Therapeutics*, vol. 4, no. 10, pp. 1595–1604, 2005.

[48] C. D'Souza-Schorey and J. W. Clancy, "Tumor-derived microvesicles: shedding light on novel microenvironment modulators and prospective cancer biomarkers," *Genes & Development*, vol. 26, no. 12, pp. 1287–1299, 2012.

[49] J. Skog, T. Würdinger, S. van Rijn et al., "Glioblastoma microvesicles transport RNA and proteins that promote tumour growth and provide diagnostic biomarkers," *Nature Cell Biology*, vol. 10, no. 12, pp. 1470–1476, 2008.

[50] S. F. Mause and C. Weber, "Microparticles: protagonists of a novel communication network for intercellular information exchange," *Circulation Research*, vol. 107, no. 9, pp. 1047–1057, 2010.

[51] G. Taraboletti, S. D'Ascenzo, P. Borsotti, R. Giavazzi, A. Pavan, and V. Dolo, "Shedding of the matrix metalloproteinases MMP-2, MMP-9, and MT1-MMP as membrane vesicle-associated components by endothelial cells," *American Journal of Pathology*, vol. 160, no. 2, pp. 673–680, 2002.

[52] V. Dolo, S. D'Ascenzo, I. Giusti, D. Millimaggi, G. Taraboletti, and A. Pavan, "Shedding of membrane vesicles by tumor and endothelial cells," *Italian Journal of Anatomy and Embryology*, vol. 110, no. 2, pp. 127–133, 2005.

[53] I. Giusti, S. D'Ascenzo, D. Millimaggi et al., "Cathepsin B mediates the pH-dependent proinvasive activity of tumor-shed microvesicles," *Neoplasia*, vol. 10, no. 5, pp. 481–488, 2008.

[54] Y. A. DeClerck and W. E. Laug, "Cooperation between matrix metalloproteinases and the plasminogen activator-plasmin system in tumor progression," *Enzyme and Protein*, vol. 49, no. 1–3, pp. 72–84, 1996.

[55] A. Ginestra, M. D. La Placa, F. Saladino, D. Cassarà, H. Nagase, and M. L. Vittorelli, "The amount and proteolytic content of vesicles shed by human cancer cell lines correlates with their *in vitro* invasiveness," *Anticancer Research*, vol. 18, no. 5A, pp. 3433–3437, 1998.

[56] J. M. Inal, E. A. Ansa-Addo, D. Stratton et al., "Microvesicles in health and disease," *Archivum Immunologiae et Therapiae Experimentalis*, vol. 60, no. 2, pp. 107–121, 2012.

[57] L. E. Graves, E. V. Ariztia, J. R. Navari, H. J. Matzel, M. S. Stack, and D. A. Fishman, "Proinvasive properties of ovarian cancer ascites-derived membrane vesicles," *Cancer Research*, vol. 64, no. 19, pp. 7045–7049, 2004.

[58] F. F. van Doormaal, A. Kleinjan, M. Di Nisio, H. R. Büller, and R. Nieuwland, "Cell-derived microvesicles and cancer," *Netherlands Journal of Medicine*, vol. 67, no. 7, pp. 266–273, 2009.

[59] M. A. Antonyak, B. Li, L. K. Boroughs et al., "Cancer cell-derived microvesicles induce transformation by transferring tissue transglutaminase and fibronectin to recipient cells," *Proceedings of the National Academy of Sciences of the United States of America*, vol. 108, no. 12, pp. 4852–4857, 2011.

[60] K. Shedden, X. T. Xie, P. Chandaroy, Y. T. Chang, and G. R. Rosania, "Expulsion of small molecules in vesicles shed by cancer cells: association with gene expression and chemosensitivity profiles," *Cancer Research*, vol. 63, no. 15, pp. 4331–4337, 2003.

[61] J. W. Kim, E. Wieckowski, D. D. Taylor, T. E. Reichert, S. Watkins, and T. L. Whiteside, "Fas ligand-positive membranous vesicles isolated from sera of patients with oral cancer induce apoptosis of activated T lymphocytes," *Clinical Cancer Research*, vol. 11, no. 3, pp. 1010–1020, 2005.

[62] R. Valenti, V. Huber, M. Iero, P. Filipazzi, G. Parmiani, and L. Rivoltini, "Tumor-released microvesicles as vehicles of immunosuppression," *Cancer Research*, vol. 67, no. 7, pp. 2912–2915, 2007.

[63] M. B. Whitlow and L. M. Klein, "Response of SCC-12F, a human squamous cell carcinoma cell line, to complement attack," *Journal of Investigative Dermatology*, vol. 109, no. 1, pp. 39–45, 1997.

[64] P. Carmeliet, "Angiogenesis in life, disease and medicine," *Nature*, vol. 438, no. 7070, pp. 932–936, 2005.

[65] K. Al-Nedawi, B. Meehan, R. S. Kerbel, A. C. Allison, and A. Rak, "Endothelial expression of autocrine VEGF upon the uptake of tumor-derived microvesicles containing oncogenic EGFR," *Proceedings of the National Academy of Sciences of the United States of America*, vol. 106, no. 10, pp. 3794–3799, 2009.

[66] V. Dolo, A. Ginestra, G. Ghersi, H. Nagase, and M. L. Vittorelli, "Human breast carcinoma cells cultured in the presence of serum shed membrane vesicles rich in gelatinolytic activities," *Journal of Submicroscopic Cytology and Pathology*, vol. 26, no. 2, pp. 173–180, 1994.

[67] A. Angelucci, S. D'Ascenzo, C. Festuccia et al., "Vesicle-associated urokinase plasminogen activator promotes invasion in prostate cancer cell lines," *Clinical and Experimental Metastasis*, vol. 18, no. 2, pp. 163–170, 2000.

[68] T. H. Lee, E. D'Asti, N. Magnus, K. Al-Nedawi, B. Meehan, and J. Rak, "Microvesicles as mediators of intercellular communication in cancer—the emerging science of cellular 'debris'," *Seminars in Immunopathology*, vol. 33, no. 5, pp. 455–467, 2011.

[69] G. Taraboletti, S. D'Ascenzo, I. Giusti et al., "Bioavailability of VEGF in tumor-shed vesicles depends on vesicle burst induced by acidic pH 1," *Neoplasia*, vol. 8, no. 2, pp. 96–103, 2006.

[70] D. Millimaggi, M. Mari, S. D'Ascenzo et al., "Tumor vesicle-associated CD147 modulates the angiogenic capability of endothelial cells," *Neoplasia*, vol. 9, no. 4, pp. 349–357, 2007.

[71] G. K. Ronquist, A. Larsson, A. Stavreus-Evers, and G. Ronquist, "Prostasomes are heterogeneous regarding size and appearance but affiliated to one DNA-containing exosome family," *Prostate*, 2012.

[72] G. Arienti, E. Carlini, A. Polci, E. V. Cosmi, and C. A. Palmerini, "Fatty acid pattern of human prostasome lipid," *Archives of Biochemistry and Biophysics*, vol. 358, no. 2, pp. 391–395, 1998.

[73] G. Arvidson, G. Ronquist, G. Wikander, and A.-C. Ojteg, "Human prostasome membranes exhibit very high cholesterol/phospholipid ratios yielding high molecular ordering," *Biochimica et Biophysica Acta*, vol. 984, no. 2, pp. 167–173, 1989.

[74] M. Stridsberg, R. Fabiani, A. Lukinius, and G. Ronquist, "Prostasomes are neuroendocrine-like vesicles in human semen," *Prostate*, vol. 29, no. 5, pp. 287–295, 1996.

[75] I. Olsson and G. Ronquist, "Nucleic acid association to human prostasomes," *Archives of Andrology*, vol. 24, no. 1, pp. 1–10, 1990.

[76] A. G. Utleg, E. C. Yi, T. Xie et al., "Proteomic analysis of human prostasomes," *Prostate*, vol. 56, no. 2, pp. 150–161, 2003.

[77] J. Nilsson, J. Skog, A. Nordstrand et al., "Prostate cancer-derived urine exosomes: a novel approach to biomarkers for prostate cancer," *British Journal of Cancer*, vol. 100, no. 10, pp. 1603–1607, 2009.

[78] G. Ronquist, "Prostasomes are mediators of intercellular communication: from basic research to clinical implications," *Journal of Internal Medicine*, vol. 271, no. 4, pp. 400–413, 2012.

[79] B. Stegmayr and G. Ronquist, "Promotive effect on human sperm progressive motility by prostasomes," *Urological Research*, vol. 10, no. 5, pp. 253–257, 1982.

[80] N. L. Cross and P. Mahasreshti, "Prostasome fraction of human seminal plasma prevents sperm from becoming acrosomally responsive to the agonist progesterone," *Systems Biology in Reproductive Medicine*, vol. 39, no. 1, pp. 39–44, 1997.

[81] G. Sahlén, A. Ahlander, A. Frost, G. Ronquist, B. J. Norlén, and B. O. Nilsson, "Prostasomes are secreted from poorly differentiated cells of prostate cancer metastases," *Prostate*, vol. 61, no. 3, pp. 291–297, 2004.

[82] B. O. Nilsson, L. Egevad, M. Jin, G. Ronquist, and C. Busch, "Distribution of prostasomes in neoplastic epithelial prostate cells," *Prostate*, vol. 39, pp. 36–40, 1999.

[83] G. Ronquist and B. O. Nilsson, "The Janus-faced nature of prostasomes: their pluripotency favours the normal reproductive process and malignant prostate growth," *Prostate Cancer and Prostatic Diseases*, vol. 7, no. 1, pp. 21–31, 2004.

[84] R. W. Kelly, P. Holland, G. Sibrinski et al., "Extracellular organelles (prostasomes) are immunosuppressive components of human semen," *Clinical and Experimental Immunology*, vol. 86, no. 3, pp. 550–556, 1991.

[85] P. O. Forsberg -., S. C. Martin, B. Nilsson, P. Ekman, U. R. Nilsson, and L. Engstrom, "*In vitro* phosphorylation of human complement factor C3 by protein kinase A and protein kinase C. Effects on the classical and alternative pathways," *Journal of Biological Chemistry*, vol. 265, no. 5, pp. 2941–2946, 1990.

[86] A. A. Babiker, G. Ronquist, B. Nilsson, and K. N. Ekdahl, "Overexpression of ecto-protein kinases in prostasomes of metastatic cell origin," *Prostate*, vol. 66, no. 7, pp. 675–686, 2006.

[87] A. A. Babiker, B. Nilsson, G. Ronquist, L. Carlsson, and K. N. Ekdahl, "Transfer of functional prostasomal CD59 of metastatic prostatic cancer cell origin protects cells against complement attack," *Prostate*, vol. 62, no. 2, pp. 105–114, 2005.

[88] J. A. Fernández, M. J. Heeb, K.-P. Radtke, and J. H. Griffin, "Potent blood coagulant activity of human semen due to prostasome-bound tissue factor," *Biology of Reproduction*, vol. 56, no. 3, pp. 757–763, 1997.

[89] Y. Sato, Y. Asada, K. Marutsuka, K. Hatakeyama, and A. Sumiyoshi, "Tissue factor induces migration of cultured aortic smooth muscle cells," *Thrombosis and Haemostasis*, vol. 75, no. 3, pp. 389–392, 1996.

[90] V. Ollivier, J. Chabbat, J. M. Herbert, J. Hakim, and D. De Prost, "Vascular endothelial growth factor production by fibroblasts in response to factor VIIa binding to tissue factor involves thrombin and factor Xa," *Arteriosclerosis, Thrombosis, and Vascular Biology*, vol. 20, no. 5, pp. 1374–1381, 2000.

[91] S. C. Heffelfinger, "The renin angiotensin system in the regulation of angiogenesis," *Current Pharmaceutical Design*, vol. 13, no. 12, pp. 1215–1229, 2007.

[92] K. Sandvig and A. Llorente, "Proteomic analysis of microvesicles released by the human prostate cancer cell line PC-3," *Molecular & Cellular Proteomics*, vol. 11, no. 7, Article ID M111.012914, 2012.

[93] D. Castellana, F. Zobairi, M. C. Martinez et al., "Membrane microvesicles as actors in the establishment of a favorable prostatic tumoral niche: a role for activated fibroblasts and CX3CL1-CX3CR1 axis," *Cancer Research*, vol. 69, no. 3, pp. 785–793, 2009.

[94] T. Itoh, Y. Ito, Y. Ohtsuki et al., "Microvesicles released from hormone-refractory prostate cancer cells facilitate mouse preosteoblast differentiation," *Journal of Molecular Histology*, pp. 1–7, 2012.

[95] M. Clemons, K. A. Gelmon, K. I. Pritchard, and A. H. Paterson, "Bone targeted agents and skeletal-related events in breast cancer patients with bone metastases: the state of the art," *Current Oncology*, vol. 19, no. 5, pp. 259–268, 2012.

[96] D. Millimaggi, C. Festuccia, A. Angelucci et al., "Osteoblast-conditioned media stimulate membrane vesicle shedding in prostate cancer cells," *International Journal of Oncology*, vol. 28, no. 4, pp. 909–914, 2006.

[97] K. Panagopoulos, S. Cross-Knorr, C. Dillard et al., "Reversal of chemosensitivity and induction of cell malignancy of a non-malignant prostate cancer cell line upon extracellular vesicle exposure," *Molecular Cancer*, vol. 12, no. 1, p. 118, 2013.

[98] E. Schiffer, "Biomarkers for prostate cancer," *World Journal of Urology*, vol. 25, no. 6, pp. 557–562, 2007.

[99] M. Chen, K. Wang, L. Zhang, C. Li, and Y. Yang, "The discovery of putative urine markers for the specific detection of prostate tumor by integrative mining of public genomic profiles," *PLoS ONE*, vol. 6, no. 12, Article ID e28552, 2011.

[100] J. Neuhaus, E. Schiffer, P. von Wilcke et al., "Seminal plasma as a source of prostate cancer peptide biomarker candidates for detection of indolent and advanced disease," *PLoS ONE*, vol. 8, no. 6, Article ID e67514, 2013.

[101] P. J. Mitchell, J. Welton, J. Staffurth et al., "Can urinary exosomes act as treatment response markers in prostate cancer?" *Journal of Translational Medicine*, vol. 7, article 4, 2009.

[102] X. Huang, M. Liang, R. Dittmar, and L. Wang, "Extracellular microRNAs in urologic malignancies: chances and challenges," *International Journal of Molecular Sciences*, vol. 14, no. 7, pp. 14785–14799, 2013.

[103] J. Li, C. A. Sherman-Baust, M. Tsai-Turton, R. E. Bristow, R. B. Roden, and P. J. Morin, "Claudin-containing exosomes in the peripheral circulation of women with ovarian cancer," *BMC Cancer*, vol. 9, p. 244, 2009.

[104] D. D. Taylor and C. Gercel-Taylor, "MicroRNA signatures of tumor-derived exosomes as diagnostic biomarkers of ovarian cancer," *Gynecologic Oncology*, vol. 110, no. 1, pp. 13–21, 2008.

[105] D. M. Smalley, N. E. Sheman, K. Nelson, and D. Theodorescu, "Isolation and identification of potential urinary microparticle biomarkers of bladder cancer," *Journal of Proteome Research*, vol. 7, no. 5, pp. 2088–2096, 2008.

[106] H. K. Kim, K. S. Song, Y. S. Park et al., "Elevated levels of circulating platelet microparticles, VEGF, IL-6 and RANTES in patients with gastric cancer: possible role of a metastasis predictor," *European Journal of Cancer*, vol. 39, no. 2, pp. 184–191, 2003.

[107] M. E. T. Tesselaar, F. P. H. T. M. Romijn, I. K. Van Der Linden, F. A. Prins, R. M. Bertina, and S. Osanto, "Microparticle-associated tissue factor activity: a link between cancer and thrombosis?" *Journal of Thrombosis and Haemostasis*, vol. 5, no. 3, pp. 520–527, 2007.

[108] D. Helley, E. Banu, A. Bouziane et al., "Platelet microparticles: a potential predictive factor of survival in hormone-refractory prostate cancer patients treated with docetaxel-based chemotherapy," *European Urology*, vol. 56, no. 3, pp. 479–485, 2009.

[109] T. P. Chendrimada, K. J. Finn, X. Ji et al., "MicroRNA silencing through RISC recruitment of eIF6," *Nature*, vol. 447, no. 7146, pp. 823–828, 2007.

[110] L. He and G. J. Hannon, "MicroRNAs: small RNAs with a big role in gene regulation," *Nature Reviews Genetics*, vol. 5, no. 7, pp. 522–531, 2004.

[111] X.-B. Shi, C. G. Tepper, and R. W. D. White, "microRNAs and prostate cancer," *Journal of Cellular and Molecular Medicine*, vol. 12, no. 5A, pp. 1456–1465, 2008.

[112] X. Chen, Y. Ba, L. Ma et al., "Characterization of microRNAs in serum: a novel class of biomarkers for diagnosis of cancer and other diseases," *Cell Research*, vol. 18, no. 10, pp. 997–1006, 2008.

[113] A. Montecalvo, A. T. Larregina, W. J. Shufesky et al., "Mechanism of transfer of functional microRNAs between mouse dendritic cells via exosomes," *Blood*, vol. 119, no. 3, pp. 756–766, 2012.

[114] J. Szczyrba, E. Löprich, S. Wach et al., "The microRNA profile of prostate carcinoma obtained by deep sequencing," *Molecular Cancer Research*, vol. 8, no. 4, pp. 529–538, 2010.

[115] A. Schaefer, M. Jung, H.-J. Mollenkopf et al., "Diagnostic and prognostic implications of microRNA profiling in prostate carcinoma," *International Journal of Cancer*, vol. 126, no. 5, pp. 1166–1176, 2010.

[116] J. C. Brase, M. Johannes, T. Schlomm et al., "Circulating miRNAs are correlated with tumor progression in prostate cancer," *International Journal of Cancer*, vol. 128, no. 3, pp. 608–616, 2011.

[117] A. Gallo, M. Tandon, I. Alevizos, and G. G. Illei, "The majority of microRNAs detectable in serum and saliva is concentrated in exosomes," *PLoS ONE*, vol. 7, no. 3, Article ID e30679, 2012.

[118] H. C. Nguyen, W. Xie, M. Yang et al., "Expression differences of circulating microRNAs in metastatic castration resistant prostate cancer and low-risk, localized prostate cancer," *Prostate*, vol. 73, no. 4, pp. 346–354, 2013.

[119] P. S. Mitchell, R. K. Parkin, E. M. Kroh et al., "Circulating microRNAs as stable blood-based markers for cancer detection," *Proceedings of the National Academy of Sciences of the United States of America*, vol. 105, no. 30, pp. 10513–10518, 2008.

[120] R. J. Bryant, T. Pawlowski, J. W. F. Catto et al., "Changes in circulating microRNA levels associated with prostate cancer," *British Journal of Cancer*, vol. 106, no. 4, pp. 768–774, 2012.

[121] I. V. Miller, G. Raposo, U. Welsch et al., "First identification of Ewing's sarcoma-derived extracellular vesicles and exploration of their biological andpotential diagnostic implications," *Biology of the Cell*, vol. 105, no. 7, pp. 289–303, 2013.

[122] M. Tsugita, N. Yamada, S. Noguchi et al., "Ewing sarcoma cells secrete EWS/Fli-1 fusion mRNA via microvesicles," *PLoS ONE*, vol. 8, no. 10, Article ID e77416, 2013.

[123] S. Khan, J. M. Jutzy, M. M. Valenzuela et al., "Plasma-derived exosomal survivin, a plausible biomarker for early detection of prostate cancer," *PLoS ONE*, vol. 7, no. 10, Article ID e46737, 2012.

[124] E. van der Pol, A. N. Boing, P. Harrison, A. Sturk, and R. Nieuwland, "Classification, functions, and clinical relevance of extracellular vesicles," *Pharmacological Reviews*, vol. 64, no. 3, pp. 676–705, 2012.

[125] N. Chaput and C. Théry, "Exosomes: immune properties and potential clinical implementations," *Seminars in Immunopathology*, vol. 33, no. 5, pp. 419–440, 2011.

[126] M. A. Morse, J. Garst, T. Osada et al., "A phase I study of dexosome immunotherapy in patients with advanced non-small cell lung cancer," *Journal of Translational Medicine*, vol. 3, article 9, 2005.

[127] B. Escudier, T. Dorval, N. Chaput et al., "Vaccination of metastatic melanoma patients with autologous dendritic cell (DC) derived-exosomes: results of the first phase 1 clinical trial," *Journal of Translational Medicine*, vol. 3, article 10, 2005.

[128] S. Dai, D. Wei, Z. Wu et al., "Phase I clinical trial of autologous ascites-derived exosomes combined with GM-CSF for colorectal cancer," *Molecular Therapy*, vol. 16, no. 4, pp. 782–790, 2008.

[129] S. Viaud, C. Théry, S. Ploix et al., "Dendritic cell-derived exosomes for cancer immunotherapy: what's next?" *Cancer Research*, vol. 70, no. 4, pp. 1281–1285, 2010.

Hindawi Publishing Corporation
BioMed Research International
Volume 2014, Article ID 627510, 16 pages
http://dx.doi.org/10.1155/2014/627510

Review Article

The Role of Single Nucleotide Polymorphisms in Predicting Prostate Cancer Risk and Therapeutic Decision Making

Thomas Van den Broeck,[1,2] Steven Joniau,[1] Liesbeth Clinckemalie,[2] Christine Helsen,[2] Stefan Prekovic,[2] Lien Spans,[2] Lorenzo Tosco,[1] Hendrik Van Poppel,[1] and Frank Claessens[2]

[1] *Department of Urology, University Hospitals Leuven, Herestraat 49, 3000 Leuven, Belgium*
[2] *Laboratory of Molecular Endocrinology, Department of Cellular and Molecular Medicine, KU Leuven, Campus Gasthuisberg O&N1, P.O. Box 901, Herestraat 49, 3000 Leuven, Belgium*

Correspondence should be addressed to Frank Claessens; frank.claessens@med.kuleuven.be

Received 6 December 2013; Accepted 7 January 2014; Published 19 February 2014

Academic Editor: Giovanni Luca Gravina

Prostate cancer (PCa) is a major health care problem because of its high prevalence, health-related costs, and mortality. Epidemiological studies have suggested an important role of genetics in PCa development. Because of this, an increasing number of single nucleotide polymorphisms (SNPs) had been suggested to be implicated in the development and progression of PCa. While individual SNPs are only moderately associated with PCa risk, in combination, they have a stronger, dose-dependent association, currently explaining 30% of PCa familial risk. This review aims to give a brief overview of studies in which the possible role of genetic variants was investigated in clinical settings. We will highlight the major research questions in the translation of SNP identification into clinical practice.

1. Introduction

Prostate cancer (PCa) is a major health care problem because of its high prevalence, health-related costs, and mortality. Even though most patients have clinically localized and indolent tumors at diagnosis, worldwide, this disease still holds second place in the leading causes of cancer deaths [1]. Despite its prevalence, lethality, and socioeconomic burden, there are still many diagnostic and therapeutic challenges in the PCa field. This is mainly due to the lack of cancer- and/or patient-specific biomarkers, currently limiting patient-tailored diagnostics/therapeutics in PCa.

Age, race, and family history remain primary risk factors for the development of PCa. It has been shown that PCa is one of the most heritable cancers with epidemiological studies suggesting the role of genetics in PCa development [2, 3].

Due to the latter, there has been an increasing focus on the role of single nucleotide polymorphisms (SNPs) in the development and progression of PCa but also on their role in diagnostics and risk prediction. A SNP is a DNA sequence variation occurring when a single nucleotide (A, T, C, or G) in the genome differs from the normally expected nucleotide. These SNPs are known to underlie differences in our susceptibility to diseases. SNPs need to be determined only once and are easy to determine, making them interesting biomarkers. The rising interest in the role of SNPs in PCa development and progression is illustrated by the number of studies being published on SNPs in the PCa field.

In 2008, an extensive genome-wide association study (GWAS) compared SNPs between PCa cases and controls. Since then, numerous GWAS studies have been conducted [4–26]. While many SNPs were only moderately associated with PCa risk, in combination, they had a stronger, dose-dependent (i.e., cumulative effect of number of SNPs) association. A total of 77 susceptibility loci are currently explaining approximately 30% of the familial risk [6]. With ongoing GWAS, we could expect that more genetic variants will be found, explaining more of the PCa familial risk. However, the question has been raised whether finding more PCa risk-associated SNPs will have added value over the currently known ones [27].

Many SNPs are connected to each other through "linkage disequilibrium," which is a nonrandom association of alleles at two or more loci, descendant from a single, ancestral

chromosome. However, the SNPs detected through GWAS studies are mostly limited to "index SNPs," excluding other SNPs which are in linkage disequilibrium. Clearly, these index SNPs are not necessarily the SNPs causative for its associated phenotype (i.e., PCa risk, risk of progression, etc). Therefore, molecular analyses will be needed to identify the exact SNP within each linkage domain which is the causative SNP. SNPs that lie within an open reading frame can lead to changes in messenger RNA stability or translation efficiency, as well as changes in structure/activity of the encoded proteins. However, most SNPs are located outside of the genes and are suspected to affect gene expression levels and genome/chromatin organization. Therefore, it is interesting to determine the role of these SNPs in the clinical field. This review aims to give a selected overview of studies on the possible role of genetic variants in clinical practice. We will highlight diagnostic and therapeutic obstacles which are currently major issues in clinical practice.

2. Evidence Synthesis

2.1. Early Detection. To detect PCa in its early stages, currently, clinicians are limited to serum PSA level measurements as a marker, which lacks sensitivity and specificity. Therefore, PSA screening (defined as mass screening of asymptomatic men) has been heavily debated. Two prospective studies (The Prostate, Lung, Colorectal, and Ovarian (PLCO) Cancer Screening Trial and The European Randomized Study of Screening for Prostate Cancer (ERSPC)) have contributed greatly to this discussion. The PLCO study concluded that PCa-related mortality did not significantly differ between patients being screened or not [3]. The ERSPC study inferred that, based on PSA-based PCa detection, 1410 men would need to be screened and 48 additional cases of PCa would need to be treated to prevent one death from PCa, resulting in a high rate of over diagnosis [28].

In reaction to these recent results, the US Preventive Services Task Force has radically recommended against PSA-based screening [29]. However, they ignored the 50% reduction in PCa-specific mortality since the introduction of PSA [28, 30]. Moreover, without PSA testing, most men would only be diagnosed when they become symptomatic, when the disease is often too far advanced to cure. Therefore, the current EAU guidelines recommend opportunistic screening to the well-informed man [31]. Furthermore, there is an urgent need for the development of novel biomarkers.

2.1.1. Opportunistic Screening. Despite the EAU guidelines' recommendation on opportunistic PSA screening, the question remains which patients would benefit the most? Rephrased, we could ask ourselves which men are at an elevated risk of PCa? Since epidemiological studies have suggested a role of genetics in PCa development, it seems tempting to speculate that genetic variations could be of interest in predicting patients' risk of PCa in clinical practice [3]. Using this, clinicians could determine which patients would benefit from PSA screening or in which patient group they should have a low threshold of performing prostate biopsies. Currently, these risk associations, detected by GWAS studies, are of limited clinical utility because the risk prediction is based on comparing groups of people. This allows for patient stratification into "risk groups," having an x-fold greater PCa risk relative to the population average. However, for the clinician, it is of greater interest to be able to calculate a patient's absolute risk to develop PCa at a certain given point based on an individual's information.

Evaluating the efficiency of detecting PCa using a model based on family history, age, and genetic variation, Zheng et al. suggested comparable efficiency in detecting PCa when compared to the predictive power of PSA level cutoff of 4.1 ng/mL (see Table 1 for an overview of all SNPs cited in this paper) [32]. At first sight, this would seem irrelevant, since the efficiency of PSA testing itself is low. However, the economic burden of genetic testing could potentially be much lower, since this should only be determined once, whereas PSA levels fluctuate over time and often require multiple testing. The combined predictive performance of PSA plus genetic testing on PCa diagnostics unfortunately did not improve diagnostics once age, PSA level, and family history were known [32, 33].

Indeed, it was argued that SNPs are not good at discriminating cases from controls but might be of better use in identifying men at high risk of PCa [34]. In light of this, Xu et al. developed a prediction model of absolute risk for PCa at a specific age based on the sum of 14 SNPs and family history [35]. Using this model, one could identify a small subset (0.5–1%) of individuals at very high risk (41% and 52% absolute risk in a US and Swedish population) of developing PCa between 55 and 74 years of age. Sun et al. studied the performance of three sets of PCa risk SNPs in predicting PCa, showing that they are efficient at discriminating men who have a considerably elevated risk for PCa (a two- and threefold increase when compared to the population median risk) [36].

These risk predictions seem to have the highest impact in young patients with a family history of PCa [37, 38]. This seems logical, since one is born with a certain inheritable subset of SNPs, which do not change throughout one's life. Therefore, it could be expected that their effects would present in the earlier stages of life. Macinnis et al. developed a risk prediction algorithm for familial PCa, using 26 common variants, predicting the cumulative PCa risk depending on family history (from incidental PCa to highly burdened PCa families) and the number of SNPs (expressed in percentile of a SNP profile) [38].

Generalized, the future role of SNP genotyping in PCa screening seems to lie in detecting men at high risk of (aggressive) disease. Men with a higher likelihood of (aggressive) PCa may choose to begin PCa screening at an earlier age and/or more frequently. They may also pursue preventative measures, including diet/lifestyle intervention and chemoprevention.

It has been estimated that, when compared to age-specific screening, personalized screening would result in 16% fewer men being eligible for screening at a cost of 3% fewer screen-detectable cases [39]. Importantly, SNPs can be determined with high accuracy, at low cost and at any age, which make

Table 1: Listing all the SNPs being discussed in the referred papers.

First author, year [ref.]	Gene(s)/loci investigated	*N*	Endpoint	Significant SNPs	Conclusion
Xu (2009) [35]	8q24, 17q12, 3p12, 7p15, 7q21, 9q33, 10q11, 11q13, 17q24, 22q13, Xp11	4674, 2329	PCa risk prediction	—	A risk prediction model, based on the number of risk alleles of 14 SNPs and family history, can predict a patients' absolute PCa risk.
Sun (2011) [36]	—	4621	PCa risk prediction	rs16901979, rs6983267, rs1447295, rs4430796, rs1855962, rs2660753, rs10486567, rs10993994, rs10896449, rs5945619, rs1465618, rs721048, rs12621278, rs10934853, rs17021918, rs7679673, rs9364554, rs2928679, rs1512268, rs16902094, rs920861, rs4962416, rs7127900, rs12418451, rs8102476, rs2735839, rs5759167	Genetic risk prediction models are interesting to identify a subset of high-risk men at early, curable stage
Salinas (2009) [33]	17q12, 17q24.3, 8q24	2574	PCa risk prediction	rs4430796, rs1859962, rs6983561, rs6983267, rs1447295	Genotyping for five SNPs plus family history is associated with a significant elevation in risk for prostate cancer. They do not improve prediction models for assessing who is at risk of getting or dying from the disease
Lindström (2012) [37]	EHBP1, THADA, ITGA6, EEFSEC, PDLIM5, TET2, SLC22A3, JAZF1, LMTK2, NKX3-1, SLC25A37, CPNE3, CNGB3, MSMB, CTBP2, TCF2, KLK3, BIK, NUDT11	15161	PCa risk prediction	rs721048, rs1465618, rs12621278, rs2660753, rs4857841, rs17021918, rs12500426, rs7679673, rs9364554, rs10486567, rs6465657, rs6465657, rs1512268, rs2928679, rs4961199, rs1016343, rs7841060, rs16901979, rs620861, rs6983267, rs1447295, rs4242382, rs7837688, rs16902094, rs1571801, rs10993994, rs4962416, rs7127900, rs12418451, rs7931342, rs10896449, rs11649743, rs4430796, rs7501939, rs1859962, rs266849, rs2735839, rs5759167, rs5945572, rs5945619	Incorporating genetic information and family history in prostate cancer risk models can be useful for identifying younger men that might benefit from prostate-specific antigen screening
Macinnis (2011) [38]	—	2885	PCa risk prediction	rs721048, rs1465618, rs12621278, rs2660753, rs17021918, rs12500426, rs7679673, rs9364554, rs10486567, rs6465657, rs10505483, rs6983267, rs1447295, rs2928679, rs1512268, rs10086908, rs620861, rs10993994, rs4962416, rs7931342, rs7127900, rs4430796, rs1859962, rs2735839, rs5759167, rs5945619	The authors developed a risk prediction algorithm for familial prostate cancer, taking into account genotyping of 26 SNPs and family history. The algorithm can be used on pedigrees of an arbitrary size or structure

Table 1: Continued.

First author, year [ref.]	Gene(s)/loci investigated	*N*	Endpoint	Significant SNPs	Conclusion
Zheng (2009) [32]	3p12, 7q15, 7q21, 8q24, 9q33, 10q11, 10q13, 17q12, 17q24.3, Xp11	4674	PCa risk prediction	rs2660753, rs10486567, rs6465657, rs16901979, rs6983267, rs1447295, rs1571801, rs10993994, rs10896449, rs4430796, rs1859962, rs5945619C	The predictive performance for prostate cancer using these genetic variants, family history, and age is similar to that of PSA levels
Loeb (2009) [48]	—	1806	Personalized PSA testing	rs10993994, rs2735839, rs2659056	Genotype influences the risk of prostate cancer per unit increase in prostate-specific antigen. Combined use could improve prostate specific antigen test performance
Helfand (2013) [49]	—	964	Personalized PSA testing	rs2736098, rs10788160, rs11067228, rs17632542	Genotyping can be used to adjust a man's measured prostate-specific antigen concentration and potentially delay or prevent unnecessary prostate biopsies
Klein (2012) [40]	JAZF1, MYC, MSMB, NCOA4, IGF2, INS, TH, TPCN2, MYEOV, HNF1B, DPF1, PPP1R14A, SPINT2, KLK3, TTLL1, BIK, NUDT11	3772	PCa risk prediction	rs10486567, rs11228565, rs17632542, rs5759167	Prostate cancer risk prediction with SNPs alone is less accurate than with PSA at baseline, with no benefit from combining SNPs with PSA.
Nam (2009) [41]	17q12, 17q24.3, 8q24, ERG, HOGG1-326, KLK2, TNF, 9p22, HPC1, ETV1	3004	Early detection	rs1447295, rs1859962, rs1800629, rs2348763	When incorporated into a nomogram, genotype status contributed more significantly than PSA. The positive predictive value of the PSA test ranged from 42% to 94% depending on the number of variant genotypes carried
Aly (2011) [42]	THADA, EHBP1, ITGA6, EEFSEC, PDLIM5, FLJ20032, SLC22A3, JAZF1, LMTK2, NKX3-1, MSMB, CTBP2, HNF1B, PPP1R14A, KLK3, TNRC6B, BIK, NUDT11, 8q24.21, 11q15.5, 11q13.2, 17q24.3	5241	PCa risk prediction	rs721048, rs12621278, rs7679673, rs10086908, rs1016343, rs13252298, rs6983561, rs16901979, rs16902094, rs6983267, rs1447295, rs10993994, rs7127900, rs10896449, rs11649743, rs4430796, rs1859962, rs8102476, rs2735839, rs5759167, rs5945619	Using a genetic risk score, implemented in a risk-prediction model, there was a 22.7% reduction in biopsies at a cost of missing a PCa diagnosis in 3% of patients characterized as having an aggressive disease
Hirata (2009) [70]	P53, p21, MDM2, PTEN, GNAS1, bcl2	167	BCR after RP	rs2279115	Bcl2 promotor region −938 C/C genotype carriers more frequently show biochemical recurrence than −938 C/A + A/A carriers

Table 1: Continued.

First author, year [ref.]	Gene(s)/loci investigated	*N*	Endpoint	Significant SNPs	Conclusion
Perez (2010) [58]	EGFR	212	BCR after RP	rs8844019	Statistically significant association between the SP and prostate biochemical recurrence after radical prostatectomy
Morote (2010) [71]	KLK2, SULT1A1, TLR4	703	BCR after RP	rs198977, rs9282861, rs11536889	Predicting biochemical recurrence after radical prostatectomy based on clinicopathological data can be significantly improved by including patient genetic information
Audet-Walsh (2011) [61]	SRD5A1, SRD5A2	846	BCR after RP	rs2208532, rs12470143, rs523349, rs4952197, rs518673, rs12470143	Multiple SRD5A1 and SRD5A2 variations are associated with increased/decreased rates of BCR after RP
Audet-Walsh (2012) [60]	HSD17B1, HSD17B2, HSD17B3, HSD17B4, HSD17B5, HSD17B12	526	BCR after RP	rs1364287, rs8059915, rs2955162, rs4243229, rs1119933, rs9934209, rs7201637, rs10739847, rs2257157, rs1810711, rs11037662, rs7928523, rs12800235, rs10838151	Twelve SNPs distributed across HSD17B2, HSD17B3, and HSD17B12 were associated with increased risk of BCR in localized PCa after RP
Jaboin (2011) [67]	MMP7	212	BCR after RP	rs10895304	The A/G genotype is predictive of decreased recurrence-free survival in patients with clinically localized prostate cancer
Wang (2009) [68]	PCGF2 (MEL-18)	124	BCR after RP	rs708692	Patients with the G/G genotype have a significantly higher rate of BCR after RP
Bachmann (2011) [69]	bcl2	290	BCR after RP	rs2279115	The −938 A/A genotype carriers more frequently show biochemical recurrence than −938 C/A + C/C carriers
Huang (2010) [64]	CTNNB1, APC	307	BCR after RP	rs3846716	There is a potential prognostic role of the GA/AA genotype of the SNP on BCR after RP
Chang (2013) [65]	IGF1, IGF1R	320	BCR after RP	rs2946834, rs2016347	A genetic interaction between IGF1 rs2946834 and IGF1R rs2016347 is associated with BCR after RP
Borque (2013) [72]	KLK3, KLK2, SULT1A1, BGLAP	670	BCR after RP	rs2569733, rs198977, rs9282861, rs1800247	A nomogram, including SNPs and clinicopathological factors, improves the preoperative prediction of early BCR after RP

Table 1: Continued.

First author, year [ref.]	Gene(s)/loci investigated	N	Endpoint	Significant SNPs	Conclusion
Langsenlehner (2011) [73]	XRCC1	603	RT toxicity	rs25489	The XRCC1 Arg280His polymorphism may be protective against the development of high-grade late toxicity after radiotherapy
Damaraju (2006) [77]	BRCA1, BRCA2, ESR1, XRCC1, XRCC2, XRCC3, NBN, RAD51, RAD2-52, LIG4, ATM, BCL2, TGFB1, MSH6, ERCC2, XPF, NR3C1, CYP1A1, CYP2C9, CYP2C19, CYP3A5, CYP2D6, CYP11B2, CYP17A1	83	RT toxicity	rs1805386, rs1052555, rs1800716	SNPs in LIG4, ERC22, and CYP2D6 are putative markers to predict individuals at risk for complications arising from radiation therapy
De Langhe (2013) [78]	TGFβ1	322	RT toxicity	rs1800469, rs1982073	Radical prostatectomy, the presence of pretreatment nocturia symptoms, and the variant alleles of TGFβ1 −509 C > T and codon 10 T > C are identified as factors involved in the development of acute radiation-induced nocturia when treated with IMRT
Fachal (2012) [79]	ATM, ERCC2, LIG4, MLH1, XRCC3	698	RT toxicity	rs1799794	The SNP and the mean dose received by the rectum are associated with the development of gastrointestinal toxicity after 3D-CRT
Fachal (2012) [80]	TGFβ1	413	RT toxicity	None	Neither of the investigated SNPs or haplotypes were found to be associated with the risk of late toxicity
Popanda (2009) [81]	XRCC1, APEX1, hOGG1, XRCC2, XRCC3, NBN, XPA, ERCC1, XPC, TP53, P21, MDM2	405	RT toxicity	rs25487, rs861539	The XRCC1 Arg399Gln polymorphism is associated with an increase in risk for heterozygous individuals and for Gln carriers. For XRCC3 Thr241Met, the Met variant increases the risk in Met carriers
Suga (2008) [82]	SART1, ID3, EPDR1, PAH, XRCC6	197	RT toxicity	rs2276015, rs2742946, rs1376264, rs1126758, rs2267437	Two-stage AUC-ROC curve reached a maximum of 0.86 (training set) in predicting late genitourinary morbidity
Cesaretti (2005) [85]	ATM	37	RT toxicity (Brachy)	—	There is a strong association between sequence variants in the ATM gene and erectile dysfunction/rectal bleeding
Cesaretti (2007) [84]	ATM	108	RT toxicity (Brachy)	—	The possession of SNPs in the ATM gene is associated with the development of radiation-induced proctitis after brachytherapy

Table 1: Continued.

First author, year [ref.]	Gene(s)/loci investigated	*N*	Endpoint	Significant SNPs	Conclusion
Peters (2008) [86]	TGFβ1	141	RT toxicity (Brachy)	rs1982073, rs1800469, rs1800471	Presence of certain TGFβ1 genotypes is associated with the development of both erectile dysfunction and late rectal bleeding in patients treated with radiotherapy.
Pugh (2009) [87]	ATM, BRCA1, ERCC2, H2AFX, LIG4, MDC1, MRE11A, RAD50	41	RT toxicity (Brachy)	rs28986317	The high toxicity group is enriched for at least one LIG4 SNP. One SNP in MDC1 is associated with increased radiosensitivity.
Burri (2008) [88]	SOD2, XRCC1, XRCC3	135	RT toxicity	rs25489, rs4880, rs861539	A XRCC1 SNP is associated with erectile dysfunction. A combination of a SNP in SOD2 and XRCC3 is associated with late rectal bleeding.
Barnett (2012) [89]	ABCA1, ALAD, APEX1, ATM, BAX, CD44, CDKN1A, DCLRE1C, EPDR1, ERCC2, ERCC4, GSTA1, GSTP1, HIF1A, IL12RB2, LIG3, LIG4, MED2L2, MAP3K7, MAT1A, MLH1, MPO, MRE11A, MSH2, NEIL3, NFE2L2, NOS3, PAH, PRKDC, PTTG1, RAD17, RAD21, RAD9A, REV3L, SART1, SH3GL1, SOD2, TGFB1, TGFB3, TP53, XPC, XRCC1, XRCC3, XRCC5, XRCC6	637	RT toxicity	None	None of the previously reported associations were confirmed by this study, after adjustment for multiple comparisons. The *P* value distribution of the SNPs tested against overall toxicity score was not different from that expected by chance.
Ross (2008) [97]	AKR1C1, AKR1C2, AKR1C3, AR, CYP11A1, CYP11B1, CYP17A1, CYP19A1, CYP21A2, CYP3A4, DHRS9, HSD17B3, HSD17B4, HSD3B1, HSD3B2, MAOA, SRD5A1, SRD5A2, SREBF2, UGT2B15	529	ADT efficacy	rs1870050, rs1856888, rs7737181	Three polymorphisms in separate genes are significantly associated with time to progression during ADT.
Teixeira (2008) [100]	EGF	275	ADT efficacy	rs4444903	EGF functional polymorphism may contribute to earlier relapse in ABT patients, supporting the involvement of EGF as an alternative pathway in hormone-resistant prostatic tumors.

Table 1: Continued.

First author, year [ref.]	Gene(s)/loci investigated	*N*	Endpoint	Significant SNPs	Conclusion
Yang (2011) [101]	SLCO2B1, SLCO1B3	538	ADT efficacy	rs12422149, rs1789693, rs1077858	Three SNPs in SLCO2B1 were associated with time to progression (TTP) on ADT. Patients carrying both SLCO2B1 and SLCO1B3 genotypes, which import androgens more efficiently, exhibited a median 2-year shorter TTP on ADT.
Teixeira (2013) [102]	TGFBR2	1765	ADT efficacy	—	TGFBR2-875GG homozygous patients have an increased risk of an early relapse after ADT. Combining clinicopathological and genetic information resulted in an increased capacity to predict the risk of ADT failure.
Kohli (2012) [103]	TRMT11, HSD17B12, PRMT3, WBSCR22, CYP3A4, PRMT2, SULT2B1, SRD5A1, AKR1D1, UGT2A1, SULT1E, HSD3B1, UGT2A3, UGT2B11, UGT2B28, CYP19A1, PRMT7, METTL2B, HSD17B3, LCMT1, UGT2B7, SRD5A2, CYP11B2, CARM1, METTL6, HSD17B1, HEMK1, CYP11B1, ESR1, UGT2B10, SERPINE1, PRMT6, HSD11B1, THBS1, SULT2A1, UGT2B4, PRMT5, PRMT8, HSD3B2, UGT1A4, ARSE, UGT1A8, UGT1A5, UGT1A10, ESR2, LCMT2, UGT1A9, AR, UGT1A6, UGT1A7, AKR1C4, STS, HSD17B8, ARSD, HSD17B2, HSD17B7, UGT1A1, UGT1A3,	304	ADT efficacy	rs1268121, rs6900796	TRMT11 showed the strongest association with time to ADT failure, with two of 4 TRMT 11 tagSNPs associated with time to ADT failure.
Bao (2011) [104]	KIF3C, CDON, ETS1, IFI30, has-mir-423, PALLD, ACSL1, GABRA1, SYT9, ZDHHC7, MTRR	601	ADT efficacy	rs6728684, rs3737336, rs1045747, rs1071738, rs998754, rs4351800	KIF3C rs6728684, CDON rs3737336, and IFI30 rs1045747 genotypes remained as significant predictors for disease progression in multivariate models that included clinicopathologic predictors. A greater number of unfavorable genotypes were associated with a shorter time to progression and worse prostate cancer-specific survival during ADT.

Table 1: Continued.

First author, year [ref.]	Gene(s)/loci investigated	*N*	Endpoint	Significant SNPs	Conclusion
Huang (2012) [106]	SPRED2, GNPDA2, BNC2, ZNF521, ZNF507, ALPK1, SKAP2, TACC2, SKAP1, KLHL14, NR4A2, FBXO32, AATF	601	ADT efficacy	rs16934641, rs3763763, rs2051778, rs3763763	Genetic variants in BNC2, TACC2, and ALPK1 are associated with clinical outcomes after ADT, with a cumulative effect on ACM following ADT of combinations of genotypes across the two loci of interest.
Huang (2012) [105]	ACTN2, NR2F1, ARRDC3, XRCC6BP1, FLT1, PSMD7, SKAP1, FBXO32, FLRT3	601	ADT efficacy	rs2939244, rs9508016, rs6504145, rs7830622, rs9508016	Genetic variants in ARRDC3, FLT1, and SKAP1 are significant predictors for PCSM and genetic variants in FBXO32 and FLT1 remained significant predictors for ACM. There was a strong combined genotype effect on PCSM and ACM.
Huang (2012) [107]	BMP5, NCOR2, IRS2, MAP2K6, RXRA, ERG, BMPR1A	601	ADT efficacy	rs4862396, rs3734444, rs7986346	Genetic variants in CASP3, BMP5, and IRS2 are associated with ACM. Genetic variation in BMP5 and IRS2 is significantly related to PCSM. Patients carrying a greater number of unfavorable genotypes at the loci of interest have a shorter time to ACM and PCSM during ADT.
Tsuchiya (2013) [108]	IGF-1	251	Metastatic PCa outcome	—	When the sum of the risk genetic factors in each LD block was considered, patients with all the risk factors had significantly shorter cancer-specific survival than those with 0–2 risk factors.
Pastina (2010) [112]	CYP1B1	60	Docetaxel response	rs1056836	The polymorphism is a possible predictive marker of response and clinical outcome to docetaxel in CRPC patients.
Sissung (2008) [113]	CYP1B1	52	Docetaxel response	rs1056836	Individuals carrying two copies of the polymorphic variant have a poor prognosis after docetaxel-based therapies compared with individuals carrying at least one copy of the allele.
Sissung (2008) [114]	ABCB1	73	Docetaxel response	—	Docetaxel-induced neuropathy, neutropenia grade, and overall survival could be linked to ABCB1 allelic variants (diplotypes).

Listing all the studies being discussed. From left to right: author (ref), genes/loci tested, number of patients included in the cohort, general endpoint of the study, significant SNPs, and conclusions.

them attractive candidates to predict an individual's risk for PCa.

2.1.2. SNPs in Interpreting (Novel) Biomarkers Levels. SNP genotyping can result in a risk prediction, that is, estimating the likelihood of developing PCa. Currently, they have no role as true diagnostic markers. However, as Klein et al. have already stated, there might be other clinical uses for SNPs [40]. Hypothetically, they could be used in combination with PSA levels, increasing its predictive role [41, 42].

Furthermore, a profound knowledge on SNPs influencing novel biomarker levels would be of great interest, since this could play a crucial role in the interpretation of novel biomarkers. Fundamental research has already identified multiple SNPs playing a role in expression and/or function of hK2, β-MSP, TMPRSS2, and so forth [43–45], which could potentially have an important impact on their interpretation.

Recent evidence has suggested that PSA levels are subject to genetic variation as well, explaining 40–45% of variability in PSA levels in the general population [46]. This variability plays an important role in the low sensitivity and specificity of PSA testing, because of which there is no generalizable threshold at which men should undergo prostate biopsies.

Attempting to explain this variability, Gudmundsson et al. detected six loci associated with PSA levels, of which four had a combined relative effect on PSA level variation [47]. Other groups have validated this work. One group suggested that genetic correction could influence the risk of PCa per unit increased/decreased PSA [48]. Another group suggested that genetic correction could alter the number of men with an abnormal PSA (based on general biopsy thresholds), preventing up to 15 to 20% of prostatic biopsies, in this way reducing complications and costs and improving quality of life [49].

With the exponentially increasing interest and development of novel biomarkers in PCa, we should keep in mind that SNPs can clearly alter biomarker levels, which is crucial for correct interpretation. If these SNPs are not taken into account, we could foresee similar obstacles as we are seeing now with PSA testing.

2.2. Localized Disease. In treating localized PCa, defined as N0 M0 disease [31], there are multiple viable treatment options, each with its indications and contraindications. Based on clinical stage of the disease, age, and comorbidities, clinicians decide to enroll a patient in an active surveillance program or to start active treatment.

2.2.1. Active Surveillance. Active surveillance (defined as close monitoring of PSA levels combined with periodic imaging and repeat biopsies) is currently the golden standard for treating PCa with the lowest risk of cancer progression (cT1-2a, PSA < 10 ng/mL, biopsy Gleason score <6 (at least 10 cores), <2 positive biopsies, minimal biopsy core involvement (< 50% cancer per biopsy)).

Although active surveillance has shown to be a viable option with excellent survival rates, reported conversion rates to active treatment range from 14% to 41%. This delayed treatment, however, has no effect on survival rates [50]. Biomarker research in the "active surveillance group" should therefore mainly focus on detecting high-risk disease with high specificity, avoiding under- and overtreatment and making prevention and early intervention possible. This topic has already been discussed in the paragraph "early detection" (see Section 2.1).

2.2.2. Active Therapy. As it has become clear that, in patients with low-risk disease, active therapy can be delayed based on active surveillance protocols, it is clear as well that therapy is required in patients with intermediate and especially in patients with high-risk disease, as defined by the EAU guidelines.

In light of this, there are two large retrospective studies, determining 15-year mortality rates in men with PCa treated with noncurative intent. Firstly, Rider et al. found that PCa mortality is low in all men diagnosed with localized low- and intermediate-risk PCa. However, death rates are much higher in all men with localized high-risk disease with a 31% mortality rate [51]. Similar results were published by Akre et al., who have shown that in men with locally advanced PCa with a Gleason score of 7–10, where the PCa is managed with noncurative intent, PCa-specific mortality rates range between 41 and 64% [52].

Reported incidence rates of high-risk PCa vary between 17% and 31%, depending on how the disease was defined [53]. After primary treatment, patients with high-risk PCa have a higher risk of disease recurrence and progression, requiring multimodality treatment [31]. Currently, the two most established treatment options with curative intent are surgery and radiotherapy, each with its obstacles.

Radical Prostatectomy. In treating patients with intermediate- and high-risk PCa, radical prostatectomy can be curative for some patients, whilst others need a multidisciplinary approach. For clinicians, it is therefore of great interest to be able to define a patient's risk for persistence or relapse of disease before they start treatment. Based on these predictions, clinicians could decide to start with or withhold from adjuvant therapy, leading to a more personalized medicine.

At this moment, these predictions are based on nomograms, integrating preoperative clinical parameters, optimizing their prognostic value [54–56]. However, current clinical parameters still lack sufficient accuracy. Therefore, there is an enormous interest in developing novel biomarkers to optimize pretreatment risk stratification [57]. Regarding this, SNPs are especially interesting, since their use avoids PCa heterogeneity in a single specimen, limiting its pathological parameter accuracy [58, 59]. Again, SNPs are not age-dependent and only need to be determined once, reducing patient burden and costs.

Multiple groups have identified SNPs that might be associated with higher rates of biochemical recurrence and/or shorter periods of biochemical-recurrence-free survival after radical prostatectomy. These polymorphisms are located in genes involved in steroid hormone biotransformation [60–62], immune response [63], Wnt [64] and IGF1 [65] signaling pathways, and other genes associated with oncogenesis [66–68]. However, conflicting results have already been reported

by Bachman et al., who found that the AA genotype of the 938 BCL2 promotor polymorphism was an independent prognostic marker of relapse-free and overall survival in a Caucasian patient group [69]. This contrasted with results published by Hirata et al., who found the CC variant of the same promotor to be predictive for biochemical recurrence in a Japanese population [70].

Despite the numerous investigations on the role of SNPs in predicting biochemical recurrence after radical prostatectomy, only a few have been developed into a clinically applicable model, integrating clinicopathological data and genetic information [71, 72].

Radiotherapy. External beam radiotherapy (EBRT) is a second treatment option with curative intent for localized PCa. Currently, there is no solid evidence suggesting superiority of surgery or radiotherapy over the other. With the development of new techniques (IMRT, tomotherapy, and so forth) with escalating radiation doses, there has been an increase in patients being treated with EBRT for localized PCa.

Still, toxicities in neighboring normal tissues remain the major limiting factor for delivering optimal tumoricidal doses [73]. Normal-tissue radiation sensitivity mainly depends on treatment-related factors, which are defined as the total irradiation dose, the fractionated regimen, the total treatment time, and the irradiated volume. However, even for similar or identical treatment protocols, the extent of side effects shows substantial variation. This interindividual variation can be explained by patient-related factors [74].

Since patients with higher rates of side effects show no specific phenotypic trait, this suggests that subclinical genetic variations could explain these interindividual differences. Therefore, there has been an increasing interest in identifying the role of genetic variation and SNPs on treatment efficacy and normal-tissue radiosensitivity, termed "radiogenomics." Detecting these genetic variations could lead to the identification of subgroups of patients at risk for developing severe radiation-induced toxicity [75].

Based on a mechanistic understanding of the radiation pathogenesis, there has been a major interest in understanding the role of genetic variation in genes involved in DNA damage sensing (e.g., ATM), fibrogenesis (e.g., TGFB1), oxidative stress (e.g., SOD1), and major DNA repair pathways (e.g., XRCC1, XRCC3, ERCC2, and MLH1), showing conflicting results [73, 76–83]. Comparable studies have been performed in patients treated with brachytherapy [84–88].

These results are of great interest, since long-term genitourinary, sexual, and gastrointestinal quality of life are major issues guiding decision making with respect to curative management of PCa. In 2012, Barnett et al. aimed to prospectively validate SNPs which were at that time reported to be associated with radiation toxicity in a population of 637 patients treated with radical prostate radiotherapy. Despite previous evidence, none of the 92 investigated SNPs were associated with late normal tissue toxicity [89].

2.3. Metastatic Prostate Cancer. Since androgens have a pivotal role in the development of PCa, the androgen receptor is the main target of systemic therapy for PCa. Androgen deprivation therapy (ADT) is the mainstay of treatment for patients with metastatic PCa, of which chemical or surgical castration is the first-line treatment. Because of comparable efficacy between chemical and surgical castration, the latter generally has been replaced by chemical castration [90–92].

2.3.1. Genetic Polymorphisms and ADT. Despite the efficiency of hormonal therapy in metastatic disease, eventually every patient will relapse, developing castration-resistant PCa (CRPC) [93]. Clinicians use well-studied clinicopathologic parameters (PSA kinetics and Gleason Score and so forth) to predict which patients will not respond well to ADT and which patients have poor prognosis [94–96]. Still, these parameters are insufficient for prediction, which is suggested by the recommendation of the EAU guidelines that LHRH agonists should be continued, even in a castration-resistant state [31]. In light of this, genetic markers could be an attractive way to improve risk stratification, predicting which patients will respond less to ADT and have poor prognosis, warranting closer follow-up.

Ross et al. underlined the importance of pharmacogenomics on an individuals' response to ADT [97]. They associated three SNPs located in/close to CYP19A1 (encodes for aromatase, a key enzyme that converts testosterone to estrogen in men), HSD3B1 (associated with PCa susceptibility) [98], and HSD17B4 (overexpression associated with higher Gleason grade) [99]. These SNPs were significantly associated with time to progression, having an additive effect when combined.

Later on, SNPs in multiple other loci have shown to be correlated with earlier relapse in patients treated with ADT. Currently known loci of interest are situated in the EGF gene [100] (known to activate several prooncogenic signaling pathways), in two androgen transporter genes (SLCO2B1 and SLCO1B3) [101] and in the TGFβR2 gene. The latter codes for a receptor involved in TGFβ signaling pathway, playing a role in carcinogenesis and tumor progression [102]. In contrast to these, some SNPs associated with time to progression under ADT, are located in genes of which the function is still unknown [103].

Moreover, a Taiwanese group developed a DNA library of 601 men with "advanced prostate cancer" treated with ADT, in which they detected 5 SNPs that were correlated with progression and 14 SNPs correlated with PCa-specific mortality under ADT [104–107]. Bao et al. detected four SNPs within miRNAs and miRNA target sites that were associated with disease progression [104]. Furthermore, Huang et al. systematically investigated 55 and 49 common SNPs in androgen- and estrogen-receptor-binding sites, after which they withheld one SNP (located in BNC2) which is correlated with progression and 5 SNPs (located in ARRDC3, FLT1, SKAP1, BNC2, and TACC2), which are correlated with PCa-specific mortality [105, 106]. Finally, Huang et al. associated a SNP in the BMP5 and IRS2 gene with survival [107]. The latter encodes a member of a family of intracellular signaling adaptor proteins that coordinate numerous biologically key extracellular signals within the cell, including insulin-like growth factor 1 (IGF1), of which the genotype seems to be correlated with survival in metastatic PCa as well [108]. This

only shows how complex and interwoven the clinical effects of genetic variation can be.

Although these results are very interesting, it should be noted that the investigated patient group is very heterogeneous. In this population with "advanced PCa," tumor characteristics show that 33% of patients have a Gleason score ranging from 2 to 6 and 31.7% of patients have T1/T2 tumors. Furthermore, the setting in which ADT was given was very heterogeneous, ranging from ADT in neoadjuvant setting to ADT for biochemical failure after radical prostatectomy. This heterogeneity limits the interpretation of genetic variation in clinical situations such as these.

Hypothetically, there are multiple potential clinical benefits of SNP genotyping with respect to ADT therapy. Firstly, it could play a prognostic role in identifying patients at high risk of therapeutic failure. This could help identify a subset of patients who may benefit from a more aggressive initial treatment strategy than ADT alone, including combinations with novel drugs [103]. Secondly, polymorphisms with functional implications on enzyme activity could be targeted with novel therapeutics, improving ADT efficacy [97].

2.3.2. Genetic Polymorphisms in the Castrate-Resistant PCa. In the castrate-resistant setting, taxane-based chemotherapy (docetaxel) has been the only treatment option for many years, based on two multicenter phase III randomized clinical trials, showing a moderate increase in overall survival [109, 110]. Over the last few years, numerous novel therapeutics have been developed in this setting. However, equally many questions regarding the optimal treatment regimen remain. Clinical evidence showing superiority to one treatment option over the other is severely lacking, keeping clinicians in the dark on the optimal treatment.

When treatment with docetaxel is started, there is a high variability in the clinical response [111]. Therefore, it would be of great interest to be able to predict this response rate before treatment is started. Based on this, the clinician could decide to withhold from docetaxel as first-line treatment and choose another treatment option.

Genetic variation in the CYP1B1 gene has shown to predict outcome in CRPC patients receiving first-line docetaxel. Pastina et al. showed that patients, carrying the CYP1B1 4326 GG genotype, had significantly shorter overall survival rates when compared to patients carrying CYP1B1 4326 GC or CC. Even after correcting for other risk factors (e.g., demographics, pathological, and biochemical characteristics), this genotype remained an independent predictive parameter of risk of death. This suggests that the 4326GG genotype might be a good pharmacogenetic marker of lower prevalence of response to docetaxel in CRPC patients [112]. It is suggested that its role probably lies in the effect it has on the levels of 4-hydroxyestradiol, which is the major CYP1B1 metabolite. The metabolite interferes with the chemotherapy-induced microtubule stabilization and structurally alters docetaxel [113]. Another gene of interest is the ABCB1 gene, which is responsible for a large portion of the systemic efflux of docetaxel. Within this gene, a combination of ABCB1 1236, 2677, and 3435 genotypes seems to be correlated with survival in CRPC patients receiving docetaxel and time to developing neuropathy in patients receiving a combination of docetaxel and thalidomide. The latter is probably due to cumulative effects on toxicity [114].

With the growing number of new treatment options, these results are very interesting for future clinical use. Using these, clinicians could individualize treatment regimens based on a patient's genotype. Similarly, the role of SNPs in predicting therapeutic efficacy of novel therapeutic agents like abiraterone and enzalutamide awaits to be assessed.

3. Conclusions

Since the definition of the human genome, the basis for genetic variations that can lead to individual risks for diseases has become more and more clear. Genome-wide association studies (GWAS) have defined groups of SNPs which partially predict increased risk for PCa. As suggested in this review, SNPs have a great potential in predicting patients' risk for PCa and/or therapy response, which could have an important impact in every day clinic.

Although many authors have suggested that genetic information can improve risk prediction and therefore be useful in clinical practice, there are several studies showing contradicting results, limiting their current clinical use. These contradicting results could be explained by multiple reasons. First, studies performed on small, heterogeneous populations might result in high rates of false positive and negative data. Secondly, most conducted studies are based on SNPs which have been correlated with PCa in GWAS studies. Since PCa phenotypes are probably determined by a spectrum of genetic variation (ranging from highly penetrant to low penetrant variations), with possible interdependencies of SNPs, GWAS studies are probably not sufficient to develop a full understanding of these variations in PCa.

Throughout this review, it has become clear that some challenges still remain for translational research on the role of SNPs in PCa. Firstly, clinical studies on SNPs should be performed in well-powered studies, which could give more conclusive results. Secondly, the important challenge for further basic research is to identify the causative SNPs within each linkage equilibrium. Hopefully, these SNPs will not only function as predictors but also give clues to important pathways in PCa development, which could be therapeutic targets.

It will only be after the enrichment of GWAS data by detailed SNP mapping and functional SNP testing that the most relevant SNPs can be analyzed in clinical research. In the future, we expect them to become critical to interpret individualized PCa risk, interindividual biomarker variation, and therapeutic response.

Conflict of Interests

The authors declare that there is no conflict of interests regarding the publication of this paper.

Acknowledgments

The authors gratefully acknowledge financial support from the company Ravago Distribution Center NV (LUOR fonds).

This study was further financially supported by the Fundacion Federico, Grant OT/09/035 from the Katholieke Universiteit Leuven, and Grant nos. G.0684.12 and G.0830.13 of the Fund for Scientific Research Flanders, Belgium (FWO-Vlaanderen). Steven Joniau is holder of a grant from the Klinisch Onderzoeksfonds (KOF) from UZ Leuven.

References

[1] R. Siegel, D. Naishadham, and A. Jemal, "Cancer statistics 2013," *CA: A Cancer Journal for Clinicians*, vol. 63, no. 1, pp. 11–30, 2013.

[2] D. J. Schaid, "The complex genetic epidemiology of prostate cancer," *Human Molecular Genetics*, vol. 13, no. 1, pp. R103–R121, 2004.

[3] P. Lichtenstein, N. V. Holm, P. K. Verkasalo et al., "Environmental and heritable factors in the causation of cancer: analyses of cohorts of twins from Sweden, Denmark, and Finland," *The New England Journal of Medicine*, vol. 343, no. 2, pp. 78–85, 2000.

[4] R. Takata, S. Akamatsu, M. Kubo et al., "Genome-wide association study identifies five new susceptibility loci for prostate cancer in the Japanese population," *Nature Genetics*, vol. 42, no. 9, pp. 751–754, 2010.

[5] J. Xu, Z. Mo, D. Ye et al., "Genome-wide association study in Chinese men identifies two new prostate cancer risk loci at 9q31. 2 and 19q13. 4.," *Nature Genetics*, vol. 44, no. 11, pp. 1231–1235, 2012.

[6] R. A. Eeles, A. A. Al Olama, S. Benlloch et al., "Identification of 23 new prostate cancer susceptibility loci using the iCOGS custom genotyping array," *Nature Genetics*, vol. 45, no. 4, pp. 385–391, 2013.

[7] J. Gudmundsson, P. Sulem, A. Manolescu et al., "Genome-wide association study identifies a second prostate cancer susceptibility variant at 8q24," *Nature Genetics*, vol. 39, no. 5, pp. 631–637, 2007.

[8] J. Gudmundsson, P. Sulem, V. Steinthorsdottir et al., "Two variants on chromosome 17 confer prostate cancer risk, and the one in TCF2 protects against type 2 diabetes," *Nature Genetics*, vol. 39, no. 8, pp. 977–983, 2007.

[9] M. Yeager, N. Orr, R. B. Hayes et al., "Genome-wide association study of prostate cancer identifies a second risk locus at 8q24," *Nature Genetics*, vol. 39, no. 5, pp. 645–649, 2007.

[10] J. Sun, S. L. Zheng, F. Wiklund et al., "Sequence variants at 22q13 are associated with prostate cancer risk," *Cancer Research*, vol. 69, no. 1, pp. 10–15, 2009.

[11] R. Eeles, Z. Kote-Jarai, and A. Al Olama, "Identification of seven new prostate cancer susceptibility loci through a genome-wide association study," *Nature Genetics*, vol. 41, no. 10, pp. 1116–1121, 2009.

[12] C. A. Haiman, G. K. Chen, W. J. Blot et al., "Genome-wide association study of prostate cancer in men of African ancestry identifies a susceptibility locus at 17q21," *Nature Genetics*, vol. 43, no. 6, pp. 570–573, 2011.

[13] J. Gudmundsson, P. Sulem, and T. Rafnar, "Common sequence variants on 2p15 and Xp11. 22 confer susceptibility to prostate cancer," *Nature Genetics*, vol. 40, no. 3, pp. 281–283, 2008.

[14] J. Gudmundsson, P. Sulem, D. F. Gudbjartsson et al., "Genome-wide association and replication studies identify four variants associated with prostate cancer susceptibility," *Nature Genetics*, vol. 41, no. 10, pp. 1122–1126, 2009.

[15] Z. Kote-Jarai, A. Al Olama, and G. Giles, "Seven prostate cancer susceptibility loci identified by a multi-stage genome-wide association study," *Nature Genetics*, vol. 43, no. 8, pp. 785–791, 2011.

[16] J. M. Murabito, C. L. Rosenberg, D. Finger et al., "A genome-wide association study of breast and prostate cancer in the NHLBI's Framingham Heart Study," *BMC Medical Genetics*, vol. 8, supplement 1, article S6, 2007.

[17] I. Cheng, G. K. Chen, H. Nakagawa et al., "Evaluating genetic risk for prostate cancer among Japanese and Latinos," *Cancer Epidemiology, Biomarkers & Prevention*, vol. 21, no. 11, pp. 2048–2058, 2012.

[18] L. M. FitzGerald, E. M. Kwon, M. P. Conomos et al., "Genome-wide association study identifies a genetic variant associated with risk for more aggressive prostate cancer," *Cancer Epidemiology Biomarkers and Prevention*, vol. 20, no. 6, pp. 1196–1203, 2011.

[19] R. K. Nam, W. Zhang, K. Siminovitch et al., "New variants at 10q26 and 15q21 are associated with aggressive prostate cancer in a genome-wide association study from a prostate biopsy screening cohort," *Cancer Biology and Therapy*, vol. 12, no. 11, pp. 997–1004, 2011.

[20] F. R. Schumacher, S. I. Berndt, A. Siddiq et al., "Genome-wide association study identifies new prostate cancer susceptibility loci," *Human Molecular Genetics*, vol. 20, no. 19, pp. 3867–3875, 2011.

[21] J. Shan, K. Al-Rumaihi, D. Rabah et al., "Genome scan study of prostate cancer in Arabs: identification of three genomic regions with multiple prostate cancer susceptibility loci in Tunisians," *Journal of Translational Medicine*, vol. 11, article 121, 2013.

[22] S. Tao, J. Feng, T. Webster et al., "Genome-wide two-locus epistasis scans in prostate cancer using two European populations," *Human Genetics*, vol. 131, no. 7, pp. 1225–1234, 2012.

[23] A. Amin Al Olama, Z. Kote-Jarai, F. R. Schumacher et al., "A meta-analysis of genome-wide association studies to identify prostate cancer susceptibility loci associated with aggressive and non-aggressive disease," *Human Molecular Genetics*, vol. 22, no. 2, pp. 408–415, 2013.

[24] D. Duggan, S. L. Zheng, M. Knowlton et al., "Two genome-wide association studies of aggressive prostate cancer implicate putative prostate tumor suppressor gene DAB2IP," *Journal of the National Cancer Institute*, vol. 99, no. 24, pp. 1836–1844, 2007.

[25] R. A. Eeles, Z. Kote-Jarai, G. G. Giles et al., "Multiple newly identified loci associated with prostate cancer susceptibility," *Nature Genetics*, vol. 40, no. 3, pp. 316–321, 2008.

[26] G. Thomas, K. B. Jacobs, M. Yeager et al., "Multiple loci identified in a genome-wide association study of prostate cancer," *Nature Genetics*, vol. 40, no. 3, pp. 310–315, 2008.

[27] S. Ren, J. Xu, T. Zhou et al., "Plateau effect of prostate cancer risk-associated SNPs in discriminating prostate biopsy outcomes," *Prostate*, vol. 73, no. 16, pp. 1824–1835, 2013.

[28] F. H. Schröder, J. Hugosson, M. J. Roobol et al., "Screening and prostate-cancer mortality in a randomized european study," *The New England Journal of Medicine*, vol. 360, no. 13, pp. 1320–1328, 2009.

[29] V. A. Moyer, "Screening for prostate cancer: U.S. Preventive Services Task Force recommendation statement," *Annals of Internal Medicine*, vol. 157, no. 2, pp. 120–134, 2012.

[30] P. C. Walsh, "Re: screening for prostate cancer: U.S. Preventive Services Task Force recommendation statement," *Journal of Urology*, vol. 188, no. 4, p. 1181, 2012.

[31] A. Heidenreich, G. Aus, M. Bolla, and S. Joniau, "EAU guidelines on prostate cancer," *European Urology*, vol. 53, pp. 31–45, 2008.

[32] S. L. Zheng, J. Sun, F. Wiklund et al., "Genetic variants and family history predict prostate cancer similar to prostate-specific antigen," *Clinical Cancer Research*, vol. 15, no. 3, pp. 1105–1111, 2009.

[33] C. A. Salinas, J. S. Koopmeiners, E. M. Kwon et al., "Clinical utility of five genetic variants for predicting prostate cancer risk and mortality," *Prostate*, vol. 69, no. 4, pp. 363–372, 2009.

[34] M. S. Pepe, H. Janes, G. Longton, W. Leisenring, and P. Newcomb, "Limitations of the odds ratio in gauging the performance of a diagnostic, prognostic, or screening marker," *American Journal of Epidemiology*, vol. 159, no. 9, pp. 882–890, 2004.

[35] J. Xu, J. Sun, A. K. Kader et al., "Estimation of absolute risk for prostate cancer using genetic markers and family history," *Prostate*, vol. 69, no. 14, pp. 1565–1572, 2009.

[36] J. Sun, A. K. Kader, F.-C. Hsu et al., "Inherited genetic markers discovered to date are able to identify a significant number of men at considerably elevated risk for prostate cancer," *Prostate*, vol. 71, no. 4, pp. 421–430, 2011.

[37] S. Lindström, F. R. Schumacher, D. Cox et al., "Common genetic variants in prostate cancer risk prediction—results from the NCI breast and prostate cancer cohort consortium (BPC3)," *Cancer Epidemiology Biomarkers and Prevention*, vol. 21, no. 3, pp. 437–444, 2012.

[38] R. J. Macinnis, A. C. Antoniou, R. A. Eeles et al., "A risk prediction algorithm based on family history and common genetic variants: application to prostate cancer with potential clinical impact," *Genetic Epidemiology*, vol. 35, no. 6, pp. 549–556, 2011.

[39] N. Pashayan, S. W. Duffy, S. Chowdhury et al., "Polygenic susceptibility to prostate and breast cancer: implications for personalised screening," *British Journal of Cancer*, vol. 104, no. 10, pp. 1656–1663, 2011.

[40] R. J. Klein, C. Hallden, A. Gupta et al., "Evaluation of multiple risk-associated single nucleotide polymorphisms versus prostate-specific antigen at baseline to predict prostate cancer in unscreened men," *European Urology*, vol. 61, no. 3, pp. 471–477, 2012.

[41] R. K. Nam, W. W. Zhang, J. Trachtenberg et al., "Utility of incorporating genetic variants for the early detection of prostate cancer," *Clinical Cancer Research*, vol. 15, no. 5, pp. 1787–1793, 2009.

[42] M. Aly, F. Wiklund, J. Xu et al., "Polygenic risk score improves prostate cancer risk prediction: results from the Stockholm-1 cohort study," *European Urology*, vol. 60, no. 1, pp. 21–28, 2011.

[43] X. Xu, C. Valtonen-André, C. Sävblom, C. Halldén, H. Lilja, and R. J. Klein, "Polymorphisms at the microseminoprotein-β locus associated with physiologic variation in β-microseminoprotein and prostate-specific antigen levels," *Cancer Epidemiology Biomarkers and Prevention*, vol. 19, no. 8, pp. 2035–2042, 2010.

[44] R. J. Klein, C. Halldén, A. M. Cronin et al., "Blood biomarker levels to aid discovery of cancer-related single-nucleotide polymorphisms: Kallikreins and prostate cancer," *Cancer Prevention Research*, vol. 3, no. 5, pp. 611–619, 2010.

[45] L. Clinckemalie, L. Spans, V. Dubois et al., "Androgen regulation of the TMPRSS2 gene and the effect of a SNP in an Androgen Response Element," *Molecular Endocrinology*, vol. 27, no. 12, pp. 2028–2040, 2013.

[46] A. Bansal, D. K. Murray, J. T. Wu, R. A. Stephenson, R. G. Middleton, and A. W. Meikle, "Heritability of prostate-specific antigen and relationship with zonal prostate volumes in aging twins," *Journal of Clinical Endocrinology and Metabolism*, vol. 85, no. 3, pp. 1272–1276, 2000.

[47] J. Gudmundsson, S. Besenbacher, P. Sulem et al., "Genetic correction of PSA values using sequence variants associated with PSA levels," *Science Translational Medicine*, vol. 2, no. 62, Article ID 62ra92, 2010.

[48] S. Loeb, H. B. Carter, P. C. Walsh et al., "Single nucleotide polymorphisms and the likelihood of prostate cancer at a given prostate specific antigen level," *Journal of Urology*, vol. 182, no. 1, pp. 101–105, 2009.

[49] B. T. Helfand, S. Loeb, Q. Hu et al., "Personalized prostate specific antigen testing using genetic variants may reduce unnecessary prostate biopsies," *Journal of Urology*, vol. 189, no. 5, pp. 1697–1701, 2013.

[50] M. R. Cooperberg, P. R. Carroll, and L. Klotz, "Active surveillance for prostate cancer: progress and promise," *Journal of Clinical Oncology*, vol. 29, no. 27, pp. 3669–3676, 2011.

[51] J. R. Rider, F. Sandin, O. Andrén, P. Wiklund, J. Hugosson, and P. Stattin, "Long-term outcomes among noncuratively treated men according to prostate cancer risk category in a nationwide, population-based study," *European Urology*, vol. 63, no. 1, pp. 88–96, 2013.

[52] O. Akre, H. Garmo, J. Adolfsson, M. Lambe, O. Bratt, and P. Stattin, "Mortality among men with locally advanced prostate cancer managed with noncurative intent: a nationwide study in PCBaSe Sweden," *European Urology*, vol. 60, no. 3, pp. 554–563, 2011.

[53] M. R. Cooperberg, J. Cowan, J. M. Broering, and P. R. Carroll, "High-risk prostate cancer in the United States, 1990–2007," *World Journal of Urology*, vol. 26, no. 3, pp. 211–218, 2008.

[54] A. Briganti, S. Joniau, P. Gontero et al., "Identifying the best candidate for radical prostatectomy among patients with high-risk prostate cancer," *European Urology*, vol. 61, no. 3, pp. 584–592, 2012.

[55] S. Joniau, C.-Y. Hsu, E. Lerut et al., "A pretreatment table for the prediction of final histopathology after radical prostatectomy in clinical unilateral T3a prostate cancer," *European Urology*, vol. 51, no. 2, pp. 388–394, 2007.

[56] M. Spahn, S. Joniau, P. Gontero et al., "Outcome predictors of radical prostatectomy in patients with prostate-specific antigen greater than 20 ng/ml: a European multi-institutional study of 712 patients," *European Urology*, vol. 58, no. 1, pp. 1–7, 2010.

[57] R. S. Svatek, C. Jeldres, P. I. Karakiewicz et al., "Pre-treatment biomarker levels improve the accuracy of post-prostatectomy nomogram for prediction of biochemical recurrence," *Prostate*, vol. 69, no. 8, pp. 886–894, 2009.

[58] C. A. Perez, H. Chen, Y. Shyr et al., "The EGFR polymorphism rs884419 is associated with freedom from recurrence in patients with resected prostate cancer," *Journal of Urology*, vol. 183, no. 5, pp. 2062–2069, 2010.

[59] S.-P. Huang, L.-C. Huang, W.-C. Ting et al., "Prognostic significance of prostate cancer susceptibility variants on prostate-specific antigen recurrence after radical prostatectomy," *Cancer Epidemiology Biomarkers and Prevention*, vol. 18, no. 11, pp. 3068–3074, 2009.

[60] É. Audet-Walsh, J. Bellemare, L. Lacombe et al., "The impact of germline genetic variations in hydroxysteroid (17-Beta) dehydrogenases on prostate cancer outcomes after prostatectomy," *European Urology*, vol. 62, no. 1, pp. 88–96, 2012.

[61] E. Audet-Walsh, J. Bellemare, G. Nadeau et al., "SRD5A polymorphisms and biochemical failure after radical prostatectomy," *European Urology*, vol. 60, no. 6, pp. 1226–1234, 2011.

[62] J. Cotignola, D. B. Leonardi, A. Shahabi et al., "Glutathione-S-transferase (GST) polymorphisms are associated with relapse after radical prostatectomy," *Prostate Cancer and Prostatic Diseases*, vol. 16, no. 1, pp. 28–34, 2013.

[63] P. J. Dluzniewski, M.-H. Wang, S. L. Zheng et al., "Variation in *IL10* and other genes involved in the immune response and in oxidation and prostate cancer recurrence," *Cancer Epidemiology, Biomarkers & Prevention*, vol. 21, no. 10, pp. 1774–1782, 2012.

[64] S.-P. Huang, W.-C. Ting, L.-M. Chen et al., "Association analysis of Wnt pathway genes on prostate-specific antigen recurrence after radical prostatectomy," *Annals of Surgical Oncology*, vol. 17, no. 1, pp. 312–322, 2010.

[65] C.-F. Chang, J.-B. Pao, C.-C. Yu et al., "Common variants in IGF1 pathway genes and clinical outcomes after radical prostatectomy," *Annals of Surgical Oncology*, vol. 20, no. 7, pp. 2446–2452, 2013.

[66] S.-P. Huang, Y.-H. Lan, T.-L. Lu et al., "Clinical significance of runt-related transcription factor 1 polymorphism in prostate cancer," *BJU International*, vol. 107, no. 3, pp. 486–492, 2011.

[67] J. J. Jaboin, M. Hwang, Z. Lopater et al., "The matrix metalloproteinase-7 polymorphism RS10895304 is associated with increased recurrence risk in patients with clinically localized prostate cancer," *International Journal of Radiation Oncology Biology Physics*, vol. 79, no. 5, pp. 1330–1335, 2011.

[68] W. Wang, T. Yuasa, N. Tsuchiya et al., "The novel tumor-suppressor Mel-18 in prostate cancer: its functional polymorphism, expression and clinical significance," *International Journal of Cancer*, vol. 125, no. 12, pp. 2836–2843, 2009.

[69] H. S. Bachmann, L. C. Heukamp, K. J. Schmitz et al., "Regulatory BCL2 promoter polymorphism (−938C>A) is associated with adverse outcome in patients with prostate carcinoma," *International Journal of Cancer*, vol. 129, no. 10, pp. 2390–2399, 2011.

[70] H. Hirata, Y. Hinoda, N. Kikuno et al., "Bcl2 -938C/A polymorphism carries increased risk of biochemical recurrence after radical prostatectomy," *Journal of Urology*, vol. 181, no. 4, pp. 1907–1912, 2009.

[71] J. Morote, J. Del Amo, A. Borque et al., "Improved prediction of biochemical recurrence after radical prostatectomy by genetic polymorphisms," *Journal of Urology*, vol. 184, no. 2, pp. 506–511, 2010.

[72] Á. Borque, J. del Amo, L. M. Esteban et al., "Genetic predisposition to early recurrence in clinically localized prostate cancer," *BJU International*, vol. 111, no. 4, pp. 549–558, 2013.

[73] T. Langsenlehner, W. Renner, A. Gerger et al., "Association between single nucleotide polymorphisms in the gene for XRCC1 and radiation-induced late toxicity in prostate cancer patients," *Radiotherapy and Oncology*, vol. 98, no. 3, pp. 387–393, 2011.

[74] O. Zschenker, A. Raabe, I. K. Boeckelmann et al., "Association of single nucleotide polymorphisms in ATM, GSTP1, SOD2, TGFB1, XPD and XRCC1 with clinical and cellular radiosensitivity," *Radiotherapy and Oncology*, vol. 97, no. 1, pp. 26–32, 2010.

[75] D. Azria, M. Betz, C. Bourgier, W. J. Sozzi, and M. Ozsahin, "Identifying patients at risk for late radiation-induced toxicity," *Critical Reviews in Oncology/Hematology*, vol. 84, supplement 1, pp. e35–e41, 2012.

[76] G. C. Barnett, C. M. L. West, A. M. Dunning et al., "Normal tissue reactions to radiotherapy: towards tailoring treatment dose by genotype," *Nature Reviews Cancer*, vol. 9, no. 2, pp. 134–142, 2009.

[77] S. Damaraju, D. Murray, J. Dufour et al., "Association of DNA repair and steroid metabolism gene polymorphisms with clinical late toxicity in patients treated with conformal radiotherapy for prostate cancer," *Clinical Cancer Research*, vol. 12, no. 8, pp. 2545–2554, 2006.

[78] S. De Langhe, K. De Ruyck, P. Ost et al., "Acute radiation-induced nocturia in prostate cancer patients is associated with pretreatment symptoms, radical prostatectomy, and genetic markers in the TGFβ1 gene," *International Journal of Radiation Oncology∗Biology∗Physics*, vol. 85, no. 2, pp. 393–399, 2013.

[79] L. Fachal, A. G. Gómez-Caamaño, P. Peleteiro et al., "Association of a XRCC3 polymorphism and rectum mean dose with the risk of acute radio-induced gastrointestinal toxicity in prostate cancer patients," *Radiotherapy & Oncology*, vol. 105, no. 3, pp. 321–328, 2012.

[80] L. Fachal, A. Gómez-Caamaño, M. Sánchez-García et al., "TGFβ1 SNPs and radio-induced toxicity in prostate cancer patients," *Radiotherapy and Oncology*, vol. 103, no. 2, pp. 206–209, 2012.

[81] O. Popanda, J. U. Marquardt, J. Chang-Claude, and P. Schmezer, "Genetic variation in normal tissue toxicity induced by ionizing radiation," *Mutation Research*, vol. 667, no. 1-2, pp. 58–69, 2009.

[82] T. Suga, M. Iwakawa, H. Tsuji et al., "Influence of multiple genetic polymorphisms on genitourinary morbidity after carbon ion radiotherapy for prostate cancer," *International Journal of Radiation Oncology Biology Physics*, vol. 72, no. 3, pp. 808–813, 2008.

[83] M. B. Parliament and D. Murray, "Single nucleotide polymorphisms of DNA repair genes as predictors of radioresponse," *Seminars in Radiation Oncology*, vol. 20, no. 4, pp. 232–240, 2010.

[84] J. A. Cesaretti, R. G. Stock, D. P. Atencio et al., "A Genetically determined dose-volume histogram predicts for rectal bleeding among patients treated with prostate brachytherapy," *International Journal of Radiation Oncology Biology Physics*, vol. 68, no. 5, pp. 1410–1416, 2007.

[85] J. A. Cesaretti, R. G. Stock, S. Lehrer et al., "ATM sequence variants are predictive of adverse radiotherapy response among patients treated for prostate cancer," *International Journal of Radiation Oncology Biology Physics*, vol. 61, no. 1, pp. 196–202, 2005.

[86] C. A. Peters, R. G. Stock, J. A. Cesaretti et al., "TGFB1 single nucleotide polymorphisms are associated with adverse quality of life in prostate cancer patients treated with radiotherapy," *International Journal of Radiation Oncology Biology Physics*, vol. 70, no. 3, pp. 752–759, 2008.

[87] T. Pugh, M. Keyes, L. Barclay et al., "Sequence variant discovery in DNA repair genes from radiosensitive and radiotolerant prostate brachytherapy patients," *Clinical Cancer Research*, vol. 15, no. 15, pp. 5008–5016, 2009.

[88] R. J. Burri, R. G. Stock, J. A. Cesaretti et al., "Association of single nucleotide polymorphisms in SOD2, XRCC1 and XRCC3 with susceptibility for the development of adverse effects resulting from radiotherapy for prostate cancer," *Radiation Research*, vol. 170, no. 1, pp. 49–59, 2008.

[89] G. C. Barnett, C. E. Coles, R. M. Elliott et al., "Independent validation of genes and polymorphisms reported to be associated

with radiation toxicity: a prospective analysis study," *The Lancet Oncology*, vol. 13, no. 1, pp. 65–77, 2012.

[90] N. J. Vogelzang, G. W. Chodak, M. S. Soloway et al., "Goserelin versus orchiectomy in the treatment of advanced prostate cancer: final results of a randomized trial," *Urology*, vol. 46, no. 2, pp. 220–226, 1995.

[91] M. S. Soloway, G. Chodak, N. J. Vogelzang et al., "Zoladex versus orchiectomy in treatment of advanced prostate cancer: a randomized trial," *Urology*, vol. 37, no. 1, pp. 46–51, 1991.

[92] J. Seidenfeld, D. J. Samson, V. Hasselblad et al., "Single-therapy androgen suppression in men with advanced prostate cancer: a systematic review and meta-analysis," *Annals of Internal Medicine*, vol. 132, no. 7, pp. 566–577, 2000.

[93] K. J. Pienta and D. Bradley, "Mechanisms underlying the development of androgen-independent prostate cancer," *Clinical Cancer Research*, vol. 12, no. 6, pp. 1665–1671, 2006.

[94] T. K. Choueiri, W. Xie, A. V. D'Amico et al., "Time to prostate-specific antigen nadir independently predicts overall survival in patients who have metastatic hormone-sensitive prostate cancer treated with androgen-deprivation therapy," *Cancer*, vol. 115, no. 5, pp. 981–987, 2009.

[95] M. Hussain, C. M. Tangen, C. Higano et al., "Absolute prostate-specific antigen value after androgen deprivation is a strong independent predictor of survival in new metastatic prostate cancer: data from Southwest Oncology Group trial 9346 (INT-0162)," *Journal of Clinical Oncology*, vol. 24, no. 24, pp. 3984–3990, 2006.

[96] A. J. Stewart, H. I. Scher, M.-H. Chen et al., "Prostate-specific antigen nadir and cancer-specific mortality following hormonal therapy for prostate-specific antigen failure," *Journal of Clinical Oncology*, vol. 23, no. 27, pp. 6556–6560, 2005.

[97] R. W. Ross, W. K. Oh, W. Xie et al., "Inherited variation in the androgen pathway is associated with the efficacy of androgen-deprivation therapy in men with prostate cancer," *Journal of Clinical Oncology*, vol. 26, no. 6, pp. 842–847, 2008.

[98] B.-L. Chang, S. L. Zheng, G. A. Hawkins et al., "Joint effect of HSD3B1 and HSD3B2 genes is associated with hereditary and sporadic prostate cancer susceptibility," *Cancer Research*, vol. 62, no. 6, pp. 1784–1789, 2002.

[99] L. True, I. Coleman, S. Hawley et al., "A molecular correlate to the Gleason grading system for prostate adenocarcinoma," *Proceedings of the National Academy of Sciences of the United States of America*, vol. 103, no. 29, pp. 10991–10996, 2006.

[100] A. L. Teixeira, R. Ribeiro, D. Cardoso et al., "Genetic polymorphism in EGF Is associated with prostate cancer aggressiveness and progression-free interval in androgen blockade-treated patients," *Clinical Cancer Research*, vol. 14, no. 11, pp. 3367–3371, 2008.

[101] M. Yang, W. Xie, E. Mostaghel et al., "SLCO2B1 and SLCO1B3 may determine time to progression for patients receiving androgen deprivation therapy for prostate cancer," *Journal of Clinical Oncology*, vol. 29, no. 18, pp. 2565–2573, 2011.

[102] A. L. Teixeira, M. Gomes, A. Nogueira et al., "Improvement of a predictive model of castration-resistant prostate cancer: functional genetic variants in TGFβ1 signaling pathway modulation," *PLoS One*, vol. 8, no. 8, Article ID e72419, 2013.

[103] M. Kohli, S. M. Riska, D. W. Mahoney et al., "Germline predictors of androgen deprivation therapy response in advanced prostate cancer," *Mayo Clinic Proceedings*, vol. 87, no. 3, pp. 240–246, 2012.

[104] B.-Y. Bao, J.-B. Pao, C.-N. Huang et al., "Polymorphisms inside MicroRNAs and MicroRNA target sites predict clinical outcomes in prostate cancer patients receiving androgen-deprivation therapy," *Clinical Cancer Research*, vol. 17, no. 4, pp. 928–936, 2011.

[105] C.-N. Huang, S.-P. Huang, J.-B. Pao et al., "Genetic polymorphisms in androgen receptor-binding sites predict survival in prostate cancer patients receiving androgen-deprivation therapy," *Annals of Oncology*, vol. 23, no. 3, pp. 707–713, 2012.

[106] C.-N. Huang, S.-P. Huang, J.-B. Pao et al., "Genetic polymorphisms in oestrogen receptor-binding sites affect clinical outcomes in patients with prostate cancer receiving androgen-deprivation therapy," *Journal of Internal Medicine*, vol. 271, no. 5, pp. 499–509, 2012.

[107] S. P. Huang, B. Bao, T. Hour et al., "Genetic variants in CASP3, BMP5, and IRS2 genes may influence survival in prostate cancer patients receiving androgen-deprivation therapy," *PLoS One*, vol. 7, no. 7, Article ID e41219, 2012.

[108] N. Tsuchiya, S. Narita, T. Inoue et al., "Insulin-like growth factor-1 genotypes and haplotypes influence the survival of prostate cancer patients with bone metastasis at initial diagnosis," *BMC Cancer*, vol. 13, no. 1, article150, 2013.

[109] I. F. Tannock, R. De Wit, W. R. Berry et al., "Docetaxel plus prednisone or mitoxantrone plus prednisone for advanced prostate cancer," *The New England Journal of Medicine*, vol. 351, no. 15, pp. 1502–1512, 2004.

[110] D. P. Petrylak, C. M. Tangen, M. H. A. Hussain et al., "Docetaxel and estramustine compared with mitoxantrone and prednisone for advanced refractory prostate cancer," *The New England Journal of Medicine*, vol. 351, no. 15, pp. 1513–1520, 2004.

[111] R. Bruno, N. Vivier, C. Veyrat-Follet, G. Montay, and G. R. Rhodes, "Population pharmacokinetics and pharmacokinetic-pharmacodynamic relationships for docetaxel," *Investigational New Drugs*, vol. 19, no. 2, pp. 163–169, 2001.

[112] I. Pastina, E. Giovannetti, A. Chioni et al., "Cytochrome 450 1B1 (*CYP1B1*) polymorphisms associated with response to docetaxel in Castration-Resistant Prostate Cancer (CRPC) patients," *BMC Cancer*, vol. 10, article 511, 2010.

[113] T. M. Sissung, R. Danesi, D. K. Price et al., "Association of the *CYP1B1***3* allele with survival in patients with prostate cancer receiving docetaxel," *Molecular Cancer Therapeutics*, vol. 7, no. 1, pp. 19–26, 2008.

[114] T. M. Sissung, C. E. Baum, J. Deeken et al., "ABCB1 genetic variation influences the toxicity and clinical outcome of patients with androgen-independent prostate cancer treated with docetaxel," *Clinical Cancer Research*, vol. 14, no. 14, pp. 4543–4549, 2008.

Hindawi Publishing Corporation
BioMed Research International
Volume 2014, Article ID 780816, 8 pages
http://dx.doi.org/10.1155/2014/780816

Research Article

Diffusion-Weighted Magnetic Resonance Diagnosis of Local Recurrences of Prostate Cancer after Radical Prostatectomy: Preliminary Evaluation on Twenty-Seven Cases

Salvatore Francesco Carbone,[1,2] Luigi Pirtoli,[1,3] Veronica Ricci,[1,2] Tommaso Carfagno,[1,3] Paolo Tini,[1,3] Augusto La Penna,[1,2] Eleonora Cacchiarelli,[1,2] and Luca Volterrani[1,2]

[1] *Istituto Toscano Tumori, via Taddeo Alderotti 26/N, 50139 Florence, Italy*
[2] *Unit of Diagnostic Imaging, University Hospital of Siena, Policlinico S. Maria alle Scotte, Viale Bracci, 53100 Siena, Italy*
[3] *Unit of Radiotherapy, University Hospital of Siena, Policlinico S. Maria alle Scotte, Viale Bracci, 53100 Siena, Italy*

Correspondence should be addressed to Salvatore Francesco Carbone; fracarb@gmail.com

Received 26 November 2013; Accepted 16 December 2013; Published 16 February 2014

Academic Editor: Giovanni Luca Gravina

Objectives. To assess the diagnostic performance of diffusion-weighted MR imaging (DWI) in patients affected by prostatic fossa (PF) relapse after radical prostatectomy (RP) for prostatic carcinoma (PC). *Methods.* Twenty-seven patients showing a nodular lesion in the PF at T2-weighted MR imaging after RP, with diagnosis of PC relapse established by biopsy or PSA determinations, were investigated by DWI. Two readers evaluated the DWI results in consensus and the apparent diffusion coefficient (ADC) of the nodules, separately; a mean value was obtained (ADCm). *Results.* Relapses did not significantly differ in size in respect of postsurgical benign nodules. The DWI qualitative evaluation showed sensitivity, specificity, accuracy, ppv, and npv values, respectively, of 83.3%, 88.9%, 85.2%, 93.7%, and 72.7% (100%, 87.5%, 95.6%, 93.7%, and 100%, for nodules >6 mm). The intraclass correlation coefficient (ICC) for ADC evaluation between the two readers was 0.852 (95% CI 0.661–0.935; $P = 0.0001$). The ADCm values for relapses and benign nodules were, respectively, $0.98 \pm 0.21 \times 10^{-3}$ mm^2/sec and $1.24 \pm 0.32 \times 10^{-3}$ mm^2/sec ($P = 0.006$). Sensitivity, specificity, accuracy, ppv and npv of ADCm were, respectively, 77.8%, 88.9%, 81.8%, 93.3%, and 66.7% (93.3%, 87.5%, 85.4%, 93.3%, and 87.5% for nodules >6 mm). *Conclusions.* Diffusion-weighted MR imaging is a promising tool in the management of a hyperintense nodule detected by T2-weighted sequences. This might have a relevant importance in contouring radiotherapy treatment volumes.

1. Introduction

Prostate cancer (PC) is second in incidence among malignancies in men in Western countries [1]; the treatment of clinical localized disease is radical prostatectomy (RP) in many cases, and the decrease of the serum total prostate-specific antigen (PSAt) values below 0.1-0.2 ng/mL within 1 month after surgery documents complete tumour eradication [2]. However, a biochemical relapse occurs in 10%–53% of the patients undergoing RP within 5 years, defined as a PSAt increase in at least three consecutive samples [3]. This is usually the first sign of recurrence, often without any clinical or imaging evidence of a tumour mass; the clinical onset of recurrence follows after a median of 5 years [4]. At present, the pattern of relapse (prostatic fossa recurrence versus metastatic disease) is established on the basis of PSAt increase (PSA velocity or PSA doubling time) with slow increasing PSAt values (i.e., doubling time >12 months) suggesting local disease.

Early postoperative radiation therapy (RT) on PF may improve metastasis free and overall survival in cases at risk for LR [5]; however, in common practice, RT is performed

in many cases at the occurrence of LR, with satisfactory results in terms of local control and prostate cancer-specific survival [6]. Radiotherapy as a salvage procedure is the treatment of choice and in such cases is usually performed on standardized volumes [7] corresponding to the PF. Presently, high doses (i.e., ≥70 Gy) are recommended and should be delivered to this whole clinical target volume [8]. However, the sophisticated RT techniques presently available, typically intensity modulated radiation therapy (IMRT), could allow such high doses to be delivered as a boost to the relapsing tumour mass, if detectable, and a lower dose (e.g., 60–64 Gy) to the "elective" volume, that is, the PF. This might result in decreasing RT side effects and complications. Thus, the detection of a mass in the PF and its reliable identification as a tumour relapse may be of the utmost importance.

Many imaging techniques have been investigated in order to individuate and characterize the local relapsing tumour mass after RP. Transrectal ultrasound (TRUS) has a poor capacity to differentiate post-surgical fibrous tissue from a relapse, but TRUS-guided biopsy is considered the gold standard of diagnosis of PC LR and should be attempted whenever possible. On the other hand, the European Association of Urology guidelines do not recommend biopsy for low level of PSA (<1 ng/mL) [9]. 18-Fluorocholine PET/CT scan is also reported to be useful, both as a follow-up procedure after RP in high-risk patients and in the case of a biochemical relapse (PSA > 1.4 ng/mL) [10].

Magnetic resonance imaging (MRI) is generally believed to be the most reliable diagnostic tool, when performed with functional imaging techniques in addition to conventional T2-weighted images. These techniques, such as dynamic contrast-enhanced MR imaging (DCE-MRI), proton spectroscopy (MRSI) [11–16], and diffusion-weighted MRI (DW-MRI, hereafter DWI), allow obtaining precious information about vascularization, metabolism, and tissue cellularity. In particular DWI, already recommended in the protocol for primary PC detection and staging [17], has recently been evaluated in identifying relapsing tumour in the PF after RP [18, 19]. In the present paper, we systematically evaluated a series of postoperative MRI examinations after RP and investigated the role of DWI in nodular lesions occurring in the PF, with the purpose of establishing the reliability of the method in diagnosis and localization of PF PC recurrences.

2. Methods and Materials

2.1. Patients. One hundred and fifty-two patients (pts) (mean age 68.2 y +/− 7.1) with a pathological staging after RP demonstrating T3a-b PCs were submitted to PSAt and MRI follow-up controls from January, 2008, to March, 2011 (i.e., from 3 to 41 months after surgery) at our institution. In 69 patients the conventional T2-weighted imaging demonstrated nodular findings in the PF: this subpopulation was the object of the present study. A PSAt value ≥ 0.2 ng/mL in three or more consecutive determinations was detected in 42 of them ("positive" cases), and an almost steady value <0.2 ng/mL in three determinations over a period of at least 18 months was observed in the other 27 ones ("negative" cases). Out of these 69 pts, only 29 entered the study: the remaining 40 were excluded due to presence of metastatic disease at nuclide bone scan, and/or CT scan, previous RT and/or hormone therapy and/or absence of DWI in the MR scan protocol. Finally, two positive cases were excluded from evaluation because of significant magnetic susceptibility artifacts (metallic clips in DWI images). The remaining 27 pts (18 cases with positive and 9 with negative PSAt determinations, as controls) are the subject of the present report. The standards of reference for positivity or negativity of the DWI results were similar to those outlined by the previous literature [13, 18]: TRUS-guided biopsy of the nodular lesions could confirm a relapsing PC in 7 pts, whereas in the other 11 ones a PSA decrease >50% was observed after RT. Out of the 83 pts with a negative T2-weighted imaging examination of the PF, 15 had positive PSAt determinations and were also submitted to RT on standard volumes. All the 27 patients included in the present study gave consent to the imaging investigations and to the anonymous use of clinical data.

2.2. Imaging. All MR examinations were obtained using a 1.5T MR scanner (Signa HDx Excite Twin Speed, GE Healthcare, USA). Images were acquired using commercially available balloon-covered expandable endorectal coils inflated with air (Endo ATD; Medrad, Pittsburgh, PA, USA) for signal reception, in combination with a four-channel phased array coil (Torso PA; GE Healthcare, USA) using a standardized protocol, as follows:

(i) T2-weighted fast spin echo (FSE) sequences on axial, sagittal, and oblique coronal planes, perpendicular and parallel to prostatic urethra (TR/TE 4600 /105 msec, bandwidth 20.8 kHz, matrix 288 × 256, FOV (cm) 24×24, thickness/gap (mm) 4/0, and NSA-6);

(ii) DWI spin echo (SE) and echo planar imaging (EPI) sequences, with 90° and 180° RF pulses, on axial plane (TR/TE 3675/119 msec, bandwidth 167 kHz, matrix 128 × 128, FOV (cm) 24 × 24, thickness/gap (mm) 4/0 mm, and NSA 4); to reduce magnetic susceptibility artifacts, a spectral fat-saturation pulse was added; diffusion motion probing gradients with b-values of 0 and 600 s/mm^2 were applied on the three orthogonal directions z, x, and y, with vectorial imaging reconstruction (DW images).

Two abdominal radiologists, each unaware of the results of the PSA values and of any other imaging examination, reviewed the MR imaging on a commercial workstation (Advantage Windows, release 4.4, GE Healthcare, USA). A locoregional relapse was suspected whenever a hyperintense nodule (compared to signal of nearest obturator muscle) in the area of PF was observed on conventional T2-weighted images, in more than one plane. The size of the nodules was measured, as the maximum diameter observed in an axial plane, and recorded. The same nodules were reevaluated in DWI (b = 600 sec/mm^2) assuming as a reference the corresponding T2-weighted images. The 1 and 0 score were

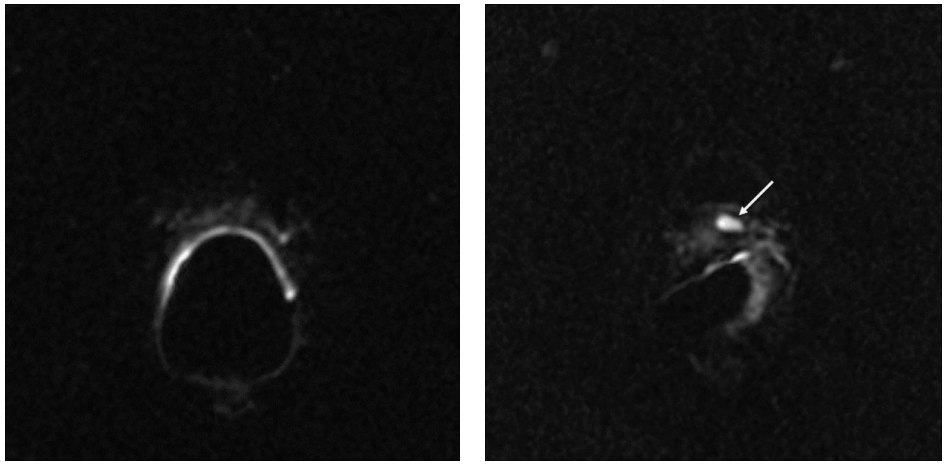

(a) (b)

Figure 1: DWI qualitative scoring. The observers attributed score 0 to the absence of clear-cut hyperintense lesion in the PF area (a) and score 1 to a focal hyperintensity (arrow, (b)) attributable to a relapse.

Table 1: Qualitative and quantitative imaging assessment in respect of the standards of reference.

	DWI (size > 6 mm)		ADC* (size > 6 mm°)	
Standard of reference	No relapse	Relapse	No relapse	Relapse
No relapse	8 (7)	1 (1)	8 (7)	1 (1)
Relapse	3 (0)	15 (15)	4 (1)	14 (14)

Data regarding PF nodules >6 mm are shown in brackets; *cut-off 1.13×10^{-3} mm^2/sec and °cut-off 1.2×10^{-3} mm^2/sec.

assigned, respectively, for presence or absence of hyperintensity, compared to background, in the site of the lesion detected in T2-weighted images (Figure 1). The two readers made this evaluation in consensus. The same operators obtained a quantitative DWI assessment separately, at least one month later, by apparent diffusion coefficient (ADC) maps, calculated using a commercially available software (Functool release 4.4.05, Advantage Windows 4.4, GE Healthcare, USA). Each operator marked an oval-shaped region of interest (ROI) on pathologic area using as a reference DWI images (b = 0 mm/sec^2) previously recognized as DWI score 1, taking into account as a reference the corresponding T2-weighted image. This ROI was automatically pasted on the ADC map, in order to obtain the ADC values of the lesion, each pixel in ADC maps resulting the application of the pixel-by-pixel Stejskal-Tanner monoexponential relationship ADC = $\mathrm{Log}(\mathrm{SI}_0 - \mathrm{SI}_1)/b_1 - b_0$ [20], where SI_0 and SI_1 are, respectively, the signal intensity at b-value of $b_0 = 0$ and $b_1 = 600$ sec/mm^2.

2.3. Statistical Analysis. We used nonparametric statistical tests (Mann-Whitney; Spearman's) due to the small number of pts included in the present reports. The intra-class correlation coefficient (ICC) [21] was used to evaluate the inter-observer agreement for ADC results. The qualitative DWI data (the 0/1 scoring system, as above) and the mean ADC values (ADCm) resulting by the separate observations of the two readers were used for further diagnostic performance evaluations, as follows. Sensitivity, specificity, accuracy, positive, and negative predictive values (ppv and npv, resp.) were calculated by the receiver-operating characteristic curves (ROC). Commercially available software for statistical analysis was used for these purposes (SSPS 17.0, Chicago, USA).

3. Results

Biochemical relapses occurred in 57 out of the 152 pts considered in the preliminary evaluation (37.5%), consistently with the available data of post-RP series of pathological stage T3 PCs [3]. As regards the subject of this paper, PSAt value was 0.29 ± 0.22 ng/mL (95% CI 0.12–0.46) for benign lesions and 1.87 ± 1.29 ng/mL (95% CI 1.22–2.51) for relapses ($P < 0.0001$). The size of the lesions at the T2-weighted sequences did not differ significantly between relapses (11.98 ± 5.05 mm; 95% CI 9.46–14.49) and benign nodules (12.1 mm ± 5.36 mm; 95% CI 7.88–16.12) ($P = 0.941$) out of the 27 cases included in the study. Nodule size was larger than 6 mm in 23 patients. The size of the "malignant" nodules and the PSA values were not significantly correlated (rho: −0.081; $P = 0.687$).

The DWI qualitative score analysis of the hyperintense nodules, carried out in consensus between the two observers, showed 15 true positives, 8 true negatives, 3 false negatives, and 1 false positive (Figure 2, Table 1). In all 3 false negatives the size of the lesion was <6 mm (Figure 3). Sensitivity, specificity, accuracy, ppv, and npv were, respectively, 83.3%, 88.9%, 85.2%, 93.7%, and 72.7%, out of the whole series. Out of the 23 patients showing nodules >6 mm, the reliability of the diagnostic parameters was improved: 100%, 87.5%, 95.6%, 93.7%, and 100%, respectively (Figure 4, Table 2).

About the quantitative evaluation, the interobserver agreement showed an ICC of 0.852 (95% CI 0.661–0.935; $P = 0.0001$). The mean ADC values (ADCm) obtained from

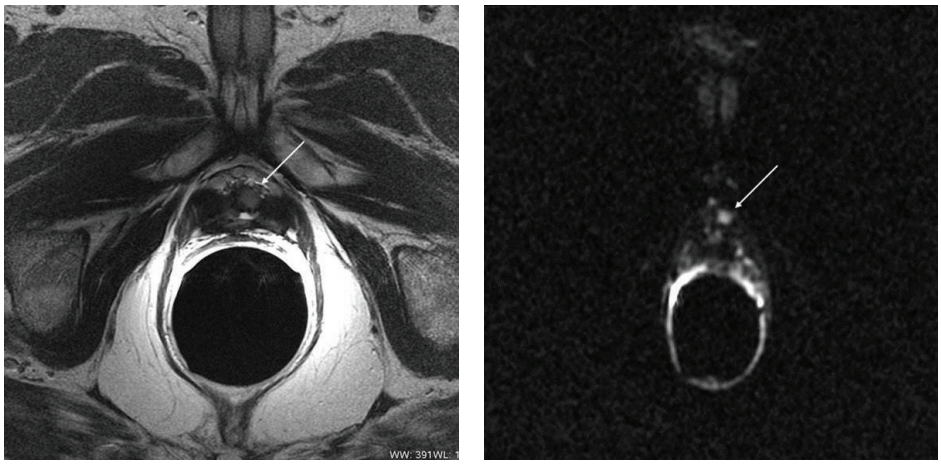

(a) (b)

Figure 2: Relapse after radical prostatectomy. Arrows show a nodular intermediate signal intensity in the T2-weighted image (a), characterized by hyperintensity in DWI (score DWI = 1: (b)).

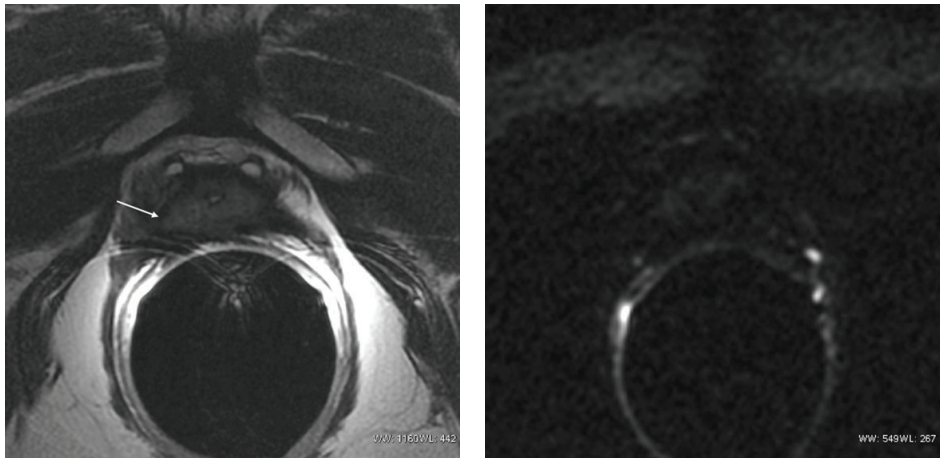

(a) (b)

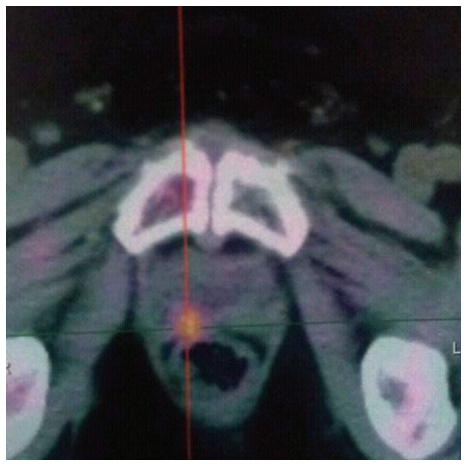

(c)

Figure 3: DWI, false negative. Patient with a glandular apical residual prostate tissue and a progressive increase of PSAt (last value before DWI: 0.61 ng/mL). The T2-weighted image (a) shows the minimal residual prostate tissue with a small bulging in the right paramedian site (arrow). No detectable hyper intensity was visualized in DW image (score DWI = 0, (b)); 18F-choline PET-CT (c) showed a focal uptake at the site of the described bulging. The post-RT decrease of PSAt under 0.2 ng/mL was a further standard of reference in this case.

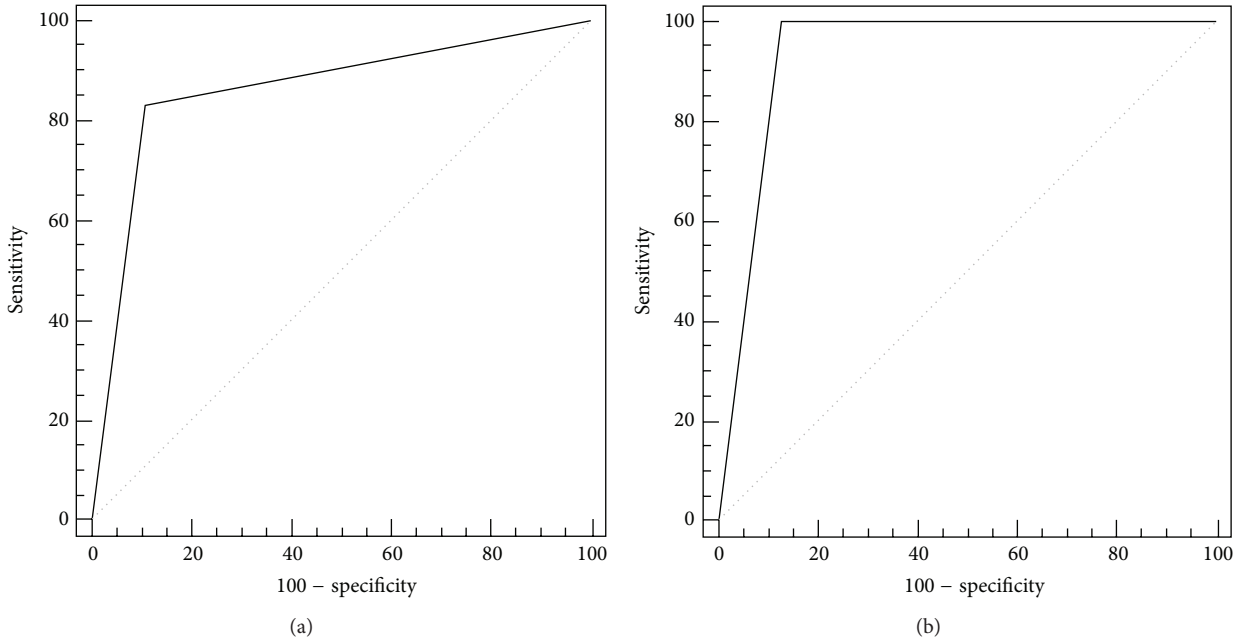

Figure 4: Receiver-operating characteristic curves of DWI score in the whole pts series (a) and in PF nodules with size >6 mm (b). The area under the curve increased for these last cases.

Table 2: Performance (%) of DWI; data regarding PF nodules >6 mm are shown in brackets.

	Sensitivity	Specificity	Accuracy	ppv	npv	Cut-off
DWI score	83.3 (100)	88.9 (87.5)	85.2 (95.6)	93.7 (93.7)	72.7 (100)	
ADCm	77.8 (93.3)	88.9 (87.5)	81.8 (85.4)	93.3 (93.3)	66.7 (87.5)	1.13 (1.2)

the observations of the two readers were $0.98 \pm 0.21 \times 10^{-3}$ mm^2/sec (95% CI 0.88–1.08) for the relapses and $1.24 \pm 0.32 \times 10^{-3}$ mm^2/sec (95% CI 0.99–1.09) for the benign nodules ($P = 0.006$), with a cut-off value of 1.13×10^{-3} mm^2/sec (Figure 5). Sensitivity, specificity, accuracy, ppv, and npv of ADCm were, respectively, 77.8%, 88.9%, 81.8%, 93.3%, and 66.7%. Also for ADCm values, as for the above DWI qualitative analysis, the diagnostic parameters showed an improved reliability in nodules >6 mm (93.3%, 87.5%, 85.4%, 93.3%, and 87.5%, resp.) (Tables 1 and 2).

4. Discussion

DWI provides reliable data concerning tissue cellularity; cell membranes, in fact, limit water proton diffusion [20]. In tumour tissues, such as PC, the hypercellularity is a constraint to proton mobility, differently from other tissues where water molecules move freely in a wide extracellular space [22]. This translates in a natural contrast-based imaging differentiation between tumour and other lesions (e.g., inflammatory or fibrotic), from a qualitative point of view. Also quantitative determinations can be achieved, with ADC values that are significantly lower in tumour than in other lesions and in normal tissue. On these bases, DWI received a considerable interest in the literature concerning primary diagnosis of PC [23–27]. Moreover, DWI has recently been considered as a useful tool in evaluation of PF in patients with biochemical relapse of PSA after primary therapy: ESUR guidelines on prostate MR recommend its use in addition to T2-weighted imaging and DCE in these cases [17].

In our experience, the qualitative DWI examinations achieved 15 true positives, 8 true negatives, 3 false negatives, and 1 false positive, with sensitivity, specificity, accuracy, ppv, and npv values, respectively of 83.3%, 88.9%, 85.2%, 93.7%, and 72.7%, out of the whole series. The three false-negative lesions had a size <6 mm; this is probably due to a low in-plane spatial resolution, as well as to a low signal-to-noise ratio in the DW images; this drawback could be overcome by a 3T MR system [18]. The only false positive could be due to the presence of urine in the urethral anastomosis, close to the lesion, leading to a shine-through artifact. The reliability of the diagnostic parameters was improved in the 23 pts showing nodules >6 mm and 100%, 87.5%, 95.6%, 93.7%, and 100% values were obtained, respectively.

The quantitative ADCm evaluation showed sensitivity, specificity, accuracy, ppv, and npv values that were, respectively, 77.8%, 88.9%, 81.8%, 93.3%, and 66.7%. Also for ADCm values, as for DWI qualitative analysis, the diagnostic parameters showed an improved reliability in nodules >6 mm (93.3%, 87.5%, 85.4%, 93.3%, and 87.5%, resp.). The ADCm values here obtained for LR (cut-off of 1.13×10^{-3} mm^2/sec) are slightly higher than those reported by other authors [19]

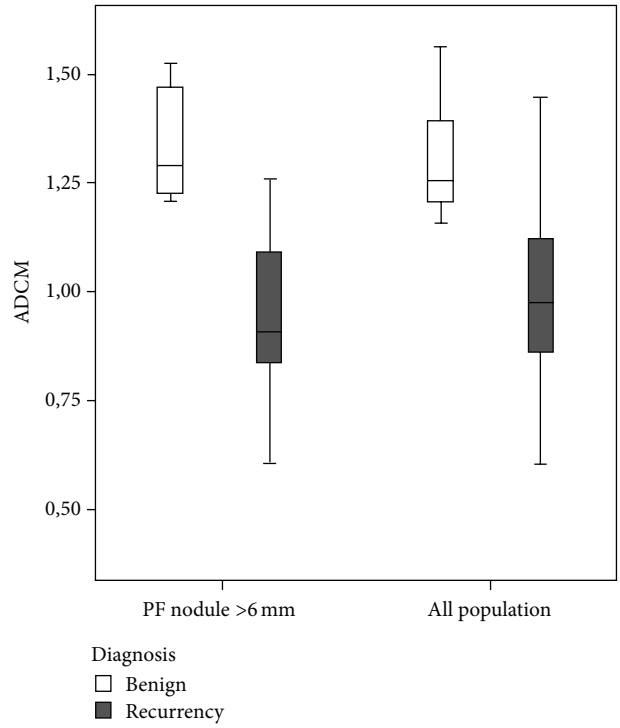

Figure 5: ADCm boxplots for nodules >6 mm and for the whole series. Note the lack of a significant overlapping between recurrences and benign nodules when nodules size <6 mm is excluded.

that used higher *b*-values for DWI. This could be explained by the decrease of pseudodiffusion, due to perfusion, that occurs by increasing *b*-values and that in turn results in reduced ADC values. However, it should be pointed out that a significant suppression of the perfusion component is generally observed even with *b*-values of 300–400 s/mm^2 [28] and that the so-called slow-component perfusion largely predominates for higher *b*-values, due to the intravoxel incoherent motion (IVIM). This, consequently, results in a further small decrease in ADC by increasing *b*-values over those adopted in the present study, high enough to provide an acceptable signal-to-noise ratio in the DW images obtained with the 1.5T MR system that we used. In fact, the choice of a *b*-value of 600 s/mm^2 can be considered low for ADC calculation, as suggested by ESUR guidelines [17]; This can explain the worst diagnostic performance of our quantitative evaluation, if compared to the DWI score that we used for qualitative one. Further acquisitions with higher *b*-values could increase the diagnostic performance. Nevertheless, it should be considered that our first goal was to assess the reliability of a fast qualitative evaluation of the PF in term of presence/absence of relapse; in this attempt an adequate signal-to-noise ratio is ensured by not exceedingly high *b*-value at 1.5T. Another technical drawbacks are magnetic susceptibility artifacts, due to metallic clips or to the air-filled balloon, in the interface with the rectum, that could lead to an unreliable evaluation of some lesions, especially in posterior portion of the PF (false positive or unsatisfactory images). Finally, a limitation of the present analysis is also the small number of patients. This aspect and the lack of significant correlations between the PSAt serum levels and the size of the relapse deserve further consideration, in the attempt to identify a useful PSAt threshold value for the reliability of DWI and of other functional MRI techniques.

Despite these limitations, our results are encouraging and they are comparable to other data regarding DWI in detecting local recurrences, obtained also with higher field MR system [18, 29]. Particularly, a single-center study documented no significant differences of 1.5T versus 3.0T in detection of local recurrences [29]; in this work the median tumour size was of 0.26 cm^3, with a significant cut-off PSAt of 0.3 ng/mL. In another single-center prospective study, authors report combined T2-weighted and DWI sensitivity 93–98%, specificity 89–96%, and accuracy 86–92%, depending on size of the lesion and *b*-value, using a 3T MR system [18]. This last MR equipment could solve problems related to low spatial resolution of DWI sequences and could give the possibility to use higher *b*-values, as the reported diagnostic performance seems to increase with higher *b*-values (b = 3000 s/mm^2) also for small lesions (4–8 mm) [18]. However, 3T MR facilities are less in current use than 1.5T systems; if our data will be confirmed by more large population studies, the translation of this technique in common clinical practice could be more feasible. DWI also shows diagnostic results comparable with other functional techniques: DCE-MR and MRSI show sensitivity, specificity, accuracy, ppv, and npv values, respectively, in the range of 84%–95%, 75%–100%, 86%–94%, 92%–100%, and 57%–88%, that are generally higher than those achieved by T2-weighted MR imaging and also by PET-CT investigations, at least for LR with mean diameters in the range from 6 mm to 15 mm [30]. Particularly, DCE-MRI seems to be more accurate if achieved with a 3T MR system [18]. On the other hand, DCE-MRI requires contrast medium administration, which sometimes could be not tolerated, and MRSI needs long acquisition and postprocessing times, and a long training period for the operator. On the contrary, DWI acquisition is achieved in 2-3 minutes and the ADC maps are automatically obtained by the workstation.

Compared with MR imaging, PET-CT scan deserves a particular mention due to the capability to differentiate local from systemic relapses. In particular, the use of choline as tracer is considered a reliable PCa biomarker for its role in cellular membrane metabolism. In a recent review, Cho-PET-CT was reported in patients with biochemical recurrence after RP or RT, with sensitivity ranging from 38% to 98%, depending on different issues like PSA value and type of treatment [10]. However, in patients treated with RP, Cho-PET-CT detection rate is too low for PSA value <1 ng/mL; at this value, salvage RT achieves suboptimal results in terms of outcome [9]. Moreover, in patients with PSA > 2 ng/mL and negative imaging, Cho-PET-CT scan is positive only in 28% cases [9]. At least, PET-CT scan is not widely available.

Of course, the present report needs confirmation on the grounds of a larger series of patients.

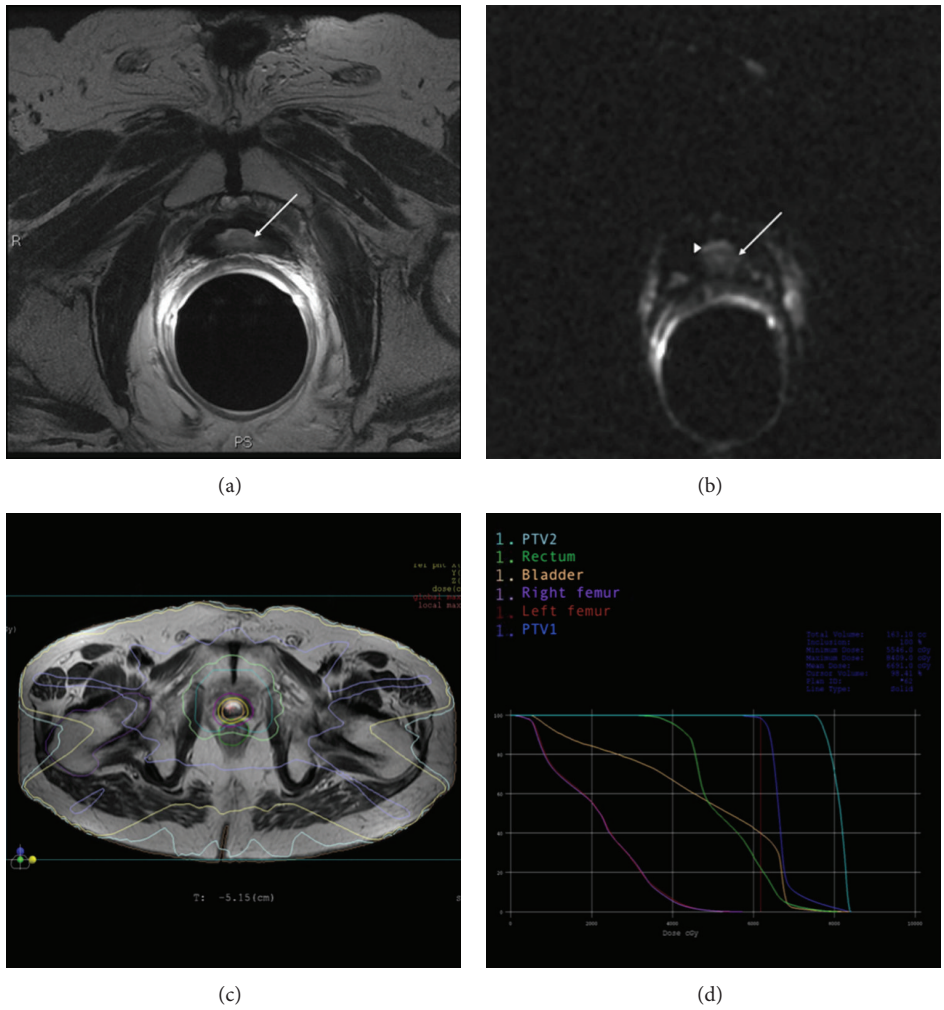

Figure 6: RT simulation plan: a paraurethral nodule suspected for relapse (white arrow) is shown by T2 images in PSA-positive patients (a); DWI score 1 qualitative evaluation (white arrow, suspected nodule; arrowhead, shine-through artifact of urine) (b); IMRT simultaneous boost (SIB) treatment plan (PTV1: 64 Gy delivered to the PF; PTV2: 74 Gy delivered to the nodule) (c); dose-volume histograms of the IMRT SIB plan (d).

5. Conclusions

Presently, the DWI characterization of a nodule in PF, detected by a previous T2-weighted MR imaging in patients showing a PSAt increase after RP for PC, can be considered appropriate as an alternative to more sophisticated MRI techniques, not widely available. Further studies are mandatory to confirm the preliminary results reported here. The reliable identification and localization of the relapse by MR imaging may be of the utmost importance mainly in RT salvage treatment (i.e., a very frequent occurrence), a useful and practical tool for targeting it with a boost dosage in the course of IMRT (Figure 6), or of other advanced irradiation techniques.

Conflict of Interests

The authors declare that there is no conflict of interests regarding the publication of this paper.

References

[1] A. Jemal, M. M. Center, C. De Santis, and E. M. Ward, "Global patterns of cancer incidence and mortality rates and trends," *Cancer Epidemiology Biomarkers and Prevention*, vol. 19, no. 8, pp. 1893–1907, 2010.

[2] C. L. Amling, E. J. Bergstralh, M. L. Blute, J. M. Slezak, and H. Zincke, "Defining prostate specific antigen progression after radical prostatectomy: what is the most appropriate cut point?" *The Journal of Urology*, vol. 165, no. 4, pp. 1146–1151, 2001.

[3] M. Han, A. W. Partin, M. Zahurak, S. Piantadosi, J. I. Epstein, and P. C. Walsh, "Biochemical (prostate specific antigen) recurrence probability following radical prostatectomy for clinically localized prostate cancer," *The Journal of Urology*, vol. 169, no. 2, pp. 517–523, 2003.

[4] S. J. Freedland, E. B. Humphreys, L. A. Mangold, M. Eisenberger, and A. W. Partin, "Time to prostate specific antigen recurrence after radical prostatectomy and risk of prostate cancer specific mortality," *The Journal of Urology*, vol. 176, no. 4, pp. 1404–1408, 2006.

[5] I. M. Thompson, C. M. Tangen, J. Paradelo et al., "Adjuvant radiotherapy for pathological T3N0M0 prostate cancer significantly reduces risk of metastases and improves survival: long-term follow-up of a randomized clinical trial," *The Journal of Urology*, vol. 181, no. 3, pp. 956–962, 2009.

[6] B. J. Trock, M. Han, S. J. Freedland et al., "Prostate cancer-specific survival following salvage radiotherapy vs observation in men with biochemical recurrence after radical prostatectomy," *The Journal of the American Medical Association*, vol. 299, no. 23, pp. 2760–2769, 2008.

[7] J. M. Michalski, C. Lawton, I. El Naqa et al., "Development of RTOG consensus guidelines for the definition of the clinical target volume for postoperative conformal radiation therapy for prostate cancer," *International Journal of Radiation Oncology Biology Physics*, vol. 76, no. 2, pp. 361–368, 2010.

[8] F. Alongi, B. De Bari, P. Franco et al., "The PROCAINA (PROstate CAncer INdication Attitudes) Project (Part I): a survey among Italian radiation oncologists on postoperative radiotherapy in prostate cancer," *La Radiologia Medica*, vol. 118, no. 4, pp. 660–678, 2013.

[9] European Association of Urology, "Guidelines 2013," http://www.uroweb.org/gls/pdf/09_Prostate_Cancer_LR.pdf.

[10] M. Picchio, A. Briganti, S. Fanti et al., "The role of choline positron emission tomography/computed tomography in the management of patients with prostate-specific antigen progression after radical treatment of prostate cancer," *European Urology*, vol. 59, no. 1, pp. 51–60, 2011.

[11] J. M. Silverman and T. L. Krebs, "MR imaging evaluation with a transrectal surface coil of local recurrence of prostatic cancer in men who have undergone radical prostatectomy," *American Journal of Roentgenology*, vol. 168, no. 2, pp. 379–385, 1997.

[12] T. Sella, L. H. Schwartz, P. W. Swindle et al., "Suspected local recurrence after radical prostatectomy: endorectal coil MR imaging," *Radiology*, vol. 231, no. 2, pp. 379–385, 2004.

[13] A. Sciarra, V. Panebianco, S. Salciccia et al., "Role of dynamic contrast enhanced magnetic resonance (MR) imaging and proton MR spectroscopic imaging in the detection of local recurrence after radical prostatectomy for prostate cancer," *European Urology*, vol. 54, no. 3, pp. 589–600, 2008.

[14] V. Panebianco, A. Sciarra, D. Lisi et al., "Prostate cancer: 1HMRS-DCEMR at 3T versus [(18)F]choline PET/CT in the detection of local prostate cancer recurrence in men with biochemical progression after radical retropubic prostatectomy (RRP)," *European Journal of Radiology*, vol. 81, no. 4, pp. 700–708, 2012.

[15] E. Casciani, E. Polettini, E. Carmenini et al., "Endorectal and dynamic contrast-enhanced MRI for detection of local recurrence after radical prostatectomy," *American Journal of Roentgenology*, vol. 190, no. 5, pp. 1187–1192, 2008.

[16] S. Cirillo, M. Petracchini, L. Scotti et al., "Endorectal magnetic resonance imaging at 1.5 Tesla to assess local recurrence following radical prostatectomy using T2-weighted and contrast-enhanced imaging," *European Radiology*, vol. 19, no. 3, pp. 761–769, 2009.

[17] J. O. Barentsz, J. Richenberg, R. Clements et al., "ESUR prostate MR guidelines 2012," *European Radiology*, vol. 22, no. 4, pp. 246–757, 2012.

[18] V. Panebianco, F. Barchetti, A. Sciarra et al., "Prostate cancer recurrence after radical prostatectomy: the role of 3-T diffusion imaging in multi-parametric magnetic resonance imaging," *European Radiology*, vol. 23, no. 6, pp. 1745–1752, 2013.

[19] G. Giannarini, D. P. Nguyen, G. N. Thalmann, and H. C. Thoeny, "Diffusion-weighted magnetic resonance imaging detects local recurrence after radical prostatectomy: initial experience," *European Urology*, vol. 61, no. 3, pp. 616–620, 2012.

[20] D. Le Bihan, R. Turner, P. Douek, and N. Patronas, "Diffusion MR imaging: clinical applications," *American Journal of Roentgenology*, vol. 159, no. 3, pp. 591–599, 1992.

[21] P. E. Shrout and J. L. Fleiss, "Intraclass correlations: uses in assessing rater reliability," *Psychological Bulletin*, vol. 86, no. 2, pp. 420–428, 1979.

[22] A. R. Padhani, G. Liu, D. M. Koh et al., "Diffusion-weighted magnetic resonance imaging as a cancer biomarker: consensus and recommendations," *Neoplasia*, vol. 11, no. 2, pp. 102–125, 2009.

[23] G. Manenti, E. Squillaci, M. Di Roma, M. Carlani, S. Mancino, and G. Simonetti, "*In vivo* measurement of the apparent diffusion coefficient in normal and malignant prostatic tissue using thin-slice echo-planar imaging," *Radiologia Medica*, vol. 111, no. 8, pp. 1124–1133, 2006.

[24] M. A. Jacobs, R. Ouwerkerk, K. Petrowski, and K. J. Macura, "Diffusion-weighted imaging with apparent diffusion coefficient mapping and spectroscopy in prostate cancer," *Topics in Magnetic Resonance Imaging*, vol. 19, no. 6, pp. 261–272, 2008.

[25] J. Yamamura, G. Salomon, R. Buchert et al., "Magnetic resonance imaging of prostate cancer: diffusion-weighted imaging in comparison with sextant biopsy," *Journal of Computer Assisted Tomography*, vol. 35, no. 2, pp. 223–228, 2011.

[26] S. Verma, A. Rajesh, H. Morales et al., "Assessment of aggressiveness of prostate cancer: correlation of apparent diffusion coefficient with histologic grade after radical prostatectomy," *American Journal of Roentgenology*, vol. 196, no. 2, pp. 374–381, 2011.

[27] D. M. Somford, J. J. Fütterer, T. Hambrock, and J. O. Barentsz, "Diffusion and perfusion MR imaging of the prostate," *Magnetic Resonance Imaging Clinics of North America*, vol. 16, no. 4, pp. 685–695, 2008.

[28] S. F. Riches, K. Hawtin, E. M. Charles-Edwards, and N. M. de Souza, "Diffusion-weighted imaging of the prostate and rectal wall: comparison of biexponential and monoexponential modelled diffusion and associated perfusion coefficients," *NMR in Biomedicine*, vol. 22, no. 3, pp. 318–325, 2009.

[29] S. L. Liauw, S. P. Pitroda, S. E. Eggener et al., "Evaluation of the prostate bed for local recurrence after radical prostatectomy using endorectal magnetic resonance imaging," *International Journal of Radiation Oncology, Biology, Physics*, vol. 85, no. 2, pp. 378–384, 2013.

[30] A. Alfarone, V. Panebianco, O. Schillaci et al., "Comparative analysis of multiparametric magnetic resonance and PET-CT in the management of local recurrence after radical prostatectomy for prostate cancer," *Critical Reviews in Oncology/Hematology*, vol. 84, no. 1, pp. 109–121, 2012.

Hindawi Publishing Corporation
BioMed Research International
Volume 2014, Article ID 323594, 14 pages
http://dx.doi.org/10.1155/2014/323594

Research Article

A Novel Role for Raloxifene Nanomicelles in Management of Castrate Resistant Prostate Cancer

Sebastien Taurin,[1] Hayley Nehoff,[1] Thalita van Aswegen,[1] Rhonda J. Rosengren,[1] and Khaled Greish[1,2]

[1] *Department of Pharmacology and Toxicology, University of Otago, Dunedin, New Zealand*
[2] *Department of Oncology, Faculty of Medicine, Suez Canal University, Ismailia, Egypt*

Correspondence should be addressed to Sebastien Taurin; sebastien.taurin@otago.ac.nz and Khaled Greish; khaled.gerish@otago.ac.nz

Received 19 November 2013; Accepted 26 December 2013; Published 6 February 2014

Academic Editor: Giovanni Luca Gravina

Of patients with castrate resistant prostate cancer (CRPC), less than 25–33% survive more than five years. Recent studies have implicated estrogen, acting either alone or synergistically with androgens in the development of castrate resistant prostate cancer. Several *in vitro* and *in vivo* studies, as well as a limited number of clinical trials, have highlighted the potential of selective estrogen receptor modulators, such as raloxifene (Ral) for the treatment of castrate resistant prostate cancer. However, the poor oral bioavailability and metabolism of selective estrogen receptor modulators limit their efficiency in clinical application. To overcome these limitations, we have used styrene co-maleic acid (SMA) micelle to encapsulate raloxifene. Compared to free drug, SMA-Ral micelles had 132 and 140% higher cytotoxicity against PC3 and DU 145 prostate cell lines, respectively. SMA-Ral effectively inhibits cell cycle progression, increases apoptosis, and alters the integrity of tumor spheroid models. In addition, the micellar system induced changes in expression and localization of estrogen receptors, epidermal growth factor receptor (EGFR), and downstream effectors associated with cell proliferation and survival. Finally, SMA-Ral treatment decreased migration and invasion of castrate resistant prostate cancer cell lines. In conclusion, SMA-Ral micelles can potentially benefit new strategies for clinical management of castrate resistant prostate cancer.

1. Introduction

Prostate cancer is the most common noncutaneous malignant neoplasm and the second leading cause of male cancer-related deaths in Oceania, Europe, and North America [1]. For the 25 to 40% of patients not cured by the initial treatments of prostatectomy or radiation therapy, the cancer inevitably reoccurs and metastasizes to distant organs [1, 2]. The standard treatment for metastatic prostate cancer is surgical or chemical castration which reduces circulating androgens (<50 ng/dL) and suppresses the activity of the androgen receptor (AR) [3]. However, despite an initial 12–18 months of regression, patients frequently relapse and a more aggressive cancer progresses to a castrate resistant status [4]. The 5-year relative survival rate for patients with castrate resistant prostate cancer (CRPC) is approximately 25–33% [5]. The initiation and progression of CRPC are not well understood and may involve multiple mechanisms such as the activation of tyrosine kinase receptors by growth factors, the loss of cell cycle regulators or genetic mutations of the androgen receptor [6]. Therapeutic options for CRPC are limited in their efficacy, as the disease inevitably progresses to metastasis.

Recently, several *in vitro* and preclinical animal studies have involved estrogens alone or synergistically with androgens in the progression of prostate cancer [6–11]. In the clinic, the significance of estrogen plasma levels as a predictor of prostate cancer development remains controversial [12]. Recently it has been demonstrated that prostate tumor growth may rely on systemic circulation levels of steroids and on local steroid production by prostate cancer cells [8, 13, 14]. Multiple isoforms of both estrogen receptor (ER)α and ERβ are differentially expressed in the prostate and contribute to cellular homeostasis. In a disease state, ERβ1 expression gradually reduces as the cancer progresses towards higher grade.

However, ERβ1 is highly expressed in prostate tumors that have metastasized to the bone and lymph nodes [15]. Less is known about the contributions of the other isoforms ERβ2–5 [16]. Other studies reported a low ERα expression in CRPC and metastatic lesions suggesting a role of ERα in tumor development and metastasis [17]. Moreover, the estrogen receptor antagonist, ICI 182, 780, inhibited the growth of the CRPC cell lines DU145 and PC3 cells [18].

In pioneering work in the early 1941s, Huggins and Hodges used diethylstilbestrol (DES), a synthetic estrogen, as a standard therapy for metastatic prostate cancer [19]. Several studies have demonstrated that estrogen receptor modulators can be valuable treatment options and recent preclinical studies have highlighted the use of selective estrogen receptor modulators (SERMs) for the prevention and treatment of CRPC [20]. Using different generations of SERMS (i.e., tamoxifen, raloxifene, or toremifene), several studies have demonstrated the potency of these drugs for the prevention of CRPC *in vitro* and in preclinical studies carried out in rat or mouse models [20–22]. Still, SERMs have shown limited efficacy in clinical trials [23–26]. Raloxifene was approved for the reduction of the risk of invasive breast cancer in postmenopausal women and postmenopausal women with osteoporosis [27], but raloxifene has been also shown to stabilize the progression of prostate cancer in a pilot phase II clinical trial (60 mg/day for 1 year) [25]. These data suggest the potential of raloxifene for the management of CRPC. However, raloxifene's effect is limited *in vivo* by low bioavailability (2%) due to poor solubility, extensive metabolism, and being prone to efflux mechanisms of various transporters such as multidrug resistance-related proteins, or organic anion transporter [28]. Therefore, we have hypothesized that the encapsulation of raloxifene in a nanodelivery platform will improve water solubility, protect the drug from metabolism, and efflux mechanisms and could potentially improve its cytotoxicity against CRPC cell lines.

We have previously developed a nanodelivery platform which exploits the amphiphilic nature of poly(styrene co-maleic acid) (SMA) for the encapsulation of highly hydrophobic drugs [29, 30]. In this study, we synthesized and characterized SMA-raloxifene (SMA-Ral) micelles relative to their drug loading, size, charge, and release rate. We examined the effect of SMA-Ral micelles compared to free raloxifene on cytotoxicity, cell proliferation, and apoptosis in two CRPC cell lines, PC3 and DU145 cells. In addition, we have shown that SMA-Ral alters the integrity of the CRPC tumor spheroids. Finally, we showed that the SMA-Ral inhibits migration and invasion of PC3 CRPC cell line as well as reducing the crosstalk between PC3 and endothelial cells.

2. Experimental Section

2.1. Materials. Raloxifene hydrochloride (99% purity), cumene terminated poly(styrene-co-maleic anhydride) with an average Mn~1600, N-(3-dimethylaminopropyl)-N-ethylcarbodiimide hydrochloride (EDAC), and sulforhodamine B were obtained from Sigma-Aldrich Ltd.

2.2. Methods

2.2.1. Cell Culture. The CRPC cell lines PC3 and DU145 and human umbilical vein endothelial cells (HUVEC) were obtained from American Type Culture Collection (Manassas USA). CRPC cells were maintained in complete growth media DMEM/Ham's F12 supplemented with 5% fetal bovine serum, 2 mM L-glutamine, 100 units/mL penicillin, 100 units/mL of streptomycin, and 2.2 g/L of $NaHCO_3$. HUVEC were seeded in complete HUVEC media (EBM-2 basal media containing FBS and growth supplements) as described by the manufacturer (Lonza, Auckland, New Zealand). For all procedures, cells were harvested using TrypLE Express (Life Technologies, Auckland, New Zealand) and were maintained at 37°C in a humidified atmosphere of 5% CO_2.

2.2.2. Preparation of SMA-Ral Micelles. SMA-Ral micelles were prepared as described previously [30]. Briefly, the hydrolyzed SMA solution was adjusted to pH 5; raloxifene-HCl was dissolved in a minimum volume of DMSO and added to the SMA solution with stirring. EDAC solubilized in distilled water was added to the mixture and allowed to stir for 20 min at pH 5. The solution was then adjusted to pH 11 with 0.1 N NaOH and stirred for 30 min. The pH was readjusted to pH 7.4 with HCl 0.1 N. The clear micelle suspension was ultrafiltered 4 times using a lab-scale ultrafiltration system mounted with a Pellicon XL filter 10 kDa (Merck Millipore, Auckland, New Zealand). The concentrated micelle solution was lyophilized to obtain the final SMA-Ral powder.

2.2.3. Loading of SMA-Ral. A standard curve of raloxifene was prepared in DMSO and measured at 287 nm. Drug content of SMA-Ral was determined by solubilizing SMA-Ral (1 mg/mL) in DMSO and measuring the absorbance at 287 nm in comparison with the standard curve. The loading was expressed as weight % of raloxifene in the final micelle compared to the total weight of recovered SMA-Ral. The SMA-Ral loading was determined as 20%.

2.2.4. Size and Charge of SMA-Ral Micelles. SMA-Ral micelles (4 mg/mL) were solubilized either in $NaHCO_3$ (0.1 M, pH 7.4) to determine the size or water to estimate the charge. All measurements for size distribution and zeta potential were carried out using the Malvern ZEN3600 Zetasizer nano series (Malvern Instruments Inc., Westborough, MA). Measurements from three independent experiments were conducted in triplicate.

2.2.5. Drug Release. The release of raloxifene from the micelle construct was evaluated using a dialysis method. SMA-Ral micelles were prepared at a concentration of 1 mg/mL in distilled water. Using a dialysis bag with a 12 kDa molecular weight cutoff, 3 mL was dialyzed against 30 mL of distilled water (pH adjusted to pH 5.5, pH 6.8, or pH 7.4). Over a period of 5 days, 2 mL of sample outside the dialysis bag was removed and the absorbance was measured at 287 nm. The percentage of release was determined by the ratio of the absorbance between the solution outside the bag at defined

time points and that within the bag at $t = 0$. All experiments were performed in triplicate. Percentage release is reported as mean ± standard error.

2.2.6. Cytotoxicity of SMA-Ral. PC3 (4×10^3 cells/well) and DU145 cells (1.8×10^4 cells/well) were seeded in 96 well-plates and incubated for 24 h at 37°C in 5% CO_2 and then treated with 0 to 30 μM concentration range of either free raloxifene or SMA-Ral. The cells were incubated for 72 h and fixed using trichloroacetic acid (TCA). Cell number was determined using the sulforhodamine B assay [31]. The concentration required to decrease cell numbers by 50% (IC_{50}) was determined by nonlinear regression using Prism software. The three independent experiments were performed in triplicate.

2.2.7. [^{3}H]-Thymidine Incorporation. DNA synthesis in cells was determined using a [^{3}H]-thymidine incorporation assay. Briefly, PC3 (20,000 cells/well) and DU145 cells (8×10^4 cells/well) were seeded in 24 well-plates and incubated for 36 h, cells were treated with SMA-Ral or free raloxifene at 2, 5, and 10 μM for 48 h. [^{3}H]-thymidine (0.5 μCi/well) was added for the last 20 h of the treatment. [^{3}H]-thymidine incorporation was measured as described previously [32].

2.2.8. Cell Cycle Analysis. PC3 (8×10^4 cells per well) and DU145 (3×10^5 cells per well) cells were seeded in 6-well culture plates in 1.5 mL of complete growth media. Cells were treated with SMA-Ral or free raloxifene at 2, 5, and 10 μM for 48 h. Cell cycle distribution was assessed using propidium iodide staining, as previously described [33]. Samples were analyzed using a FACScalibur flow cytometer (BD Biosciences, San Jose, CA, USA) and the proportion of cells in each of G0/G1-, S- and G2/M-phases were determined using CellQuest Pro software (BD Biosciences, San Jose, CA, USA).

2.2.9. Apoptosis Analysis. PC3 (8×10^4 cells per well) and DU145 (3×10^5 cells per well) cells were seeded in 6-well culture plates in 1.5 mL of complete growth media. Cells were treated with SMA-Ral or free raloxifene at 2, 5 and 10 μM for 48 h. Apoptosis was assessed using Annexin-V-FLUOS/propidium iodide staining, as described previously [33]. Samples were analyzed using a FACScalibur flow cytometer and the proportion of apoptotic cells was determined using CellQuest Pro software.

2.2.10. Western Blot. PC3 cells (4×10^4 cells per well) were seeded in 12-well culture plates in 1 mL of complete growth media and incubated for 36 h. PC3 cells were treated with SMA-Ral or free raloxifene at 2, 5, and 10 μM for 48 h. Cells were lysed in buffer containing 50 mM Tris-HCl (pH 8), 150 mM NaCl, and 1% Triton X-100, 1% SDS, 1 mM NaF, 200 μM sodium orthovanadate, and protease inhibitors (1 μg/mL leupeptin, 1 μg/mL aprotinin, 1 mM PMSF). The lysates were cleared from insoluble material by centrifugation at 20,000 g for 10 min, boiled in Laemmli buffer, subjected to polyacrylamide gel electrophoresis, and analyzed by Western blotting.

2.2.11. Indirect Immunofluorescence Microscopy. Immunofluorescence was performed as described previously [34]. PC3 cells (20,000 cells/well) seeded on glass slides were incubated for 36 h and treated with SMA-Ral or free raloxifene at 5 or 10 μM for 48 h. Cells were washed twice with ice-cold PBS, fixed in 4% paraformaldehyde in PBS for 15 min at room temperature, washed again with PBS, and permeabilized in 0.2% Triton-X100 in PBS for 5 min, followed by incubation with 1% bovine serum albumin in PBS for 1 h. The cells were then incubated with antiestrogen receptor β antibody (5 μg/mL in PBS/bovine serum albumin, as above) overnight at 4°C for 1 h and washed four times with PBS, followed by incubation with fluorescein-conjugated goat anti-mouse IgG (10 μg/mL in PBS/bovine serum albumin, as above) for 1 h at room temperature. The slides were washed four more times with PBS, and the coverslips were mounted using Gel/Mount aqueous mounting medium (Fisher, Pittsburgh, PA). The images were taken under a confocal fluorescent microscope.

2.2.12. Cell Migration. Migration of PC3 cells was measured using the *in vitro* cell scratch assay. After cells grown in 6-well plates had reached confluence, a scratch was made with a pipette tip followed by extensive washing with serum-free medium to remove cell debris. SMA-Ral or free raloxifene at 5 and 10 μM or controls (SMA or DMSO) were then added. Cells were allowed to migrate into the scrapped area for up to 20 h at 37°C. At the indicated times, cells were photographed.

2.2.13. Cell Invasion. PC3 cells (4×10^4 cells/mL) were seeded onto growth factor-reduced matrigel invasion chambers (8 μm pore; BD Biosciences) with or without free raloxifene or SMA-Ral 10 μM for 20 h. Lower chambers contained DMEM/Ham's F12 supplemented with the chemoattractant, 5% FBS. Filters were fixed in methanol and stained using Diff Quick staining solutions. Cells from each well were counted under an inverted microscope at 20x magnification. The invasion was expressed as the percentage of cells passing through the matrigel layer over the number of cells counted in the control well without matrigel. Data were collected from three independent experiments, each done in triplicate. Migrated cells were counted, and mean differences (±S.E.) between groups were analyzed using the Student's t test.

2.2.14. MMP-9 Activity Assay. PC3 cells were seeded in 6-well plate (1.2×10^5 cells/well) and incubated for 36 h. The cells were washed with PBS and then incubated in serum free media. Cells were treated with either free raloxifene or SMA-Ral 10 μM, DSMO (0.05%) or SMA for 24 h and 48 h. Media was collected, centrifuged to remove cell debris, and freeze dried for 12 h. Samples were rehydrated and mixed with loading buffer (0.4 mol/L Tris, pH 6.8, 5% SDS, 20% glycerol, 0.03% bromophenol blue). Samples were loaded on a 10% SDS-polyacrylamide gel containing 1 mg/mL of gelation. After electrophoresis, the gels were incubated in renaturing solution (2.5% Triton-X-100) for 30 minutes at room temperature and then for 24 h at 37°C in a developing buffer containing 50 mmol/L Tris, pH 7.5, 200 mmol/L NaCl, 4 mmol/L $CaCl_2$, and 0.02% NP40. The gels were then stained with

Coomassie blue R250, and regions without staining were indicative of gelatin lysis. The gels were briefly rinsed and scanned.

2.2.15. Endothelial Tube Formation Assay and PC3 Coculture. Tube formation was carried out using HUVEC. Briefly, Geltrex (Invitrogen, Auckland, NZ) was allowed to thaw on ice at 4°C overnight. 40 μL was pipetted into a 96-well plate and kept for 30 min at 37°C to allow gelling. HUVECs were seeded in triplicate on the top of Geltrex layer at a density of 1.5×10^4 cells/well. Various concentrations of raloxifene or SMA-Ral (5 and 10 μM) were added into the wells and incubated for 20 h at 37°C in 5% CO_2 atmosphere. After incubation time, pictures were taken. For the co-culture study. HUVEC (1.5×10^4 cells/well) and PC3 cells (6×10^3 cells/well) were seeded on Geltrex as previously described and treated with free raloxifene or SMA-Ral 10 μM. Following treatments, the cells were incubated for 20 h at 37°C in 5% CO_2 atmosphere. After incubation time, pictures were taken. The three independent experiments were performed in triplicate.

2.2.16. Tumor Spheroids and Cell Viability via Acid Phosphatase Assay. Tumor spheroids were produced as previously described [35]. Briefly, PC3 cells were trypsinized and the cell suspension (8000 cells) was transferred to a 96-well plate precoated with agarose (1.5% w/v). Cells were incubated for 4 days to generate spheroids of 400 μm in diameter. They were then treated with 2, 5, or 10 μM of free raloxifene or SMA-Ral for 15 days. Media and treatment were renewed every three days. At the end of the treatment period, photographs were taken and cell viability of the tumor spheroids was assessed by an acid phosphatase assay as previously described [35]. Briefly, tumor spheroids were collected, washed in phosphate buffered saline, and incubated in the presence of acid phosphatase buffer (0.1 M sodium acetate, 0.1% Triton X-100, and p-nitrophenyl phosphate (2 mg/mL)) for 90 min at 37°C. The reaction was stopped with NaOH (1 N) and quantified at 405 nm on a microplate reader. The results are expressed as percentage of control. The three independent experiments were performed in sextuplicate.

2.2.17. Statistics. Groups were compared using a one-way ANOVA. In all cases, the ANOVA was coupled with the Student-Newman-Keuls post hoc test. For all analyses, $P < 0.05$ was the minimal requirement for a statistically significant difference.

3. Results

3.1. Characterization of SMA-Ral. The poor solubility of raloxifene can be significantly improved by forming polymeric micelles from assembled amphiphilic SMA block copolymers. While free raloxifene is insoluble in water, the SMA-Ral micelles could be easily dissolved with an apparent solubility of 10.6 mg/mL (Table 1). The UV-spectrophotometry profile of the micellar drug was similar to that of free raloxifene. In the current study, we achieved loading of 20% as determined by the weight ratio of raloxifene over SMA. SMA-Ral had a mean micelle diameter of 65.34 ± 30.89 nm and a polydispersity index of 0.135 as measured by dynamic light scattering (Table 1). Nanomedicines with diameters greater than 7 nm evade renal filtration and urinary excretion [36]. The charge of SMA-Ral was near neutral with a zeta potential of −0.0165 mV (Table 1). Having a neutral zeta potential is helpful in decreasing the recognition of the micelle by the reticuloendothelial system (RES) composed of macrophages [37] and could prolong its presence in the circulation upon parenteral administration.

Table 1: SMA-Ral micelles characterization.

SMA-Ral	Measurement
Drug loading efficiency (%)	87
Drug loading (% w/w)	20
Mean micelle diameter (nm)	65.34 ± 30.89
Polydispersity index	0.135 ± 0.021
Zeta potential (mV)	−0.0165 ± 4.59
Solubility (mg/mL)	10.6

3.2. Release of Raloxifene from SMA-Ral. We compared the release rate of raloxifene at pH 5.5, 6.8 and 7.4 (Figure 1). At pH 7.4, similar to that of plasma, the cumulative release of raloxifene was 11.6% over 5 days of incubation. At pH 6.8, a comparable value to the surrounding of tumor tissue, the release of raloxifene was similar to that of pH 7.4 (11.9%). This release rate is optimal for a prolonged circulation time, protection from metabolizing enzymes, and ultimate tumor accumulation. The SMA-Ral had a faster release profile at pH 5.5, which corresponds to that found in the lumen of late endosomes with a cumulative release of 16.2% after 5 days of incubation (Figure 1). The stable micelles would thus benefit protecting raloxifene until it reaches tumor cells and then could be internalized and released through membrane hydrophobic partition, a unique intracellular release mechanism of SMA micellar system as described by Nakamura et al. [38].

3.3. Cytotoxicity of SMA-Ral. The cytotoxicity of SMA-Ral micelles was assessed *in vitro* over 72 h in CRPC cell lines, namely, PC3 and DU145 cells, and compared to the free drug. Treatment with SMA-Ral showed a higher cytotoxic effect in both cell lines compared to free raloxifene (Table 2). SMA (24 μg/mL) and DMSO (0.05%) controls showed no cytotoxicity in both cell lines over the same period of treatment.

The effects of specific concentrations of free raloxifene and SMA-Ral were assessed over a time course of 72 h in PC3 and DU145 cells. PC3 cells were more sensitive to raloxifene than DU145 cells (Figure 2). In both cell lines, the SMA-Ral treatments were more potent than free raloxifene (Figure 2). The differences between the cell lines in their sensitivity to raloxifene may be dependent on their gene expression patterns, where PC3 cells express both ERα and ERβ but DU145 cells only have ERβ [39].

After 48 h, a significant difference in the cell numbers was observed between controls and SMA-Ral treatments at 5 μM and 10 μM in both PC3 and DU145 cells (Figure 2). Taken

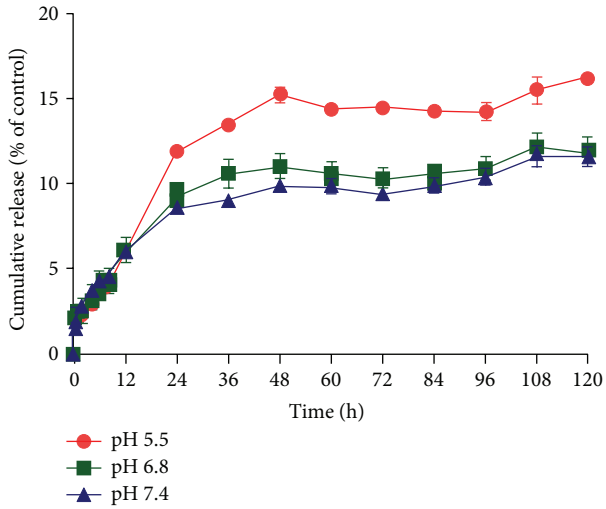

Figure 1: Release rate of raloxifene from SMA-Ral at pH 5.5, 6.8, and 7.4. The release of raloxifene was evaluated using dialysis method and compared to raloxifene present inside the dialysis bag at $t = 0$ h. The released was assessed over a period of 5 days. Data are expressed as mean ± SEM ($n = 3$) ($P < 0.05$ for pH 5.5 versus pH 6.8 and 7.4 from 24 to 120 h).

Table 2: IC_{50} values for raloxifene free drug and SMA-Ral in HRPC cells lines.

Cells	SMA-Ral (M)	Free drug (M)
PC3	$7.75E-06$	$1.03E-05$
DU145	$1.03E-05$	$1.46E-05$

together, these data indicate that the effects of free raloxifene and SMA-Ral were cell specific and time dependent.

3.4. Effect of Raloxifene and SMA-Ral on DNA Synthesis and Cell Proliferation. In order to determine the effect of raloxifene and SMA-Ral on DNA synthesis, PC3 and DU145 cells were treated for 48 h with specific concentrations of free raloxifene and SMA-Ral and [^{3}H]-Thymidine incorporation was measured. Exposing PC3 and DU145 cells to free raloxifene (2–10 μM) did not alter DNA synthesis when normalized to protein content (Figure 3). However, treatment with SMA-Ral significantly decreased DNA synthesis in both cell lines. At concentrations of 5 and 10 μM, [^{3}H]-Thymidine incorporation was decreased by 15 and 44%, respectively, in PC3 cells and by 29 and 47%, respectively, in DU145 cells (Figure 3).

To determine whether SMA-Ral micelles were capable of inducing cell cycle arrest, flow cytometry was used on both PC and DU145 cell lines. As shown in Figure 4, the treatment of CRPC cells with SMA-Ral was associated with a higher number of cells in the G0/G1 phase of the cell cycle. In PC3 cells, free raloxifene did not affect cell cycle progression at concentrations below 10 μM. At 10 μM a small increase of cells in G0/G1 phase of the cell cycle was observed (10%) with a concomitant decrease of cells in S-phase (−3%) and G2/M-phase (−7%) (Figure 4(a)). However, treatment of PC3 cells with SMA-Ral 5 and 10 μM potentiated G0/G1 arrest and increased the percentage of cells by 15 and 20% in G1/G0 phase with a concomitant reduction of S-phase (−5 and 7%) and G2M phase (−10 and 13%), respectively (Figure 4(a)). In DU145 cells, free raloxifene treatments did not affect the cell cycle progression at the concentrations here used (Figure 4(b)). SMA-Ral treatment slightly increased the number of cells in G0/G1 phase of the cell cycle by 4 and 7% for SMA-Ral concentration of 5 and 10 μM, respectively (Figure 4(b)).

Overall, SMA-Ral treatment was more potent compared to free raloxifene in PC3 and DU145 cells. SMA-Ral reduced DNA synthesis as well as halted the progression of cells through the cell cycle. The effect of SMA-Ral was concentration dependent and more potent in PC3 cells compared to DU145 cells.

3.5. Effect of Raloxifene and SMA-Ral on Apoptosis and Necrosis. We used flow cytometry to determine if free raloxifene or SMA-Ral treatments were able to induce apoptosis or necrosis. Apoptosis was measured using FITC-Annexin V which recognized the externalization of phosphatidylserine, a common characteristic of apoptotic cells. The proportion of necrotic cells was determined by propidium iodide. Treatment of PC3 cells with free raloxifene did not promote apoptosis but triggered a concentration-dependent necrosis, with 2-fold and 6-fold increase of necrotic cells with 5 and 10 μM, respectively (Figure 5(a)). Interestingly, SMA-Ral treatment promotes apoptosis in PC3 cells, with 7- and 11-fold increase of apoptotic cells following treatment with 5 and 10 μM, respectively (Figure 5(a)). In addition, cell necrosis was concentration dependent with 1.5- and 4-fold increase following 5 and 10 μM raloxifene, respectively. The sensitivity of DU145 cells to treatment with raloxifene differed largely from the sensitivity of PC3 cells. Free raloxifene or SMA-Ral failed to trigger necrosis at 5 or 10 μM. Free raloxifene increased apoptosis by 2-fold following 10 μM treatment (Figure 5(b)) whereas SMA-Ral increased the occurrence of apoptosis by 2- and 6-fold following treatment with 5 and 10 μM SMA-Ral (Figure 5(b)).

Overall, these data demonstrated that the mechanisms of inducing cell death differ between free raloxifene and SMA-Ral in PC3 cells. SMA-Ral induces apoptosis while free raloxifene elicits necrosis. DU145 cells are less sensitive to raloxifene treatment but SMA-Ral potentiates apoptosis. The difference in sensitivity between PC3 and DU145 cells may also involve different signaling mechanisms leading to different internalization and subcellular localization inherent to the endocytic process characteristic of macromolecular cell uptake.

3.6. Effect of SMA-Ral on the Expression of Protein Involved in Proliferation and Protein Synthesis. To determine the mechanism for the higher sensitivity of PC3 cells to SMA-Ral treatment, we examined the effect of free raloxifene and SMA-Ral on the expression of several proteins involved in cell proliferation and protein synthesis. As shown in Figure 6, treatment with free raloxifene or SMA-Ral did not affect the expressions

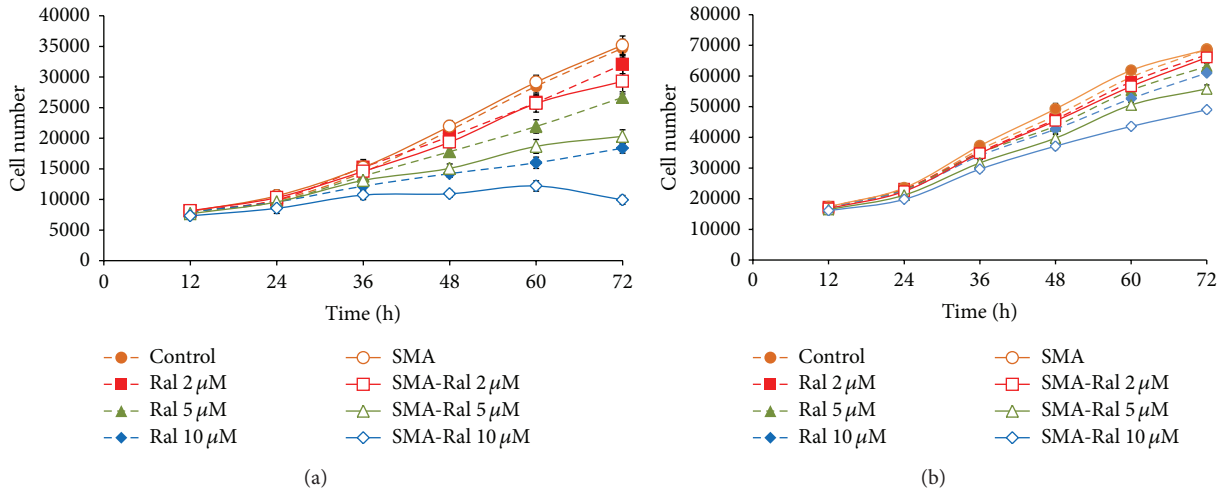

Figure 2: Comparison of the effect of various concentrations of raloxifene (Ral) and SMA-Ral (SMA-Ral) on the proliferation of PC3 (a) and DU145 (b) cells. Cells were treated over a period of 72 h with specific concentrations of raloxifene or SMA-Ral. At the indicated time point, cells were fixed and cell number was determined using the sulforhodamine B assay. Data are expressed as mean ± SEM ($n = 3$).

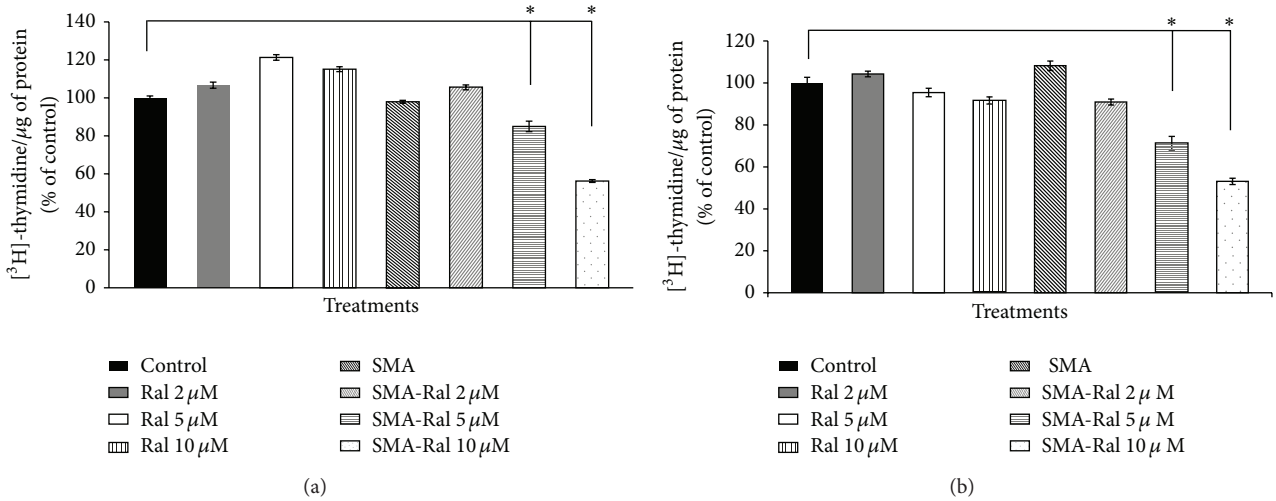

Figure 3: DNA synthesis following treatment of PC3 (a) and DU145 cells (b) with free raloxifene or SMA-Ral. Cells were treated with various concentrations of free raloxifene (Ral) or SMA-Ral for 48 h. DNA synthesis was evaluated by [^{3}H] thymidine incorporation during the last 20 h of the treatment. Data are expressed as mean ± SEM ($n = 3$).

of ERα (66 kDa). However, the expression of a Δ5ERα, a splice variant of ERα, was decreased by 70% following free raloxifene (10 μM) treatment. SMA-Ral further potentiates the decreased expression of Δ5ERα and that at a lower concentration. Δ5ERα expression was decreased by 60 and 90% following 5 and 10 μM SMA-Ral treatment. The expression of ERβ was not modified by raloxifene; however, its nuclear localization was decreased both by raloxifene and SMA-Ral (Figure 6(b)), suggesting a decrease of ERβ binding to the estrogen response element (ERE). Crosstalk has been documented between ERα, ERβ, and other signaling proteins involved in cell proliferation and protein synthesis such as the epidermal growth factor receptor (EGFR), mitogen activated protein kinase (MAPK, ERK1/2), or serine/threonine kinase (AKT). We examined the effect of free raloxifene and SMA-Ral on the expression of these proteins. Treatment with free raloxifene from 2 to 10 μM had no effect on EGFR protein expression; however, 10 μM of free raloxifene promoted the appearance of an EGFR fragment of approximately 65 kDa. Treatment with 5 and 10 μM SMA-Ral resulted in a decrease in EGFR expression by 27 and 36%, respectively. The appearance of a truncated form of EGFR (65 kDa) was also observed with SMA-Ral 10 μM and this concentration also decreased ERK1/2 as well as AKT phosphorylation and expression, both signaling pathways involved in cell proliferation and inhibition of apoptosis, along with other proteins involved in protein synthesis such as NFκB and mTOR. In addition, treatment with 5 and 10 μM SMA-Ral promoted the activation of caspase-3, a marker for apoptosis mediated cell death while free raloxifene treatment 10 μM only showed a faint activation of caspase-3 (Figure 6(a)).

In DU145 cells, mechanisms implicated in the reduction of cell proliferation and increased apoptosis are mediated through different pathways as the proteins modified by

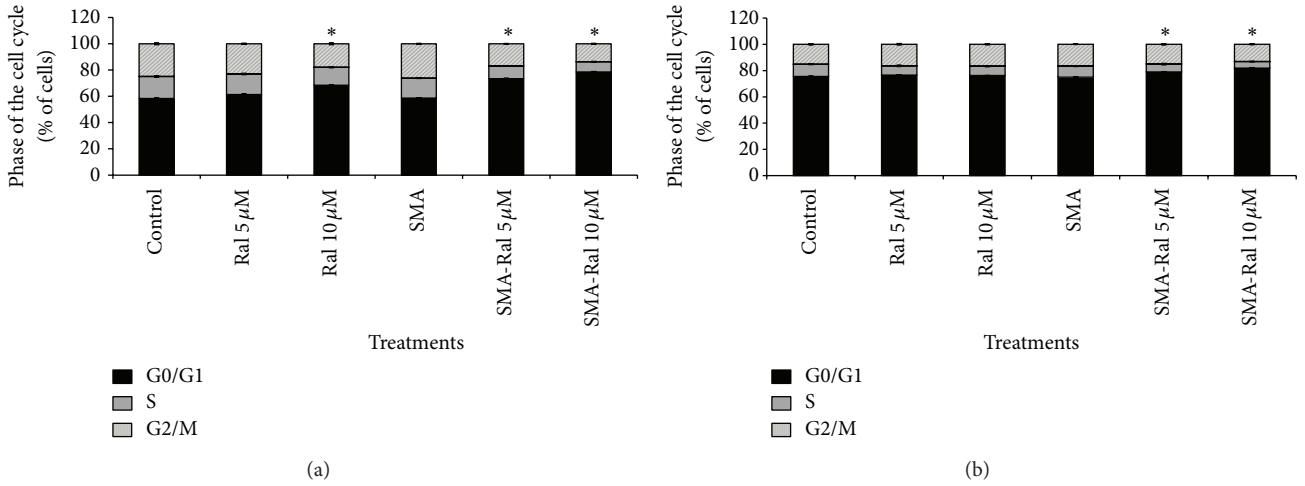

Figure 4: Effect of free raloxifene and SMA-Ral on cell cycle progression. PC3 (a) and DU145 cells (b) were treated for 48 h with either free raloxifene, SMA-Ral at 5 or 10 μM, or controls (SMA or DMSO). Data are expressed as mean ± SEM ($n = 3$). $^*P < 0.05$ compared to controls.

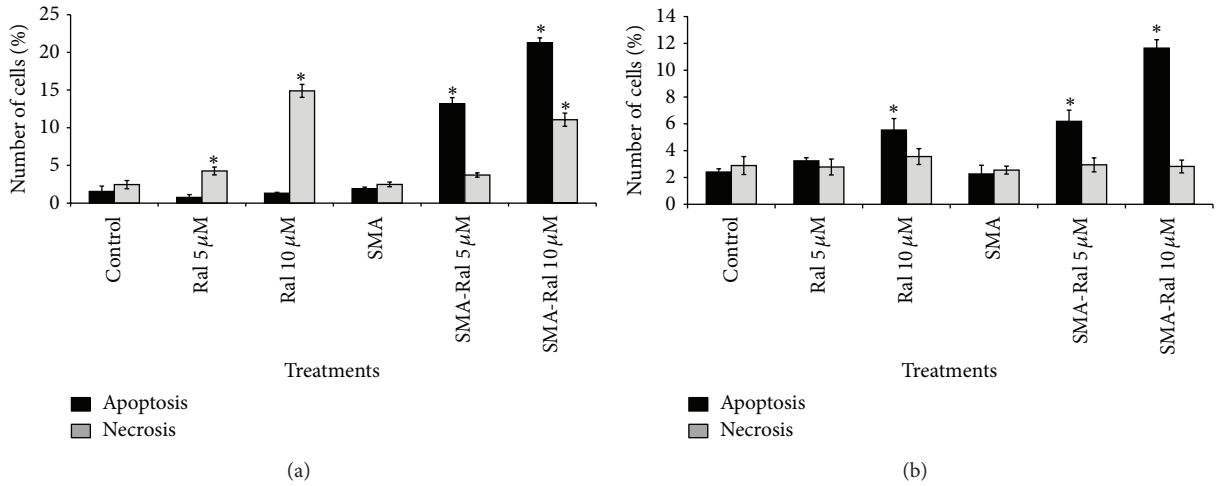

Figure 5: Effect of free raloxifene and SMA-Ral on apoptosis and necrosis. PC3 (a) and DU145 cells (b) were treated for 48 h with either free raloxifene (Ral), SMA-Ral at 5 or 10 μM, or controls (SMA or DMSO). Data are expressed as mean ± SEM ($n = 3$). ($^*P < 0.05$ compared to control).

SMA-Ral treatment in PC3 were not affected in DU145 cells. In DU145 cells, raloxifene did not affect EGFR expression; however, with free raloxifene (10 μM) and SMA-Ral (5 and 10 μM), cleaved forms appeared with apparent molecular weights of 85 kDa and 65 kDa (Figure 6(c)). In addition, treatment with SMA-Ral 10 μM specifically promoted endocytosis of EGFR (Figure 6(d)).

Overall, the effect of SMA-Ral on downstream signaling effectors appeared dependent on cell type. SMA-Ral decreased the expression and activation of proteins involved in the regulation of cell proliferation and protein synthesis in PC3 cells. In DU145 cells, cells are less sensitive to SMA-Ral treatment and the mechanisms may be mediated through a decreased expression of the EGFR at the membrane and subsequent downstream effectors.

3.7. Effect of Raloxifene and SMA-Ral on the Integrity of PC3 Tumor Spheroids. We compared the efficacy of free raloxifene and SMA-Ral using PC3 tumor spheroids since, as previously reported by Friedrich et al. [35], growth of DU145 tumor spheroids failed. PC3 tumor spheroids were treated over a period of 15 days with either free raloxifene or SMA-Ral at 2, 5 and 10 μM. As shown in Figure 7, morphologies of PC3 tumor spheroids was not modified upon free raloxifene treatment with 2 or 5 μM (Figure 7(a)). Concentrations of free raloxifene up to 10 μM decreased the spheroid volume by 16% and by 38% the activity of acid phosphatase, a marker of cell viability (Figure 7(b)). In contrast, treatment with SMA-Ral 5 μM reduced the spheroid volume by 11% and decreased acid phosphatase activity by 29% compared to control or SMA and 15% compared to free raloxifene 5 μM. The effect of SMA-Ral on the integrity of tumor spheroids was concentration dependent; SMA-Ral (10 μM) abolished their spherical morphology resulting in cellular aggregates without defined structure (Figure 7(a)). This was accompanied by a decrease in cell viability of 69% compared to control or SMA and 30% compared to free raloxifene 10 μM (Figure 7(b)). These results provided further evidence of the potency of SMA-Ral.

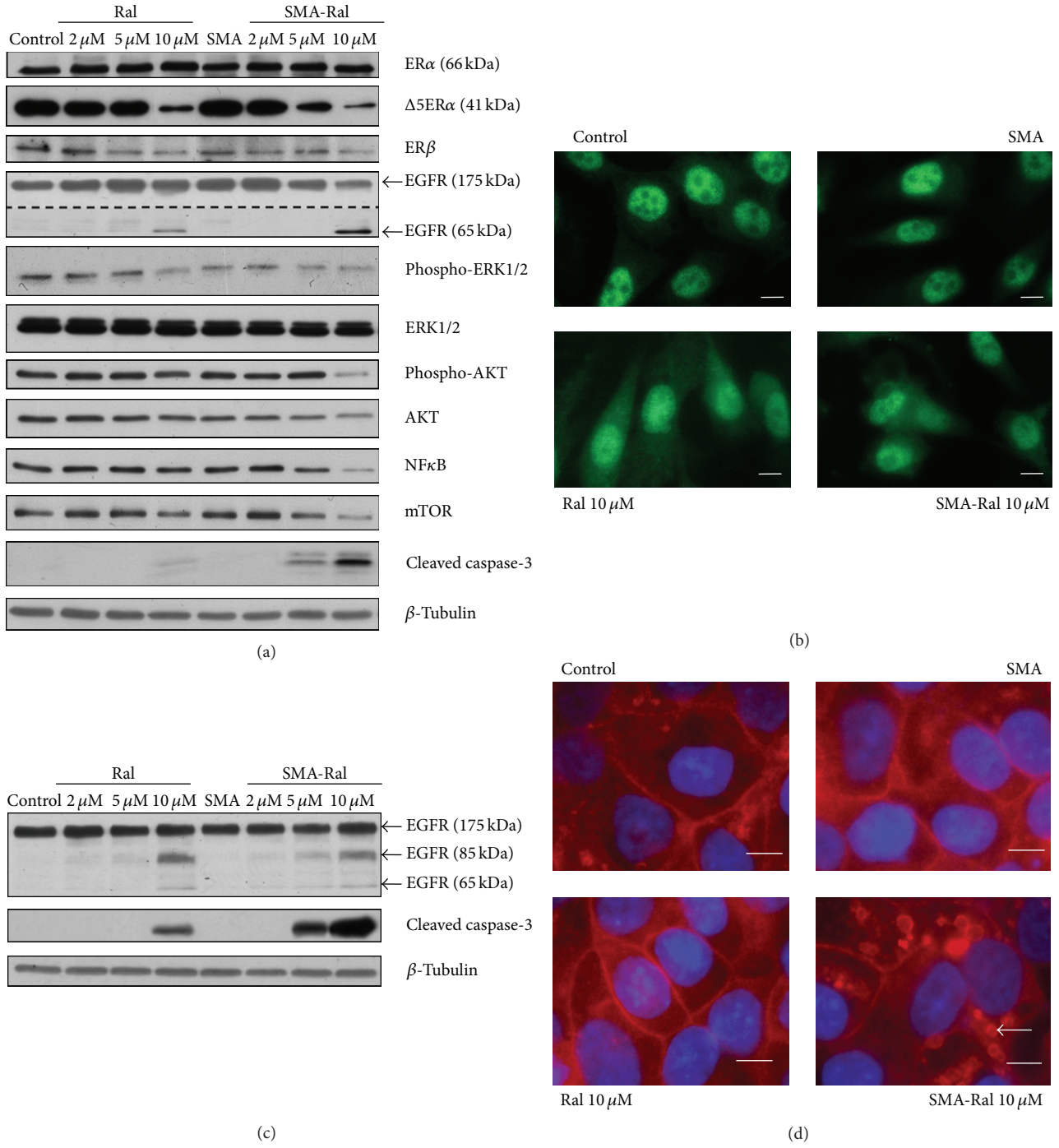

Figure 6: Effect of free raloxifene and SMA-Ral on ERα and ERβ protein expressions and proteins involved in cell cycle progression and protein synthesis. Western blot of proteins following treatment with free raloxifene or SMA-Ral at 2, 5, and 10 μM for 48 h in PC3 cells (a). Immunocytochemistry of ERβ following treatment with free raloxifene or SMA-Ral 10 μM (b). Western blot of EGFR in DU145 cells treated with free raloxifene or SMA-Ral at 2, 5, and 10 μM for 48 h (c). Localization of EGFR in DU145 cells treated with free raloxifene or SMA-Ral 10 μM for 48 h (d).

3.8. Effect of Free Raloxifene and SMA-Ral on PC3 Cell Migration and Invasion and MMP-9 Secretion. We have demonstrated that SMA-Ral decreased cell viability, proliferation and affected the integrity and viability of tumor spheroids. Next, we tested the effect of free raloxifene and SMA-Ral on the migration, and invasion of PC3 cells. Migration was determined using a scratch assay. Treatment with free raloxifene 5 and 10 μM, decreased migration of PC3 cells in a concentration-dependent manner (Figure 8(a)). Moreover, SMA-Ral reduced migration by 50 and 90% when treated with 5 and 10 μM, respectively (Figure 8(a)). SMA-Ral also elicited a concentration dependent reduction of matrigel

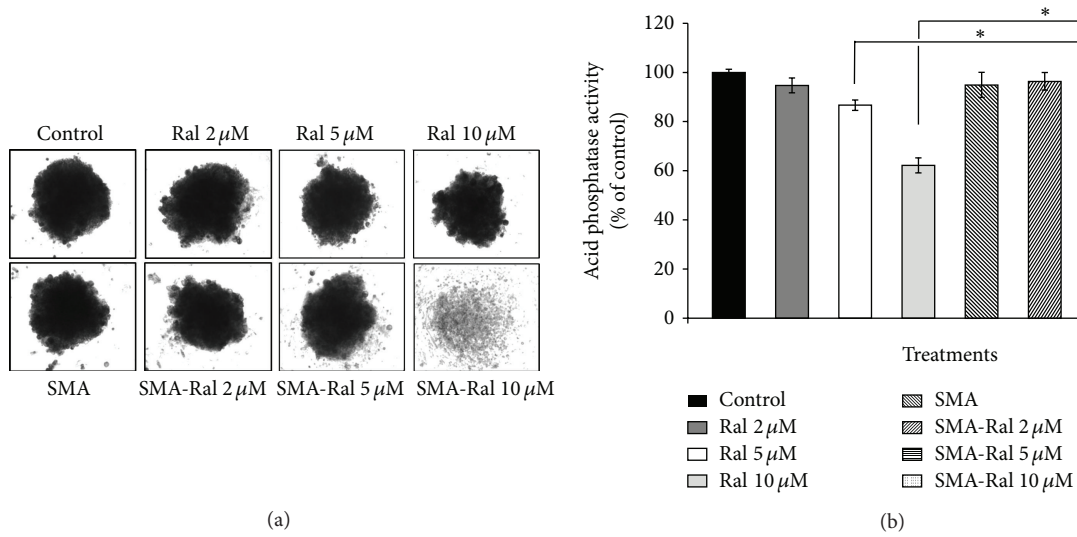

Figure 7: Morphologies and viability of PC3 tumor spheroids after 15 days of treatment with free raloxifene or SMA-Ral. Representative pictures of tumor spheroids were taken following treatment with free raloxifene or SMA-Ral at 2, 5, and 10 μM or controls (DMSO or SMA) (a). Tumor spheroid viability was measured by the activity of acid phosphatase (b). $^{*}P < 0.05$.

invasion. While 5 μM free raloxifene had no effect, treatment at 10 μM decreased invasion by 1.6-fold (Figure 8(b)). In contrast, SMA-Ral reduced cell invasion by 1.9- and 3-fold following treatment with 5 and 10 μM (Figure 8(b)). Matrix metalloproteinase (MMP) secretion has been implicated with cancer invasiveness and tumor progression [40]. Analysis of the secretion level of MMP-9 in the conditioned media after 24 and 48 h by gelatin zymography showed that free raloxifene and SMA-Ral 10 μM decreased MMP-9 secretion after 24 and 48 h incubation. Additionally, after 48 h incubation, MMP-9 secretion was decreased by 53% and 83% by 10 μM of free raloxifene and SMA-Ral, respectively (Figures 8(c)-8(d)). We also compared the effect of raloxifene and SMA-Ral on endothelial tube formation using HUVEC cells. While raloxifene 10 μM decreased endothelial tube-like formation, SMA-Ral 5 μM abolished tube-forming capability (Figure 8(e)). In addition, the coculture of PC3 cells and endothelial cells on a basement membrane matrix surface promoted the interaction between the two cell lines and the formation of tubule (Figure 8(f)). These interactions were decreased efficiently by the treatment with SMA-Ral 10 μM (Figure 8(f)) suggesting that the treatment with SMA-Ral will decrease neoangiogenesis in the tumor.

4. Discussion

In the present study, we report a new raloxifene formulation with higher cytotoxicity against CRPC cell lines compared to free raloxifene. The encapsulation of raloxifene into SMA micelles resulted in reduced CRPC cell proliferation, promoted cell death, impaired tumor spheroid formation, decreased interaction with endothelial cells, reduced cell migration and invasion more effectively than the free drug.

Free raloxifene transport into the cell depends on active and saturable carriers belonging to the organic anion transporting polypeptide family (OATP). Two well-studied members of this family, OATP1B1 and OATP1B3, have been implicated in the internalization of raloxifene [41]. Interestingly, in prostate cancer, the expression of OATP1B3 has been shown to be upregulated [42]. SMA-Ral crosses the plasma membrane independently of carriers, delivering raloxifene to the cytoplasm away from the plasma membrane and the efflux drug transporters such as P-glycoprotein (Pgp), multidrug resistance-related protein (MRP), and OATP are also involved in the excretion of raloxifene [43, 44]. MRP was also found to be expressed in PC3 and DU145 cells [45].

Many studies have demonstrated that the cellular uptake of nanoparticles involves either clathrin-mediated or caveolae-mediated endocytosis [46, 47]. Treatment of PC3 cells with 10 μM SMA-Ral triggered the formation of caveolin-1 vesicles after 48 h of incubation but did not promote the formation of clathrin vesicles (data not shown). Endocytosis is a multistep process that leads to lysosome formation which promotes the degradation of nanoparticles due to the acidic environment (lumen pH 5.5), releasing their content into the cytosol [48]. Once raloxifene is delivered by endocytosis into the cytosol, it modulates signaling pathways that are different from those mediated by the free drug resulting in the decrease of cell proliferation and/or the increase of cell death.

We have also shown that SMA-Ral treatment reduced DNA synthesis (Figure 3) and cell proliferation by promoting the accumulation of cells in the G1 phase of the cell cycle for PC3 and DU145 cells (Figure 4). In addition, we showed that free raloxifene and SMA-Ral induced cell death potentially through different mechanisms (Figure 5). In PC3 cells, while free raloxifene treatment mediated cell death through a necrotic process, the treatment with SMA-Ral implicated mainly apoptosis (Figure 5(a)). Previous studies have shown that SERMs can induce cell death through multiple mechanisms [49]; in addition, treatment with high concentration of

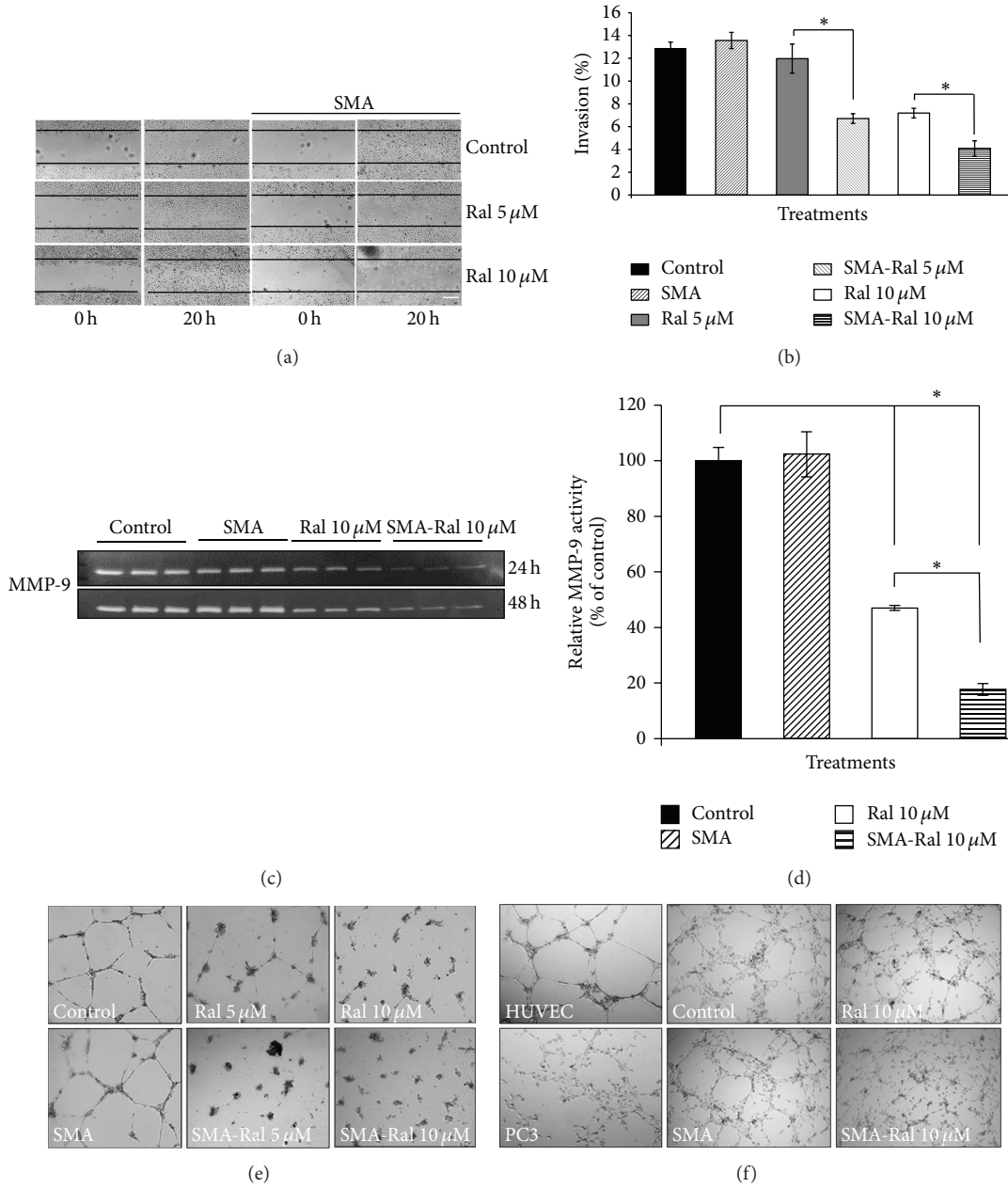

Figure 8: Effect of free raloxifene or SMA-Ral treatment on cell migration and invasion. PC3 monolayer of cells was scratched and treated with either free raloxifene or SMA-Ral at 5 or 10 μM or controls (DMSO or SMA) and incubated for 20 h. Representative pictures were taken at $t = 0$ h and at 20 h (a). For cell invasion, PC3 cells were treated with either free raloxifene or SMA-Ral at indicated concentrations. After 20 h-the cells migrating to the lower surface were fixed and stained with Diff Quick. Bars represent the mean ± SEM of three independent experiments (b). Conditioned mediums were collected from cultures following 24 and 48 h and analyzed by gelatin zymography (c). Bars indicate the relative MMP-9 activity in the conditioned media and represent the mean ± SEM of three independent experiments (d). Effects of free raloxifene and SMA-Ral on the formation of capillary-like structures by HUVEC. Cells were treated with either free raloxifene or SMA-Ral at 5 or 10 μM or controls (DMSO or SMA) for 24 h. Representative pictures were taken (e). PC3 cells cocultured with endothelial cells were treated with either free raloxifene or SMA-Ral at 10 μM or controls (DMSO or SMA) for 24 h. Representative pictures were taken (f). $^{*}P < 0.05$.

SERM may also promote cell death independently of the activation of caspase [50]. As shown in Figure 6, caspase-3 is activated following treatment with SMA-Ral 10 μM. In DU145, free raloxifene and SMA-Ral treatments induced apoptosis; however, the SMA-Ral treatment appeared more potent compared to free raloxifene. Previous studies using PC3 and DU145 cells have demonstrated cytotoxicity of free raloxifene at a low concentration (1 μM) in cells incubated in steroids-stripped media [51]. These data suggested that raloxifene mediated cell death is dependent on the presence

of steroids as higher concentrations of raloxifene are required to readily elicit potent cytotoxicity. The higher efficacy of the SMA-Ral might be explained by the release of the drug in the cytoplasm and direct targeting of ERα and ERβ.

SMA-Ral cytotoxicity appeared more potent against PC3 cells that express both ERα and ERβ,compared to only ERβ in DU145 cells. Previous studies have hypothesized that the clinical benefit of SERMs for the treatment of CRPC relies on targeting ERα [52]. Moreover, raloxifene has a 17-fold higher affinity for ERα compared to ERβ [53]. An additional parameter to consider is that the cellular localization of ERα and ERβ differs where ERα is both cytoplasmic and nuclear in PC3 cells [54], while ERβ is mainly localized in the nucleus of cells (Figure 6). The endocytosis process of SMA-Ral and the release of raloxifene in the cytoplasm may promote its interaction with the ERα. However, ERβ is significantly expressed in human prostate cancer cells (including PC3 and DU145) and its potential as a raloxifene target in CRPC remains to be determined. Therefore, we cannot exclude a synergy between ERα and ERβ to promote strong raloxifene-induced cytotoxicity.

To gain better understanding of the signaling mechanisms behind the effect of SMA-Ral in PC3 cells, we examined the expression of ERα and ERβ. SMA-Ral treatment did not significantly alter the expression of full length ERα. However, ER$\alpha\Delta5$ expression, one of the splice variant of ERα characterized by the deletion of the ligand binding domain (exon 5, AF2 domain), was decreased in PC3 cells (Figure 6). Conflicting reports have associated the specific increased ER$\alpha\Delta5$ expression to the stimulation of gene expression in tumors [55]. SMA-Ral treatment decreased the expression of ER$\alpha\Delta5$ at concentrations as low as 5 μM compared to 10 μM with free raloxifene (Figure 6). ERβ protein level was slightly decreased by free raloxifene or SMA-Ral treatment. ERβ protein is essentially localized in the nucleus but treatment by both free raloxifene and SMA-Ral causes ERβ to accumulate in the cytoplasm (Figure 6), suggesting that raloxifene might reduce the expression of genes normally targeted by ERβ binding to their promoter. Analyzing the expression and/or activation of downstream signaling pathways in PC3 cells revealed that SMA-Ral treatment decreased activation or lowered expression of proteins involved in the proliferation or inhibition of apoptosis such AKT and ERK1/2 as well as in protein synthesis such as NFκB and mTOR at concentrations equivalent to 5 μM raloxifene. These data suggest the specificity and potential of SMA-Ral treatment for the treatment of CRPC expressing ERα and ERβ.

In contrast, the mechanisms by which SMA-Ral treatment caused cytotoxicity to DU145 cells appeared to be mediated through different pathways all together, as none of the proteins examined in PC3 cells were affected by raloxifene. However, treatment with free raloxifene and SMA-Ral promoted the appearance of truncated EGFR protein, the role of which needs to be characterized in further studies. In addition, SMA-Ral induced the endocytosis of EGFR and its localization in cytoplasmic vesicles as shown by immunofluorescence analysis (Figure 6(d)). SMA-Ral treatment also triggered the formation of cytoplasmic vesicles containing EGFR in PC3 cells (data not shown). EGFR is highly expressed in DU145 cells compared to PC3 cells [56] and has been demonstrated to contribute to the proliferation of androgen independent prostate cancer cells [57]. Generation of the truncated form of EGFR receptors as well as its delocalization into cytoplasmic vesicle may delay proliferation and induce cytotoxicity in DU145 cells.

In addition, using the PC3 tumor spheroid model, we demonstrated that SMA-Ral destroyed the integrity and reduced the cell viability of the spheroids (Figure 7). Tumor spheroids are an advantageous *in vitro* model used to mimic specific characteristics of tumor development and the complex cellular interactions observed *in vivo* [58]. Tumor spheroids are also used to more accurately predict drug efficacy prior to examination *in vivo*. The potency of SMA-Ral against CRPC prostate tumor spheroids suggests strong potential and the need to further assess its value in preclinical animal models. Furthermore, SMA-Ral also decreased cell migration, cell invasion, and MMP-9 protein excretion in conditioned media of PC3 cells. The activity of MMPs has been repeatedly associated with the metastatic potential of tumor cells [59]. These data suggest the potency of SMA-Ral for the prevention of the appearance of metastasis *in vivo*. In addition, the interaction of PC3 cells with endothelial cells was significantly altered by the treatment with SMA-Ral which abolishes the tubule formation suggesting a potent antiangiogenic effect of SMA-Ral (Figure 8(e)).

Raloxifene is characterized by low bioavailability (approximately 2%) due to extensive metabolism [60] which essentially occurs via glucuronidation catalyzed by UDP-glucuronosyltransferases (UGTs) present in the liver [60]. Raloxifene encapsulation into the SMA micelles is plausibly protected from the liver metabolizing enzymes and could hypothetically improve its plasma level. These water soluble nanoparticles should promote the accumulation of raloxifene at the tumor site while protecting the drug from metabolic deactivation. In addition, the stability of SMA-Ral, demonstrated by the low release rate over 5 days (Figure 1), should increase its internalization by the prostate cancer cells. Further *in vivo* testing of these assumptions is currently being pursued in our laboratory.

The passive accumulation of nanoparticles at tumor sites has been demonstrated by Matsumura and Maeda [61] who established the concept of the enhanced permeability and retention (EPR) effect. The EPR effect is associated with irregular blood vessel morphology inherent to tumor tissues and characterized by large fenestration between the endothelial cells. The EPR effect promotes the accumulation of nanomedicine at tumor sites by passive targeting while its particle size prevents extravasation from normal vessels. Passive targeting can prolong retention of a drug in the tumor interstitium over days to weeks [62]. In addition, the reduced clearance of SMA-Ral due to its size and charge will contribute to its accumulation at the tumor site as well as in distant metastatic secondary tumors. A nanoparticle diameter larger than 7 nm will escape the renal filtration through the glomerular slits and remain in the systemic circulation for a longer period [63–65]. In the systemic circulation, the micellar charge dictates the molecules interaction with blood

components, vascular endothelium, or the reticuloendothelial system (RES). A neutral zeta potential as measured for SMA-Ral is expected to decrease recognition of the micelle by the components of the RES and prolong its circulation [66]. The stability of the SMA-Ral as observed by the low release rate (only 12% release after 5 days incubation at physiological pH 7.4) (Figure 1) will extend its circulation time and may promote drug localization at the tumor site.

5. Conclusion

Together, the data obtained in this study demonstrated the advantages of encapsulating raloxifene into SMA and its cytotoxic potency in two CRPC cell lines differing in the level of ERα and ERβ expression. Compared to free drug, SMA-Ral more effectively inhibits cell cycle progression, increases apoptosis, and alters the integrity of tumor spheroid models. SMA-Ral treatment decreased migration and invasion of a CRPC cells. The micellar system could possibly have different mechanisms of action compared to free drug. This hypothesis is supported by the distinct pattern of expression and localization of estrogen receptors, EGFR, and downstream signaling of cell proliferation and survival. This new formulation could potentially confer a superior efficacy and pharmacokinetic profile to raloxifene and thus warrants further examination *in vivo*.

Conflict of Interests

The authors declare that there is no conflict of interests regarding the publication of this paper.

Acknowledgments

This work was supported by grants from the Otago Medical Research Foundation (ST, KG, RR), UORG (ST, RR), Health Research Council of New Zealand (ST, RR), and Lottery Health (ST). The authors would like to thank Ms. Céline Bourdon for the editorial assistance.

References

[1] P. C. Walsh, T. L. DeWeese, and M. A. Eisenberger, "Localized prostate cancer," *The New England Journal of Medicine*, vol. 357, no. 26, pp. 2696–2705, 2007.

[2] K. Kelly and J. J. Yin, "Prostate cancer and metastasis initiating stem cells," *Cell Research*, vol. 18, no. 5, pp. 528–537, 2008.

[3] G. Attard, A. H. M. Reid, D. Olmos, and J. S. De Bono, "Anti-tumor activity with CYP17 blockade indicates that castration-resistant prostate cancer frequently remains hormone driven," *Cancer Research*, vol. 69, no. 12, pp. 4937–4940, 2009.

[4] C. R. Pound, A. W. Partin, M. A. Eisenberger, D. W. Chan, J. D. Pearson, and P. C. Walsh, "Natural history of progression after PSA elevation following radical prostatectomy," *Journal of the American Medical Association*, vol. 281, no. 17, pp. 1591–1597, 1999.

[5] O. W. Brawley, "Prostate cancer epidemiology in the United States," *World Journal of Urology*, vol. 30, no. 2, pp. 195–200, 2012.

[6] S. M. Ho, M. T. Lee, H. M. Lam, and Y. K. Leung, "Estrogens and prostate cancer: etiology, mediators, prevention, and management," *Endocrinology and Metabolism Clinics of North America*, vol. 40, no. 3, pp. 591–614, 2011.

[7] R. L. Noble, "Production of Nb rat carcinoma of the dorsal prostate and response of estrogen-dependent transplants to sex hormones and tamoxifen," *Cancer Research*, vol. 40, no. 10, pp. 3547–3550, 1980.

[8] W. A. Ricke, S. J. McPherson, J. J. Bianco, G. R. Cunha, Y. Wang, and G. P. Risbridger, "Prostatic hormonal carcinogenesis is mediated by in situ estrogen production and estrogen receptor alpha signaling," *The FASEB Journal*, vol. 22, no. 5, pp. 1512–1520, 2008.

[9] M. C. Bosland, H. Ford, and L. Horton, "Induction of high incidence of ductal prostate adenocarcinomas in NBL/Cr and Sprague-Dawley Hsd:SD rats treated with a combination of testosterone and estradiol-17β or diethylstilbestrol," *Carcinogenesis*, vol. 16, no. 6, pp. 1311–1317, 1995.

[10] I. Leav, S. M. Ho, P. Ofner, F. B. Merk, P. W. L. Kwan, and D. Damassa, "Biochemical alterations in sex hormone-induced hyperplasia and dysplasia of the dorsolateral prostates of noble rats," *Journal of the National Cancer Institute*, vol. 80, no. 13, pp. 1045–1053, 1988.

[11] M. Yu, B. A. Leav, I. Leav, F. B. Merk, H. J. Wolfe, and S.-M. Ho, "Early alterations in ras protooncogene mRNA expression in testosterone and estradiol-17β induced prostatic dysplasia of Noble rats," *Laboratory Investigation*, vol. 68, no. 1, pp. 33–44, 1993.

[12] J. L. Nelles, W. Y. Hu, and G. S. Prins, "Estrogen action and prostate cancer," *Expert Review of Endocrinology and Metabolism*, vol. 6, no. 3, pp. 437–451, 2011.

[13] S. J. Ellem, J. F. Schmitt, J. S. Pedersen, M. Frydenberg, and G. P. Risbridger, "Local aromatase expression in human prostate is altered in malignancy," *Journal of Clinical Endocrinology and Metabolism*, vol. 89, no. 5, pp. 2434–2441, 2004.

[14] R. B. Montgomery, E. A. Mostaghel, R. Vessella et al., "Maintenance of intratumoral androgens in metastatic prostate cancer: a mechanism for castration-resistant tumor growth," *Cancer Research*, vol. 68, no. 11, pp. 4447–4454, 2008.

[15] I. Leav, K. Lau, J. Adams et al., "Comparative studies of the estrogen receptors β and α and the androgen receptor in normal human prostate glands, dysplasia, and in primary and metastatic carcinoma," *The American Journal of Pathology*, vol. 159, no. 1, pp. 79–92, 2001.

[16] Y.-K. Leung, H.-M. Lam, S. Wu et al., "Estrogen receptor β2 and β5 are associated with poor prognosis in prostate cancer, and promote cancer cell migration and invasion," *Endocrine-Related Cancer*, vol. 17, no. 3, pp. 675–689, 2010.

[17] M. J. Linja, K. J. Savinainen, T. L. J. Tammela, J. J. Isola, and T. Visakorpi, "Expression of ERα and ERβ in prostate cancer," *Prostate*, vol. 55, no. 3, pp. 180–186, 2003.

[18] K.-M. Lau, M. LaSpina, J. Long, and S.-M. Ho, "Expression of estrogen receptor (ER)-α and ER-β in normal and malignant prostatic epithelial cells: regulation by methylation and involvement in growth regulation," *Cancer Research*, vol. 60, no. 12, pp. 3175–3182, 2000.

[19] C. Huggins and C. V. Hodges, "Studies on prostatic cancer. I. The effect of castration, of estrogen and of androgen injection on serum phosphatases in metastatic carcinoma of the prostate," *Cancer Research*, vol. 1, pp. 293–297, 1941.

[20] H. Bonkhoff and R. Berges, "The evolving role of oestrogens and their receptors in the development and progression of prostate cancer," *European Urology*, vol. 55, no. 3, pp. 533–542, 2009.

[21] V. Rossi, G. Bellastella, C. de Rosa et al., "Raloxifene induces cell death and inhibits proliferation through multiple signaling pathways in prostate cancer cells expressing different levels of estrogen receptorα and β," *Journal of Cellular Physiology*, vol. 226, no. 5, pp. 1334–1339, 2011.

[22] C. Rohlff, M. V. Blagosklonny, E. Kyle et al., "Prostate cancer cell growth inhibition by tamoxifen is associated with inhibition of protein kinase C and induction of p21(waf1/cip1)," *The Prostate*, vol. 37, no. 1, pp. 51–59, 1998.

[23] R. C. Bergan, E. Reed, C. E. Myers et al., "A phase II study of high-dose tamoxifen in patients with hormone- refractory prostate cancer," *Clinical Cancer Research*, vol. 5, no. 9, pp. 2366–2373, 1999.

[24] P. Lissoni, P. Vigano, M. Vaghi et al., "A phase II study of tamoxifen in hormone-resistant metastatic prostate cancer: possible relation with prolactin secretion," *Anticancer Research*, vol. 25, no. 5, pp. 3597–3599, 2005.

[25] R. L. Shazer, A. Jain, A. V. Galkin et al., "Raloxifene, an oestrogen-receptor-β-targeted therapy, inhibits androgen-independent prostate cancer growth: results from preclinical studies and a pilot phase II clinical trial," *BJU International*, vol. 97, no. 4, pp. 691–697, 2006.

[26] S. Stein, B. Zoltick, T. Peacock et al., "Phase II trial of toremifene in androgen-independent prostate cancer: a penn cancer clinical trials group trial," *The American Journal of Clinical Oncology*, vol. 24, no. 3, pp. 283–285, 2001.

[27] M. B. Sporn, S. A. Dowsett, J. Mershon, and H. U. Bryant, "Role of raloxifene in breast cancer prevention in postmenopausal women: clinical evidence and potential mechanisms of action," *Clinical Therapeutics*, vol. 26, no. 6, pp. 830–840, 2004.

[28] H. K. Lim, M. Yang, W. Lam et al., "Free radical metabolism of raloxifene in human liver microsomes," *Xenobiotica*, vol. 42, pp. 737–747, 2012.

[29] K. Greish, A. Nagamitsu, J. Fang, and H. Maeda, "Copoly(styrene-maleic acid)-pirarubicin micelles: high tumor-targeting efficiency with little toxicity," *Bioconjugate Chemistry*, vol. 16, no. 1, pp. 230–236, 2005.

[30] K. Greish, T. Sawa, J. Fang, T. Akaike, and H. Maeda, "SMA-doxorubicin, a new polymeric micellar drug for effective targeting to solid tumours," *Journal of Controlled Release*, vol. 97, no. 2, pp. 219–230, 2004.

[31] V. Vichai and K. Kirtikara, "Sulforhodamine B colorimetric assay for cytotoxicity screening," *Nature Protocols*, vol. 1, no. 3, pp. 1112–1116, 2006.

[32] N. Thorin-Trescases, Y. Ono, J. Tremblay, P. Hamet, and S. N. Orlov, "Dual effect of adenosine on vascular smooth muscle [3H]-thymidine DNA labeling: receptor-mediated modulation of DNA synthesis and inhibition of thymidine uptake," *Journal of Vascular Research*, vol. 37, no. 6, pp. 477–484, 2000.

[33] T. J. Somers-Edgar, S. Taurin, L. Larsen, A. Chandramouli, M. A. Nelson, and R. J. Rosengren, "Mechanisms for the activity of heterocyclic cyclohexanone curcumin derivatives in estrogen receptor negative human breast cancer cell lines," *Investigational New Drugs*, vol. 29, no. 1, pp. 87–97, 2011.

[34] S. Taurin, N. Sandbo, Y. Qin, D. Browning, and N. O. Dulin, "Phosphorylation of β-catenin by cyclic AMP-dependent protein kinase," *Journal of Biological Chemistry*, vol. 281, no. 15, pp. 9971–9976, 2006.

[35] J. Friedrich, C. Seidel, R. Ebner, and L. A. Kunz-Schughart, "Spheroid-based drug screen: considerations and practical approach," *Nature Protocols*, vol. 4, no. 3, pp. 309–324, 2009.

[36] S. Taurin, H. Nehoff, and K. Greish, "Anticancer nanomedicine and tumor vascular permeability, where is the missing link?" *Journal of the Controlled Release Society*, vol. 164, pp. 265–275, 2012.

[37] S. M. Moghimi, A. C. Hunter, and J. C. Murray, "Long-circulating and target-specific nanoparticles: theory to practice," *Pharmacological Reviews*, vol. 53, no. 2, pp. 283–318, 2001.

[38] H. Nakamura, J. Fang, B. Gahininath, K. Tsukigawa, and H. Maeda, "Intracellular uptake and behavior of two types zinc protoporphyrin (ZnPP) micelles, SMA-ZnPP and PEG-ZnPP as anticancer agents; unique intracellular disintegration of SMA micelles," *Journal of Controlled Release*, vol. 155, no. 3, pp. 367–375, 2011.

[39] A. Pravettoni, O. Mornati, P. G. V. Martini et al., "Estrogen receptor beta (ERbeta) and inhibition of prostate cancer cell proliferation: studies on the possible mechanism of action in DU145 cells," *Molecular and Cellular Endocrinology*, vol. 263, no. 1-2, pp. 46–54, 2007.

[40] B. L. Lokeshwar, M. G. Selzer, N. L. Block, and Z. Gunja-Smith, "Secretion of matrix metalloproteinases and their inhibitors (tissue inhibitor of metalloproteinases) by human prostate in explant cultures: reduced tissue inhibitor of metalloproteinase secretion by malignant tissues," *Cancer Research*, vol. 53, no. 18, pp. 4493–4498, 1993.

[41] T. Trdan Lusin, B. Stieger, J. Marc et al., "Organic anion transporting polypeptides OATP1B1 and OATP1B3 and their genetic variants influence the pharmacokinetics and pharmacodynamics of raloxifene," *Journal of Translational Medicine*, vol. 10, article 76, 2012.

[42] M. Svoboda, J. Riha, K. Wlcek, W. Jaeger, and T. Thalhammer, "Organic anion transporting polypeptides (OATPs): regulation of expression and function," *Current Drug Metabolism*, vol. 12, no. 2, pp. 139–153, 2011.

[43] J. H. Chang, C. J. Kochansky, and M. Shou, "The role of P-glycoprotein in the bioactivation of raloxifene," *Drug Metabolism and Disposition*, vol. 34, no. 12, pp. 2073–2078, 2006.

[44] E. J. Jeong, H. Lin, and M. Hu, "Disposition mechanisms of raloxifene in the human intestinal Caco-2 model," *Journal of Pharmacology and Experimental Therapeutics*, vol. 310, no. 1, pp. 376–385, 2004.

[45] J. P. van Brussel, G. J. van Steenbrugge, J. C. Romijn, F. H. Schröder, and G. H. J. Mickisch, "Chemosensitivity of prostate cancer cell lines and expression of multidrug resistance-related proteins," *European Journal of Cancer*, vol. 35, no. 4, pp. 664–671, 1999.

[46] G. J. Doherty and H. T. McMahon, "Mechanisms of endocytosis," *Annual Review of Biochemistry*, vol. 78, pp. 857–902, 2009.

[47] N. M. Zaki and N. Tirelli, "Gateways for the intracellular access of nanocarriers: a review of receptor-mediated endocytosis mechanisms and of strategies in receptor targeting," *Expert Opinion on Drug Delivery*, vol. 7, no. 8, pp. 895–913, 2010.

[48] H. Maeda, H. Nakamura, and J. Fang, "The EPR effect for macromolecular drug delivery to solid tumors: Improvement of tumor uptake, lowering of systemic toxicity, and distinct tumor imaging in vivo," *Advanced Drug Delivery Reviews*, vol. 65, pp. 71–79, 2013.

[49] S. Mandlekar and A. N. Kong, "Mechanisms of tamoxifen-induced apoptosis," *Apoptosis*, vol. 6, no. 6, pp. 469–477, 2001.

[50] M. Obrero, D. V. Yu, and D. J. Shapiro, "Estrogen receptor-dependent and estrogen receptor-independent pathways for tamoxifen and 4-hydroxytamoxifen-induced programmed cell death," *Journal of Biological Chemistry*, vol. 277, no. 47, pp. 45695–45703, 2002.

[51] I. Y. Kim, B.-C. Kim, D. H. Seong et al., "Raloxifene, a mixed estrogen agonist/antagonist, induces apoptosis in androgen-independent human prostate cancer cell lines," *Cancer Research*, vol. 62, no. 18, pp. 5365–5369, 2002.

[52] D. Price, B. Stein, P. Sieber et al., "Toremifene for the prevention of prostate cancer in men with high grade prostatic intraepithelial neoplasia: results of a double-blind, placebo controlled, phase IIB clinical trial," *Journal of Urology*, vol. 176, no. 3, pp. 965–971, 2006.

[53] A. Zou, K. B. Marschke, K. E. Arnold et al., "Estrogen receptor β activates the human retinoic acid receptor promoter in response to tamoxifen and other estrogen receptor antagonists, but not in response to estrogen," *Molecular Endocrinology*, vol. 13, no. 3, pp. 418–430, 1999.

[54] A. Rimler, Z. Culig, Z. Lupowitz, and N. Zisapel, "Nuclear exclusion of the androgen receptor by melatonin," *Journal of Steroid Biochemistry and Molecular Biology*, vol. 81, no. 1, pp. 77–84, 2002.

[55] S. E. Taylor, P. L. Martin-Hirsch, and F. L. Martin, "Oestrogen receptor splice variants in the pathogenesis of disease," *Cancer Letters*, vol. 288, no. 2, pp. 133–148, 2010.

[56] S. S. El Sheikh, J. Domin, P. Abel, G. Stamp, and E.-N. Lalani, "Phosphorylation of both EGFR and ErbB2 is a reliable predictor of prostate cancer cell proliferation in response to EGF," *Neoplasia*, vol. 6, no. 6, pp. 846–853, 2004.

[57] D. Carrion-Salip, C. Panosa, J. A. Menendez et al., "Androgen-independent prostate cancer cells circumvent EGFR inhibition by overexpression of alternative HER receptors and ligands," *International Journal of Oncology*, vol. 41, pp. 1128–1138, 2012.

[58] F. Hirschhaeuser, H. Menne, C. Dittfeld, J. West, W. Mueller-Klieser, and L. A. Kunz-Schughart, "Multicellular tumor spheroids: an underestimated tool is catching up again," *Journal of Biotechnology*, vol. 148, no. 1, pp. 3–15, 2010.

[59] F. A. Attiga, P. M. Fernandez, A. T. Weeraratna, M. J. Manyak, and S. R. Patierno, "Inhibitors of prostaglandin synthesis inhibit human prostate tumor cell invasiveness and reduce the release of matrix metalloproteinases," *Cancer Research*, vol. 60, no. 16, pp. 4629–4637, 2000.

[60] H. E. Cubitt, J. B. Houston, and A. Galetin, "Prediction of human drug clearance by multiple metabolic pathways: integration of hepatic and intestinal microsomal and cytosolic data," *Drug Metabolism and Disposition*, vol. 39, no. 5, pp. 864–873, 2011.

[61] Y. Matsumura and H. Maeda, "A new concept for macromolecular therapeutics in cancer chemotherapy: mechanism of tumoritropic accumulation of proteins and the antitumor agent smancs," *Cancer Research*, vol. 46, no. 12, pp. 6387–6392, 1986.

[62] K. Greish, "Enhanced permeability and retention of macromolecular drugs in solid tumors: a royal gate for targeted anticancer nanomedicines," *Journal of Drug Targeting*, vol. 15, no. 7-8, pp. 457–464, 2007.

[63] H. S. Choi, W. Liu, P. Misra et al., "Renal clearance of quantum dots," *Nature Biotechnology*, vol. 25, no. 10, pp. 1165–1170, 2007.

[64] H. Sarin, "Physiologic upper limits of pore size of different blood capillary types and another perspective on the dual pore theory of microvascular permeability," *Journal of Angiogenesis Research*, vol. 2, article 14, 2010.

[65] K. Greish, J. Fang, T. Inutsuka, A. Nagamitsu, and H. Maeda, "Macromolecular therapeutics: advantages and prospects with special emphasis on solid tumour targeting," *Clinical Pharmacokinetics*, vol. 42, no. 13, pp. 1089–1105, 2003.

[66] X. Li, X. Tian, J. Zhang et al., "In vitro and in vivo evaluation of folate receptor-targeting amphiphilic copolymer-modified liposomes loaded with docetaxel," *International Journal of Nanomedicine*, vol. 6, pp. 1167–1184, 2011.

Hindawi Publishing Corporation
BioMed Research International
Volume 2013, Article ID 252939, 9 pages
http://dx.doi.org/10.1155/2013/252939

Research Article

Evaluation of the PI-RADS Scoring System for Classifying mpMRI Findings in Men with Suspicion of Prostate Cancer

Daniel Junker,[1] Georg Schäfer,[2,3] Michael Edlinger,[4] Christian Kremser,[1] Jasmin Bektic,[3] Wolfgang Horninger,[3] Werner Jaschke,[1] and Friedrich Aigner[1]

[1] *Department of Radiology, Medical University of Innsbruck, Anichstraße 35, 6020 Innsbruck, Austria*
[2] *Department of Pathology, Medical University of Innsbruck, Anichstraße 35, 6020 Innsbruck, Austria*
[3] *Department of Urology, Medical University of Innsbruck, Anichstraße 35, 6020 Innsbruck, Austria*
[4] *Department of Medical Statistics, Informatics and Health Economics, Medical University of Innsbruck, Schöpfstraße 41/1, 6020 Innsbruck, Austria*

Correspondence should be addressed to Daniel Junker; daniel.junker@uki.at

Received 19 September 2013; Revised 31 October 2013; Accepted 2 November 2013

Academic Editor: Giovanni Luca Gravina

Purpose. To evaluate the ESUR scoring system (PI-RADS) for multiparametric MRI of the prostate in clinical routine and to define a reliable way to generate an overall PI-RADS score. *Methods*. Retrospective analysis of all patients with a history of negative prebiopsies, who underwent 3 Tesla multiparametric MRI from October 2011 to April 2013 ($n = 143$): PI-RADS scores for each single modality were defined. To generate the overall PI-RADS score, an algorithm based approach summing up each single-modality score to a sum-score was compared to a more subjective approach, weighting the single modalities dependent on the radiologist's impression. Because of ongoing cancer suspicion 73 patients underwent targeted mpMRI-ultrasound image fusion rebiopsy. For this group thresholds for tumor incidences and malignancy were calculated. *Results*. 39 (53%) out of 73 targeted rebiopsies were cancer positive. The PI-RADS score correlated well with tumor incidence (AUC of 0.86, 95% CI 0.78 to 0.94) and malignancy (AUC 0.84, 95% CI 0.68 to 0.99). Regarding the sum-score a threshold of ≥10 turned out to be reliable for cancer detection (sensitivity 90%, specificity 62%) and for ≥13 for indicating higher malignancy (Gleason ≥ 4 + 3) (sensitivity 80%, specificity 86%). To generate the overall PI-RADS score, the use of an algorithm based approach was more reliable than that of the approach based on the radiologist's impression. *Conclusion*. The presented scoring system correlates well with tumor incidence and malignancy. To generate the overall PI-RADS score, it seems to be advisable to use an algorithm based instead of a subjective approach.

1. Introduction

Due to the increasing availability of multiparametric magnetic resonance imaging (mpMRI) in general, the improved image quality at 3 Tesla, and the increasing number of studies confirming the diagnostic reliability of mpMRI for prostate cancer (PCa) detection, mpMRI proceeds to become an important and widely used tool for PCa diagnosis [1–5]. In Austria we recognize a growing urological demand for mpMRI of the prostate especially in patients with negative systematic prebiopsies but ongoing tumor suspicion.

The multiparametric approach using three different MRI techniques (T2-weighted MRI (T2W-MRI), diffusion-weighted imaging (DWI), and dynamic contrast-enhanced MRI (DCE-MRI)) can improve the diagnostic accuracy. However its complexity and the sometimes contradictory findings of the different single modalities may result in a wide scope of possible interpretations of mpMRI findings leading to heterogeneities between different readers and different diagnostic centers [6–9].

To overcome these problems, the European Society of Urogenital Radiology (ESUR) has called a panel of experts and published a guideline providing recommendations for the performance of mpMRI investigations and a structured reporting scheme named Prostate Imaging Reporting and Data System (PI-RADS) in February 2012 [10]. Inspired by the BI-RADS system for breast cancer detection [11, 12], this scheme is based on Likert scales, scoring each single modality

Table 1: Patient characteristics at the date of mpMRI.

	All patients ($n = 143$)	Patients with rebiopsy ($n = 73$)
Age (years), mean (s.d.)	62 (7.8)	62 (7.4)
Prostate volume (cm^3), median (interquartile range)	45 (34–60)	45 (34 to 61)
Negative prebiopsies, *n* (%)		
1	51 (36%)	17 (23%)
2	50 (35%)	31 (42%)
3	23 (16%)	15 (21%)
4	13 (9%)	6 (8%)
≥5	6 (4%)	4 (5%)
PSA (ng/mL), median (IQR)	6.4 (5.0–11.3)	7.0 (5.1 to 12.9)
Free PSA (%), median (IQR)	13.8 % (11.0%–18.45%)	13.4% (10%–18.6%)

Table 2: mpMRI parameters.

	T2W-MRI	DWI	DCE-MRI
Sequence	Fast spin echo	Spin echo EPI	T1w-3D FLASH
TR (ms)	4891	6800	2.89
TE (ms)	101	67	1.12
Flip angle (°)	160	90	2
FoV (mm^2)	200 × 200	210 × 210	380 × 285
Resolution	320 × 320	160 × 132	256 × 192
Slice thickness (mm)	3	3	4
b-values	—	50/400/1000	—

TR: relaxation time, TE: emission time, FoV: field of view, and FLASH: fast low angle shot magnetic resonance imaging.

from 1 to 5 (single-scores) and then generating the final PI-RADS score (1–5 points: overall PI-RADS). Similar to BI-RADS, the PI-RADS score involves individual risk stratification for the absence or presence of a clinically relevant disease and should be part of the written report. Although the ESUR guideline provides explicit criteria for how to generate each single-score, it lacks a consistent instruction on how to calculate the overall PI-RADS score [10, 13, 14].

The aim of this study was to evaluate the PI-RADS scoring system in our patient population and to find the best way of generating the overall PI-RADS score.

2. Materials and Methods

2.1. Patients. From October 2011 to May 2013, 143 consecutive patients with a history of at least one negative systematic prebiopsy, who underwent 3 Tesla mpMRI of the prostate because of ongoing tumor suspicion, were included in this retrospective single-center study in Innsbruck. None of the patients were under treatment with 5-alpha-reductase inhibitors at the time the MRI was performed. Of these 143 patients, 73 underwent systematic and targeted rebiopsy within 3 months after mpMRI. Patient characteristics are summarized in Table 1. A positive vote of the local ethical committee was obtained.

2.2. mpMRI Technique. mpMRI was performed on a 3 Tesla whole body scanner (Magnetom Skyra, Siemens AG, Erlangen, Germany) using an 18-channel phased array body coil with 18 integrated preamplifiers. Examinations included 2D and 3D T2W-MRI, DWI, and DCE-MRI. MRI parameters are shown in Table 2. 2D T2W-MR images were obtained in axial orientation using T2W turbo spin echo (TSE) sequences covering the entire prostate and the seminal vesicles. For 3D T2W images a 3D TSE sequence with variable flip angle (3D SPACE sequence) was used in sagittal orientation. DWI was obtained in axial orientation using a spin echo-echo planar imaging (SE-EPI) sequence with three *b*-values (50, 400, and 1000 s/mm^2) and restriction of diffusion was quantified by the apparent diffusion coefficient (ADC) value [15, 16]. DCE-MR images were obtained using fast 3D T1-weighted (T1-VIBE) gradient echo sequence in axial orientation every 7 seconds for about 10 minutes. As a contrast agent Gadobutrol (Gadovist, Bayer Schering Pharma, Germany) was used with a dose of 0.1 mL/kg body weight. Bolus injection was performed using a power injector (3T Tennessee, Ulrich, Germany) with a flow rate of 0.1 mL/s. Perfusion curves were generated with the commercial software TISSUE4D (Siemens AG, Erlangen, Germany) [17] which was available on the MR scanner console.

2.2.1. Image Interpretation. The mpMRI datasets were analyzed by two experienced uroradiologists with at least 6 years of experience in prostate MRI interpretation, who compared two different approaches to generate an overall PI-RADS score.

In a first step the three single-scores (1–5) for T2W-MRI, DWI, and DCE-MRI for each patient were defined according to the ESUR guidelines (Table 3) by the two radiologists in consensus.

Subsequently, in a first algorithm based approach the first radiologist calculated a PI-RADS sum-score (scale from 3 to 15) by summation of the 3 single-scores. The overall PI-RADS score (1–5) was obtained by classifying the sum-score according to the algorithm proposed by Röthke et al. [13] (Table 4, column 3).

In a second more subjective approach the second radiologist independently generated an overall PI-RADS score by subjectively weighting the results of the single-scores according to the definitions of the ESUR panel (Table 4, column 2), but without deriving it from a strict algorithm. So whenever the results of the three single-scores were incoherent, the analyzing radiologist had to prefer one of the single modalities over the others.

Image interpretation and scoring were done before biopsy, so the radiologists were blinded to the histopathological outcomes. For reporting and localization of findings

Table 3: Single-modality scores according to the ESUR panel [10].

(A1) T2W imaging for the peripheral zone
(1) Uniform high signal intensity
(2) Linear, wedge-shaped, or geographical areas of lower signal intensity, usually not well demarcated
(3) Intermediate appearances not in categories 1/2 or 4/5
(4) Discrete, homogeneous low-signal focus/mass confined to the prostate
(5) Discrete, homogeneous low-signal-intensity focus with extracapsular extension/invasive behavior or mass effect on the capsule (bulging) or broad (>1.5 cm) contact with the surface
(A2) T2W imaging for the transition zone
(1) Heterogeneous transition zone adenoma with well-defined margins: "organized chaos"
(2) Areas of more homogeneous low signal intensity, however, well marginated, originating from the transition zone/benign prostatic hyperplasia
(3) Intermediate appearances not in categories 1/2 or 4/5
(4) Areas of more homogeneous low signal intensity, ill defined: "erased charcoal sign"
(5) Same as 4, but involving the anterior fibromuscular stroma or the anterior horn of the peripheral zone, usually lenticular or water-drop shaped
(B) Diffusion-weighted imaging
(1) No reduction in ADC compared with normal glandular tissue; no increase in signal intensity on any high-*b*-value image ($\geq b800$)
(2) Diffuse, hyper signal intensity on $\geq b800$ image with low ADC; no focal features; however, linear, triangular, or geographical features are allowed
(3) Intermediate appearances not in categories 1/2 or 4/5
(4) Focal area(s) of reduced ADC but isointense signal intensity on high-*b*-value images ($\geq b800$)
(5) Focal area/mass of hyper signal intensity on the high-*b*-value images ($\geq b800$) with reduced ADC
(C) Dynamic contrast-enhanced MRI
(1) Type 1 enhancement curve
(2) Type 2 enhancement curve
(3) Type 3 enhancement curve
(+1) For focal enhancing lesion with curve types 2-3
(+1) For asymmetric lesion or lesion at an unusual place with curve types 2-3

previous to targeted biopsies the prostate was divided into 27 regions as recommended by the ESUR guidelines according to a scheme presented by Röthke et al. [10, 13].

2.2.2. Rebiopsy. Within 3 months after mpMRI 73 patients underwent re-biopsy, which was indicated in consideration of radiological and clinical findings by the attending urologist. Within one re-biopsy setting one of the uroradiologists, who interpreted the mpMRI images, took 5 targeted cores of those lesions that were suspicious on at least one single modality (PI-RADS sum-score $\geq$ 7). Additionally the urologist, who was unaware of the mpMRI imaging results, took 10 systematic cores of all patients. All rebiopsies were taken with an ultrasound system equipped with an endfire endorectal biopsy probe (Logiq 9 ultrasound unit, GE Healthcare, Little Chalfont, United Kingdom, or EUB 8500 Hitachi ultrasound unit, Hitachi Medical Systems, Tokyo, Japan). Targeted re-biopsy was performed with mpMRI-ultrasound fusion. Registration of suspicious lesions was done with a combined approach of cognitive evaluation on the basis of zonal anatomy and imaging landmarks as well as computerized real-time 3D transrectal US-MRI image fusion by uploading the SPACE 3D T2W sequence to the Logiq 9 ultrasound system [18–20] (Figure 1).

For histopathological analysis all biopsy specimens were numbered, reviewed by a pathologist with >10 years of experience in prostate characterization, and reported as PCa with an assigned Gleason score, prostatitis, adenomyomatosis, benign prostatic hyperplasia, or atrophy.

2.3. Statistical Analysis. Summary statistics are provided using the appropriate measures of location and measures of variation for all 143 patients. The D'Agostino-Pearson test was used to test for normal distribution. Mean values ± standard deviations were given for normal distributed data and otherwise median with interquartile range. The different approaches to generate the overall PI-RADS score were compared regarding number and distribution of score levels for all patients within the collective.

Correlation of mpMRI findings and histopathological findings was performed only for the collective of 73 patients, who underwent re-biopsy: to assess a possible positive association between the number of biopsies conducted before the re-biopsy and the relative number of tumor cases,

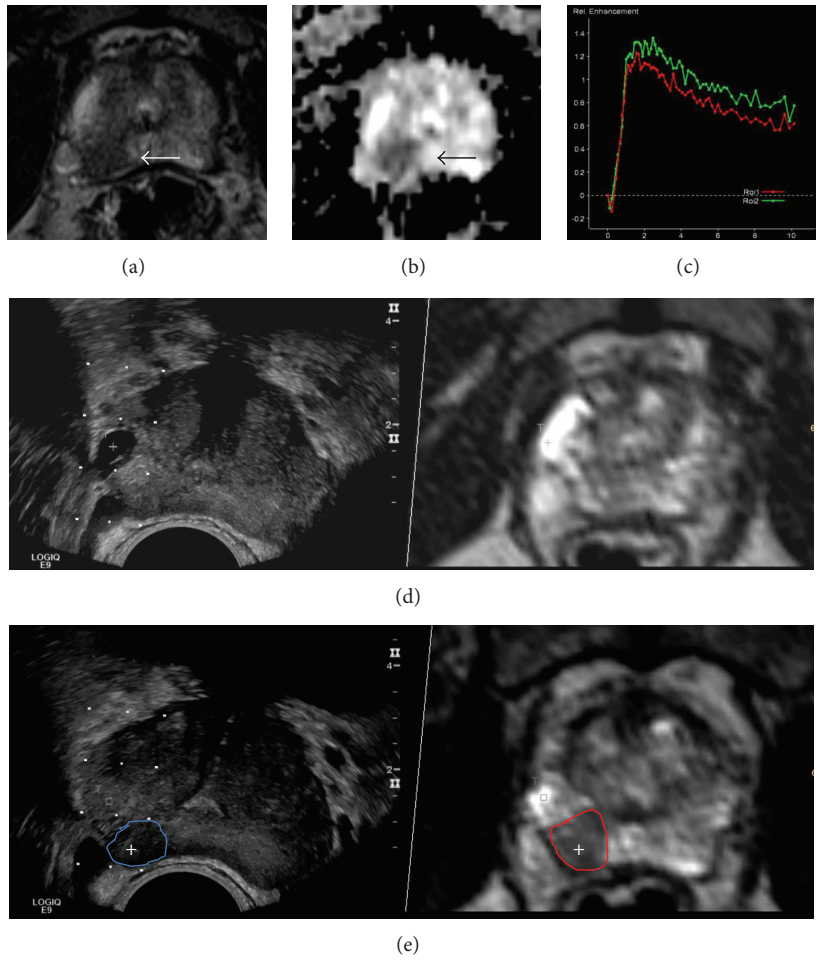

(a) (b) (c)

(d)

(e)

Figure 1: mpMRI-ultrasound image fusion: suspicious lesion (arrows) on T2W (a), on DWI with low ADC (b), and washout curve on DCE (c). Correlation of an anatomical landmark (cyst) for registration of *b*-mode ultrasound and SPACE 3D T2W-MRI (d). Target point (+) in the center of the suspicious lesion on *b*-mode ultrasound and SPACE 3D T2W-MRI (e). Note the slight deformation of the lesion (circle) on the ultrasound due to compression by the endorectal probe.

Table 4: Calculation of the overall PI-RADS score according to the definitions of the ESUR panel compared to the algorithm presented by Röthke et al. [13].

Overall PI-RADS	Definition of the ESUR panel	Sum-score of T2W, DWI, and DCE
Score 1	Clinically significant disease highly unlikely to be present	3, 4
Score 2	Clinically significant cancer is unlikely to be present	5, 6
Score 3	Clinically significant cancer is equivocal	7–9
Score 4	Clinically significant cancer is likely to be present	10–12
Score 5	Clinically significant cancer is highly likely to be present	13–15

a Chi-squared test for trend was applied. A receiver operating characteristic (ROC) analysis was performed to evaluate sensitivity and specificity of the scoring system with regard to tumor incidence and tumor malignancy. For statistical analysis respective to tumor malignancy, histopathologic results were split into two groups (Gleason score level $\leq 3 + 4$ versus Gleason score level $\geq 4 + 3$). Additionally, an assessment of cutoff levels was made. Two-sided $P < 0.05$ was considered statistically significant. The statistical calculations were performed using SPSS 19.0.

3. Results

3.1. Biopsy Results. After performing mpMRI, 39 (53%) out of 73 targeted rebiopsies were positive for prostate cancer. Of the 39 tumors, 22 (56%) were located in anterior parts of the prostate, and 17 (44%) in the transitional zone (TZ) while 17 tumors (44%) were located in the posterior parts and 22 (56%) in the peripheral zone (PZ). Regarding tumor malignancy, 29 (74%) were cancers with Gleason $\leq 3 + 4$ and 10 (26%) cancers with Gleason $\geq 4 + 3$. Chi-squared trend

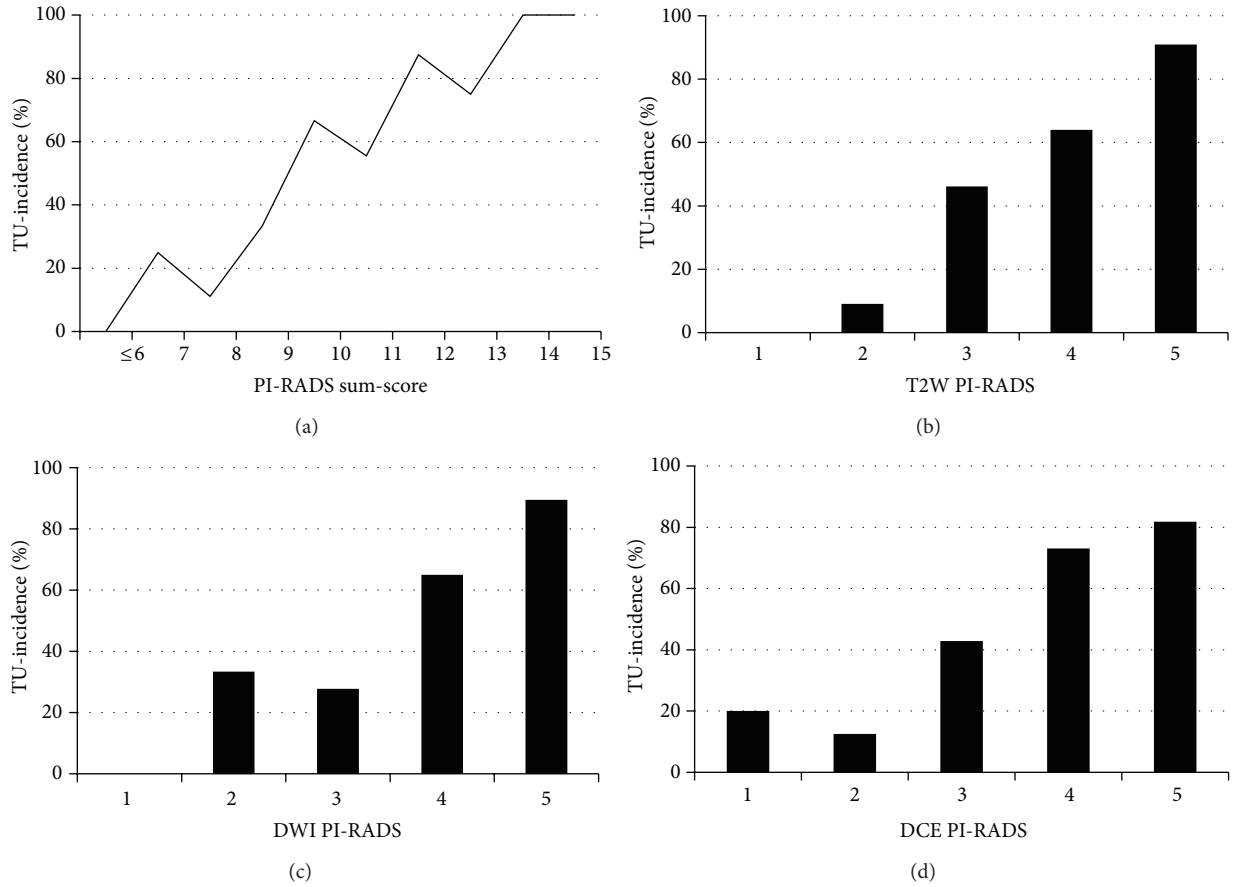

Figure 2: Distribution of tumor incidences for PI-RADS single-scores and sum-scores.

analysis revealed a significant association between increasing tumor incidence and increasing number of negative pre-biopsies ($P < 0.05$). Targeted biopsies of suspicious lesions revealed markedly more negative findings within the TZ (83%) than in the PZ (17%) and were caused by the presence of adenomas (58%) or inflammations (42%).

3.2. Evaluation of the PI-RADS Single- and Sum-Scores. After evaluating the 3 single modalities and adding the single-scores, the collective of 143 patients revealed sum-scores with a median of 8 (range 4–15, IQR 6 to 10). In the group of patients with targeted re-biopsy the PI-RADS sum-score was positively related to the number of cancer positive cores ($P < 0.05$). Each of the single-scores generally showed a tendency to a higher tumor incidence at higher score levels (Figure 2). The ROC analyses revealed a rather large area under the curve (AUC) of 0.86 (95% CI 0.78 to 0.94) regarding tumor incidence and 0.84 (95% CI 0.68 to 0.99) regarding tumor malignancy (Figure 3). When analyzing the balance between sensitivity and specificity to calculate a reliable threshold for tumor incidence for the PI-RADS sum-score, the score level of ≥10 with an accent on sensitivity (90%) rather than specificity (62%) was the highest possible threshold with more sensitivity than specificity. The threshold of ≥11 already showed a markedly lower sensitivity (69%), but better specificity (82%). Tumor incidences differed significantly for score levels below both thresholds compared to those above ($P < 0.005$). Regarding tumor malignancy a threshold was calculated for a score level of ≥13, which revealed high sensitivity (80%) and specificity (86%) for the prediction of cancers with Gleason score ≥4+3. The number of cancers with high Gleason scores ($\geq 4 + 3$) differed significantly for score levels below this threshold compared to those above ($P < 0.005$) (Figure 4).

3.3. Comparison of Two Different Approaches to Generate the Overall PI-RADS Score (Table 5). Both, the first approach based on the algorithm of Röthke et al. (PI-RADS scheme 1) and the second approach (PI-RADS scheme 2), based on the overall impression of the radiologist, revealed overall PI-RADS scores, which showed increasing tumor incidence with increasing score levels. When classified according to the algorithm of Röthke et al., it is noticeable that their cutoff between overall PI-RADS 3 and 4 corresponds to the calculated threshold for tumor incidence on the PI-RADS sum-score and their cutoff between 4 and 5 to our calculated threshold for higher tumor malignancy. According to this approach, the prostates of 47 (33%) patients revealed cancer suspicious lesions (PI-RADS scores of either 4 or 5) of which 35 (82%) proved to be cancer positive after targeted biopsy. When generating the overall PI-RADS score simply by the radiologist's impression on the other hand 55

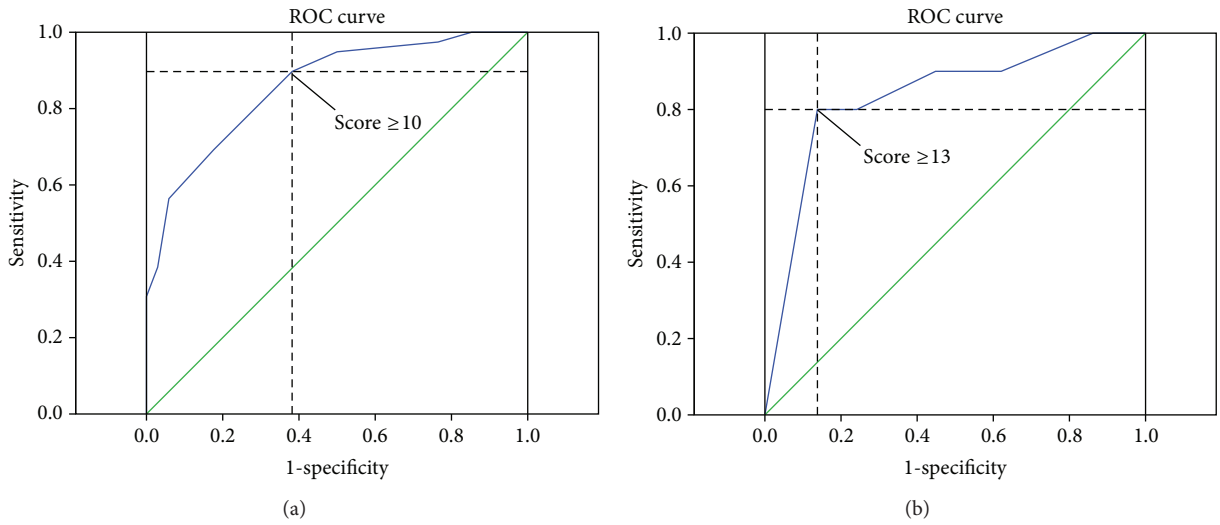

Figure 3: Receiver operation characteristic (ROC) curves for the PI-RADS sum-score, regarding thresholds for tumor incidence with a cutoff at 10 (a) and for tumor malignancy with a cutoff at 13 (b).

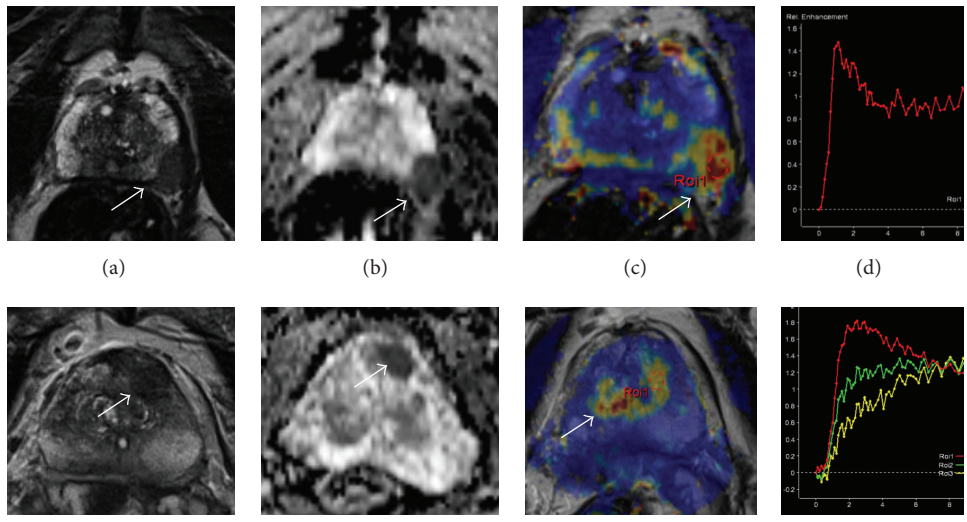

Figure 4: Suspicious lesions (arrows) on mpMRI with different PI-RADS sum-scores. Gleason 8 carcinoma: 5 points on T2W for hypointensity and bulging (a), 5 points on DWI for focal very low ADC (b), and 5 points on DCE-MRI for washout curve in a focal lesion (c, d) = sum-score of 15 points. Gleason 7 (3 + 4) carcinoma with 4 points on T2W for focal hypointensity (e), 5 points on DWI for focal very low ADC (f), and 3 points on DCE-MRI for symmetrical washout curve without focal lesion (g, h) = sum-score of 12 points.

Table 5: Overall PI-RADS score according to Röthke et al. [13] (calculation based on sum-score results) compared to the one based on the overall impression of the radiologist.

Overall PI-RADS score level (1–5)	Score based on Röthke et al.		Score based on radiologist's impression	
	Frequency of patients *n* (%)	Tumor incidence (% of biopsies)	Frequency of patients *n* (%)	Tumor incidence (% of biopsies)
1	1 (1%)	—	0 (<1%)	—
2	43 (30%)	0%	38 (27%)	0%
3	52 (36%)	19%	50 (35%)	17%
4	31 (22%)	65%	38 (27%)	54%
5	16 (11%)	94%	17 (12%)	100%

(38%) prostates revealed cancer suspicious lesions, but only 37 (67%) of these proved to be cancer positive after targeted biopsy. Regarding the frequency of PI-RADS 3 lesions, both approaches assigned a similar number of patients to this score level. Nevertheless with 19% compared to 17% biopsy proved tumor incidence in PI-RADS 3 patients was slightly higher for PI-RADS scheme 1. PI-RADS 1 and 2, which mean low suspicion for clinically relevant disease, were diagnosed in 44 (31%) patients when using PI-RADS scheme 1 and in only 38 (27%) patients with PI-RADS scheme 2. None of the biopsies taken from these patients revealed cancer positive cores. The very rare diagnosis of PI-RADS 1 in both approaches can be explained by the presence of multiple tissue alterations in this collective of patients with negative prebiopsies (Table 5).

4. Discussion

With this study we could demonstrate a good reliability of the PI-RADS risk stratification system for the interpretation of mpMRI in our patient population: all 3 single-scores and thus the calculated PI-RADS sum-score of 3–15 points showed a clear association with tumor incidence and tumor malignancy with large AUC in ROC curve analysis. In concordance with the other studies, which recently evaluated the PI-RADS classification system with slightly different approaches, this suggests high reliability for the use of a system with fixed criteria for mpMRI interpretation [14, 21, 22]. Similar to the findings of Portalez et al. the T2W single-score proportionally increased with tumor incidence [22]. However, DWI and DCE-MRI single-scores showed indentations at score levels 2 and 3. For DCE-MRI this was mainly due to the observation of several symmetrical or asymmetrical plateau curves in TZ regions, which consequently received 2 points for the DCE-MRI single-score but still were cancer negative after targeted biopsy. This finding mainly corresponded to the presence of adenomas. Low cancer incidences at DWI score level 3 could probably be explained by the existence of fibrous tissue and inflammation in nearly all prostates after systematic prebiopsies, which lead to a certain extent of asymmetrical diffusion restriction and thus were scored with 3 points. All tumors that were found in single-score levels <4 on T2W-MRI, DWI, or DCE-MRI were only carcinomas ≤ Gleason 3 + 4.

Regarding sensitivity and specificity levels of the PI-RADS sum-score on ROC analysis, our results suggest either ≥10 or ≥11 as possible thresholds for the increase of tumor incidence. The question of which of these two values should be used as a threshold to indicate distinct cancer suspicion was discussed with our clinicians, who clearly favored the threshold of ≥10 points for its very high sensitivity level of 90% with an acceptable specificity level of 62%. This goes along to the findings of Schimmöller et al., who also evaluated the sum-score level of ≥10 to be the threshold for tumor incidence and reported a sensitivity of 85.7% and a specificity of 67.6% [21]. However there are some differences when compared to the findings of Portalez et al., who proposed a threshold of ≥9, because of an overall lower sensitivity. This can be explained by the different approaches of our studies, as the main goal of the study of Portalez et al. was to compare targeted biopsy cores with systematically taken cores, and thus they took the single biopsy core as the smallest comparable unit for statistical analysis [22]. We on the other hand wanted to evaluate the PI-RADS scale for its reliability as a risk stratification system for the patient and thus we compared mpMRI findings to the findings of the complete targeted biopsy set (at least 2 cores) in the style of other studies, which dealt with mpMRI/US fusion targeted biopsies [18, 23].

The second goal of this study was to find a reliable approach to generate the overall PI-RADS score, which in the end shall be part of the clinical report as a simplified risk stratification system and which could provide recommendations for further diagnostic procedures. Regarding this issue, the ESUR guidelines lack a consistent instruction of how to generate the overall PI-RADS score [10]. Therefore Röthke et al. published a suggestion to flesh out the ESUR guidelines. According to this proposal the single modalities are added up to a sum-score, which then is classified according to a separate algorithm [13]. However, the authors noted that no evidence-based data exist for certain thresholds (≥10 and ≥13). Rosenkrantz et al. on the other hand presented a study, where the sum-score was not separately classified but interpreted for itself, and additionally an overall PI-RADS score (1–5) was derived from an overall impression by the radiologist according to the definitions provided by the ESUR panel [10, 14].

Comparing the algorithm of Röthke et al. [13] it turns out that their cutoffs between overall PI-RADS 3 and 4 and between 4 and 5 are exactly consistent with our calculated thresholds for tumor incidence (sum-score ≥10) and tumor malignancy (sum-score ≥13), and thus their approach to classify the overall PI-RADS from the sumscore seems to be reliable in accordance with our data.

The second approach to generate an overall PI-RADS score, based on the radiologist's impression, showed less association with the thresholds of the sum-score, and the evaluating radiologist assigned more prostates to PI-RADS 4 and 5, which lead to lower tumor incidences (67% compared to 82%) in these categories and thus less specificity. Regarding PI-RADS 4 and 5 as possible indications for re-biopsy this would have led to a higher number of interventions with a higher percentage of negative results. Therefore, according to our data, an algorithm based approach, which derives the overall PI-RADS score from the sum-score seems to be more reliable.

However, the overall PI-RADS score, recommended by Röthke et al. [13], also led to a noticeable amount of PI-RADS 3 (36%) scores and at the same time showed low cancer incidences in this group (19%). Keeping in mind that PI-RADS 3 is defined as equivocal cancer suspicion and compared to the BI-RADS scoring system of the breast could lead to certain management challenges [24]. To reduce the number of PI-RADS 3, without substantially reducing specificity, we recommend lifting the threshold between PI-RADS 2 and 3 from sum-score levels ≥7 to ≥8. Applied to our patient collective 16 mpMRIs would be reduced from PI-RADS 3 to PI-RADS 2 and thus the rate of PI-RADS 3 scores would be reduced from 36% to 25%. With this correction

Table 6: Recommendation to calculate an overall PI-RADS score, based on division from the sum-score, with tumor incidences derived from our data.

Overall PI-RADS score	Sum-score of T2W, DWI, and DCE-MRI	Number of patients (%)	Tumor incidence (% of biopsies)	Definition of the ESUR panel
1	3, 4	1 (1%)	—	Clinically significant disease highly unlikely to be present
2	5, 6, 7	59 (41%)	11%	Clinically significant cancer unlikely to be present
3	8-9	36 (25%)	19%	Clinically significant cancer is equivocal
4	10–12	31 (22%)	65%	Clinically significant cancer likely to be present
5	13–15	16 (11%)	94%	Clinically significant cancer highly likely to be present

Changes in comparison to the system of Röthke et al. [13] are underlined (threshold between PI-RADS 2 and 3).

one Gleason 6 (3 + 3) tumor would have been assigned to score level PI-RADS 2 elevating the tumor incidence to 11% (Table 6).

This study is prone to some limitations. This study was designed as an evaluation of our clinical routine and not every patient underwent re-biopsy of the prostate. This might have led to a verification bias, since patients with few or no abnormalities on mpMRI less frequently underwent re-biopsy. Furthermore in patients without suspicious lesion on at least one single modality (sum-score <7) no targeted biopsies could be performed and systematic re-biopsy had to be used as a gold standard. Therefore all tumor incidences, calculated for low PI-RADS score levels (sum-score <7 or overall Pi-RADS 1 and 2), should be regarded as uncertain. Further studies with data based on a long followup will be necessary to evaluate reliable tumor incidences for these low suspicion groups. Additionally, since each of the evaluating radiologists used a different approach for scoring, we do not have data about interobserver variability within the same approach. For this we refer to a recent study of Schimmöller et al. [21].

5. Conclusion

The PI-RADS sum-score (3–15) shows a strong relation to tumor incidence and malignancy in our routine setting for PCa diagnosis. A score level of ≥10 seems to be an important threshold for a positive tumor diagnosis and of ≥13 for the existence of high Gleason scores (≥ 4+3). For generating the overall PI-RADS score, which is part of the clinical report, our results indicate a recommendation for a number based algorithm with a slightly elevated threshold between PI-RADS 2 and 3 compared to that of Röthke et al. [13].

Conflict of Interests

The authors declare that they have no conflict of interests.

References

[1] K. Kitajima, Y. Kaji, Y. Fukabori, K. Yoshida, N. Suganuma, and K. Sugimura, "Prostate cancer detection with 3 T MRI: comparison of diffusion-weighted imaging and dynamic contrast-enhanced MRI in combination with T2-weighted imaging," *Journal of Magnetic Resonance Imaging*, vol. 31, no. 3, pp. 625–631, 2010.

[2] M. Sertdemir, S. O. Schoenberg, S. Sourbron et al., "Interscanner comparison of dynamic contrast-enhanced MRI in prostate cancer: 1.5 versus 3 T MRI," *Investigative Radiology*, vol. 48, no. 2, pp. 92–97, 2013.

[3] C. M. Hoeks, M. G. Schouten, J. G. R. Bomers et al., "Three-Tesla magnetic resonance-guided prostate biopsy in men with increased prostate-specific antigen and repeated, negative, random, systematic, transrectal ultrasound biopsies: detection of clinically significant prostate cancers," *European Urology*, vol. 62, no. 5, pp. 902–909, 2012.

[4] A. B. Rosenkrantz, T. C. Mussi, M. S. Borofsky, S. S. Scionti, M. Grasso, and S. S. Taneja, "3.0 T multiparametric prostate MRI using pelvic phased-array coil: utility for tumor detection prior to biopsy," *Urologic Oncology*, vol. 31, no. 8, pp. 1430–1435, 2013.

[5] B. K. Park, B. Kim, C. K. Kim, H. M. Lee, and G. Y. Kwon, "Comparison of phased-array 3.0-T and endorectal 1.5-T magnetic resonance imaging in the evaluation of local staging accuracy for prostate cancer," *Journal of Computer Assisted Tomography*, vol. 31, no. 4, pp. 534–538, 2007.

[6] H. P. Schlemmer, "Multiparametric MRI of the prostate: method for early detection of prostate cancer?" *Fortschr Röntgenstr*, vol. 182, no. 12, pp. 1067–1075, 2010.

[7] L. Dickinson, H. U. Ahmed, C. Allen et al., "Magnetic resonance imaging for the detection, localisation, and characterisation of prostate cancer: recommendations from a European consensus meeting," *European Urology*, vol. 59, no. 4, pp. 477–494, 2011.

[8] C. M. Hoeks, J. O. Barentsz, T. Hambrock et al., "Prostate cancer: multiparametric MR imaging for detection, localization, and staging," *Radiology*, vol. 261, no. 1, pp. 46–66, 2011.

[9] L. Dickinson, H. U. Ahmed, C. Allen et al., "Scoring systems used for the interpretation and reporting of multiparametric MRI for prostate cancer detection, localization, and characterization: could standardization lead to improved utilization of imaging within the diagnostic pathway?" *Journal of Magnetic Resonance Imaging*, vol. 37, no. 1, pp. 48–58, 2013.

[10] J. O. Barentsz, J. Richenberg, R. Clements et al., "ESUR prostate MR guidelines 2012," *European Radiology*, vol. 22, no. 4, pp. 746–757, 2012.

[11] C. Balleyguier, S. Ayadi, K. Van Nguyen, D. Vanel, C. Dromain, and R. Sigal, "BIRADSŮ classification in mammography," *European Journal of Radiology*, vol. 61, no. 2, pp. 192–194, 2007.

[12] S. Obenauer, K. P. Hermann, and E. Grabbe, "Applications and literature review of the BI-RADS classification," *European Radiology*, vol. 15, no. 5, pp. 1027–1036, 2005.

[13] M. Röthke, D. Blondin, H. P. Schlemmer, and T. Franiel, "PI-RADS classification: structured reporting for MRI of the prostate," *Fortschr Röntgenstr*, vol. 185, no. 3, pp. 253–261, 2013.

[14] A. B. Rosenkrantz, S. Kim, R. P. Lim et al., "Prostate cancer localization using multiparametric MR imaging: comparison of prostate imaging reporting and data system (PI-RADS) and likert scales," *Radiology*, vol. 269, no. 2, pp. 482–492, 2013.

[15] J. H. Koo, C. K. Kim, D. Choi, B. K. Park, G. Y. Kwon, and B. Kim, "Diffusion-weighted magnetic resonance imaging for the evaluation of prostate cancer: optimal B value at 3T," *Korean Journal of Radiology*, vol. 14, no. 1, pp. 61–69, 2013.

[16] C. K. Kim, B. K. Park, and B. Kim, "High-b-value diffusion-weighted imaging at 3 T to detect prostate cancer: comparisons between b values of 1,000 and 2,000 s/mm2," *American Journal of Roentgenology*, vol. 194, no. 1, pp. W33–W37, 2010.

[17] N. B. Delongchamps, M. Rouanne, T. Flam et al., "Multiparametric magnetic resonance imaging for the detection and localization of prostate cancer: combination of T2-weighted, dynamic contrast-enhanced and diffusion-weighted imaging," *BJU International*, vol. 107, no. 9, pp. 1411–1418, 2011.

[18] M. M. Siddiqui, S. Rais-Bahrami, H. Truong et al., "Magnetic resonance imaging/ultrasound-fusion biopsy significantly upgrades prostate cancer versus systematic 12-core transrectal ultrasound biopsy," *European Urology*, vol. 64, no. 5, pp. 713–719, 2013.

[19] S. Vourganti, A. Rastinehad, N. K. Yerram et al., "Multiparametric magnetic resonance imaging and ultrasound fusion biopsy detect prostate cancer in patients with prior negative transrectal ultrasound biopsies," *Journal of Urology*, vol. 188, no. 6, pp. 2152–2157, 2012.

[20] T. H. Kuru, M. C. Röthke, J. Seidenader et al., "Critical evaluation of magnetic resonance imaging targeted, transrectal ultrasound guided transperineal fusion biopsy for detection of prostate cancer," *Journal of Urology*, vol. 190, no. 4, pp. 1380–1386, 2013.

[21] L. Schimmöller, M. Quentin, C. Arsov et al., "Inter-reader agreement of the ESUR score for prostate MRI using in-bore MRI-guided biopsies as the reference standard," *European Radiology*, vol. 23, no. 11, pp. 3185–3190, 2013.

[22] D. Portalez, P. Mozer, F. Cornud et al., "Validation of the European Society of Urogenital Radiology scoring system for prostate cancer diagnosis on multiparametric magnetic resonance imaging in a cohort of repeat biopsy patients," *European Urology*, vol. 62, no. 6, pp. 986–996, 2012.

[23] P. Puech, O. Rouvière, R. Renard-Penna et al., "Prostate cancer diagnosis: multiparametric MR-targeted biopsy with cognitive and transrectal US-MR fusion guidance versus systematic biopsy—prospective multicenter study," *Radiology*, vol. 268, no. 2, pp. 461–469, 2013.

[24] M. D. Dorrius, R. M. Pijnappel, M. C. Jansen-van der Weide, and M. Oudkerk, "Breast magnetic resonance imaging as a problem-solving modality in mammographic BI-RADS 3 lesions," *Cancer Imaging A*, vol. 10, pp. S54–S58, 2010.

Hindawi Publishing Corporation
BioMed Research International
Volume 2013, Article ID 460546, 6 pages
http://dx.doi.org/10.1155/2013/460546

Review Article

Strategies for Imaging Androgen Receptor Signaling Pathway in Prostate Cancer: Implications for Hormonal Manipulation and Radiation Treatment

Gravina Giovanni Luca,[1,2,3] Claudio Festuccia,[1] Pierluigi Bonfili,[1] Mario Di Staso,[1] Pietro Franzese,[1] Valeria Ruggieri,[1] Vladimir M. Popov,[3] Vincenzo Tombolini,[4,5] Carlo Masciocchi,[6] Eleonora Carosa,[7] Andrea Lenzi,[2] Emmanuele A. Jannini,[7] and Ernesto Di Cesare[1]

[1] *Department of Applied, Clinical and Biotechnological Sciences, Laboratory of Radiobiology and Division of Radiotherapy, University of L'Aquila, Via Vetoio, Coppito 2, L'Aquila, Italy*
[2] *Department of Experimental Medicine, Section of Medical Pathophysiology, Food Science and Endocrinology, Sapienza University of Rome, Italy*
[3] *LIPOGEN LLC, Mount Laurel, NJ, USA*
[4] *Division of Radiotherapy, University of Rome, University Hospital "Policlinico Umberto I", Italy*
[5] *Department of Radiological Sciences, Division of Radiotherapy, University of Rome "La Sapienza", Spencer-Lorillard Foundation, Rome, Italy*
[6] *Department of Applied, Clinical and Biotechnological Sciences, Division of Radiology, University of L'Aquila, L'Aquila, Italy*
[7] *Course of Endocrinology and Medical Sexology, Department of Applied, Clinical and Biotechnological Sciences, University of L'Aquila, L'Aquila, Italy*

Correspondence should be addressed to Claudio Festuccia; claudio.festuccia@univaq.it

Received 30 July 2013; Accepted 16 September 2013

Academic Editor: David Sherris

Prostate cancer (Pca) is a heterogeneous disease; its etiology appears to be related to genetic and epigenetic factors. Radiotherapy and hormone manipulation are effective treatments, but many tumors will progress despite these treatments. Molecular imaging provides novel opportunities for image-guided optimization and management of these treatment modalities. Here we reviewed the advances in targeted imaging of key biomarkers of androgen receptor signaling pathways. A computerized search was performed to identify all relevant studies in Medline up to 2013. There are well-known limitations and inaccuracies of current imaging approaches for monitoring biological changes governing tumor progression. The close integration of molecular biology and clinical imaging could ease the development of new molecular imaging agents providing novel tools to monitor a number of biological events that, until a few years ago, were studied by conventional molecular assays. Advances in translational research may represent the next step in improving the oncological outcome of men with Pca who remain at high risk for systemic failure. This aim may be obtained by combining the anatomical properties of conventional imaging modalities with biological information to better predict tumor response to conventional treatments.

1. Molecular Imaging as Tool for Translating Biological Information into Oncological Practice

Pca is one of the most commonly diagnosed cancers in men. Its etiology appears to be related to lifestyle patterns, genetic, epigenetic factors, and hormones [1, 2]. Surgery and external beam radiation therapy (EBRT) remain to be two of the major milestones for the treatment of localized or locally advanced Pca [3]. Despite their technical improvements, Pca recurrence is not uncommon [3] after these treatments. Historically, hormonal manipulation has been used for the management

of advanced and/or recurrent Pca [3] especially in association with radiotherapy [4]. We now have a greater understanding of mechanisms sustaining CRPC upon hormonal manipulation [5]. Biological evidence supports the idea that androgen receptor (AR) drives the transition towards an androgen independent and radioresistant phenotype [6]. However, we are aware that the improvement in oncological outcome of men who remain at high risk for systemic failure may also be achieved by improving the diagnostic performances of conventional imaging modalities by making them more suitable for predicting tumor response to conventional treatments. There are well-known limitations and inaccuracies in current imaging approaches for monitoring biological changes governing tumor progression and radioresistant phenotypes [7]. The growing number of alternative treatments and the need for an early identification of nonresponders have considerably stimulated and renewed the interest to use molecular imaging techniques [7]. The close integration between molecular biology and clinical imaging may ease the development of new molecular imaging agents useful to monitor a number of biological events that, until a few years ago, were studied by conventional molecular assays [8]. With regard to Pca, progress in quantification, characterization, and timing of biological processes could create novel opportunities to more fully characterize many biological events and to monitor the performance of well-established as well as novel treatment modalities [8]. However, there are theoretical and practical challenges in attempting to translate these imaging strategies into clinical practice [9]. Some of these challenges include the need to overcome problems related to the amplification of low level signals of *in vivo* biological events, the development of integrated imaging platforms with sufficiently high spatial and temporal resolution [9], and the need to reach the target *in vivo* to achieve satisfactory specificity [7–9]. The advances in the molecular based approaches in radiology are specifically evident in oncological treatments [10]. One of the most striking examples of foregoing statements is attested by the development of the enormous amount of specific drugs and inhibitors, the ability to genetically modify cellular systems, and the introduction of a multitude of diagnostic tools able to monitor individual molecular and biological processes [8]. These achievements have dramatically augmented our understanding of molecular oncology and this body of knowledge can now be translated into new drugs or agents for molecular imaging by allowing detection of patients with specific molecular profiles and improving patient care [11]. However the question of whether radiology will be able to integrate the molecular imaging into the mainstream molecular research and really translate biological knowledge and discoveries into clinical practice is still open. Historically, although most radiological research has been focused on the attempt to improve technological quality, substantial advances in MR spectroscopy, diffusion weighted imaging, dynamic contrast enhanced methods, and contrast agents as well as radiochemistry advances in tumor targeting agents such as antibodies and PET radiopharmaceuticals have greatly improved the overall diagnostic performance [8–11]. Today's medical imaging technology has improved significantly in terms of resolution and speed reaching a stage where cell trafficking can be efficiently imaged. Among the many putative biological targets for imaging cancer, angiogenesis, apoptosis, signal transduction, and metabolic pathways have been the subject of intense research [5, 7, 12]. Conventional anatomic [13, 14] and some molecular imaging techniques [15–17] are currently used in the common clinical practice to study patients suffering from Pca. All these diagnostic tools have advantages and disadvantages although they play a rather limited role in monitoring men with Pca [7, 15–17]. These limitations are imputable to inability to distinguish Pca from the surrounding nonmalignant tissue. Thus, molecular imaging, providing biologically relevant information, may allow more accurate patient stratification with a more accurate therapeutic monitoring. Among all of molecular imaging modalities, PET represents a robust imaging technique because it provides noninvasive qualitative and quantitative information and requires very low levels of molecular probes to obtain images in intact living subjects [17]. Additionally, the imaging of tumor receptor poses specific challenges for the design of radiopharmaceuticals. Since most receptors have high affinities for their ligands, radiopharmaceuticals with high specific activity are essential since small molar quantities of an imaging agent may saturate a receptor and limit the ability to visualize receptor expression [17]. This paper is intended as a review of recent advances in molecular imaging of key biomarkers of androgen receptor signaling pathways and their implications for hormonal manipulation and radiation treatment in Pca.

2. Methods

2.1. Search Strategy. A computerized search was performed to identify all relevant studies in Medline up to 2013. The following search terms were used in Medline: "prostate cancer AND molecular imaging," "prostate cancer AND radiotherapy," "prostate cancer AND hormonal manipulation," "PET-CT and prostate cancer," "ProstaScint SPECT and prostate cancer," "molecular imaging AND androgen receptor," and "molecular imaging AND radiotherapy." Additional articles were extracted based on recommendations from an expert panel of authors.

3. Imaging AR Signaling Pathway

3.1. 18F-Fluoro-5α-dihydrotestosterone (18F-FDHT). F-FDHT, a ligand that targets the ligand-binding domain of AR, assesses receptor occupancy but not downstream activity. Recent studies of 18F-FDHT PET in CRPC patients treated with MDV3100 found that tumors in nearly all patients showed a decrease in 18F-FDHT binding, indicating that MDV3100 can occupy the AR ligand-binding domain and preclude 18F-FDHT binding. However, these 18F-FDHT PET "responses" did not correlate with declines in serum PSA or tumor response [6]. Therefore, 18F-FDHT PET may have utility in optimizing the dose of antiandrogen required for complete blockade of androgen binding to AR, but it cannot assess AR pathway activity. Changes in AR levels may be measured by 18F-FDHT, a structural analog of 5α-dihydrotestosterone (DHT), in Pca patients undergoing therapy [18]. Among

fluorinated androgen analogs studied in animals, 18F-FDHT uptake was reduced by about 10-fold by the coadministration of testosterone. Thus, 18F-FDHT appears to bind specifically to AR *in vivo* and to have the most favorable targeting properties for imaging among AR-binding radiotracers studied [18]. Currently, a direct biopsy of a metastatic lesion may be required to assess the AR status especially when treatment is being considered. This procedure is technically feasible, but due to its invasiveness it is not considered as a part of routine practice. Moreover, the AR status determined histopathologically in one metastasis may not be representative of all metastatic lesions. A PET ligand which provides signals able to predict and measure AR expression levels not only would have great potential in the diagnostic environment but also could have implications in tailoring the appropriate therapy and in assessing its efficacy. Preliminary clinical experience suggests that [18]F-FDHT PET is a simple way to estimate AR concentration in men suffering from CRPC metastatic disease and treated by hormonal manipulation [18]. The group of Larson, at the Memorial Sloan-Kettering Cancer Center [19, 20], confirmed that [18]F-FDHT may be a promising radiotracer for the study and imaging of AR during the progression to CRPC. This team found that [18]F-FDHT-PET detected 58 of the 59 lesions identified using conventional imaging procedures [21]. In a second study [18], at the Washington University, a team led by Dehdashti found that 10 of the 15 patients with advanced Pca and studied with [18]F-FDHT-PET, computed tomography (CT) and bone scintigraphy had tumors that took up [18]F-FDHT. In 10 patients with positive [18]F-FDHT-PET, the tumor [18]F-FDHT uptake after one single dose of flutamide was significantly decreased with a mean drop in intensity around 60% [18]. Whether this early response to antiandrogens predicts the long-term therapy response to hormonal manipulation remains unclear. However, the evidence that after flutamide treatment tumors which disappear on FDHT-PET are still visible on conventional imaging suggests that this radiotracer may be used as an early marker of tumor response. This evidence is confirmed by studies in CRPC patients treated with MDV3100 showing that tumors in nearly all patients had a decrease in 18F-FDHT binding, indicating that MDV3100 occupies the AR ligand-binding domain and precludes 18F-FDHT binding. However, these 18F-FDHT PET "responses" did not correlate with declines in serum PSA or tumor response [22].

3.2. Radiotracer Targeting Free Prostate-Specific Antigen. By quantitatively assessing expression of a downstream AR target gene, PET tracers targeting PSA subforms or PSMA may identify those patients whose tumors retain AR activity despite blockade of the AR ligand-binding domain and therefore would be ideal candidates for additional therapies to fully inhibit AR signaling. PSA is one of the downstream mediators whose expression reflects AR transcriptional activity in normal and cancerous prostatic cells, although additional factors regulating the PSA promoter have been identified [23]. However, even though it is used as tumor marker, PSA exhibits certain limitations. As a primary screening tool, this marker is unable to distinguish between normal pathological conditions especially in the so-called "grey zone" (PSA value from 2.5 to 10 ng/mL) [24]. For the range above 20 ng/mL or in clinical conditions characterized as androgen independent, it has been shown to be a good indicator of metastatic disease [24]. Apart from a few clinical contexts, changes in PSA levels are hard to interpret and over the last few years new PSA fractions have increasingly been used to improve the PSA diagnostic performance. Clinical and biological data suggest that tumor tissue produces greater amount of free PSA (fPSA) than normal one and this seems to improve the predictive value of this marker in detecting Pca [24]. In a recent report, a team led by Ulmert et al. [25] pointed out that the use of a monoclonal antibody, the 5A10, is conjugated with 89ZR that specifically binds fPSA and features the AR-driven prostate tumor activity. Of great interest is the fact that 89Zr-5A10 is suitable for the quantification of AR transcriptional activity in preclinical models of androgen independent models. Additionally, 89Zr-5A10 is colocalized in PSA- and AR-positive Pca models and quantitatively predicted response to antiandrogen therapy [25]. This radiotracer appears to preferentially target malignant tumor cells and therefore may become a more predictive imaging biomarker in prostate cancer [26].

3.3. Imaging Strategies Targeting Prostate-Specific Membrane Antigen. Another surrogate of AR transcriptional activity is the prostate-specific membrane antigen (PSMA) [26]. The molecular basis for downregulation of PSMA expression by AR may be related to the presence of an enhancer region although no androgen response elements have been identified [27]. Recent AR ChIP-Seq reveals four peaks of AR binding among multiple introns of PSMA in LNCaP [28]. Preliminary data indicated that PSMA, a membrane glycoprotein, was specifically expressed on Pca cells as a noncovalent homodimer and, for this reason, was regarded as specific for prostate tissue [29]. More recently, its expression has been documented in a few other tissues reducing its specificity for prostate [29]. Although PSMA is no longer considered prostate specific, the literature indicates that this glycoprotein may be useful in nuclear medicine for imaging benign and malignant prostate tissue [29]. Little is known about its function in the biology of normal and pathological conditions although some evidence suggests a role of this glycoprotein as oncosuppressor. This hypothesis is supported by the evidence that PC3 cells, transfected with full length PSMA cDNA and then orthotopically implanted into nude mice, gave rise to lower tumor volumes with reduced incidence of metastases with respect to mice implanted with wild-type PC3 cells [30]. Interestingly, its activity and expression are increased as tumor becomes more androgen independent [31]. This clearly indicates that there is a link between PSMA and androgen independent phenotype [30]. From a clinical point of view this may have a significant impact on the possibility to select men with CRPC who can be at risk of resistance to hormonal manipulation and/or radiation therapy. This statement may be confirmed by reports indicating that changes in PSMA expression can also serve as a noninvasive marker for imaging AR signaling and monitoring response to conventional treatments [29, 32]. Additionally, the molecular imaging strategy using tracers

directed towards PSMA could also have a more significant clinical impact considering that PSMA is upregulated in response to antiandrogen therapy [33]. This may have important therapeutic implications since a toxin-conjugated PSMA-targeted mAb could be an effective combination therapy with antiandrogens. Indeed, J591 has been adapted for radioimmunotherapy, and Ab-drug conjugates and therapeutic doses are well tolerated in patients [34, 35]. A well-known Food and Drug Administration (FDA) approved that agent targeting PSMA is capromab pendetide (ProstaScint) [36]. It consists of a murine monoclonal antibody (mAb) (mAb 7E11) labeled with 111In [36]. The overall diagnostic performance of ProstaScint for detecting Pca is variable in function according to different reports with an average sensitivity, specificity, and positive and negative predictive value of 60%, 70%, 60%, and 70%, respectively [7, 36]. The relatively disappointing results of these studies are partially due to the murine monoclonal antibody properties. This antibody binds to the internal epitope of PSMA and therefore shows limited effectiveness in targeting viable prostate tumor cancer cells. Thus, only cells with damaged cell membranes bind mAb 7E11, explaining the decreased overall performance of this imaging modality [36]. More recently, radiolabeled mAbs that bind the extracellular PSMA domain have been developed [37]. The second-generation of antibodies targeting PSMA provide higher performance than capromab pendetide. Among these, the monoclonal antibody J591 [38] has provided outstanding results in imaging bone metastatic disease. J591 has been extensively utilized and evaluated in different preclinical models, demonstrating higher specificity in identifying tumor tissue [38]. Clinical trials, using J591 labeled with 99mTc, demonstrated the detection of distant metastases, including bone metastases, in patients with CRPC [39]. Several other novel mAbs targeting PSMA have been developed for molecular imaging. Among these, four new IgG mAbs (3/F11, 3/A12, 3C6, and 3/E7) with strong affinity for three different extracellular PSMA epitopes [40, 41] have been developed. The 3/A12 antibody labeled with 64Cu (64Cu-3/A12) demonstrated a good tumor-to-background ratio in preclinical models [42]. However, the slow tumor uptake and plasma clearance of mAbs in men necessitate the use of long-lived radioisotopes for imagining at the expense of increased radiation dose to the patients [43]. A further disadvantage is the need to bring the patient for a second visit several days after injection for imaging [43]. Low-molecular-weight radiopharmaceutical agents have better pharmacokinetic properties than radiolabeled mAbs [43]. These low-molecular-weight molecules have encouraged the generation of a new class of PSMA targeting molecules for single-photon emission computed tomography (SPECT) and PET imaging [31, 44–46]. Among these, the PSMA tracer N-[N-[(S)-1,3-dicarboxypropyl]-carbamoyl]-S-[11C] methyl-l-cysteine (DCFBC) has been developed for PET imaging [47–50]. This radiotracer has been used successfully for imaging preclinical xenograft models expressing PSMA antigen [47–50]. More recently, Mease and colleagues [51] and Lapi and coworkers [52] labeled DCFBC and phosphoramidates compounds, respectively, with 18F. Biodistribution and imaging studies showed a PSMA-expression dependent tumor uptake of this radiotracer with higher uptake in PSMA expressing tumor cells [51, 52]. Other promising small-molecule inhibitors for Pca imaging are MIP-1072 and MIP-1095 [53]. These agents are urea based compounds and exhibit high affinity for PSMA [29, 53]. When labeled with 123I, they have been successfully used as radiotracers with SPECT/CT in human Pca xenografts [53]. Finally, limited experience with thermally cross-linked SPION (TCL-SPION), able to both detect Pca cells and deliver targeted chemotherapeutic agents directly to Pca cells, has been reported [47–50]. Differential uptake of the TCL-SPION-Apt bioconjugates by PSMA-expressing LnCaP cells or non-PSMA-expressing PC3 cells was documented confirming that TCL-SPION-Apt bioconjugates can differentially target PSMA-expressing Pca cells [47–50]. This agent, in addition to the efficient identification of Pca cells *in vivo* by magnetic resonance imaging (MRI), is able to selectively deliver cytotoxic drugs to the tumor tissue, providing an excellent compromise in terms of diagnostic and therapeutic capabilities [47–50].

4. Conclusions

New imaging modalities allowing the investigation of molecular events in terms of the spatiotemporal dimension may be useful to follow the intracellular signaling pathways both in the tumor itself as well as in the surrounding normal tissues. Molecular imaging comprises a cluster of technologies allowing the measurement of biological events that are relevant for the understanding and the monitoring of prostate cancer, especially when it becomes resistant to treatments. Each different imaging modality presents its unique set of advantages and disadvantages in terms of sensitivity, resolution, and type of information provided. To overcome these drawbacks, innovative technologies, allowing the integration of different imaging modalities, have been developed. Further advances are also expected to be in the way tracers are conceived to widen the number of biological events that can be studied and monitored by molecular imaging. Among them, PET-based and, to a lesser extent, MRI-based technologies are promising modalities which have opened up new avenues for visualizing and understanding the biological changes occurring in patients that do not respond to hormonal and radiation treatment. Obviously, the information obtained in such manner could not be sufficient to unravel the molecular pathways that govern the mechanisms involved in the resistance to treatments but might represent a powerful tool for visualizing and understanding differences in the cancer biology that become manifested between a responding patient and a nonresponding patient. Hopefully, the knowledge of critical molecular events involved in these biological processes will allow us to identify unique signatures useful to inspire development of new therapeutic strategies for overcoming the problem of resistance to conventional treatments.

Conflict of Interests

Gravina Giovanni Luca is the Lead Guest Editor of the special issue "Advances in Prostate Cancer Research and Treatment."

Other authors declare that there is no conflict of interests regarding the publication of this paper.

References

[1] J. Ferlay, D. M. Parkin, and E. Steliarova-Foucher, "Estimates of cancer incidence and mortality in Europe in 2008," *European Journal of Cancer*, vol. 46, no. 4, pp. 765–781, 2010.

[2] P. A. Jones and S. B. Baylin, "The fundamental role of epigenetic events in cancer," *Nature Reviews Genetics*, vol. 3, no. 6, pp. 415–428, 2002.

[3] R. Siegel, C. De Santis, K. Virgo, K. Stein, A. Mariotto, and T. Smith, "Cancer treatment and survivorship statistics, 2012," *Cancer Journal for Clinicians*, vol. 62, no. 4, pp. 220–241, 2012.

[4] P. Milecki, P. Martenka, A. Antczak, and Z. Kwias, "Radiotherapy combined with hormonal therapy in prostate cancer: the state of the art," *Cancer Management and Research*, vol. 2, no. 1, pp. 243–253, 2010.

[5] G. L. Gravina, F. Marampon, M. Piccolella et al., "Hormonal therapy promotes hormone-resistant phenotype by increasing DNMT activity and expression in prostate cancer models," *Endocrinology*, vol. 152, no. 12, pp. 4550–4561, 2011.

[6] G. L. Gravina, C. Festuccia, F. Marampon et al., "Biological rationale for the use of DNA methyltransferase inhibitors as new strategy for modulation of tumor response to chemotherapy and radiation," *Molecular Cancer*, vol. 9, pp. 305–321, 2010.

[7] G. L. Gravina, V. Tombolini, M. Di Staso, P. Franzese, P. Bonfili, and A. Gennarelli, "Advances in imaging and in non-surgical salvage treatments after radiorecurrence in prostate cancer: what does the oncologist, radiotherapist and radiologist need to know?" *European Radiology*, vol. 22, no. 12, pp. 2848–2858, 2012.

[8] L. Fass, "Imaging and cancer: a review," *Molecular Oncology*, vol. 2, no. 2, pp. 115–152, 2008.

[9] M. G. Pomper, "Translational molecular imaging for cancer," *Cancer Imaging A*, vol. 5, pp. S16–S26, 2005.

[10] S. Kumar, A. Mohan, and R. Guleria, "Biomarkers in cancer screening, research and detection: present and future: a review," *Biomarkers*, vol. 11, no. 5, pp. 385–405, 2006.

[11] D. A. Mankoff, "Molecular imaging to select cancer therapy and evaluate treatment response," *Quarterly Journal of Nuclear Medicine and Molecular Imaging*, vol. 53, no. 2, pp. 181–192, 2009.

[12] M. L. Thakur, "Genomic biomarkers for molecular imaging: predicting the future," *Seminars in Nuclear Medicine*, vol. 39, no. 4, pp. 236–246, 2009.

[13] H. Hricak, P. L. Choyke, S. C. Eberhardt, S. A. Leibel, and P. T. Scardino, "Imaging prostate cancer: a multidisciplinary perspective," *Radiology*, vol. 243, no. 1, pp. 28–53, 2007.

[14] L. M. Wu, J. R. Xu, Y. Q. Ye, Q. Lu, and J. N. Hu, "The clinical value of diffusion-weighted imaging in combination with T2-weighted imaging in diagnosing prostate carcinoma: a systematic review and meta-analysis," *American Journal of Roentgenology*, vol. 199, no. 1, pp. 103–110, 2012.

[15] H. A. Vargas, C. Wassberg, O. Akin, and H. Hricak, "MR imaging of treated prostate cancer," *Radiology*, vol. 262, no. 1, pp. 26–42, 2012.

[16] V. Ambrosini, M. Fani, S. Fanti, F. Forrer, and H. R. Maecke, "Radiopeptide imaging and therapy in Europe," *Journal of Nuclear Medicine*, vol. 52, supplement 2, pp. 42S–55S, 2011.

[17] H. Jadvar, "Molecular imaging of prostate cancer: PET radiotracers," *American Journal of Roentgenology*, vol. 199, no. 2, pp. 278–291, 2012.

[18] F. Dehdashti, J. Picus, J. M. Michalski et al., "Positron tomographic assessment of androgen receptors in prostatic carcinoma," *European Journal of Nuclear Medicine and Molecular Imaging*, vol. 32, no. 3, pp. 344–350, 2005.

[19] J. J. Fox, E. Autran-Blanc, M. J. Morris et al., "Practical approach for comparative analysis of multilesion molecular imaging using a semiautomated program for PET/CT," *Journal of Nuclear Medicine*, vol. 52, no. 11, pp. 1727–1732, 2011.

[20] J. J. Fox, M. J. Morris, S. M. Larson, H. Schöder, and H. I. Scher, "Developing imaging strategies for castration resistant prostate cancer," *Acta Oncologica*, vol. 50, supplement 1, pp. 39–48, 2011.

[21] S. M. Larson, M. Morris, I. Gunther et al., "Tumor localization of 16β-18F-fluoro-5α- dihydrotestosterone versus 18F-FDG in patients with progressive, metastatic prostate cancer," *Journal of Nuclear Medicine*, vol. 45, no. 3, pp. 366–373, 2004.

[22] H. I. Scher, A. Anand, D. Rathkopf et al., "Antitumour activity of MDV3100 in castration-resistant prostate cancer: a phase 1-2 study," *The Lancet*, vol. 375, no. 9724, pp. 1437–1446, 2010.

[23] L. Van Neste, J. G. Herman, G. Otto, J. W. Bigley, J. I. Epstein, and W. Van Criekinge, "The epigenetic promise for prostate cancer diagnosis," *Prostate*, vol. 72, no. 11, pp. 1248–1261, 2012.

[24] D. Ilic, D. O'Connor, S. Green, and T. J. Wilt, "Screening for prostate cancer: an updated Cochrane systematic review," *BJU International*, vol. 107, no. 6, pp. 882–891, 2011.

[25] D. Ulmert, M. J. Evans, J. P. Holland, S. L. Rice, J. Wongvipat, and K. Pettersson, "Imaging androgen receptor signaling with a radiotracer targeting free prostate-specific antigen," *Cancer Discovery*, vol. 4, pp. 320–327, 2012.

[26] P. Mhawech-Fauceglia, D. J. Smiraglia, W. Bshara et al., "Prostate-specific membrane antigen expression is a potential prognostic marker in endometrial adenocarcinoma," *Cancer Epidemiology Biomarkers and Prevention*, vol. 17, no. 3, pp. 571–577, 2008.

[27] K. R. Noss, S. A. Wolfe, and S. R. Grimes, "Upregulation of prostate specific membrane antigen/folate hydrolase transcription by an enhancer," *Gene*, vol. 285, no. 1-2, pp. 247–256, 2002.

[28] J. Yu, J. Yu, R. Mani et al., "An integrated network of androgen receptor, polycomb, and TMPRSS2-ERG gene fusions in prostate cancer progression," *Cancer Cell*, vol. 17, no. 5, pp. 443–454, 2010.

[29] R. M. Taylor, V. Severns, D. C. Brown, M. Bisoffi, and L. O. Sillerud, "Prostate cancer targeting motifs: expression of $\alpha v\beta 3$, neurotensin receptor 1, prostate specific membrane antigen, and prostate stem cell antigen in human prostate cancer cell lines and xenografts," *Prostate*, vol. 72, no. 5, pp. 523–532, 2012.

[30] P. Laidler, J. Dulińska, M. Lekka, and J. Lekki, "Expression of prostate specific membrane antigen in androgen-independent prostate cancer cell line PC-3," *Archives of Biochemistry and Biophysics*, vol. 435, no. 1, pp. 1–14, 2005.

[31] C. A. Foss, R. C. Mease, H. Fan et al., "Radiolabeled small-molecule ligands for prostate-specific membrane antigen: in vivo imaging in experimental models of prostate cancer," *Clinical Cancer Research*, vol. 11, no. 11, pp. 4022–4028, 2005.

[32] U. Elsässer-Beile, P. Bühler, and P. Wolf, "Targeted therapies for Prostate cancer against the prostate specific membrane antigen," *Current Drug Targets*, vol. 10, no. 2, pp. 118–125, 2009.

[33] M. J. Evans, P. M. Smith-Jones, J. Wongvipat et al., "Noninvasive measurement of androgen receptor signaling with a positron-emitting radiopharmaceutical that targets prostate-specific membrane antigen," *Proceedings of the National Academy of Sciences of the United States of America*, vol. 108, no. 23, pp. 9578–9582, 2011.

[34] N. H. Bander, M. I. Milowsky, D. M. Nanus, L. Kostakoglu, S. Vallabhajosula, and S. J. Goldsmith, "Phase I trial of 177Lutetium-labeled J591, a monoclonal antibody to prostate-specific membrane antigen, in patients with androgen-independent prostate cancer," *Journal of Clinical Oncology*, vol. 23, no. 21, pp. 4591–4601, 2005.

[35] M. D. Galsky, M. Eisenberger, S. Moore-Cooper et al., "Phase I trial of the prostate-specific membrane antigen-directed immunoconjugate MLN2704 in patients with progressive metastatic castration-resistant prostate cancer," *Journal of Clinical Oncology*, vol. 26, no. 13, pp. 2147–2154, 2008.

[36] A. B. Apolo, N. Pandit-Taskar, and M. J. Morris, "Novel tracers and their development for the imaging of metastatic prostate cancer," *Journal of Nuclear Medicine*, vol. 49, no. 12, pp. 2031–2041, 2008.

[37] J. K. Troyer, M. L. Beckett, and G. L. Wright, "Location of prostate-specific membrane antigen in the LNCaP prostate carcinoma cell line," *Prostate*, vol. 30, no. 4, pp. 232–242, 1997.

[38] D. M. Nanus, M. I. Milowsky, L. Kostakoglu et al., "Clinical use of monoclonal antibody HuJ591 therapy: targeting prostate specific membrane antigen," *Journal of Urology*, vol. 170, supplement 6, part 2, pp. S84–S89, 2003.

[39] V. Nargund, D. Al Hashmi, P. Kumar et al., "Imaging with radiolabelled monoclonal antibody (MUJ591) to prostate-specific membrane antigen in staging of clinically localized prostatic carcinoma: comparison with clinical, surgical and histological staging," *BJU International*, vol. 95, no. 9, pp. 1232–1236, 2005.

[40] P. Wolf, N. Freudenberg, P. Bühler et al., "Three conformational antibodies specific for different PSMA epitopes are promising diagnostic and therapeutic tools for prostate cancer," *Prostate*, vol. 70, no. 5, pp. 562–569, 2010.

[41] C. A. Regino, K. J. Wong, D. E. Milenic et al., "Preclinical evaluation of a monoclonal antibody (3C6) specific for prostate-specific membrane antigen," *Current Radiopharmaceuticals*, vol. 2, no. 1, pp. 9–17, 2009.

[42] K. Alt, S. Wiehr, W. Ehrlichmann et al., "High-resolution animal PET imaging of prostate cancer xenografts with three different64Cu-labeled antibodies against native cell-adherent PSMA," *Prostate*, vol. 70, no. 13, pp. 1413–1421, 2010.

[43] K. Chen and P. S. Conti, "Target-specific delivery of peptide-based probes for PET imaging," *Advanced Drug Delivery Reviews*, vol. 62, no. 11, pp. 1005–1022, 2010.

[44] M. Eder, M. Schäfer, U. Bauder-Wüst et al., "68Ga-complex lipophilicity and the targeting property of a urea-based PSMA inhibitor for PET imaging," *Bioconjugate Chemistry*, vol. 23, no. 4, pp. 688–697, 2012.

[45] K. Graham, R. Lesche, A. V. Gromov, N. Böhnke, M. Schäfer, and J. Hassfeld, "Radiofluorinated derivatives of 2-(Phosphonomethyl)pentanedioic acid as inhibitors of prostate specific membrane antigen (PSMA) for the imaging of prostate cancer," *Journal of Medicinal Chemistry*, vol. 55, no. 22, pp. 9510–9520, 2012.

[46] S. R. Banerjee, M. Pullambhatla, Y. Byun et al., "68 Ga-labeled inhibitors of prostate-specific membrane antigen (PSMA) for imaging prostate cancer," *Journal of Medicinal Chemistry*, vol. 53, no. 14, pp. 5333–5341, 2010.

[47] H. Lee, K. Y. Mi, S. Park et al., "Thermally cross-linked superparamagnetic iron oxide nanoparticles: synthesis and application as a dual imaging probe for cancer in vivo," *Journal of the American Chemical Society*, vol. 129, no. 42, pp. 12739–12745, 2007.

[48] K. Min, H. Jo, K. Song et al., "Dual-aptamer-based delivery vehicle of doxorubicin to both PSMA (+) and PSMA (-) prostate cancers," *Biomaterials*, vol. 32, no. 8, pp. 2124–2132, 2011.

[49] M. Li, H. S. Kim, L. Tian, M. K. Yu, S. Jon, and W. K. Moon, "Comparison of two ultrasmall superparamagnetic iron oxides on cytotoxicity and MR imaging of tumors," *Theranostics*, vol. 2, no. 1, pp. 76–85, 2012.

[50] A. Z. Wang, V. Bagalkot, C. C. Vasilliou et al., "Superparamagnetic iron oxide nanoparticle-aptamer bioconjugates for combined prostate cancer imaging and therapy," *ChemMedChem*, vol. 3, no. 9, pp. 1311–1315, 2008.

[51] R. C. Mease, C. L. Dusich, C. A. Foss et al., "N-[N-[(S)-1,3-dicarboxypropyl]carbamoyl]-4-[18F]fluorobenzyl-L- cysteine, [18F]DCFBC: a new Imaging probe for prostate cancer," *Clinical Cancer Research*, vol. 14, no. 10, pp. 3036–3043, 2008.

[52] S. E. Lapi, H. Wahnishe, D. Pham et al., "Assessment of an 18F-labeled phosphoramidate peptidomimetic as a new prostate-specific membrane antigen-targeted imaging agent for prostate cancer," *Journal of Nuclear Medicine*, vol. 50, no. 12, pp. 2042–2048, 2009.

[53] Y. Chen, C. A. Foss, Y. Byun et al., "Radiohalogenated prostate-specific membrane antigen (PSMA)-based ureas as imaging agents for prostate cancer," *Journal of Medicinal Chemistry*, vol. 51, no. 24, pp. 7933–7943, 2008.